COPY NO. 36

AD 740740

TECHNICAL REPORT 4309

THE STATISTICAL PROPERTIES AND CORRELATIONS OF DIMENSIONAL VARIATIONS AND INERTIAL PROPERTIES OF 175 MM. M437 PROJECTILES

HENRY E. HUDGINS, JR.

MARCH 1972

APPROVED FOR PUBLIC RELEASE: DISTRIBUTION UNLIMITED

PICATINNY ARSENAL
DOVER, NEW JERSEY

344

The findings in this report are not to be construed as an official Department of the Army position.

DISPOSITION

Destroy this report when no longer needed. Do not return it to the originator.

Technical Report 4309

SOME STATISTICAL PROPERTIES AND CORRELATIONS OF DIMENSIONAL VARIATIONS AND INERTIAL PROPERTIES OF 175MM, M437 PROJECTILES

by

Henry E. Hudgins, Jr.

AMCMS Code 4810.16.2911.8

Engineering Sciences Division
Feltman Research Laboratories
Picatinny Arsenal
Dover, New Jersey

UNCLASSIFIED
Security Classification

DOCUMENT CONTROL DATA - R & D

(Security classification of title, body of abstract and indexing annotation must be entered when the overall report is classified)

1. ORIGINATING ACTIVITY (Corporate author) Feltman Research Laboratories Picatinny Arsenal Dover, New Jersey	2a. REPORT SECURITY CLASSIFICATION Unclassified 2b. GROUP

3. REPORT TITLE
SOME STATISTICAL PROPERTIES AND CORRELATIONS OF DIMENSIONAL VARIATIONS AND INERTIAL PROPERTIES OF 175MM, M437 PROJECTILES

4. DESCRIPTIVE NOTES (Type of report and inclusive dates)

5. AUTHOR(S) (First name, middle initial, last name)
Henry E. Hudgins, Jr.

6. REPORT DATE	7a. TOTAL NO. OF PAGES	7b. NO. OF REFS
March 1972	346	3

8a. CONTRACT OR GRANT NO. b. PROJECT NO. AMCMS Code 4810.16.2911.8 c. d.	9a. ORIGINATOR'S REPORT NUMBER(S) TR 4309 9b. OTHER REPORT NO(S) (Any other numbers that may be assigned this report)

10. DISTRIBUTION STATEMENT
Approved for public release; distribution unlimited

11. SUPPLEMENTARY NOTES	12. SPONSORING MILITARY ACTIVITY
None	Feltman Research Laboratories Picatinny Arsenal Dover, New Jersey

13. ABSTRACT A large number of M437, 175mm, projectiles were extensively measured dimensionally and their inertial properties determined experimentally, in cooperation with Frankford Arsenal and Aberdeen Proving Ground. These shells had been separated into two dimensionally "acceptable" and three dimensionally "unacceptable" groups at their production sites. This report presents a statistical evaluation of that data and preliminary attempts at analyzing and correlating the data. The clearest relations found at this preliminary stage of the study are: the "corkscrew" pattern resulting from the correlation of the azimuthal angle locating the minimum wall thickness with the longitudinal station, and, the correlation of the wall thickness variation in the body/boattail region with the static unbalance. Considering the high correlation of the "cork-screw" effect and its physical connections to the next most highly correlated pairs of parameters, the production processes should be examined for possible cause should the planned firing tests show the unbalance levels resulting to be causing unacceptable dispersion. It is also clear that what determines a "good" group from a "bad" group is the skewing of their unbalance histograms not their ranges. Thus, a "good" group has more of low unbalance than a "bad" group even though the maximum and minimum unbalance values are nearly equal for both "good" and "bad" groups. Maximum values of static and dynamic unbalances found for loaded projectiles are .017 inches and .001 radians.

DD FORM 1 NOV 65 1473 REPLACES DD FORM 1473, 1 JAN 64, WHICH IS OBSOLETE FOR ARMY USE.

UNCLASSIFIED
Security Classification

UNCLASSIFIED

Security Classification

14. KEY WORDS	LINK A		LINK B		LINK C	
	ROLE	WT	ROLE	WT	ROLE	WT
STATISTICS						
UNBALANCE						
DYNAMIC UNBALANCE						
STATIC UNBALANCE						
SHELL TOLERANCES						

UNCLASSIFIED

Security Classification

ACKNOWLEDGEMENT

The cooperation and help of personnel from other installations, Mr. Spencer Hirshman of Frankford Arsenal, and Mr. Stephen Zuchor of Aberdeen Proving Ground, in particular, is gratefully acknowledged.

The development of the normal distance least squares and of the correlation/plotting computer codes essential to this study was done by, SP5 Harry Rutman of the Aeroballistics Branch, Picatinny Arsenal.

Mr. Eugene Friedman of the Aeroballistics Branch, Picatinny Arsenal, was responsible for selecting and defining the types of physical measurements and the procedures for obtaining them; and frequent discussions with him on the definitions of and limitations of the various types of data were invaluable in performing this study.

TABLE OF CONTENTS

Page

Page

Page

Page

Page

	Page

Page

Page

		Page
261.	Mean Azimuth of Minimum Wall Thickness Versus Azimuth of Static Unbalance, Series 5000, Region 2, Empty	305
262.	Mean Azimuth of Minimum Wall Thickness Versus Azimuth of Static Unbalance, Series 5000, Region 3, Empty	306
263.	Mean Azimuth of Minimum Wall Thickness Versus Azimuth of Static Unbalance, Series 6000, Region 1, Empty	307
264.	Mean Azimuth of Minimum Wall Thickness Versus Azimuth of Static Unbalance, Series 6000, Region 2, Empty	308
265.	Mean Azimuth of Minimum Wall Thickness Versus Azimuth of Static Unbalance, Series 6000, Region 3, Empty	309
266.	Mean Azimuth of Minimum Wall Thickness Versus Azimuth of Static Unbalance, Series 7000, Region 1, Empty	310
267.	Mean Azimuth of Minimum Wall Thickness Versus Azimuth of Static Unbalance, Series 7000, Region 2, Empty	311
268.	Mean Azimuth of Minimum Wall Thickness Versus Azimuth of Static Unbalance, Series 7000, Region 3, Empty	312
269.	Mean Azimuth of Minimum Wall Thickness Versus Azimuth of Static Unbalance, Series 8000, Region 1, Empty	313
270.	Mean Azimuth of Minimum Wall Thickness Versus Azimuth of Static Unbalance, Series 8000, Region 2, Empty	314

NOMENCLATURE

a	Constant in linear fit to data
a_3	Coefficient of skewness
a_4	Coefficient of kurtosis
b	Slope in linear fit to data
d	Normal distance from line $y = ax + b$ to point (x_i, y_i)
D	Sum of the squares of d_i
M.D.	Sample mean deviation
N	Number of data points
r_{xy}	Linear correlation coefficient of a sample
s	Sample standard deviation
$\overline{\Delta t}$	Average wall thickness variation over a region
$\bar{x}$	Sample mean
x	Independent variable
y	Dependent variable
α	Dynamic unbalance
$\bar{\beta}_{min}$	Average over a region of the azimuthal angle locating the minimum wall thickness
ϵ	Static unbalance
λ	Azimuthal angle locating the static unbalance
σ_x	In Appendix A, $\sum_{i=1}^{N} x_i$

σ_y In Appendix A, $\sum_{i=1}^{N} y_i$

σ_{xy} In Appendix A, $\sum_{i=1}^{N} x_i y_i$

σ_{xx} In Appendix A, $\sum_{i=1}^{N} x_i^2$

σ_{yy} In Appendix A, $\sum_{i=1}^{N} y_i^2$

τ Azimuthal angle locating the plane of dynamic unbalance

Subscripts

i i^{th} data point

ABSTRACT

A large number of M437, 175mm, projectiles were extensively measured dimensionally and their inertial properties determined experimentally, in cooperation with Frankford Arsenal and Aberdeen Proving Ground. These shells had been separated into two dimensionally "acceptable" and three dimensionally "unacceptable" groups at their production sites. This report presents a statistical evaluation of that data and preliminary attempts at analyzing and correlating the data. The clearest relations found at this preliminary stage of the study are: the "corkscrew" pattern resulting from the correlation of the azimuthal angle locating the minimum wall thickness with the longitudinal station, and, the correlation of the wall thickness variation in the body/boattail region with the static unbalance. Considering the high correlation of the "corkscrew" effect and its physical connections to the next most highly correlated pairs of parameters, the production processes should be examined for possible cause should the planned firing tests show the unbalance levels resulting to be causing unacceptable dispersion. It is also clear that what determines a "good" group from a "bad" group is the skewing of their unbalance histograms not their ranges. Thus, a "good" group has more shell of low unbalance than a "bad" group even though the maximum and minimum unbalance values are nearly equal for both "good" and "bad" groups. Maximum values of static and dynamic unbalances found for loaded projectiles are .017 inches and .001 radians.

INTRODUCTION

As part of the study of the effects of asymmetries and the resulting unbalances in 175mm, M437, shell, several sample groups of shell of different "quality" were collected. All of these groups met the minimum and or maximum dimensions specified but failed to meet the wall thickness variation specifications. These groups were ranked in order of "badness" as defined by how much the wall thickness varied in regions where this property was controlled by the production specifications.

The first step in any analysis would be to clarify the vague concept of "badness" implicit in the above. Clearly in an operational sense, "badness" means dispersion in range and azimuth and the shell mass properties which contribute to these are the static and dynamic unbalances and the weight variation.

The current production design philosophy is that controlling certain dimensions and the wall thickness variation in some locations to within specified tolerances will keep the above parameters under sufficient control to result in acceptable dispersion. This is desireable from the current production point of view since it eliminates actual measurements of static and dynamic unbalances on the production line. It might be desireable, however, to directly measure the unbalances instead of making many dimensional measurements on future production lines. One purpose of this study is to examine possible relationships between the unbalances and the projectile dimensions and their variations. Therefore, the second step would be to attempt to correlate these properties with the dimensional variations of the shell to see if such a procedure is actually useful. Thus the following preliminary statistical analysis was undertaken as a necessary step in the solution process.

ANALYSIS

The sample groups available represented an acceptable production group and three groups made from unaccepted shell from Gateway Army Ordnance Plant (GAAP) and one accepted production group from Scranton Army Ordnance Plant (SOP). In all cases the deciding criterion for acceptance or rejection was wall thickness variation in the body/boattail regions, since all the sampled shell were within the minimum or maximum dimensions specified. The groups are shown in Table I in order of increasing variation with the different sample groups assigned a distinctive series number. The tolerance on and the dimensional extend of the regions on the shell are given in Table II.

TABLE I

Thickness Variations in Different Series

SERIES	BODY/BOATTAIL REGION VARIATION	GROUP SIZE
SOP	Acceptable, <0.036 in.	50
3000 (GAAP)	Acceptable, <0.036 in.	100
5000 (GAAP)	0.040 to 0.050 in.	88
6000 (GAAP)	< 0.050 in.	57
7000 (GAAP)	0.040 to 0.80 in.	51
8000 (GAAP)	All GAAP Shell	296

All of these shell had their wall thicknesses and their azimuthal angles of minimum wall thickness determined at 24 longitudinal positions and either 2 or 3 other evenly spaced azimuths at each longitudinal station by Frankford Arsenal personnel. These shell were then sent to the Material Test Directorate, Aberdeen Proving Ground, where their dynamic and static unbalance parameters were experimentally measured.

TABLE II

Definitions of Regions of Shell

REGION	WALL VARIATION TOL. (inches)	BOUNDARIES OF REGION (inches from nose of shell w/o fuze)
1	$\pm$ 0.036	20 to 29.5 (body/boattail)
2	$\pm$ 0.060	4 to 13 (ogive)
3	-	complete shell

The first phase of the statistical analysis consisted of constructing histograms and cumulative frequency polygons for each shell series for the following measured properties:

a. dynamic unbalance (rad. x 10^4): empty and full

b. static unbalance (in. x 10^3): empty and full

c. azimuthal angle of static unbalance (deg.): empty and full

d. azimuthal angle of dynamic unbalance (deg.): empty and full

A histogram for a given variable is constructed by deciding that the complete range (maximum value-minimum value) of the sample of the variable will be divided into some finite number of cells. Then the numbers of times the sample values fall within each cell is plotted as the ordinate and the value of the mid-point of each cell is plotted as the abscissa. A cumulative frequency polygon is constructed by summing from left to right the number in each cell and plotting this accumulating sum as the ordinate versus the upper (right-most) value of the cell boundaries.

The dynamic unbalance is the angle between the shell's nominal principle axis of symmetry and the actual major principle axis of

the ellipsoid of inertia; while the static unbalance is the perpendicular distance which the actual center-of-gravity is off-set from the nominal axis of symmetry. The azimuthal angles of static unbalance and of dynamic unbalance are explicitly defined in Reference 4. For practical purposes, they are the angles about the axis of symmetry, beginning from a common arbitrary zero reference, which locate the off-set center of gravity and the positive axis of the longitudinal principle axis of inertia in a plane perpendicular to the symmetry axis and passing through the center of gravity.

These histograms and cumulative frequency polygons are plotted automatically during runs of a statistical analysis program, STATCS, which also computes the sample mean, variance, standard deviation, skewness coefficient, kurtosis coefficient, and mean deviation for each property. The statistical parameters computed are standard; but for completeness, the definitions will be repeated here.

For a sample of size N the definitions are:

Sample Mean:

$$\bar{x} \triangleq \sum_{i=1}^{N} x_i / N \qquad (1)$$

Sample Variance

$$s^2 \triangleq \sum_{i=1}^{N} (x_i - \bar{x})^2 / (N-1) \qquad (2)$$

Sample Standard Deviation

$$s \triangleq \sqrt{s^2} \qquad (3)$$

Sample Mean Deviation

$$M.D. = \sum_{i=1}^{N} | x_i - \bar{x} | / (N-1) \qquad (4)$$

The skewness and kurtosis coefficients deserve a bit more discussion. Skewness is a measure of the departure from symmetry of the distribution. A distribution which has a longer "tail" to the right of the central maximum than to the left is said

to have positive skewness and one which has the longer "tail" to the left has negative skewness. The coefficient of skewness is defined as the third moment of the distribution nondimensionalized by the cube of the standard deviation or:

$$a_3 \triangleq \left[\sum_{i=1}^{N} (x_i - \bar{x})^3 / (N-1) \right] / s^3 \qquad (5)$$

Note: A normal distribution has a skewness of zero.

Kurtosis is a measure of the "peakedness" of a distribution and the coefficient of kurtosis is defined by a non-dimensionalized fourth moment:

$$a_4 \triangleq \left[\sum_{i=1}^{N} (x_i - \bar{x})^4 / (N-1) \right] / s^4 \qquad (6)$$

With this definition, a normal distribution yields an a_4 of 3.

One of the primary uses of the coefficients of skewness and kurtosis is to estimate the probability of the given sample being from a normally distributed population by such means as Geary and Pearson's tables, available in a number of statistics texts.

A family of computer codes were written and used to compute the sample linear single independent variable correlation coefficients of the samples and to plot the results. In general, the sample linear correlation coefficient between two series of values x_i and y_i is given by

$$r_{xy} = \frac{N \sum_{i=1}^{N} x_i y_i - \sum_{i=1}^{N} x_i \sum_{i=1}^{N} y_i}{\sqrt{\left[N \sum_{i=1}^{N} x_i^2 - \left(\sum_{i=1}^{N} x_i \right)^2 \right] \left[N \sum_{i=1}^{N} y_i^2 - \left(\sum_{i=1}^{N} y_i \right)^2 \right]}} \qquad (7)$$

where N is the number of (x_i, y_i) data points and the equation is symmetric in x an y so that the question of which is the independent variable does not enter.

Equation (7) is the computational form for the linear single independent variable correlation coefficient of a sample from a population. The actual definition of a linear r_{xy} is, in words,

$$r_{xy} \triangleq \sqrt{1 - \frac{\text{unassociated variation}}{\text{total variation}}}$$

where the unassociated variation is that variation which cannot be explained by making y a linear function of x as determined by a least squares procedure. For a further and more complete discussion see Chapter 18 of Reference 2.

It is well known in the least squares fitting of a straight line to data that interchanging the dependent and independent variables (where the least squares criterion is applied to the dependent variable) will, in general, result in different "best-fits" to the same data. In the process of analyzing the shell data it was found that sometimes one and sometimes the other of the two possible forms was clearly superior. Since which form would work best for a given set of variables could not be readily predicted in advance, a least squares method which does not require this choice was used. The method is that of determining the coefficients which minimize the sum of the squares of the distances along the normal from the line to the data points. The detailed deriviation is given in Appendix A, while it is outlined here.

If the line is given by:

$$y = ax + b \tag{8}$$

then the normal distance from the line to the point (x_i, y_i) is

$$d_i = \frac{ax_i - y_i + b}{\sqrt{a^2 + 1}} \tag{9}$$

then if

$$D(a,b) \equiv \sum_{i=1}^{N} d_i^2 \tag{10}$$

but for a minimum value of D

$$\frac{\partial D(a,b)}{\partial a} = 0 \tag{11}$$

and

$$\frac{\partial D(a,b)}{\partial b} = 0 \tag{12}$$

The final result is,

$$a = G \pm \sqrt{G^2 + 1} \tag{13}$$

where,

$$G = \frac{\left(\sum_{i=1}^{N} y_i\right)^2 - \left(\sum_{i=1}^{N} x_i\right)^2 + N\left(\sum_{i=1}^{N} x_i^2 - \sum_{i=1}^{N} y_i^2\right)}{2\left(N \sum_{i=1}^{N} x_i y_i - \sum_{i=1}^{N} x_i \sum_{i=1}^{N} y_i\right)} \tag{14}$$

and the proper root is determined by matching the value of D(a, b) when

$$b = \frac{1}{N}\left(\sum_{i=1}^{N} y_i - a \sum_{i=1}^{N} x_i\right) \tag{15}$$

This is equivalent to requiring that the denominator of D be > 0.

The correlation effort in this study was principally directed at linear correlation since the method of Reference 1 is currently restricted to linearity.

The primary correlations sought were:

1. the mean azimuthal angle of minimum wall thickness at a given station for each series versus longitudinal position of that station

2. the wall thickness variation, $\overline{\Delta t}$, (averaged for regions and complete shell for all series) versus static unbalance, ϵ, and dynamic unbalance, α

3. the azimuthal angle of minimum wall thickness, $\bar{\beta}$ min, (averaged over complete shell for all series) versus the azimuthal angle of static unbalance, λ, and the azimuthal angle of dynamic unbalance, τ

4. the azimuthal angle of static unbalance, λ, versus the azimuthal angle of dynamic unbalance, τ

5. the dynamic unbalance, α, versus the static unbalance, ϵ

The parameters in the above attempted correlations have been defined earlier; and the series mentioned are those in Table I, while the term region refers to an area in the shell of differing tolerance, as defined in Table II. (Note that the terms complete shell and Region 3 mean the same.)

The lowest value of the correlation coefficient which is required to meet a certain level of significance is a function of sample size. The values computed for the various size series, using the tabulated values in Appendix II of Reference 2 are shown in Table III.

TABLE III

Minimum Absolute Values of Sample Correlation Coefficients for Different Series Versus Significance Level

Series (SIZE)	SIGNIFICANCE LEVELS		
	0.05	0.02	0.01
3000 (100)	0.1967	0.2325	0.2567
5000 (88)	0.2099	0.2579	0.2736
6000 (57)	0.2616	0.3083	0.3394
7000 (51)	0.2761	0.3251	0.3577
8000 (296)*	0.115	0.132	0.150

*Extrapolated values from Appendix VII of Reference 2

Significance ɾel in this usage is defined so that the probability of the true popula..on correlation coefficient being zero is, at most, "the significance level value" when the sample correlation coefficient is equal to or greater than the tabulated minimum value (Table III). For example let us consider Series 3000 which has a sample size of 100. If we are trying to determine if the true (population) correlation coefficient is non-zero and we are willing to accept 2 chances in 100 that it is zero (i.e., a significance level of .02), then the sample correlation coefficient must have an absolute value of at least 0.2325, as shown in Table III. Alternatively for a 95% confidence level (0.05 significance level) the sample correlation coefficient for the 3000 series need only be 0.1967. Further statistical analysis can

yield estimates of the true correlation coefficients not just their probability of being non-zero. The general results are available in Appendix VIII of Reference 2.

RESULTS AND DISCUSSION

In order to make the preliminary results and the data gathered for this study available, this report is being published before the program is completed. No claim is made that the statistical manipulation of the data is exhaustive or that realistic limits on the unbalances can be set until the firing data from these shell has been analyzed.

The histograms computed by the STATCS code are shown in Figures 1 to 40 and the cumulative frequency polygons are shown in Figures 41 to 80. The statistical moments and/or their coefficients as defined and discussed in the Analysis Section and as computed for each property of each series are tabulated in Figure 81. It can be seen that all properties are highly non-normal in their distributions.

As an example, let us consider the 3000 and 7000 series in their loaded condition. The 3000 series is a dimensionally "acceptable" sample group and the 7000 series is the dimensionally "worst" sample group from GAAP. If one looks at the dynamic and static unbalances of these series as presented in Table IV, it can be seen that the ranges, that is, the maximum values less the minimum values, of both static and dynamic unbalances, are practically the same in the two series. However, the "good" series (3000) has both its dynamic and static unbalances much more highly skewed toward zero than does the "bad" (7000) series.

The linear regression lines and the data points for the various correlations sought are shown in Figures 82 to 286. The correlation coefficients are tabulated in Figures 287 to 291.

It can be seen from these tabulations that the correlations which are both <u>significant</u>, at levels less than 0.01, and also appear to account for a <u>majority</u> of the variation are (for all shell, 8000 series):

1. the longitudinal station versus the mean angle of the minimum wall thickness

TABLE IV

Comparison of "Best" and "Worst" Series from GAAP (Loaded)

Level of Static Unbalance (in. X 10^3)	Cumulative Frequency (%)		Level of Dynamic Unbalance (rad. X 10^4)	Cumulative Frequency (%)	
	3000 Series	7000 Series		3000 Series	7000 Series
2 or less	8	0	1 or less	20	4
4 or less	32	7	2 or less	40	19
8 or less	69	35	4 or less	80	51
12 or less	97	71	6 or less	95	82
15 or less	100	94	8 or less	100	90
17 or less	-	100	10 or less	-	100

2. the static unbalance versus the mean thickness variation for all except the shell ogive region

One may surmise that the first item in correlation rank (see also Results), the mean angle of minimum wall thickness versus longitudinal station, is an artifact of the current production process at GAAP. This "corkscrew" effect amounts to 150° in 22 inches of shell length for the 8000 series (all GAAP shell) as shown in Figure 86. This effect could be caused by, for example, differential rotation of a round punch and die which are off-center with respect to each other, or by an out-of-round punch and/or die.

The second item shows that the static unbalance is more strongly effected by wall thickness variations in the body/boattail section than it is by variations in the ogive section. This is as would be expected, since greater masses at larger radii are involved in the aft shell sections. At least part of this correlation can probably be attributed to the "corkscrew" effect since the data shows that the azimuthal angle of minimum wall is confined within the same 180° around the shell for the entire length of the cavity.

While the correlations for the following are still significant, at the .01 level or less, they appear to explain a smaller part of the variations:

3. the static versus the dynamic unbalance, both empty and full

4. both the azimuthal angles of static and the azimuthal angles of dynamic unbalance with the mean angle of minimum wall thickness.

These seem to indicate that a shell does not often have both large (or small) static unbalance and large (or small) dynamic unbalance. Since the histograms of Figures 1 to 40 show that the shell series do not cluster tightly about one value of either static or dynamic unbalance, the negative correlation between static and dynamic unbalance would tend to increase dispersion since the effects of the two unbalances on a trajectory are at right angles and vary differently with range (See Reference 3). It is also suggested that the correlation between the azimuthal angles of static and

dynamic unbalance is, at least in part, due to their physical linkage with the fact that the minimum wall thickness tends to occur in the same angular half of a shell over its cavity length.

The extremely high correlation between the mean angle of minimum wall thickness and longitudinal station, or the "corkscrew" effect, and its physical connections with the next most highly correlated pairs of parameters seems to indicate that effort spent examining the production processes for the causes and cures of this close relationship would be well spent if the magnitudes of the unbalances being produced are shown to result in unacceptable dispersion in the test firings of these shell. It would seem from the shell data gathered to date that variation limitation type dimensional controls are not very effective in limiting dynamic unbalance while they are fairly effective in limiting static unbalance with current production methods since the correlation coefficients for complete shell of the 8000 series (all GAAP shell) are (See also Figure 291):

mean wall thickness variation vs. dynamic unbalance = -0.0967

mean wall thickness variation vs. static unbalance = 0.698

However, it is yet to be determined whether the large range of dynamic unbalance resulting would still have an acceptable dispersion level. This is to be settled by a series of test firings using the shell which are reported on here.

Examination of the correlation coefficients for the individual series shows that the first group remains both highly significant and highly correlated for all series whereas those in the second group drop to being significant only at the 0.05 level or higher for some conditions and explain only a small part of the variation.

It seems necessary at this point to emphasize that lack of linear correlation does not mean that the particular variables involved are necessarily unrelated. It may mean that they can be related in a nonlinear manner. On the other hand a strong linear correlation may be false in that the variables really correlate, not to each other, but with some other factor(s).

CONCLUSIONS

The primary conclusion to be drawn from the statistical quantities for the different mass properties is that all the properties are highly non-normal in their distribution and, hence, the application of statistical theorems and methods which assume normality is questionable.

The implication of the loaded 3000/7000 series unbalances study in the Results is that meeting or not meeting the wall thickness variations specifications, even in this extreme situation, does not significantly alter the maximum unbalances found in a group. However, the acceptable series has more shell of low unbalances than does the unacceptable series.

The very high correlation between the mean angle of minimum wall thickness and longitudinal station for the GAAP shell, resulting in a "corkscrew effect" suggests a physical cause in the manufacturing process.

The second highest correlation is between static unbalance and wall thickness variation, particularly in the body/boattail region. Since the "corkscrew effect" above is restricted to the same 180° around the shell, it contributes to this correlation.

The next two highest correlations indicate a negative correlation between static and dynamic unbalance, empty and full, which will increase free flight dispersion; and a correlation between the azimuthal angles of static and dynamic unbalance possibly due, in part, to the "corkscrew effect". This again emphasizes the desireability of examining the production process for causes of the "corkscrew effect" if these magnitudes of unbalance produce unacceptable dispersion in the test firings.

The data gathered to date seems to indicate that variation limitation type dimensional controls are not very effective in limiting dynamic unbalance while they are fairly effective in limiting static unbalance.

It should be kept in mind that a lack of linear correlation does not mean that the variables do not have a nonlinear correlation. Conversely, a good linear correlation may be false in that the variables realiy correlate with some unexamined factor(s) which have remained the same.

A firing program will be conducted to determine the actual operational restrictions on static and dynamic unbalance and weight imposed by acceptable dispersion limits. These values can be used as input to the OPTOL code (Reference 1) which computes the loosest and least costly tolerances which will statistically meet these requirements. An alternative method is to use the unbalance and weight limitations directly by measuring them on the production shell and using them as acceptance or rejection criteria.

REFERENCES

1. Friedman, E., Lacher, E., and Ng, C., "A Method of Choosing Projectile Manufacturing Tolerances so as to Minimize Costs of Production While Satisfying Functional Requirements", PA TM 1982, December 1970.

2. Richmond, S.B., Principles of Statistical Analysis, The Ronald Press Company, New York, N. Y., 1957

3. Loeb, Alfred A., "A Preliminary Investigation of the Mass Asymmetry Effects on Exterior Ballistics for the 175mm, M437 Projectile", ESL IR 445, August 1969

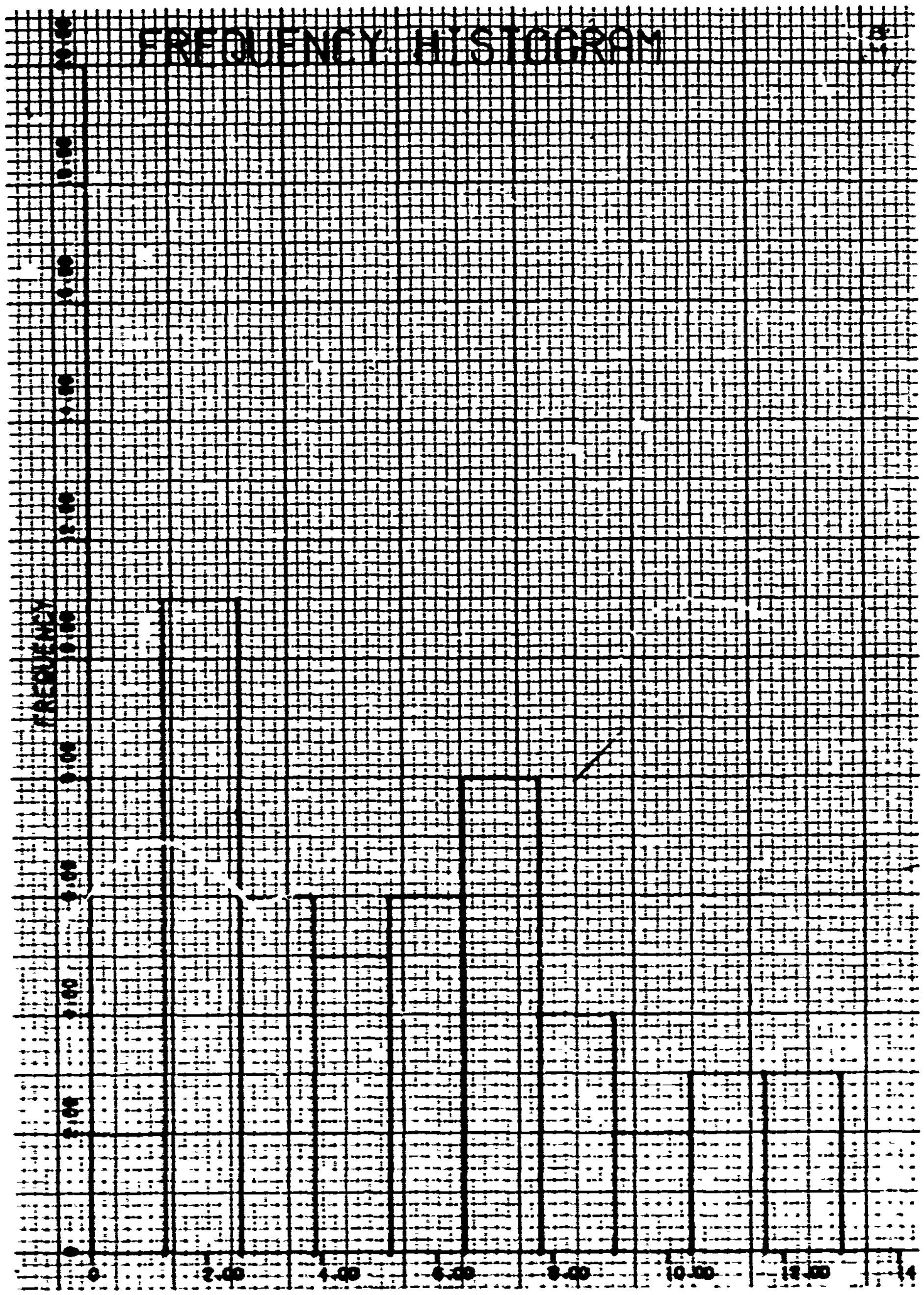

Figure 1 - Frequency Histogram for Dynamic Unbalance of Empty SOP Series Shell

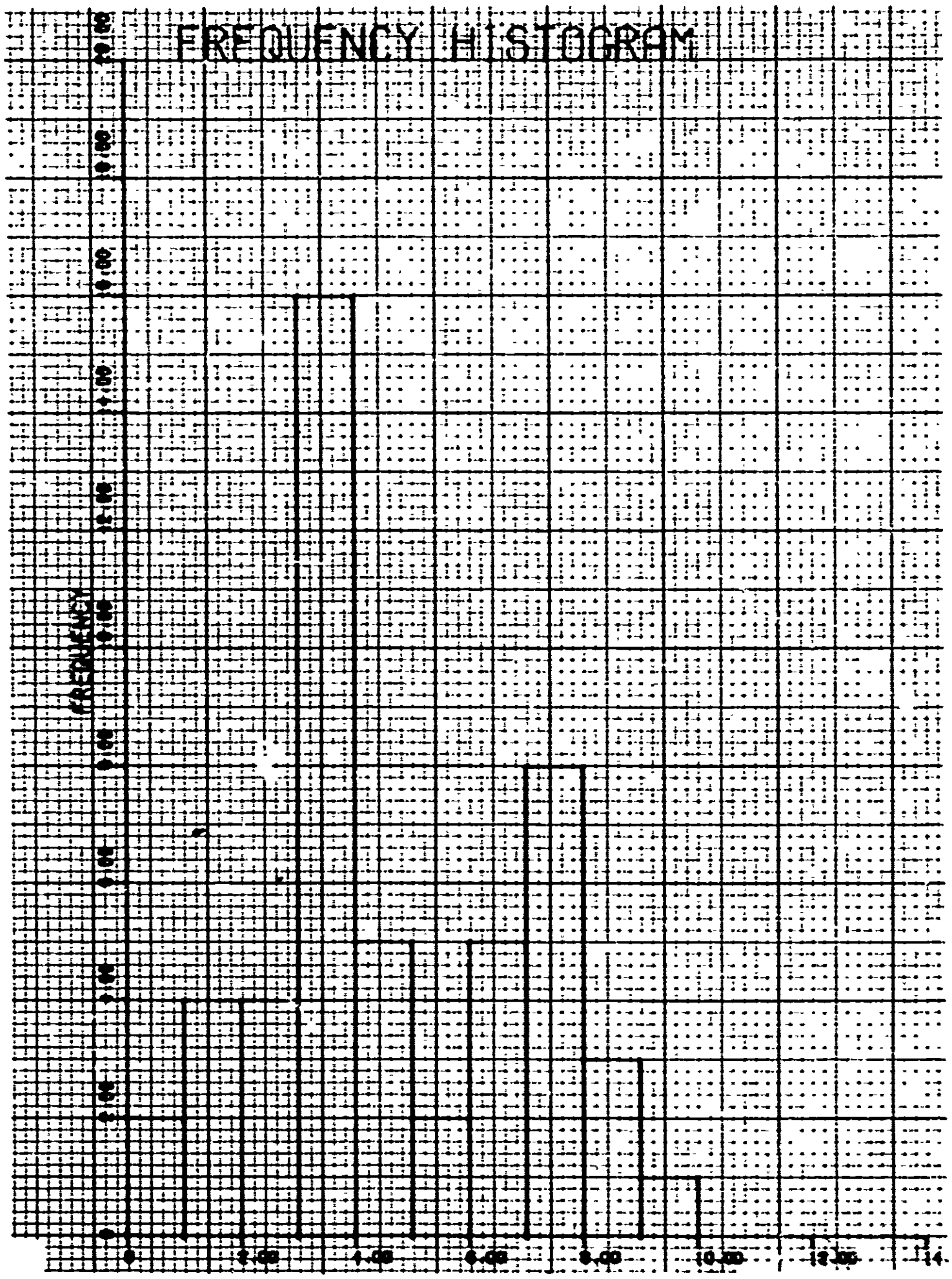

Figure 2 - Frequency Histogram for Dynamic Unbalance of Full SOP Series Shell

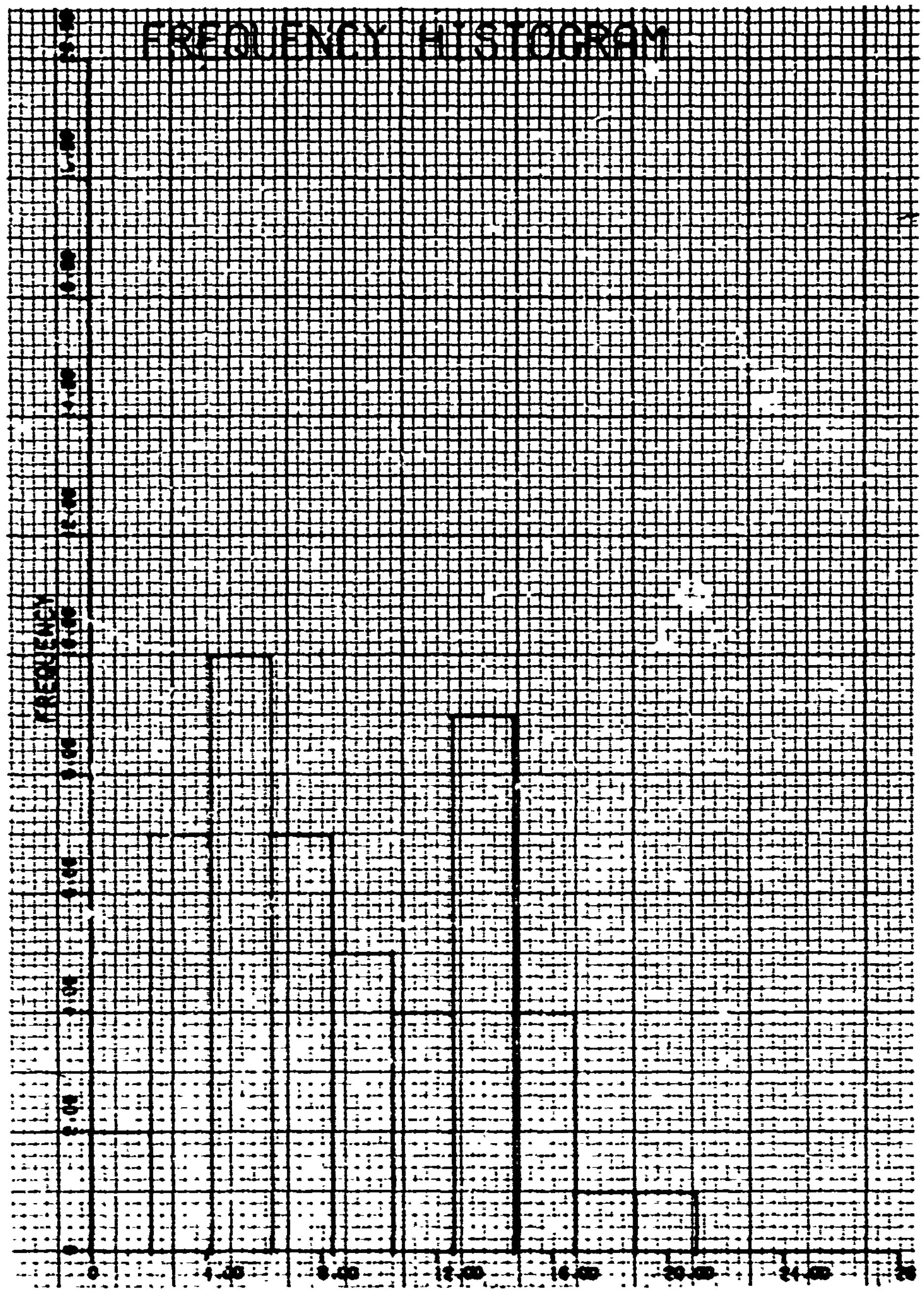

Figure 3 - Frequency Histogram for Static Unbalance of Empty SOP Series Shell

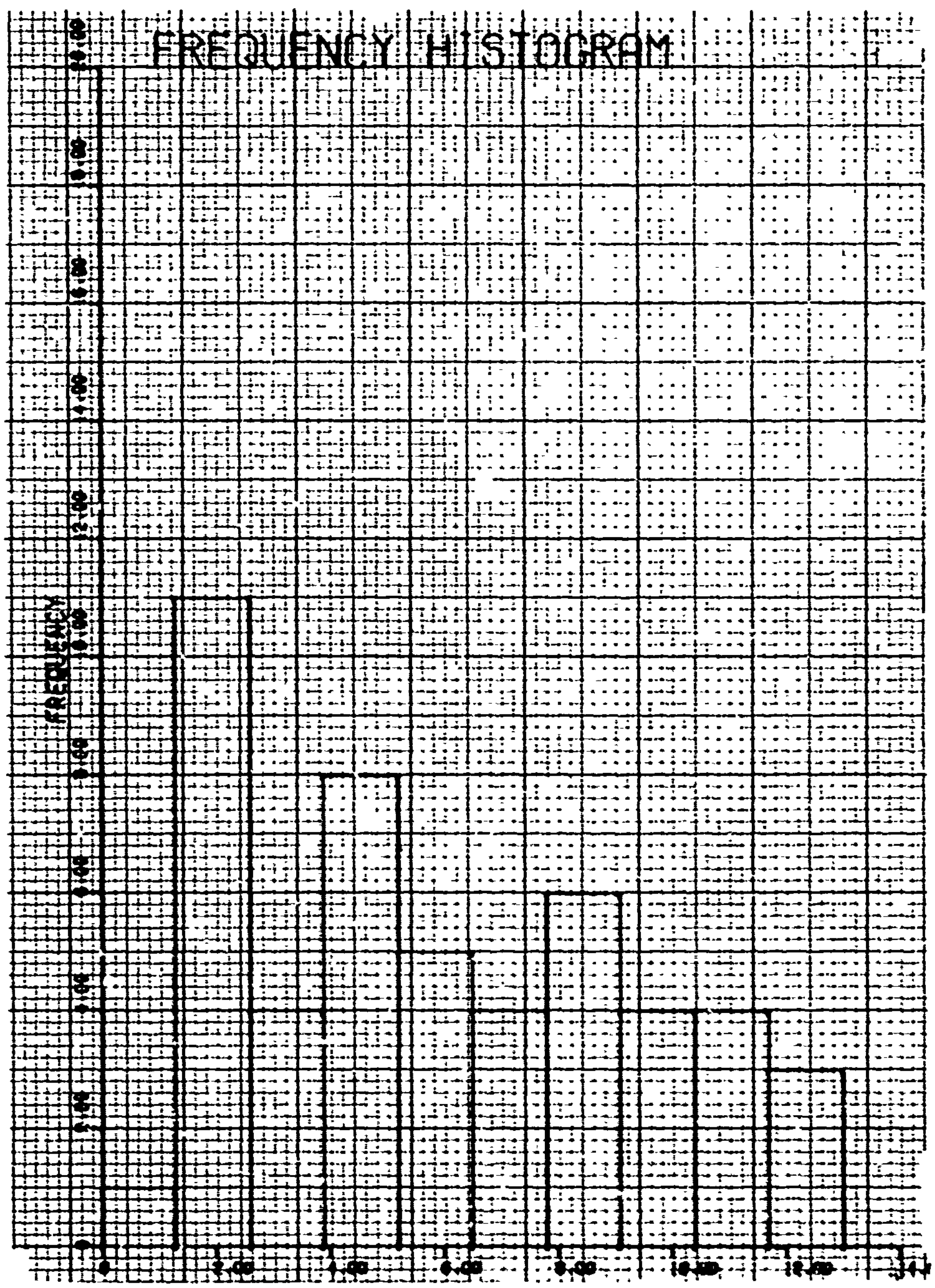

Figure 4 - Frequency Histogram for Static Unbalance of Full SOF Series Shell

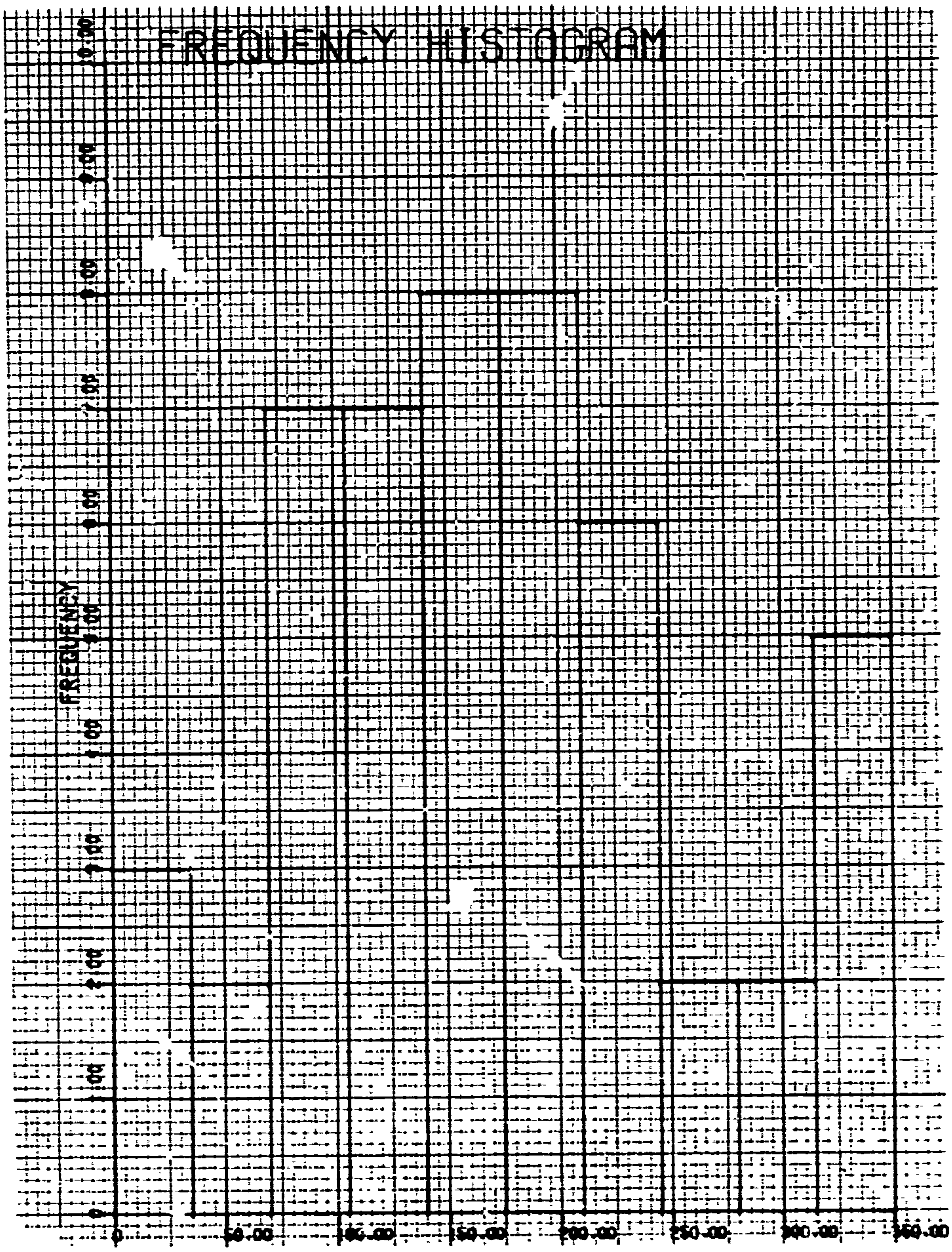

Figure 5 - Frequency Histogram for Azimuth of Dynamic Unbalance of Empty SOP Series Shell

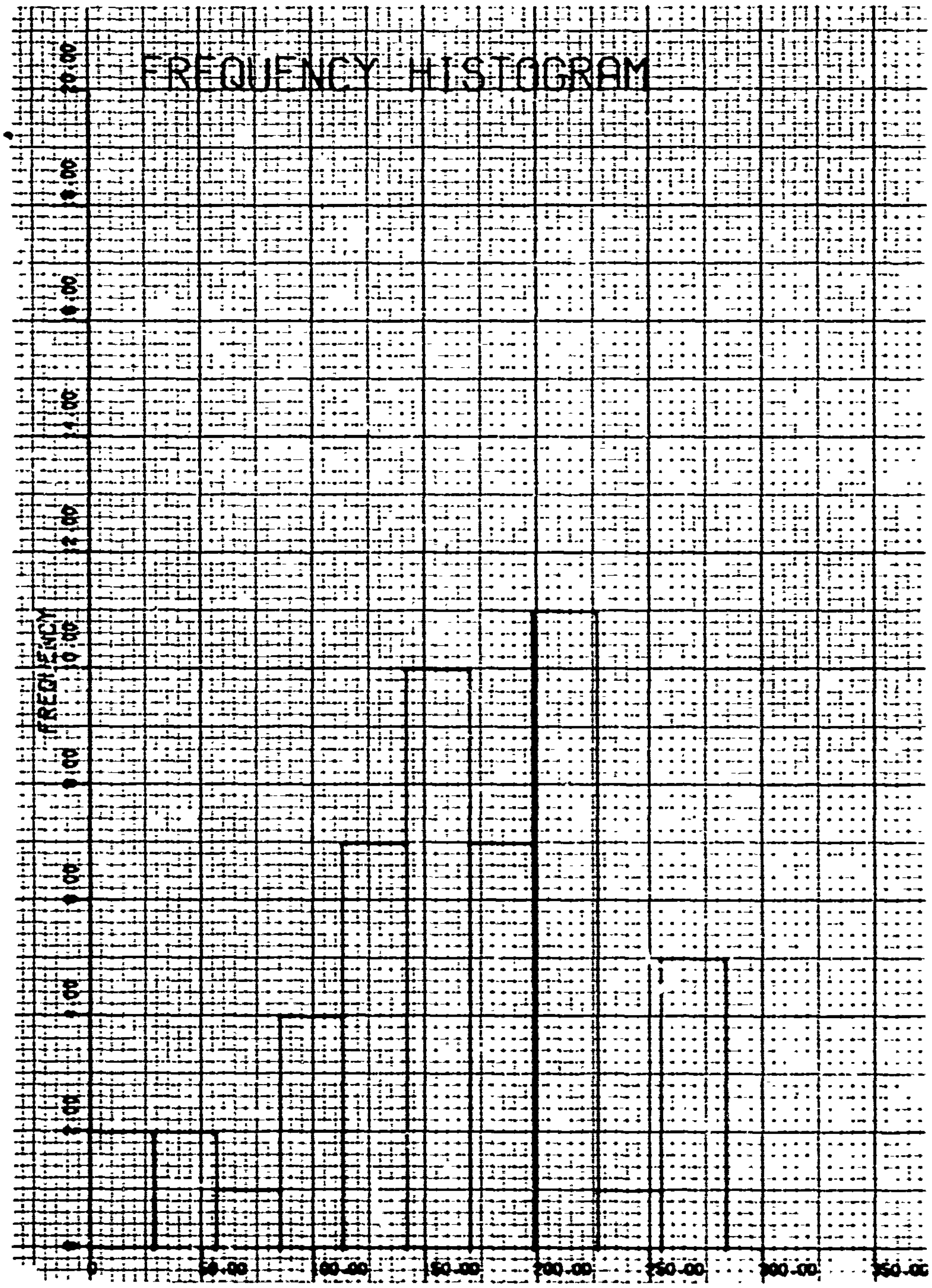

Figure 6 - Frequency Histogram for Azimuth of Dynamic Unbalance of Full SOP Series Shell

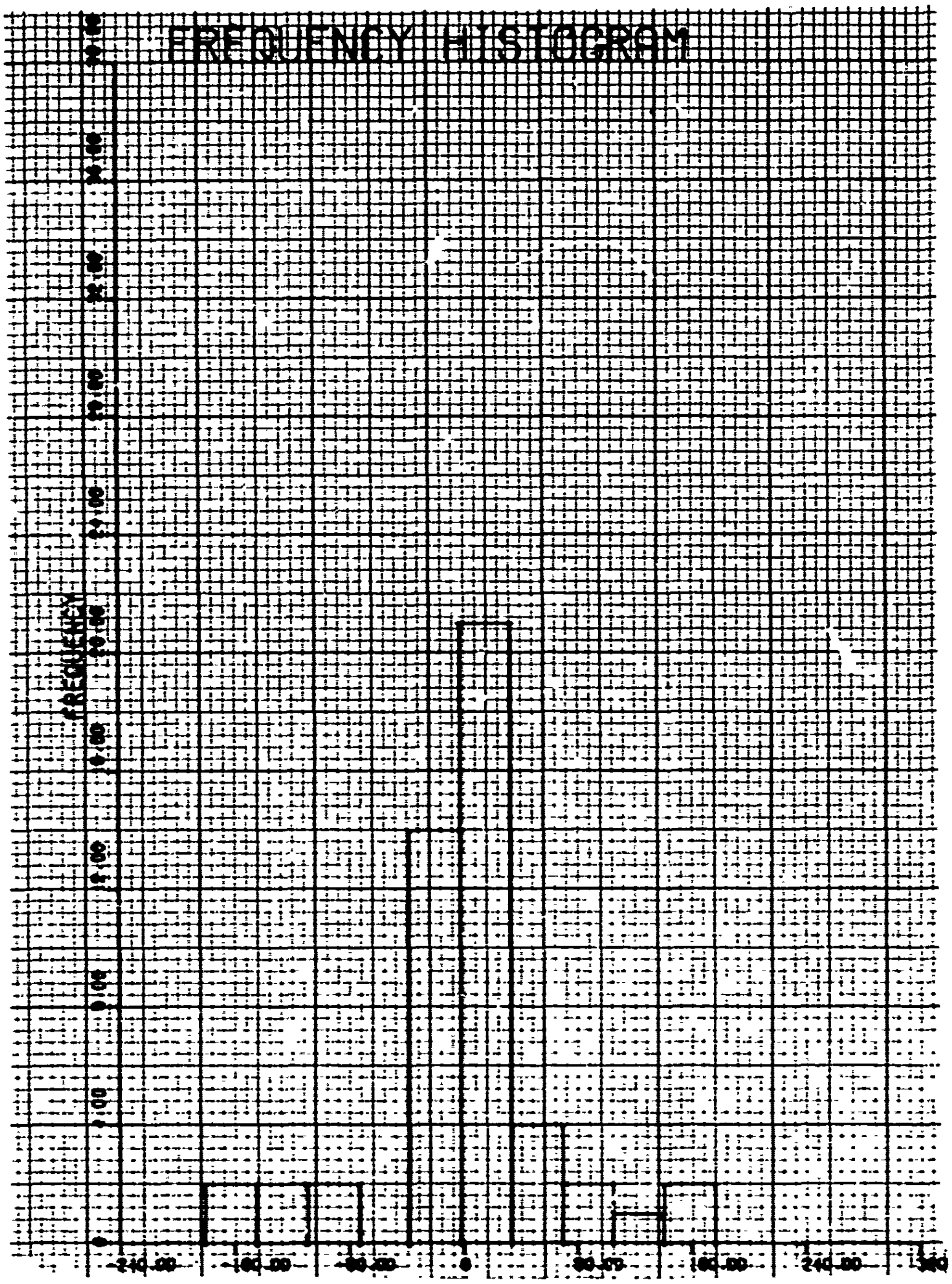

Figure 7 - Frequency Histogram for Azimuth of Static Unbalance of Empty SOP Series Shell

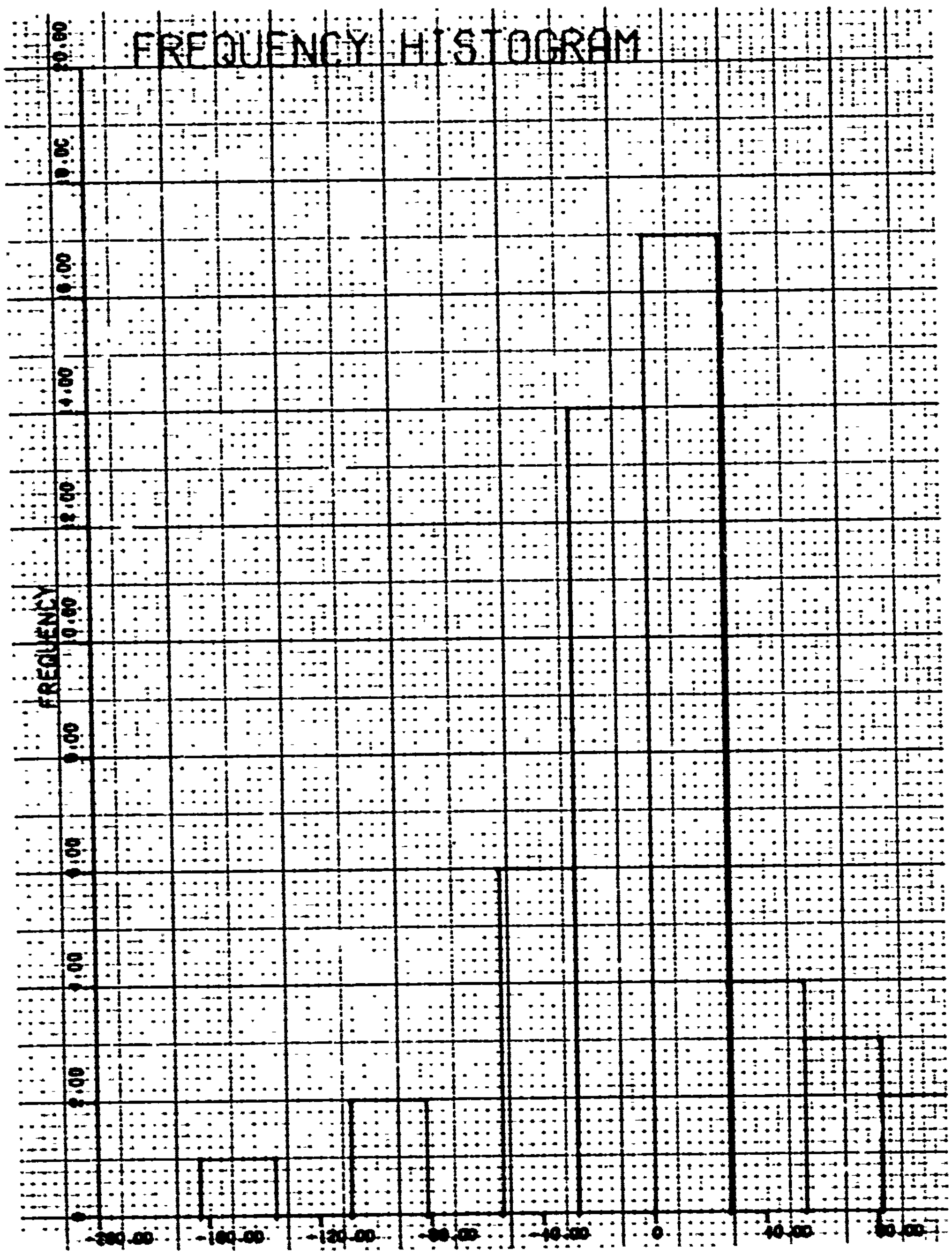

Figure 8 - Frequency Histogram for Azimuth of Static Unbalance of Full SOP Series Shell

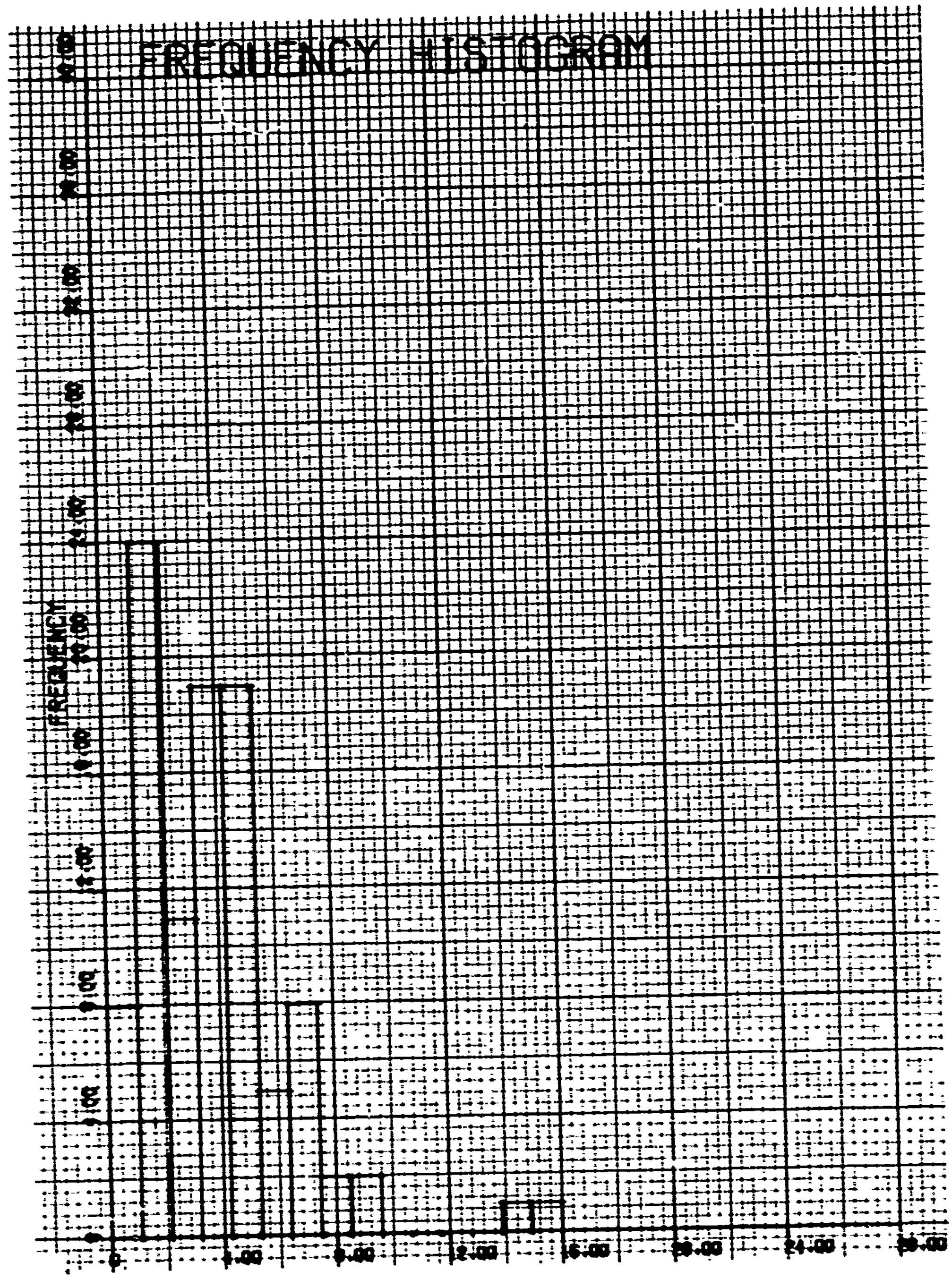

Figure 9 - Frequency Histogram for Dynamic Unbalance of Empty 3000 Series Shell

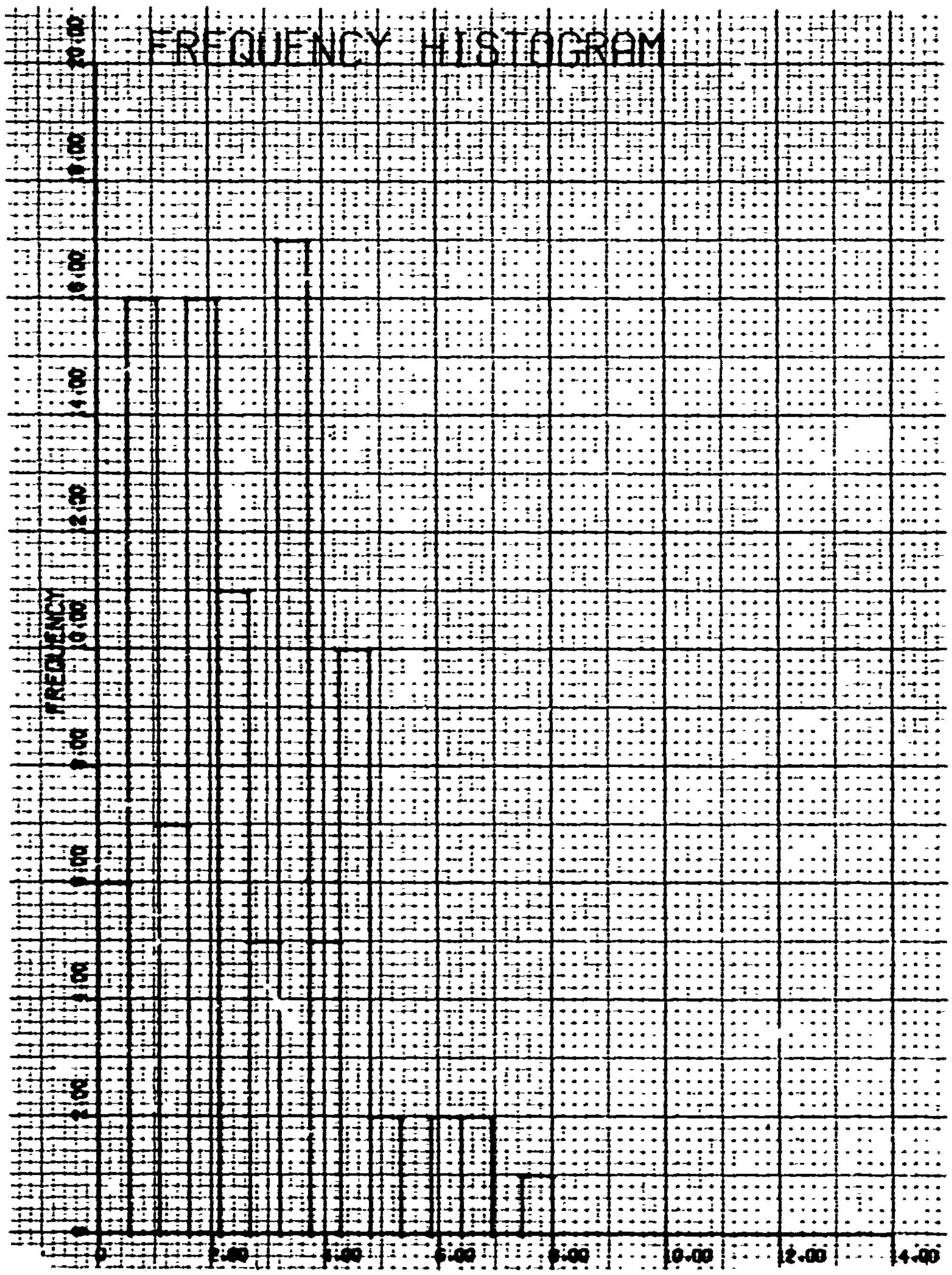

Figure 10 - Frequency Histogram for Dynamic Unbalance of Full 3000 Series Shell

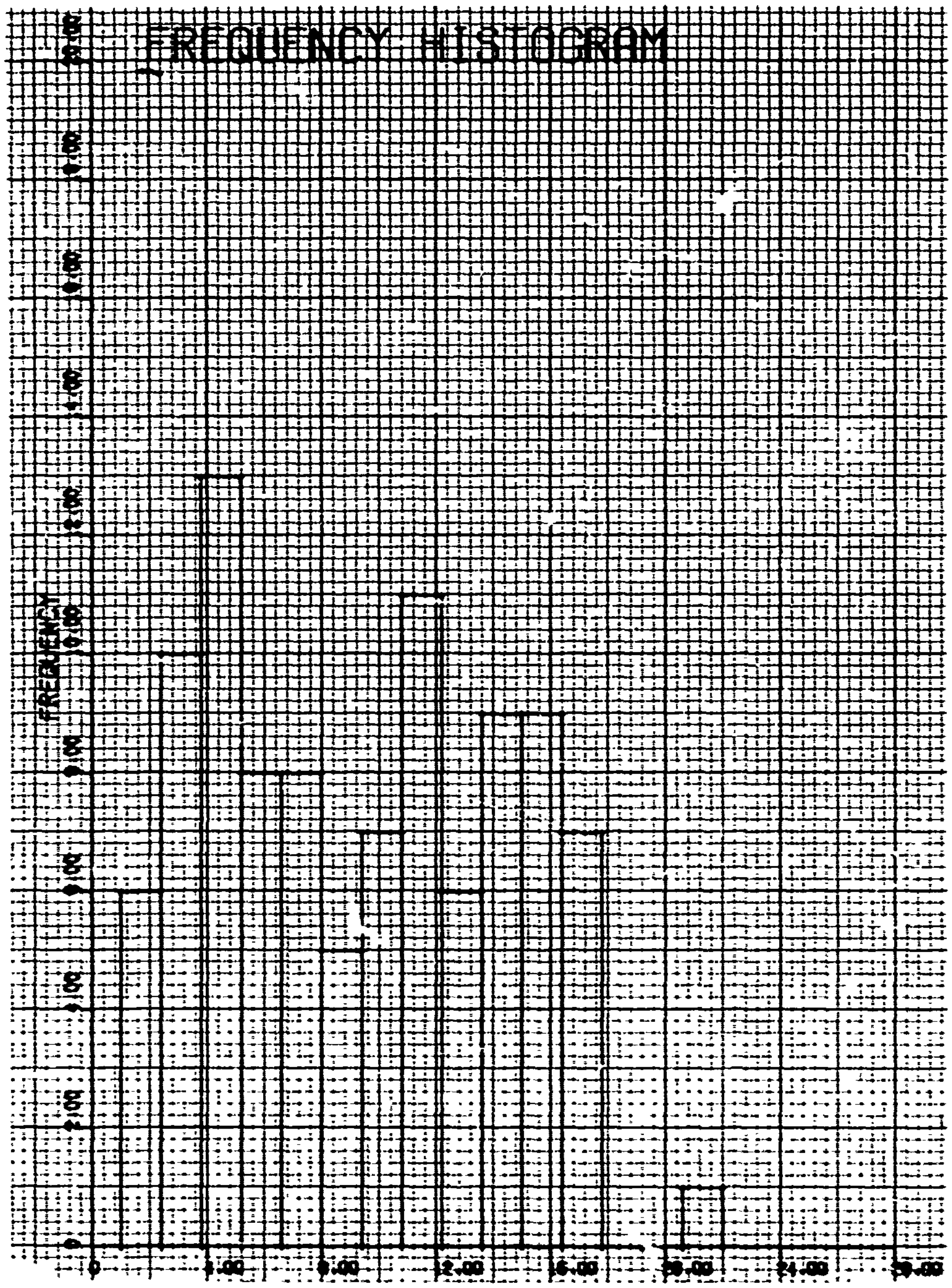

Figure 11 - Frequency Histogram for Static Unbalance of Empty 3000 Series Shell

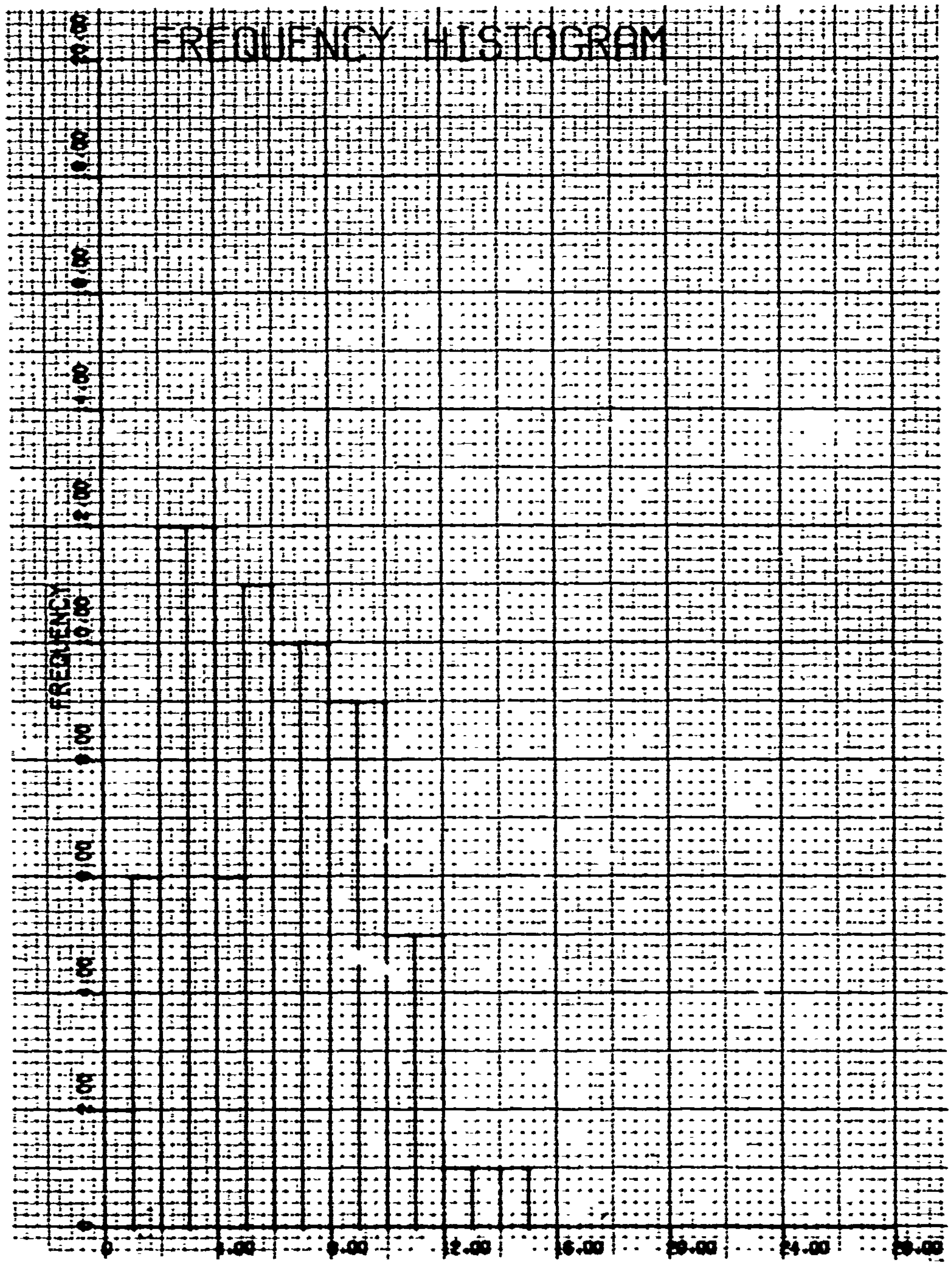

Figure 12 - Frequency Histogram for Static Unbalance of Full 3000 Series Shell

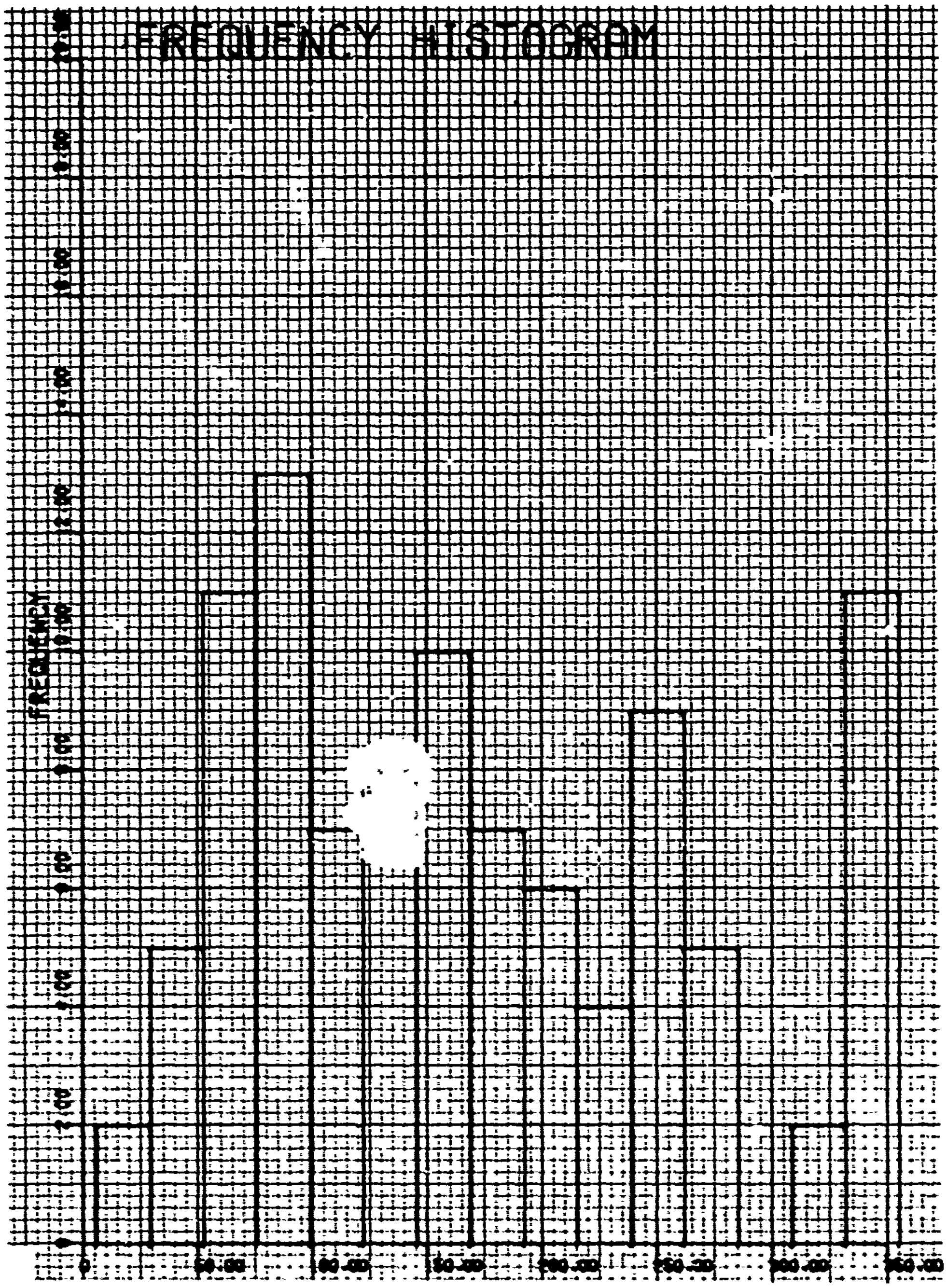

Figure 13 - Frequency Histogram for Azimuth of Dynamic Unbalance of Empty 3000 Series Shell

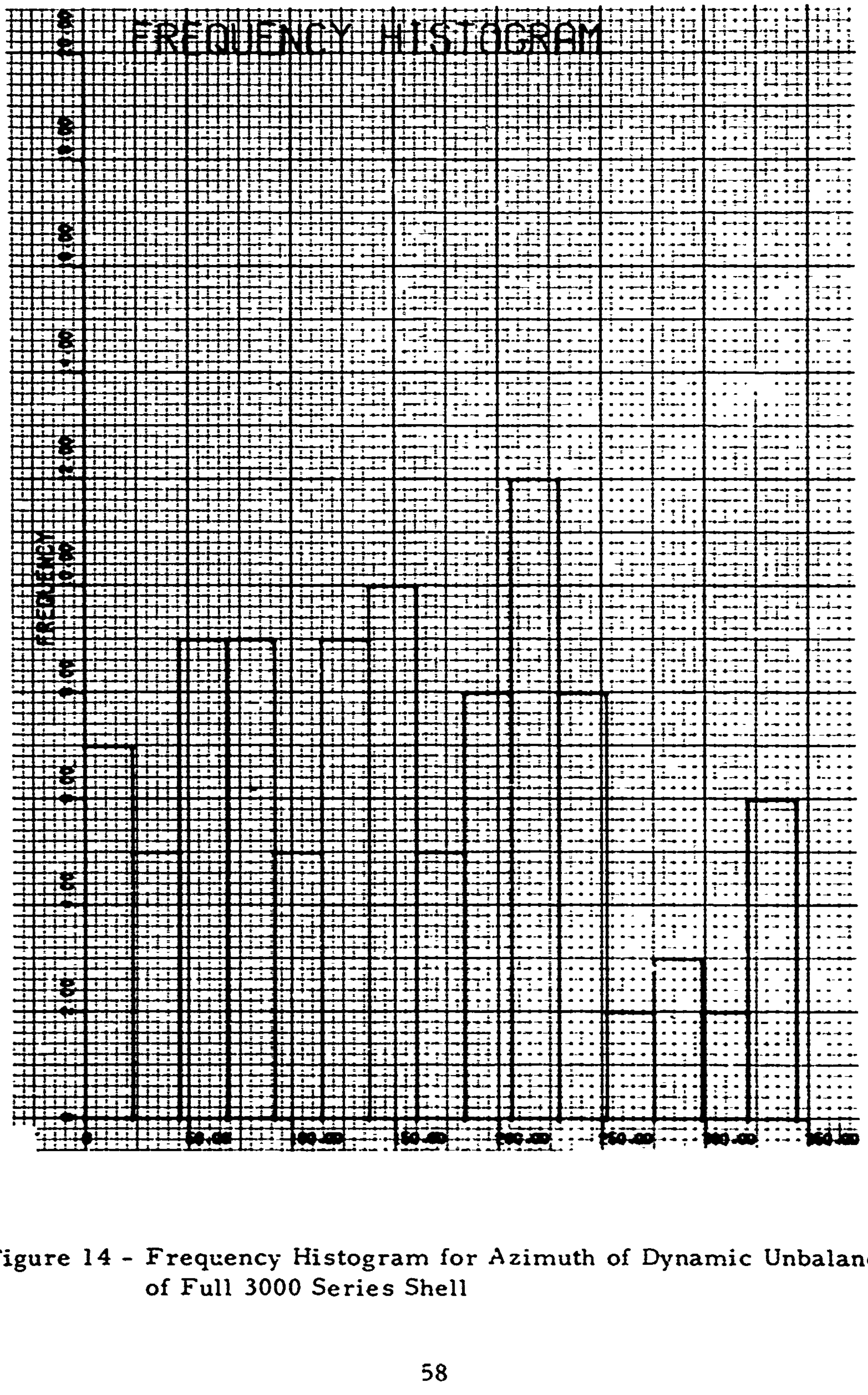

Figure 14 - Frequency Histogram for Azimuth of Dynamic Unbalance of Full 3000 Series Shell

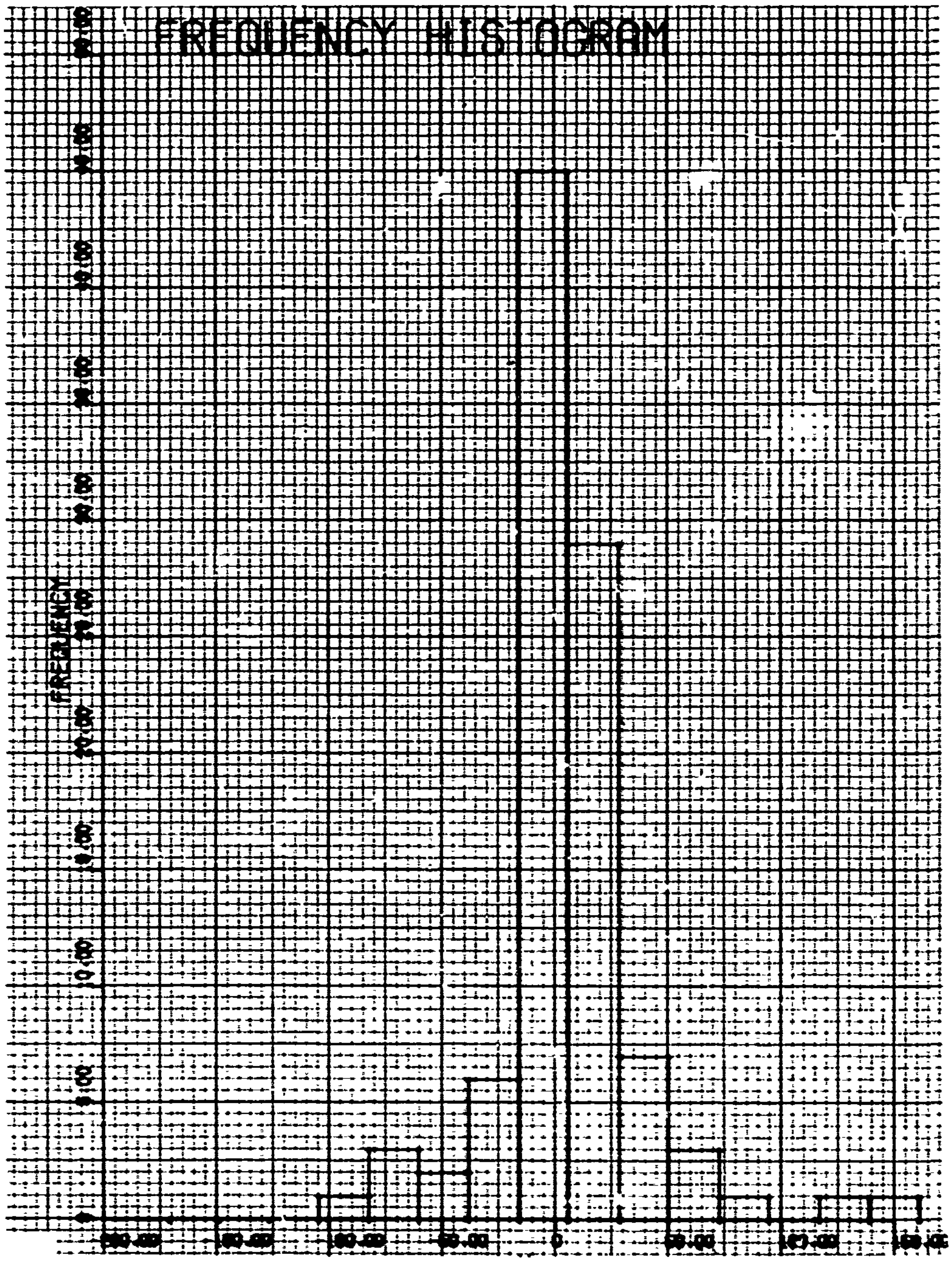

Figure 15 - Frequency Histogram for Azimuth of Static Unbalance of Empty 3000 Series Shell

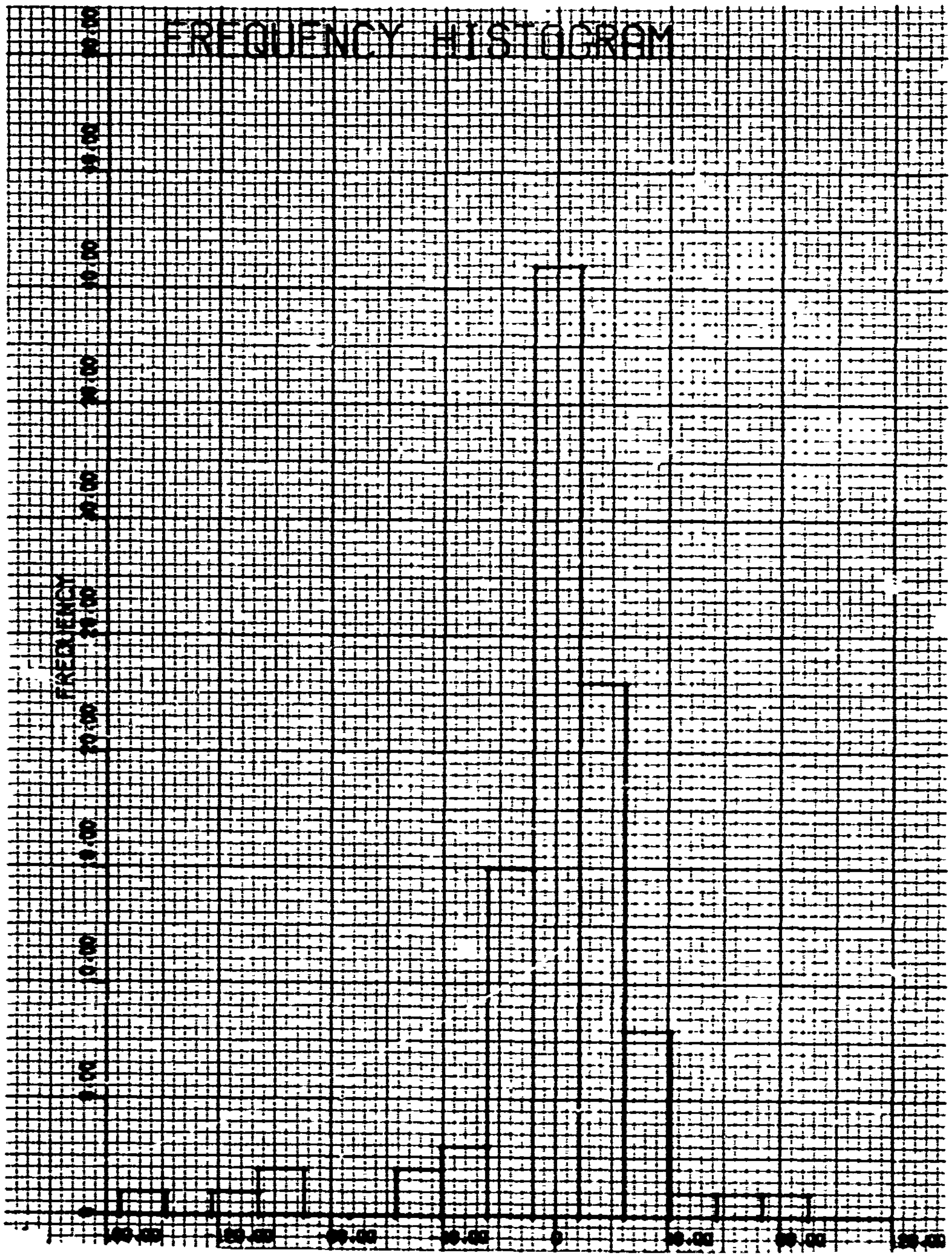

Figure 16 - Frequency Histogram for Azimuth of Static Unbalance of Full 3000 Series Shell

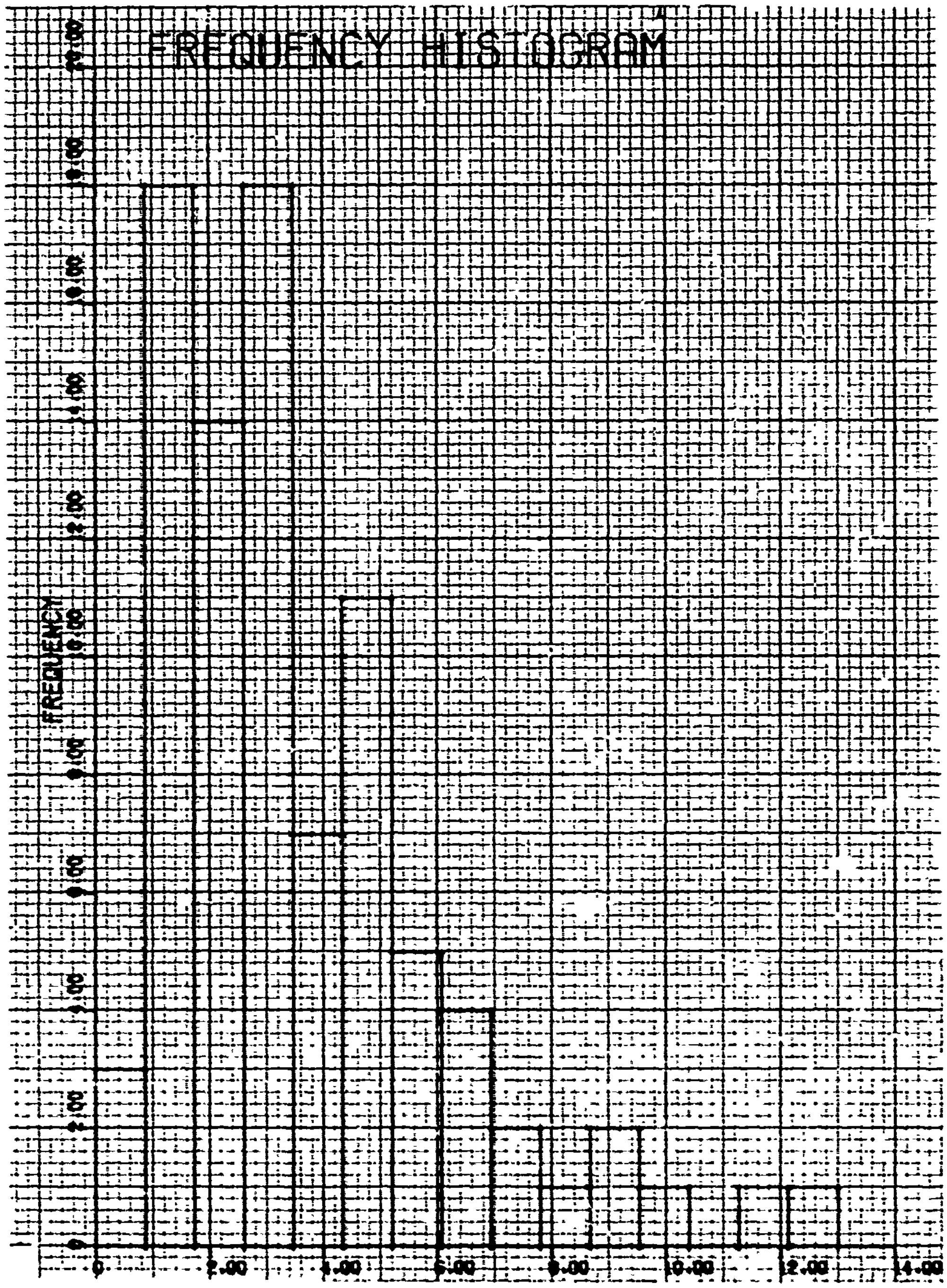

Figure 17 - Frequency Histogram for Dynamic Unbalance of Empty 5000 Series Shell

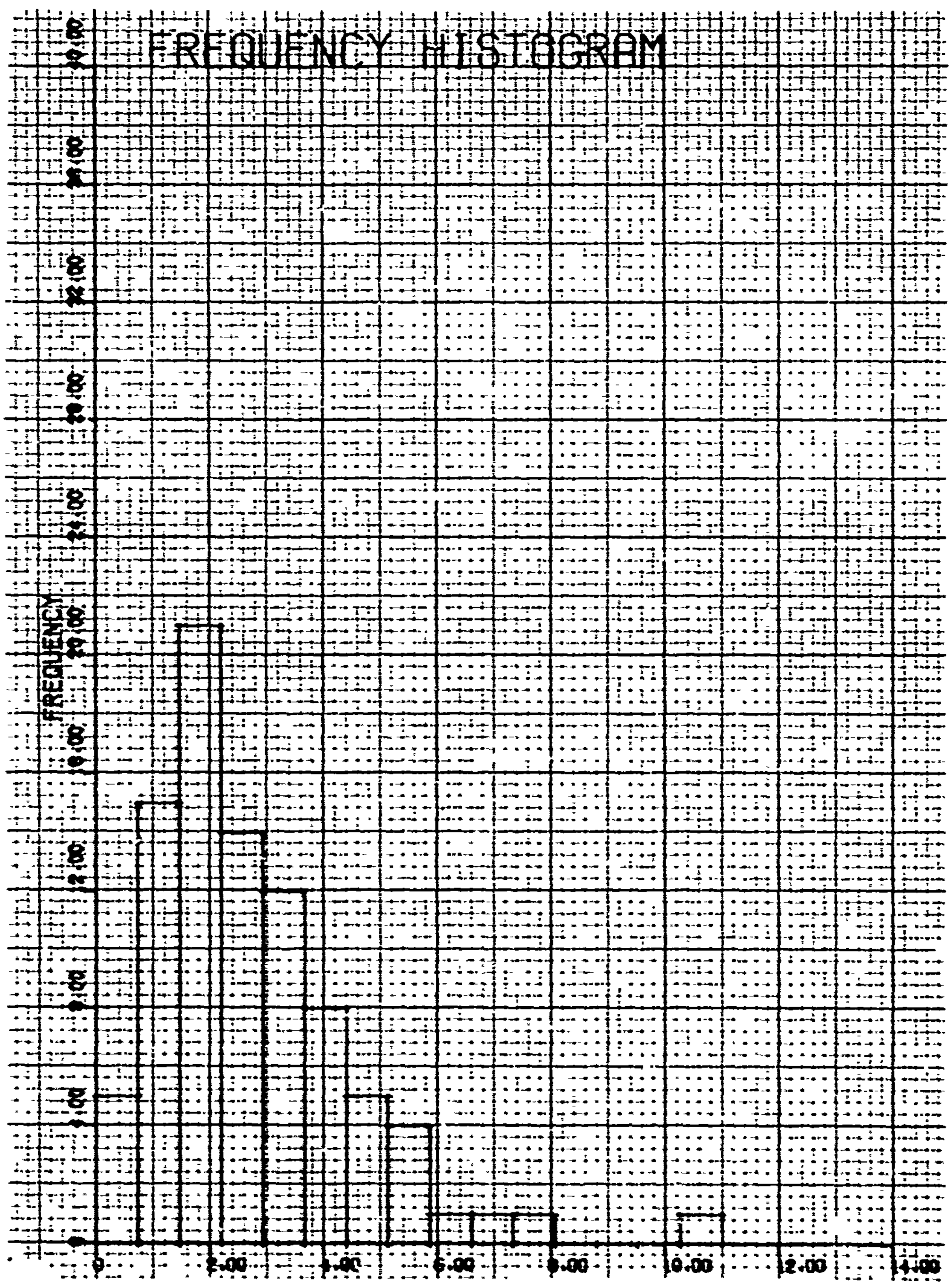

Figure 18 - Frequency Histogram for Dynamic Unbalance of Full 5000 Series Shell

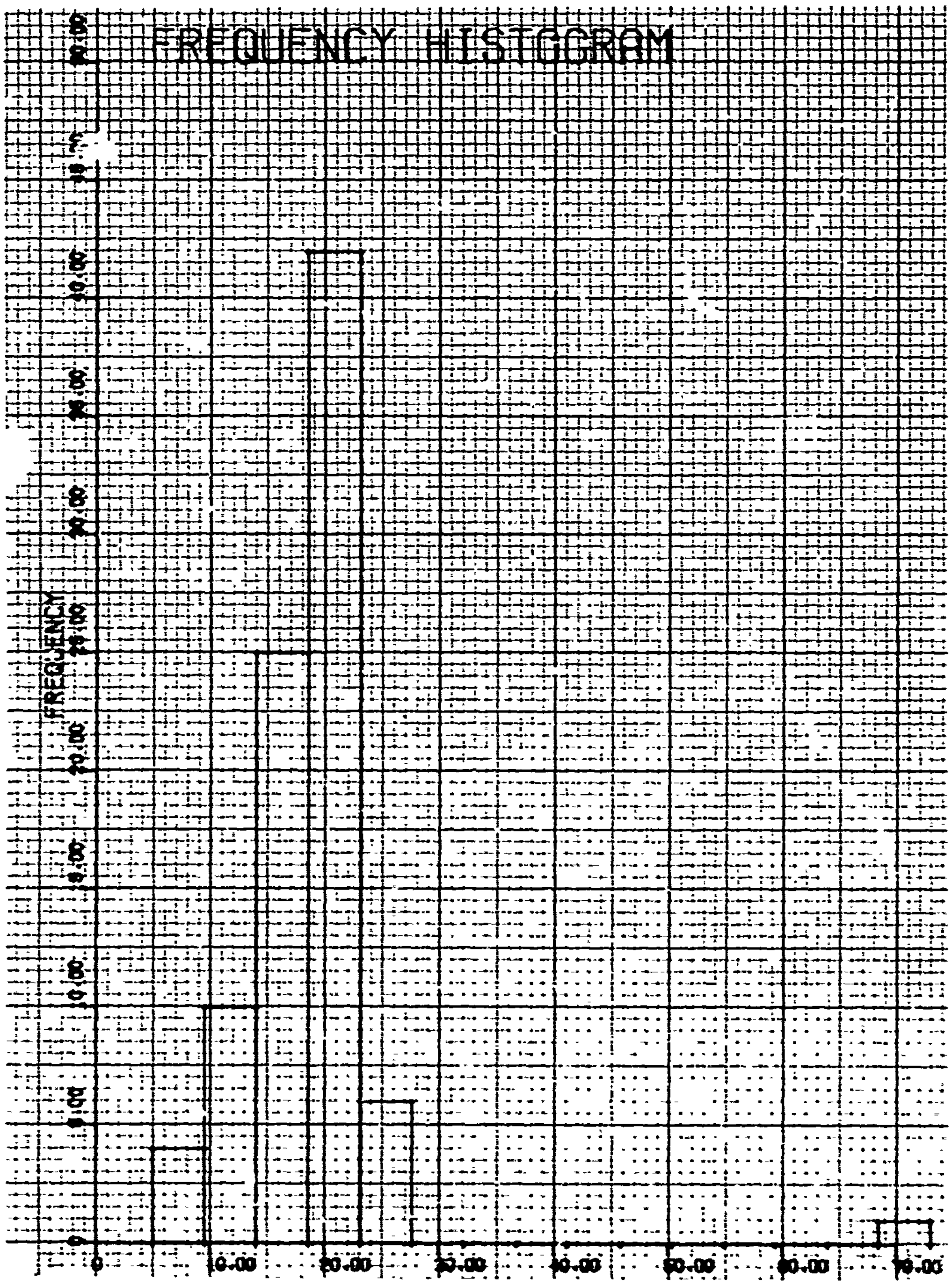

Figure 19 - Frequency Histogram for Static Unbalance of Empty 5000 Series Shell

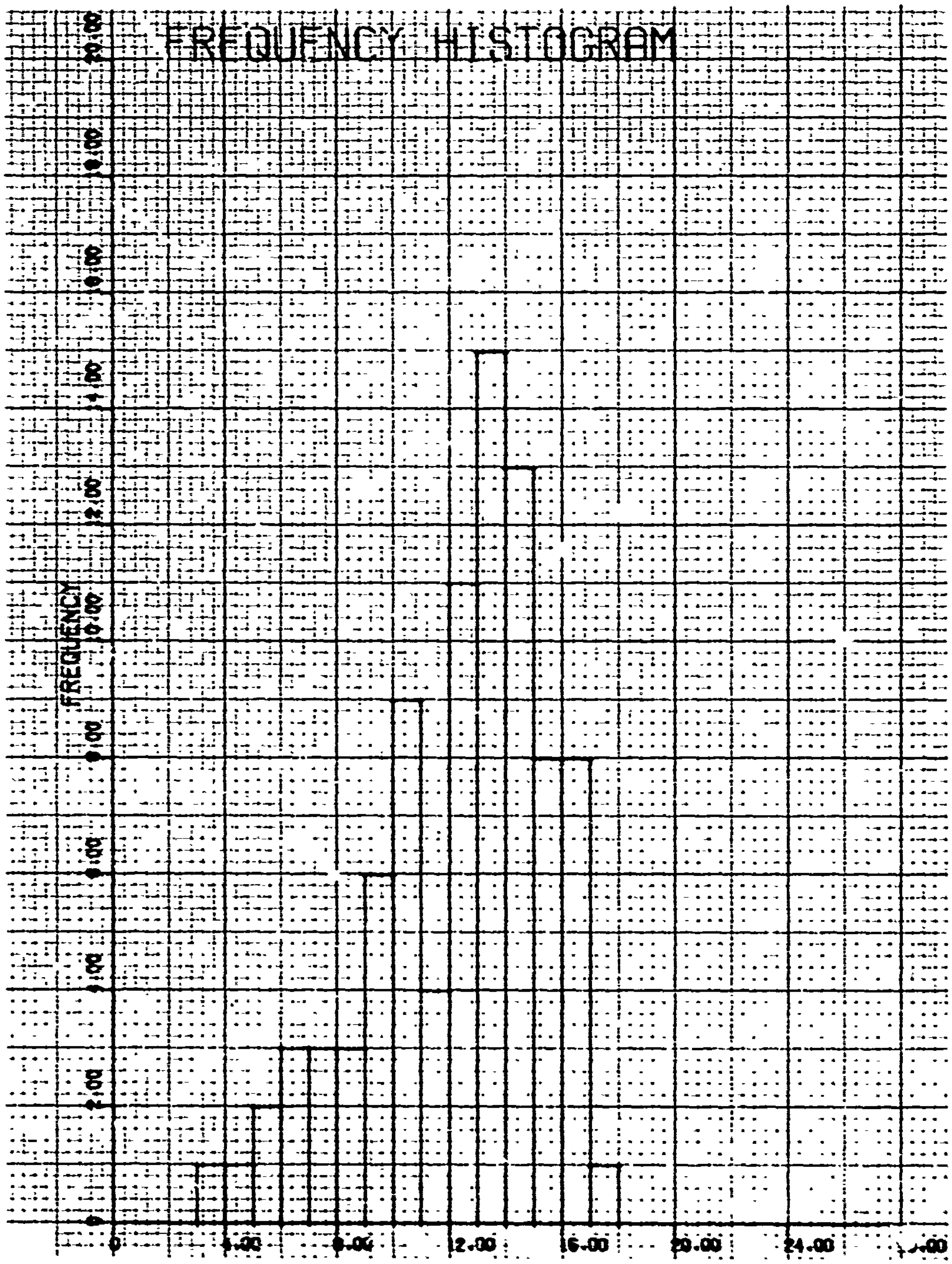

Figure 20 - Frequency Histogram for Static Unbalance of Full 5000 Series Shell

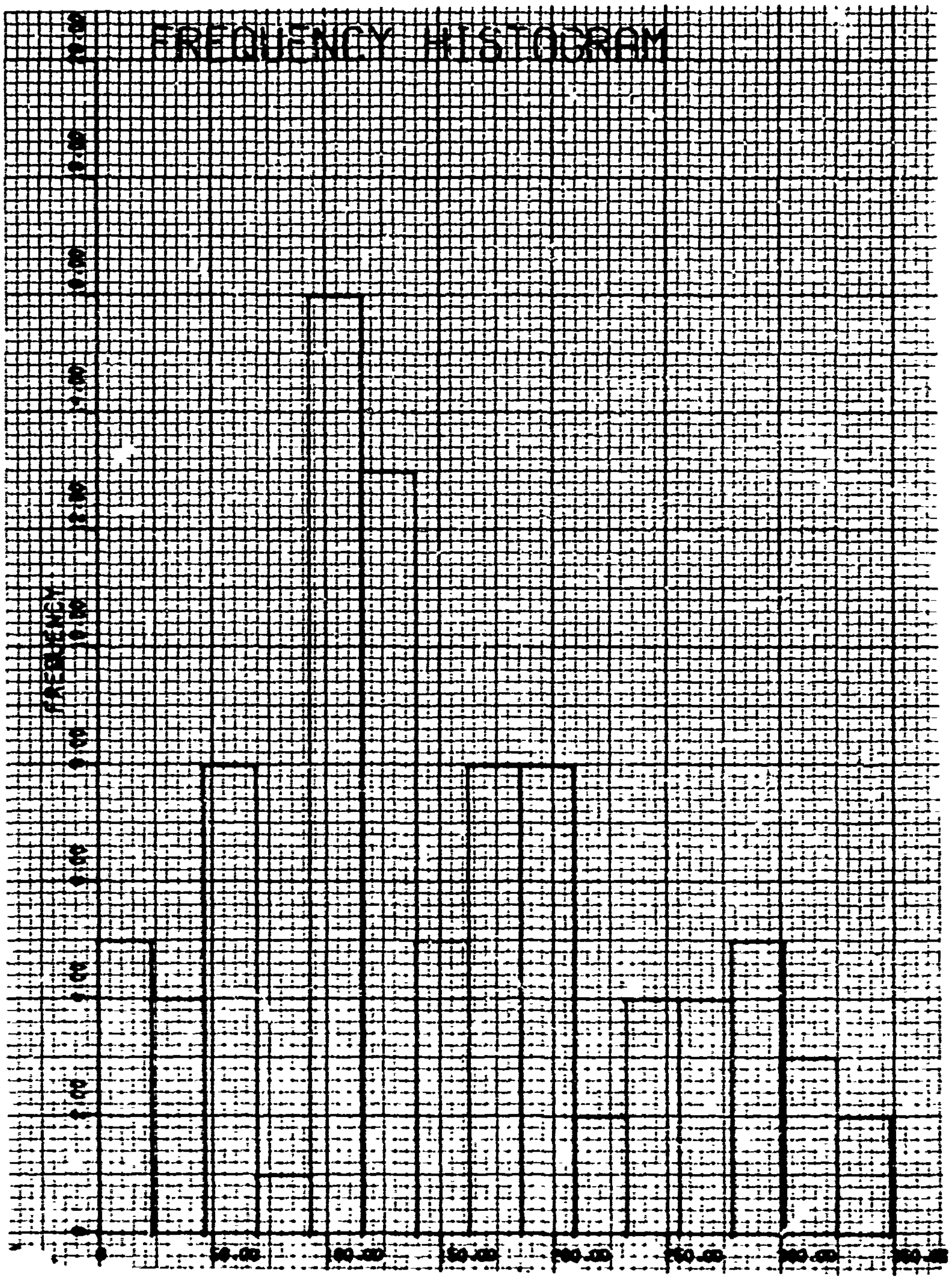

Figure 21 - Frequency Histogram for Azimuth of Dynamic Unbalance of Empty 5000 Series Shell

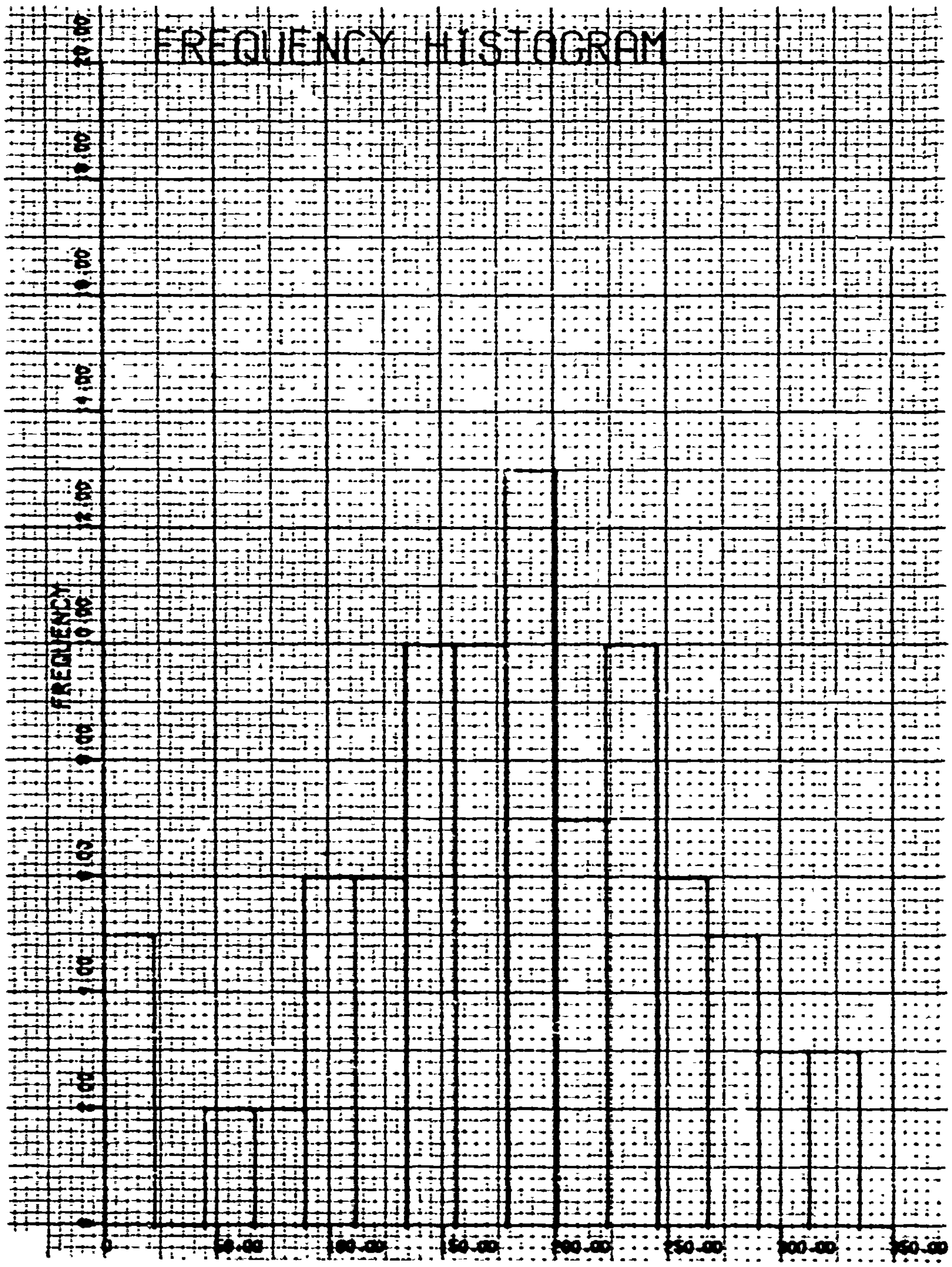

Figure 22 - Frequency Histogram for Azimuth of Dynamic Unbalance of Full 5000 Series Shell

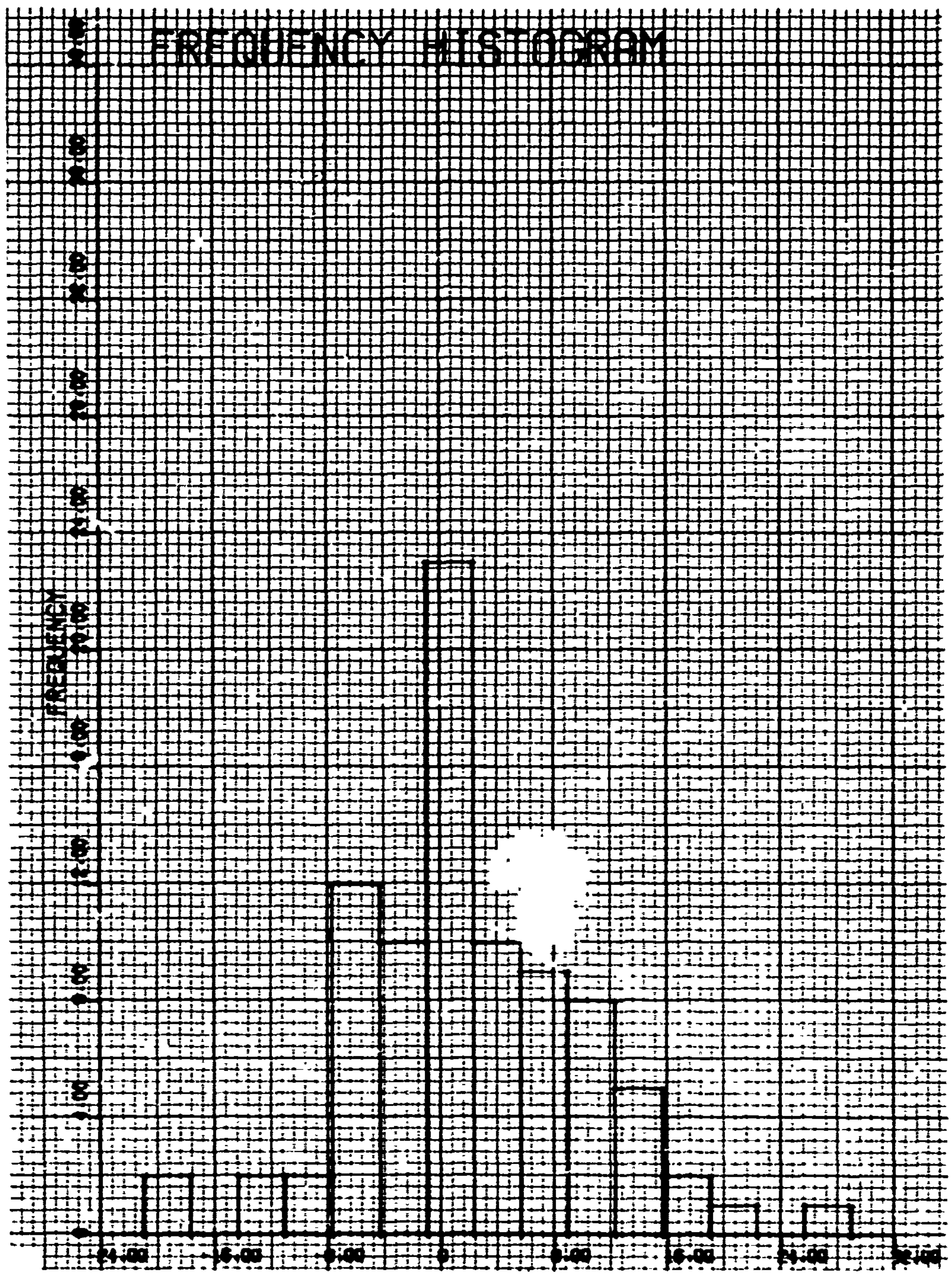

Figure 23 - Frequency Histogram for Azimuth of Static Unbalance of Empty 5000 Series Shell

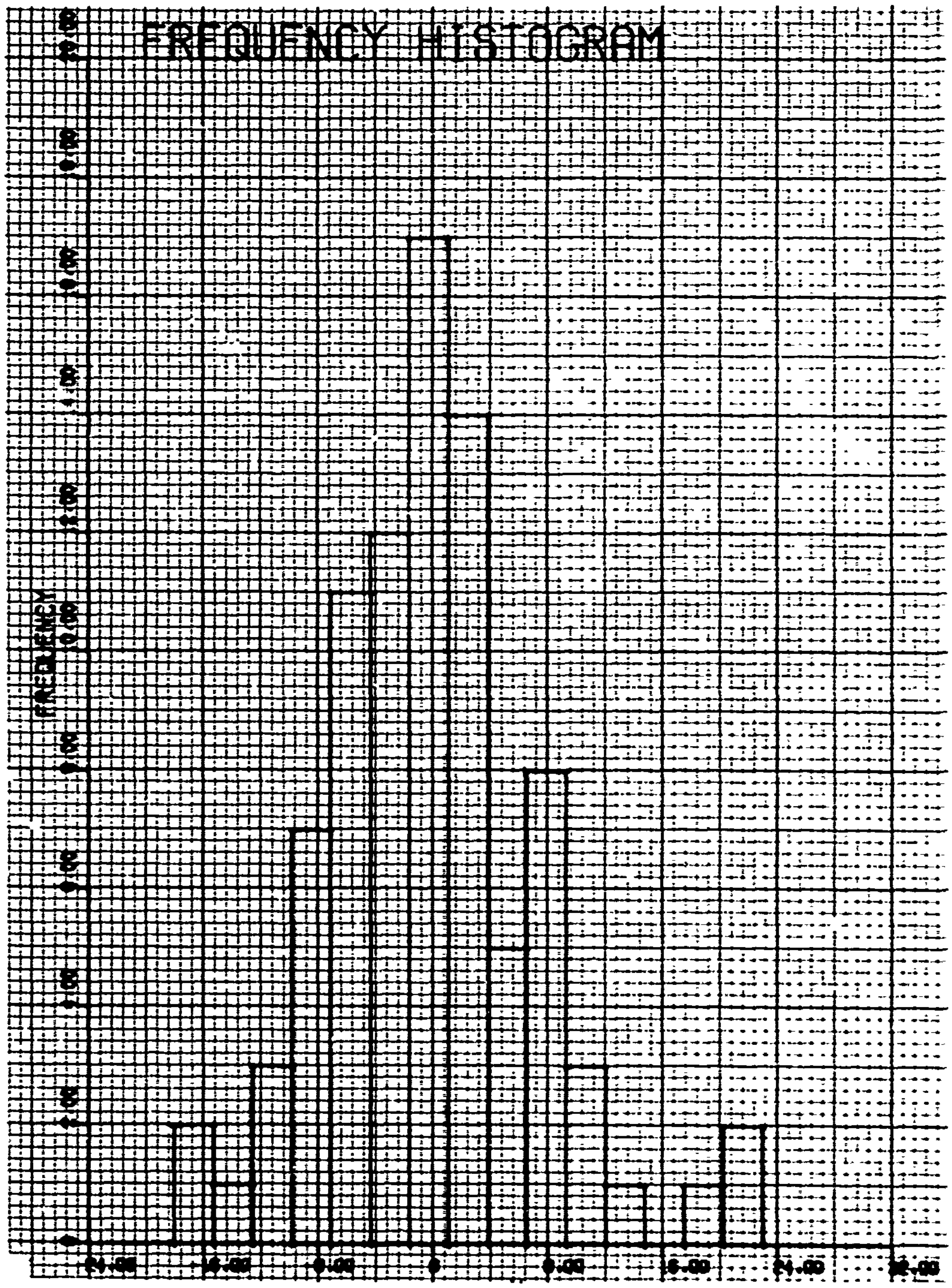

Figure 24 - Frequency Histogram for Azimuth of Static Unbalance of Full 5000 Series Shell

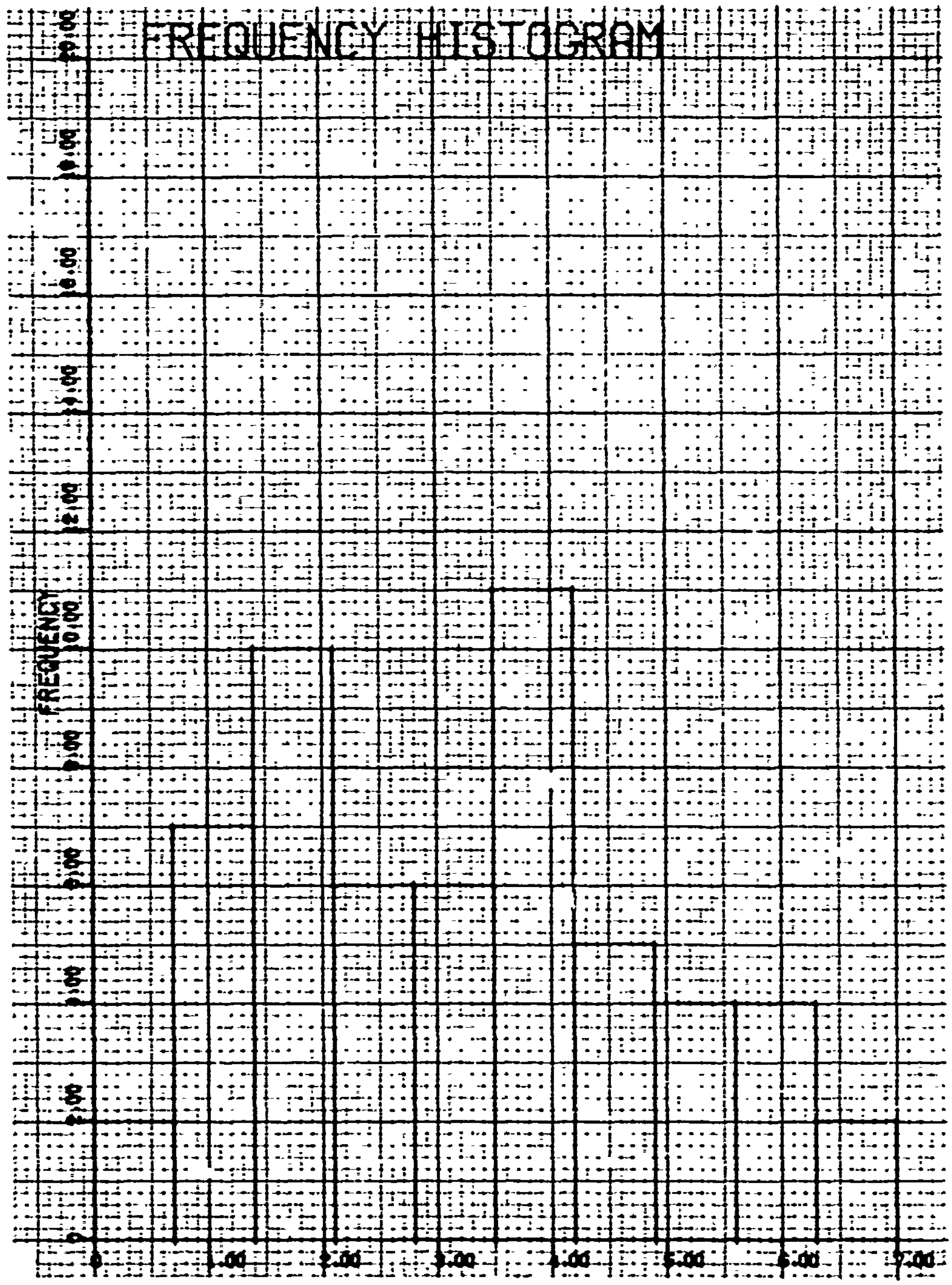

Figure 25 - Frequency Histogram for Dynamic Unbalance of Empty 6000 Series Shell

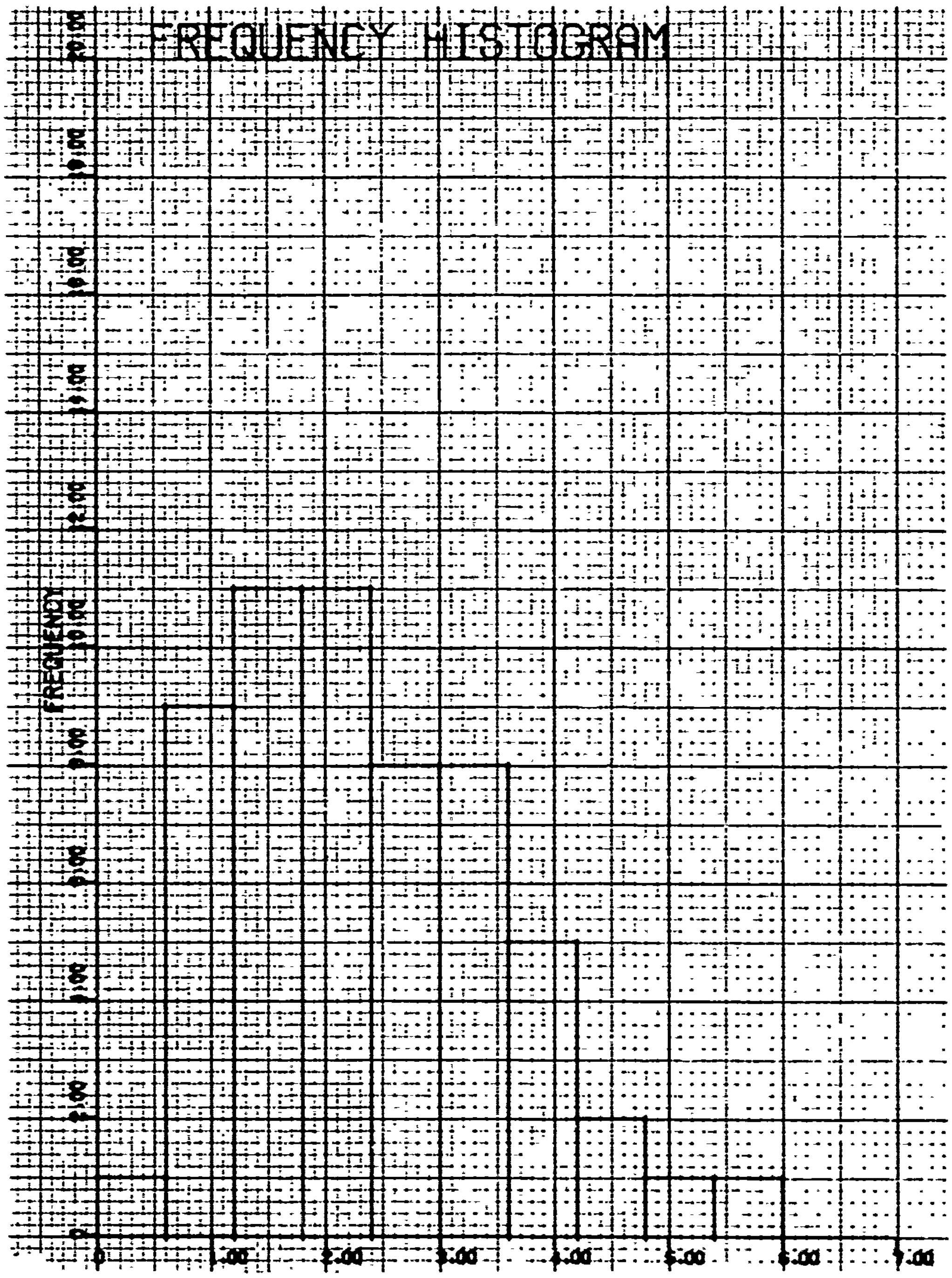

Figure 26 - Frequency Histogram for Dynamic Unbalance of Full 6000 Series Shell

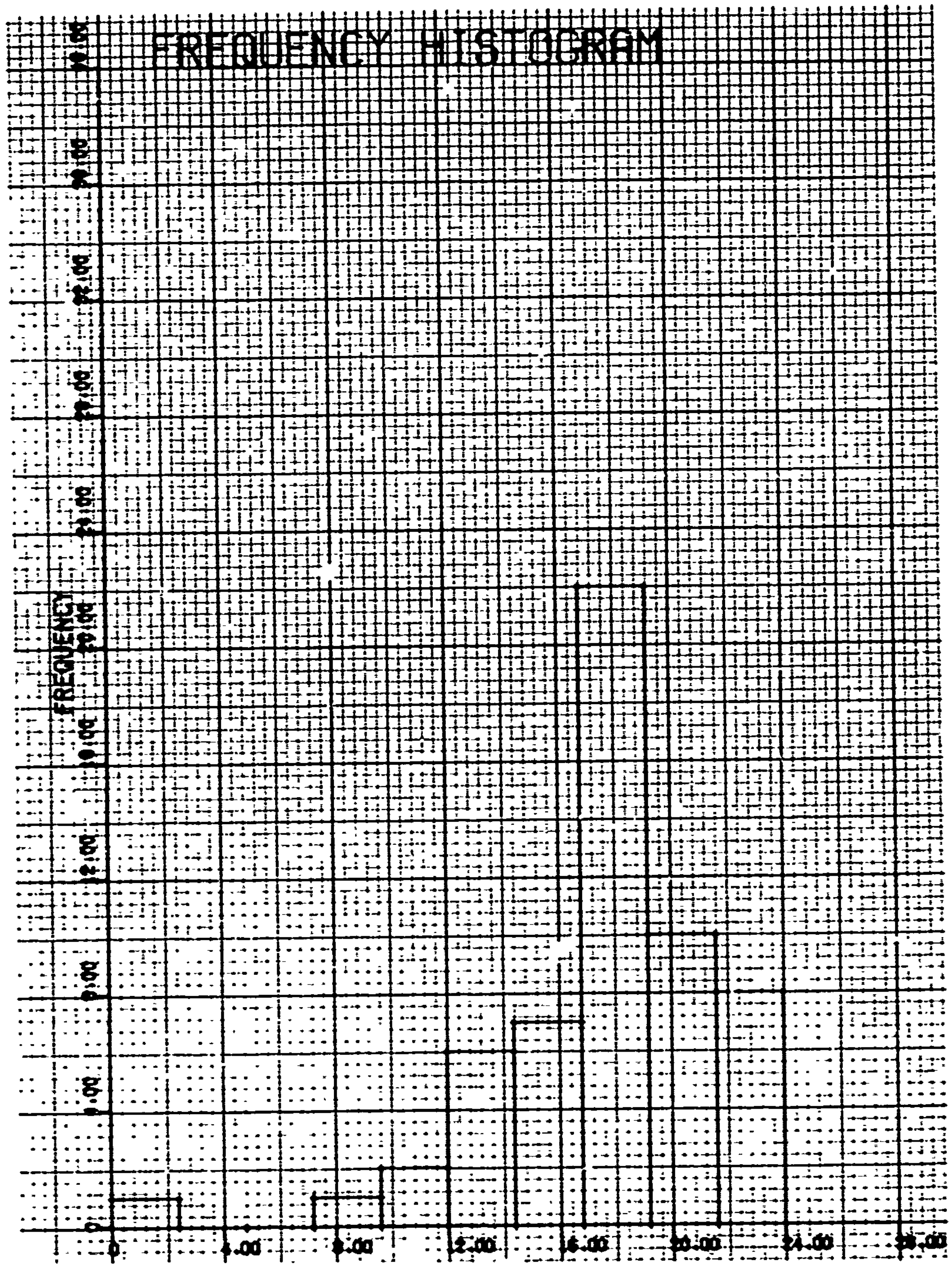

Figure 27 - Frequency Histogram for Static Unbalance of Empty 6000 Series Shell

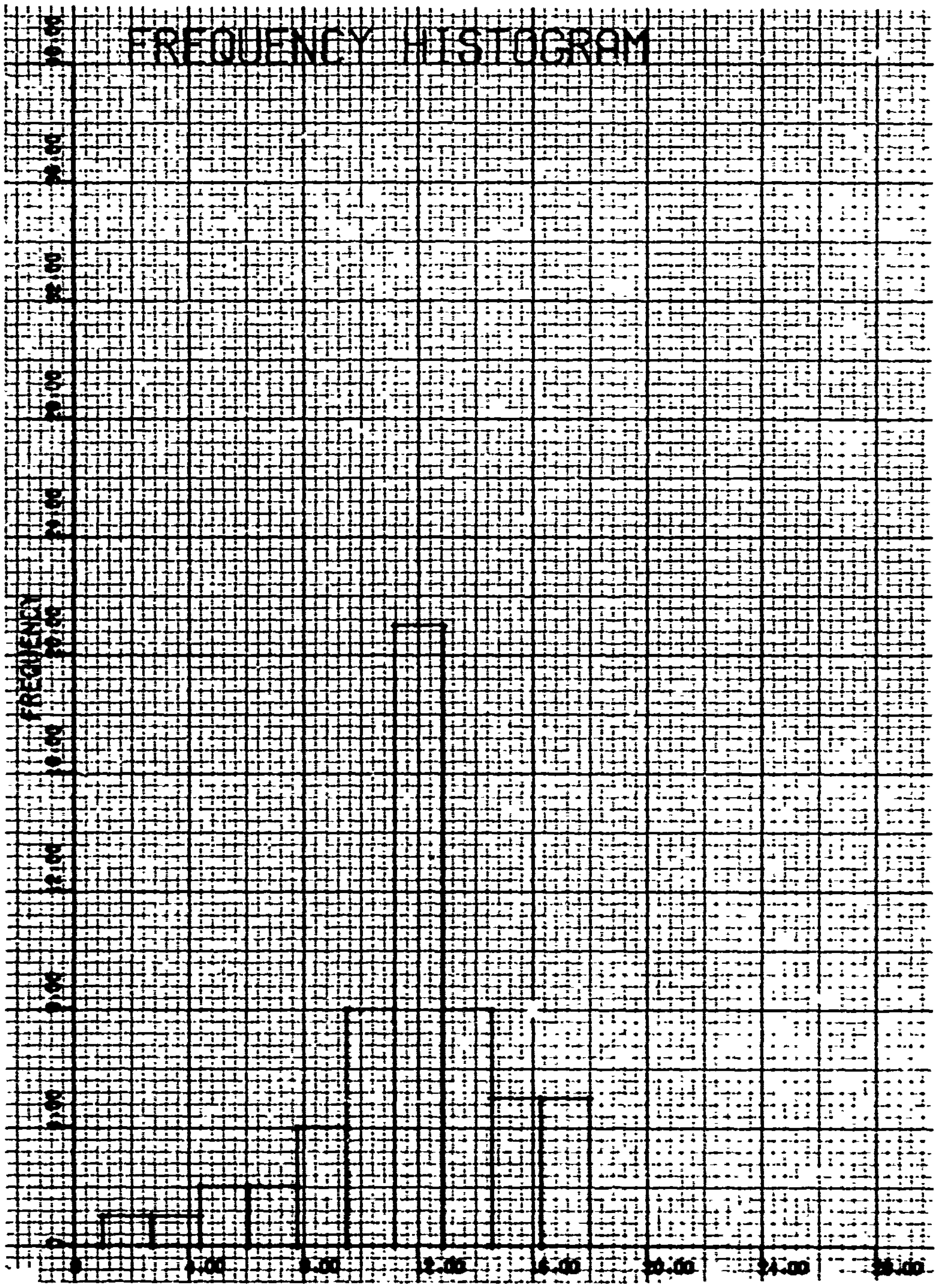

Figure 28 - Frequency Histogram for Static Unbalance of Full 6000 Series Shell

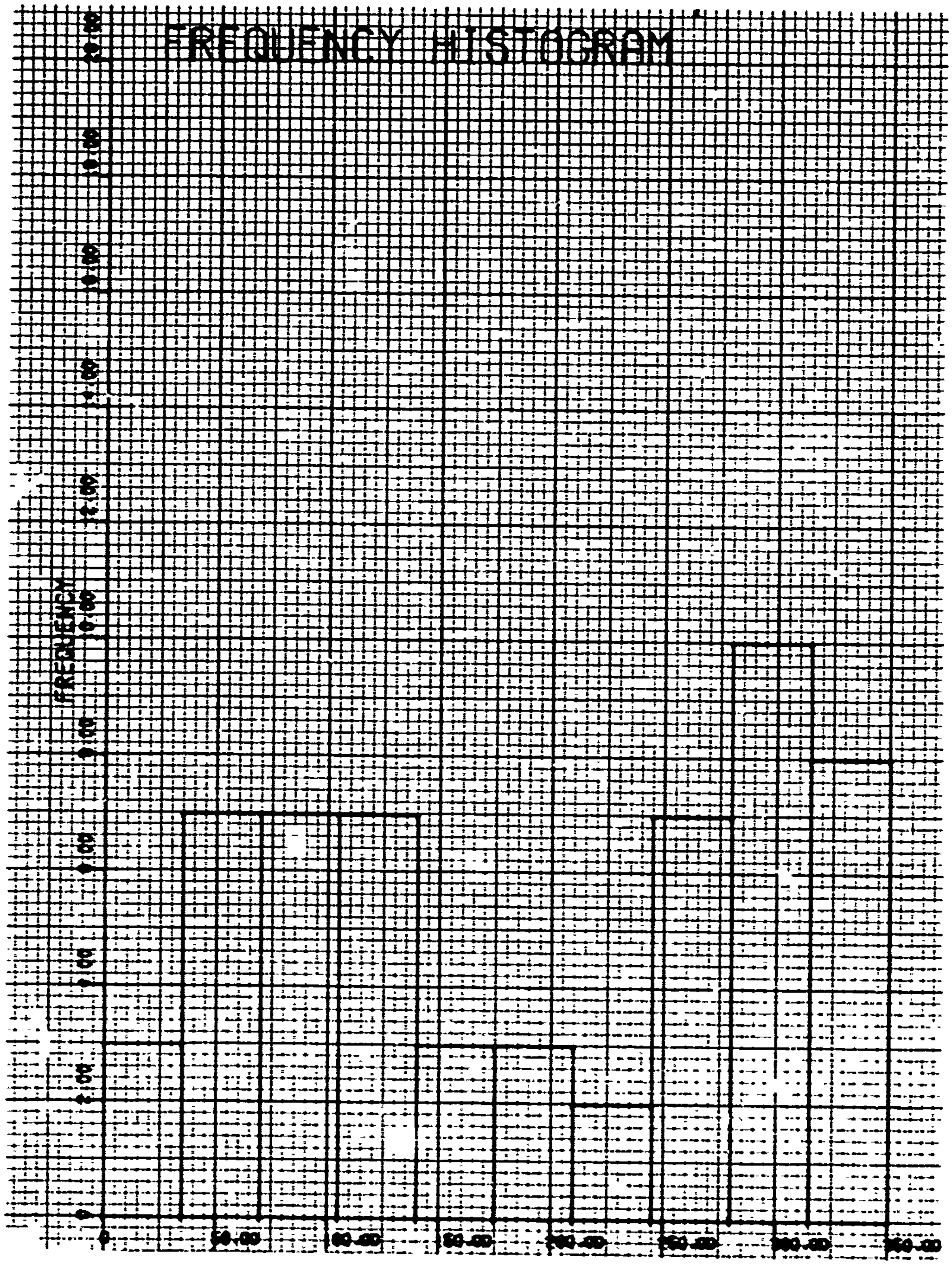

Figure 29 - Frequency Histogram for Azimuth of Dynamic Unbalance of Empty 6000 Series Shell

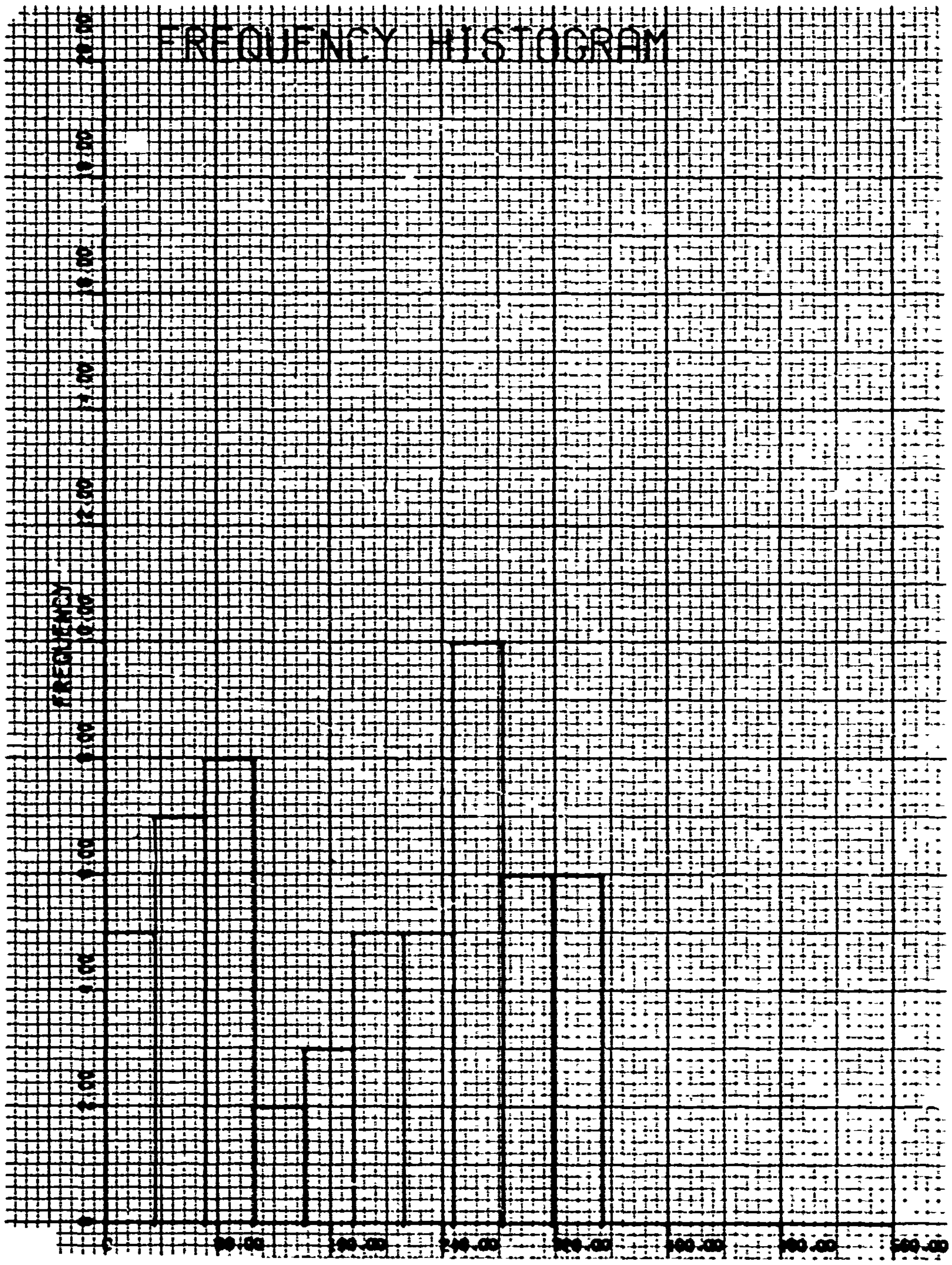

Figure 30 - Frequency Histogram for Azimuth of Dynamic Unbalance of Full 6000 Series Shell

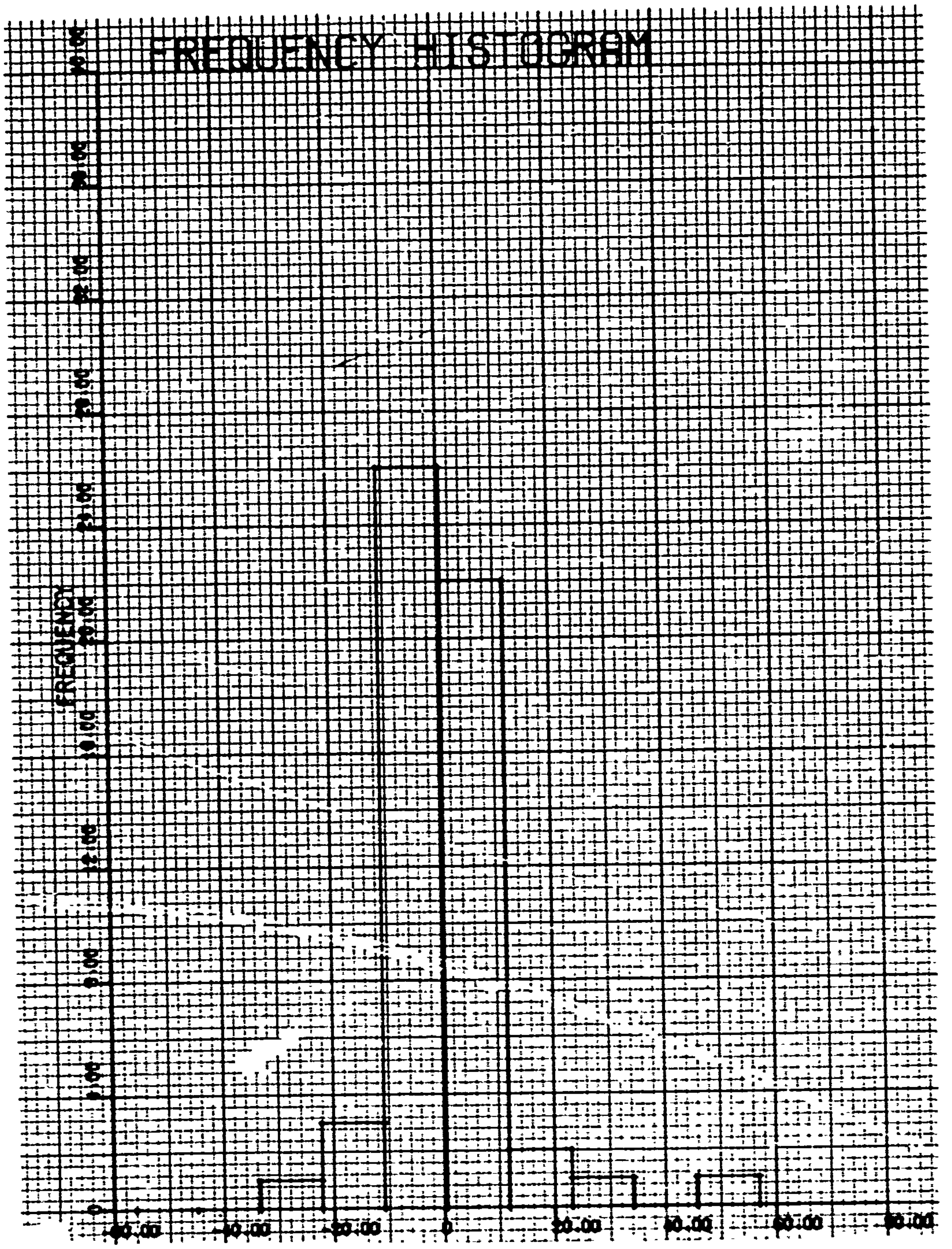

Figure 31 - Frequency Histogram for Azimuth of Static Unbalance of Empty 6000 Series Shell

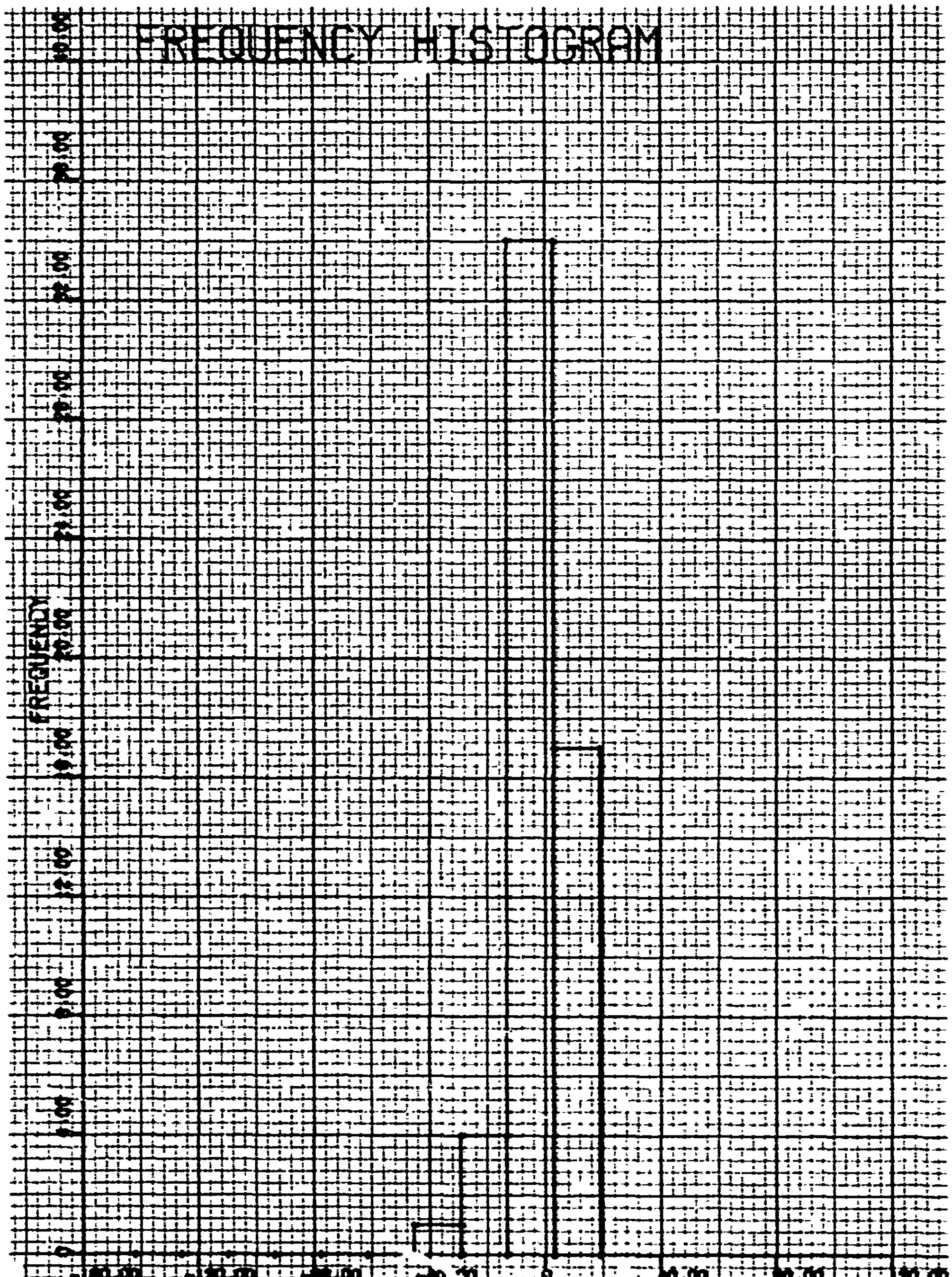

Figure 32 - Frequency Histogram for Azimuth of Static Unbalance of Full 6000 Series Shell

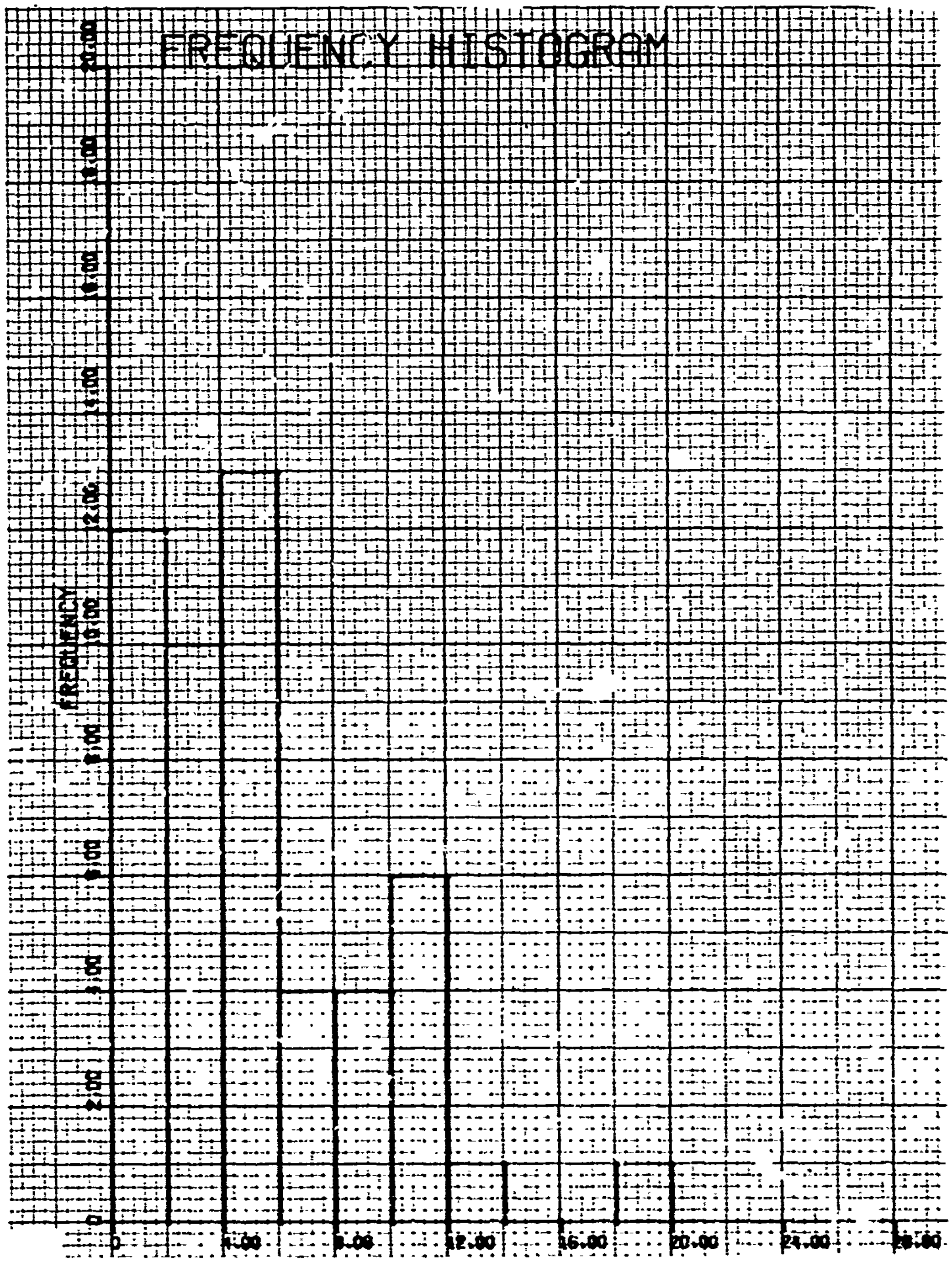

Figure 23 - Frequency Histogram for Dynamic Unbalance of Empty 7000 Series Shell

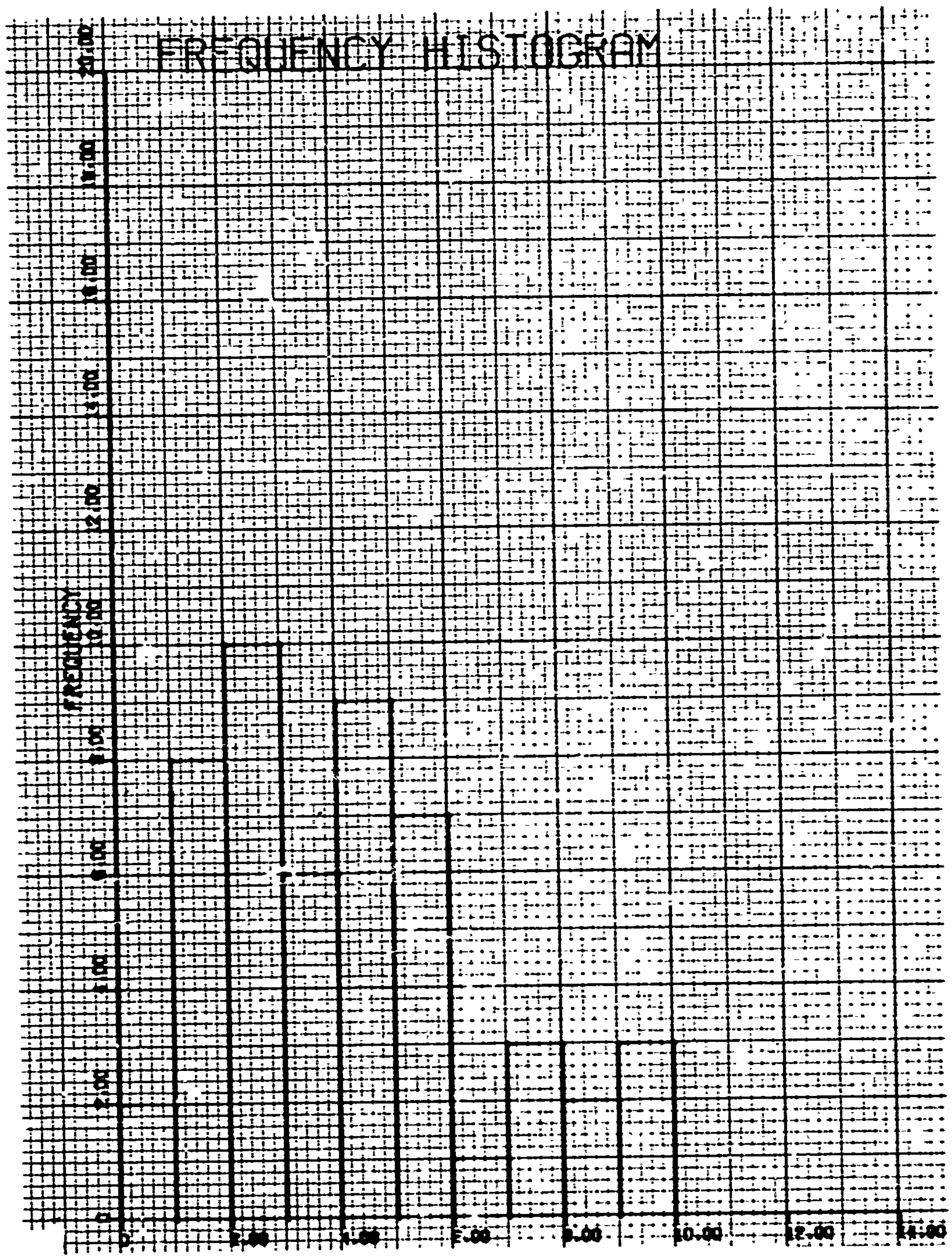

Figure 34 - Frequency Histogram for Dynamic Unbalance of Full 7000 Series Shell

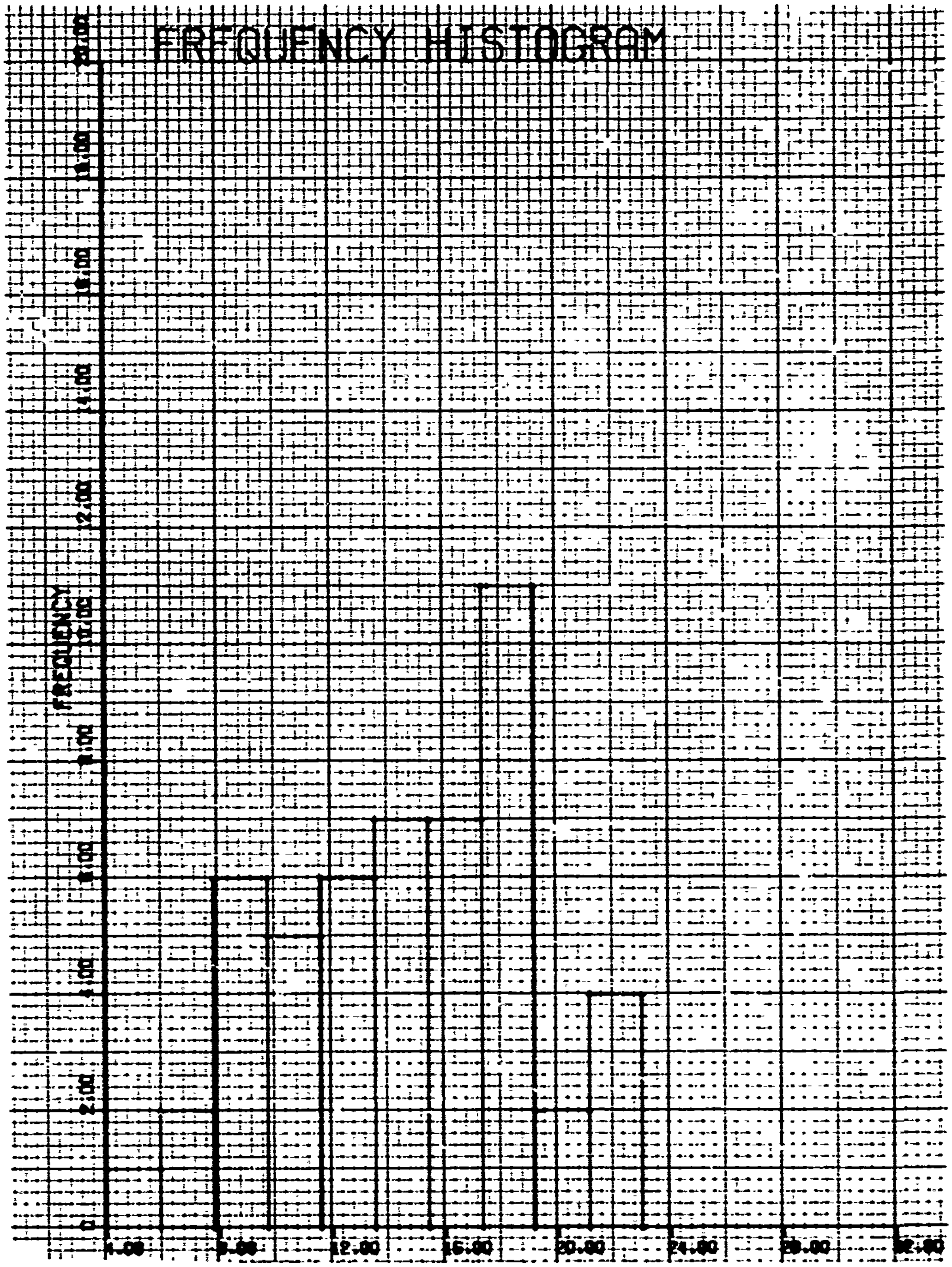

Figure 35 - Frequency Histogram for Static Unbalance of Empty 7000 Series Shell

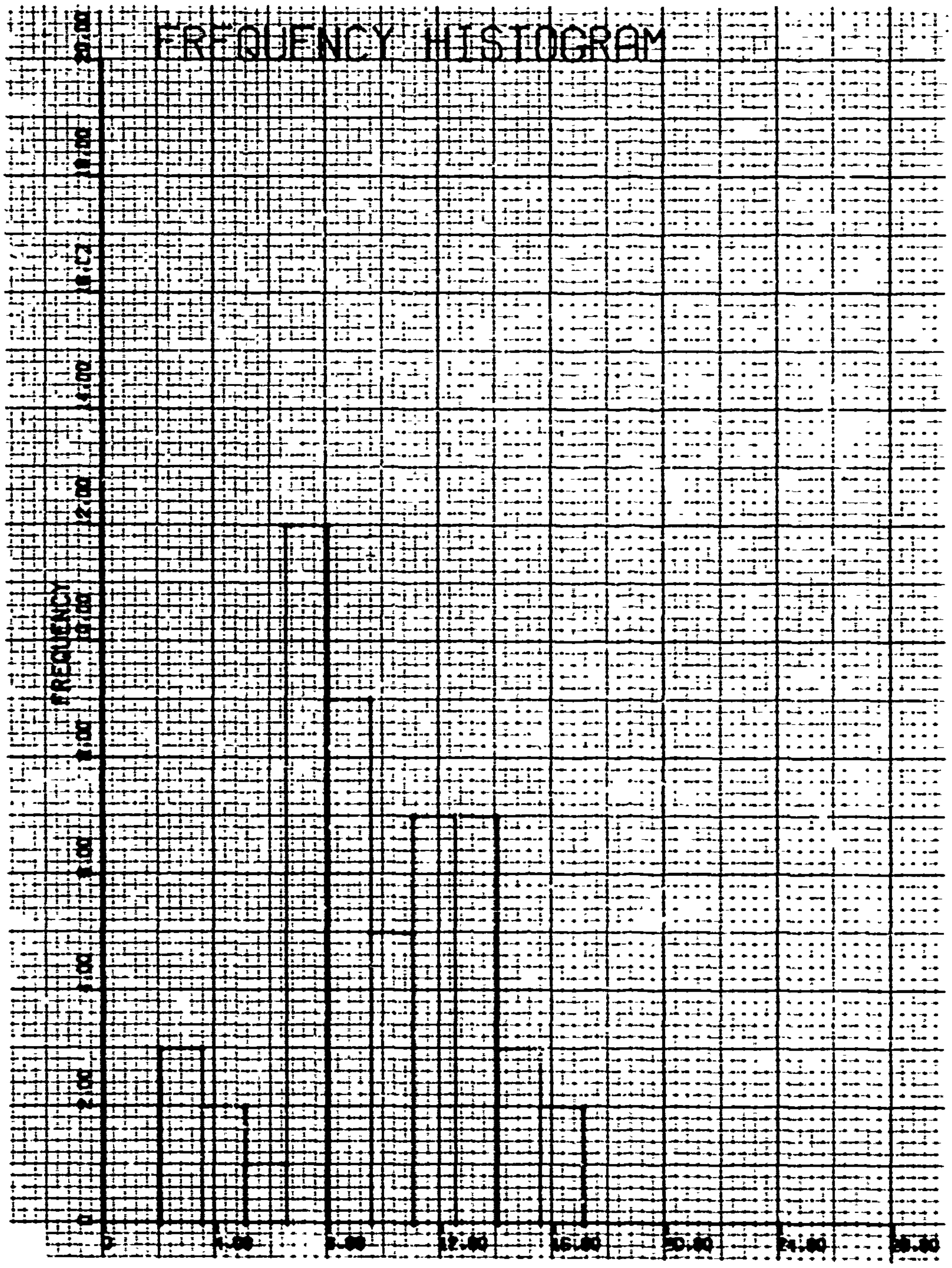

Figure 36 - Frequency Histogram for Static Unbalance of Full 7000 Series Shell

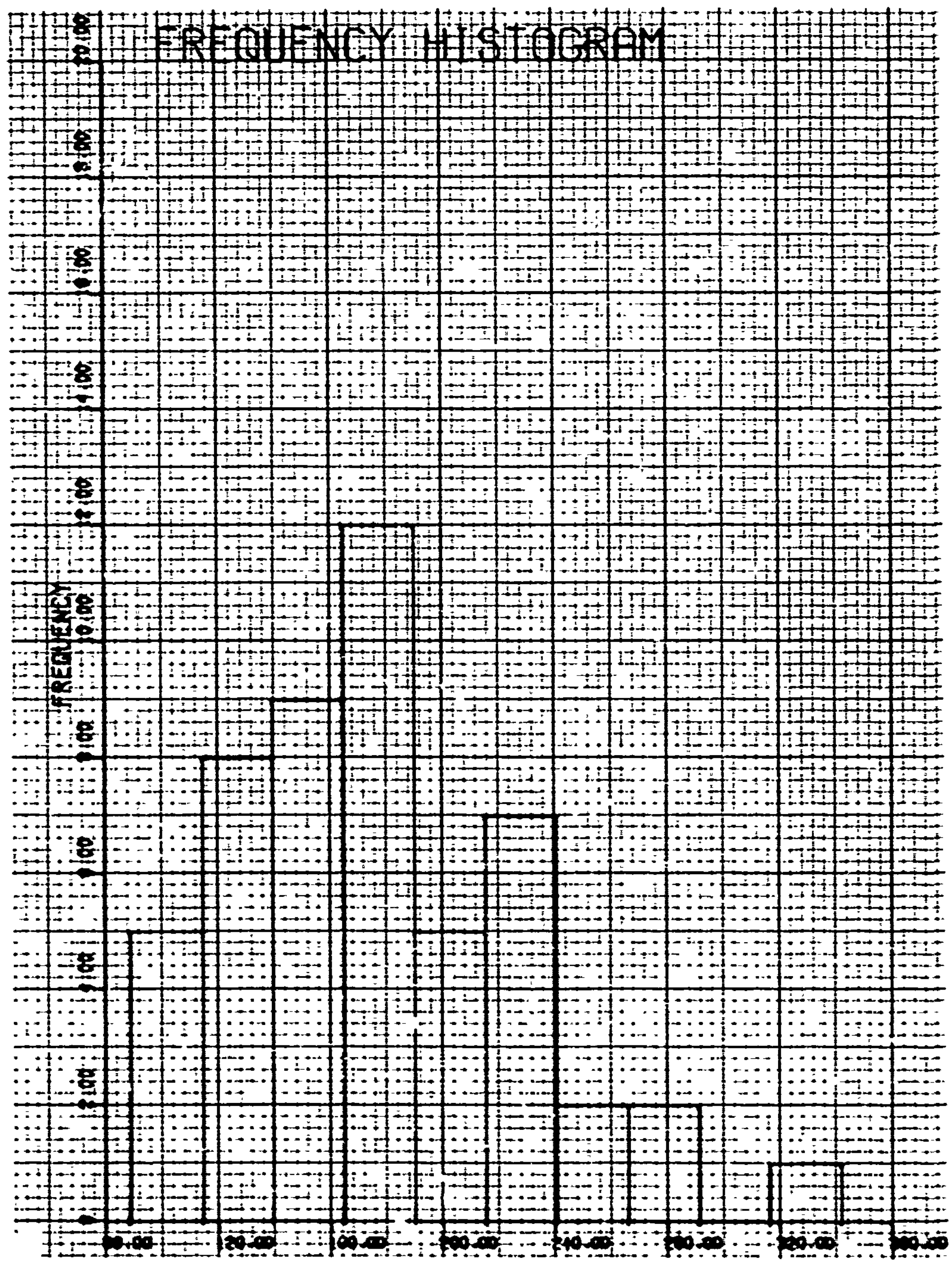

Figure 37 - Frequency Histogram for Azimuth of Dynamic Unbalance of Empty 7000 Series Shell

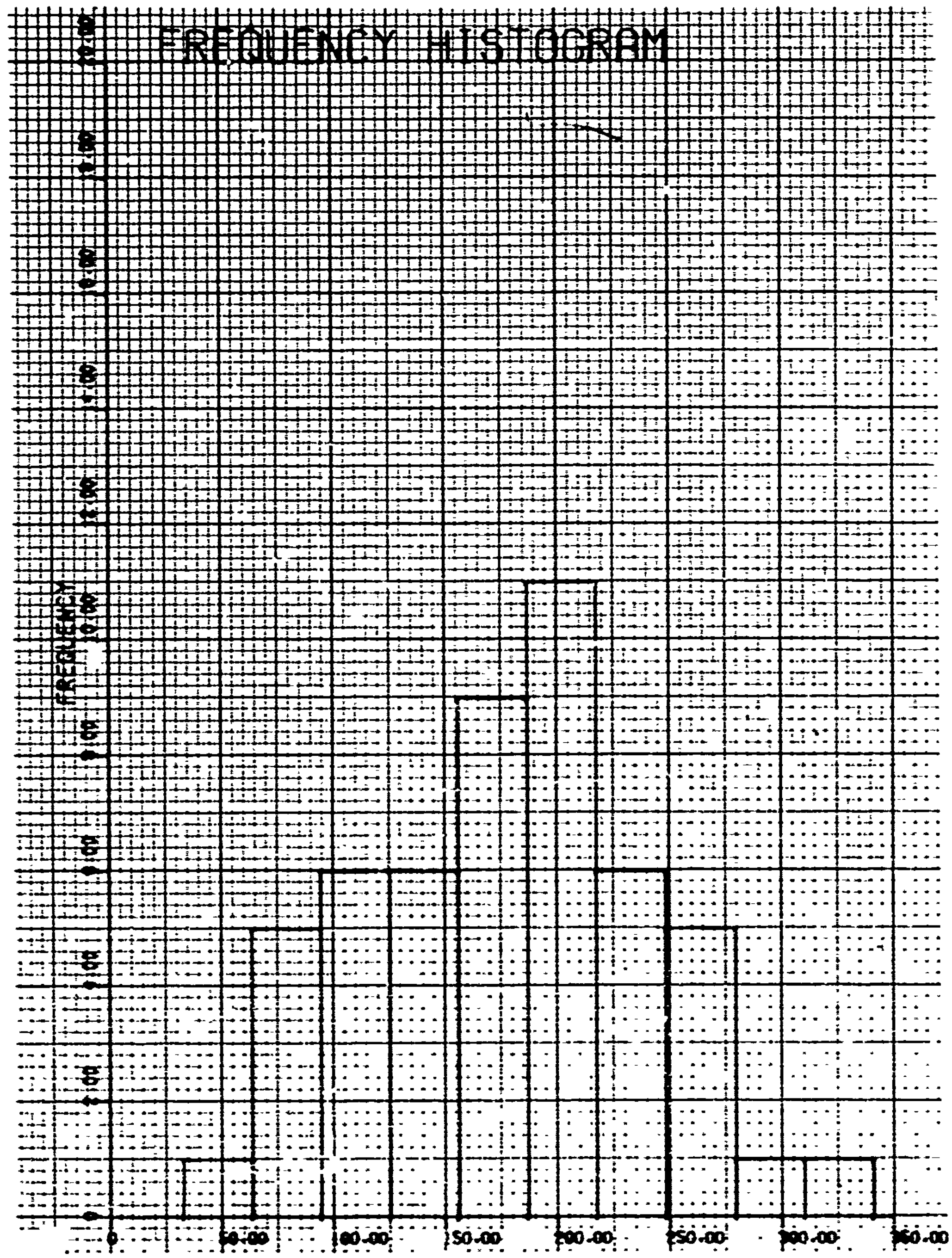

Figure 38 - Frequency Histogram for Azimuth of Dynamic Unbalance of Full 7000 Series Shell

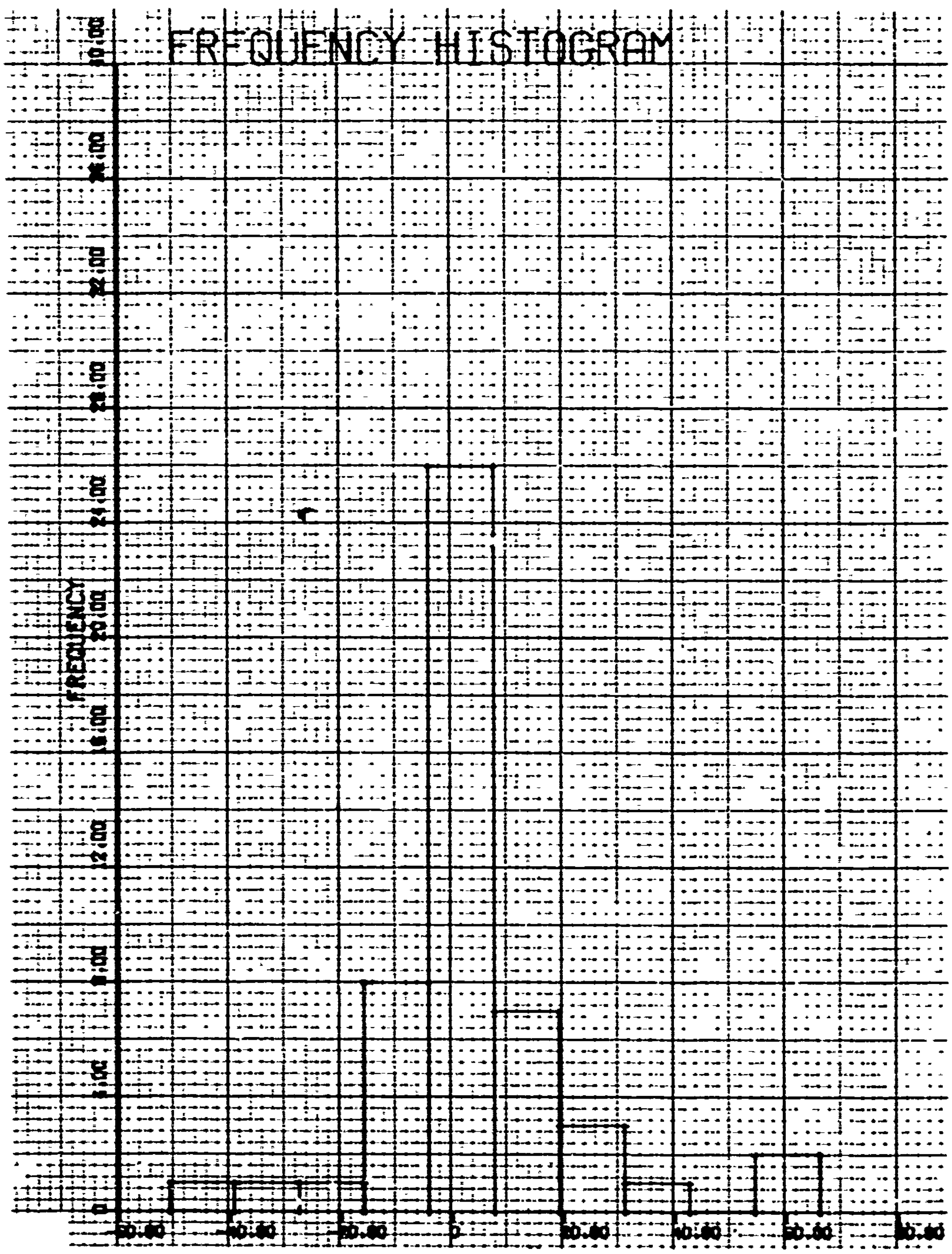

Figure 39 - Frequency Histogram for Azimuth of Static Unbalance of Empty 7000 Series Shell

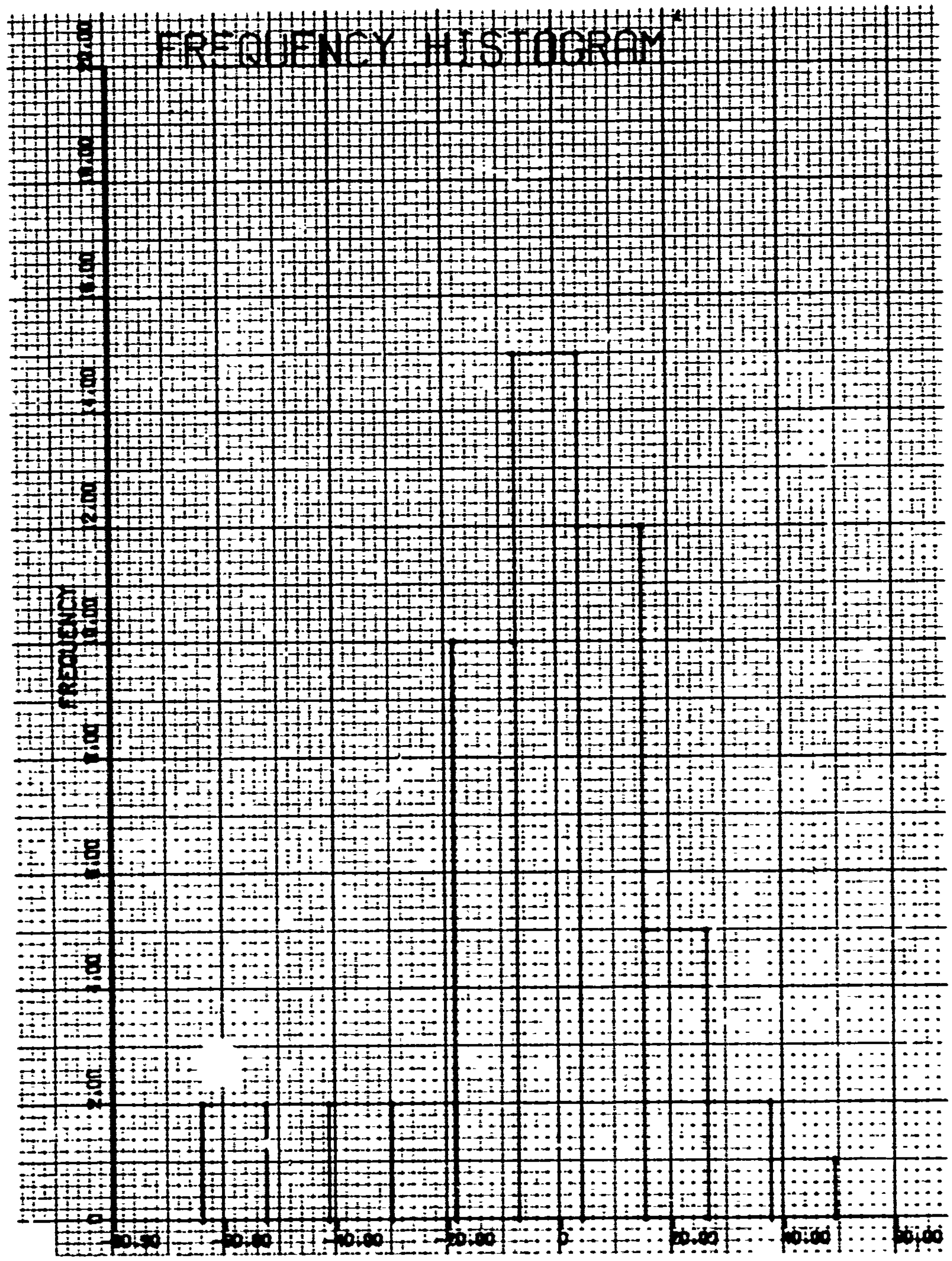

Figure 40 - Frequency Histogram for Azimuth of Static Unbalance of Full 7000 Series Shell

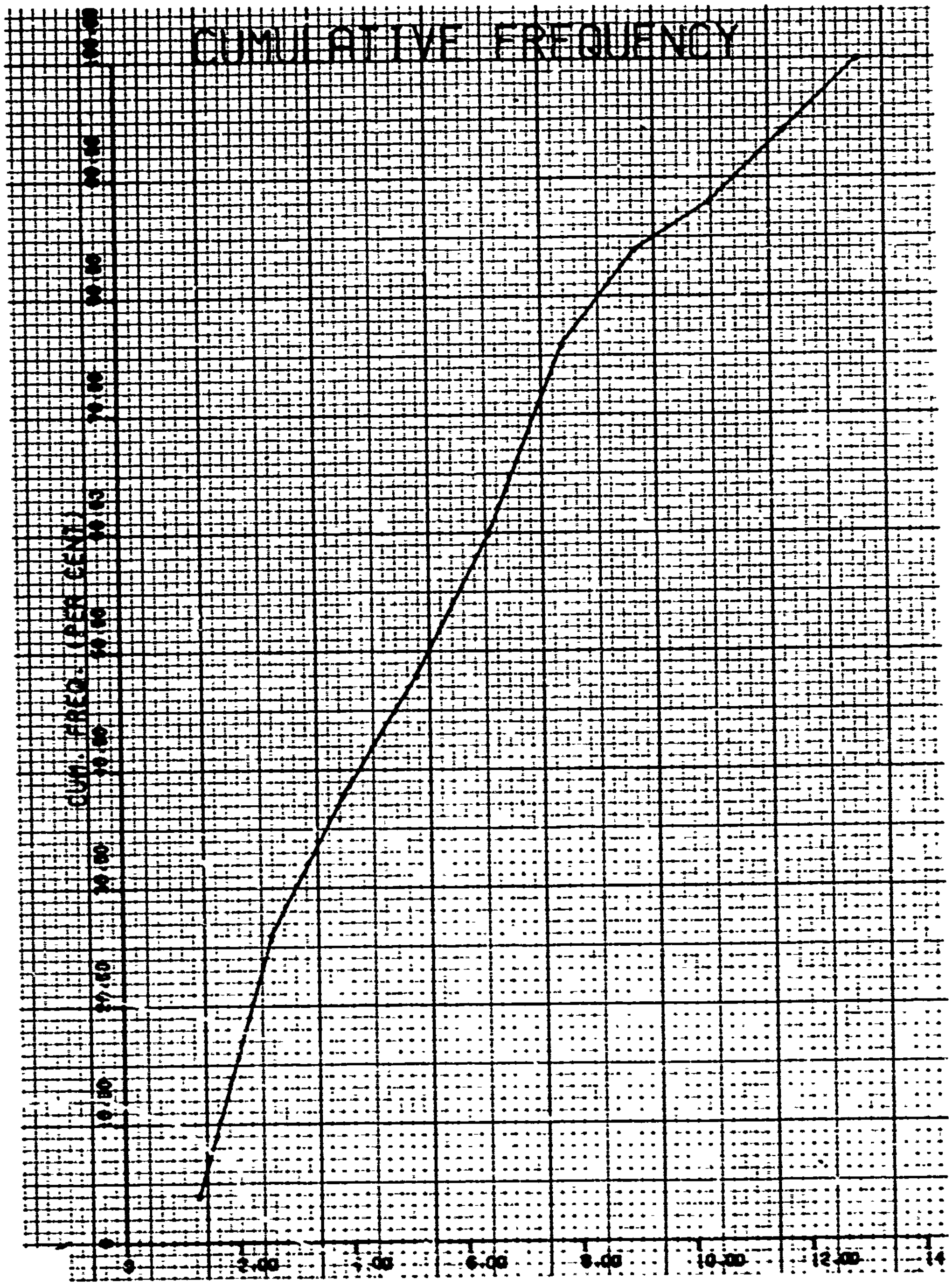

Figure 41 - Cumulative Frequency Polygon for Dynamic Unbalance of Empty SOP Series Shell

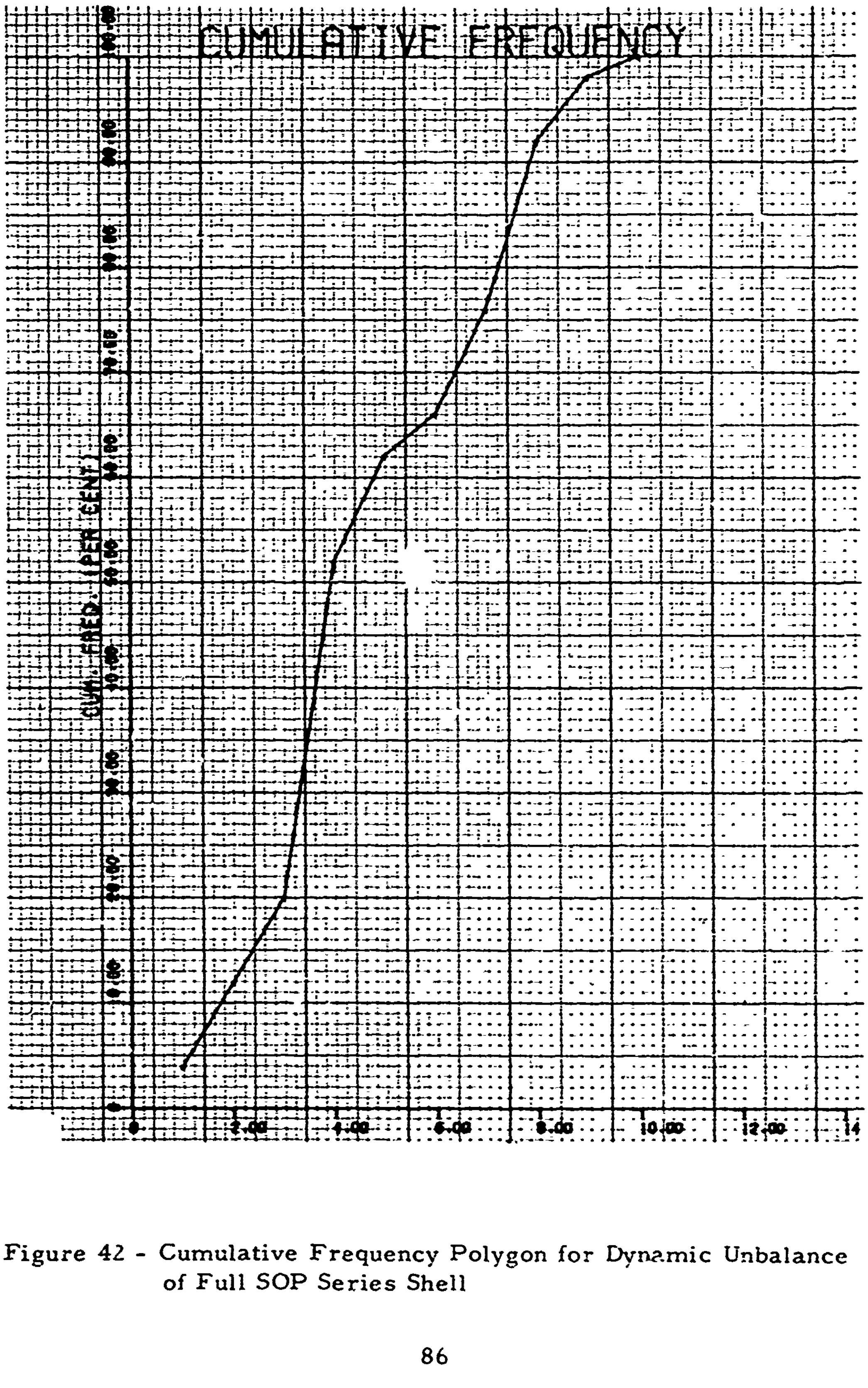

Figure 42 - Cumulative Frequency Polygon for Dynamic Unbalance of Full SOP Series Shell

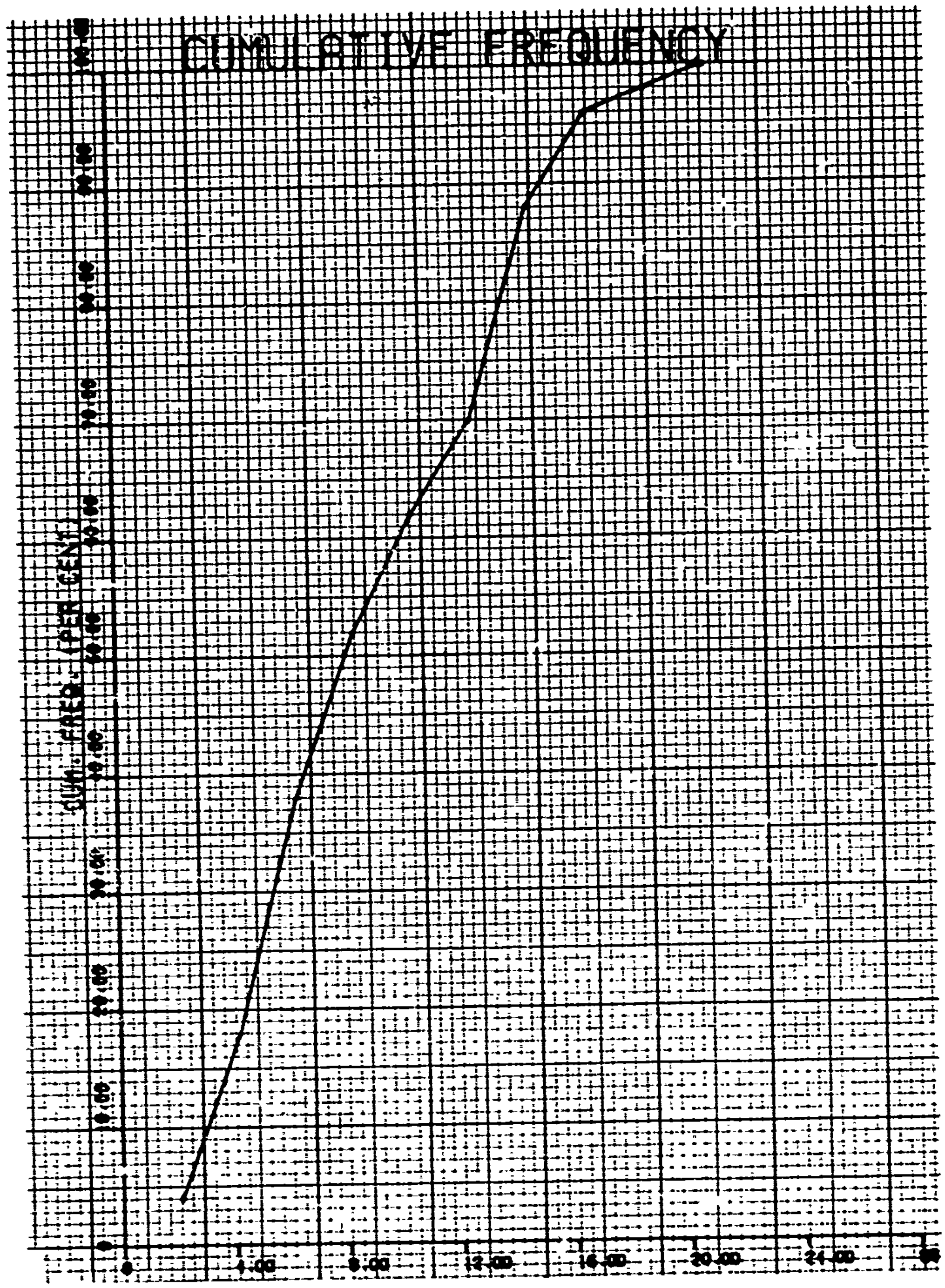

Figure 43 - Cumulative Frequency Polygon for Static Unbalance of Empty SOP Series Shell

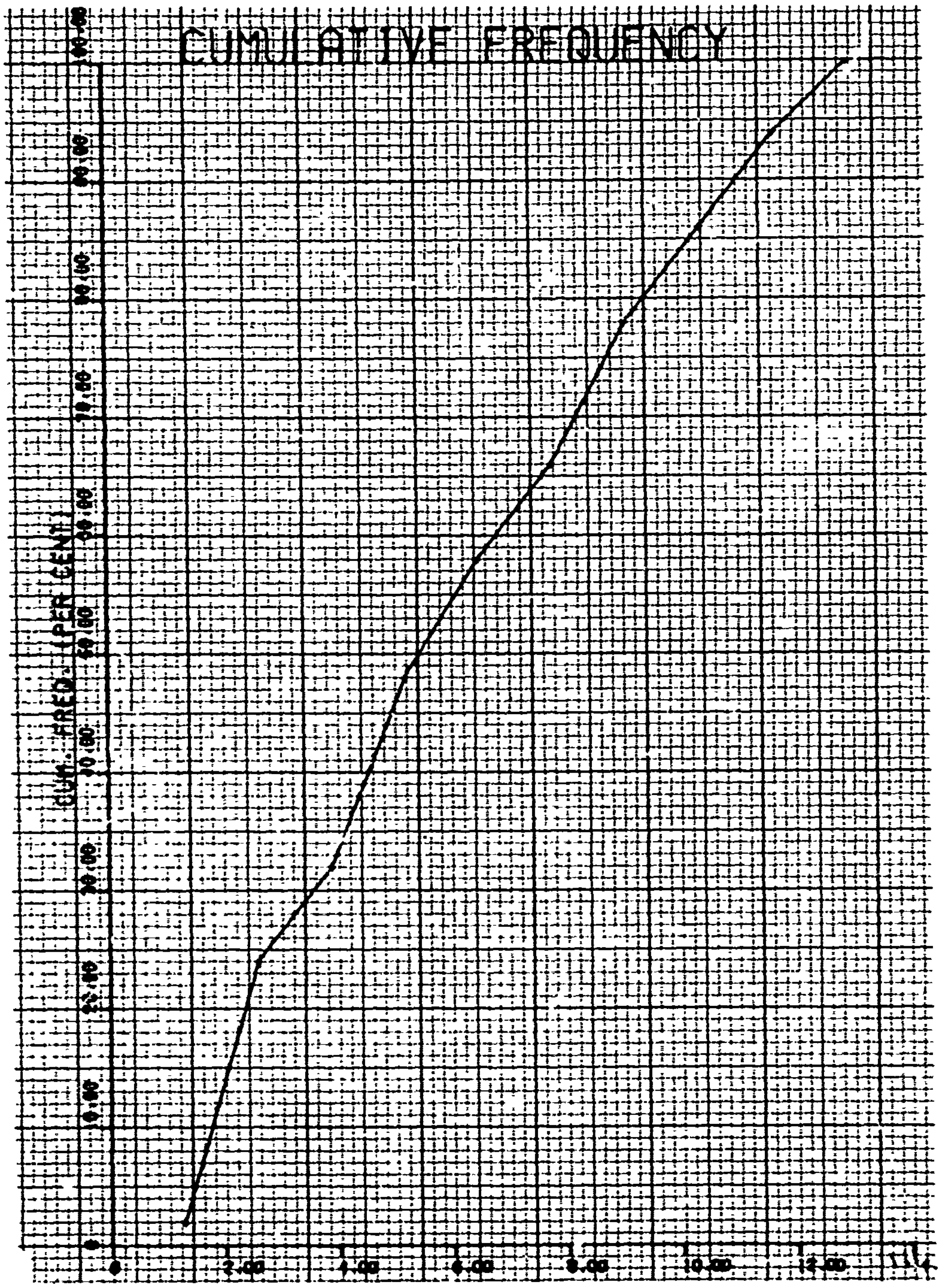

Figure 44 - Cumulative Frequency Polygon for Static Unbalance of Full SOP Series Shell

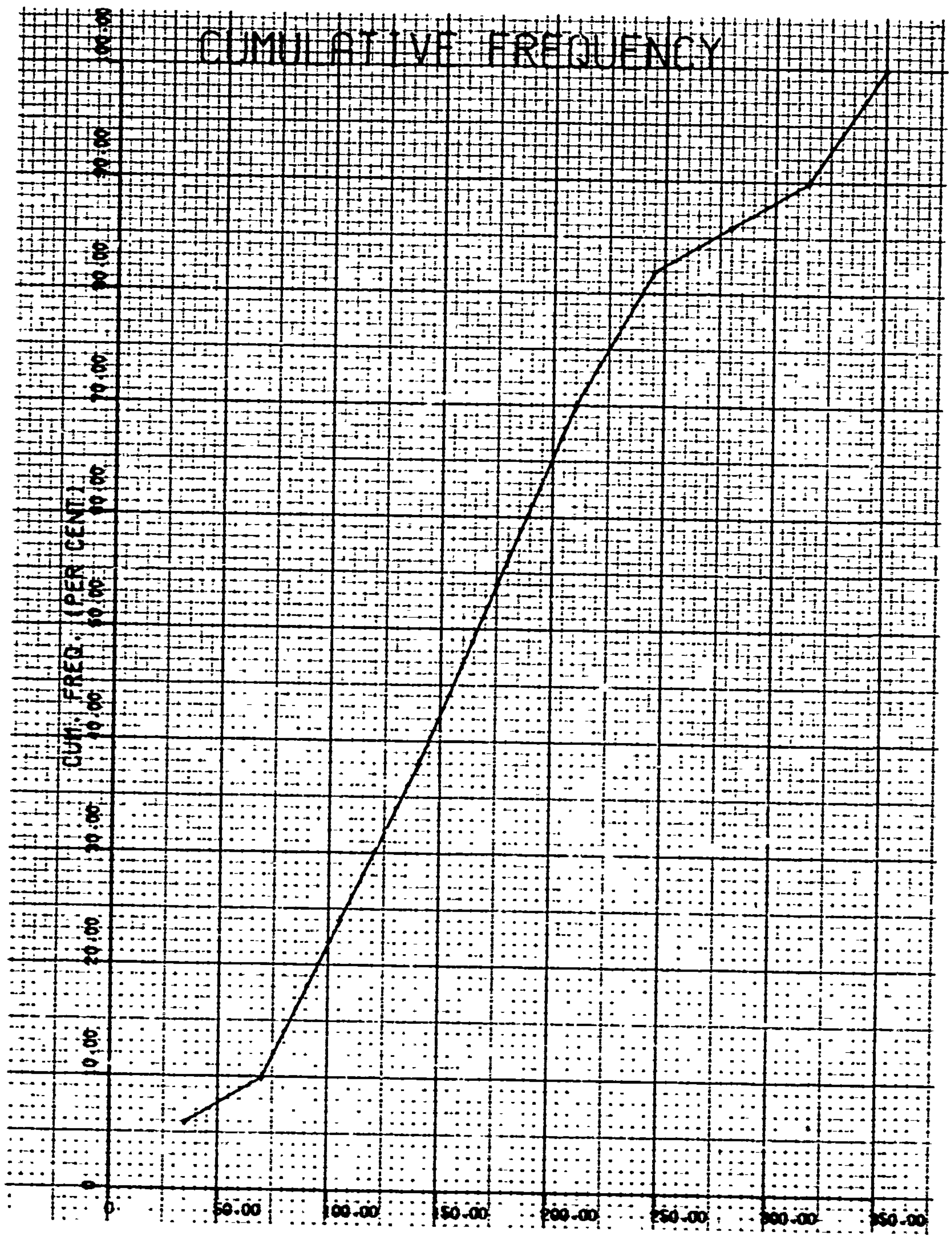

Figure 45 - Cumulative Frequency Polygon for Azimuth of Dynamic Unbalance of Empty SOP Series Shell

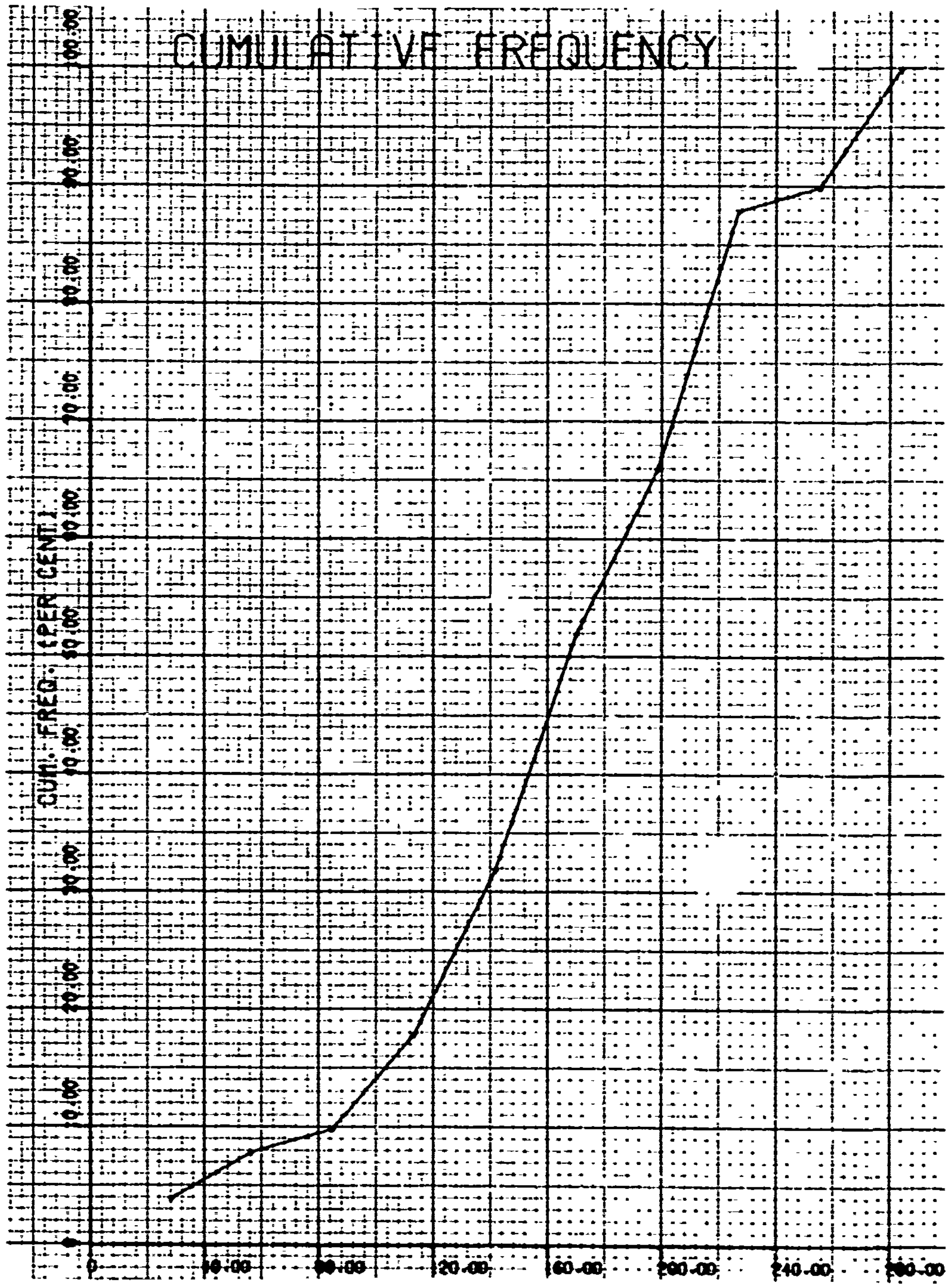

Figure 46 - Cumulative Frequency Polygon for Azimuth of Dynamic Unbalance of Full SOP Series Shell

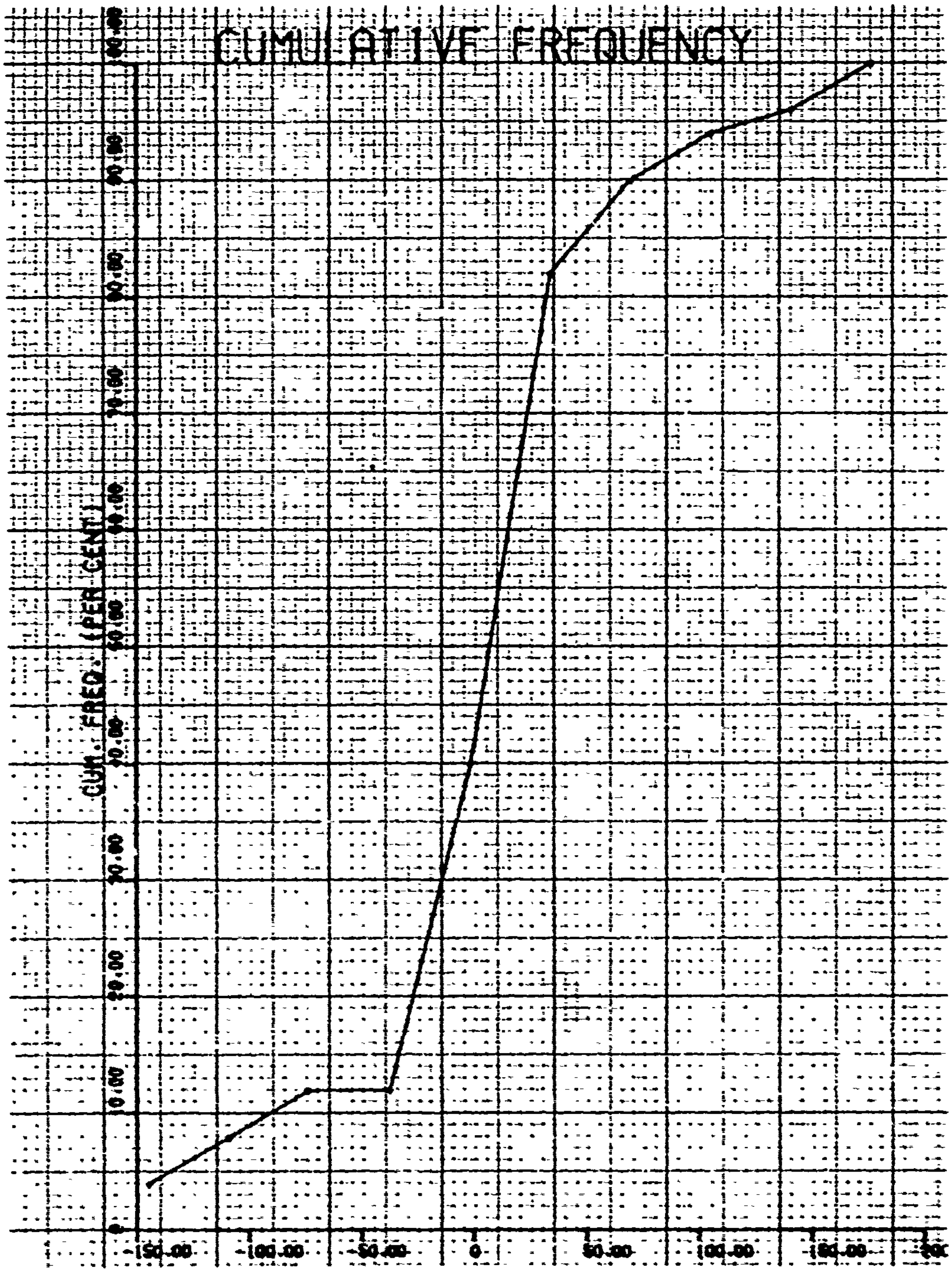

Figure 47 - Cumulative Frequency Polygon for Azimuth of Static Unbalance of Empty SOP Series Shell

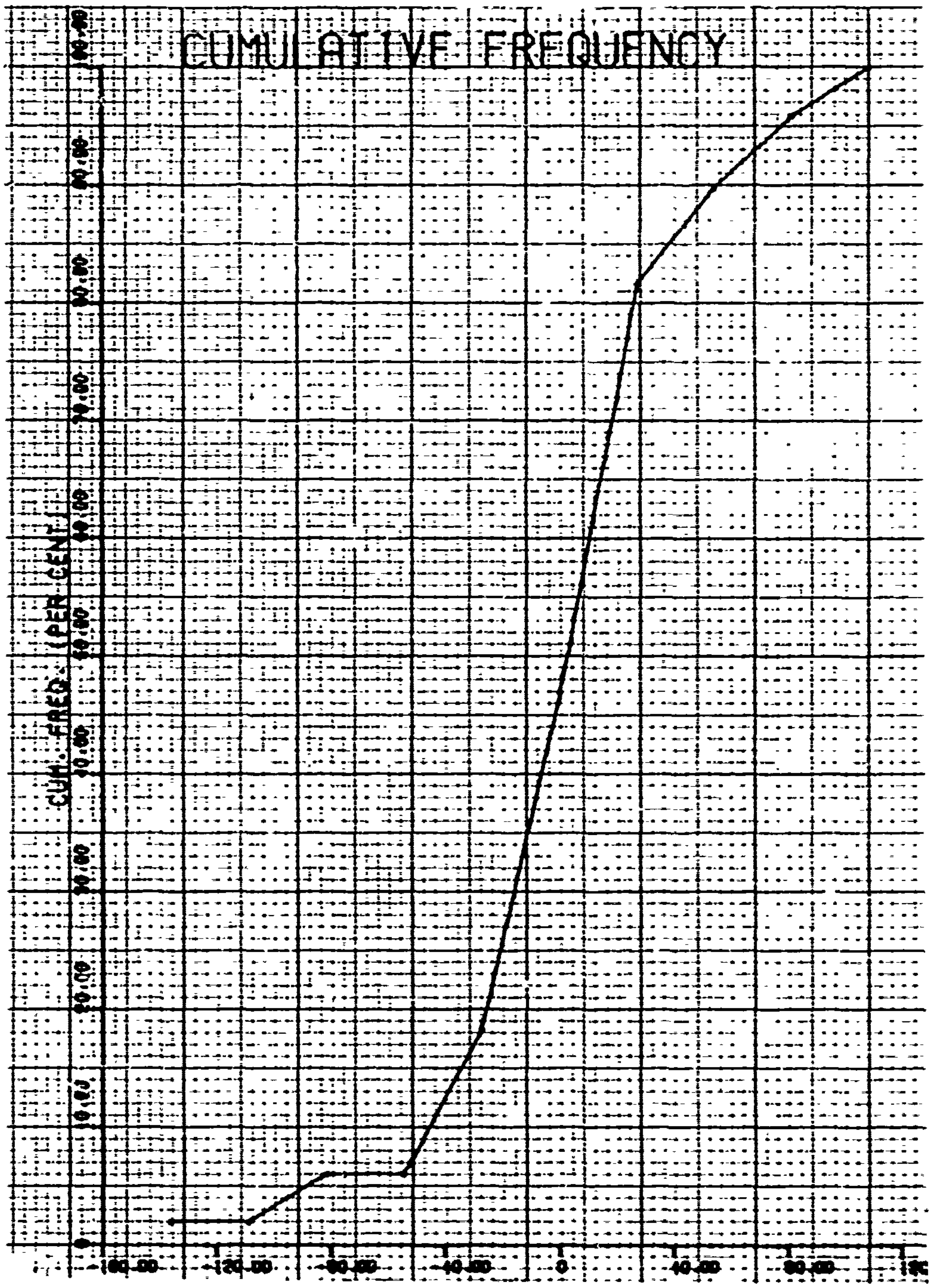

Figure 48 - Cumulative Frequency Polygon for Azimuth of Static Unbalance of Full SOP Series Shell

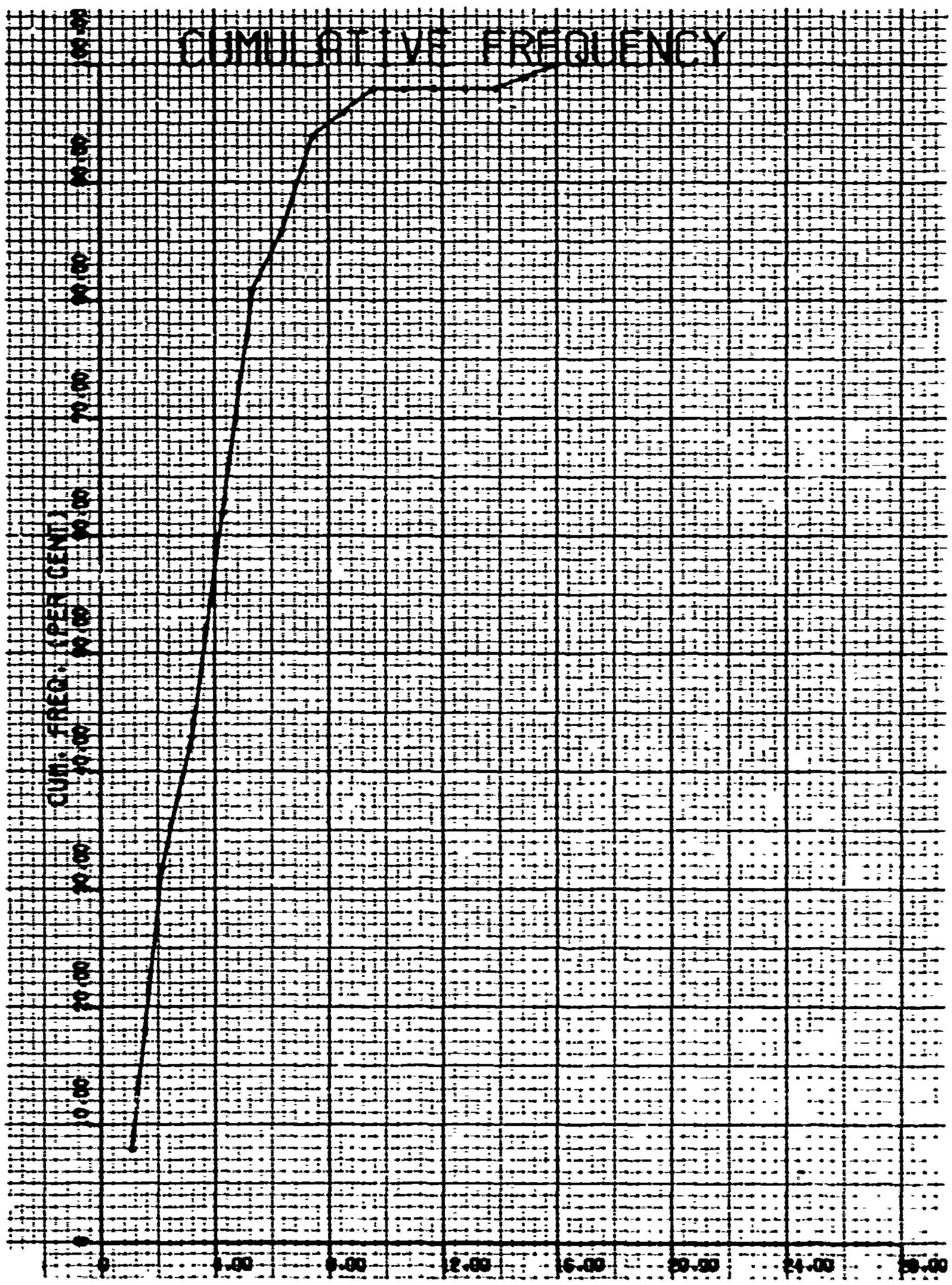

Figure 49 - Cumulative Frequency Polygon for Dynamic Unbalance of Empty 3000 Series Shell

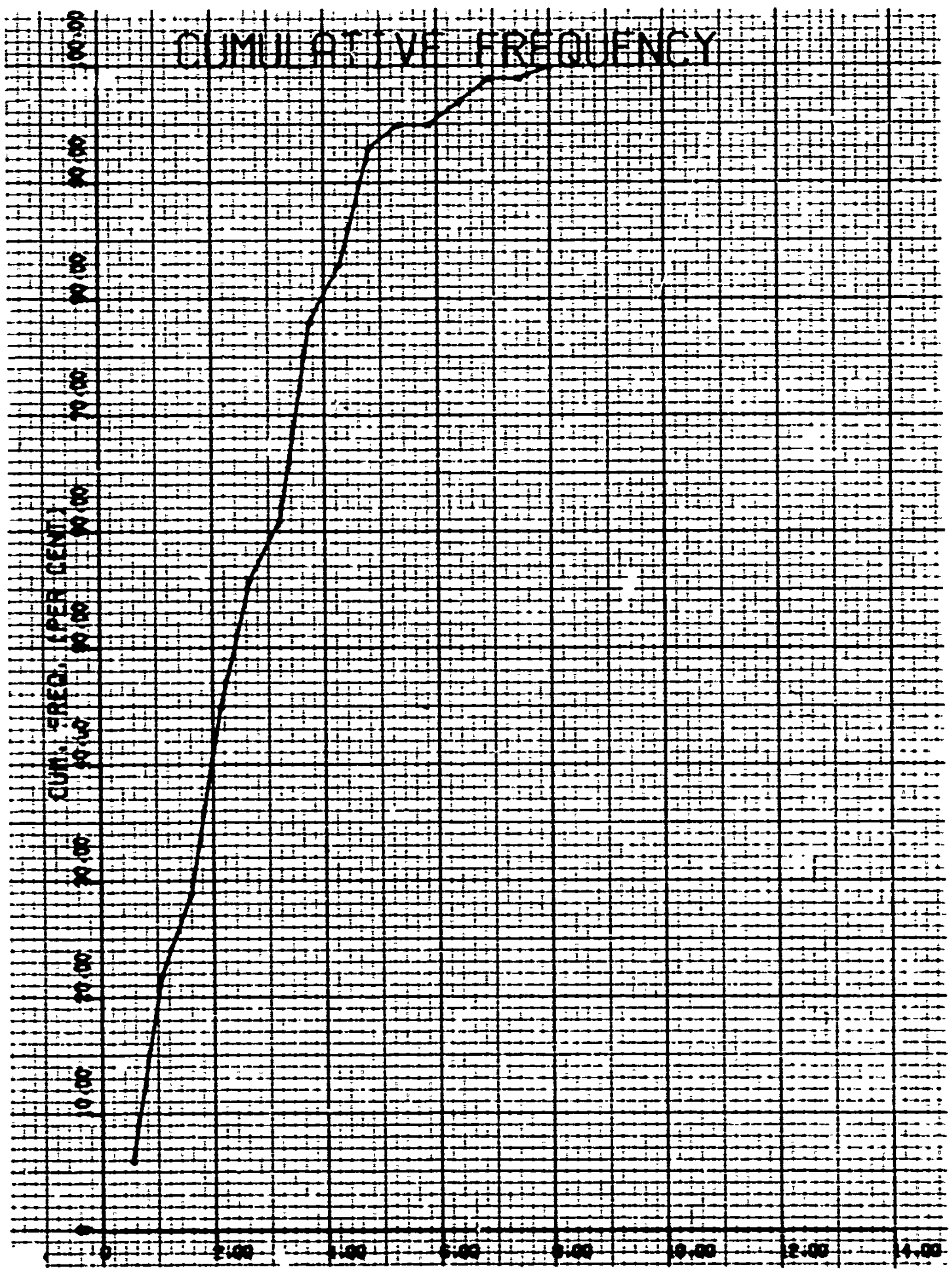

Figure 50 - Cumulative Frequency Polygon for Dynamic Unbalance of Full 3000 Series Shell

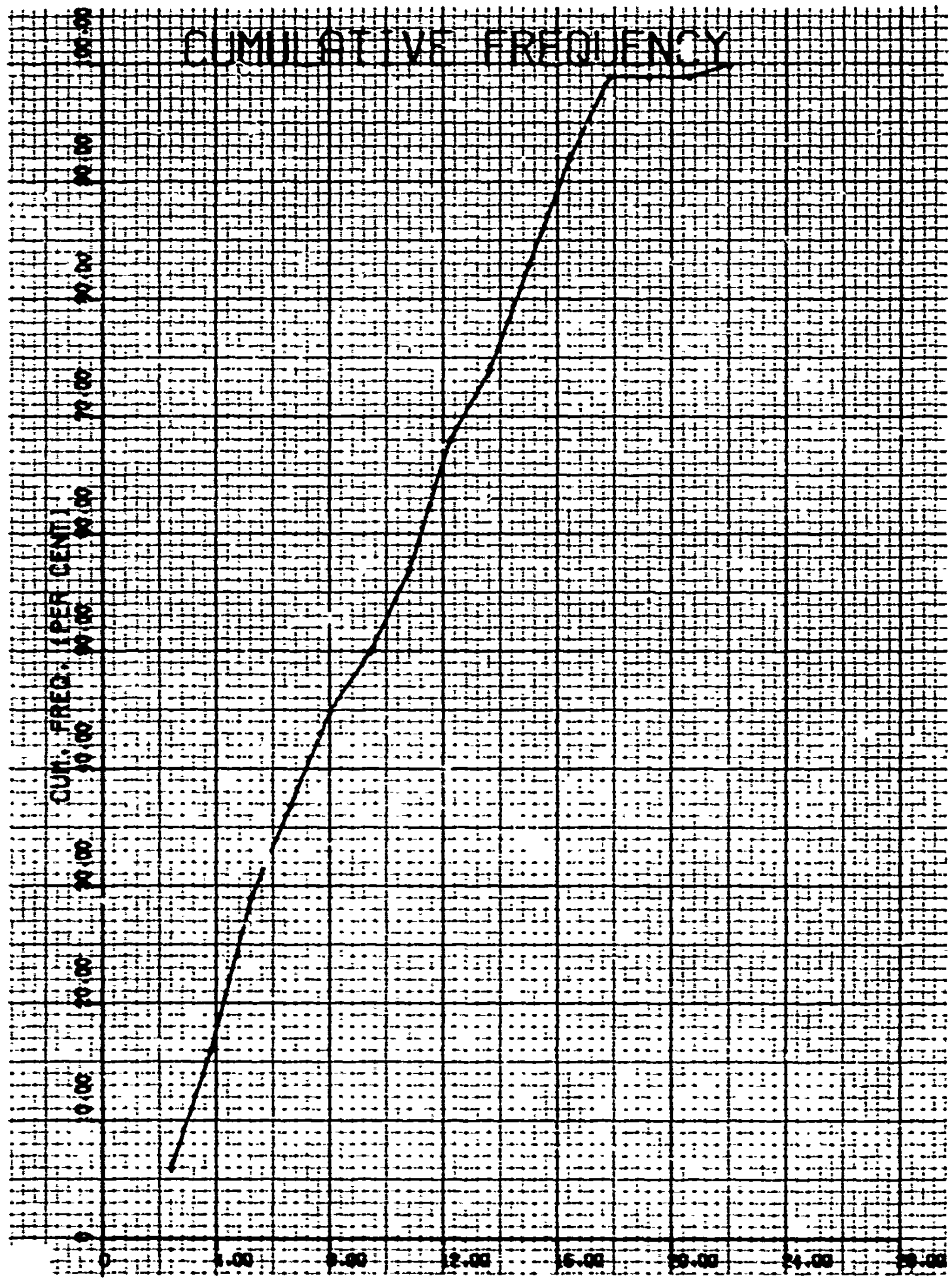

Figure 51 - Cumulative Frequency Polygon for Static Unbalance of Empty 3000 Series Shell

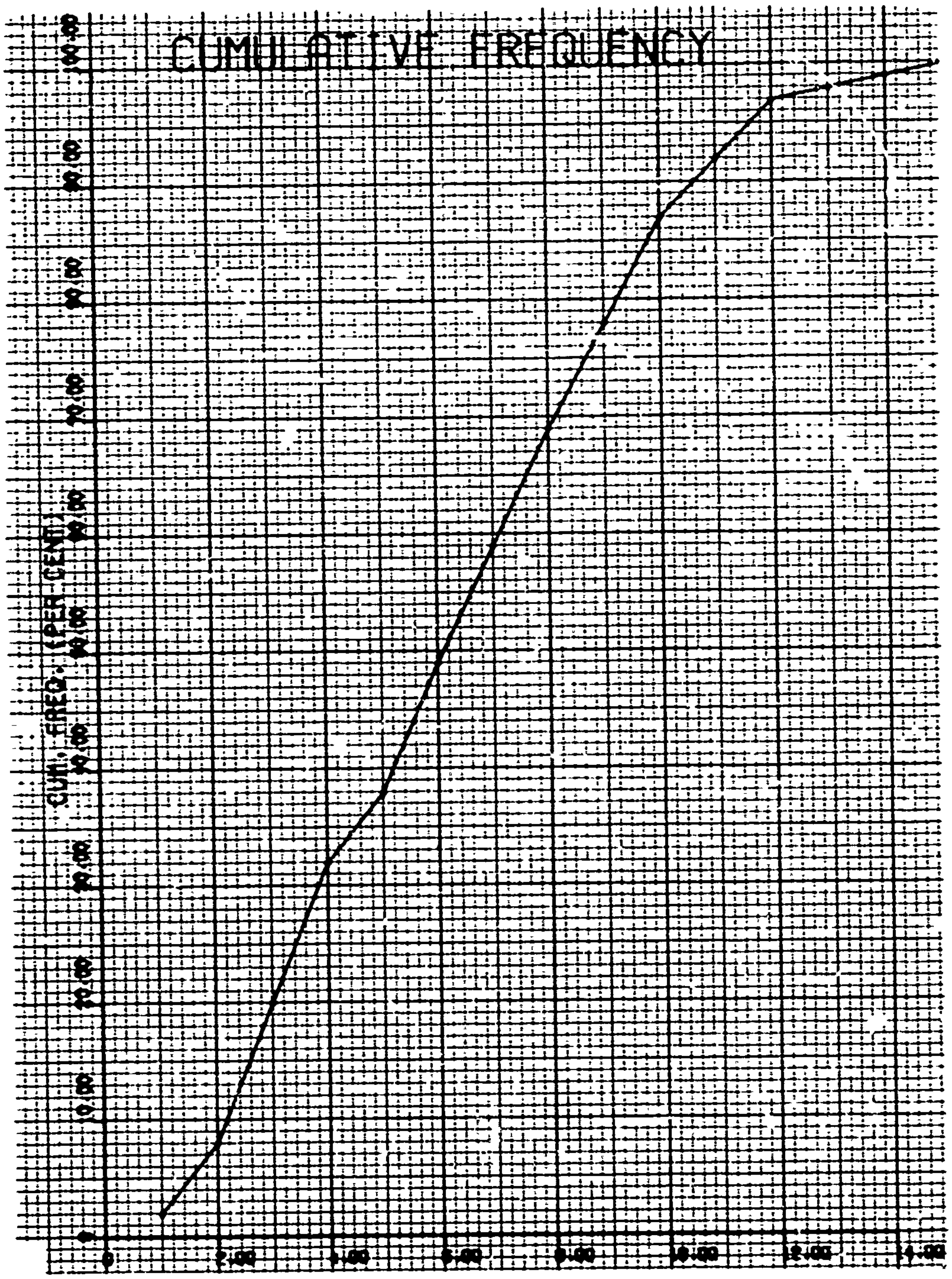

Figure 52 - Cumulative Frequency Polygon for Static Unbalance of Full 3000 Series Shell

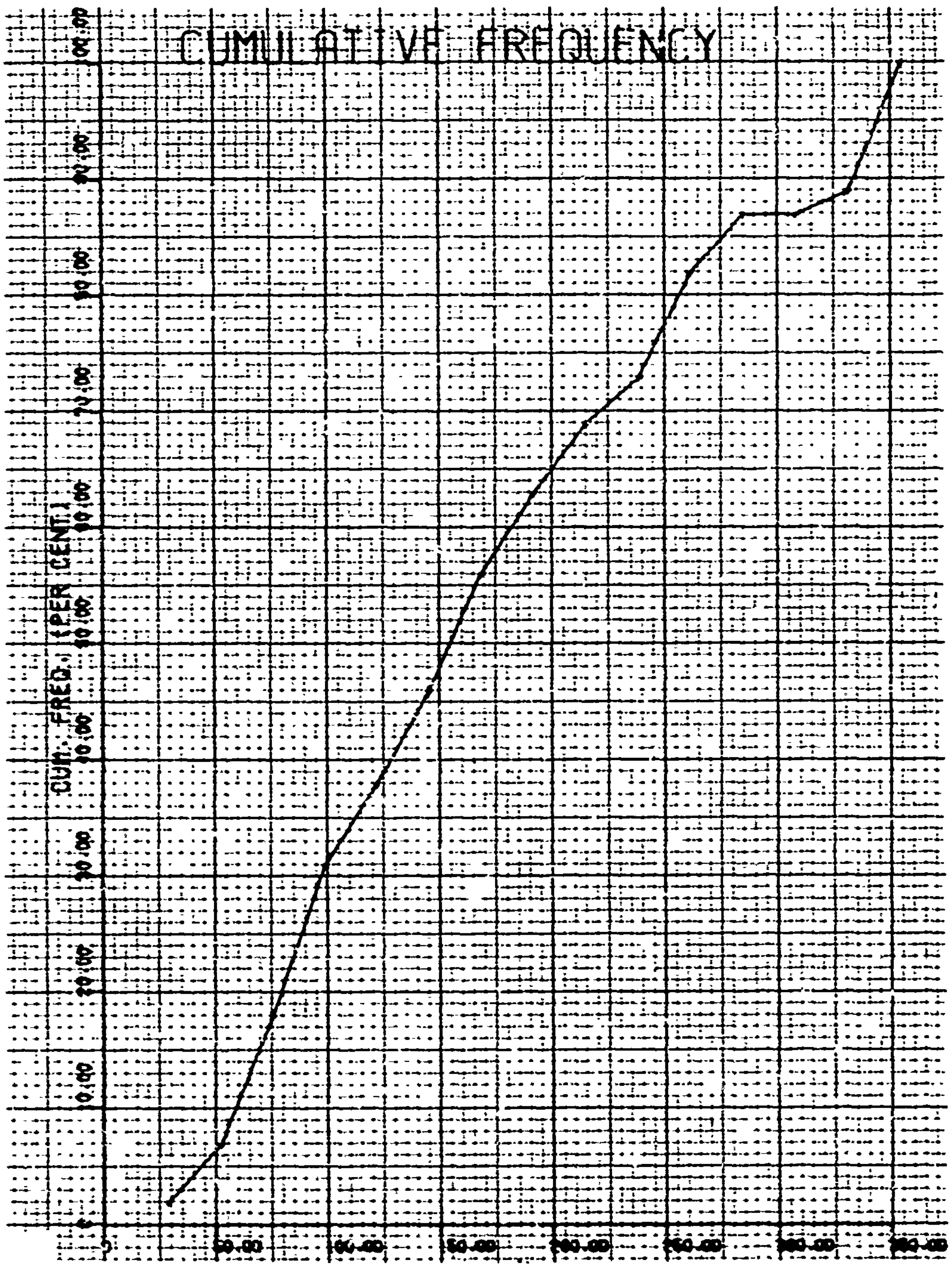

Figure 53 - Cumulative Frequency Polygon for Azimuth of Dynamic Unbalance of Empty 3000 Series Shell

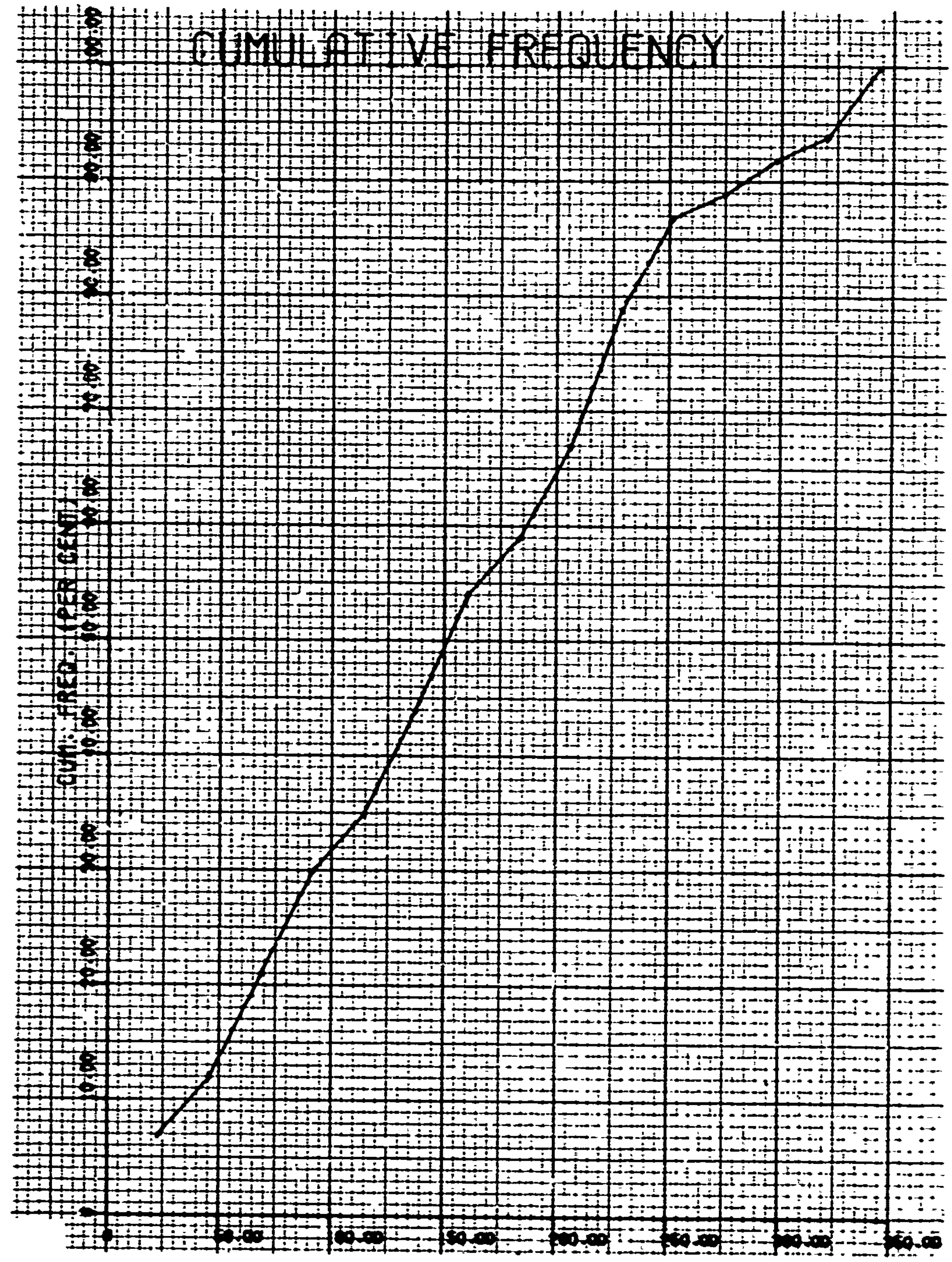

Figure 54 - Cumulative Frequency Polygon for Azimuth of Dynamic Unbalance of Full 3000 Series Shell

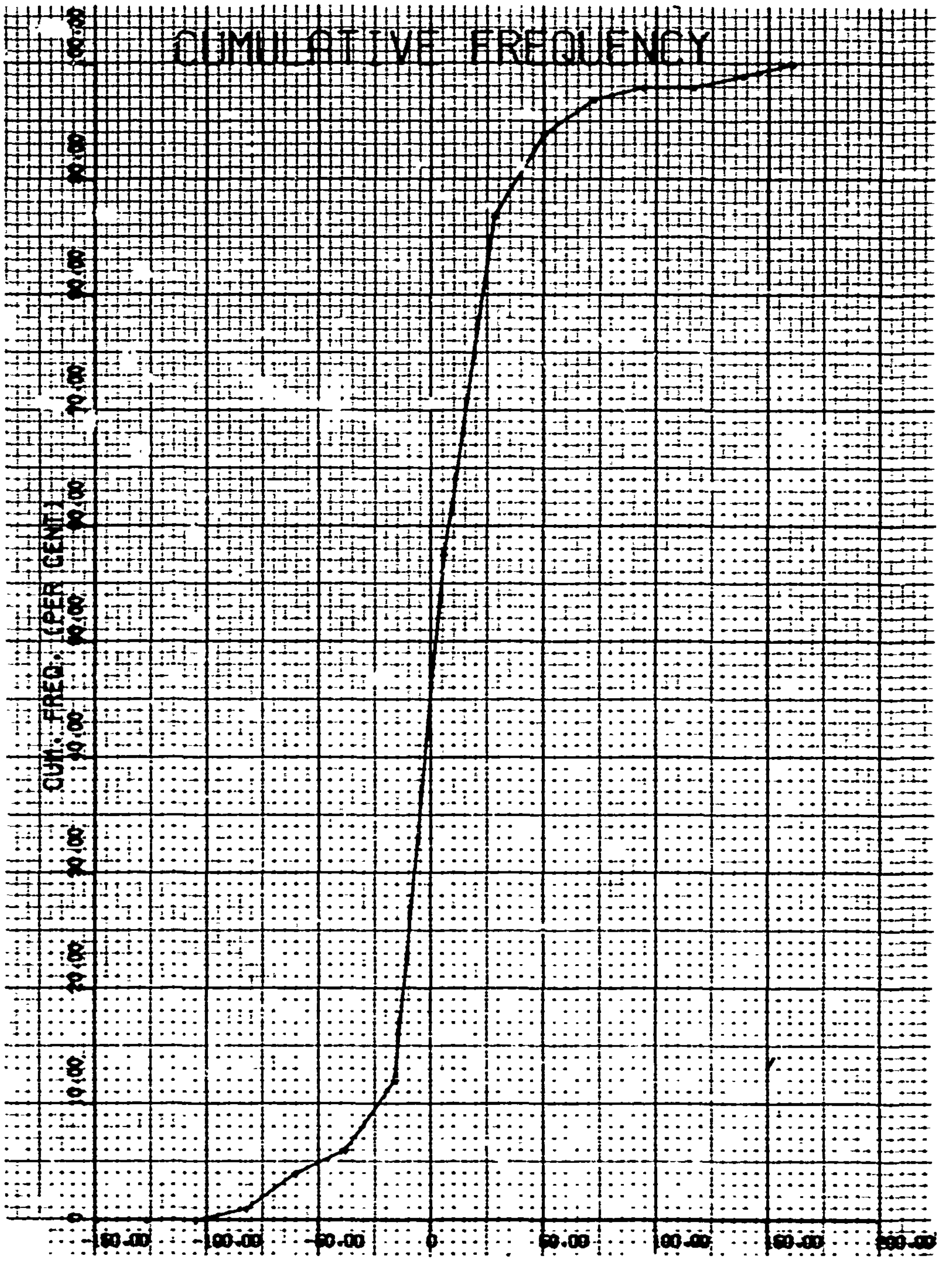

Figure 55 - Cumulative Frequency Polygon for Azimuth of Static Unbalance of Empty 3000 Series Shell

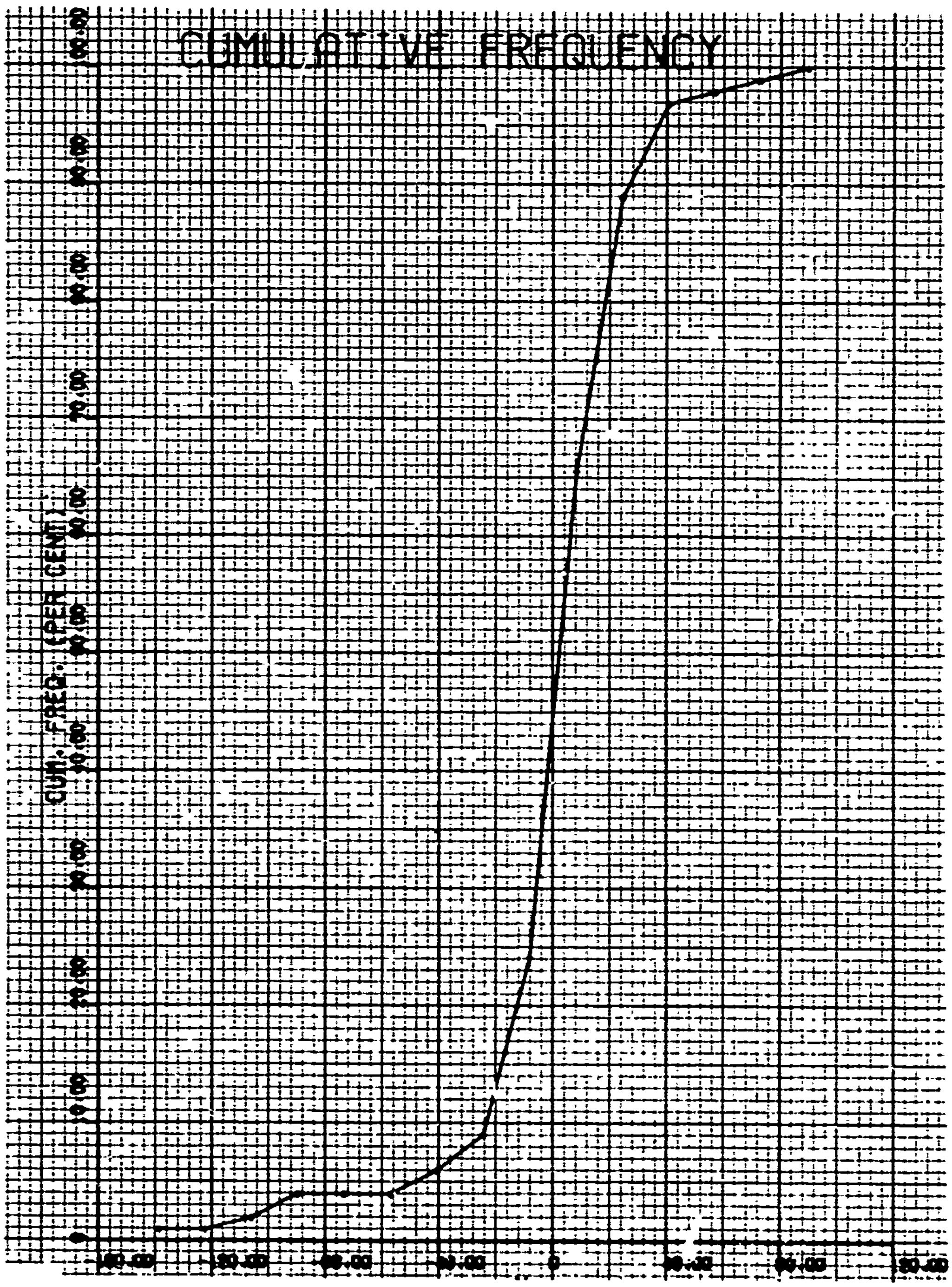

Figure 56 - Cumulative Frequency Polygon for Azimuth of Static Unbalance of Full 3000 Series Shell

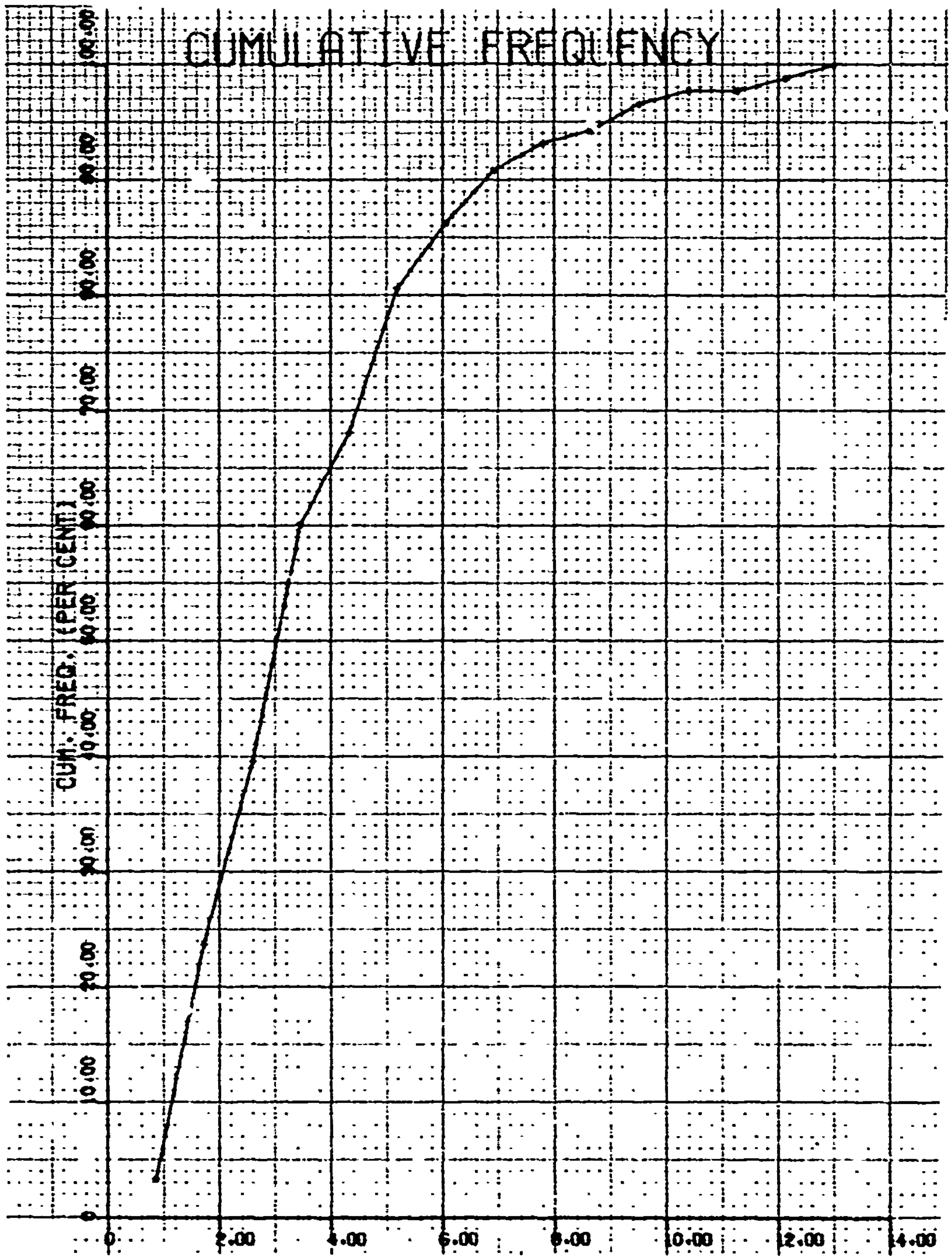

Figure 57 - Cumulative Frequency Polygon for Dynamic Unbalance of Empty 5000 Series Shell

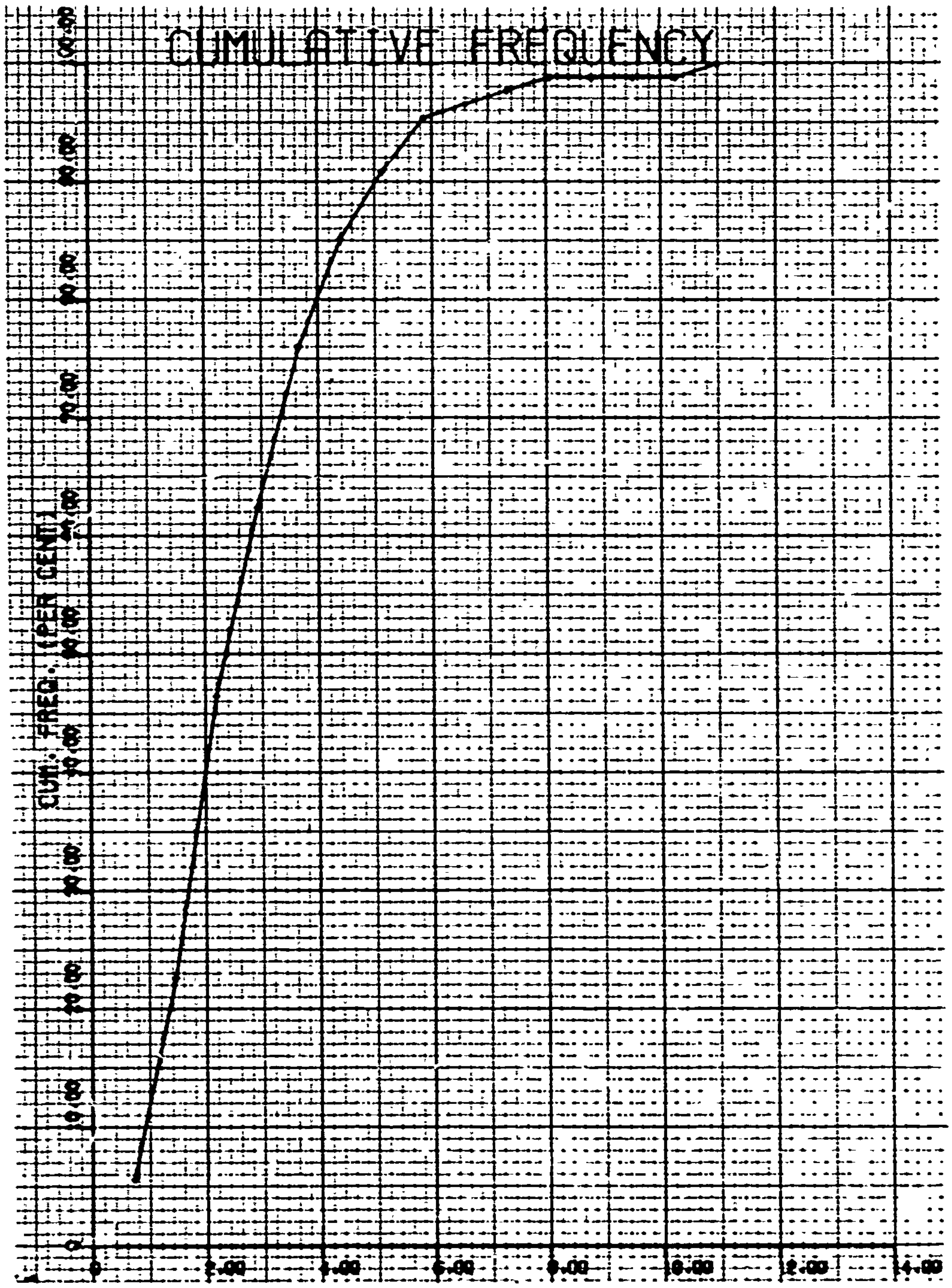

Figure 58 - Cumulative Frequency Polygon for Dynamic Unbalance of Full 5000 Series Shell

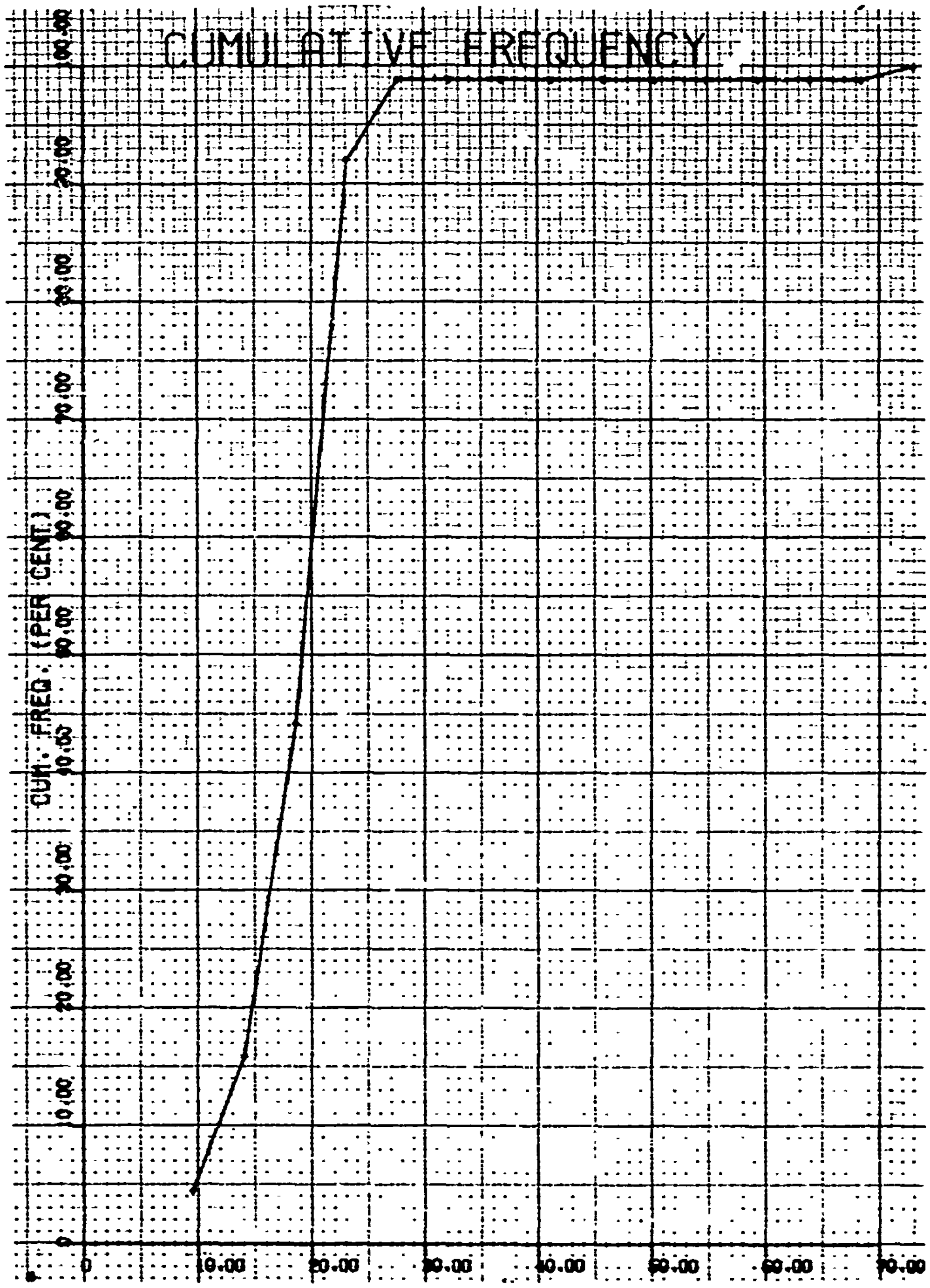

Figure 59 - Cumulative Frequency Polygon for Static Unbalance of Empty 5000 Series Shell

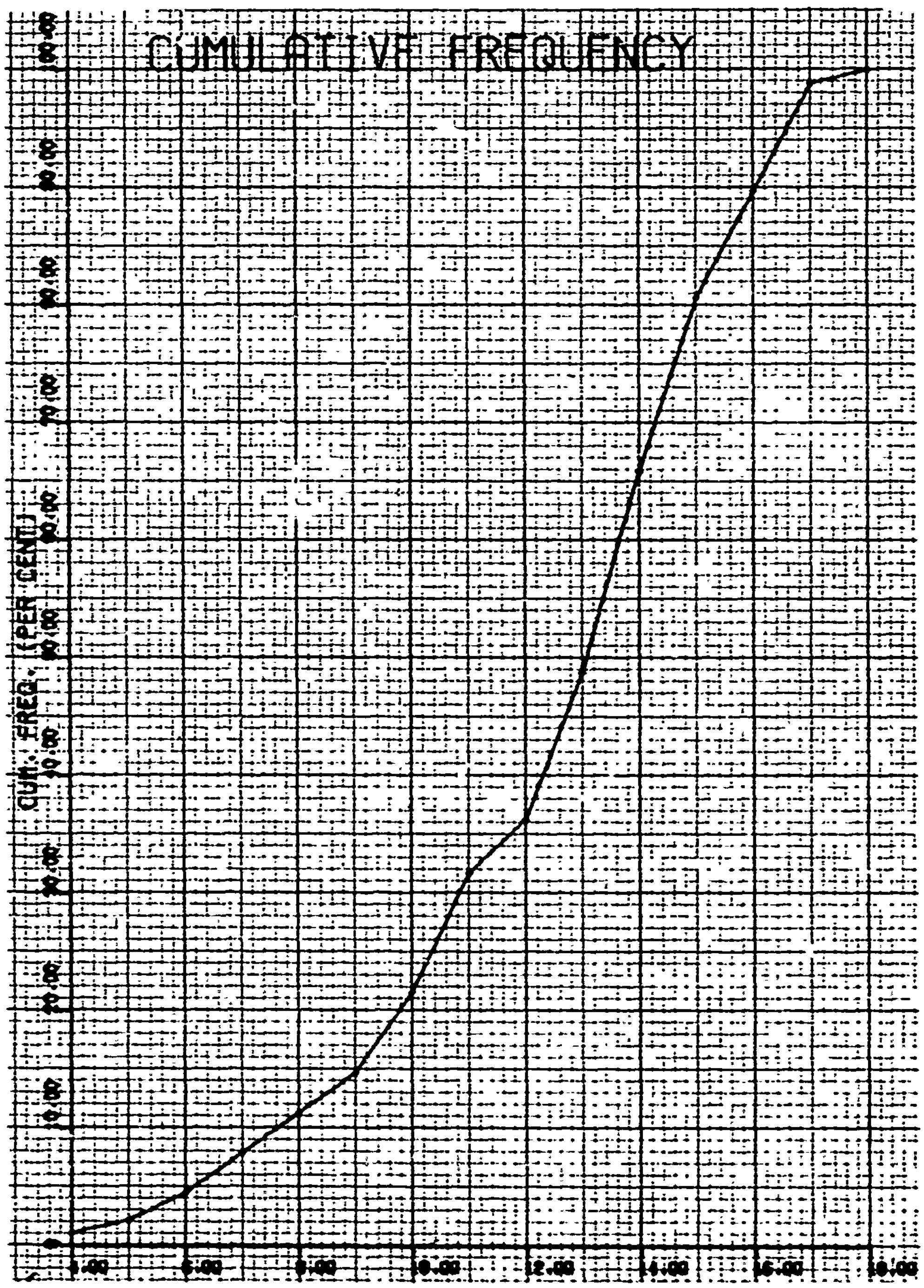

Figure 60 - Cumulative Frequency Polygon for Static Unbalance of Full 5000 Series Shell

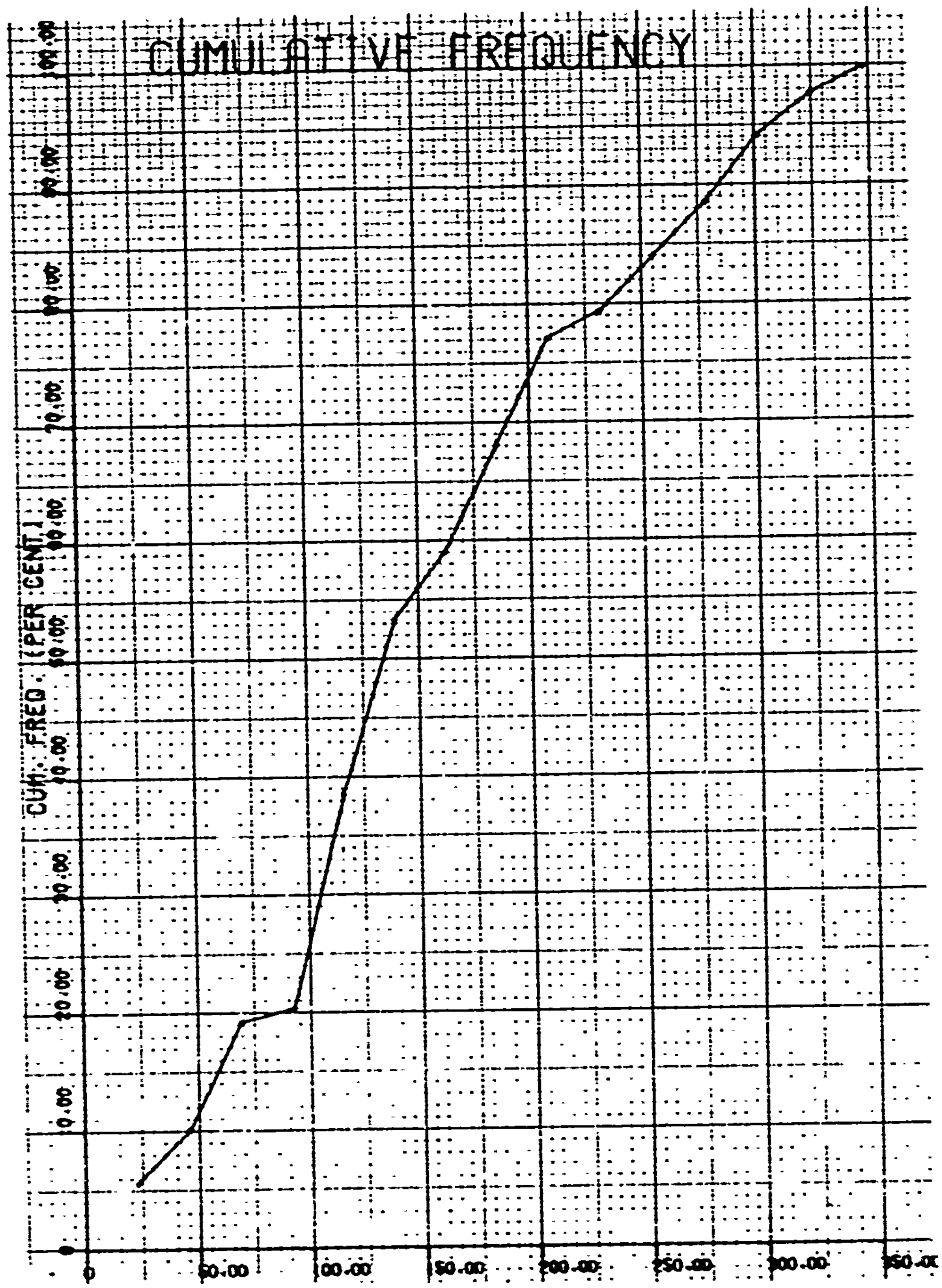

Figure 61 - Cumulative Frequency Polygon for Azimuth of Dynamic Unbalance of Empty 5000 Series Shell

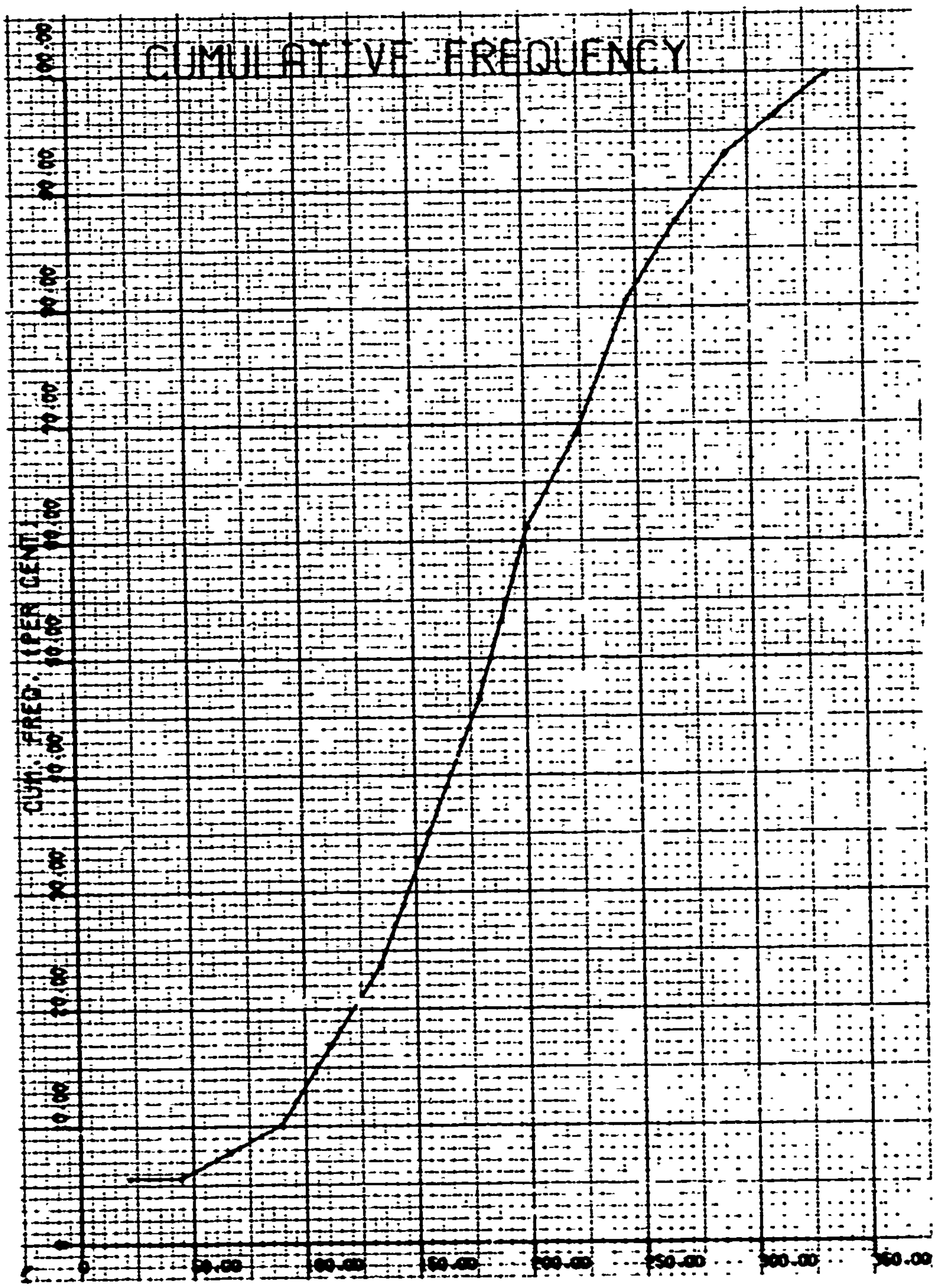

Figure 62 - Cumulative Frequency Polygon for Azimuth of Dynamic Unbalance of Full 5000 Series Shell

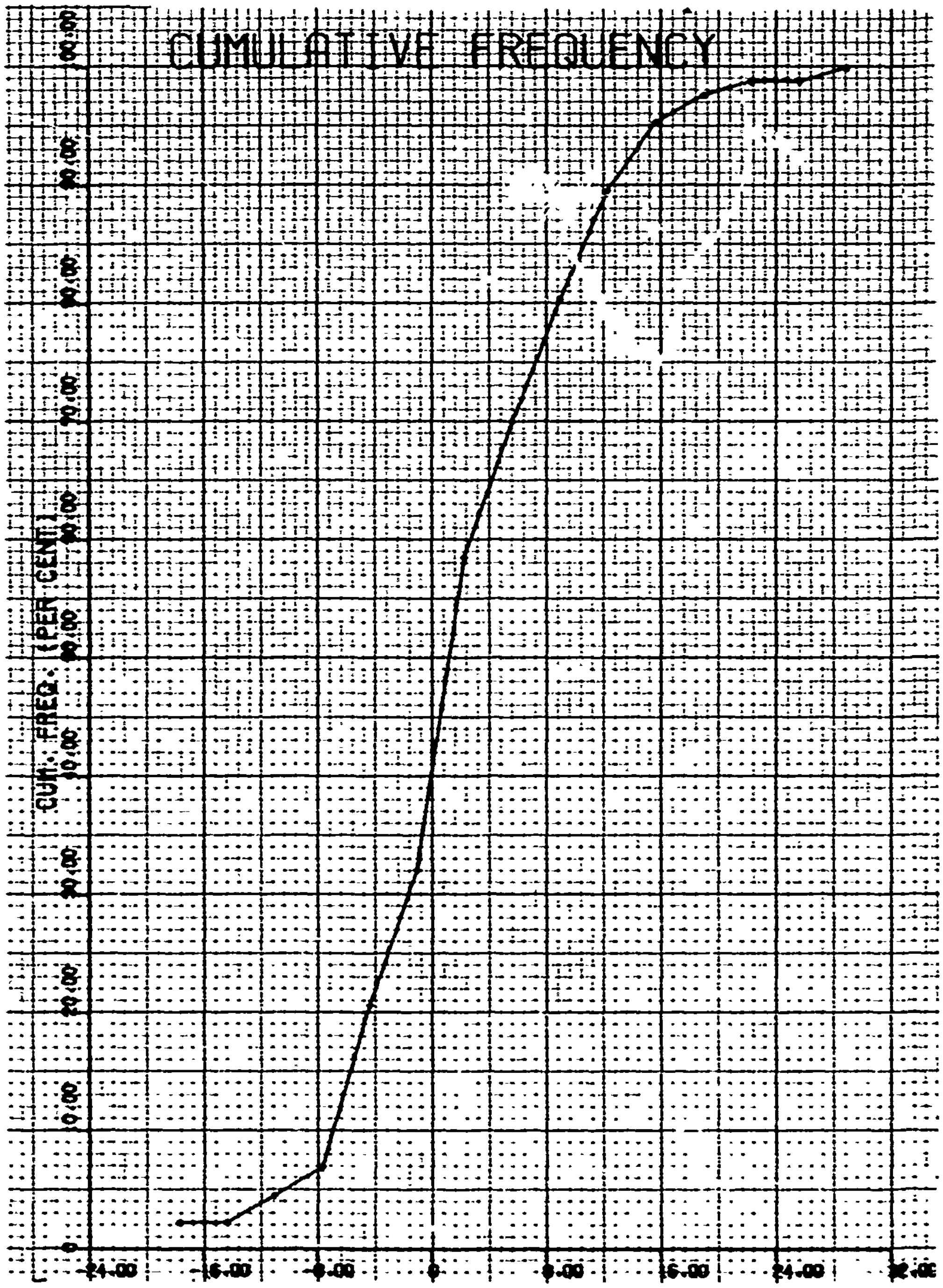

Figure 63 - Cumulative Frequency Polygon for Azimuth of Static Unbalance of Empty 5000 Series Shell

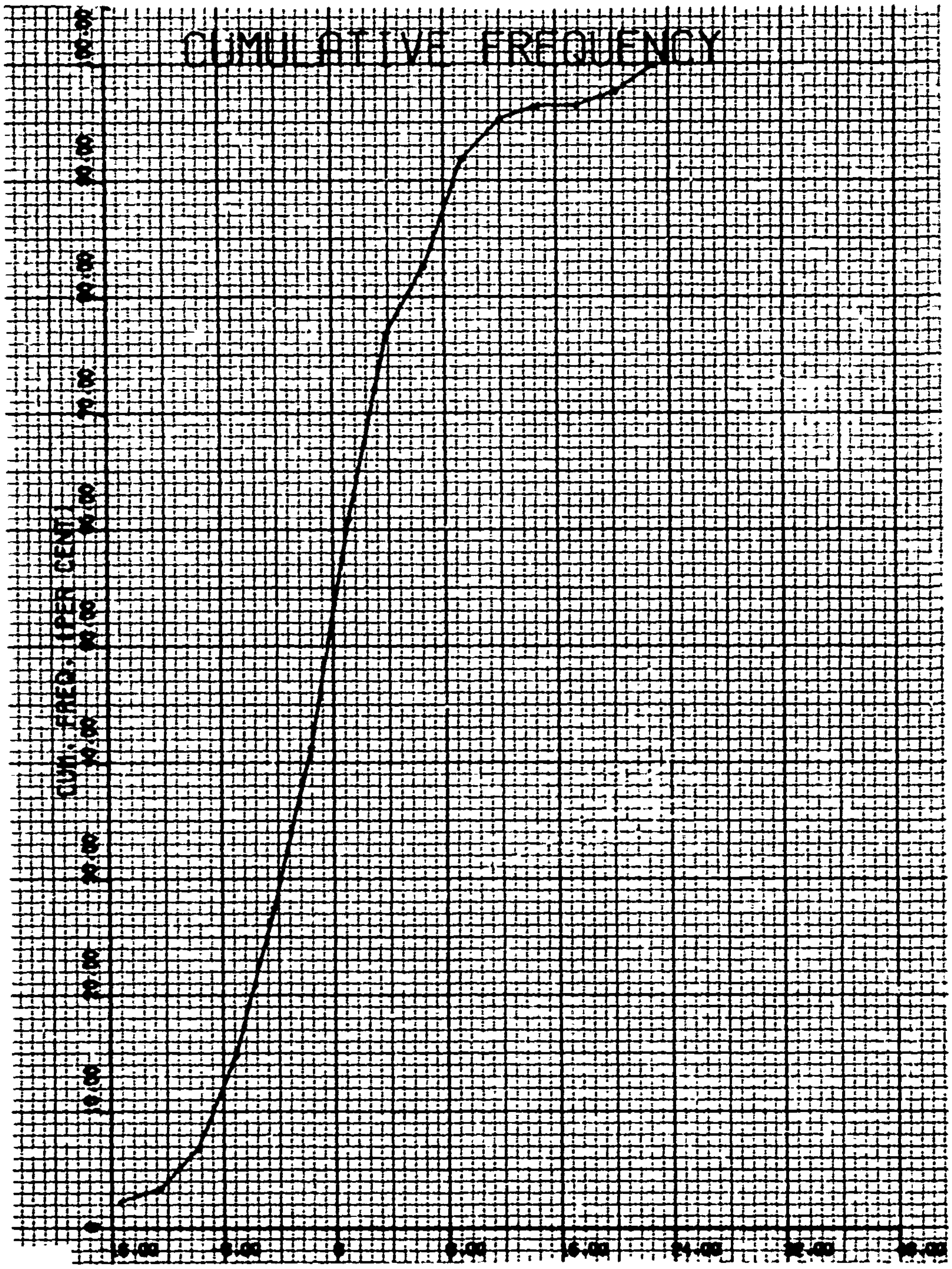

Figure 64 - Cumulative Frequency Polygon for Azimuth of Static Unbalance of Full 5000 Series Shell

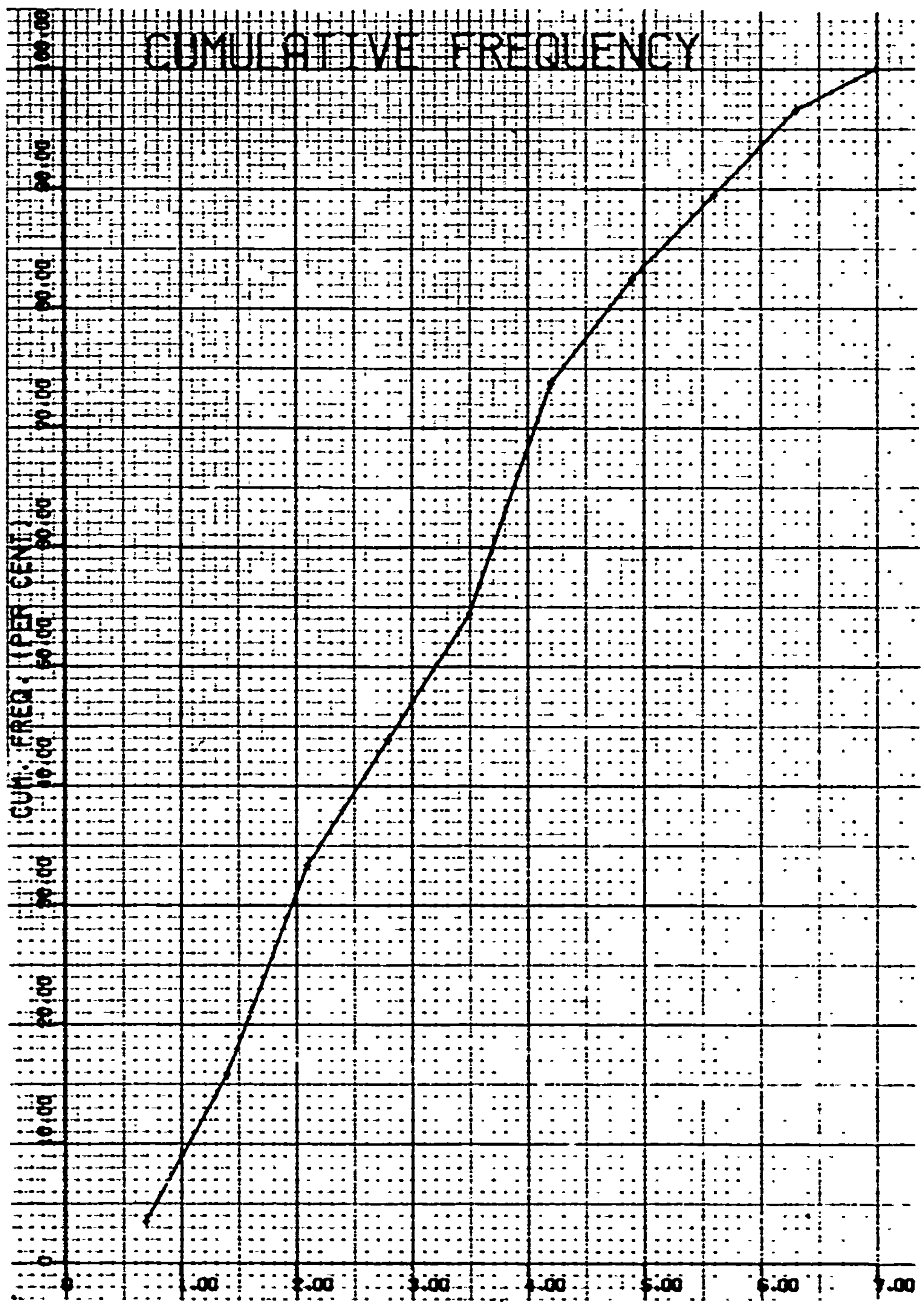

Figure 65 - Cumulative Frequency Polygon for Dynamic Unbalance of Empty 6000 Series Shell

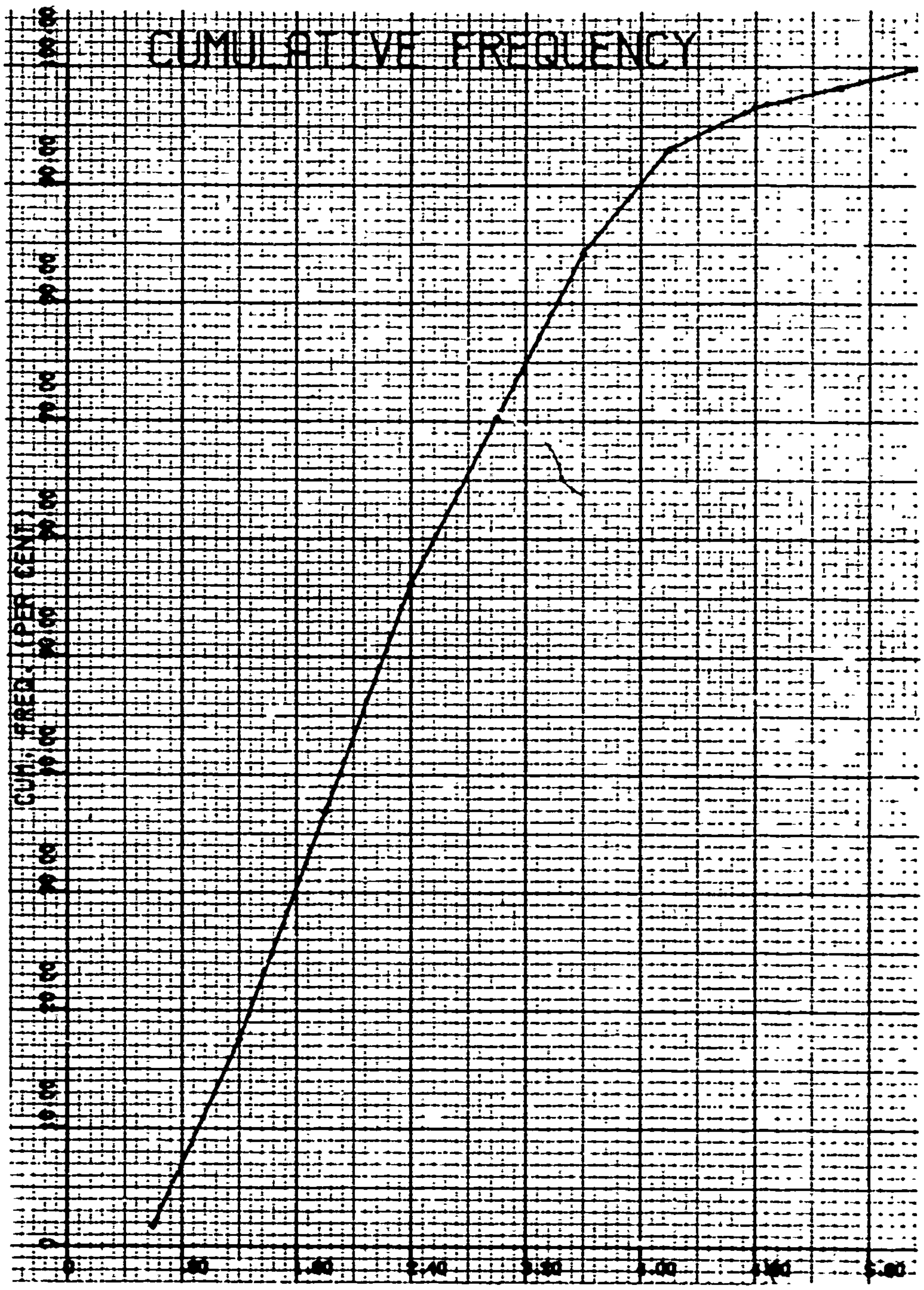

Figure 66 - Cumulative Frequency Polygon for Dynamic Unbalance of Full 6000 Series Shell

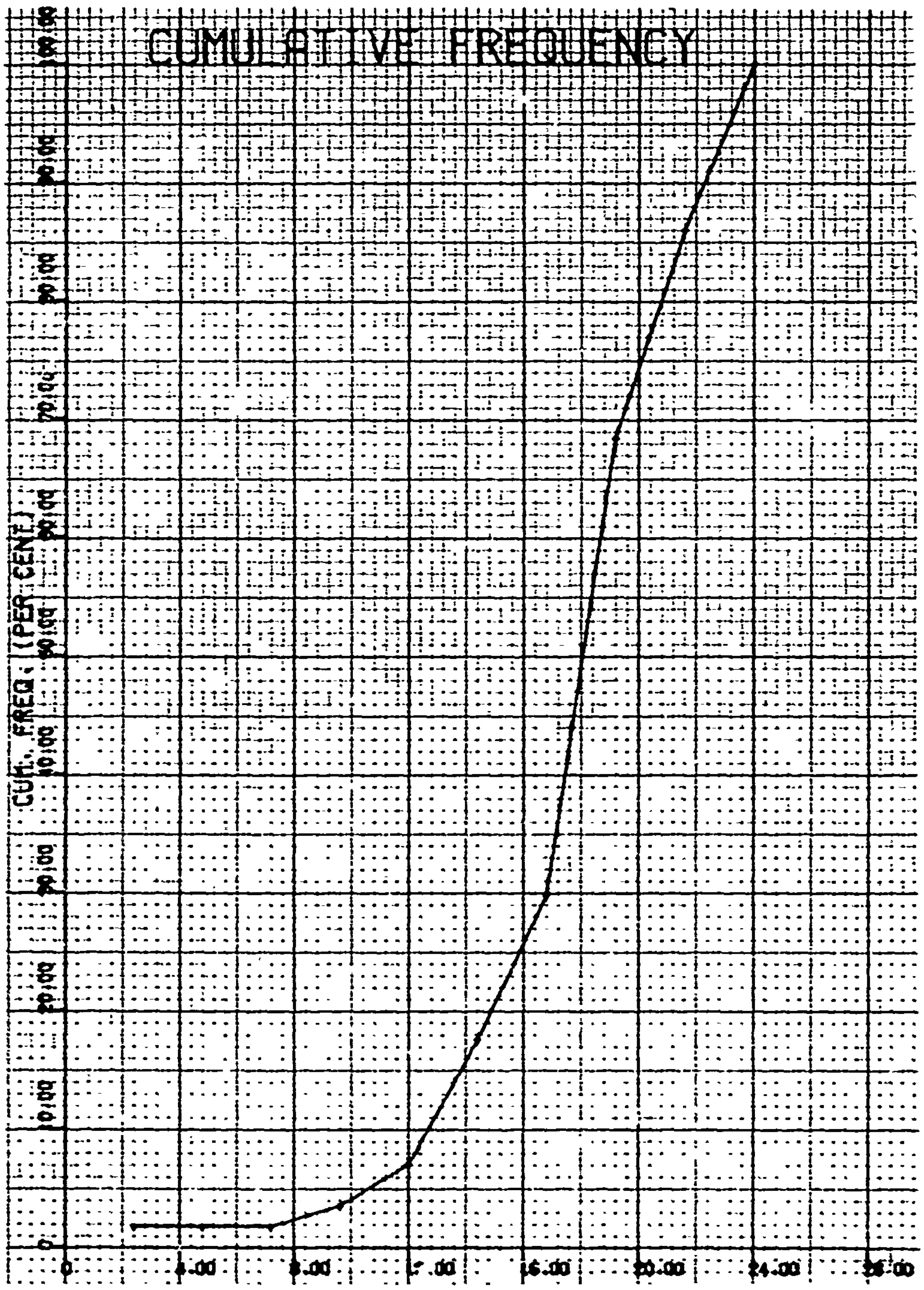

Figure 67 - Cumulative Frequency Polygon for Static Unbalance of Empty 6000 Series Shell

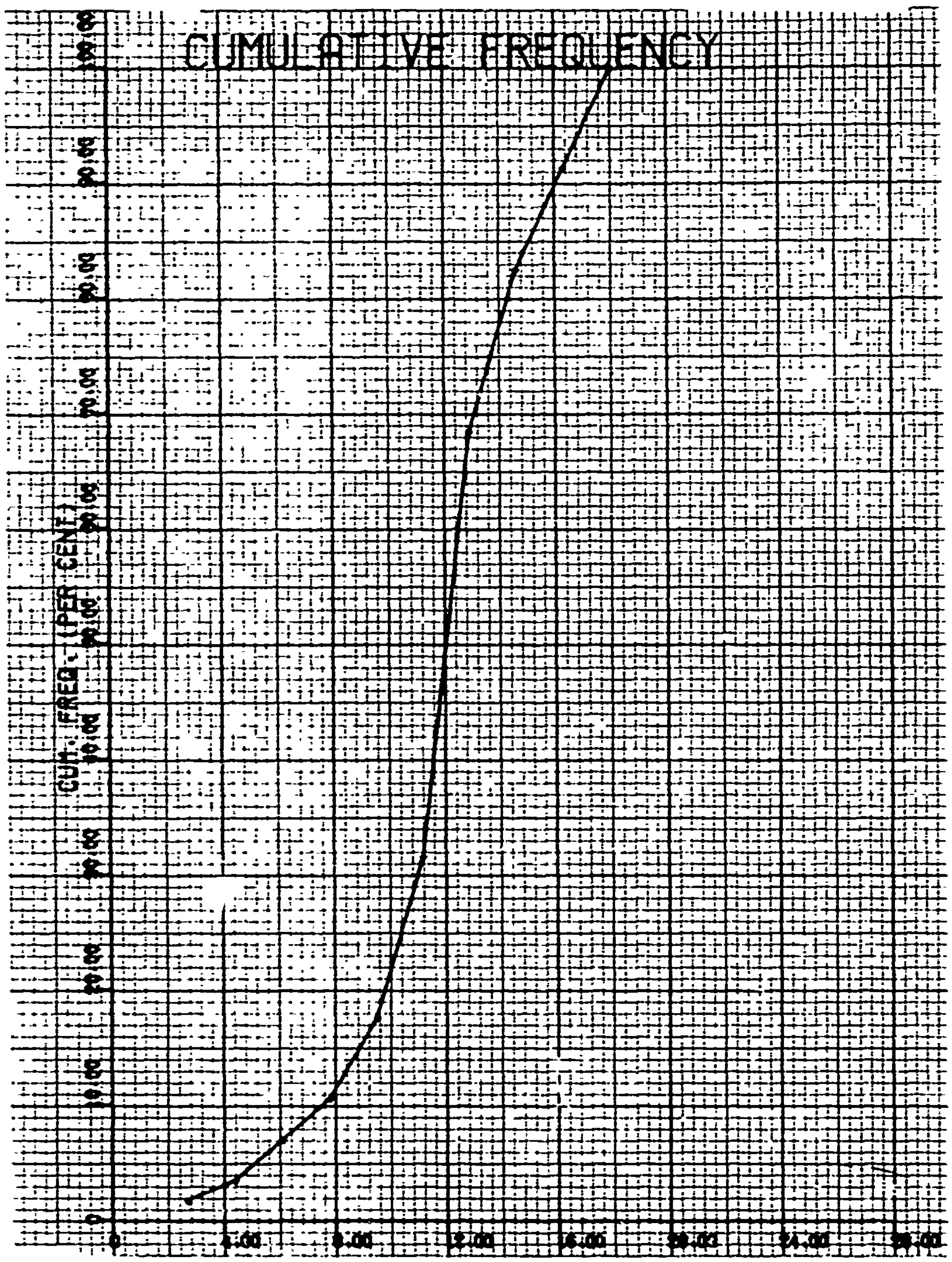

Figure 68 - Cumulative Frequency Polygon for Static Unbalance of Full 6000 Series Shell

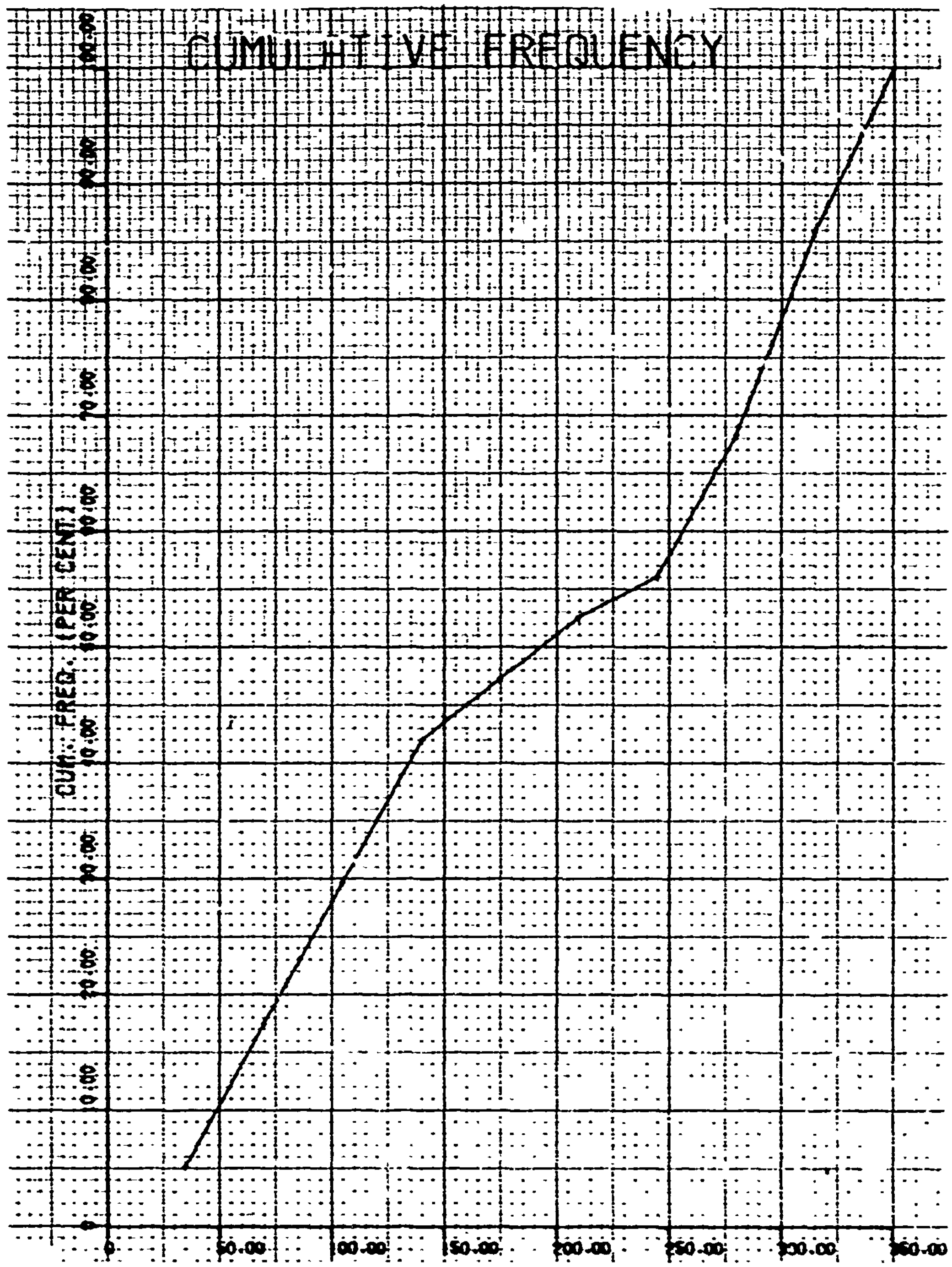

Figure 69 - Cumulative Frequency Polygon for Azimuth of Dynamic Unbalance of Empty 6000 Series Shell

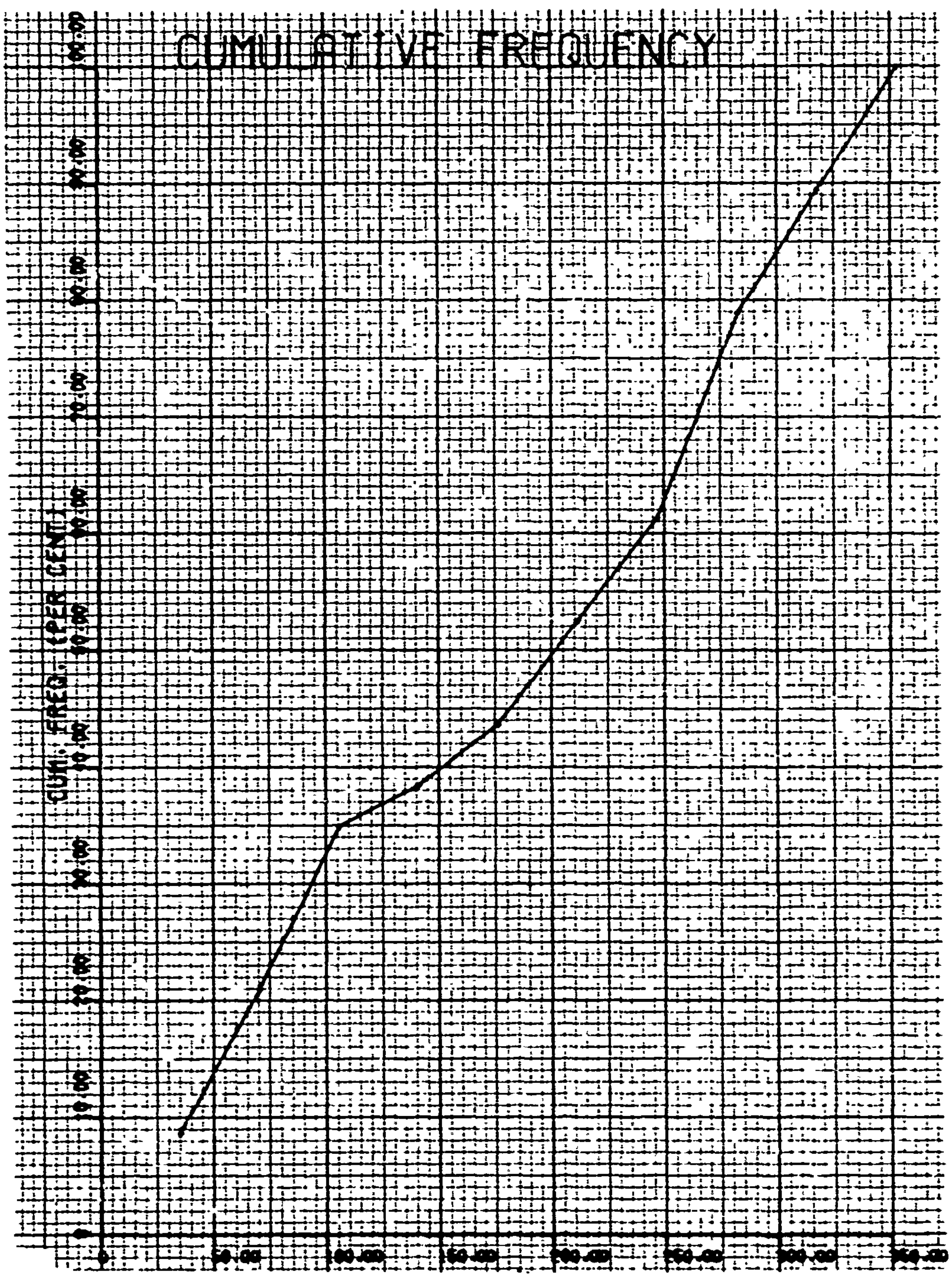

Figure 70 - Cumulative Frequency Polygon for Azimuth of Dynamic Unbalance of Empty 6000 Series Shell

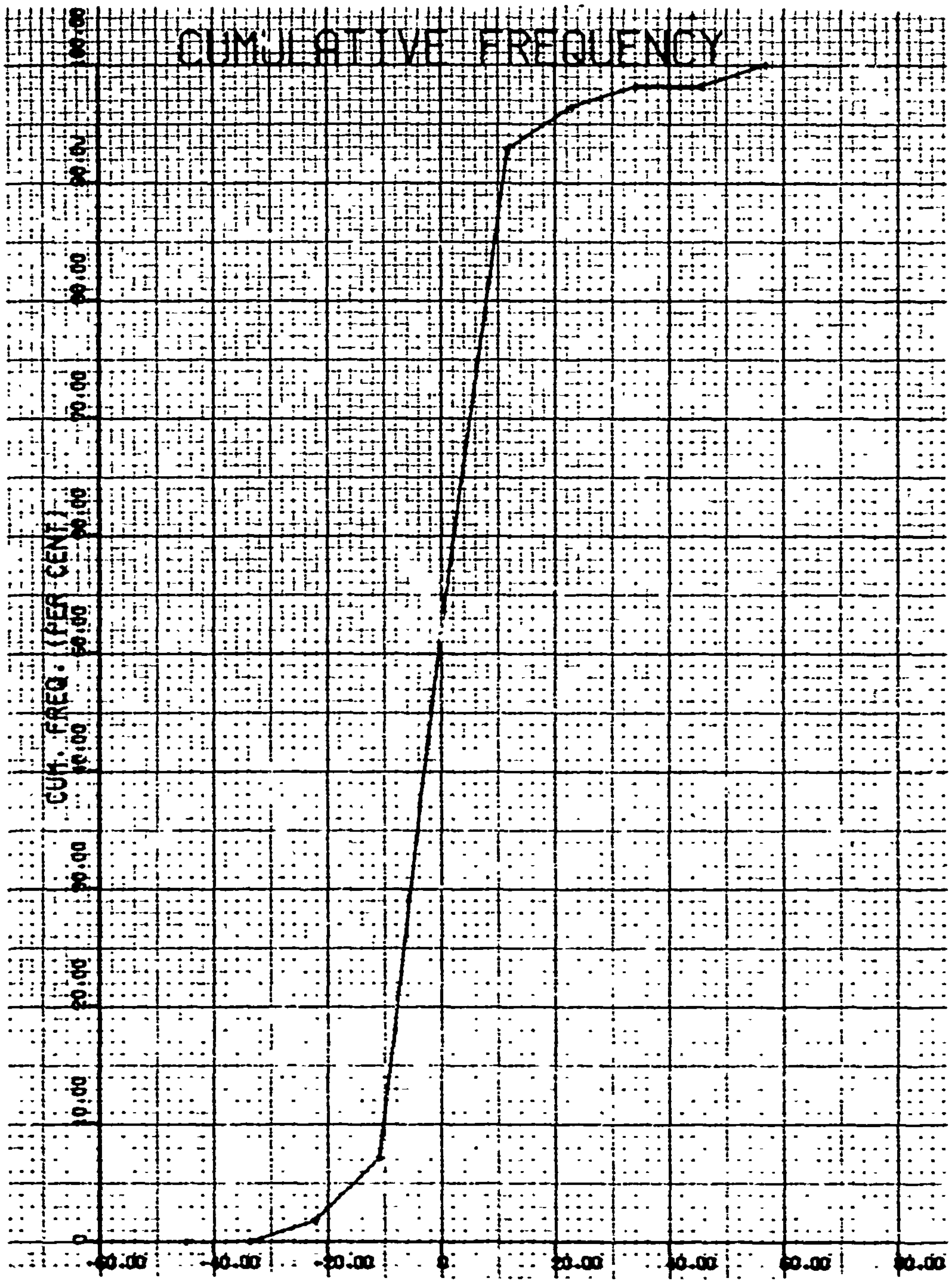

Figure 71 - Cumulative Frequency Polygon for Azimuth of Static Unbalance of Empty 6000 Series Shell

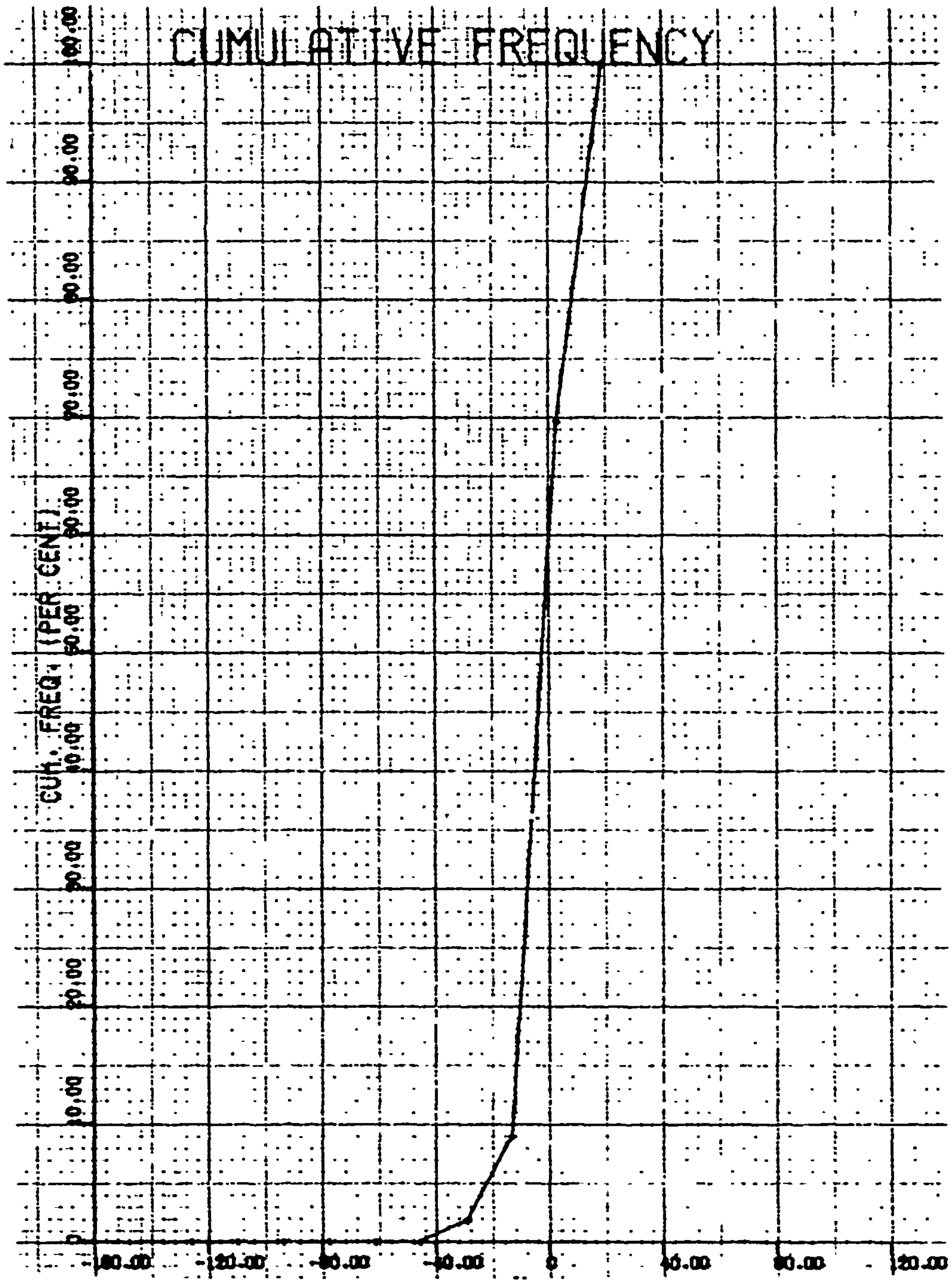

Figure 72 - Cumulative Frequency Polygon for Azimuth of Static Unbalance of Full 6000 Series Shell

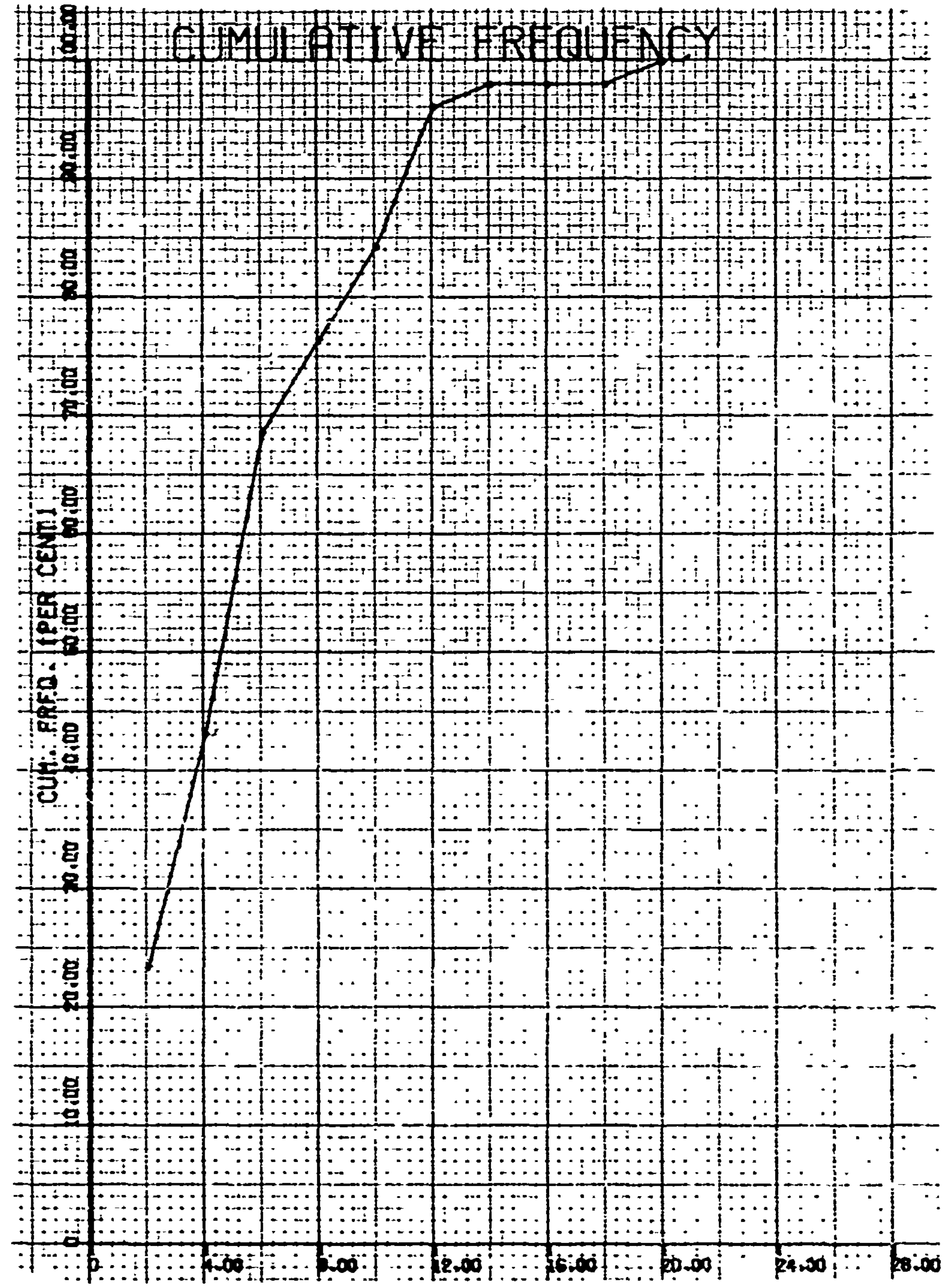

Figure 73 - Cumulative Frequency Polygon for Dynamic Unbalance of Empty 7000 Series Shell

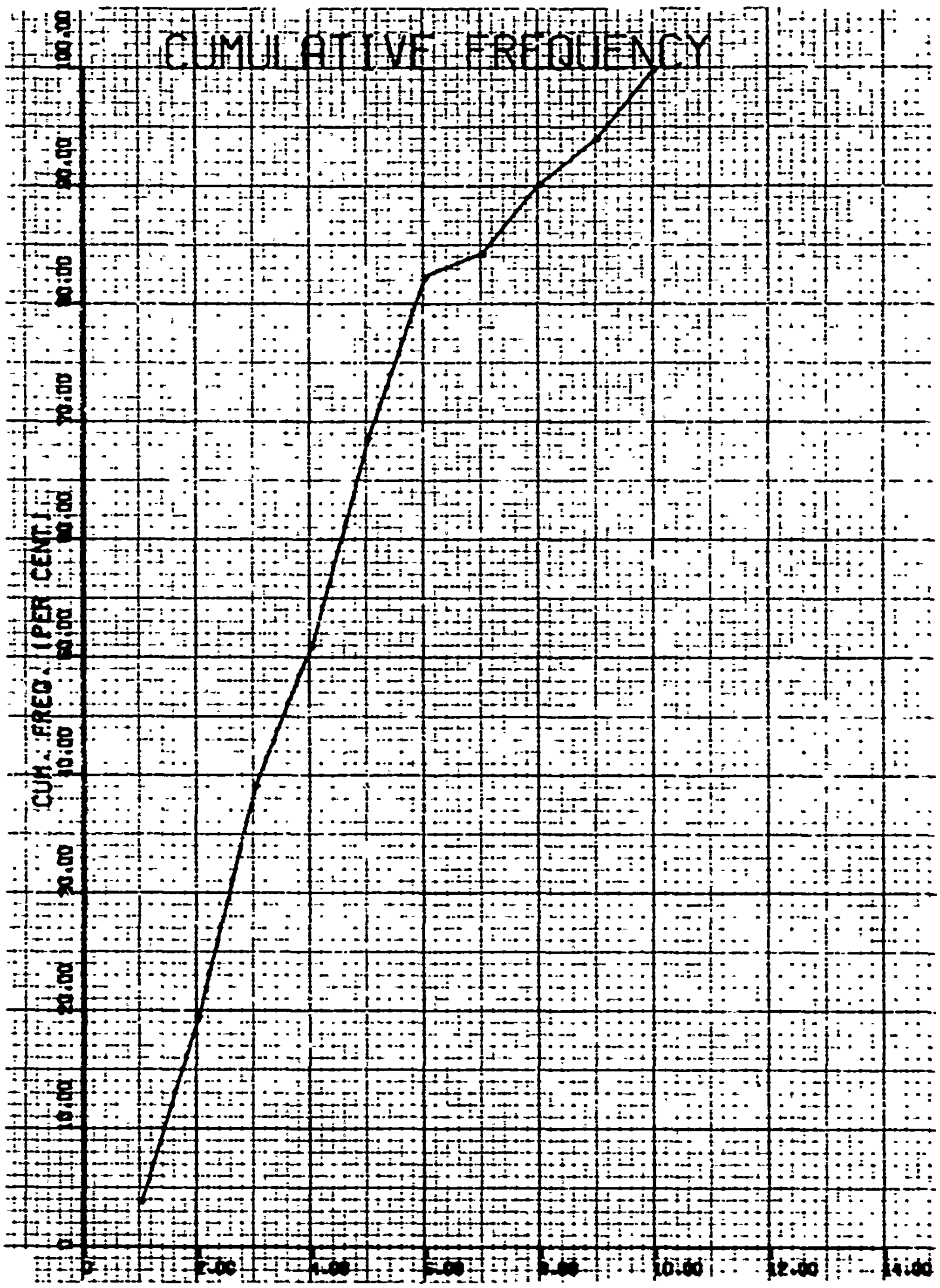

Figure 74 - Cumulative Frequency Polygon for Dynamic Unbalance of Full 7000 Series Shell

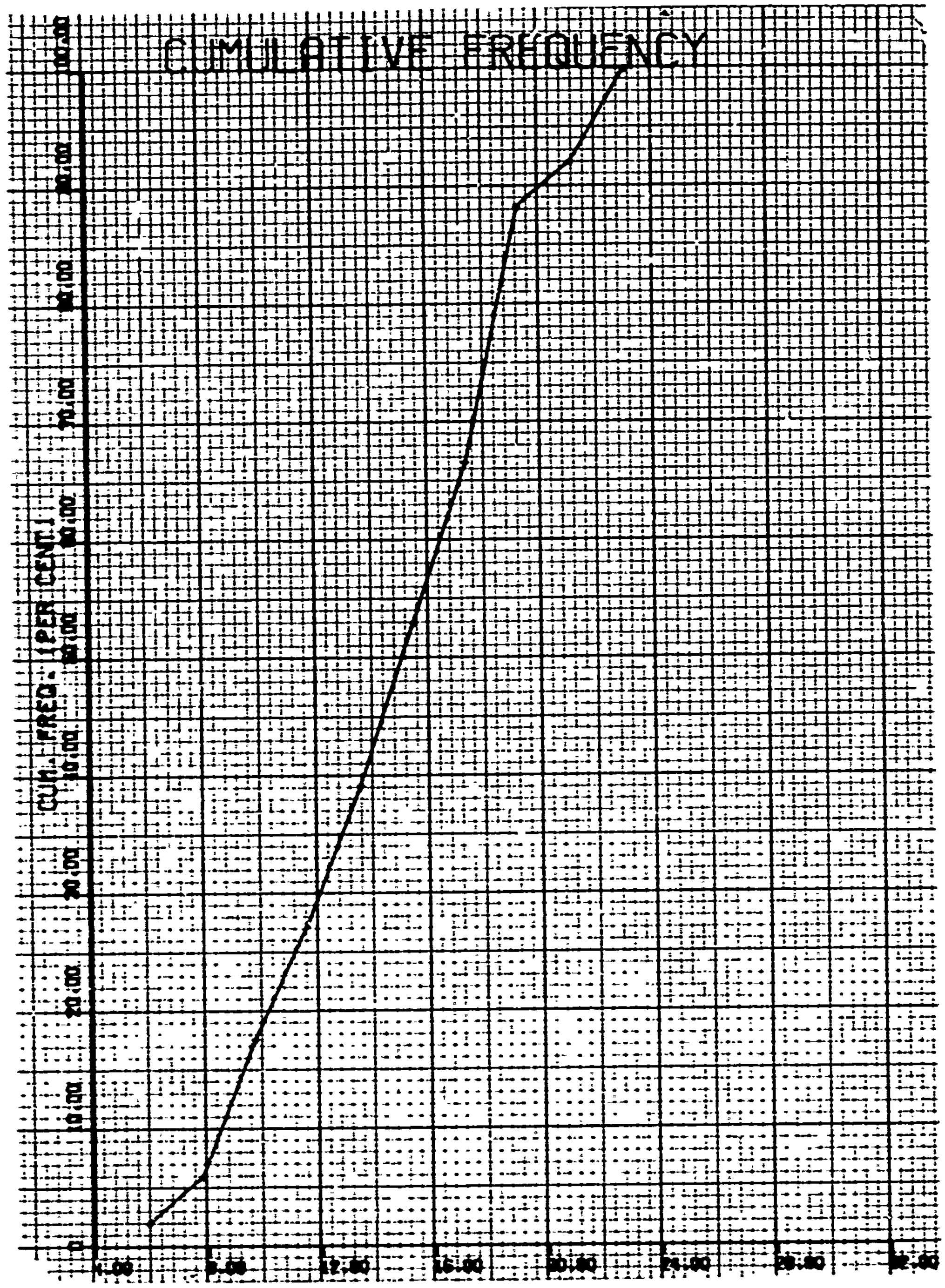

Figure 75 - Cumulative Frequency Polygon for Static Unbalance of Empty 7000 Series Shell

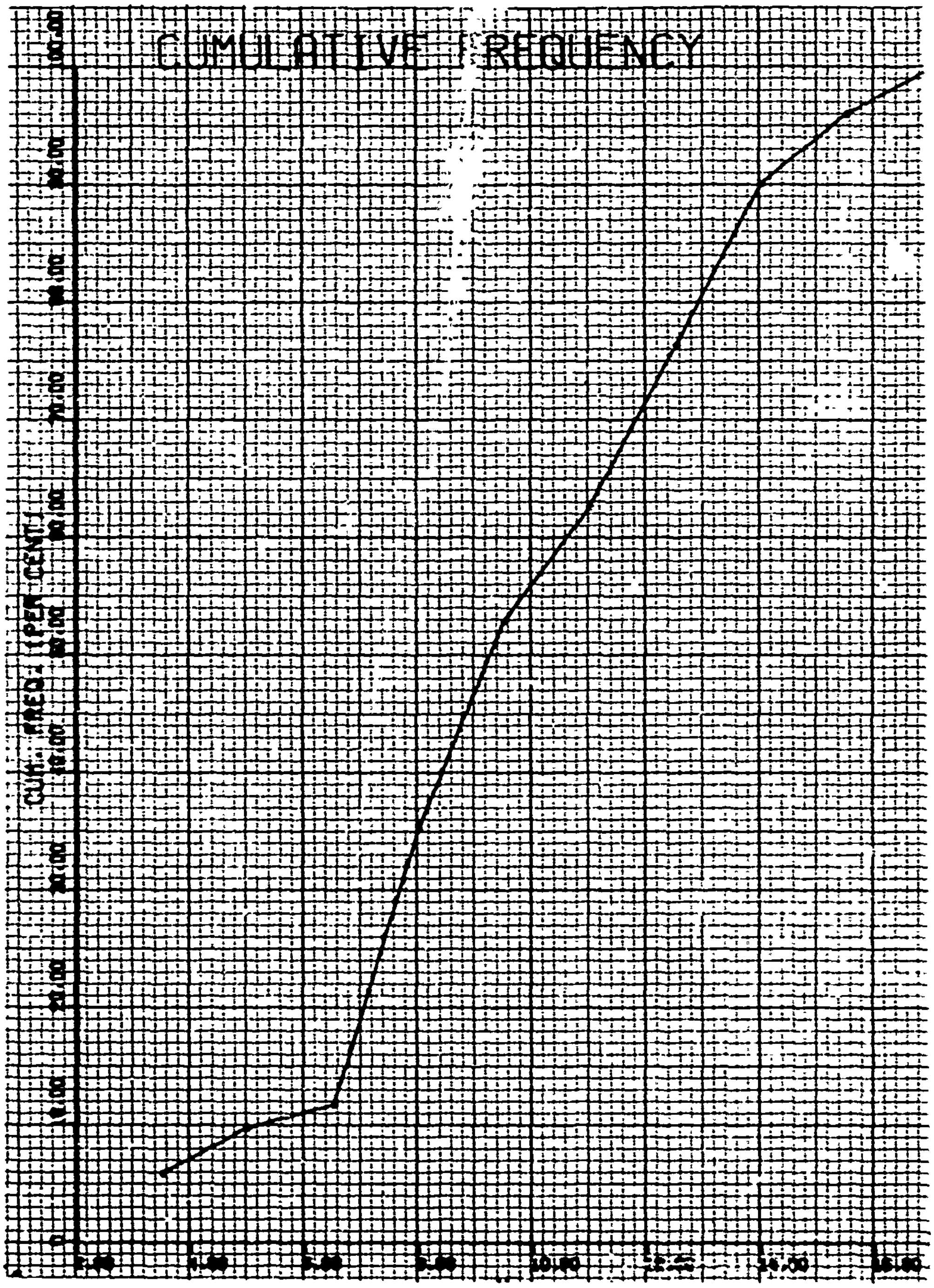

Figure 76 - Cumulative Frequency Polygon for Static Unbalance of Full 7000 Series Shell

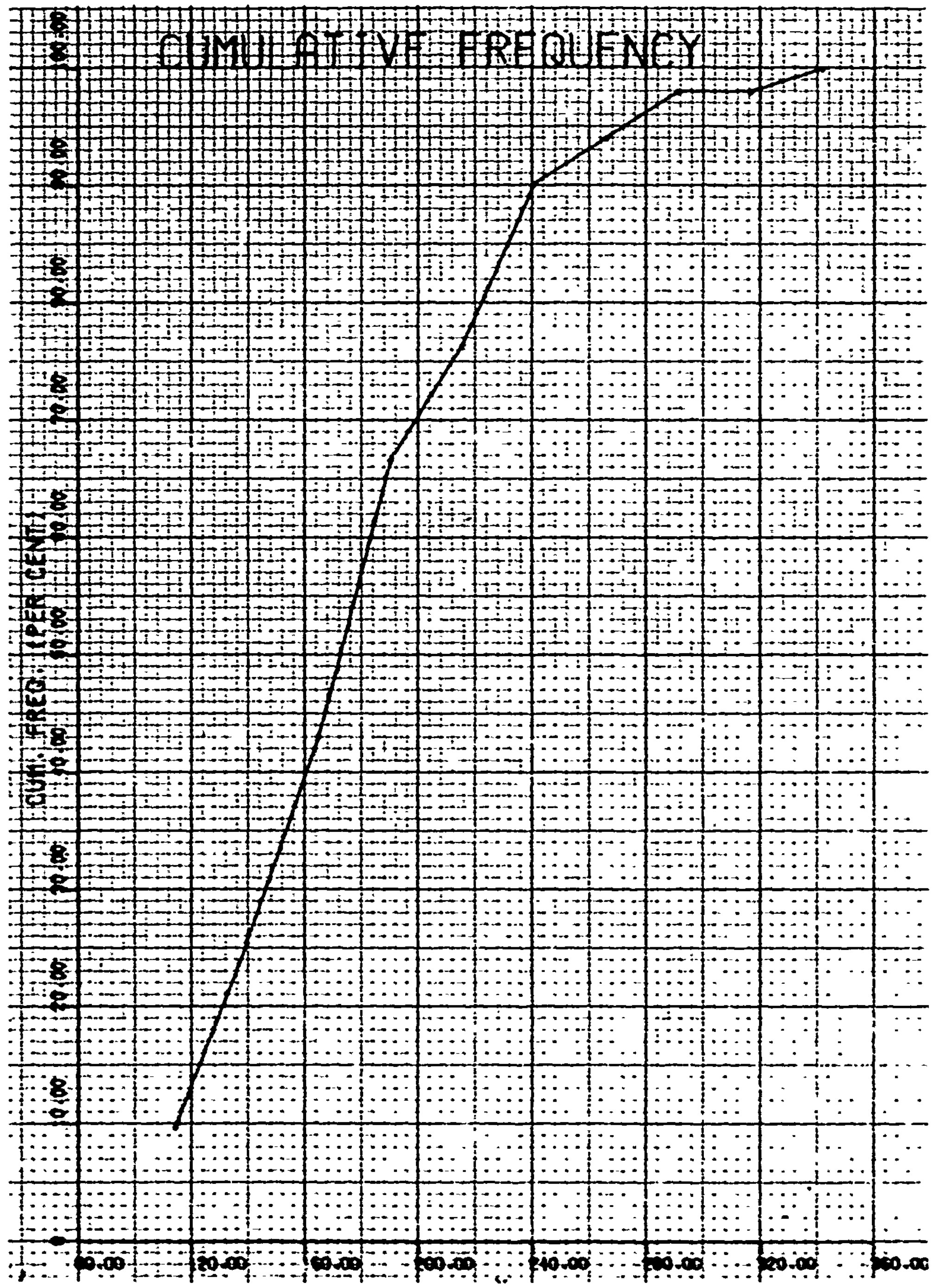

Figure 77 - Cumulative Frequency Polygon for Azimuth of Dynamic Unbalance of Empty 7000 Series Shell

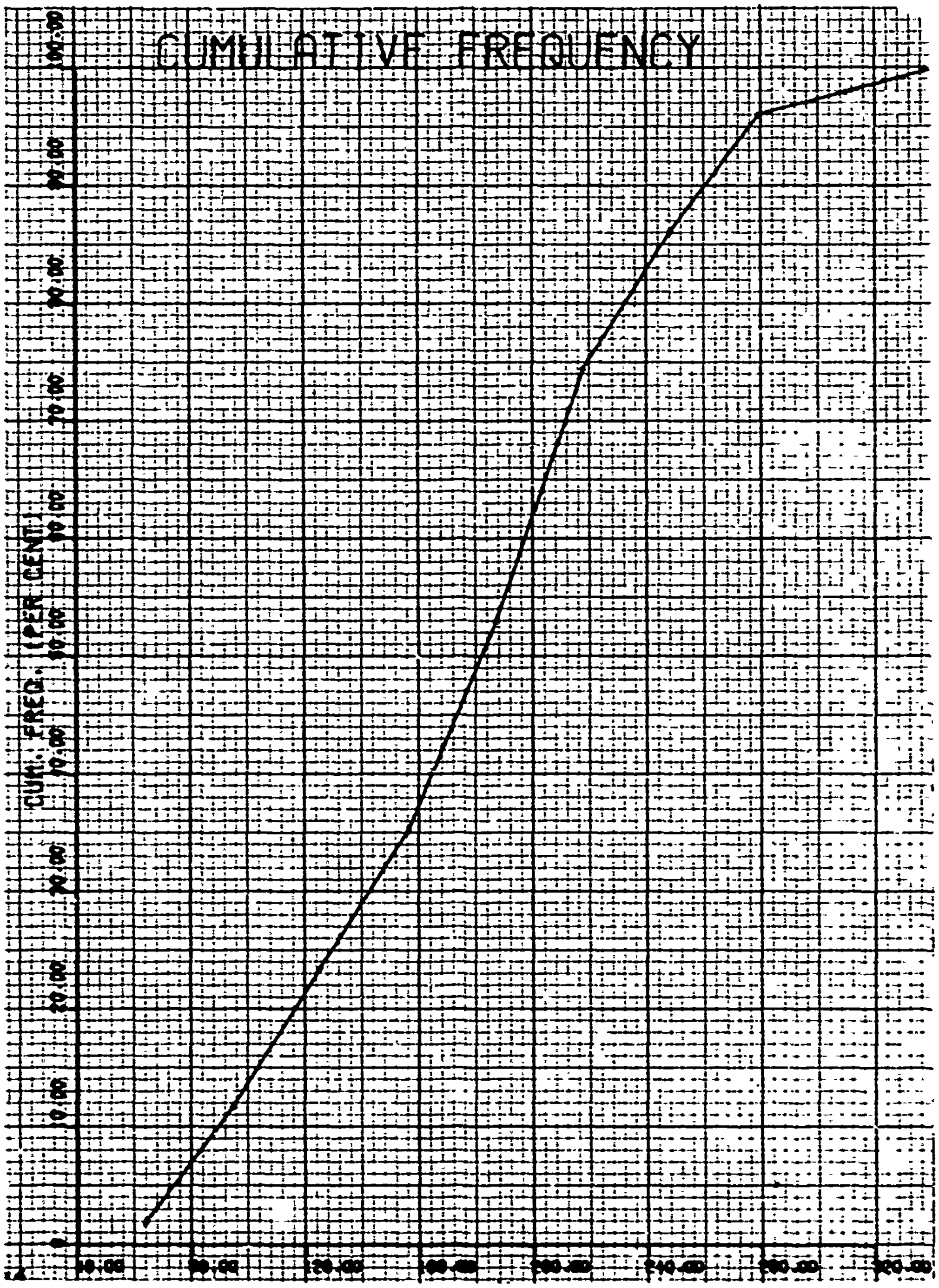

Figure 78 - Cumulative Frequency Polygon for Azimuth of Dynamic Unbalance of Full 7000 Series Shell

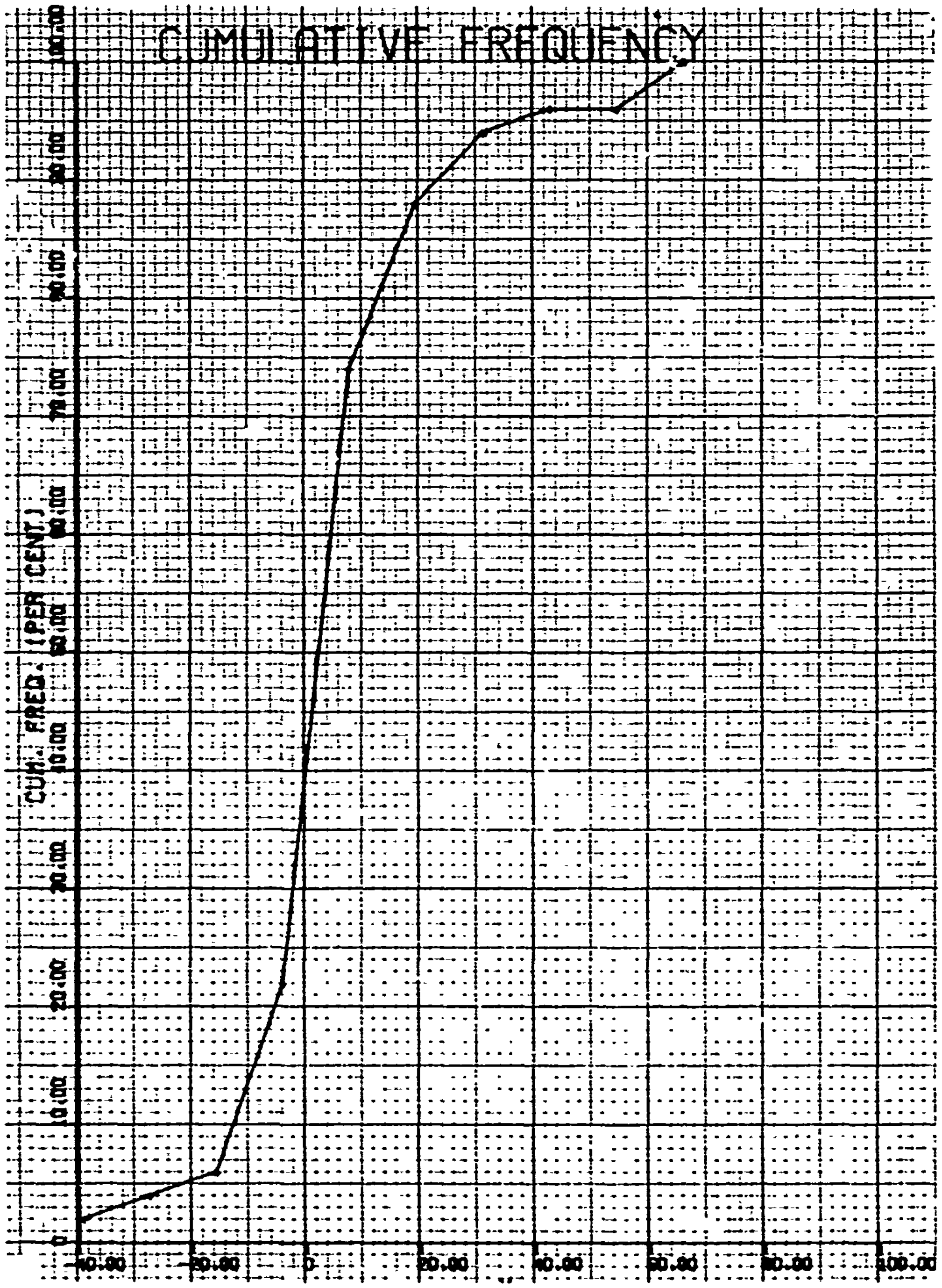

Figure 79 - Cumulative Frequency Polygon for Azimuth of Static Unbalance of Empty 7000 Series Shell

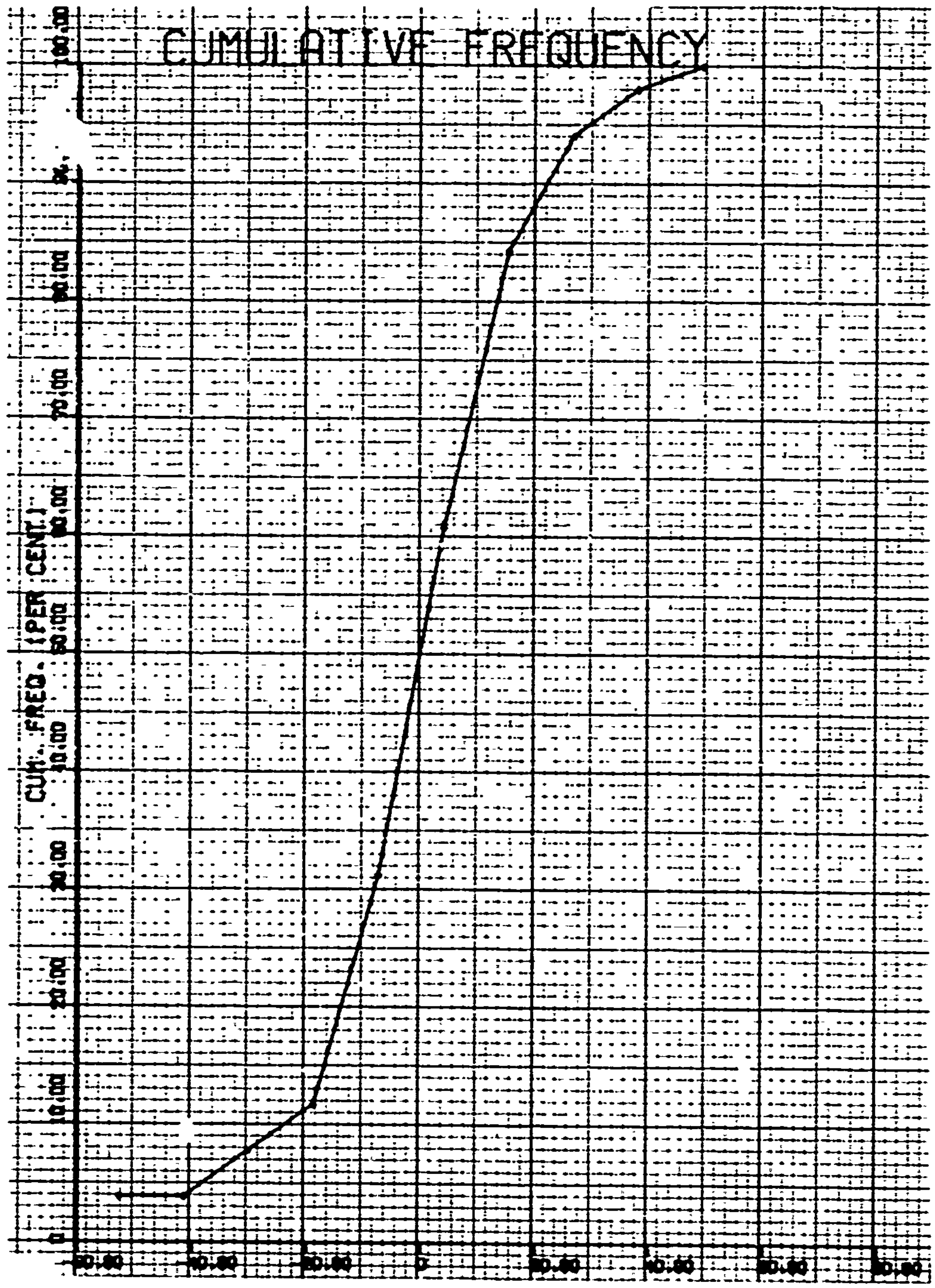

Figure 80 - Cumulative Frequency Polygon for Azimuth of Static Unbalance of Full 7000 Series Shell

SERIES (SIZE)	VARIABLE	MEAN		STD. DEV.		COEF. SKEW.		COEF. KURT.		MEAN DEV.	
		Empty	Full	Empty	Full	Empty	Full	Empty	Full	Empty	Full
SOP (50)	α, rad x 10^4	5.552	4.666	3.266	2.341	0.3996	0.2881	2.087	1.964	0.8560	0.8766
	ϵ, in. x 10^3	3.936	6.002	4.851	3.376	0.2298	0.3073	1.980	1.857	0.8872	0.8712
	τ, deg. (>0)	164.6	169.6	67.37	85.58	-0.4061	0.2281	2.998	2.546	0.7845	0.8090
	λ, deg.	2.642	-2.086	63.80	50.37	-0.1681	-0.7433	5.098	5.165	0.6177	0.6778
3000 (100)	α, rad x 10^4	3.828	2.645	2.607	1.692	1.818	0.7118	8.549	3.243	0.7285	0.8288
	ϵ, in. x 10^3	9.363	6.243	4.961	3.173	0.1599	0.3282	1.935	2.429	0.8741	0.8412
	τ, deg. (>0)	169.8	156.8	94.46	92.04	0.4404	0.1799	2.150	2.135	0.8467	0.8470
	λ, deg.	4.017	-1.739	36.92	34.39	-0.1737	-2.049	10.86	10.22	0.5834	0.5966
5000 (88)	α, rad x 10^4	3.603	2.733	2.477	1.758	1.501	1.441	5.479	6.154	0.7589	0.7624
	ϵ, in. x 10^3	18.79	12.43	7.014	3.141	4.819	-0.7594	39.07	2.925	0.5279	0.8117
	τ, deg. (>0)	180.2	150.9	76.50	85.84	-0.3413	0.4185	2.917	2.372	0.7853	0.8247
	λ, deg.	1.980	-0.2205	8.422	7.480	0.0941	0.3942	3.902	4.037	0.7430	0.7505
6000 (57)	α, rad x 10^4	3.195	2.349	1.686	1.197	0.2522	0.7132	2.156	2.891	0.8503	0.8315
	ϵ, in. x 10^3	17.63	11.70	4.054	3.220	-1.464	-0.8428	6.702	4.209	0.7129	0.7174
	τ, deg. (>0)	188.1	182.5	109.4	107.8	-0.0766	-0.1506	1.463	1.590	0.9253	0.9055
	λ, deg.	0.5790	4.050	13.63	20.	-0.1044	-5.322	11.31	35.79	0.6307	0.4747
7000 (51)	α, rad x 10^4	5.382	4.159	3.968	2.403	1.131	0.7017	4.223	2.692	0.7980	0.8199
	ϵ, in. x 10^3	14.66	9.860	4.526	3.478	-0.2567	-0.1547	2.339	2.556	0.8303	0.8257
	τ, deg. (>0)	178.2	177.5	53.05	63.07	0.5985	0.1089	3.367	2.700	0.7834	0.8054
	λ, deg.	2.184	-1.545	19.94	19.26	0.4550	-0.6581	6.297	5.209	0.6201	0.7002

Figure 81 - Statistical Parameters of All Series, Empty and Full

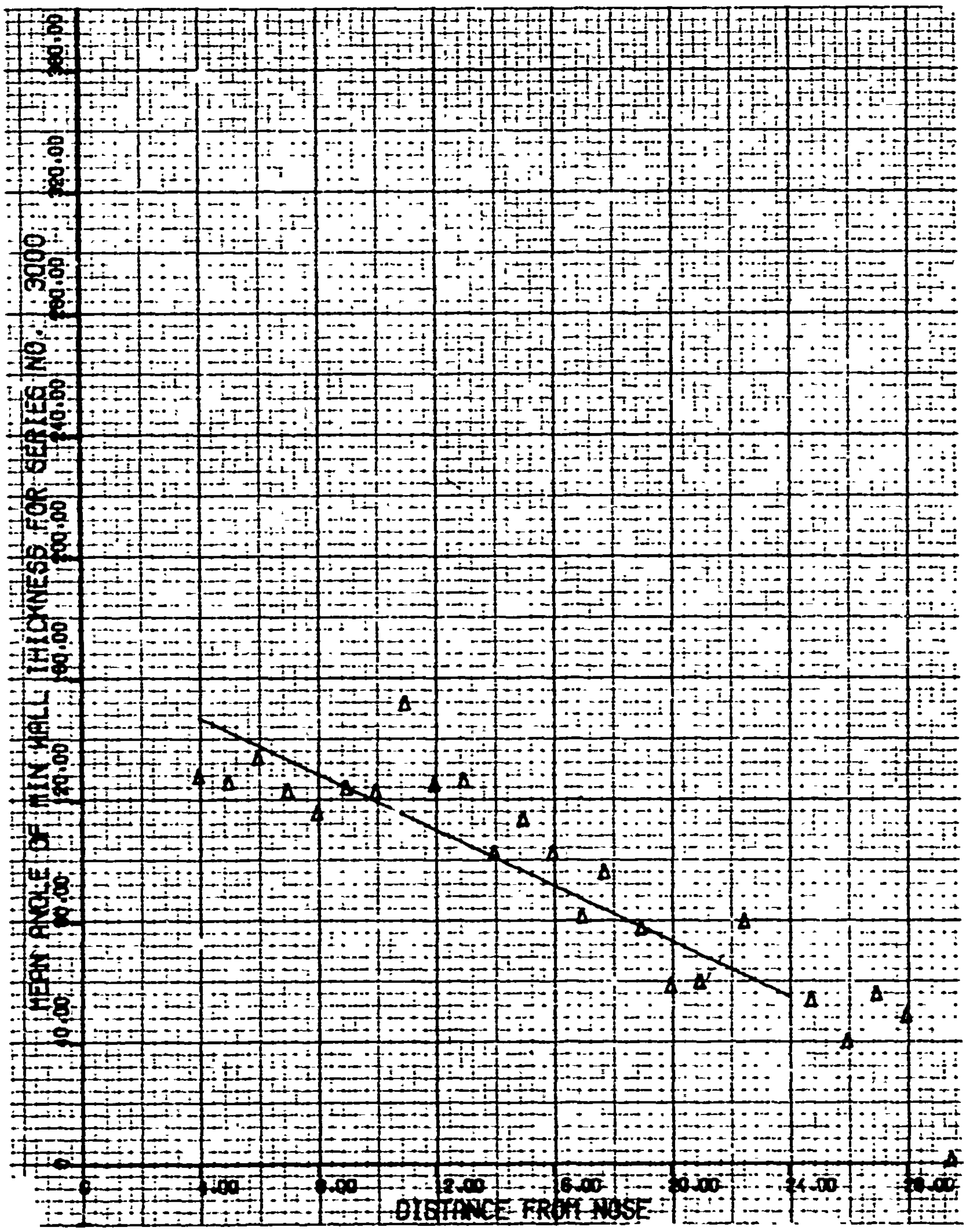

Figure 82 - Mean Angle of Minimum Wall Thickness Versus
Longitudinal Station, 3000 Series

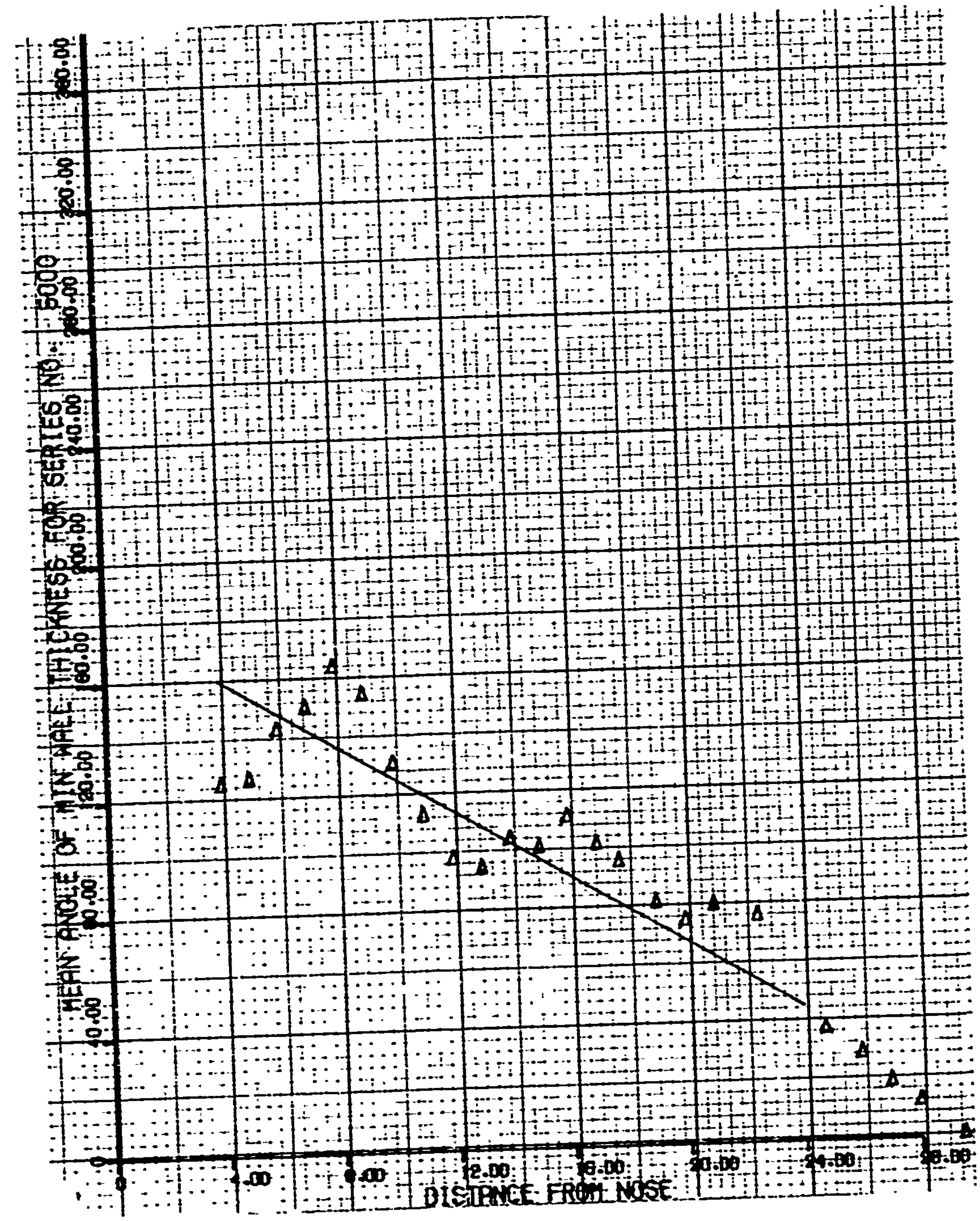

Figure 83 - Mean Angle of Minimum Wall Thickness Versus Longitudinal Station, 5000 Series

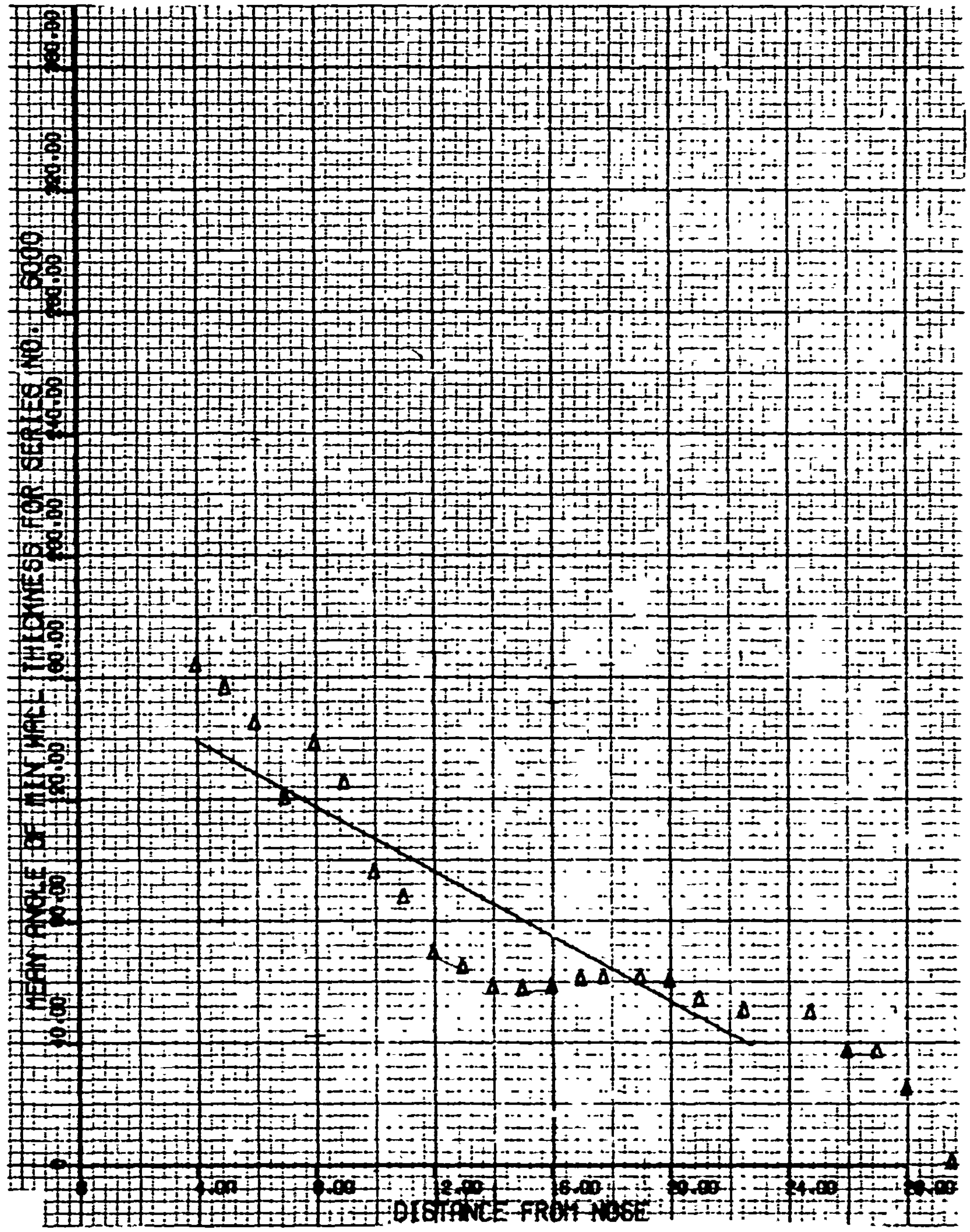

Figure 84 - Mean Angle of Minimum Wall Thickness Versus Longitudinal Station, 6000 Series

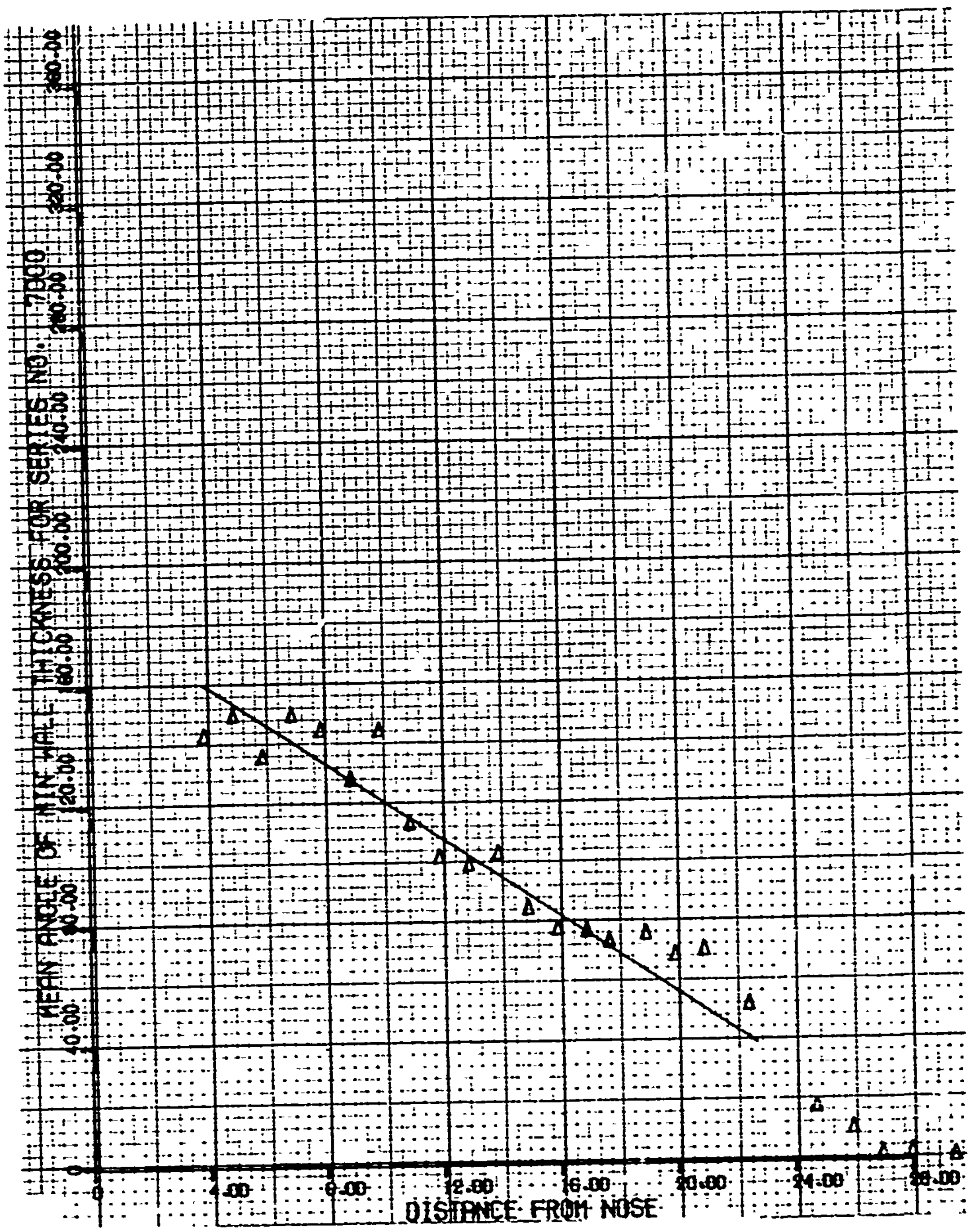

Figure 85 - Mean Angle of Minimum Wall Thickness Versus Longitudinal Station, 7000 Series

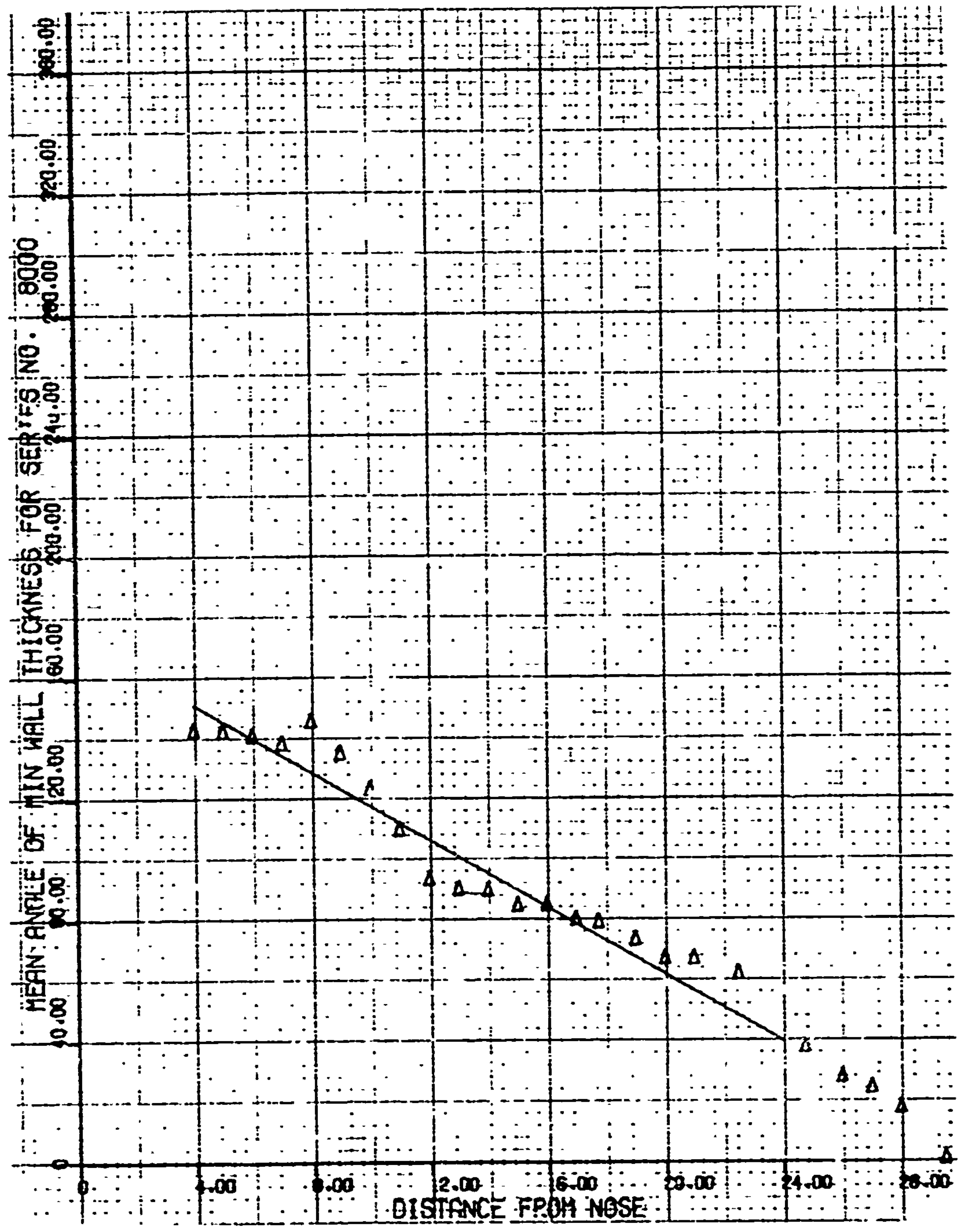

Figure 86 - Mean Angle of Minimum Wall Thickness Versus Longitudinal Station, 8000 Series

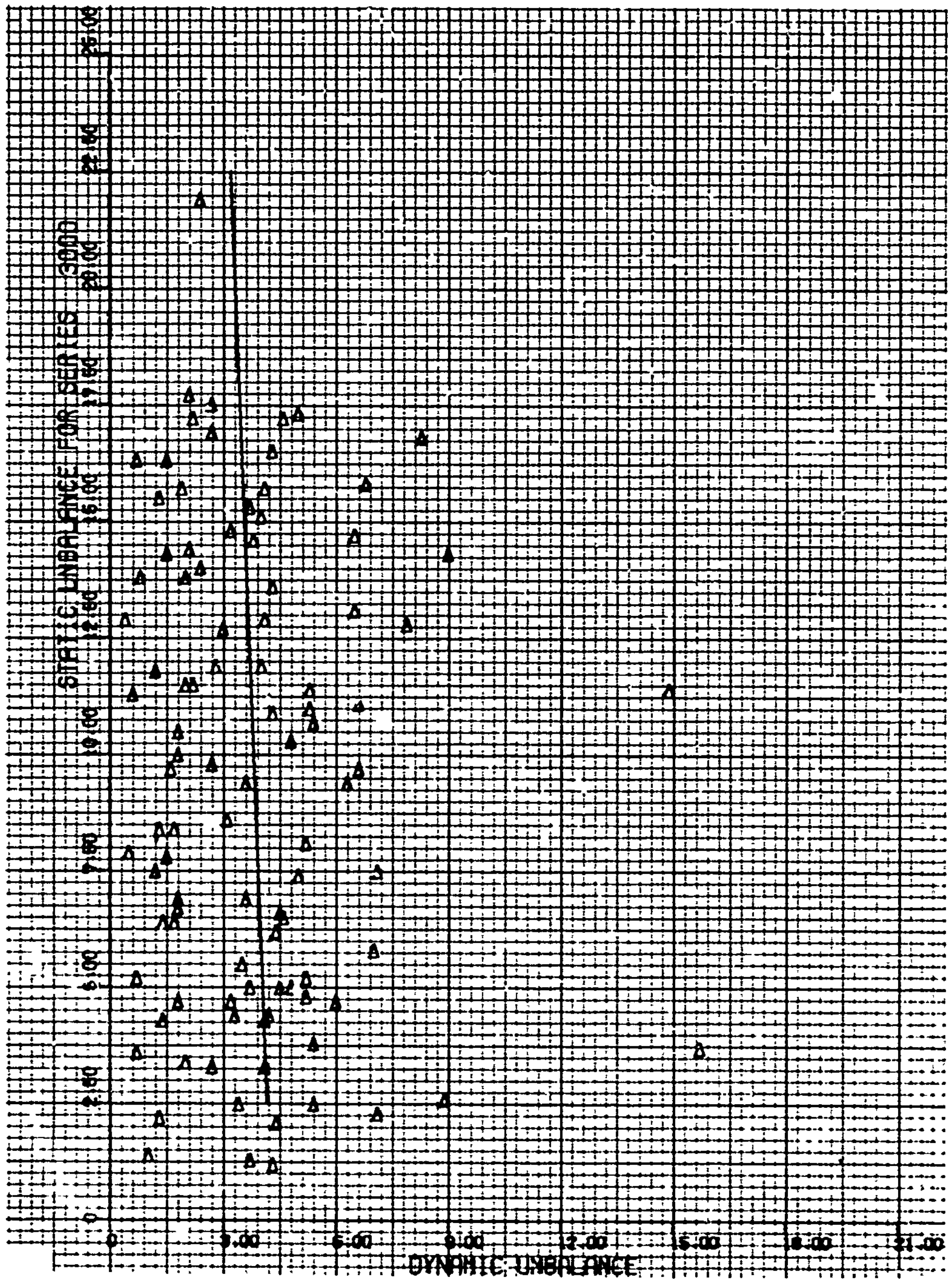

Figure 87 - Static Unbalance Versus Dynamic Unbalance,
3000 Series, Empty

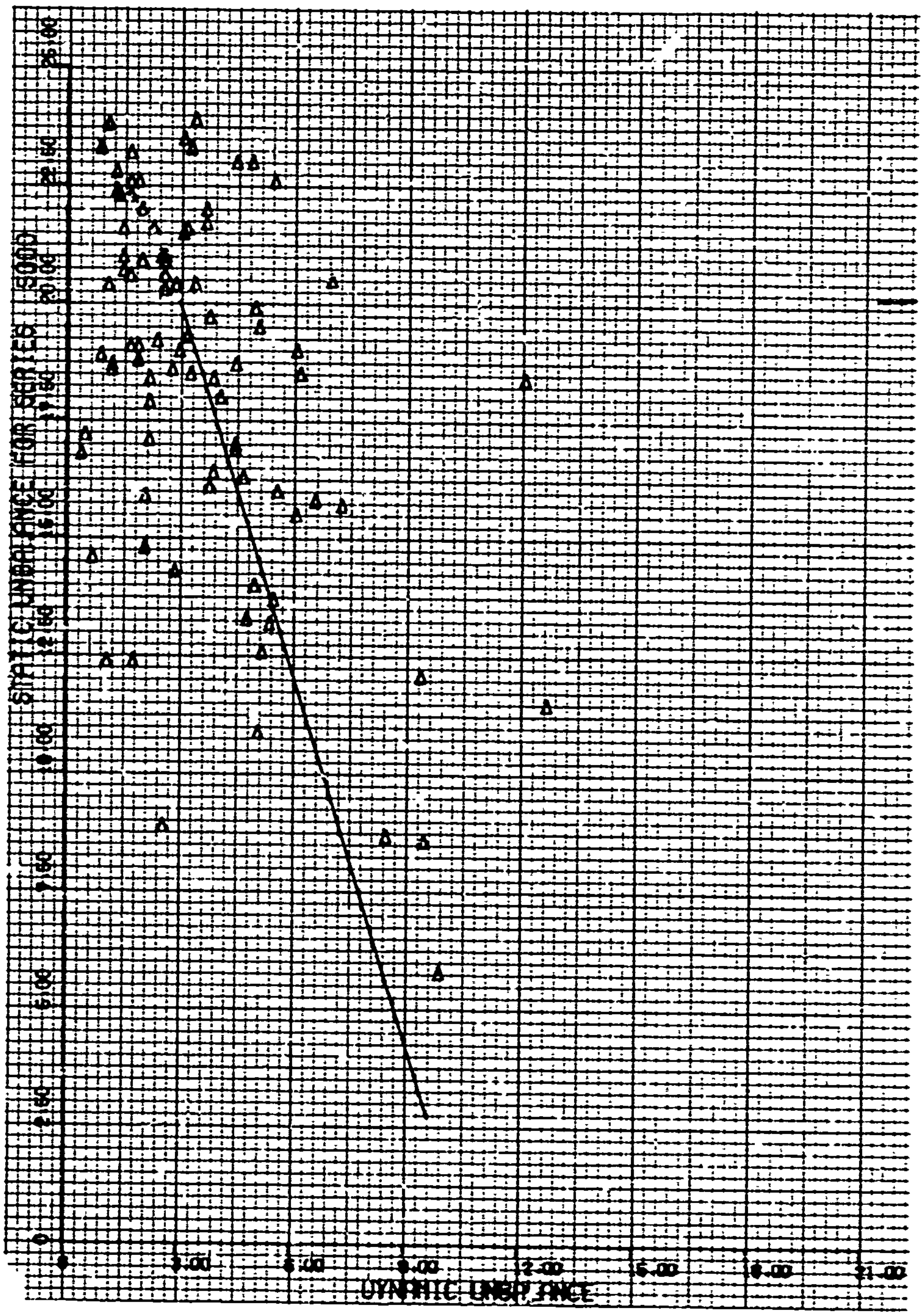

Figure 88 - Static Unbalance Versus Dynamic Unbalance, 5000 Series, Empty

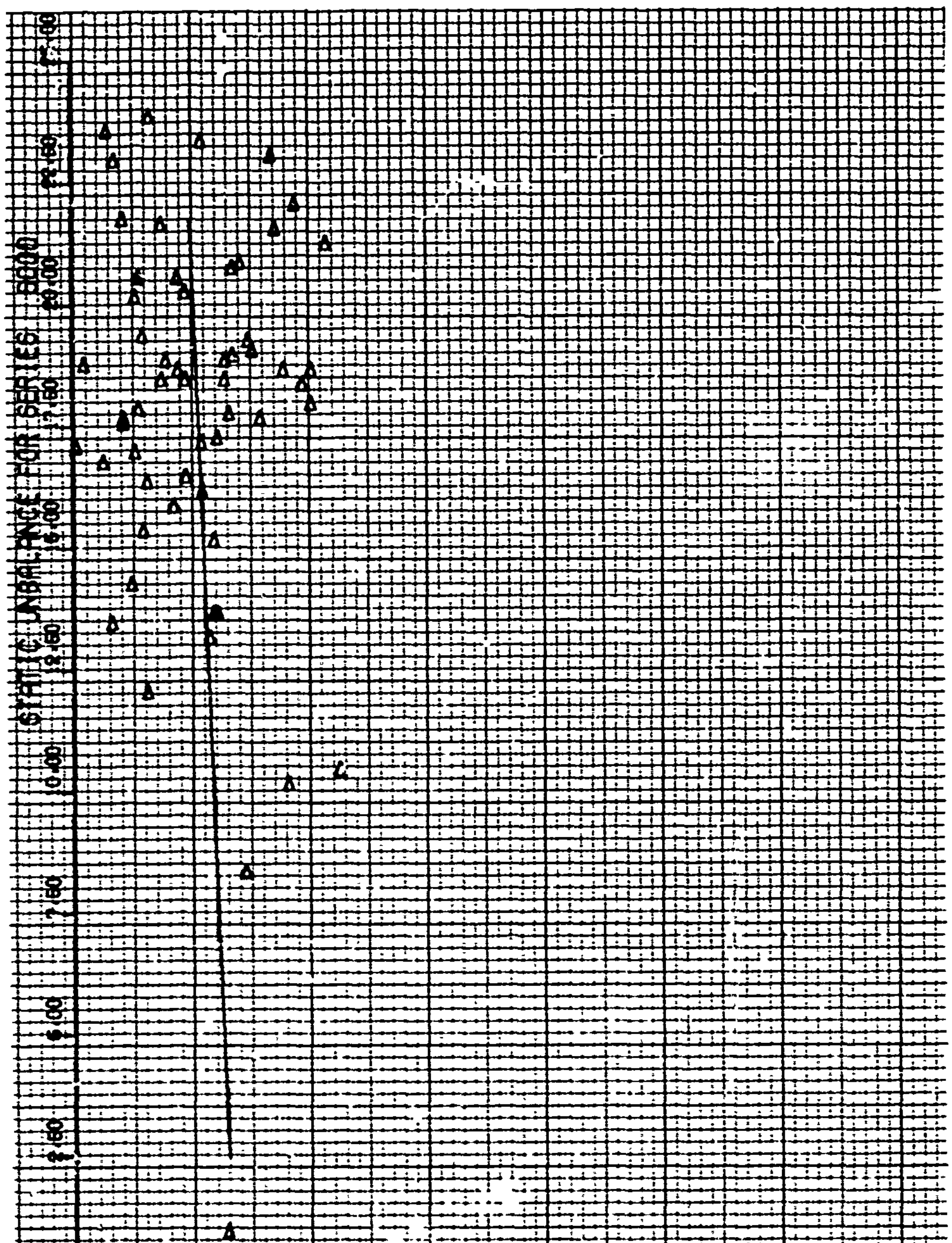

Figure 89 - Static Unbalance Versus Dynamic Unbalance, 6000 Series, Empty

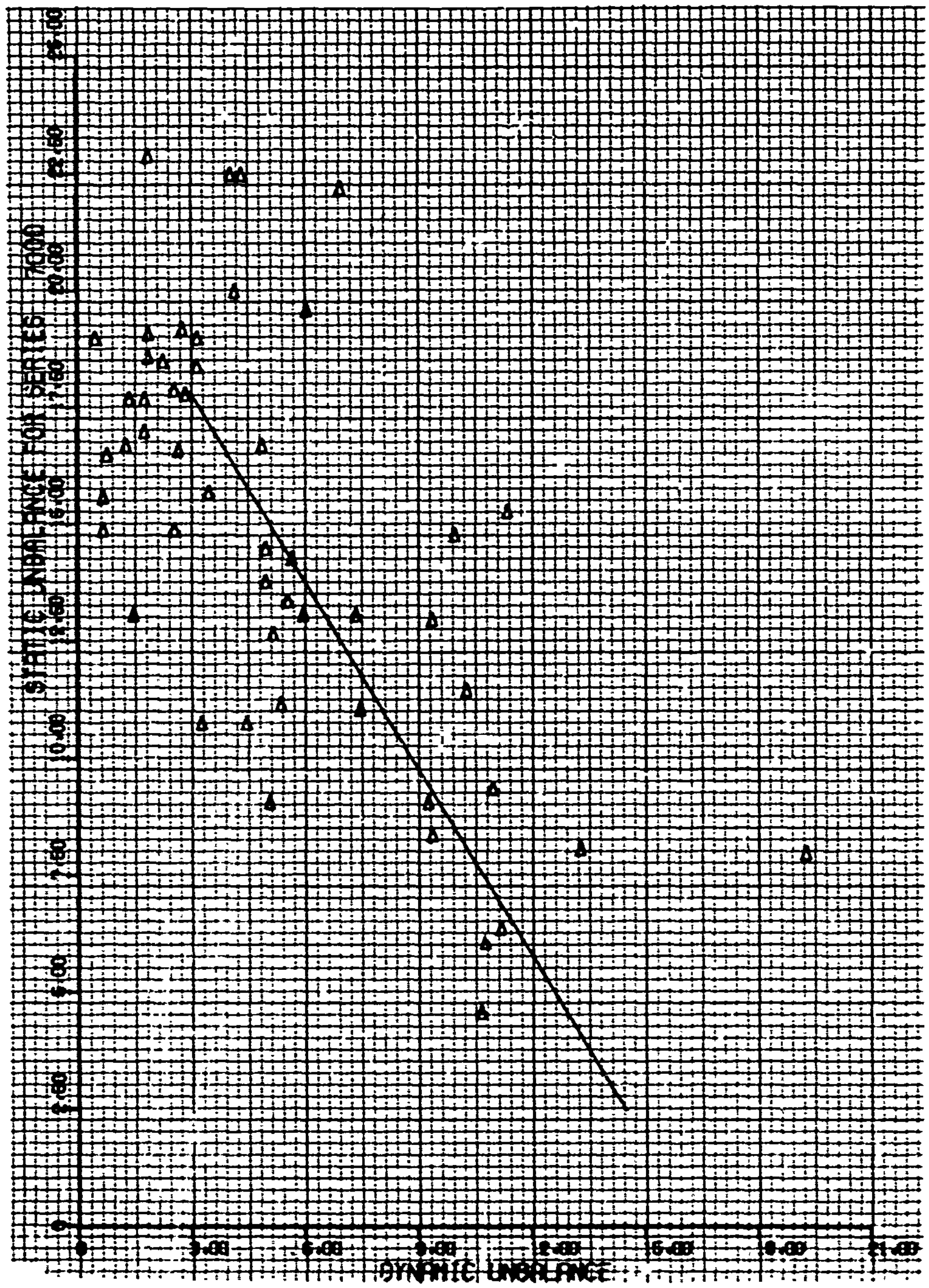

Figure 90 - Static Unbalance Versus Dynamic Unbalance, 7000 Series, Empty

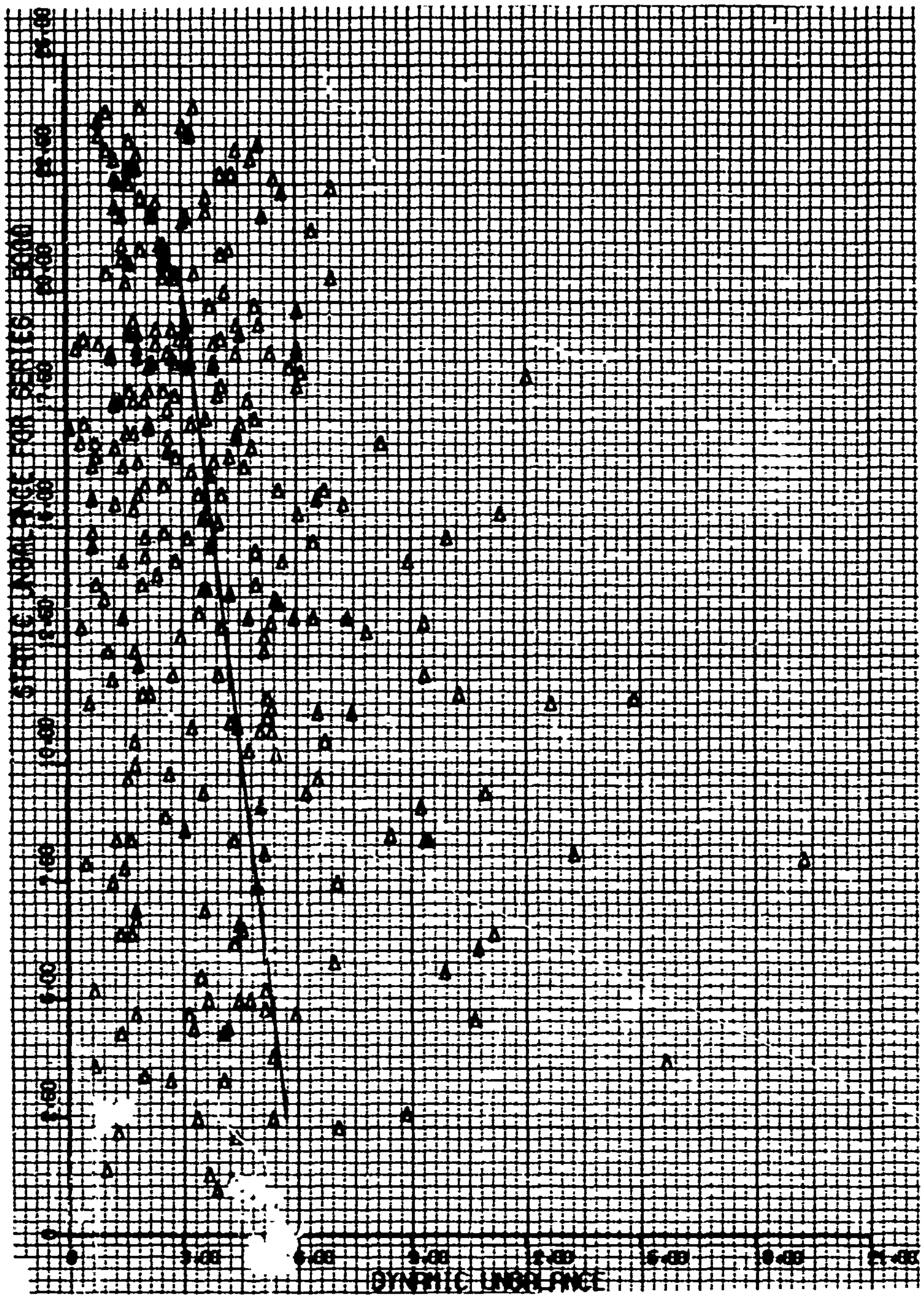

Figure 91 - Static Unbalance Versus Dynamic Unbalance, 8000 Series, Empty

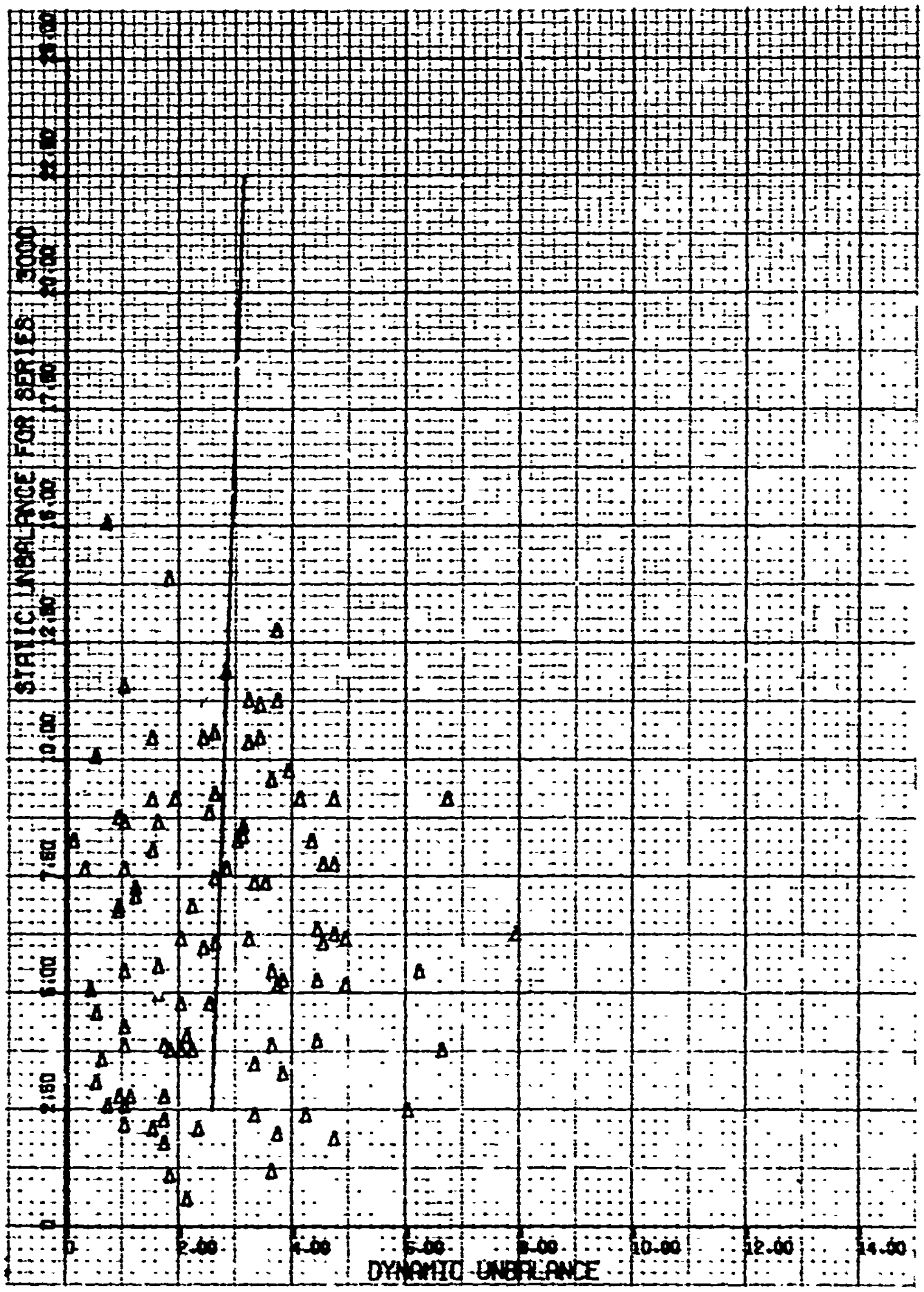

Figure 92 - Static Unbalance Versus Dynamic Unbalance, 3000 Series, Full

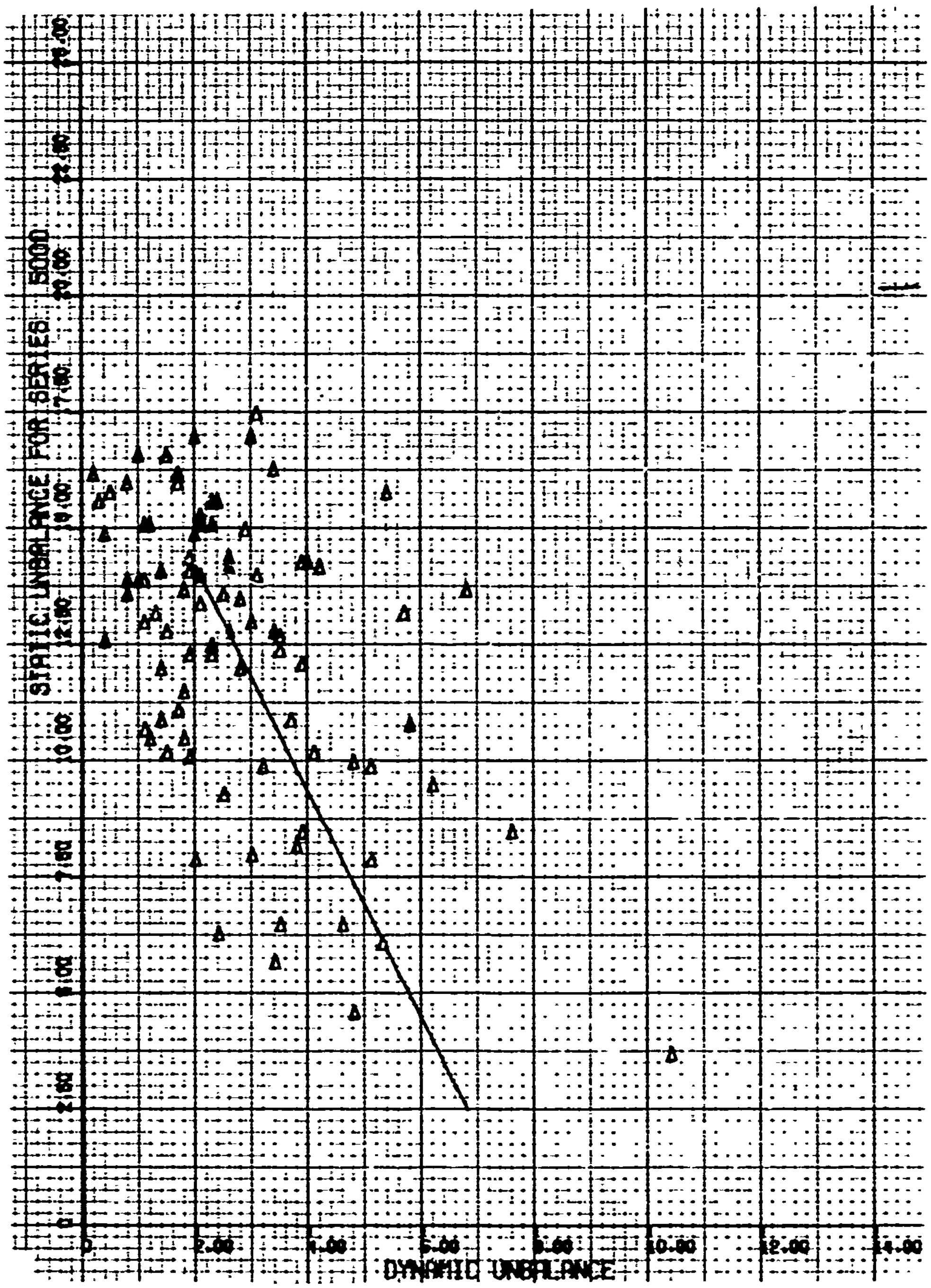

Figure 93 - Static Unbalance Versus Dynamic Unbalance,
5000 Series, Full

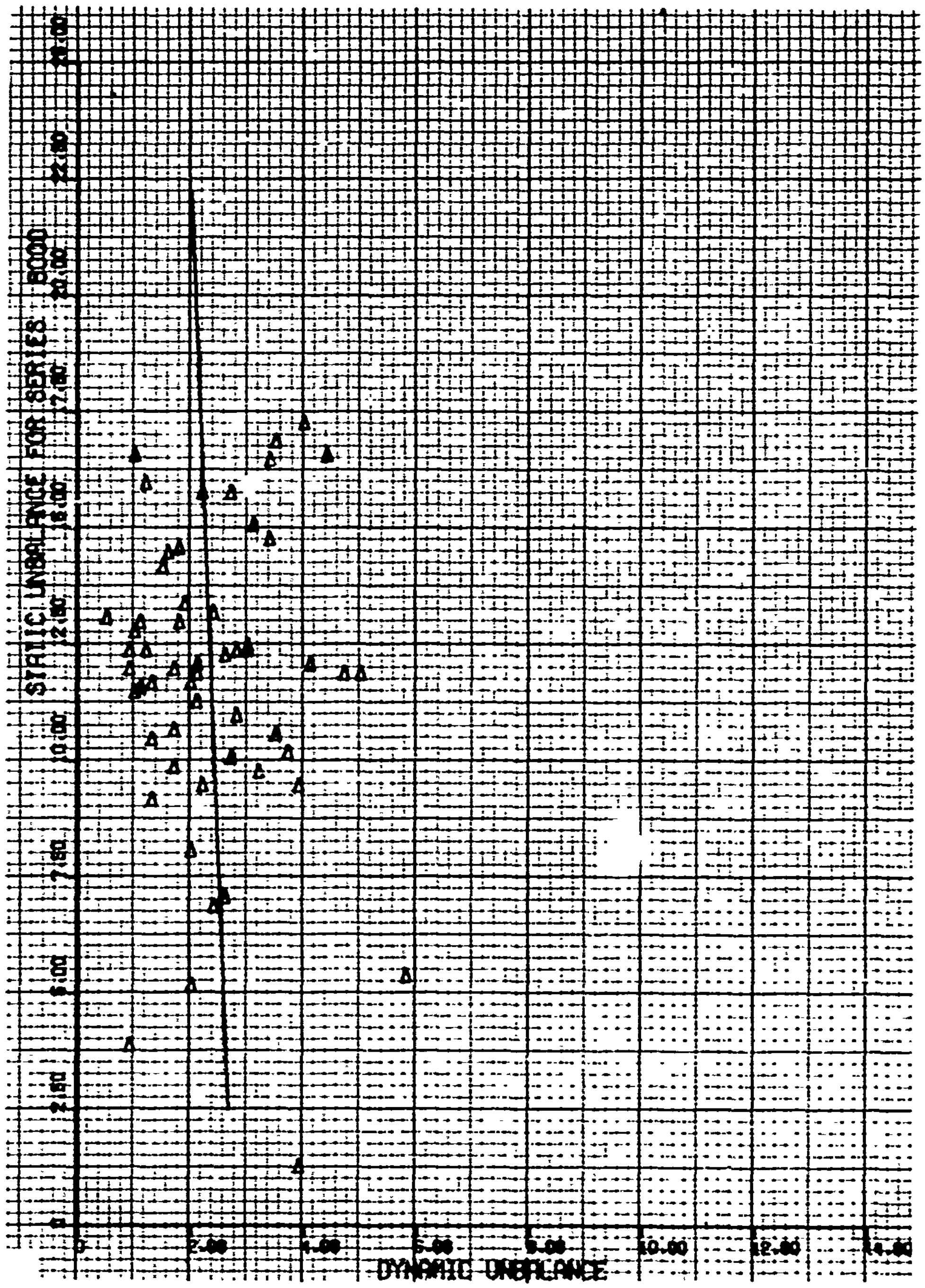

Figure 94 - Static Unbalance Versus Dynamic Unbalance
6000 Series, Full

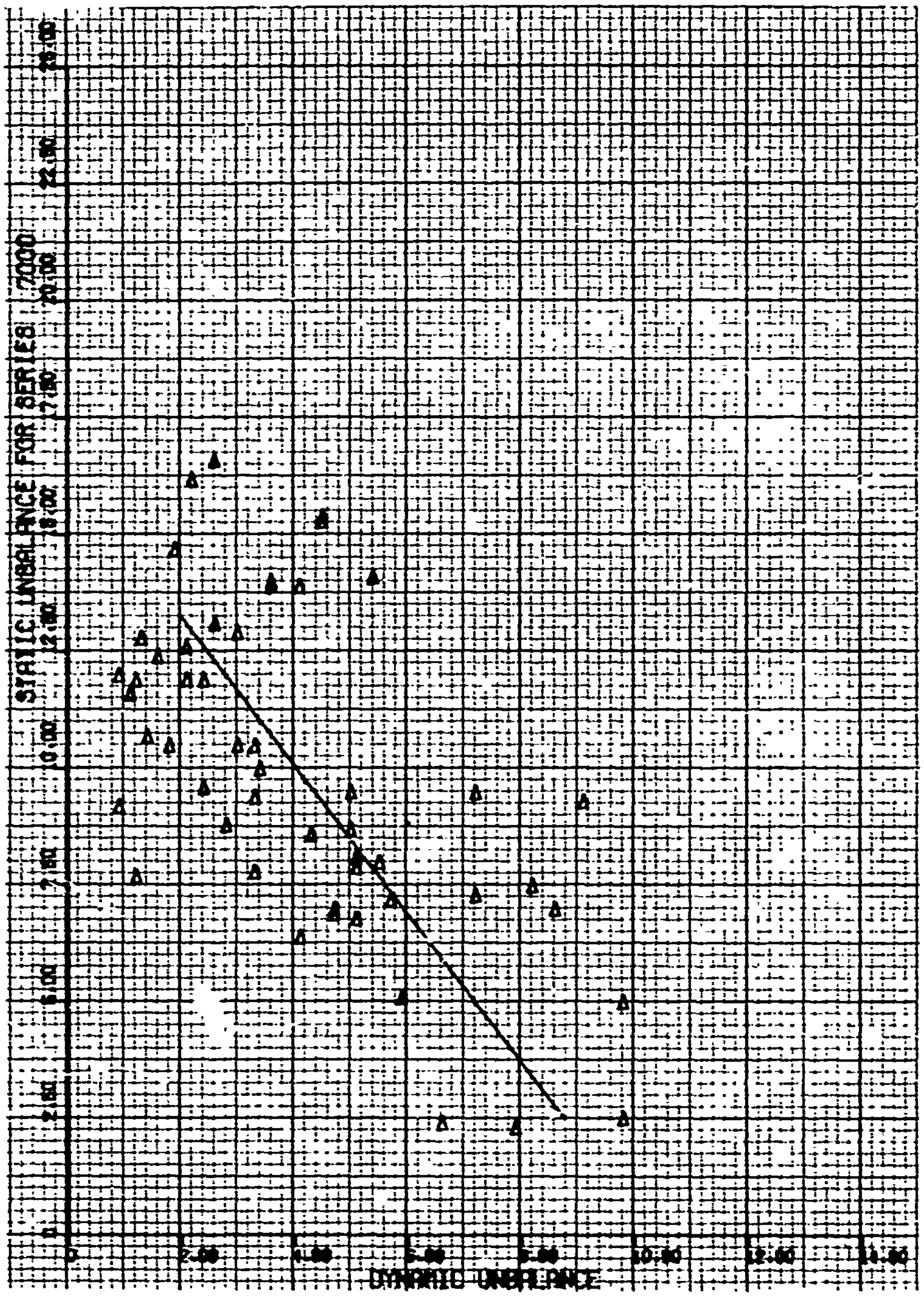

Figure 95 - Static Unbalance Versus Dynamic Unbalance
7000 Series, Full

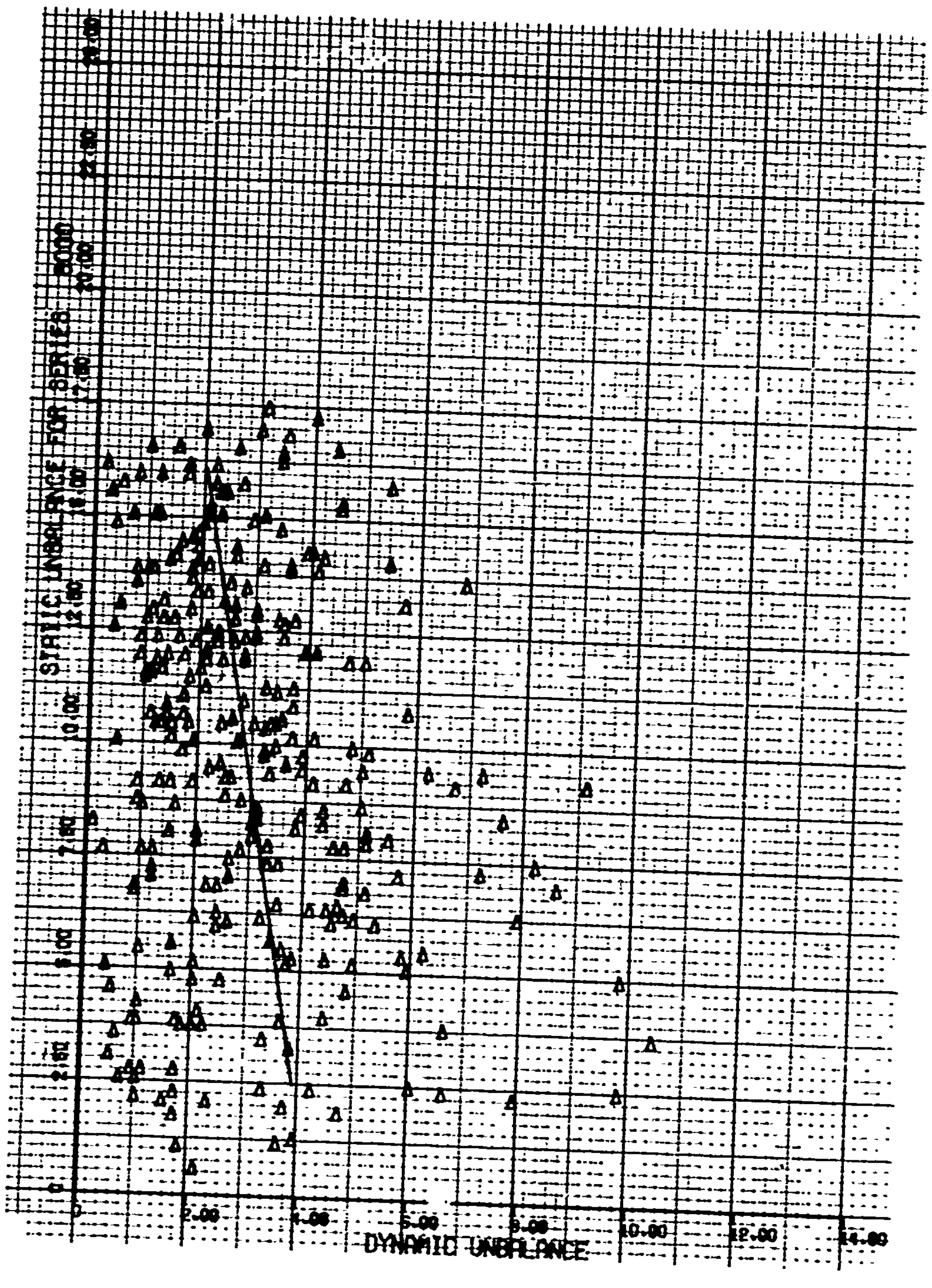

Figure 96 - Static Unbalance Versus Dynamic Unbalance
8000 Series, Full

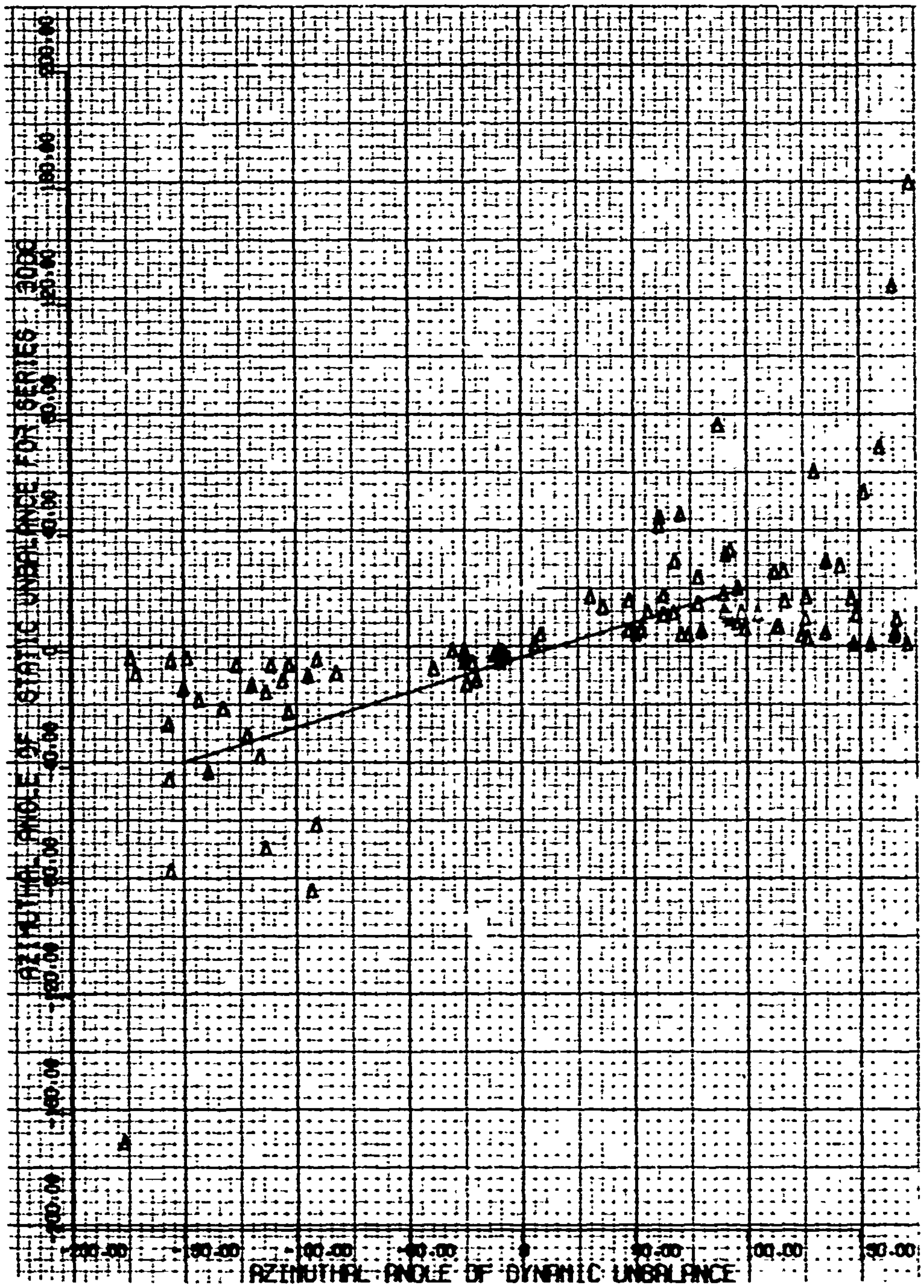

Figure 97 - Azimuth of Static Unbalance Versus Azimuth of Dynamic Unbalance, 3000 Series, Empty

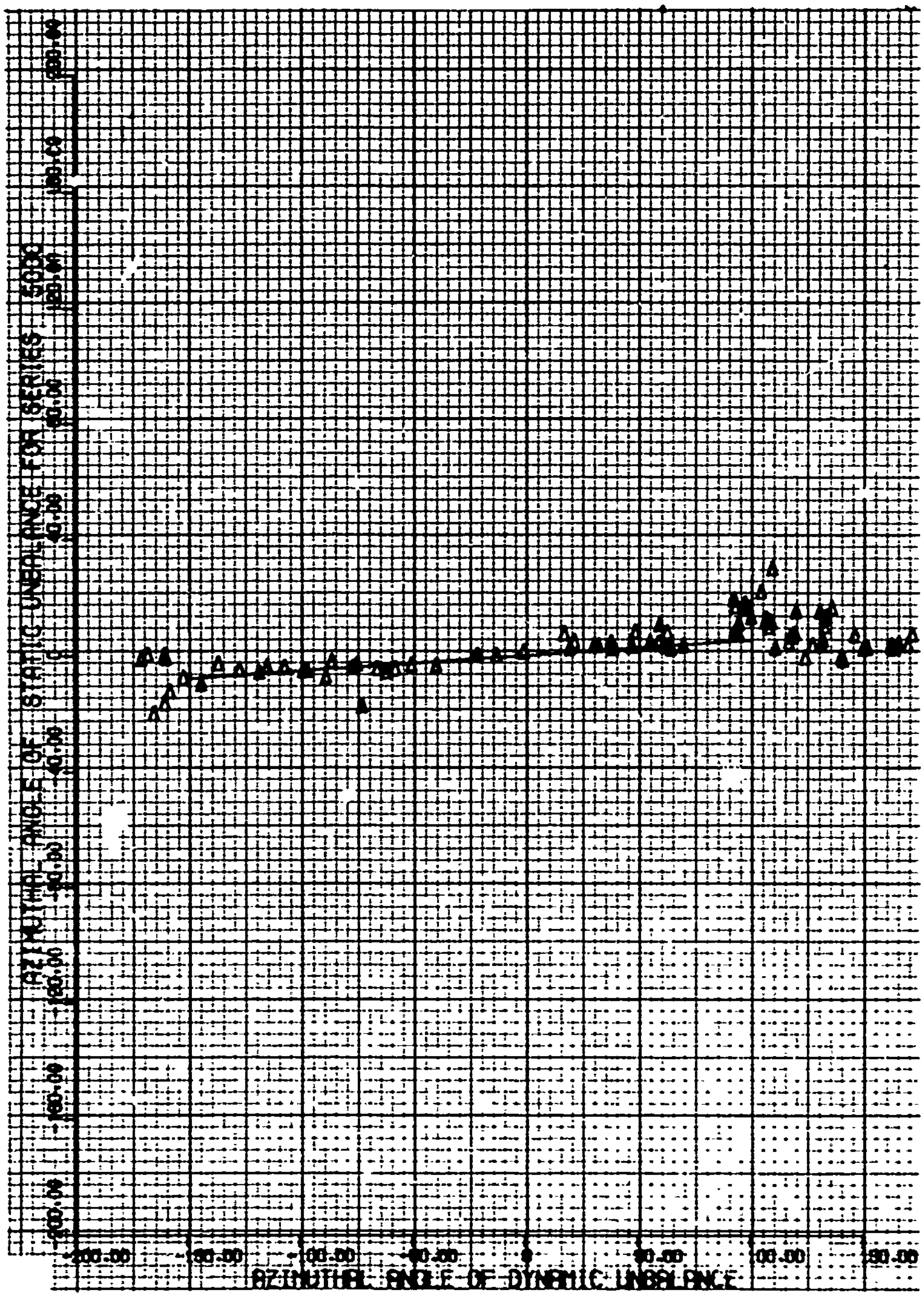

Figure 98 - Azimuth of Static Unbalance Versus Azimuth of Dynamic Unbalance, 5000 Series, Empty

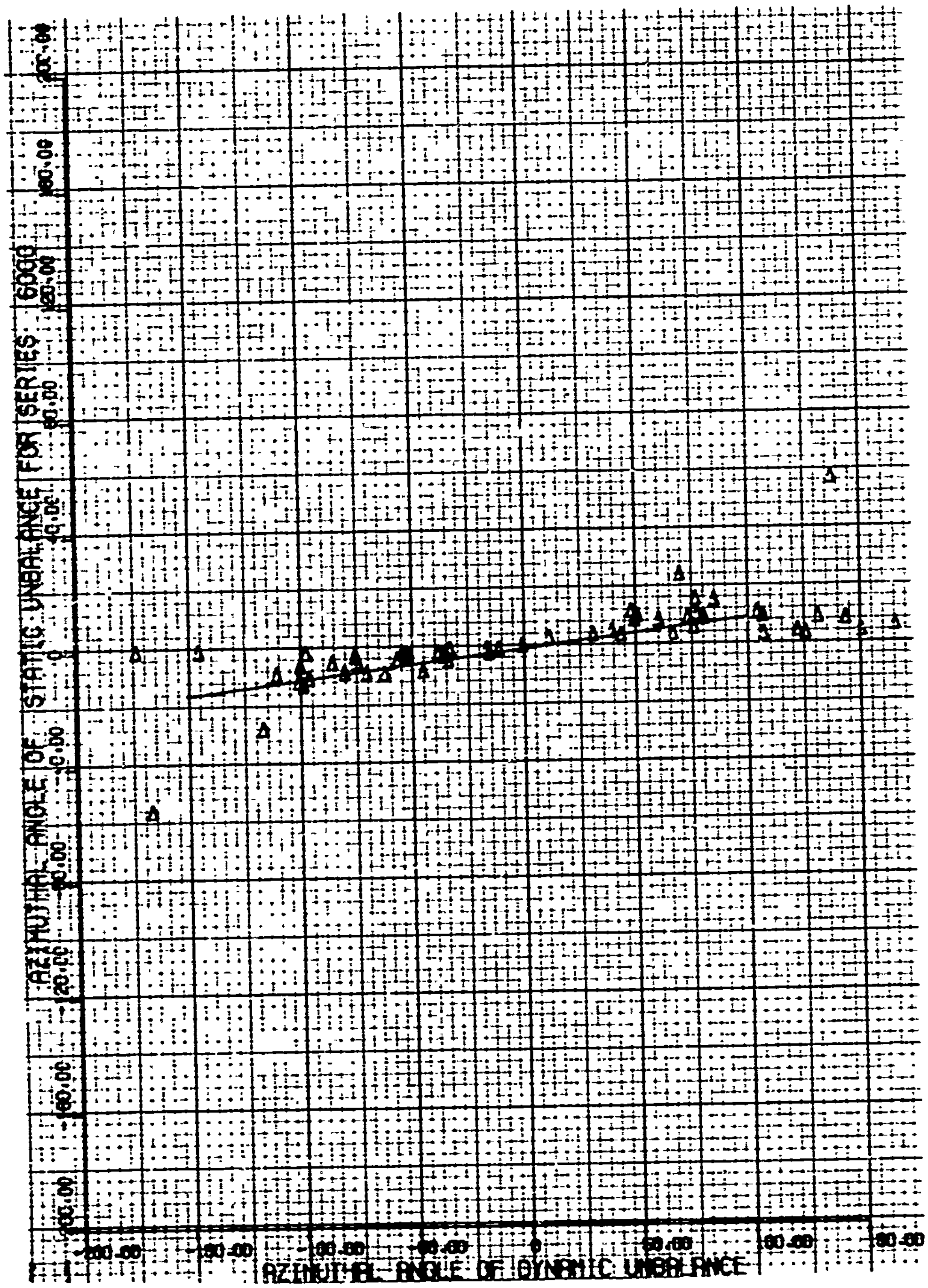

Figure 99 - Azimuth of Static Unbalance Versus Azimuth of Dynamic Unbalance, 6000 Series, Empty

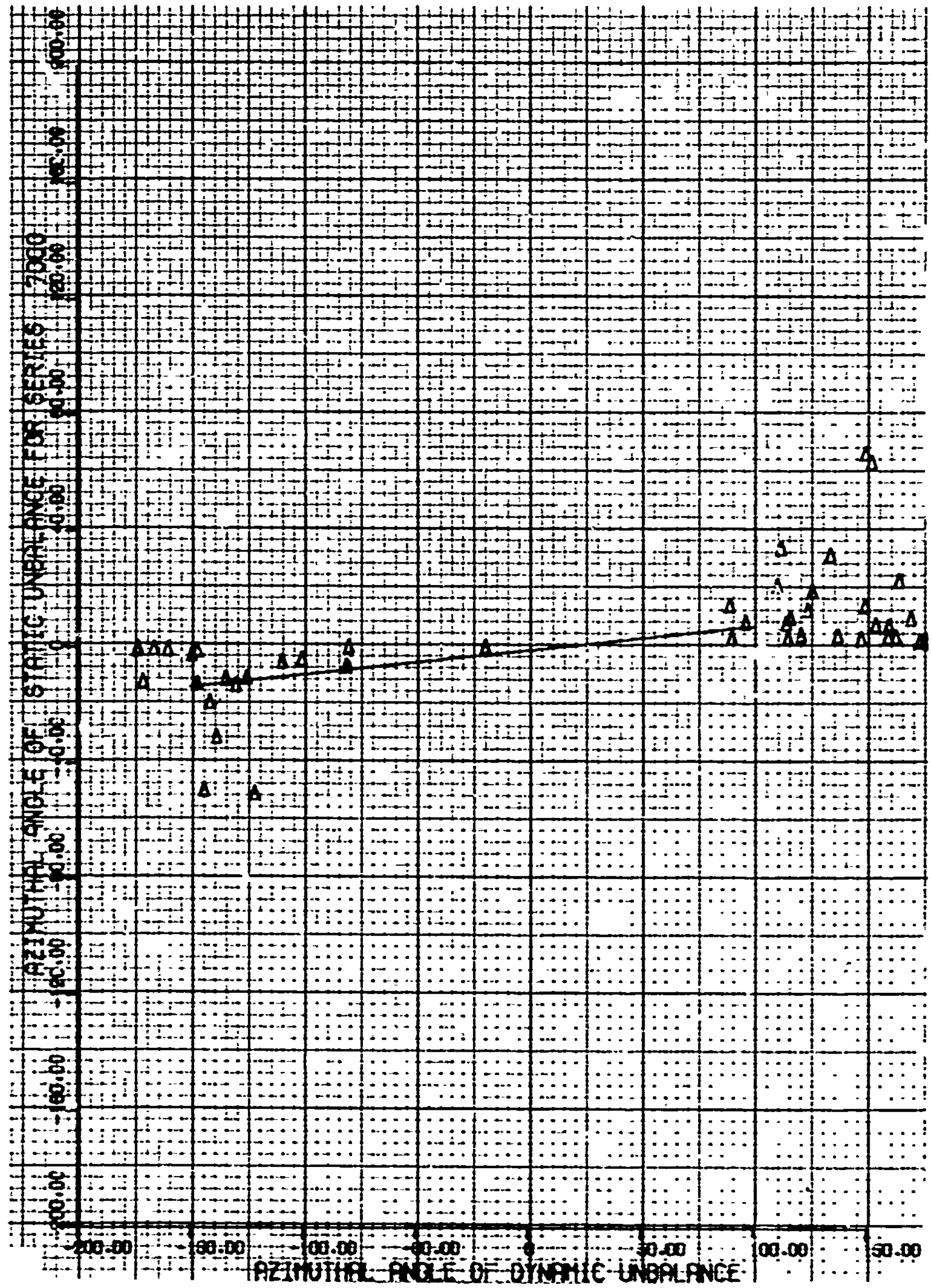

Figure 100 - Azimuth of Static Unbalance Versus Azimuth of Dynamic Unbalance, 7000 Series, Empty

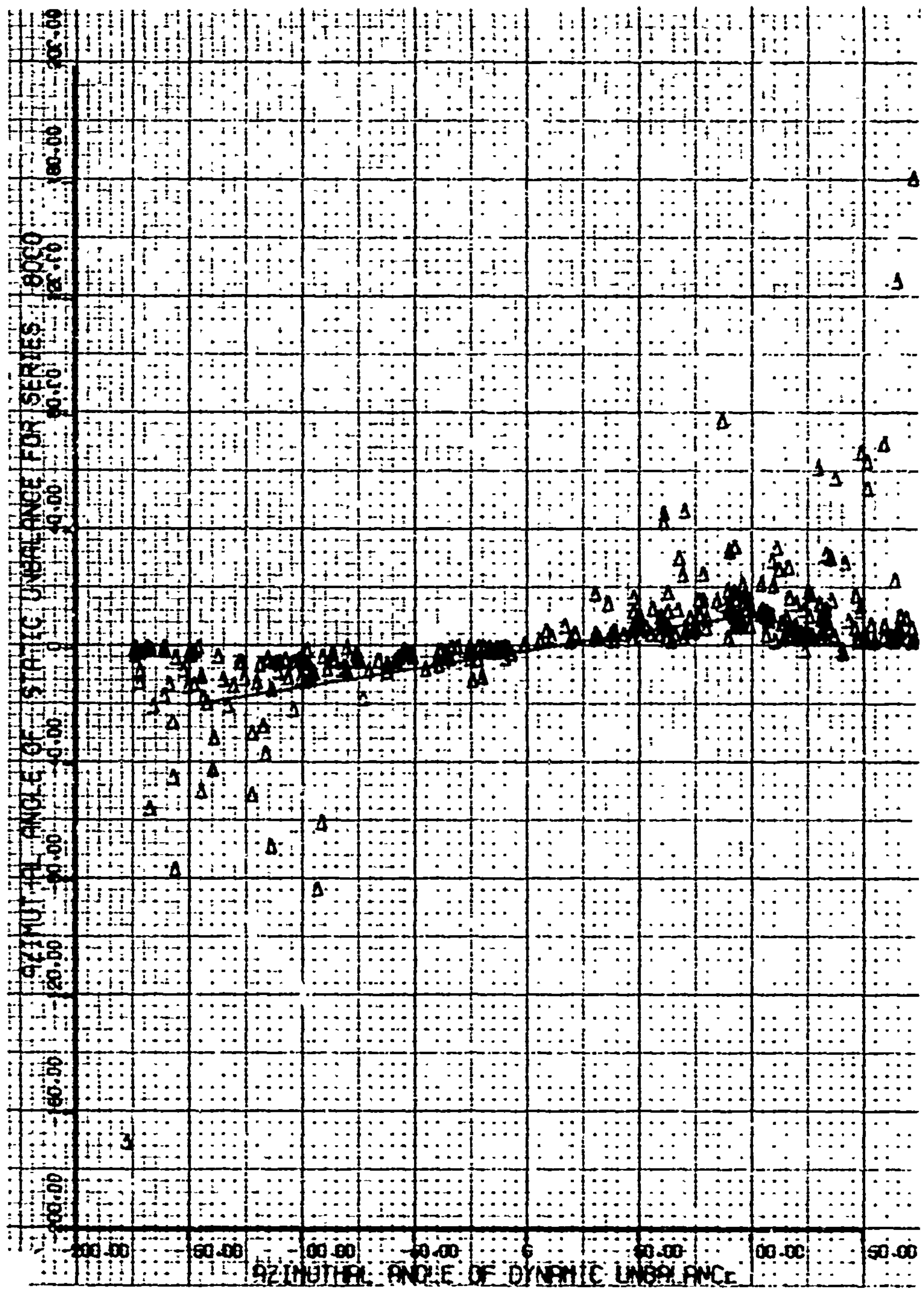

Figure 101 - Azimuth of Static Unbalance Versus Azimuth of Dynamic Unbalance, 8000 Series, Empty

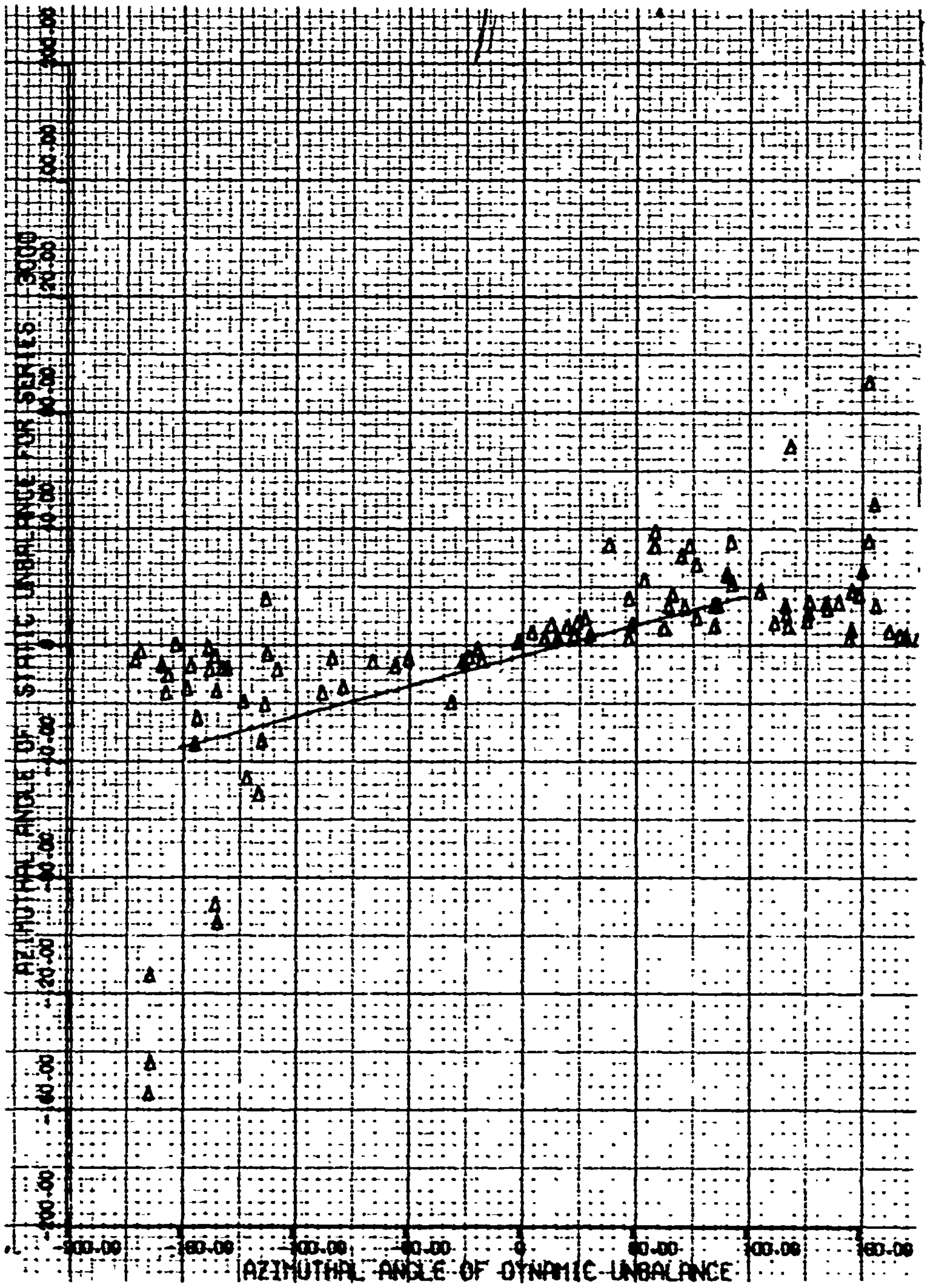

Figure 102 - Azimuth of Static Unbalance Versus Azimuth of Dynamic Unbalance, 3000 Series, Full

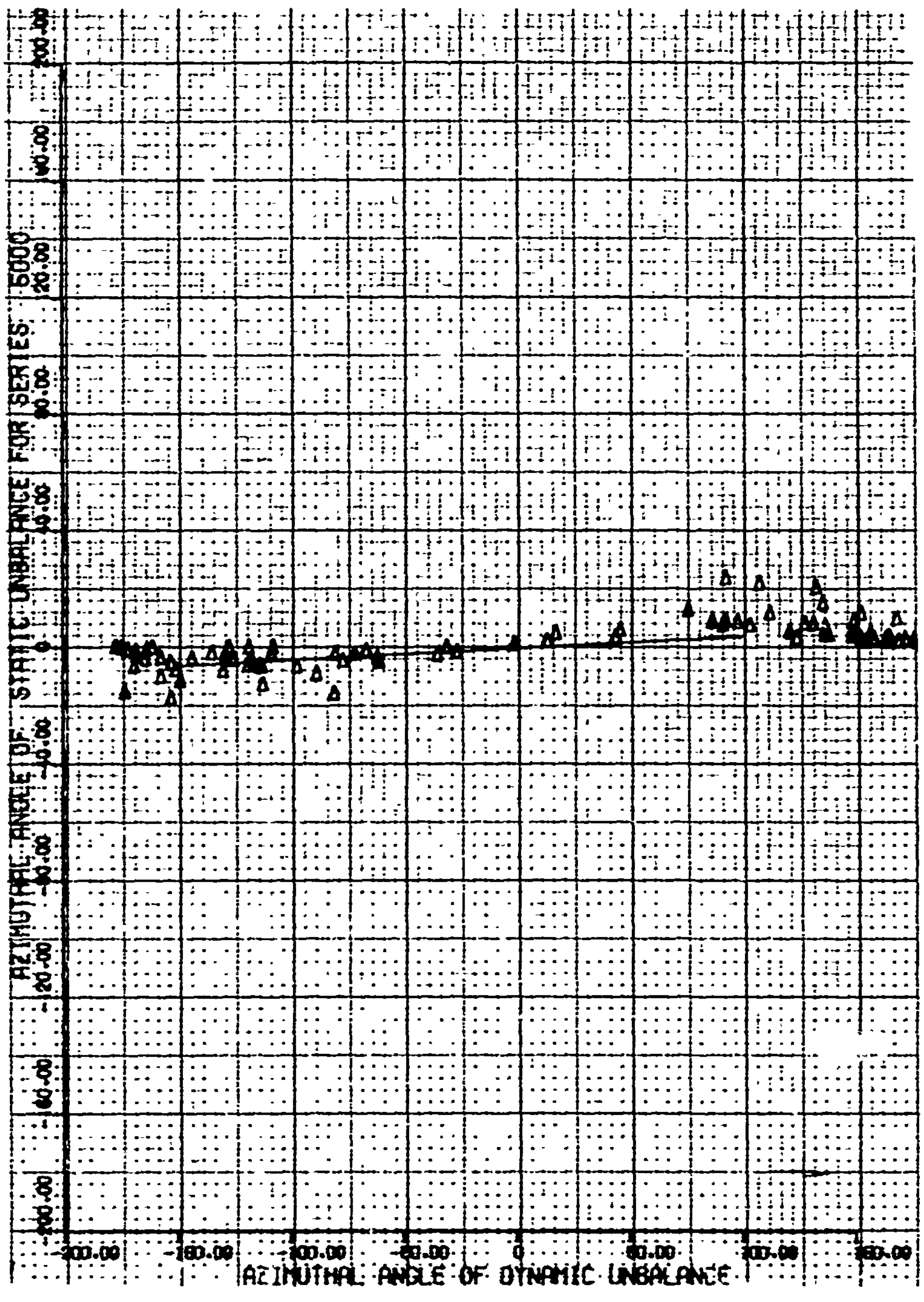

Figure 103 - Azimuth of Static Unbalance Versus Azimuth of Dynamic Unbalance, 5000 Series, Full

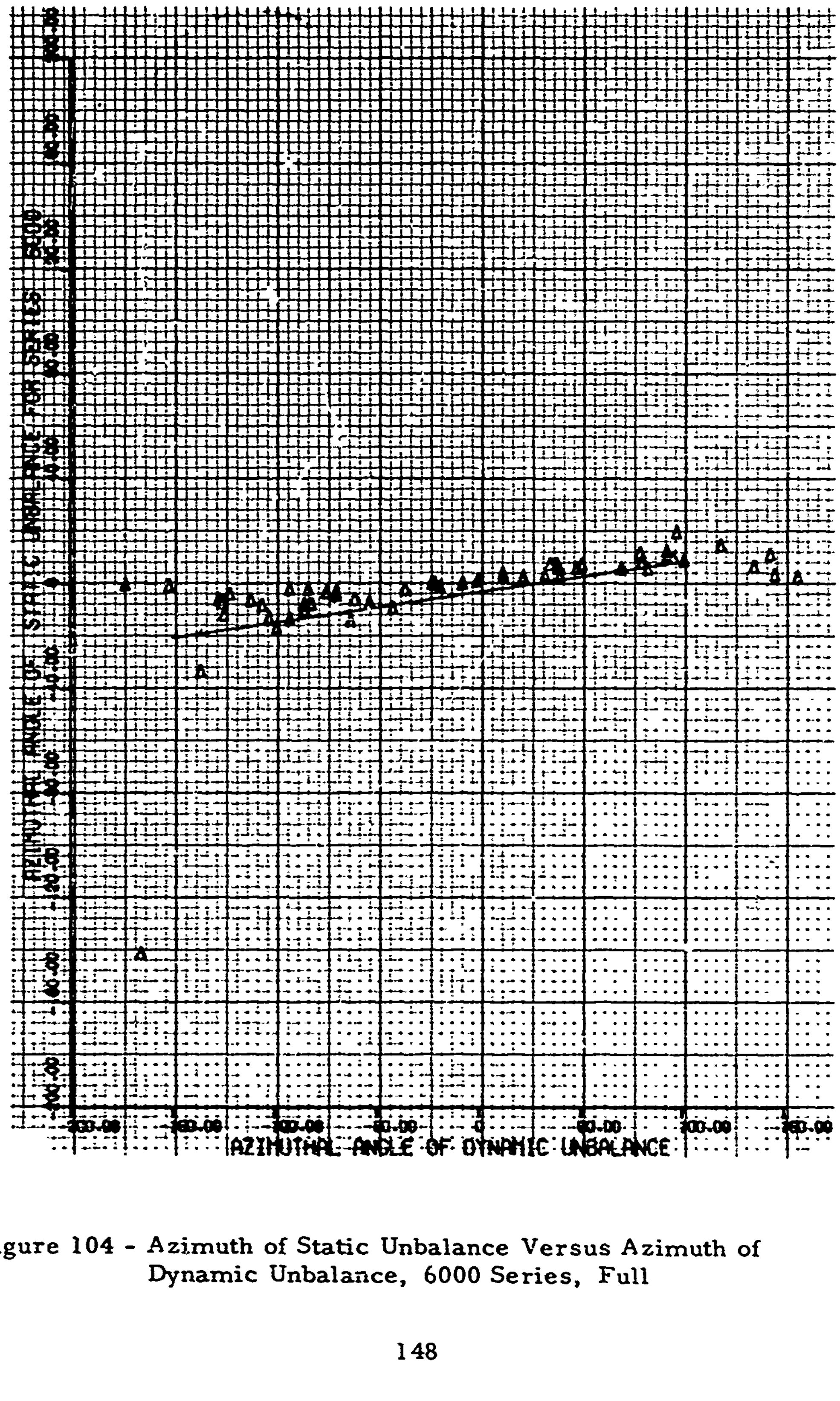

Figure 104 - Azimuth of Static Unbalance Versus Azimuth of Dynamic Unbalance, 6000 Series, Full

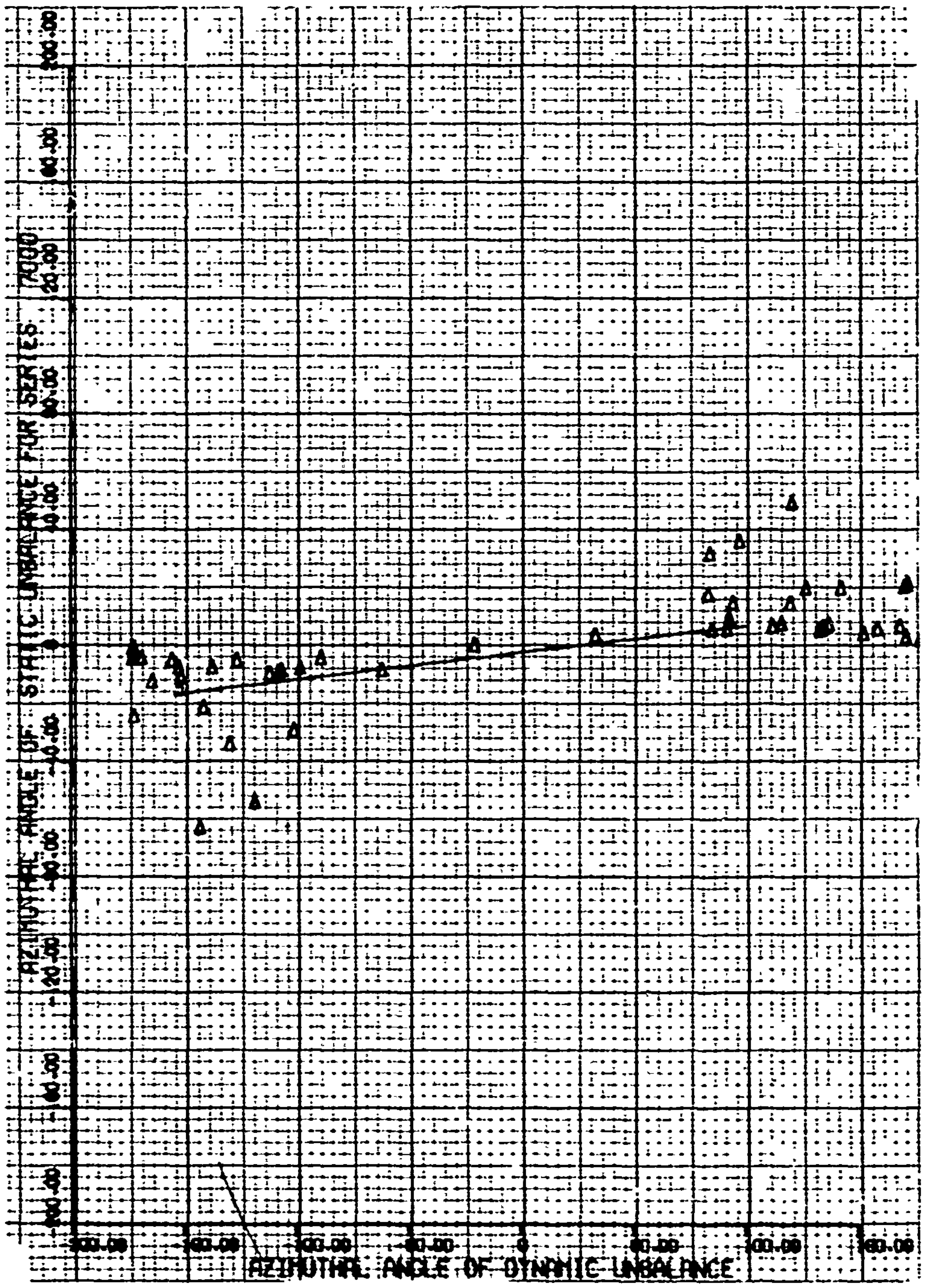

Figure 105 - Azimuth of Static Unbalance Versus Azimuth of Dynamic Unbalance, 7000 Series, Full

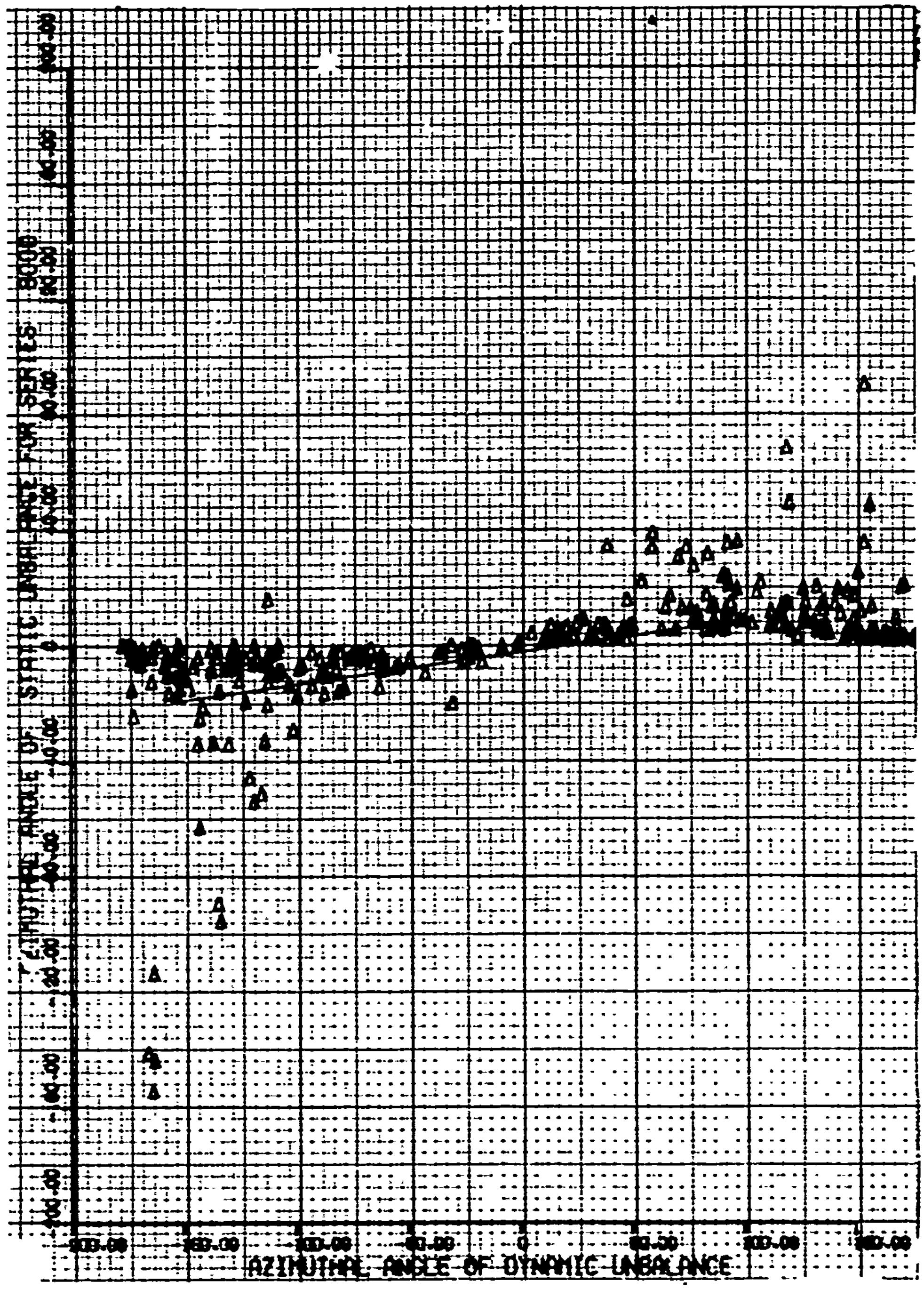

Figure 106 - Azimuth of Static Unbalance Versus Azimuth of Dynamic Unbalance, 8000 Series, Full

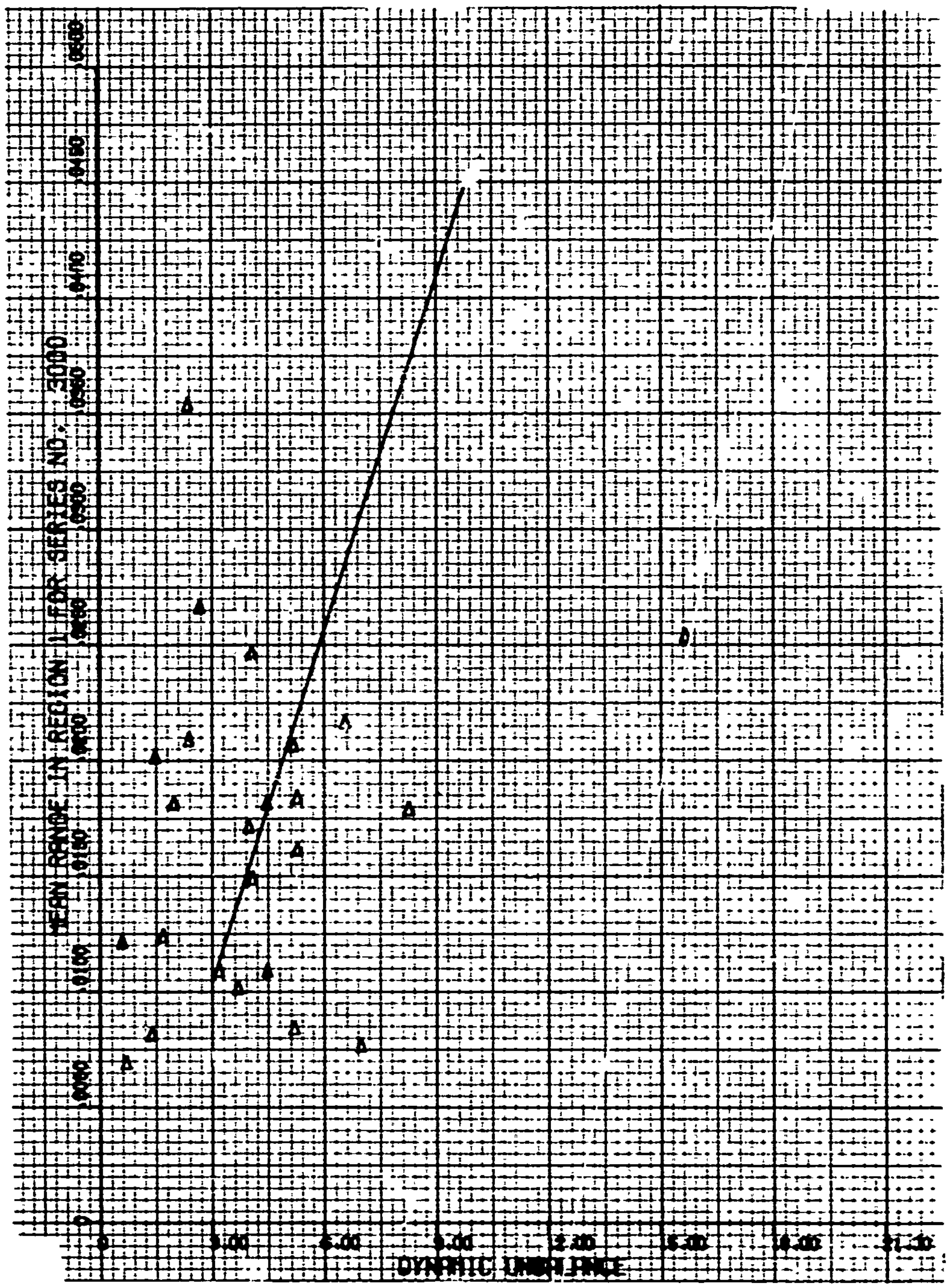

Figure 107 - Mean Wall Thickness Variation Versus Dynamic Unbalance, 3000 Series, Region 1, Empty

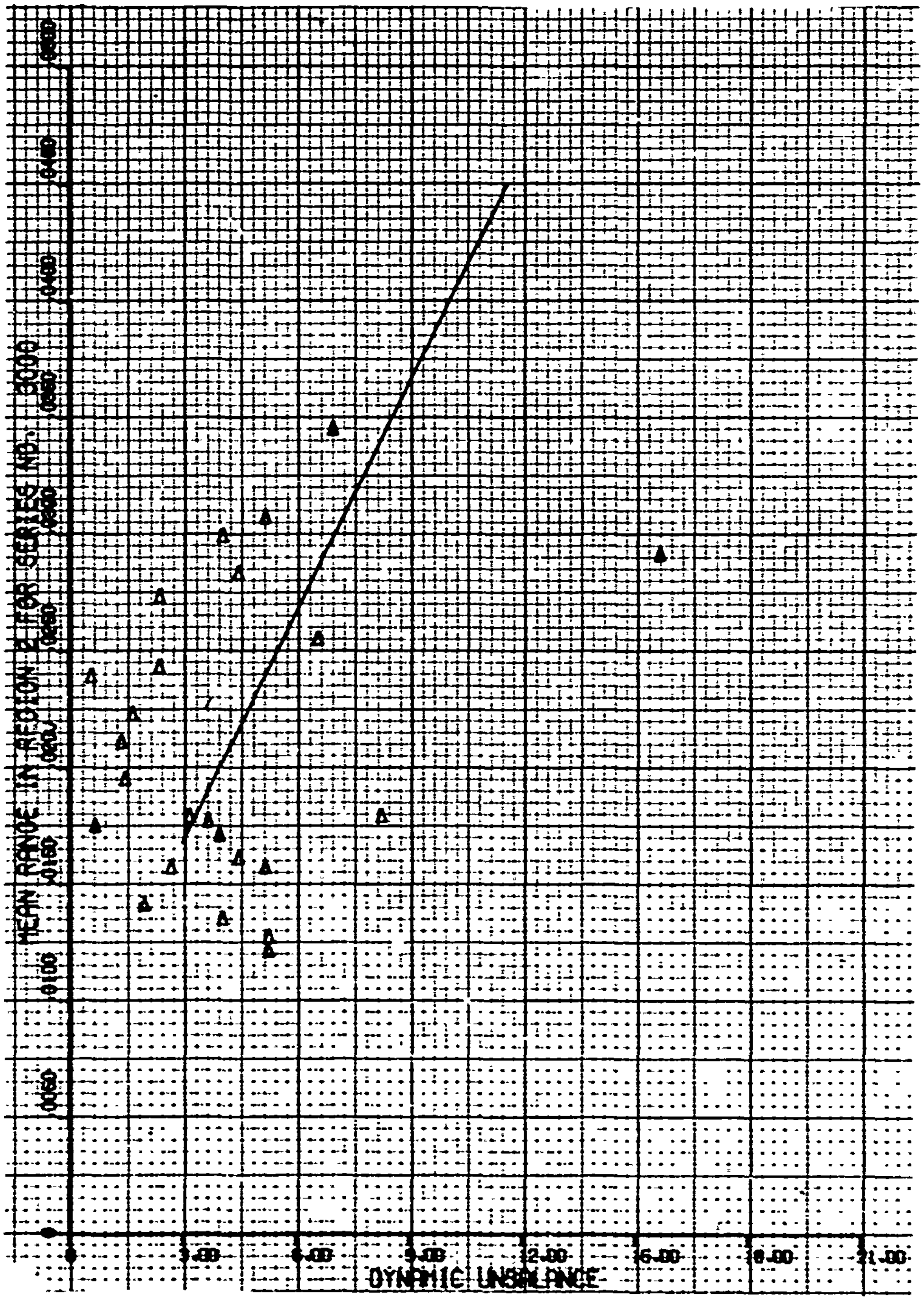

Figure 108 - Mean Wall Thickness Variation Versus Dynamic Unbalance, 3000 Series, Region 2, Empty

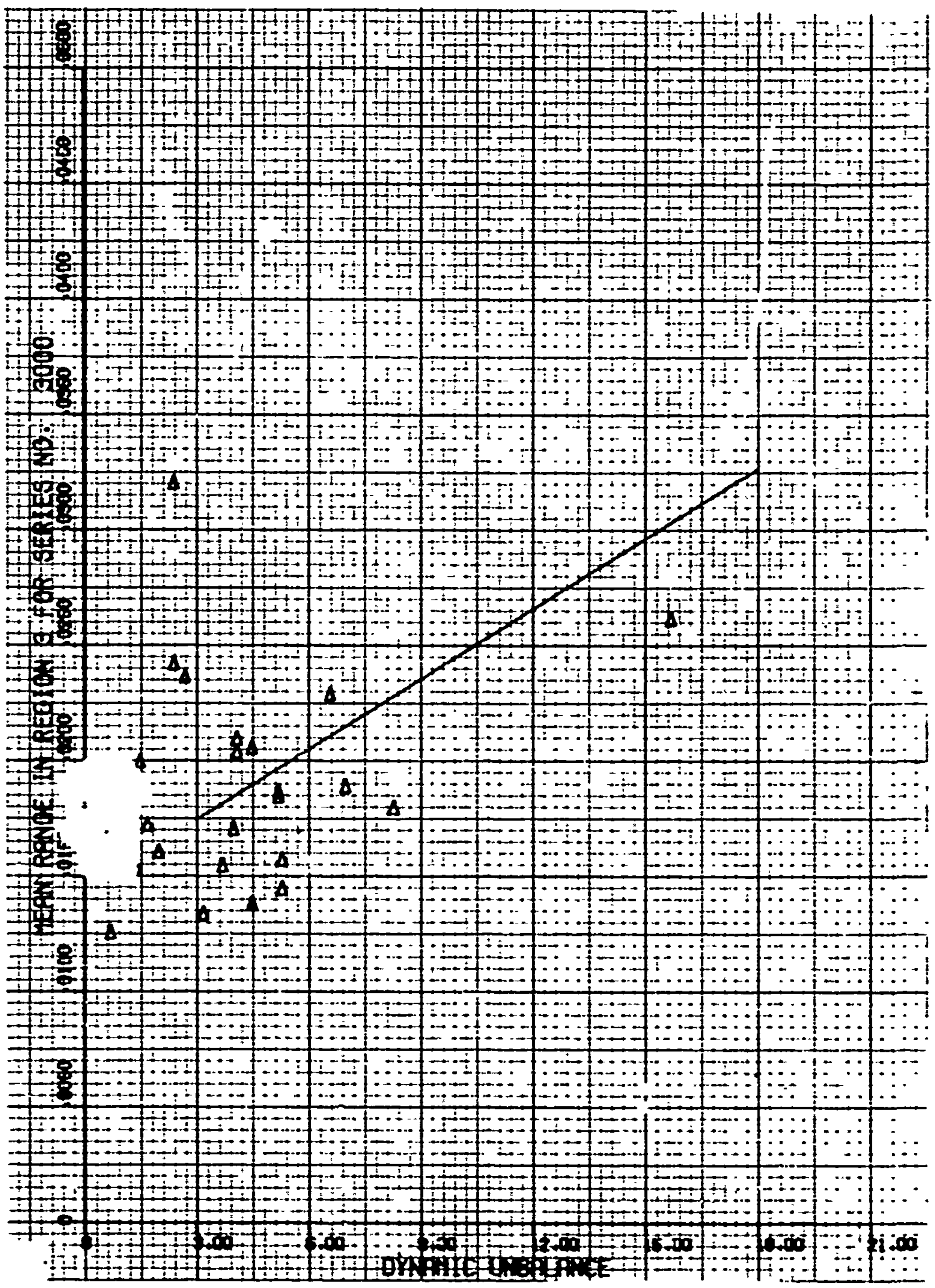

Figure 109 - Mean Wall Thickness Variation Versus Dynamic Unbalance, 3000 Series, Region 3, Empty

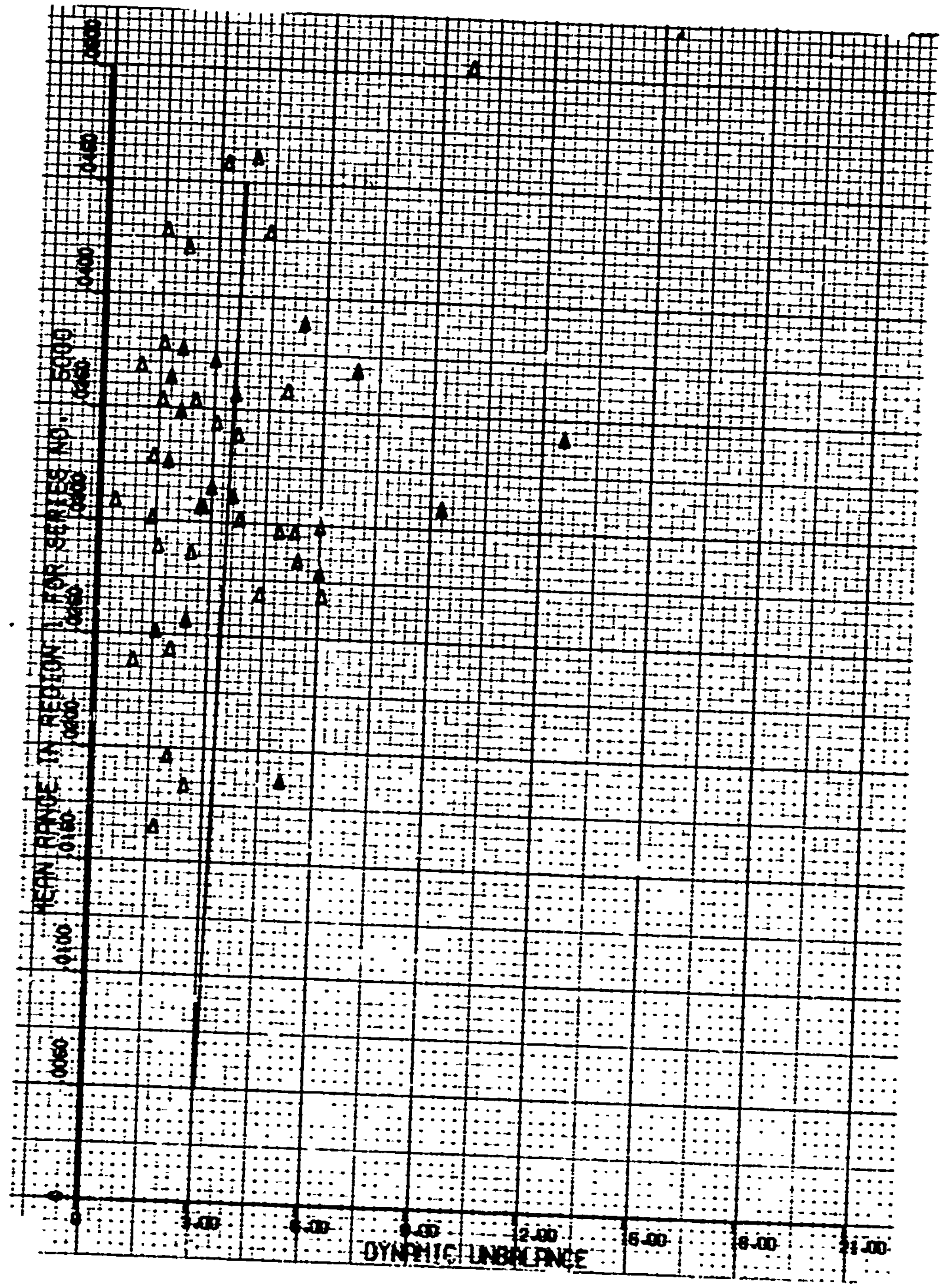

Figure 110 - Mean Wall Thickness Variation Versus Dynamic Unbalance, 5000 Series, Region 1, Empty

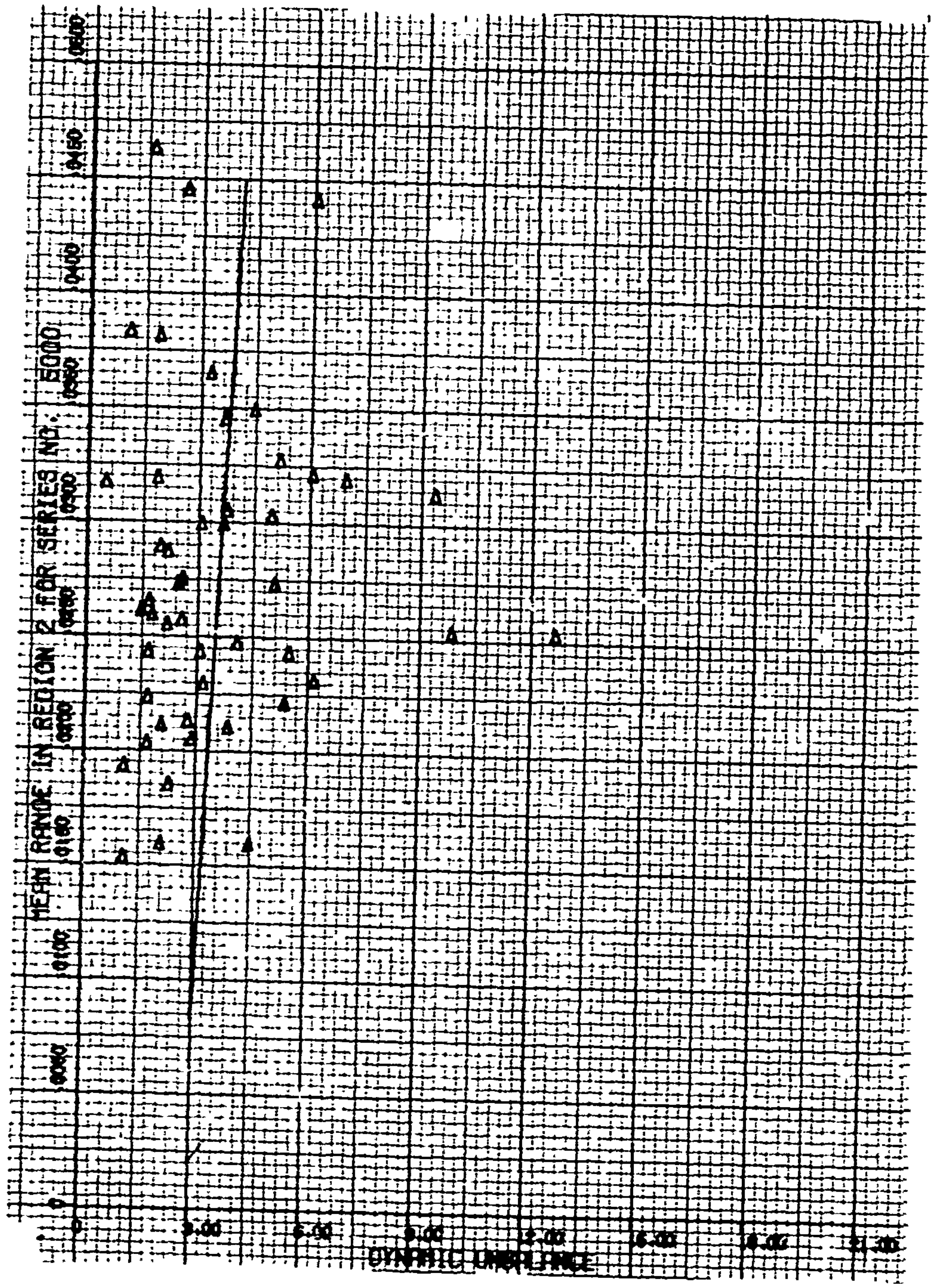

Figure 111 - Mean Wall Thickness Variation Versus Dynamic Unbalance, 5000 Series, Region 2, Empty

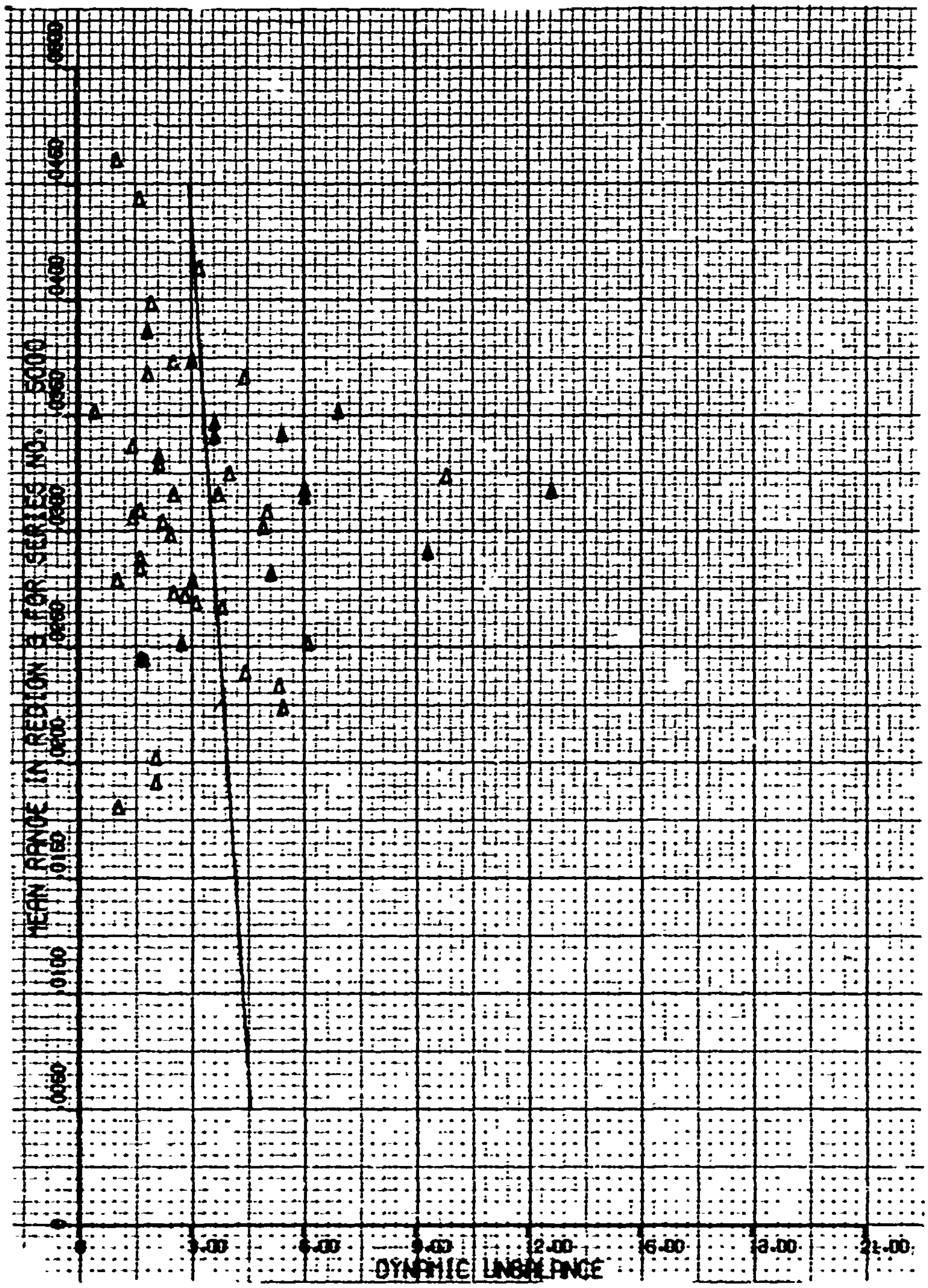

Figure 112 - Mean Wall Thickness Variation Versus Dynamic Unbalance, 5000 Series, Region 3, Empty

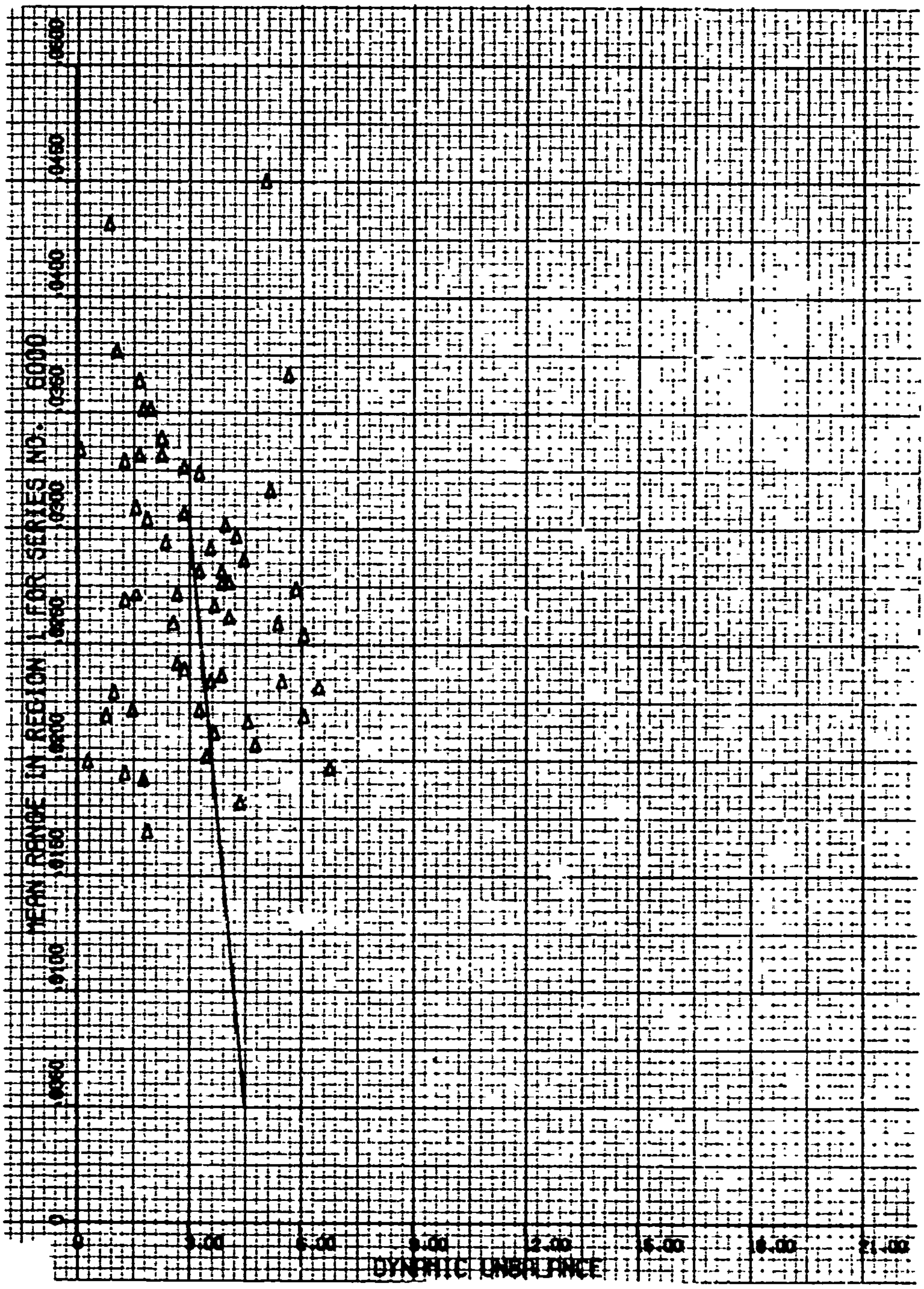

Figure 113 - Mean Wall Thickness Variation Versus Dynamic Unbalance, 6000 Series, Region 1, Empty

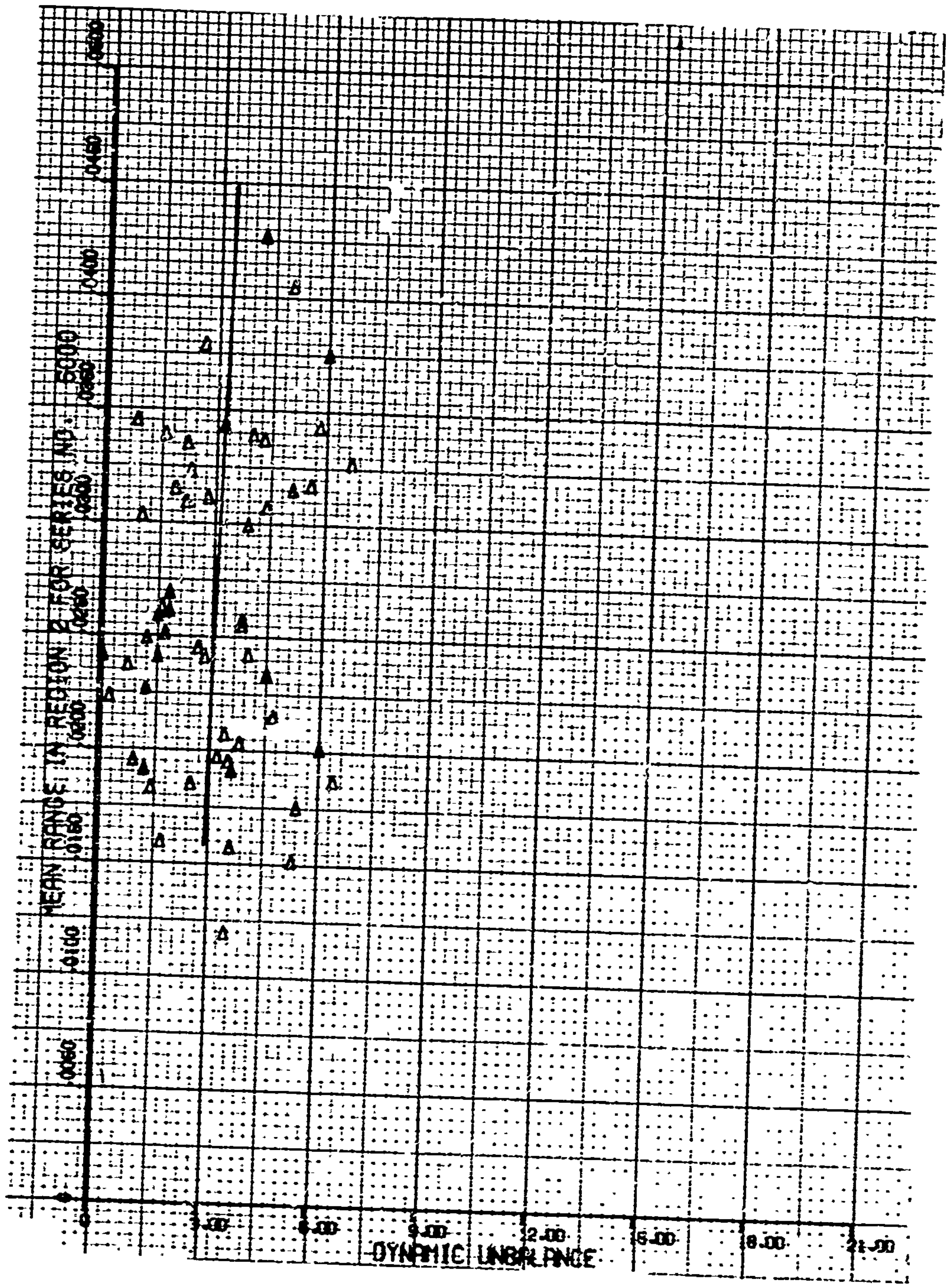

Figure 114 - Mean Wall Thickness Variation Versus Dynamic Unbalance, 6000 Series, Region 2, Empty

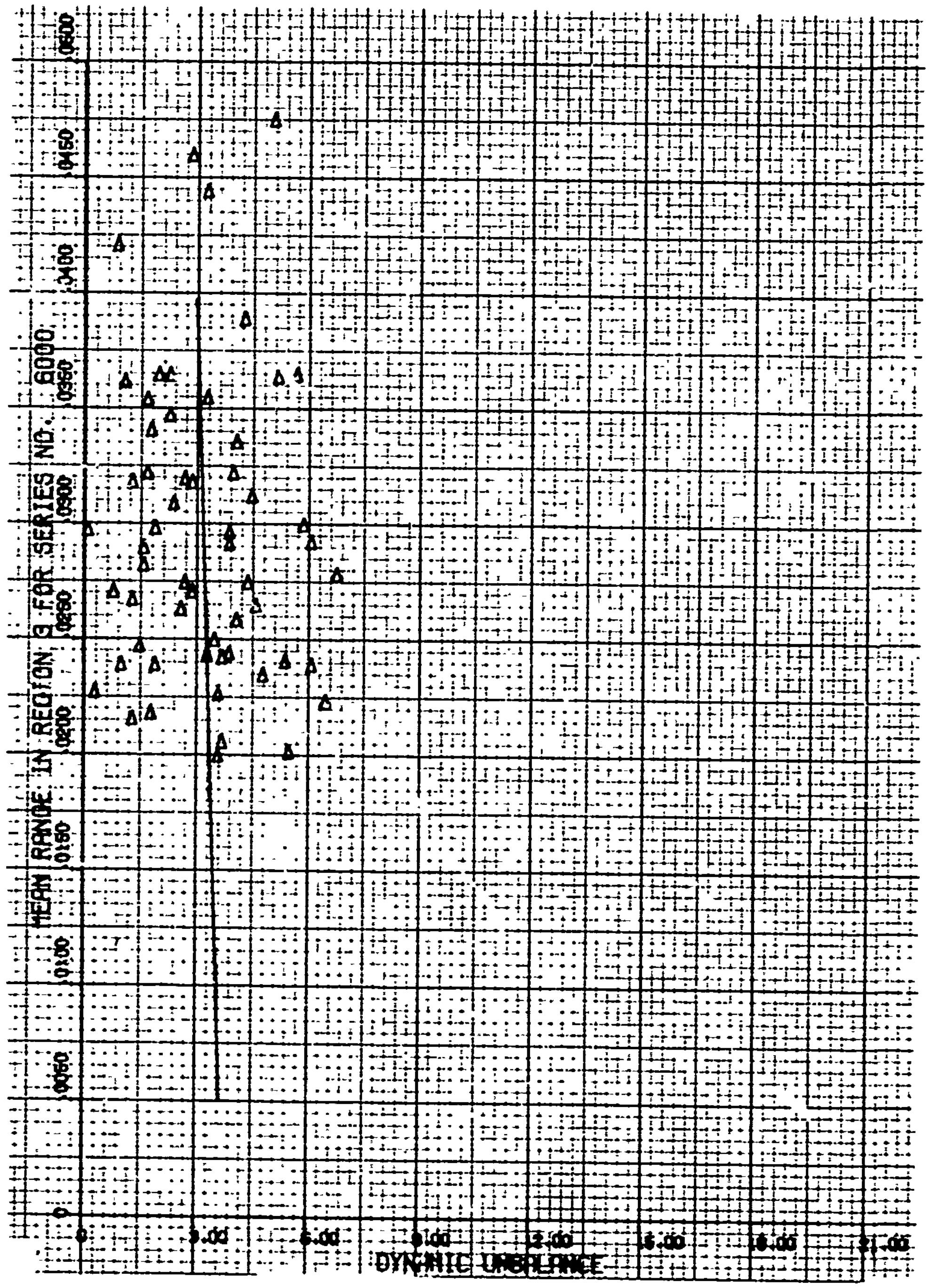

Figure 115 - Mean Wall Thickness Variation Versus Dynamic Unbalance, 6000 Series, Region 3, Empty

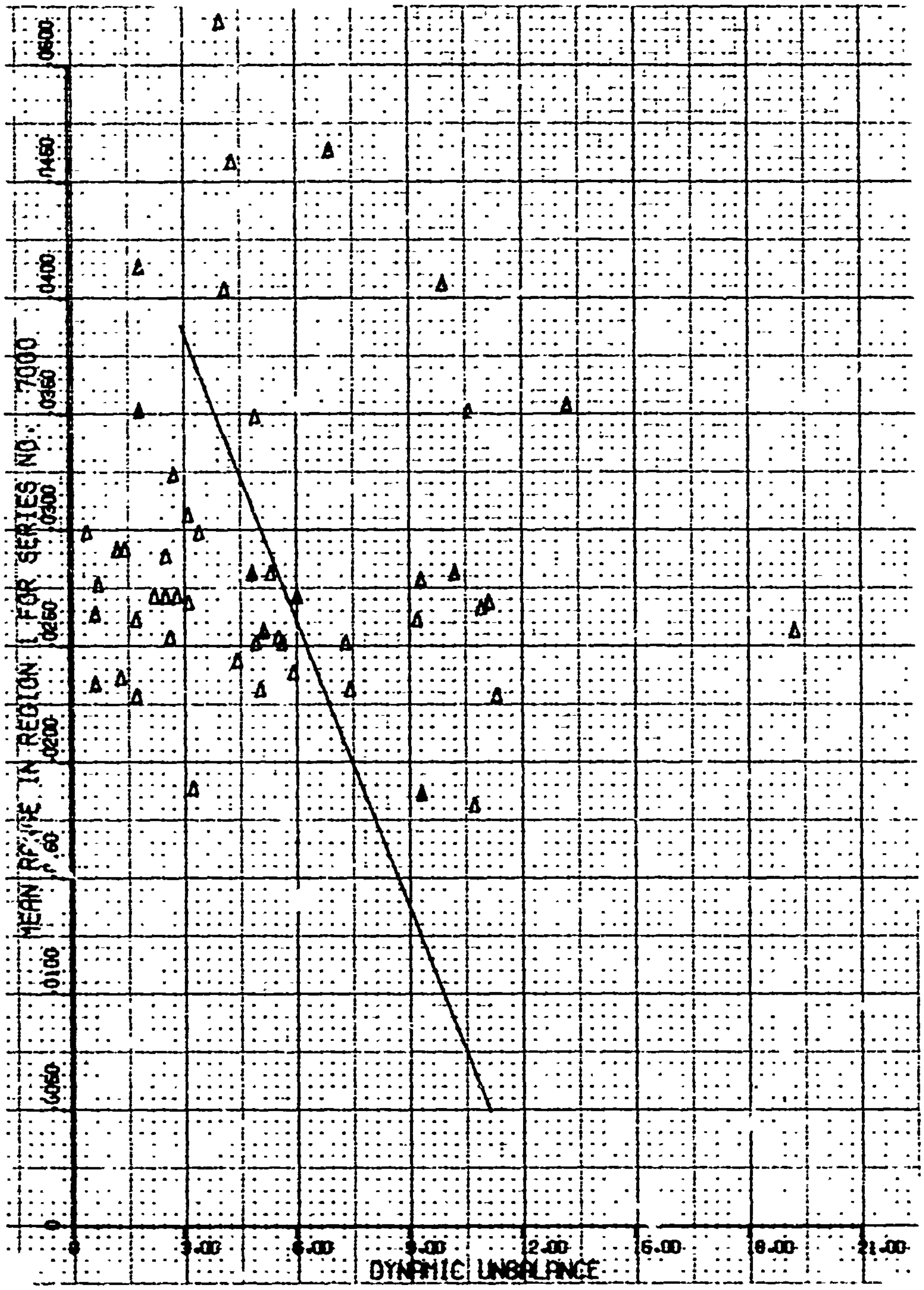

Figure 116 - Mean Wall Thickness Variation Versus Dynamic Unbalance, 7000 Series, Region 1, Empty

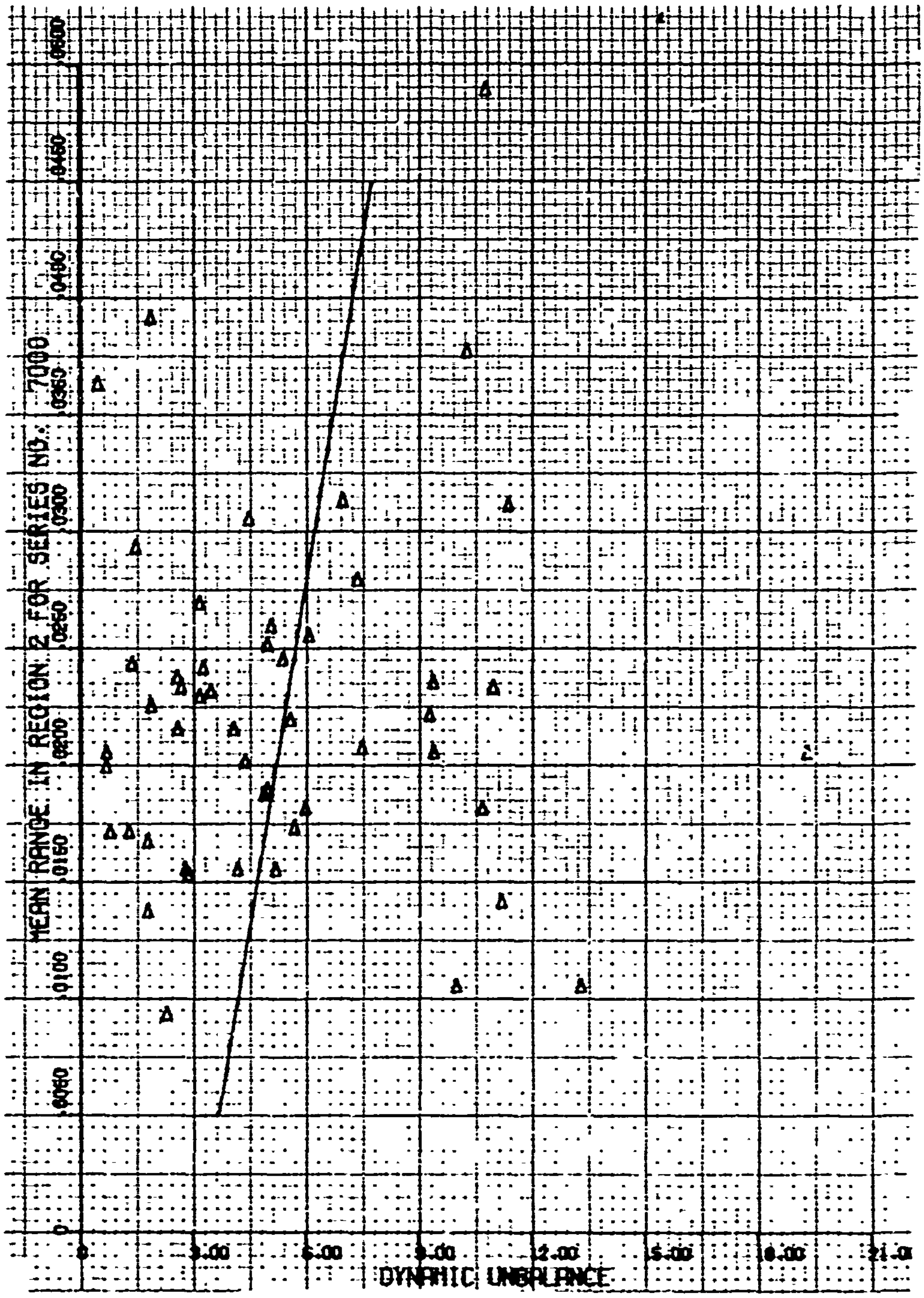

Figure 117 - Mean Wall Thickness Variation Versus Dynamic Unbalance, 7000 Series, Region 2, Empty

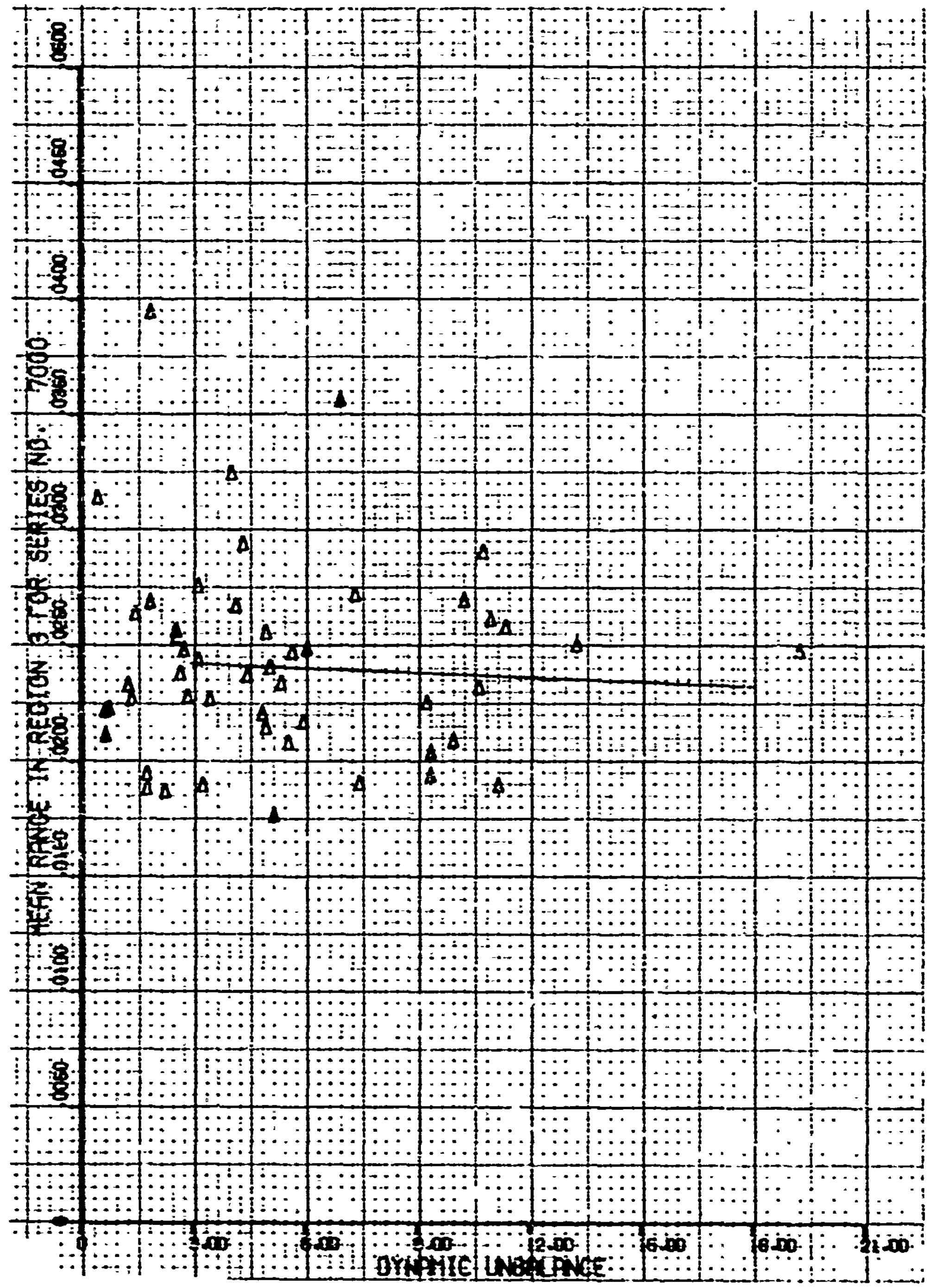

Figure 118 - Mean Wall Thickness Variation Versus Dynamic Unbalance, 7000 Series, Region 3, Empty

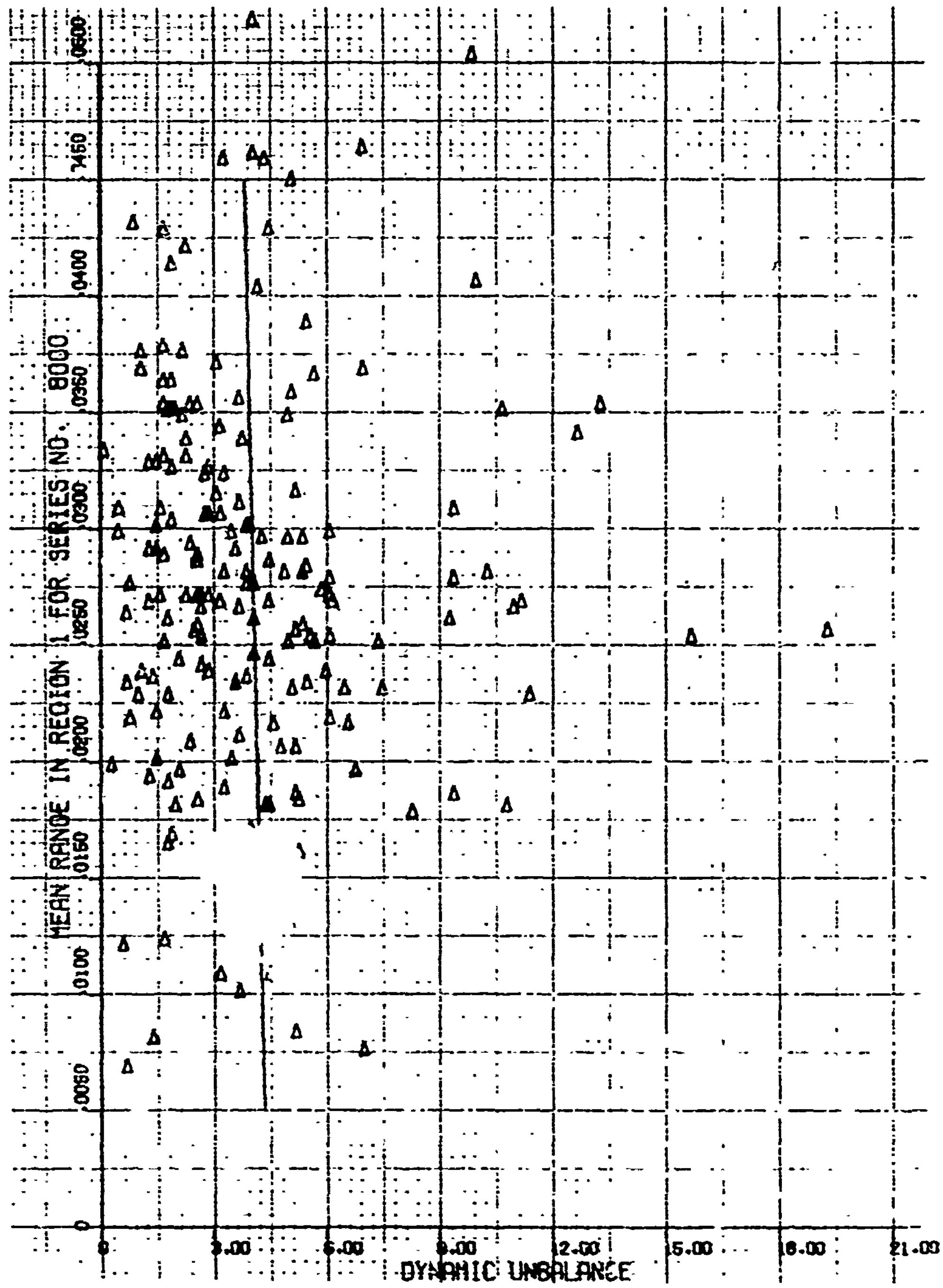

Figure 119 - Mean Wall Thickness Variation Versus Dynamic Unbalance, 8000 Series, Region 1, Empty

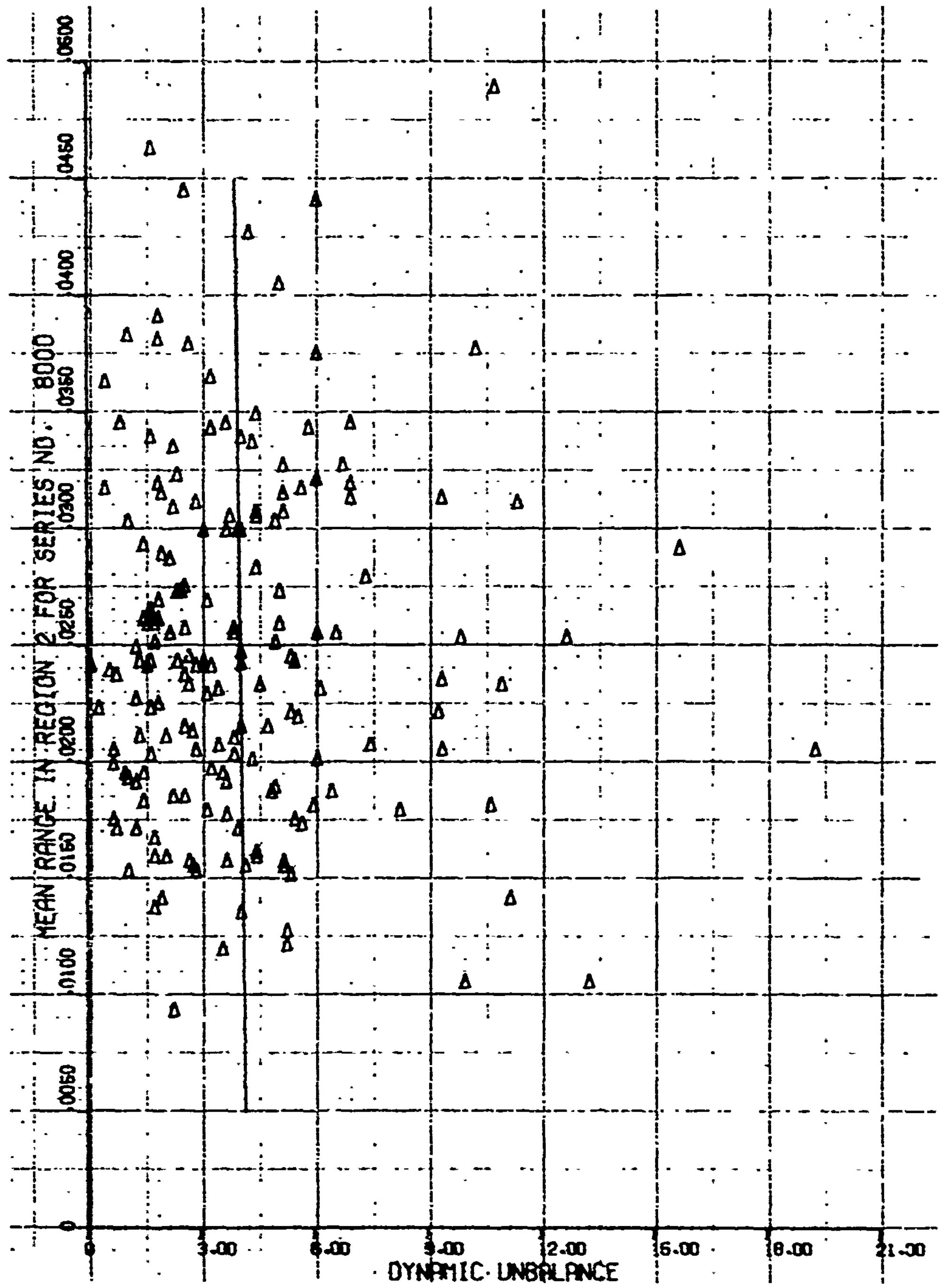

Figure 120 - Mean Wall Thickness Variation Versus Dynamic Unbalance, 8000 Series, Region 2, Empty

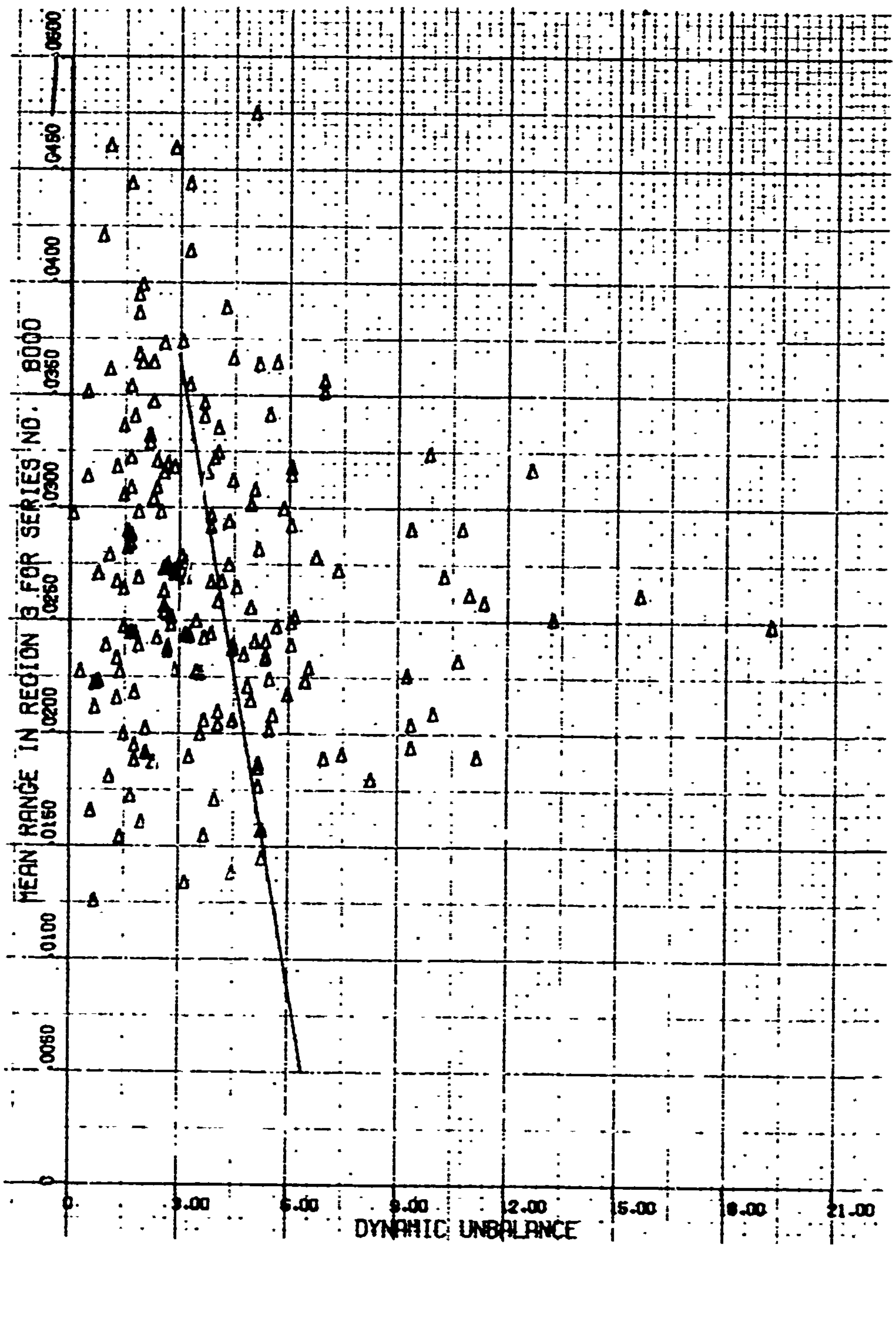

Figure 121 - Mean Wall Thickness Variation Versus Dynamic Unbalance, 8000 Series, Region 3, Empty

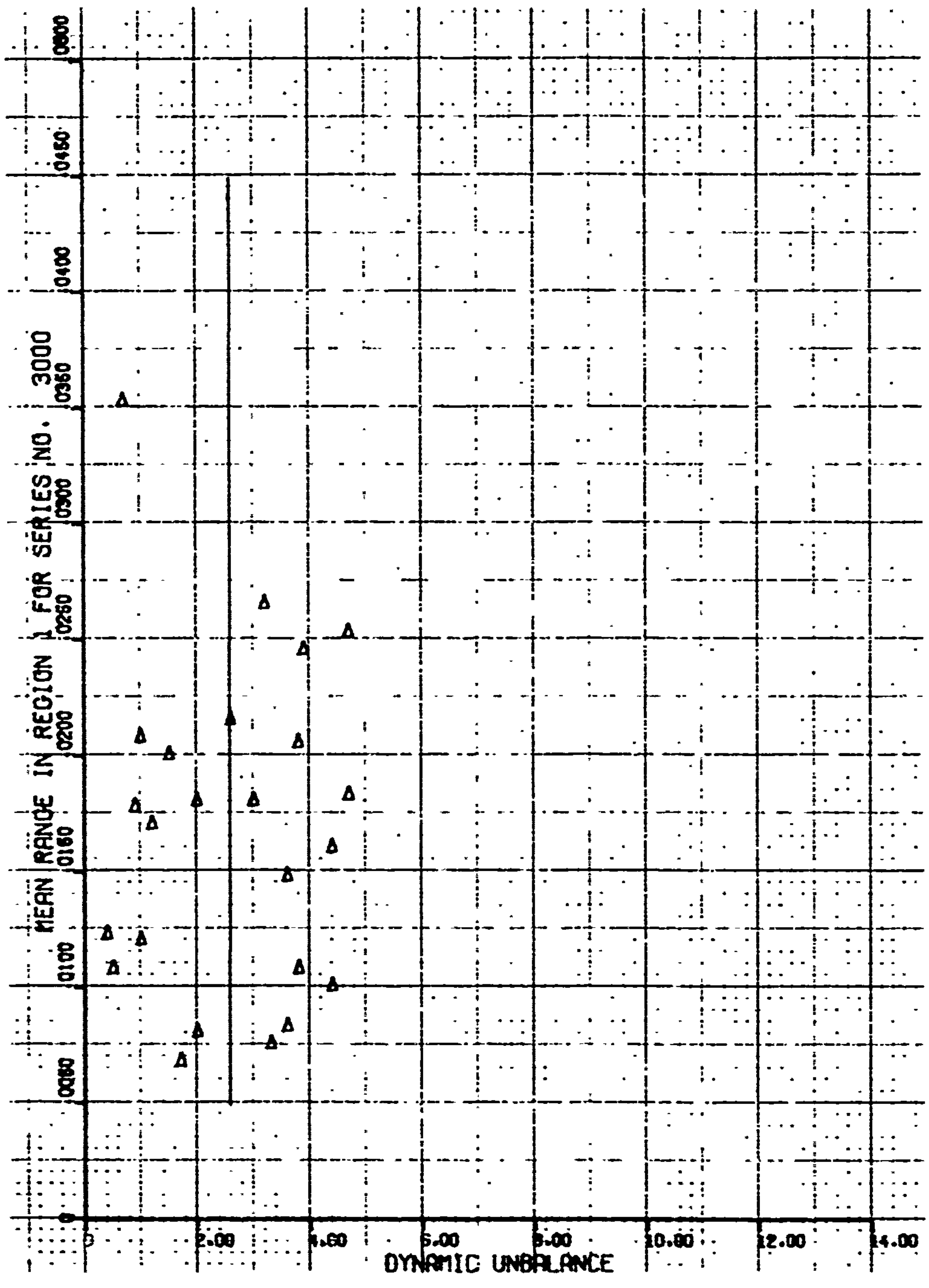

Figure 122 - Mean Wall Thickness Variation Versus Dynamic Unbalance,
3000 Series, Region 1, Full

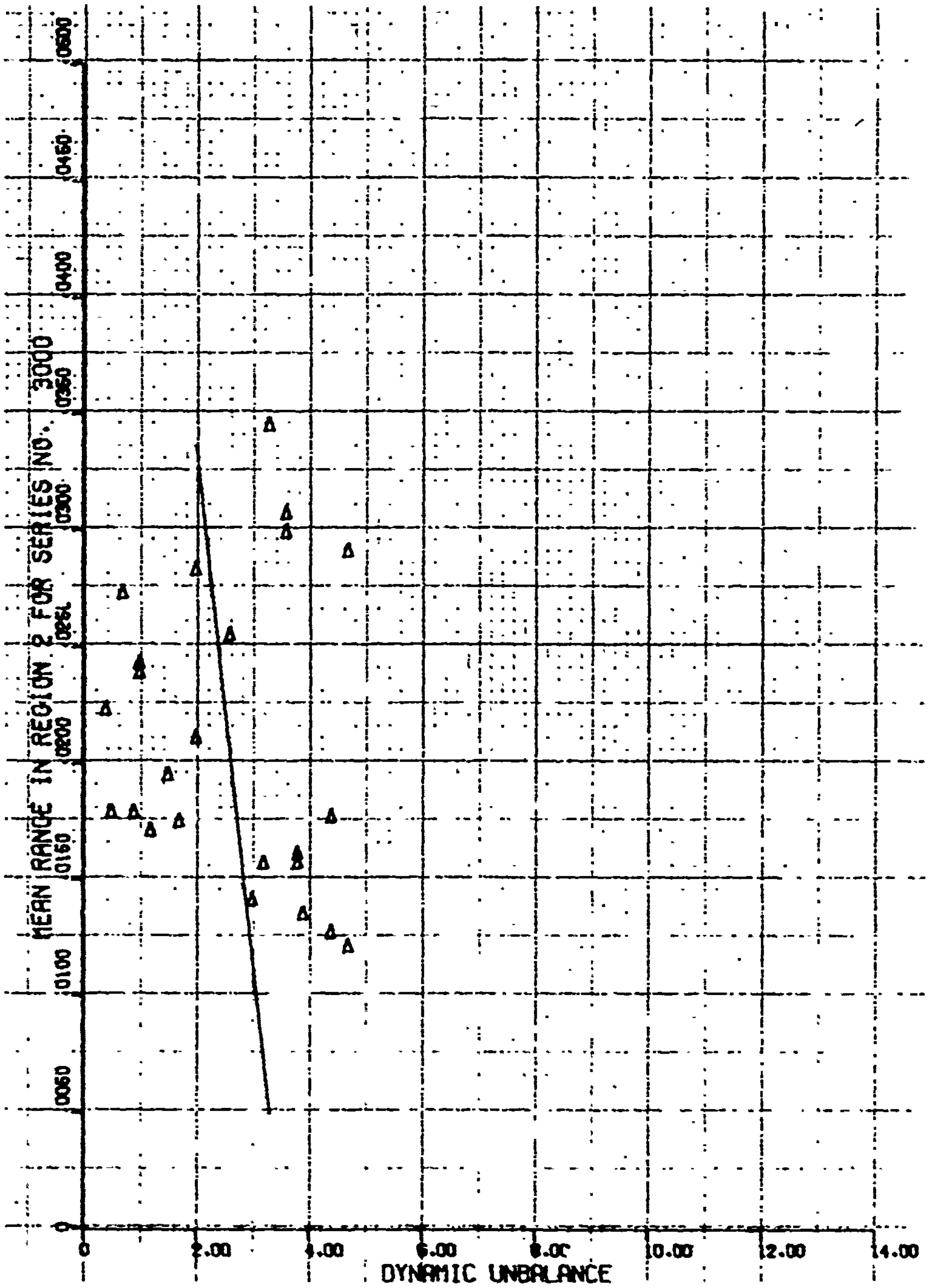

Figure 123 - Mean Wall Thickness Variation Versus Dynamic Unbalance, 3000 Series, Region 2, Full

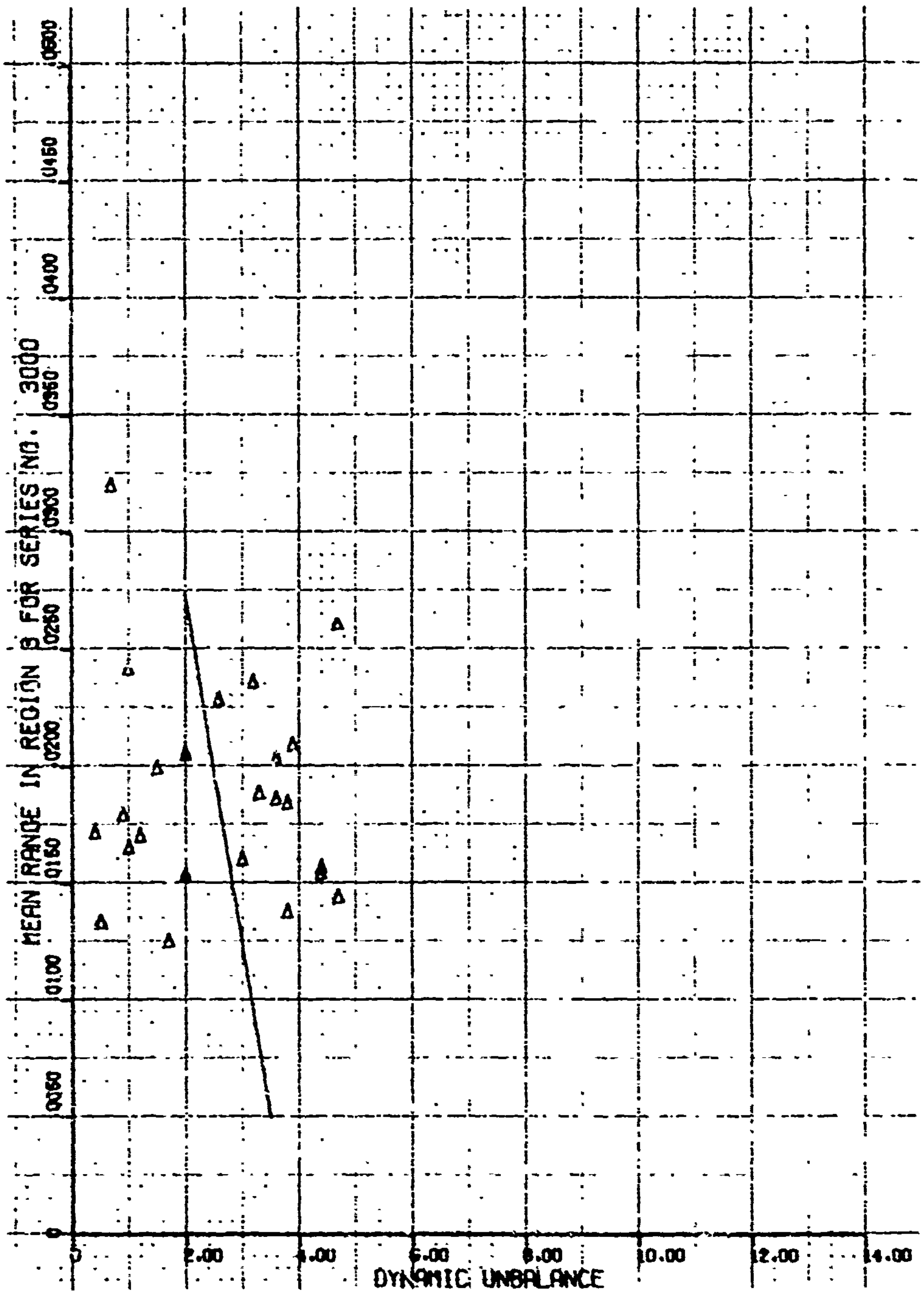

Figure 124 - Mean Wall Thickness Variation Versus Dynamic Unbalance, 3000 Series, Region 3, Full

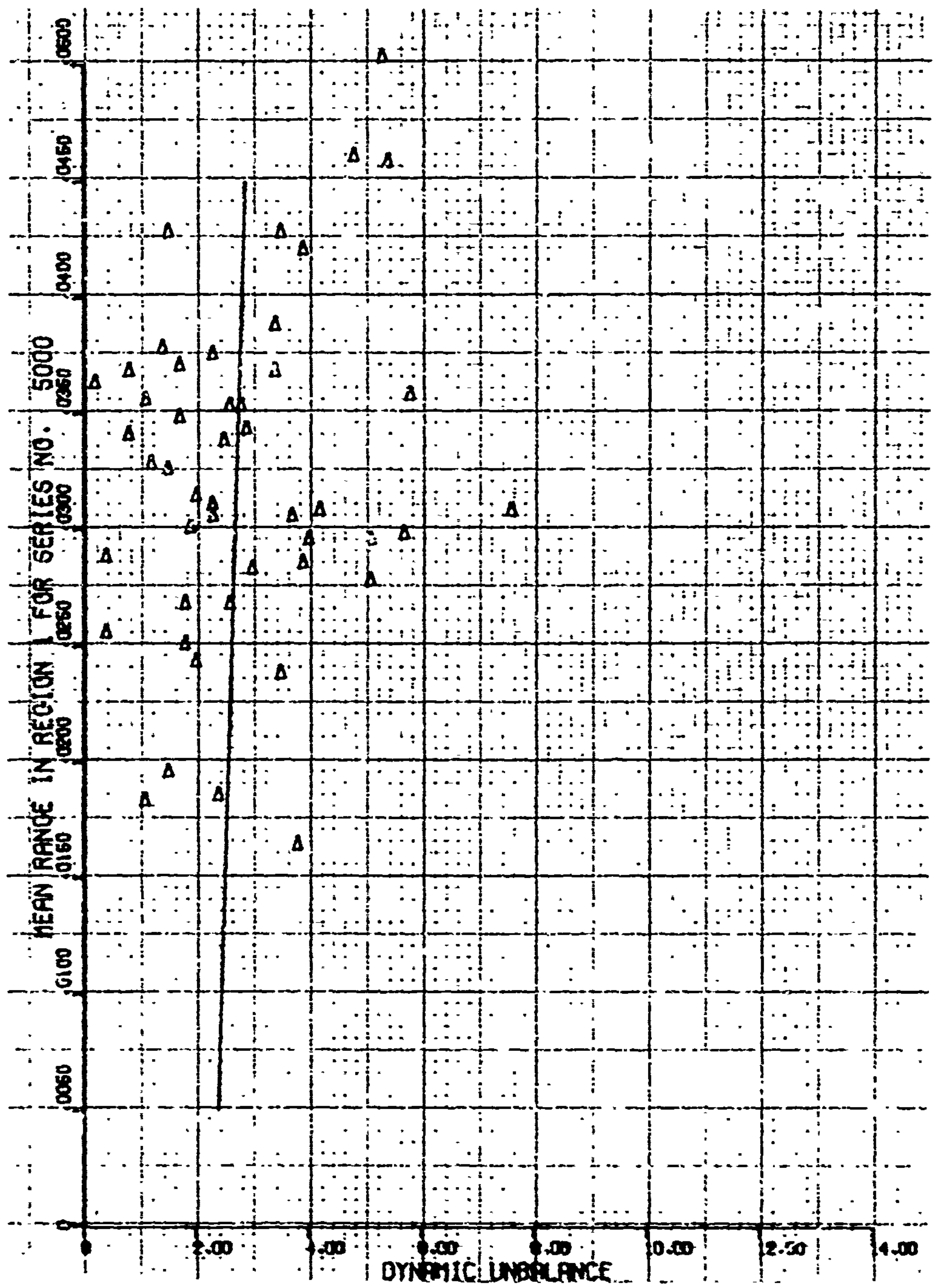

Figure 125 - Mean Wall Thickness Variation Versus Dynamic Unbalance, 5000 Series, Region 1, Full

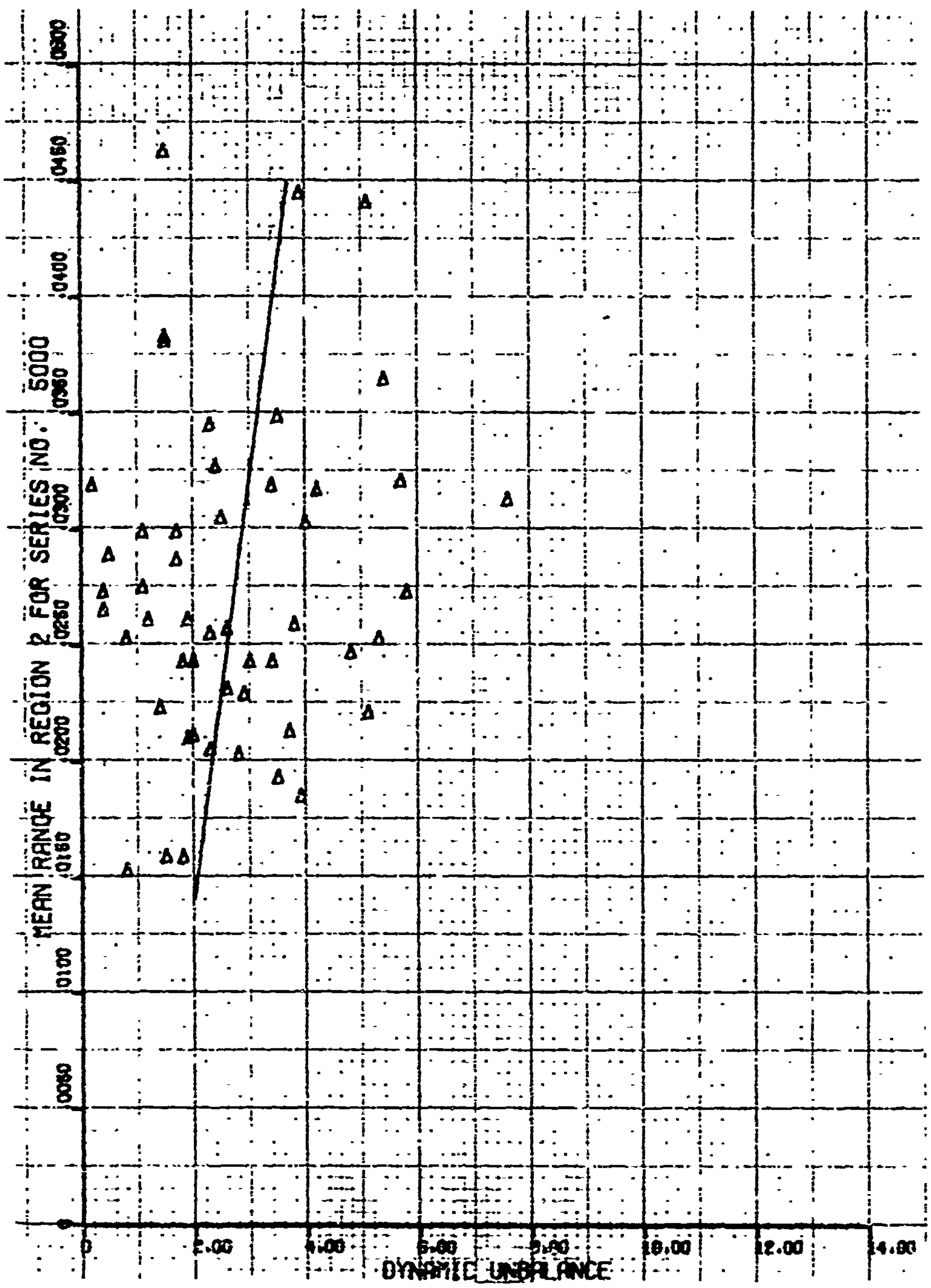

Figure 126 - Mean Wall Thickness Variation Versus Dynamic Unbalance, 5000 Series, Region 2, Full

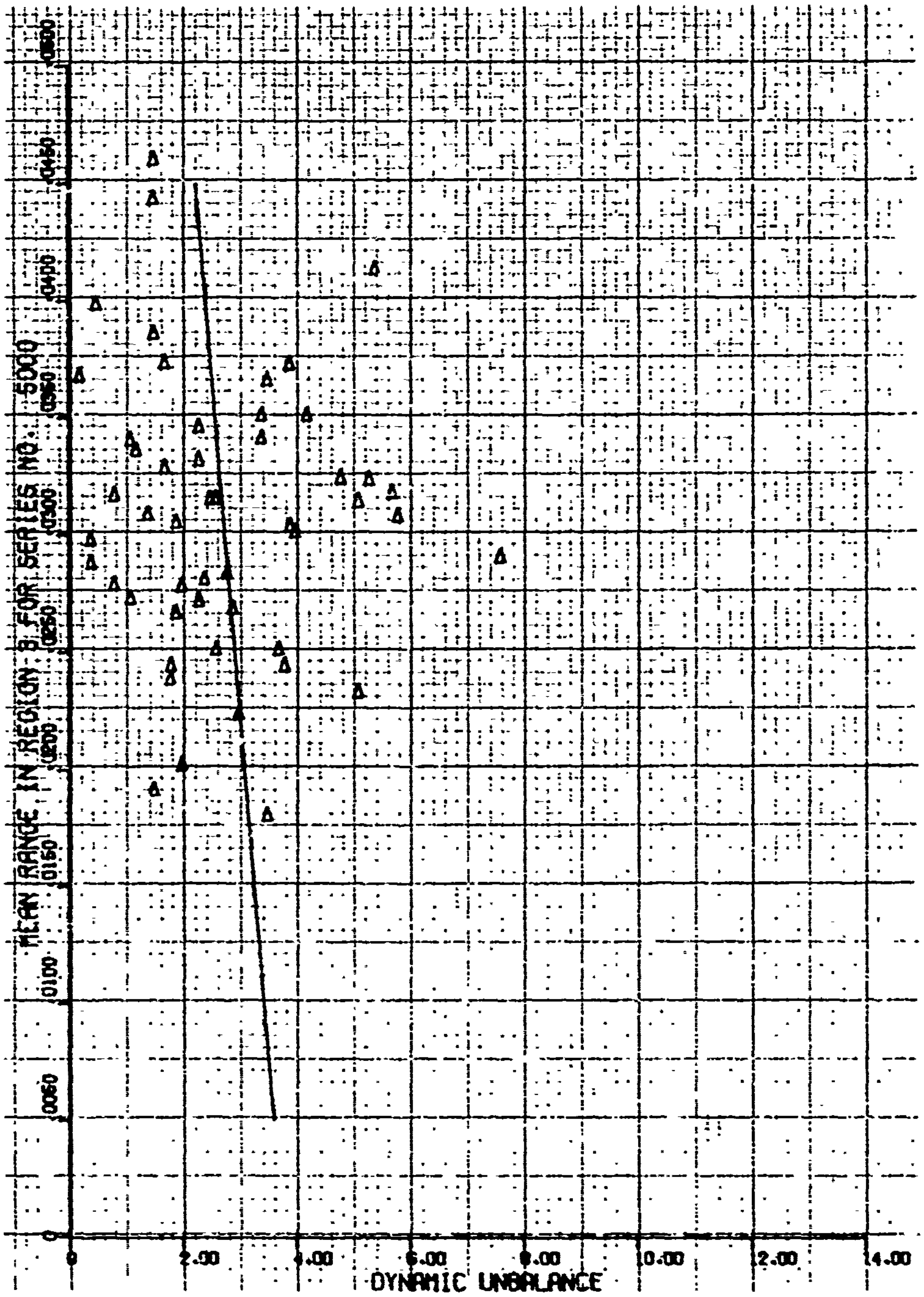

Figure 127 - Mean Wall Thickness Variation Versus Dynamic Unbalance, 5000 Series, Region 3, Full

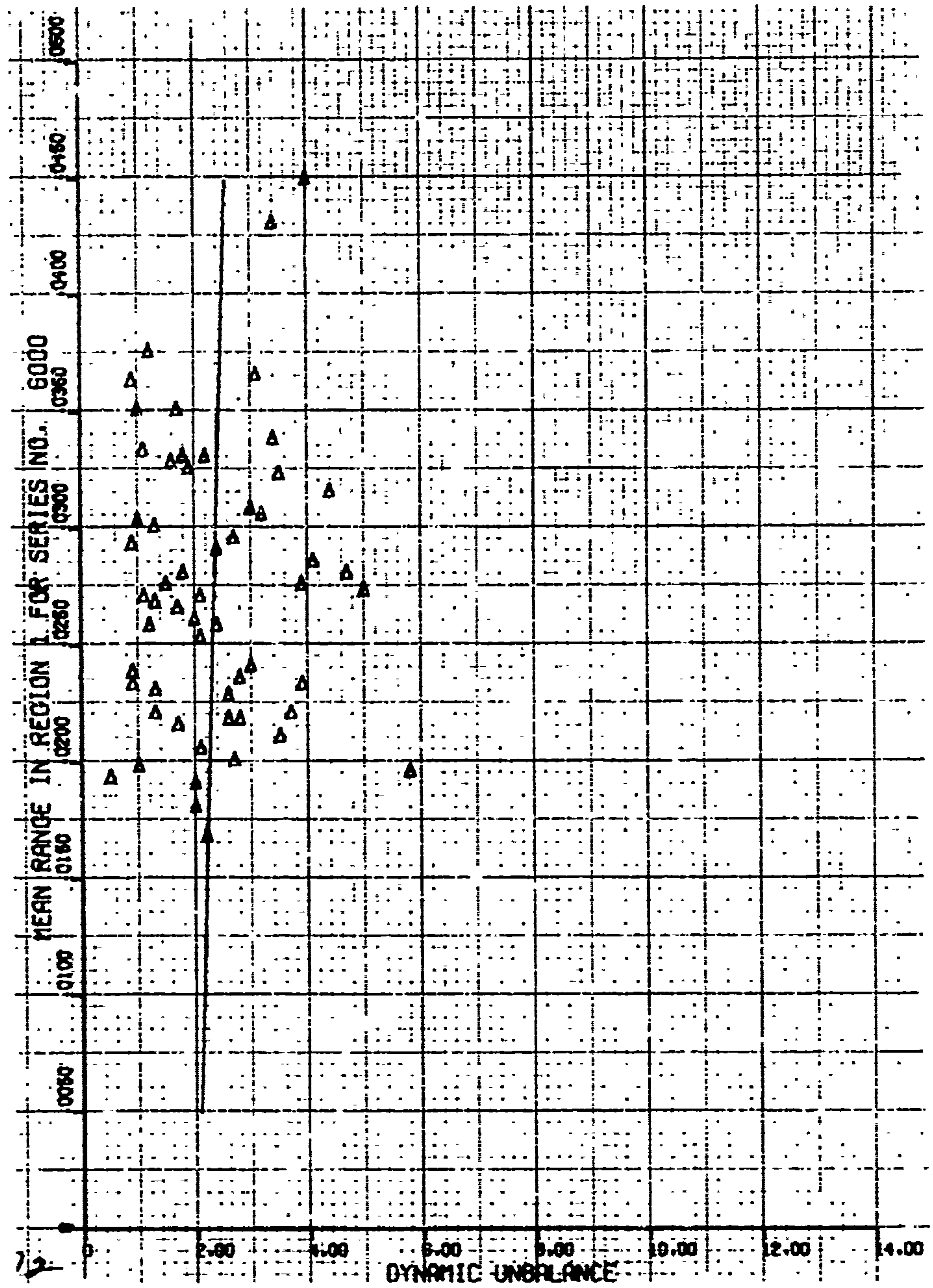

Figure 128 - Mean Wall Thickness Variation Versus Dynamic Unbalance, 6000 Series, Region 1, Full

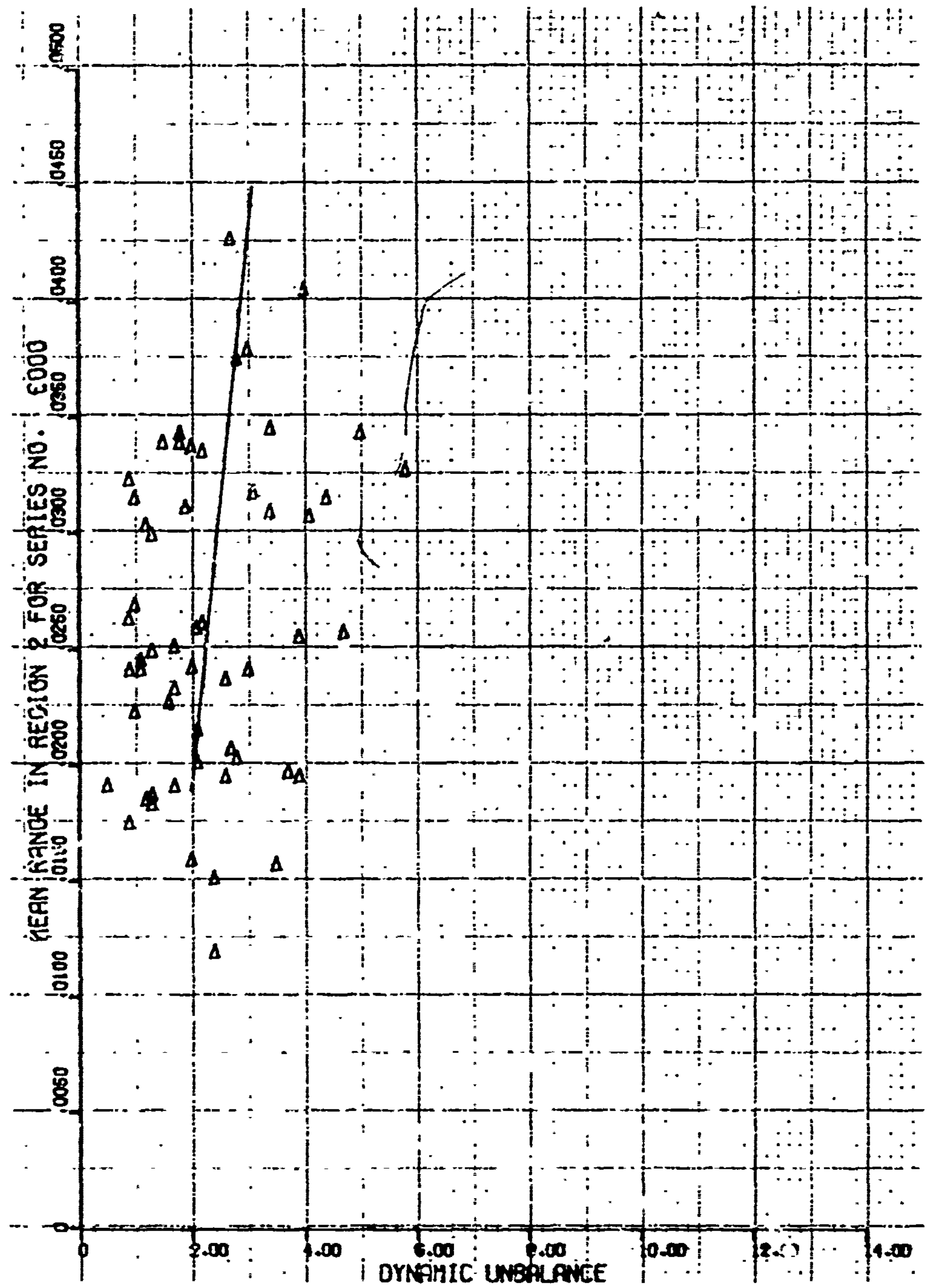

Figure 129 - Mean Wall Thickness Variation Versus Dynamic Unbalance, 6000 Series, Region 2, Full

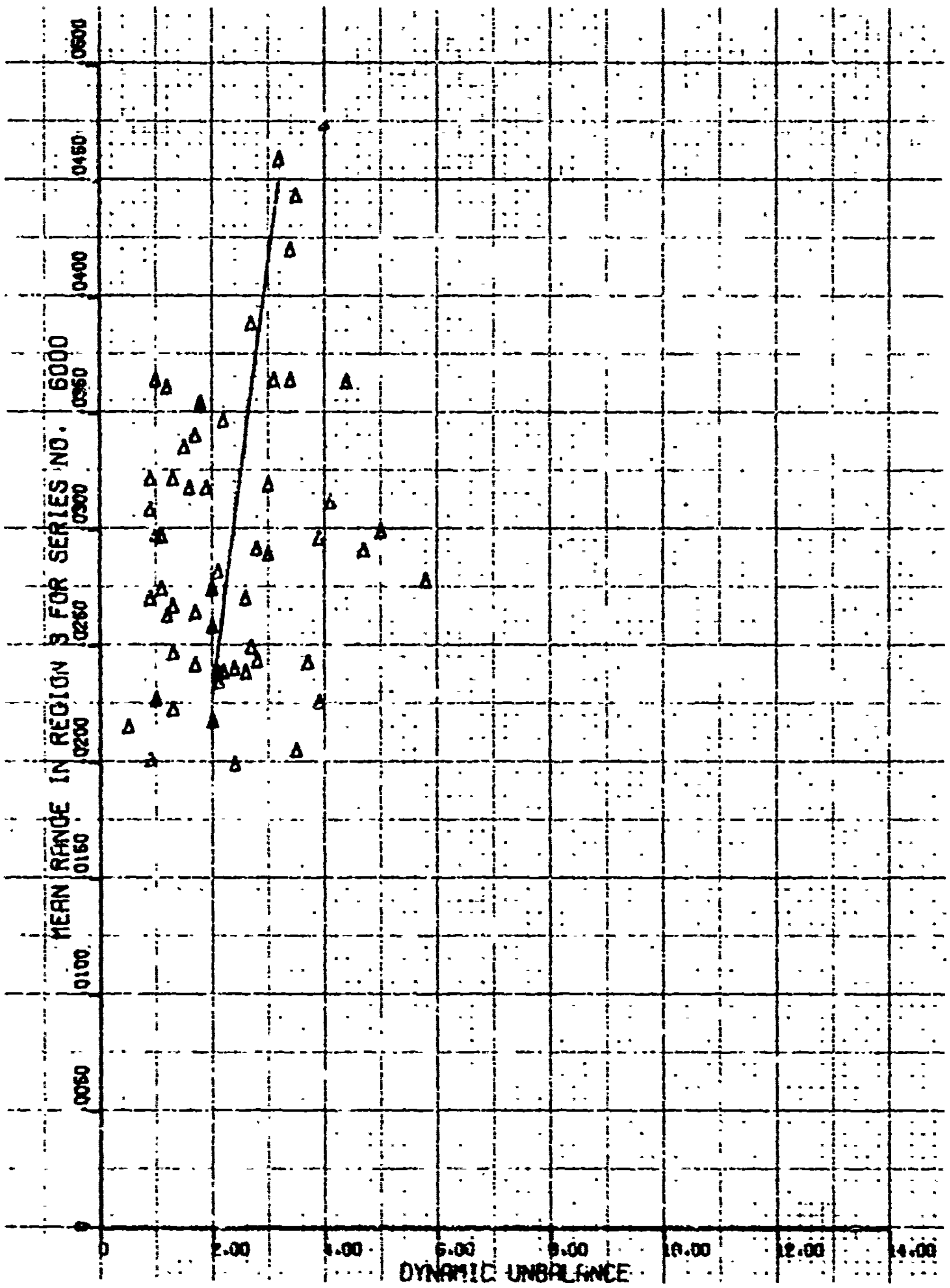

Figure 130 - Mean Wall Thickness Variation Versus Dynamic Unbalance, 6000 Series, Region 3, Full

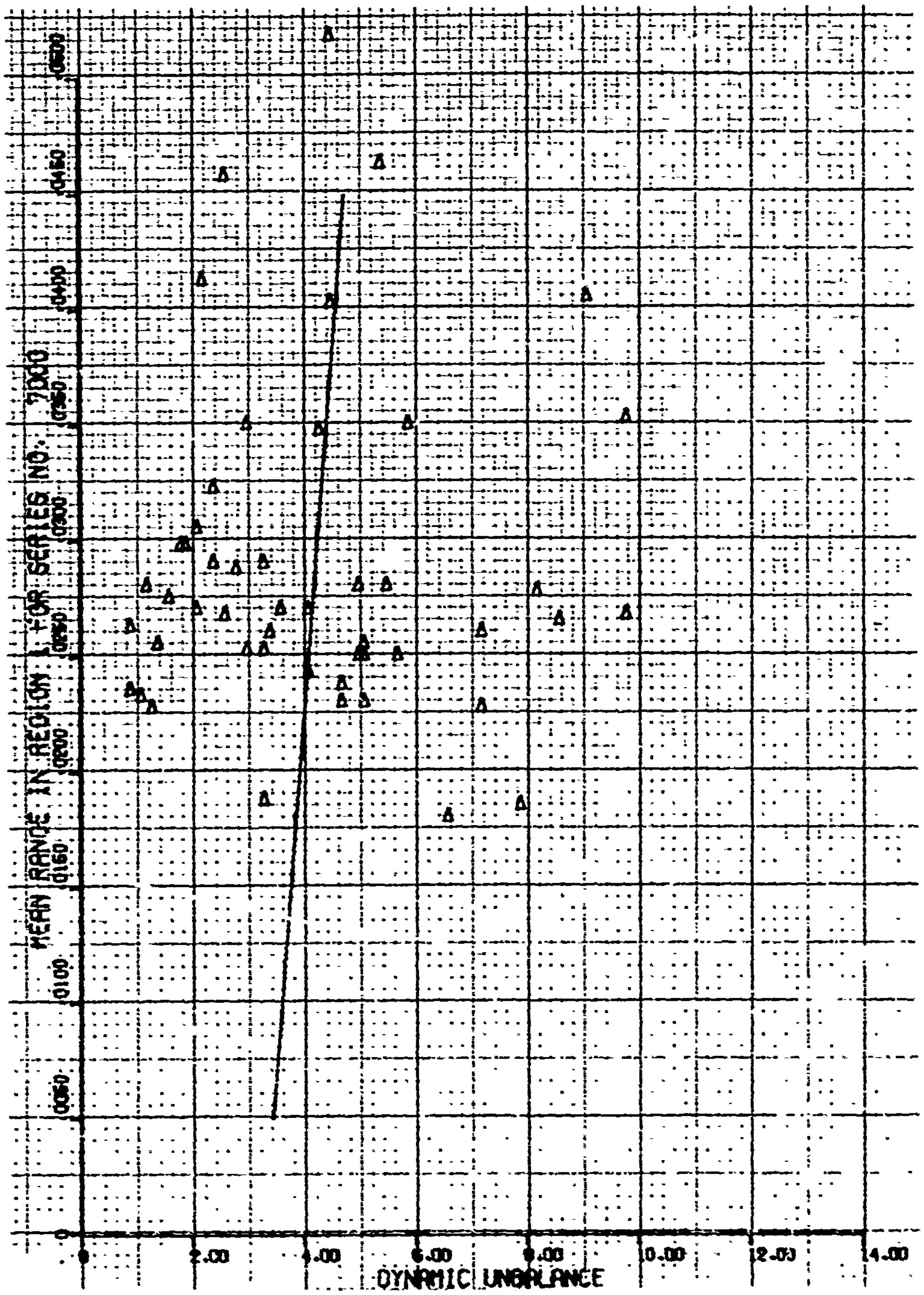

Figure 131 - Mean Wall Thickness Variation Versus Dynamic Unbalance, 7000 Series, Region 1, Full

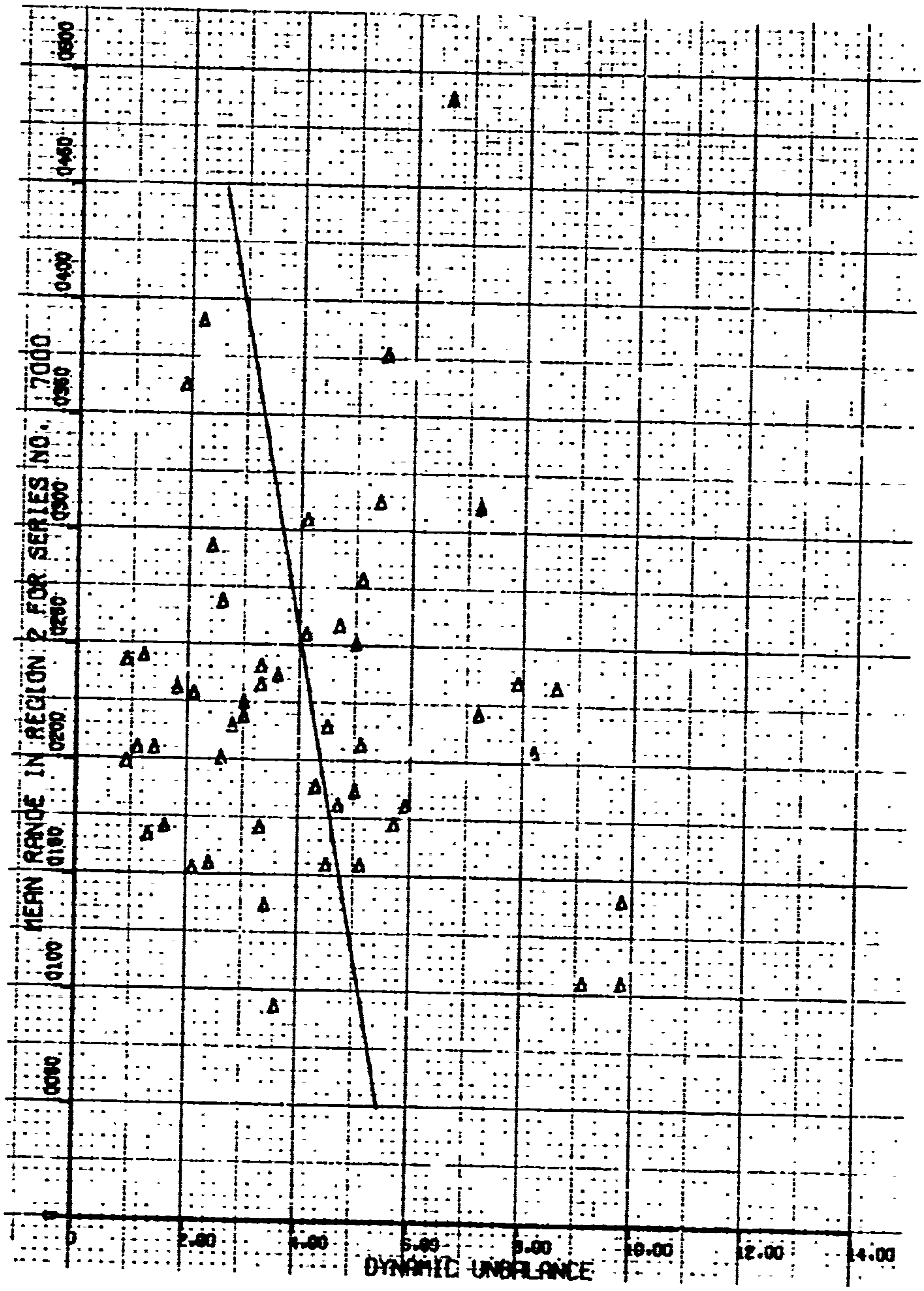

Figure 132 - Mean Wall Thickness Variation Versus Dynamic Unbalance, 7000 Series, Region 2, Full

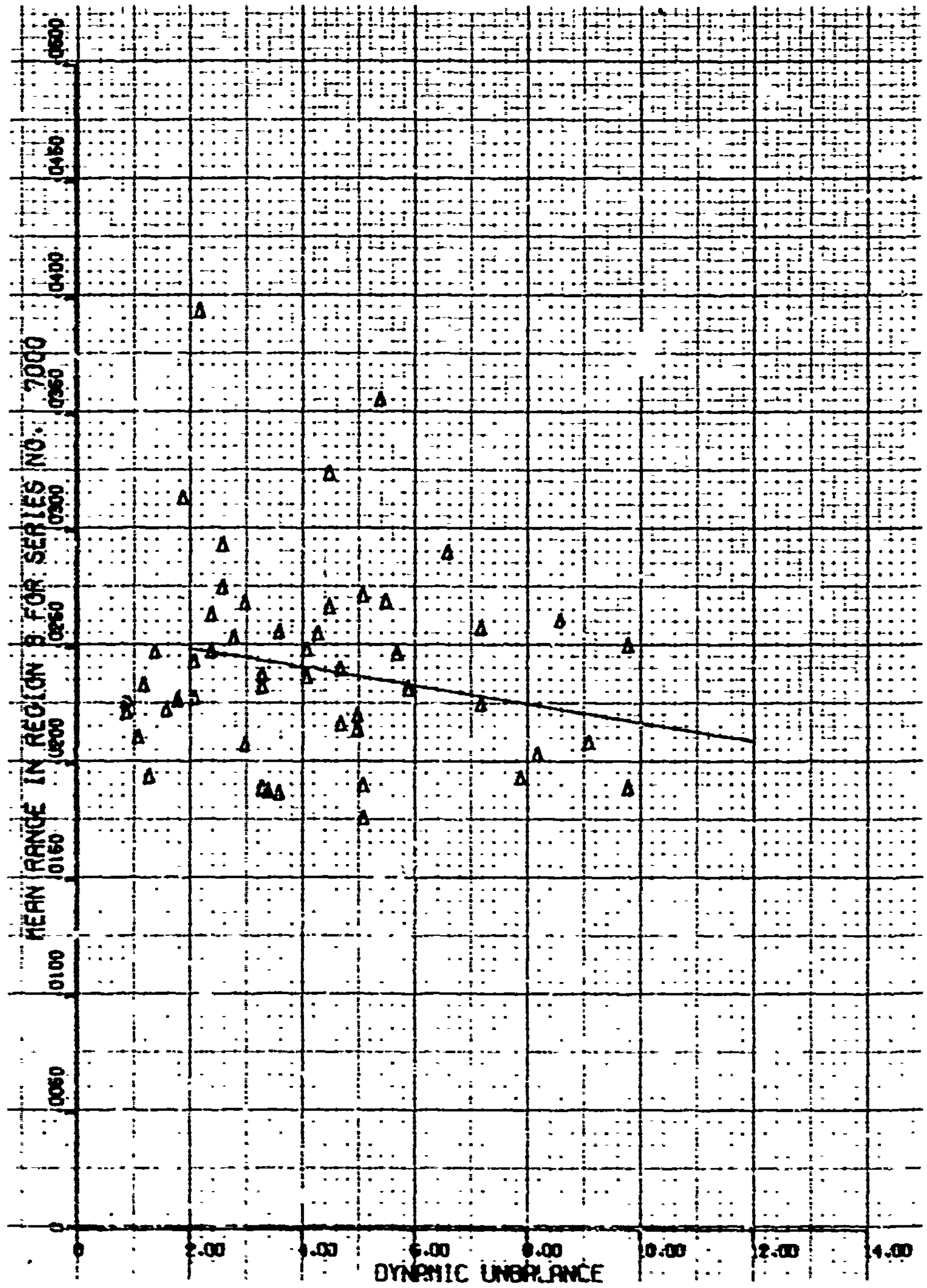

Figure 133 - Mean Wall Thickness Variation Versus Dynamic Unbalance, 7000 Series, Region B, Full

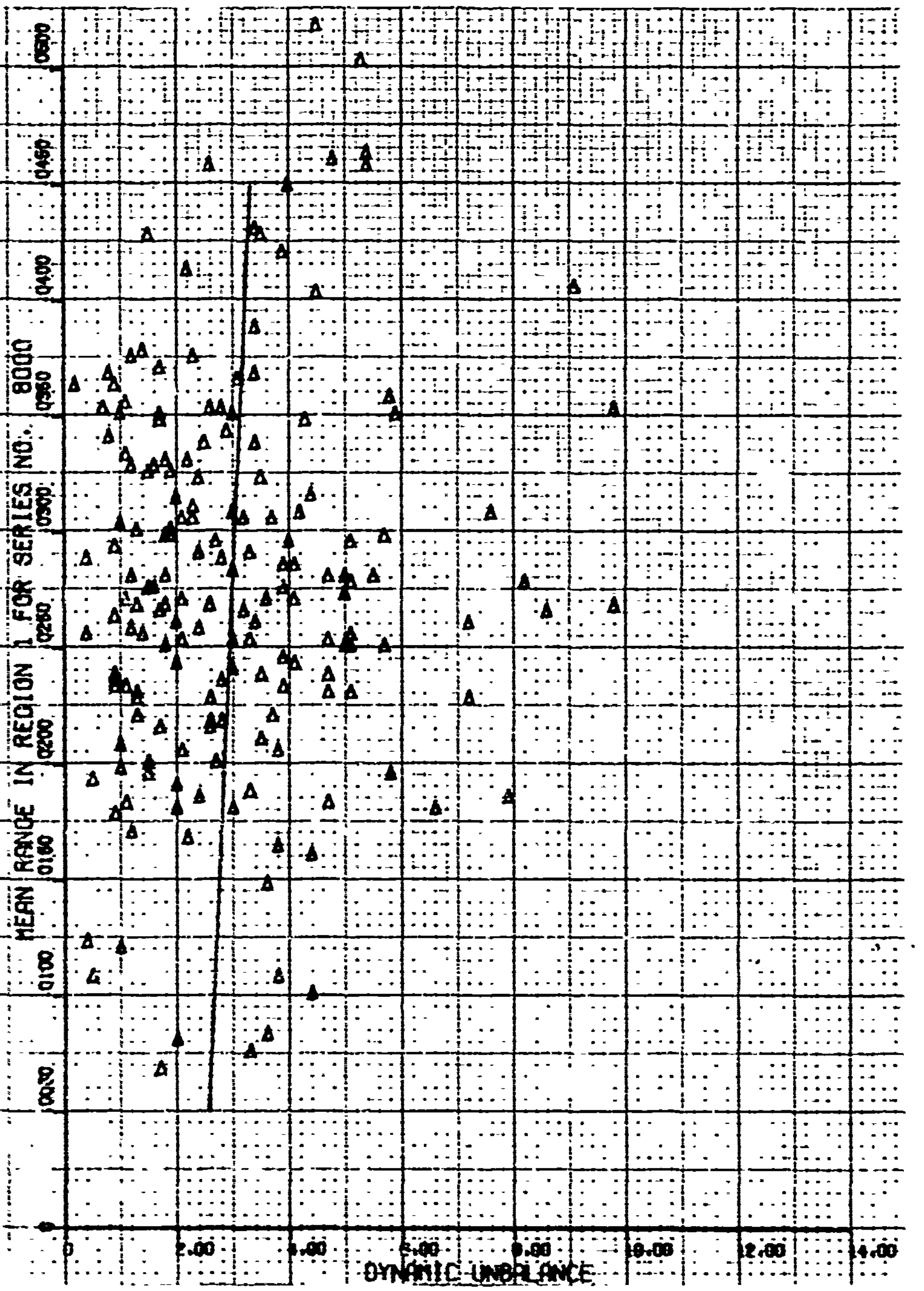

Figure 134 - Mean Wall Thickness Variation Versus Dynamic Unbalance, 8000 Series, Region 1, Full

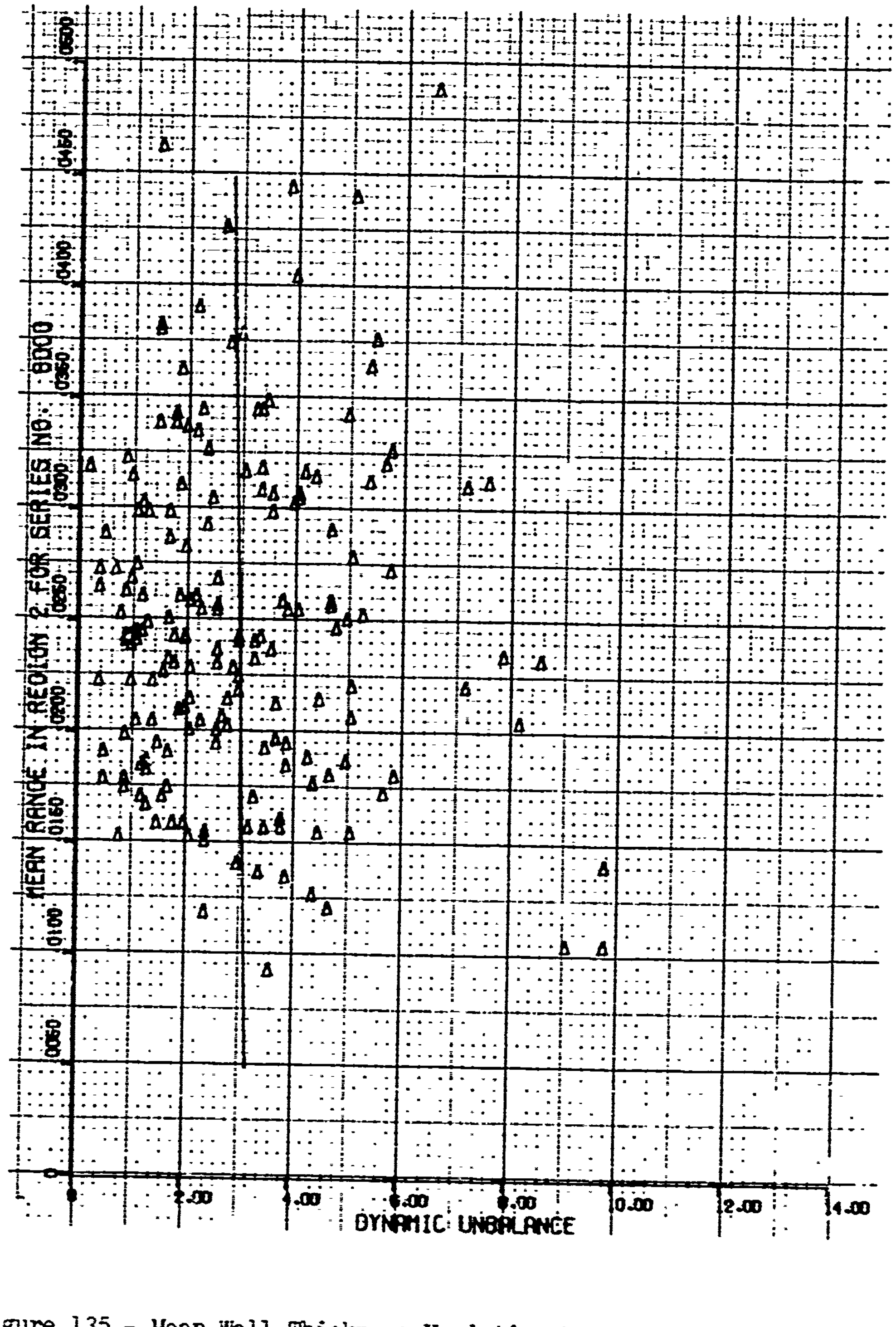

Figure 135 - Mean Wall Thickness Variation Versus Dynamic Unbalance, 8000 Series, Region 2, Full

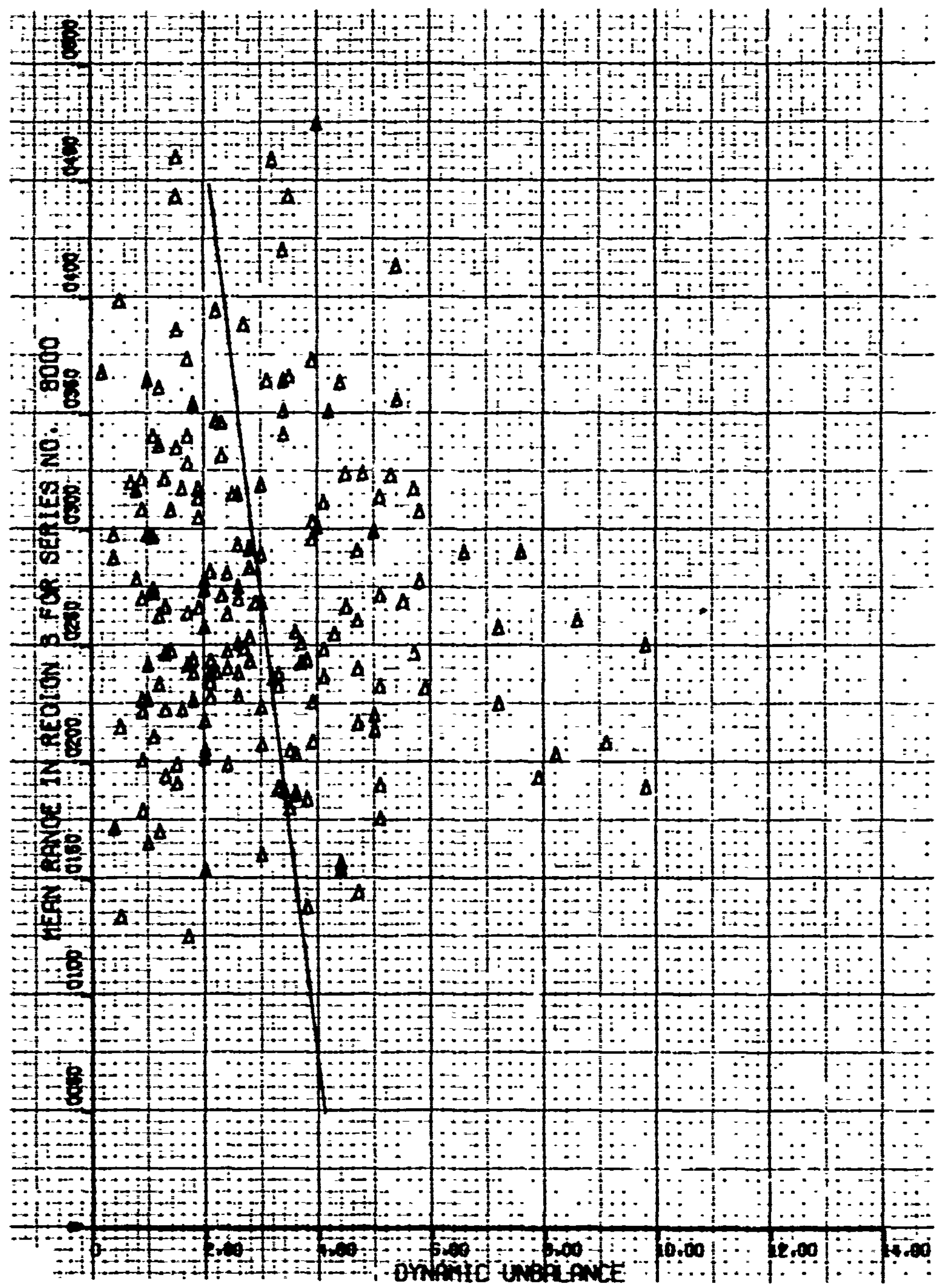

Figure 136 - Mean Wall Thickness Variation Versus Dynamic Unbalance, 8000 Series, Region 3, Full

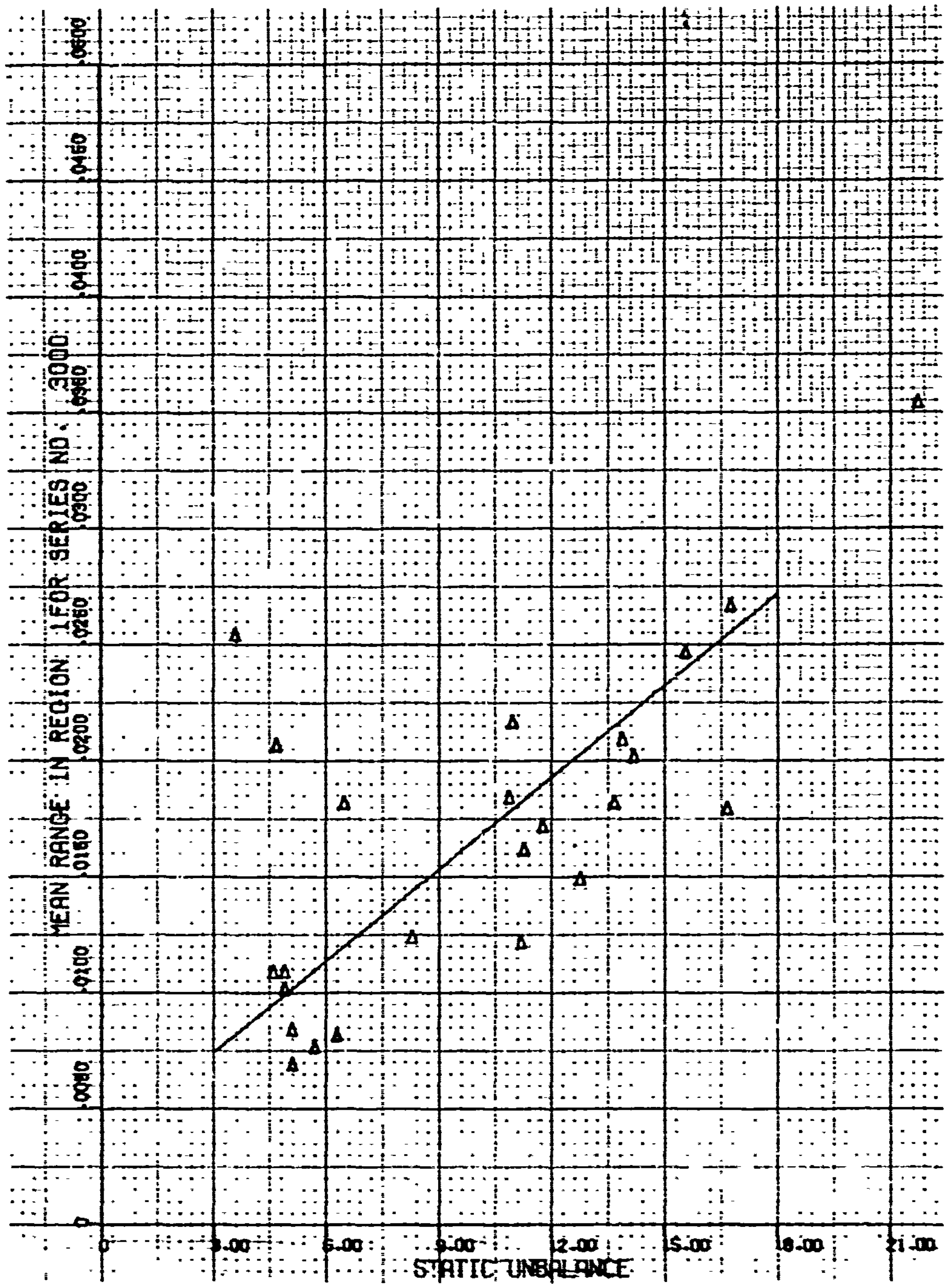

Figure 137 - Mean Wall Thickness Variation Versus Static Unbalance, 3000 Series, Region 1, Empty

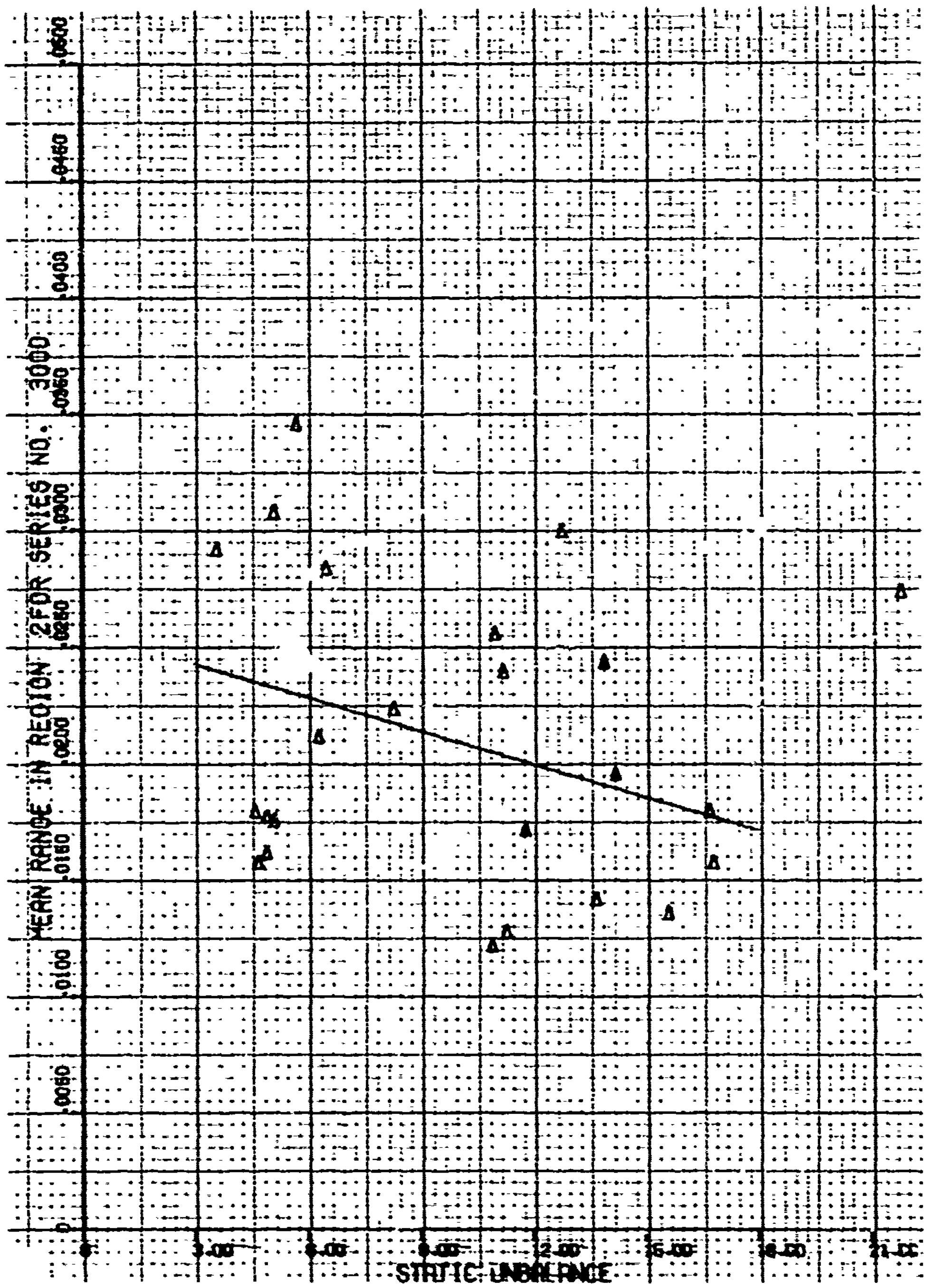

Figure 138 - Mean Wall Thickness Variation Versus Static Unbalance, 3000 Series, Region 2, Empty

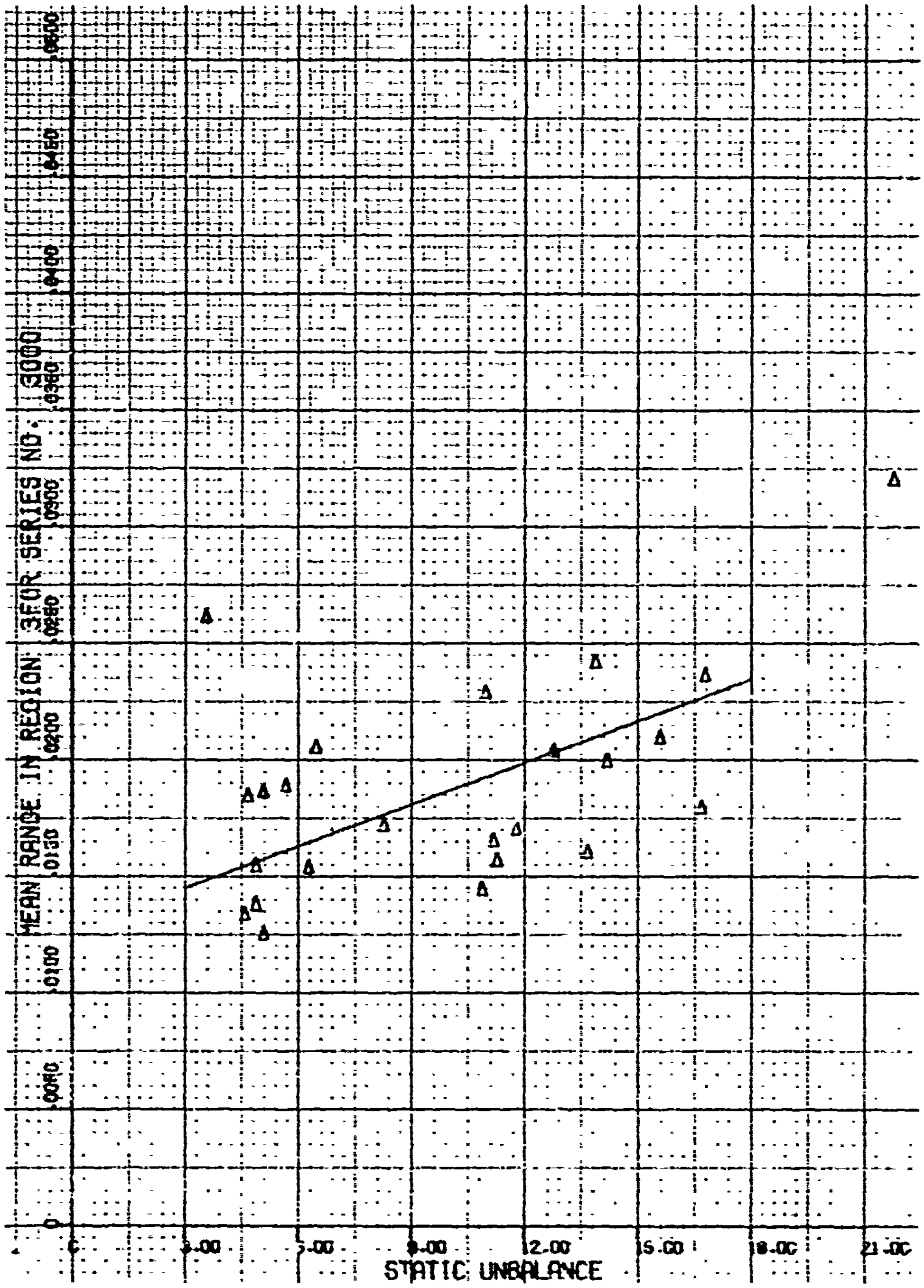

Figure 139 - Mean Wall Thickness Variation Versus Static Unbalance, 3000 Series, Region 3, Empty

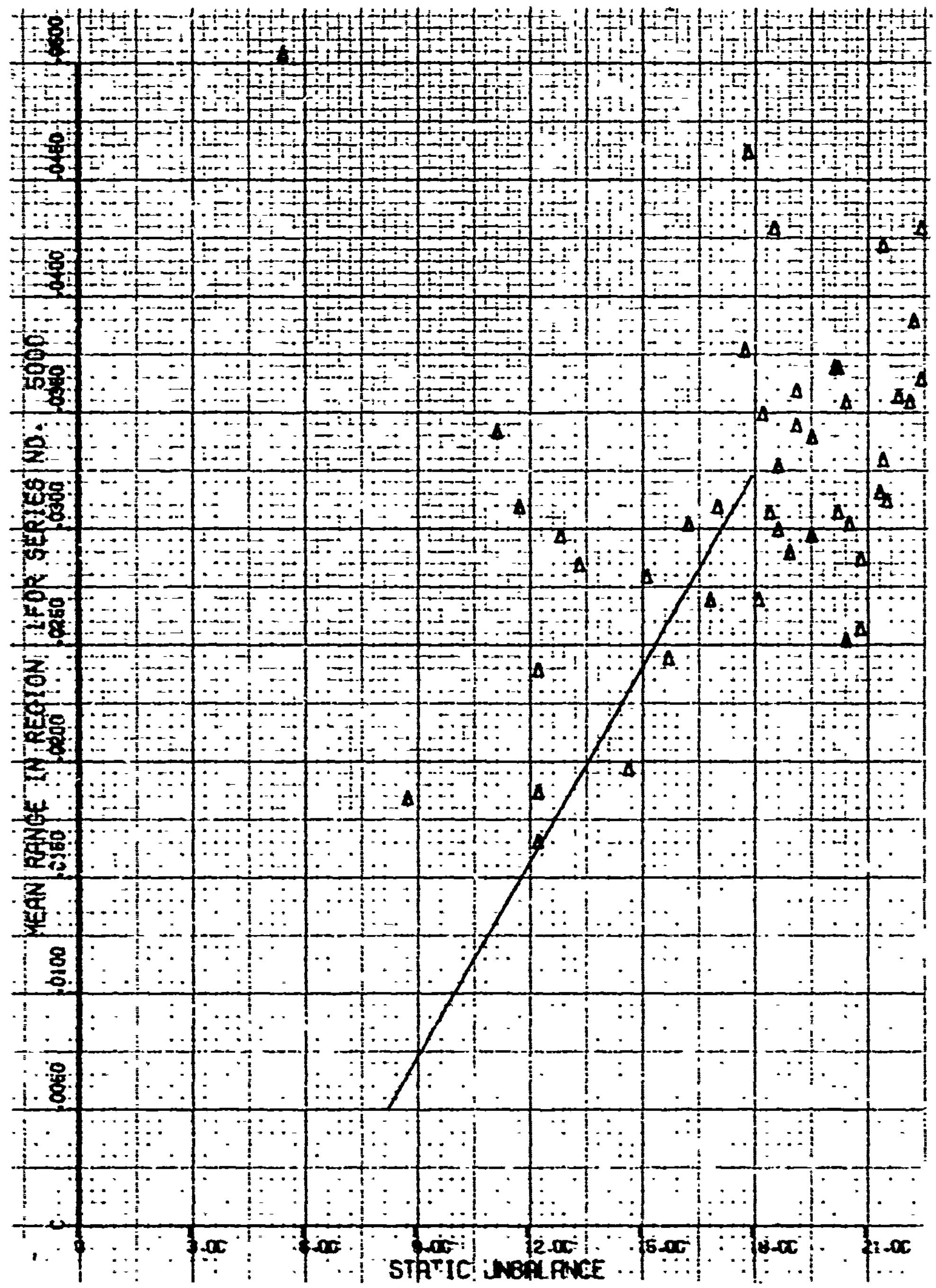

Figure 140 - Mean Wall Thickness Variation Versus Static Unbalance, 5000 Series, Region 1, Empty

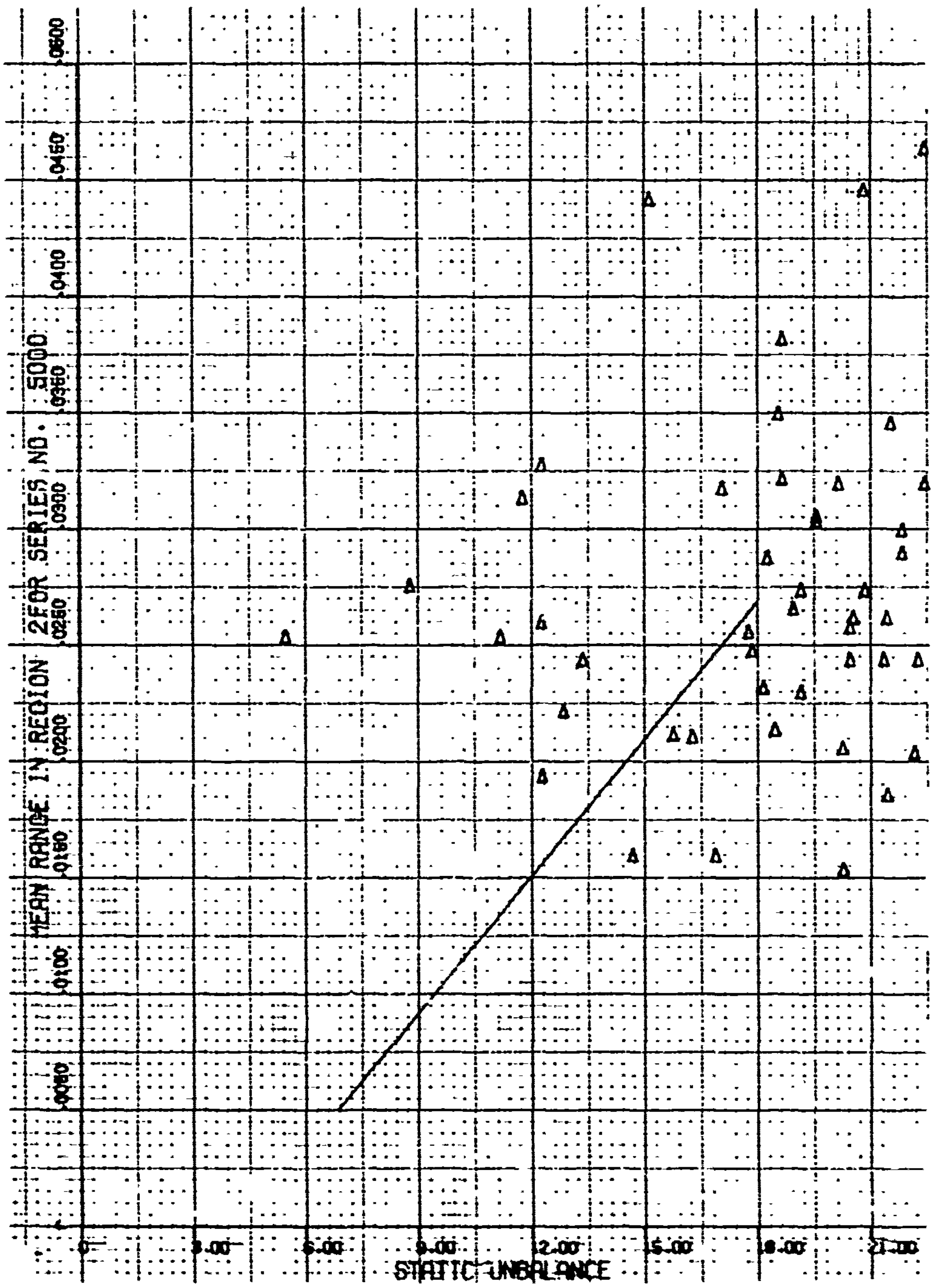

Figure 141 - Mean Wall Thickness Variation Versus Static Unbalance, 5000 Series, Region 2, Empty

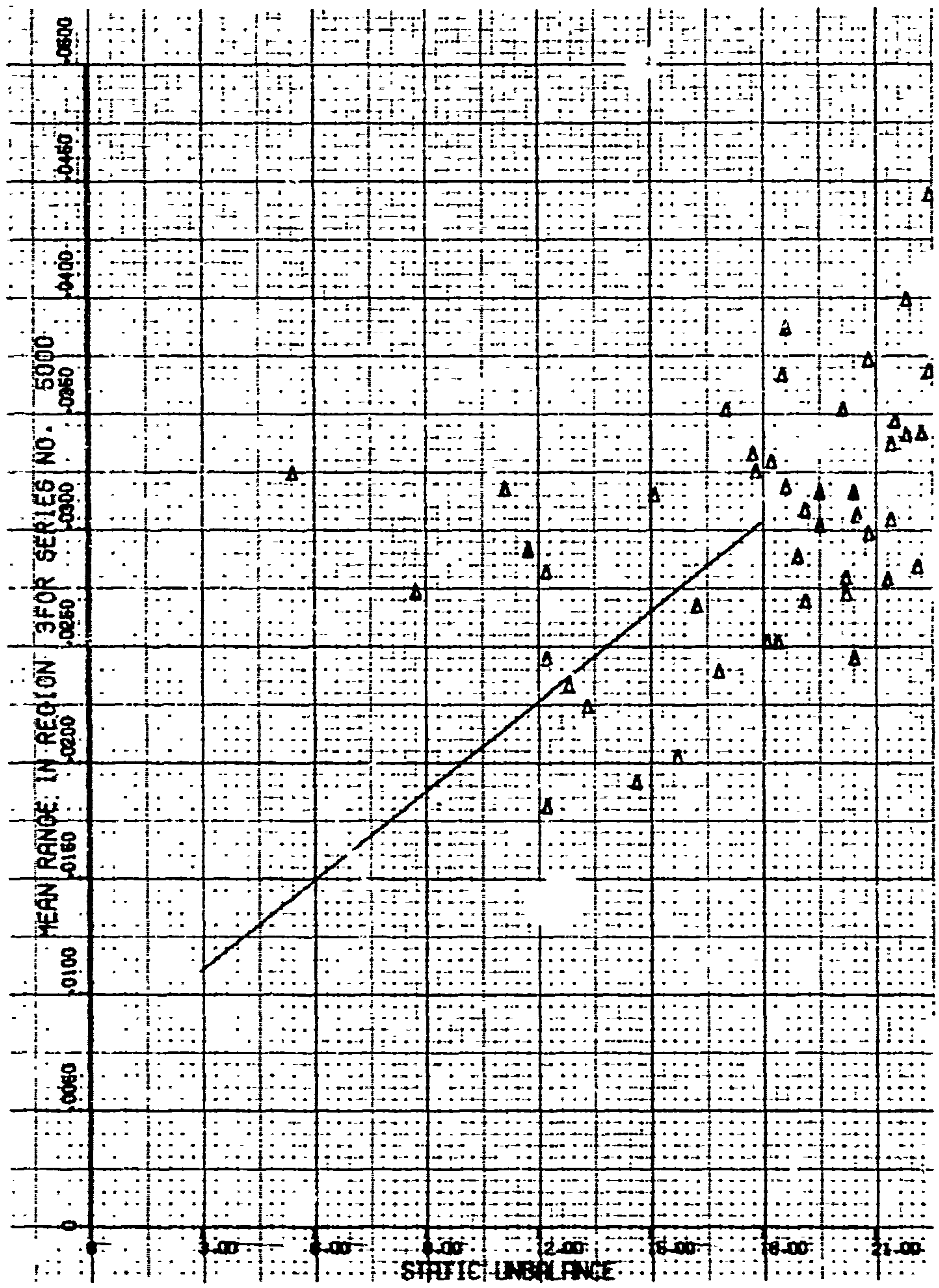

Figure 142 - Mean Wall Thickness Variation Versus Static Unbalance,
5000 Series, Region 3, Empty

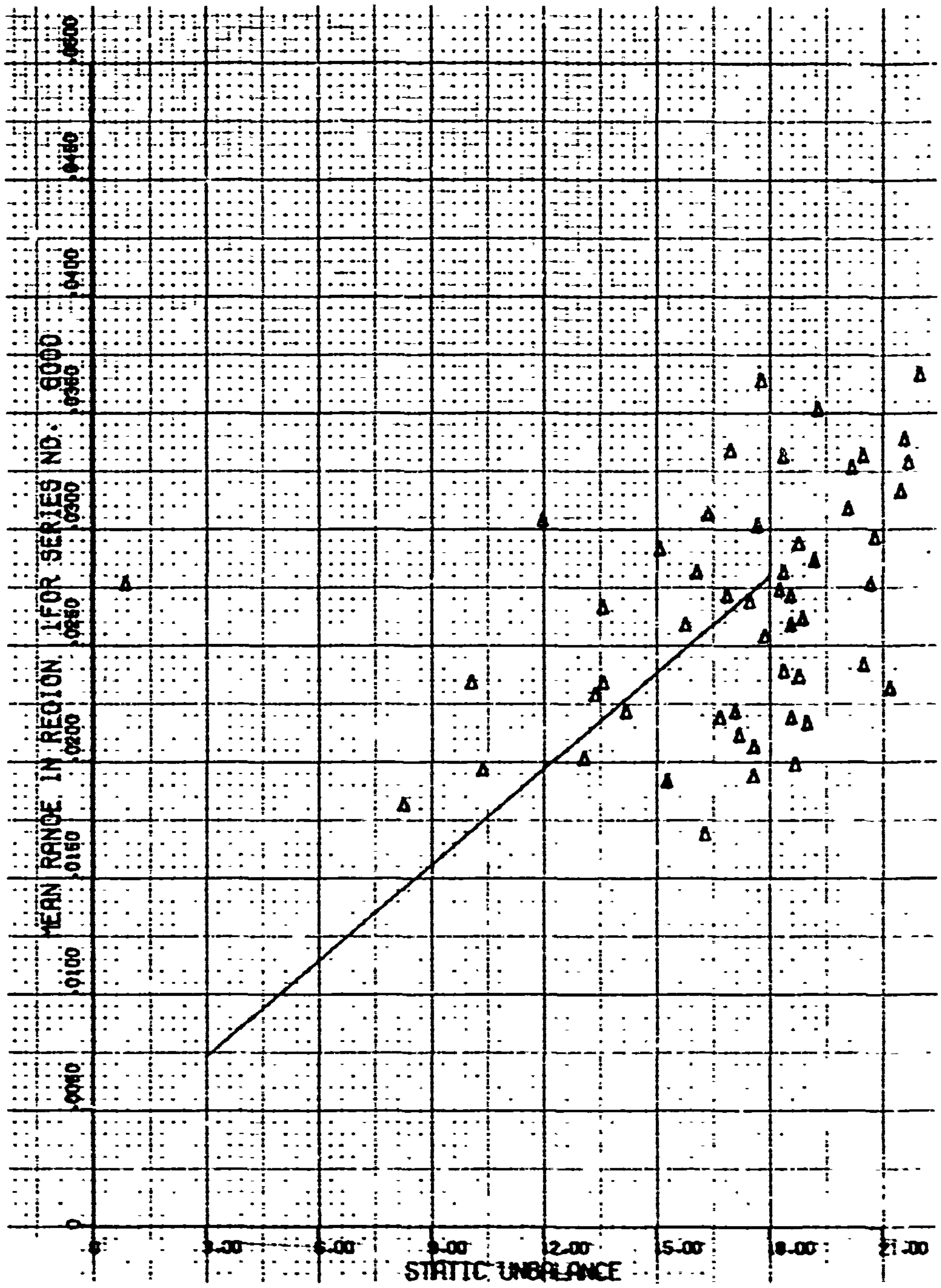

Figure 143 - Mean Wall Thickness Variation Versus Static Unbalance, 6000 Series, Region 1, Empty

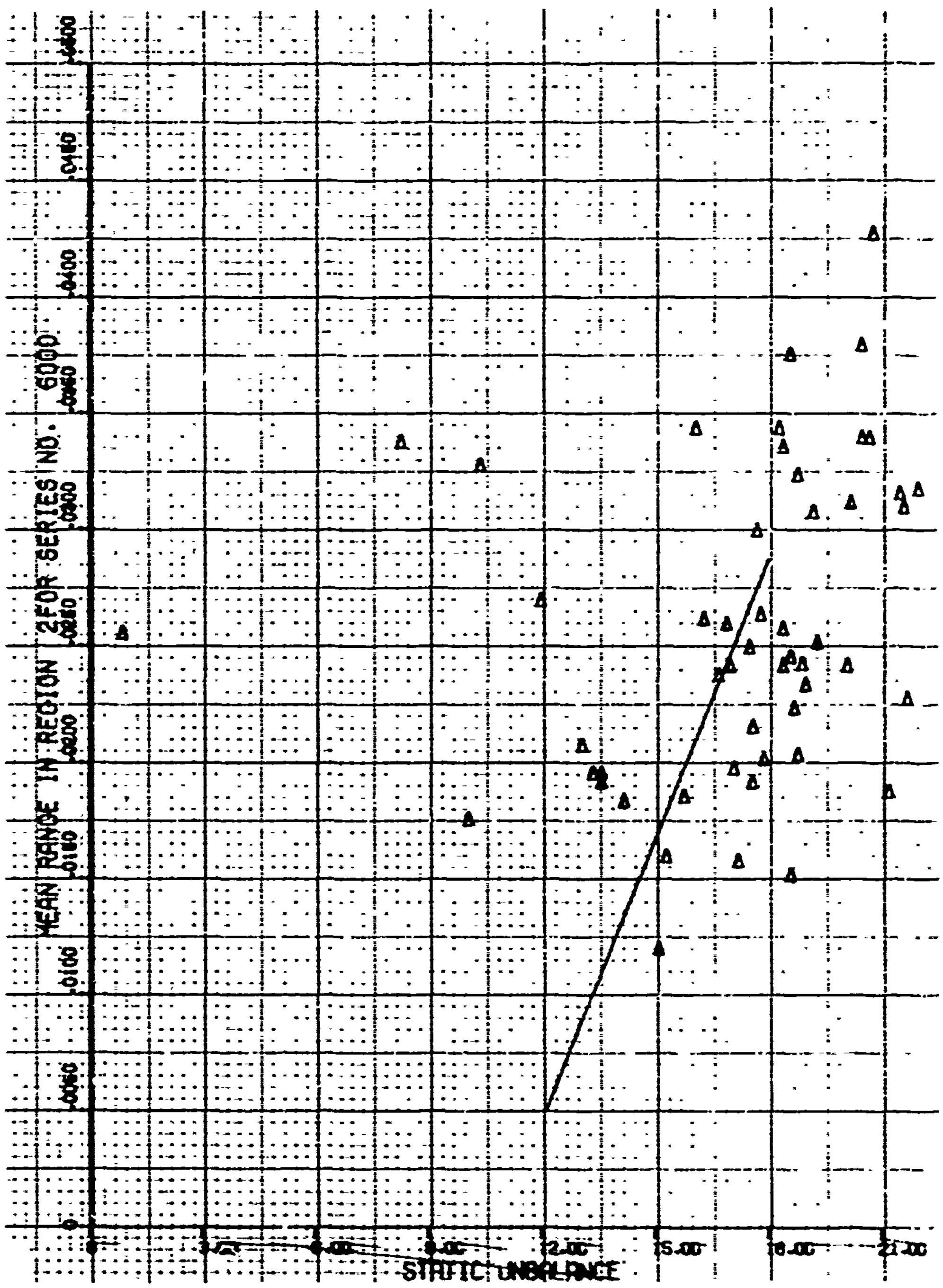

Figure 144 - Mean Wall Thickness Variation Versus Static Unbalance, 6000 Series, Region 2, Empty

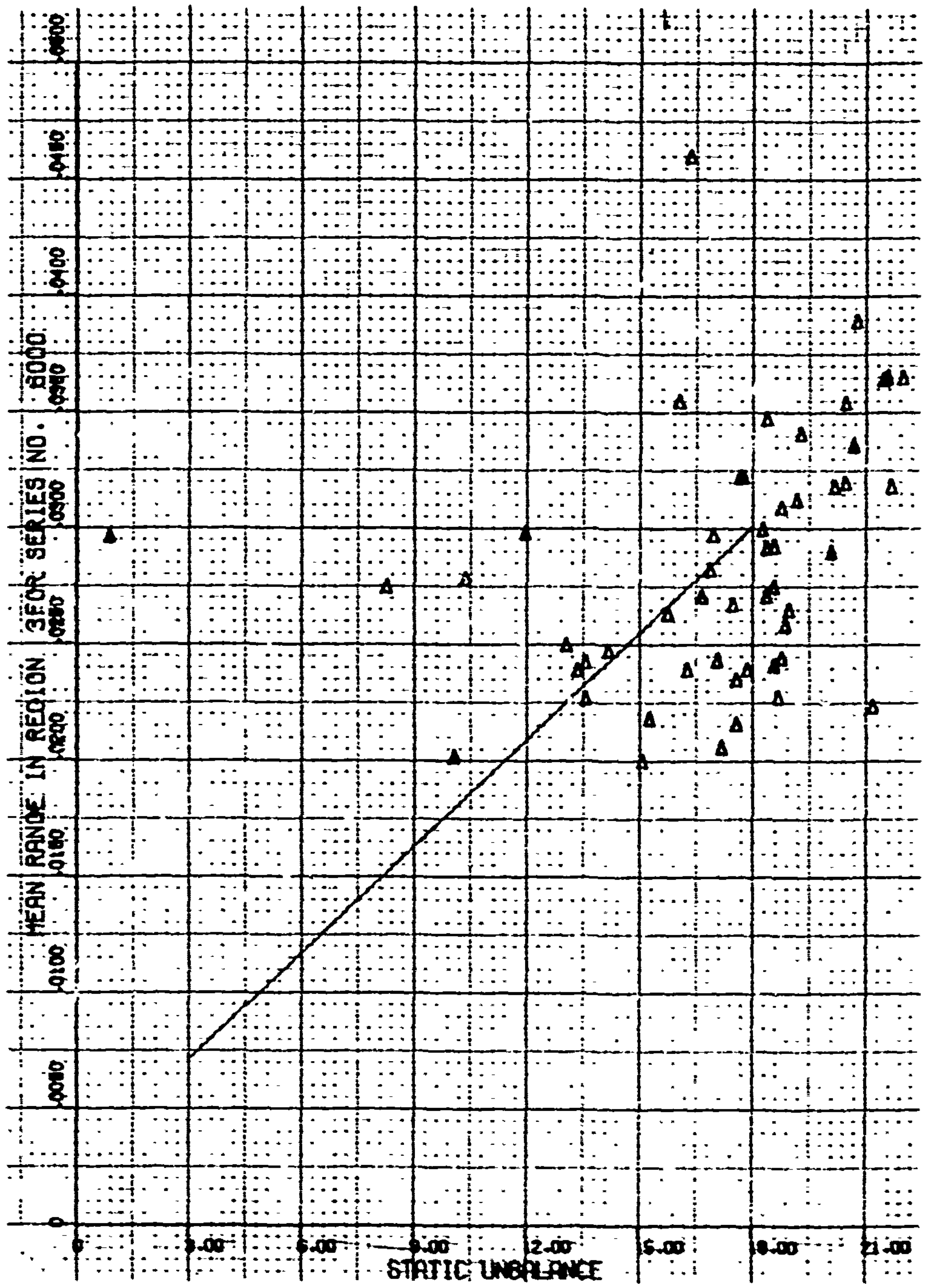

Figure 145 - Mean Wall Thickness Variation Versus Static Unbalance, 6000 Series, Region 3, Empty

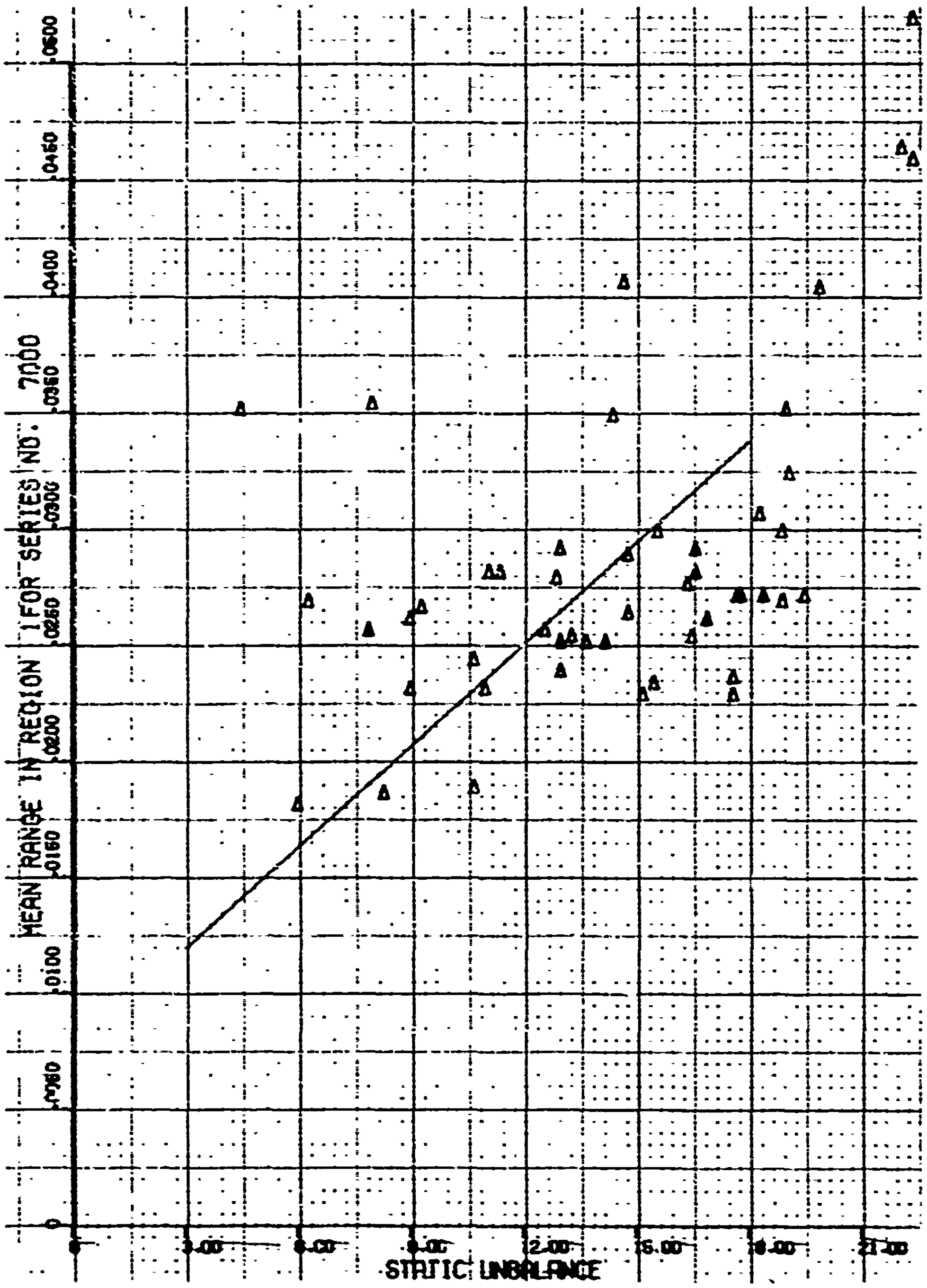

Figure 146 - Mean Wall Thickness Variation Versus Static Unbalance, 7000 Series, Region 1, Empty

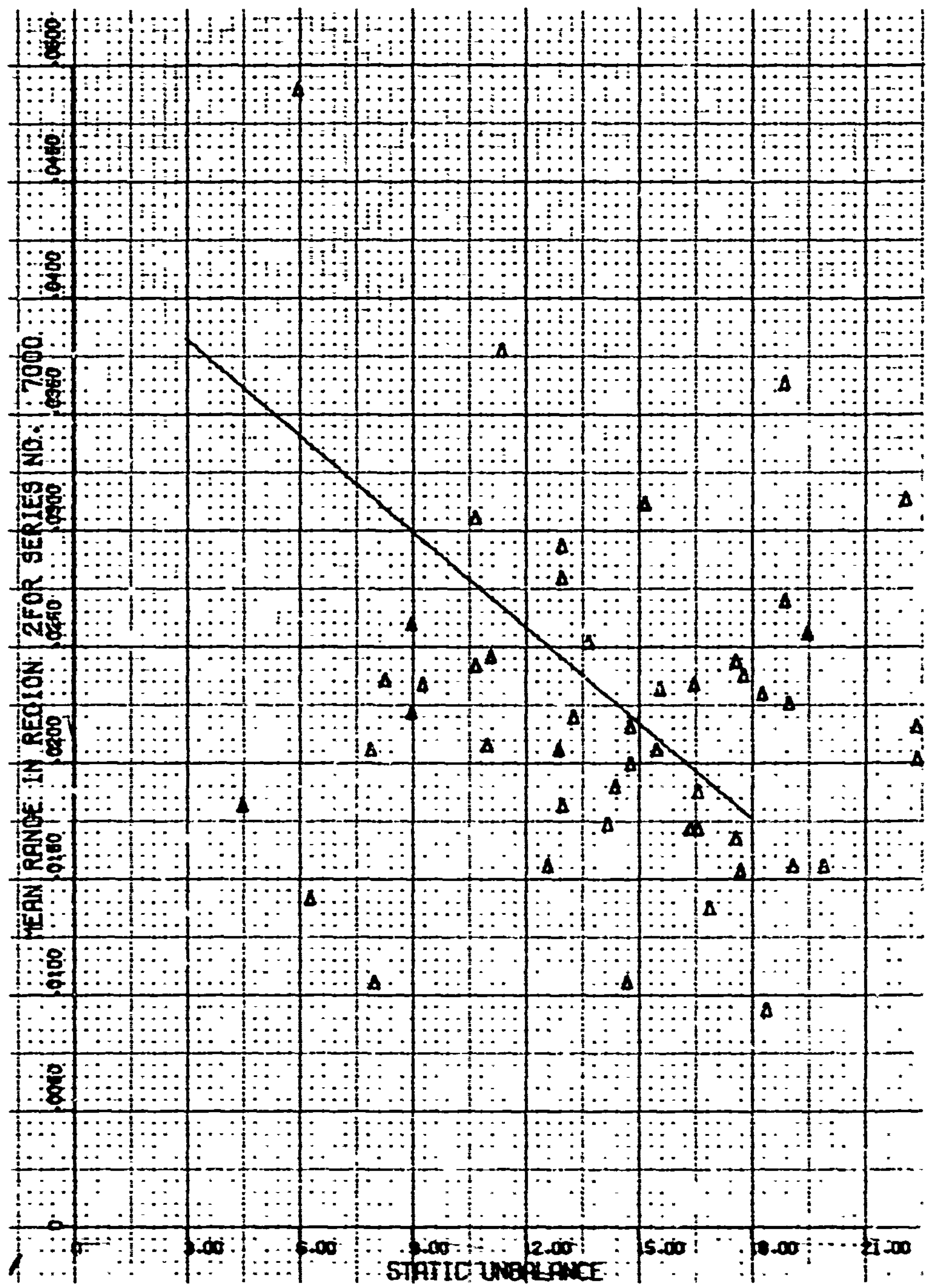

Figure 147 - Mean Wall Thickness Variation Versus Static Unbalance, 7000 Series, Region 2, Empty

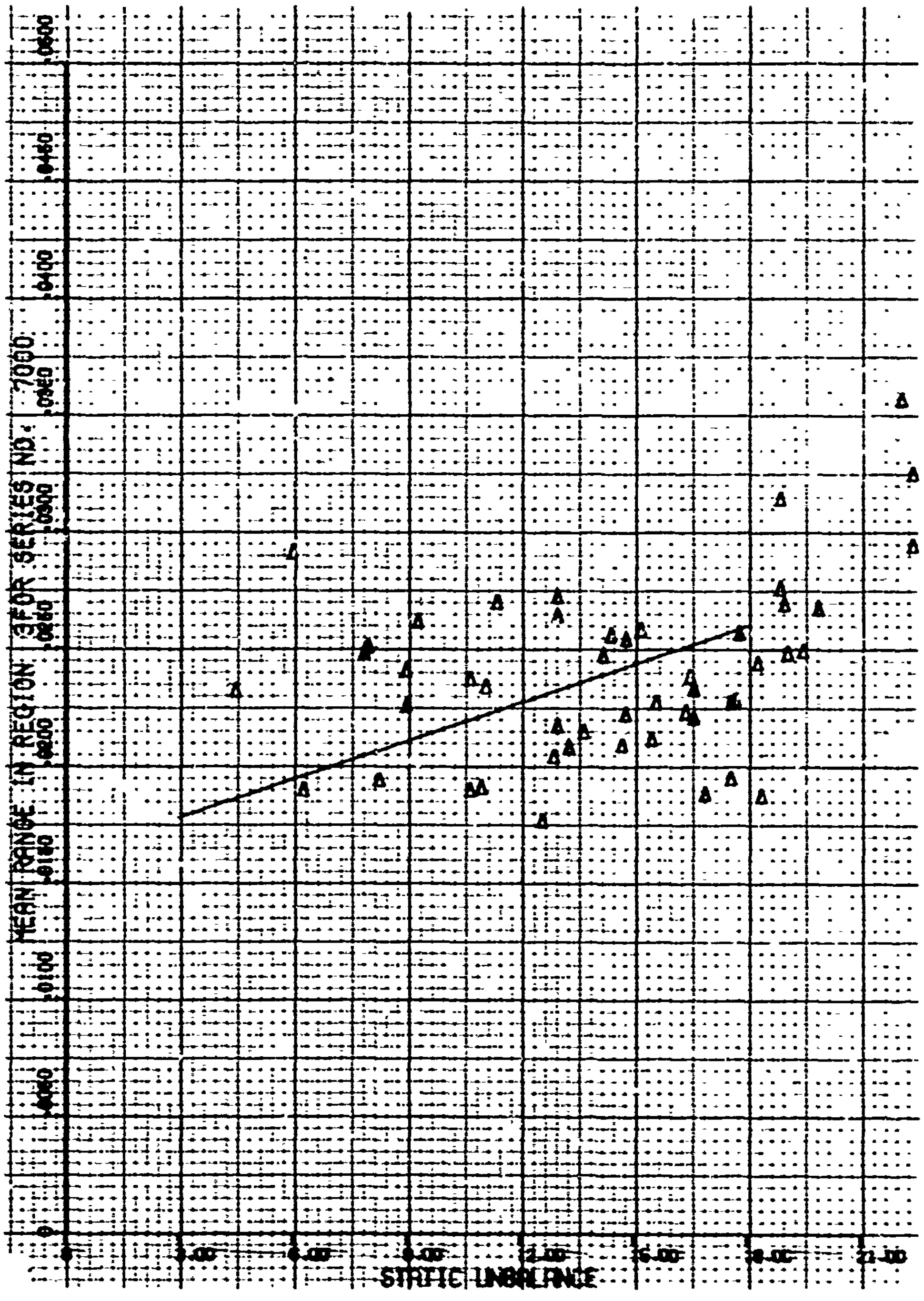

Figure 1.48 - Mean Wall Thickness Variation Versus Static Unbalance, 7000 Series, Region 3, Empty

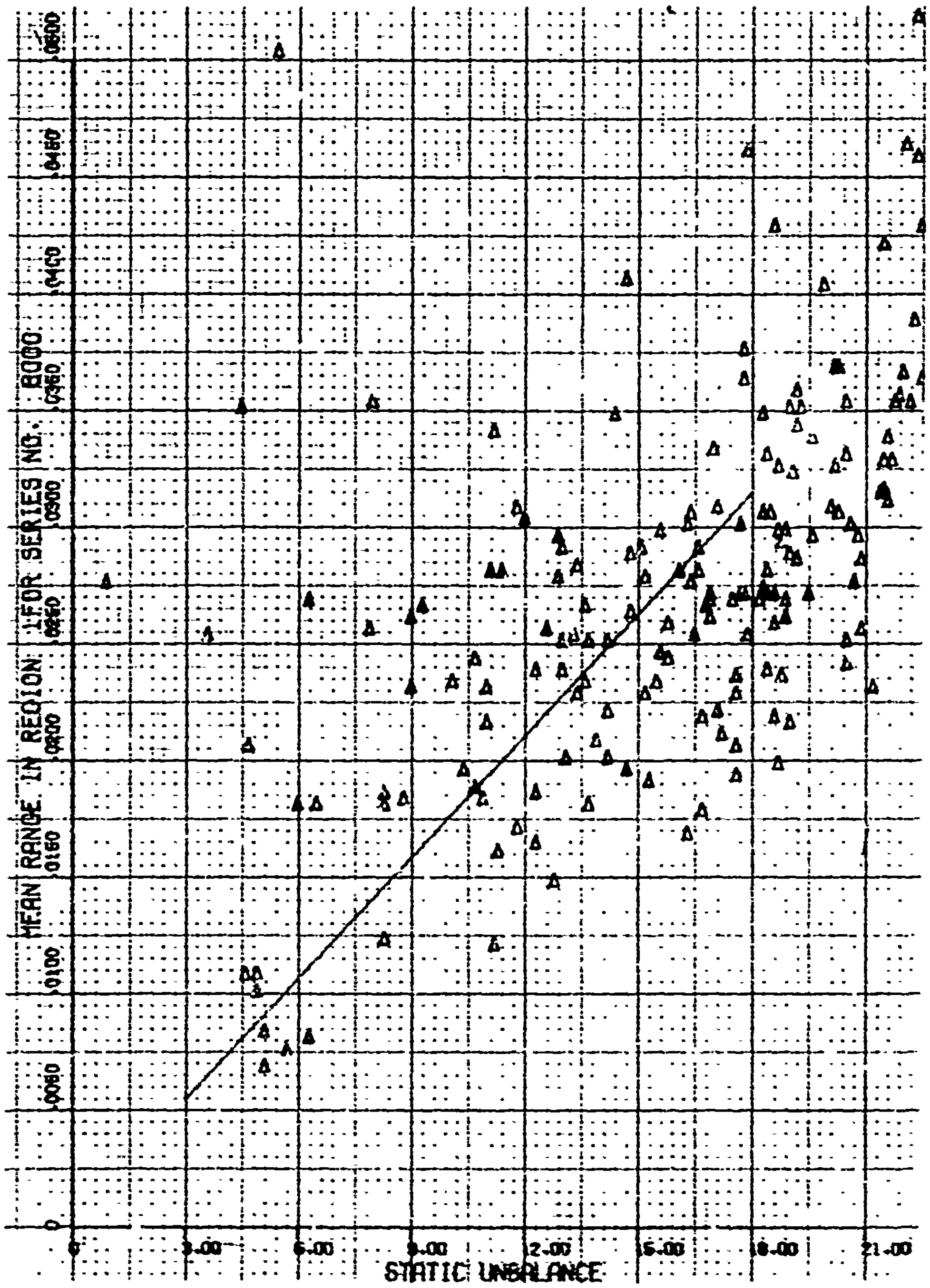

Figure 149 - Mean Wall Thickness Variation Versus Static Unbalance, 8000 Series, Region 1, Empty

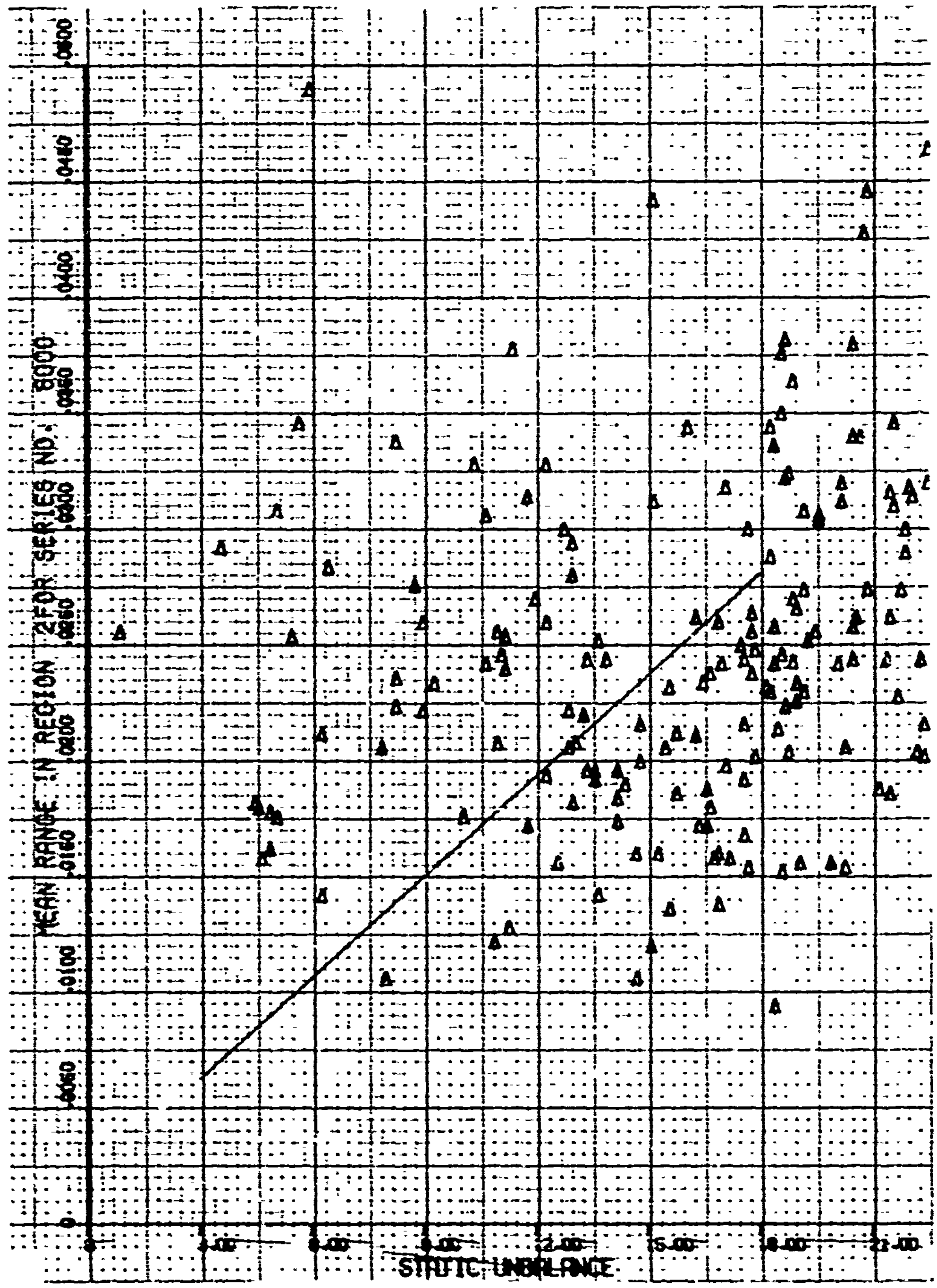

Figure 150 - Mean Wall Thickness Variation Versus Static Unbalance, 8000 Series, Region 2, Empty

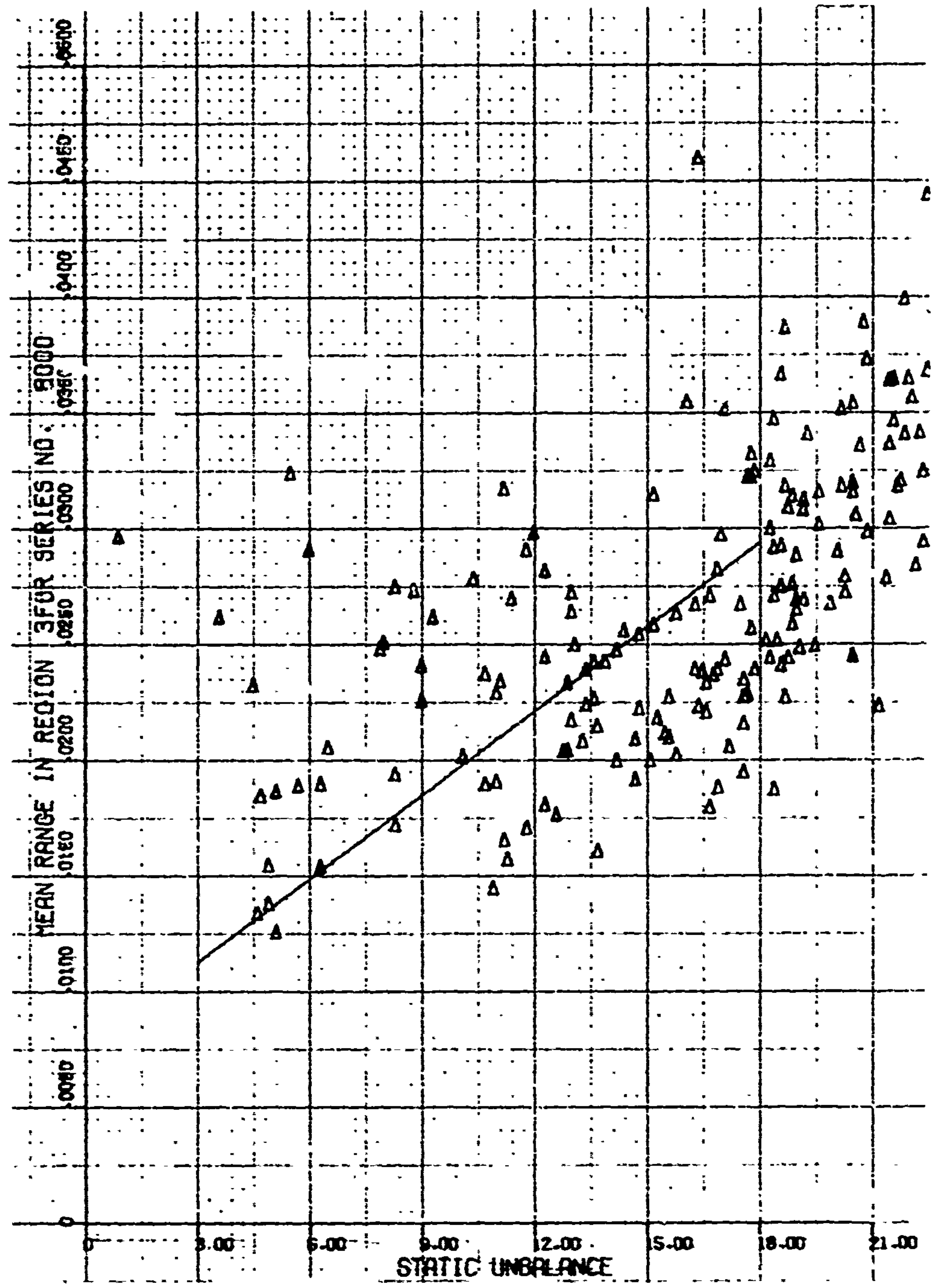

Figure 151 - Mean Wall Thickness Variation Versus Static Unbalance,
8000 Series, Region 3, Empty

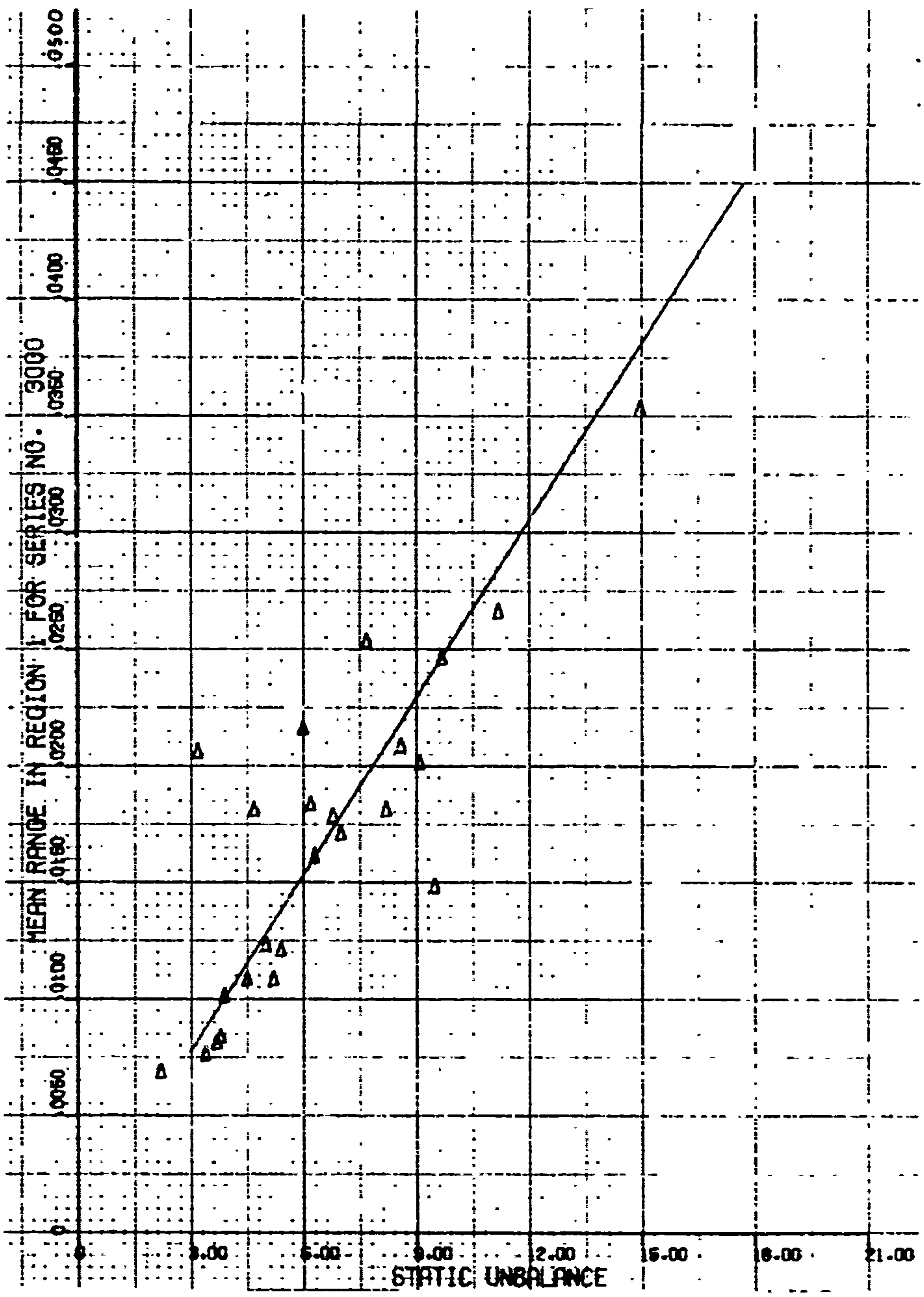

Figure 152 - Mean Wall Thickness Variation Versus Static Unbalance, 3000 Series, Region 1, Full

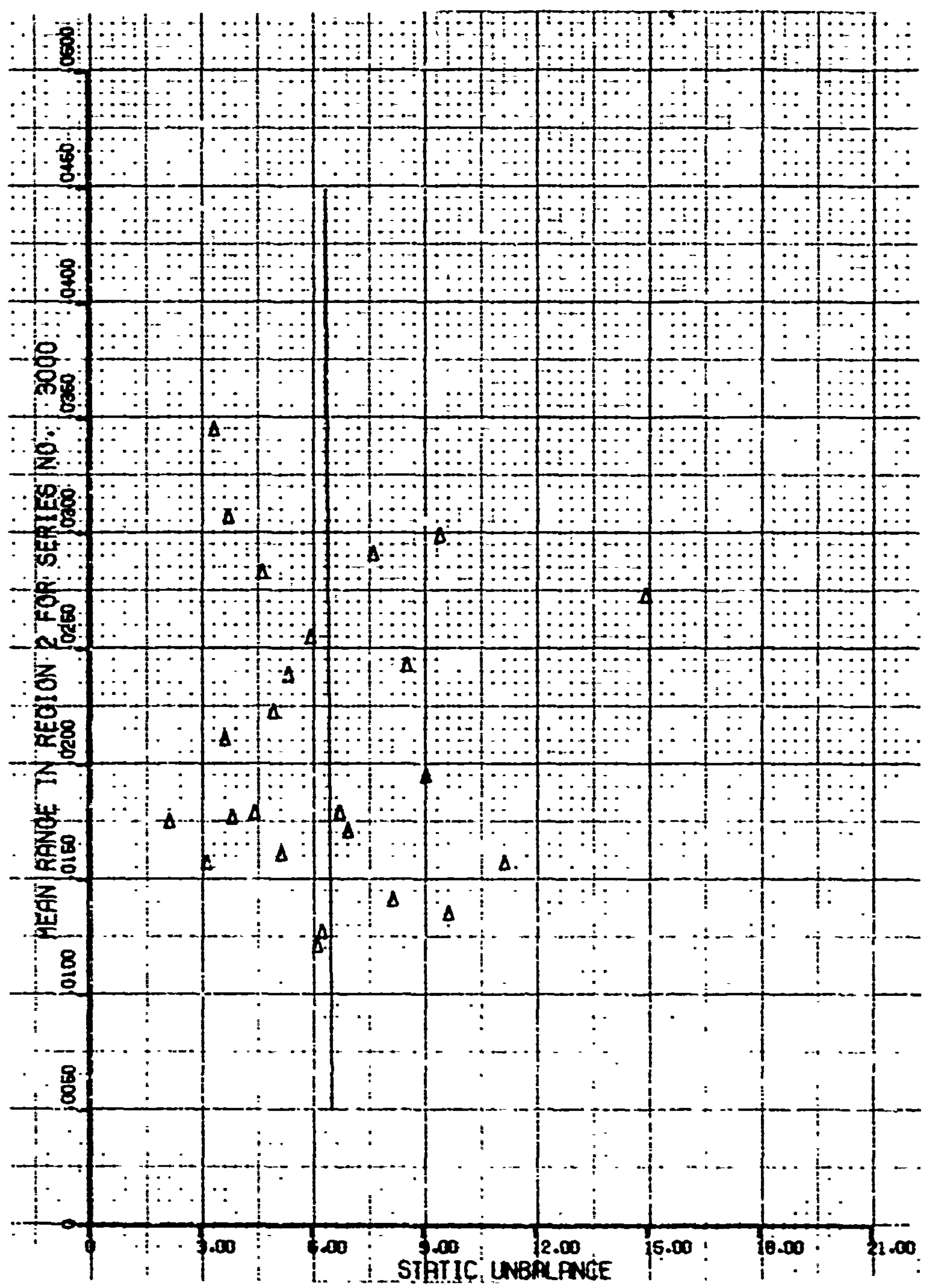

Figure 153 - Mean Wall Thickness Variation Versus Static Unbalance, 3000 Series, Region 2, Full

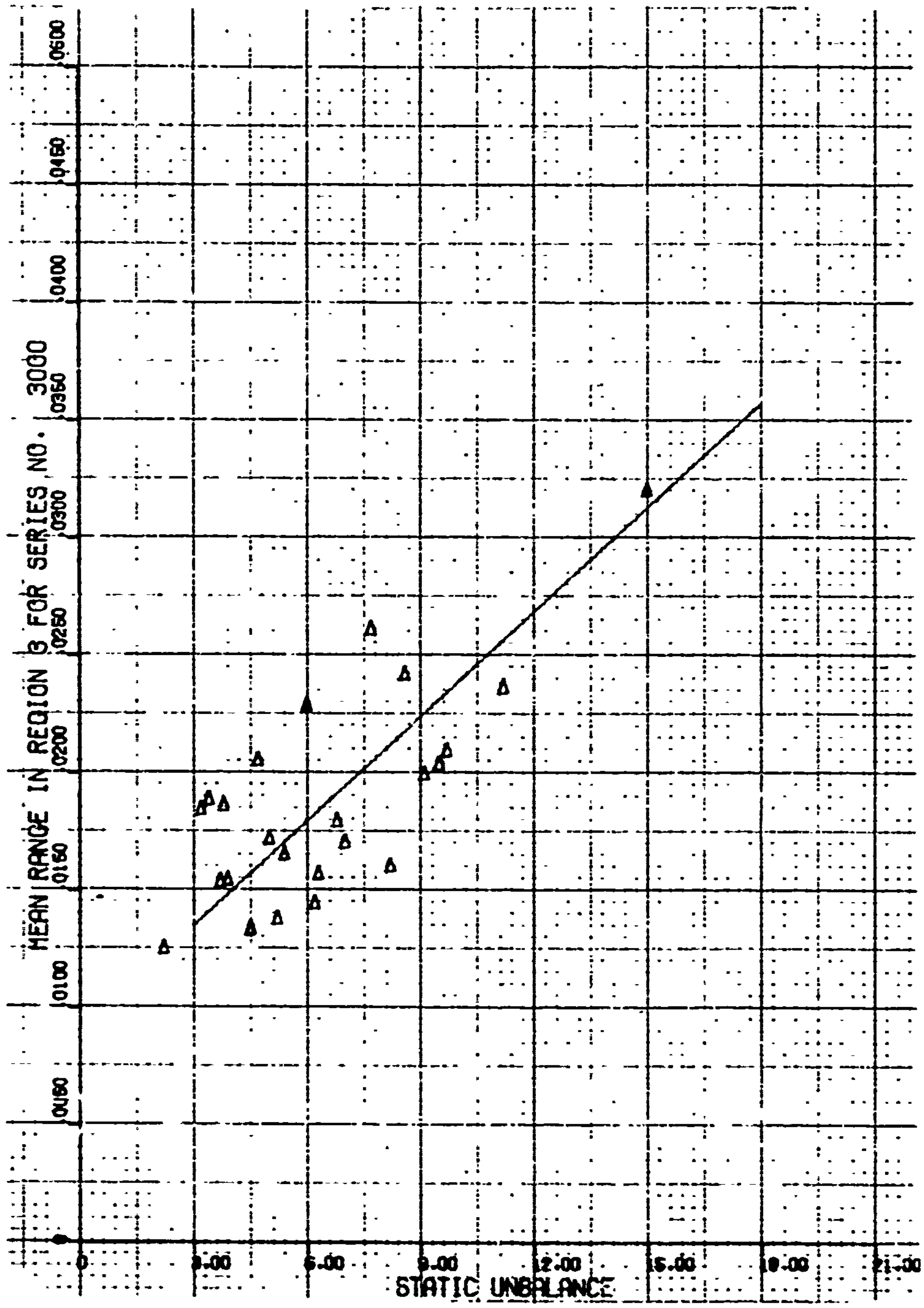

Figure 154 - Mean Wall Thickness Variation Versus Static Unbalance, 3000 Series, Region 3, Full

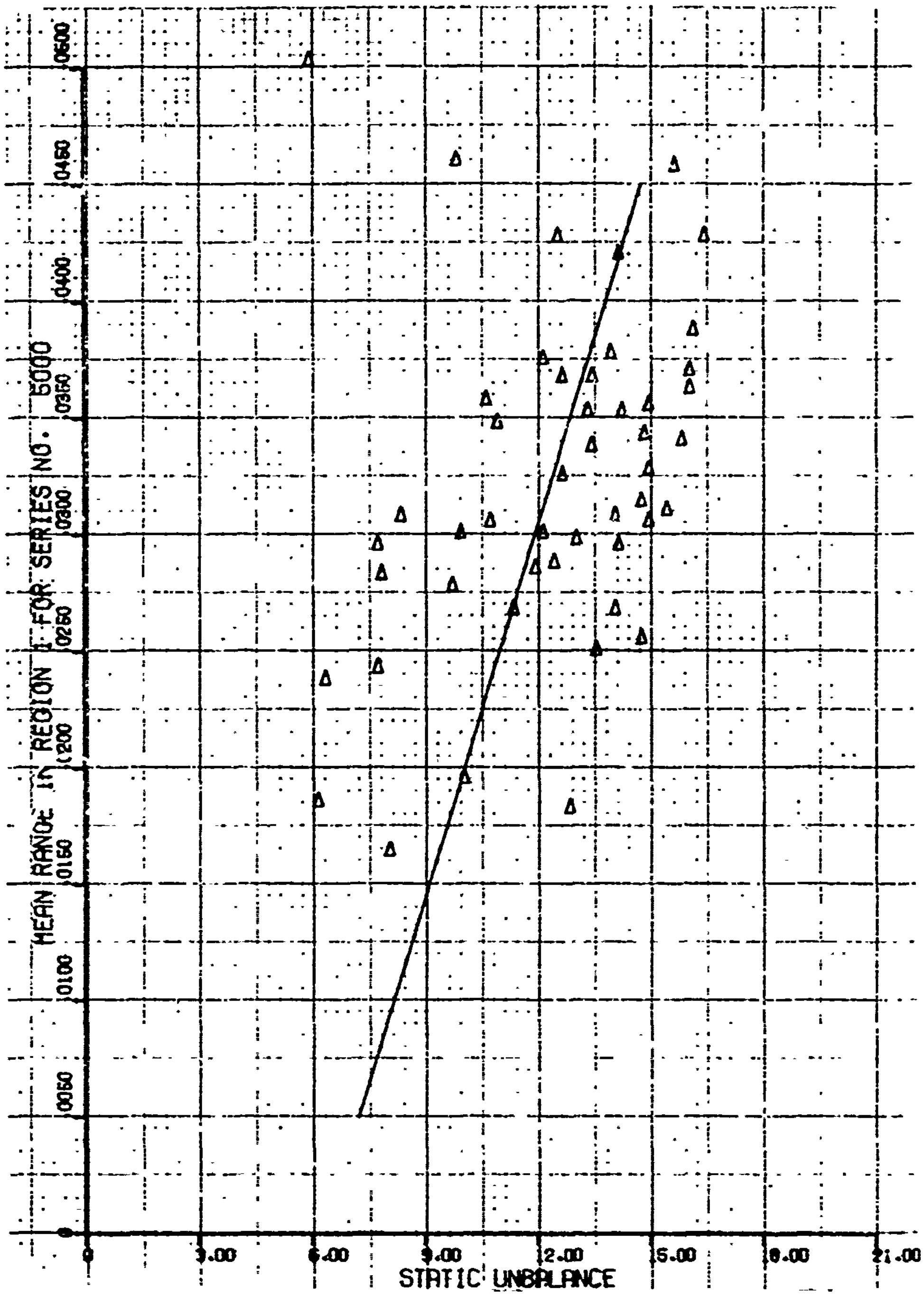

Figure 155 - Mean Wall Thickness Variation Versus Static Unbalance, 5000 Series, Region 1, Full

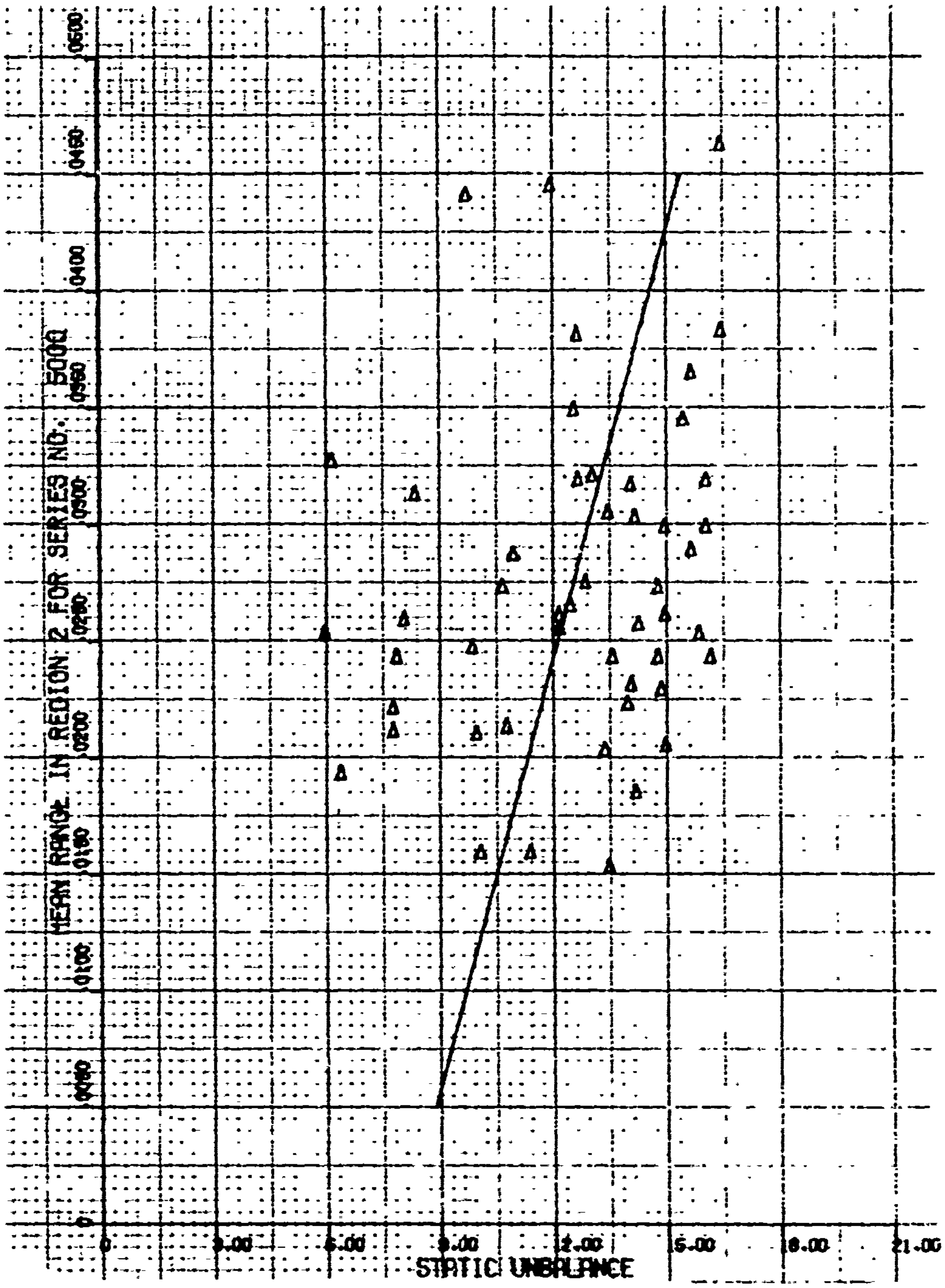

Figure 156 - Mean Wall Thickness Variation Versus Static Unbalance, 5000 Series, Region 2, Full

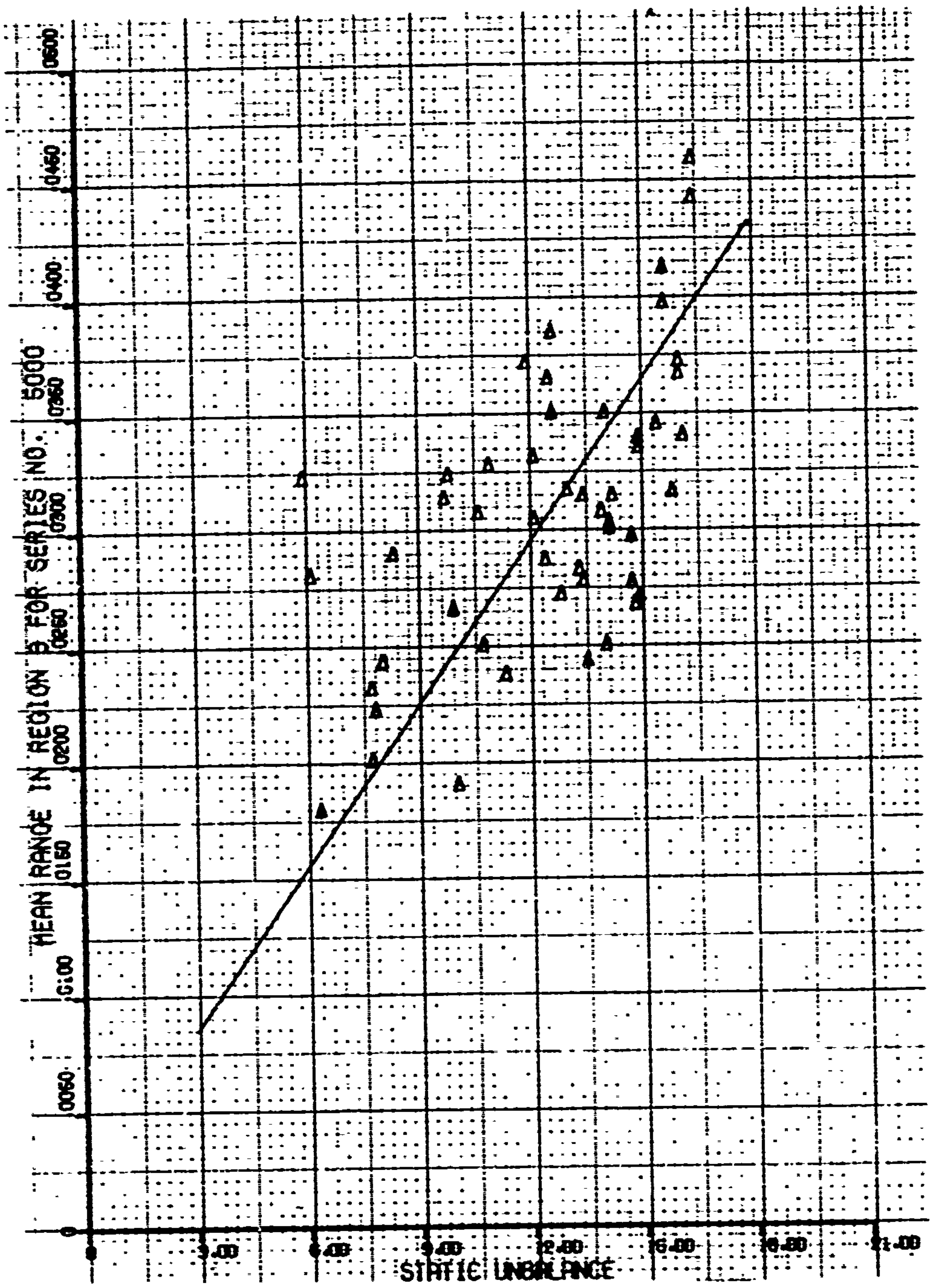

Figure 157 - Mean Wall Thickness Variation Versus Static Unbalance, 5000 Series, Region 3, Full

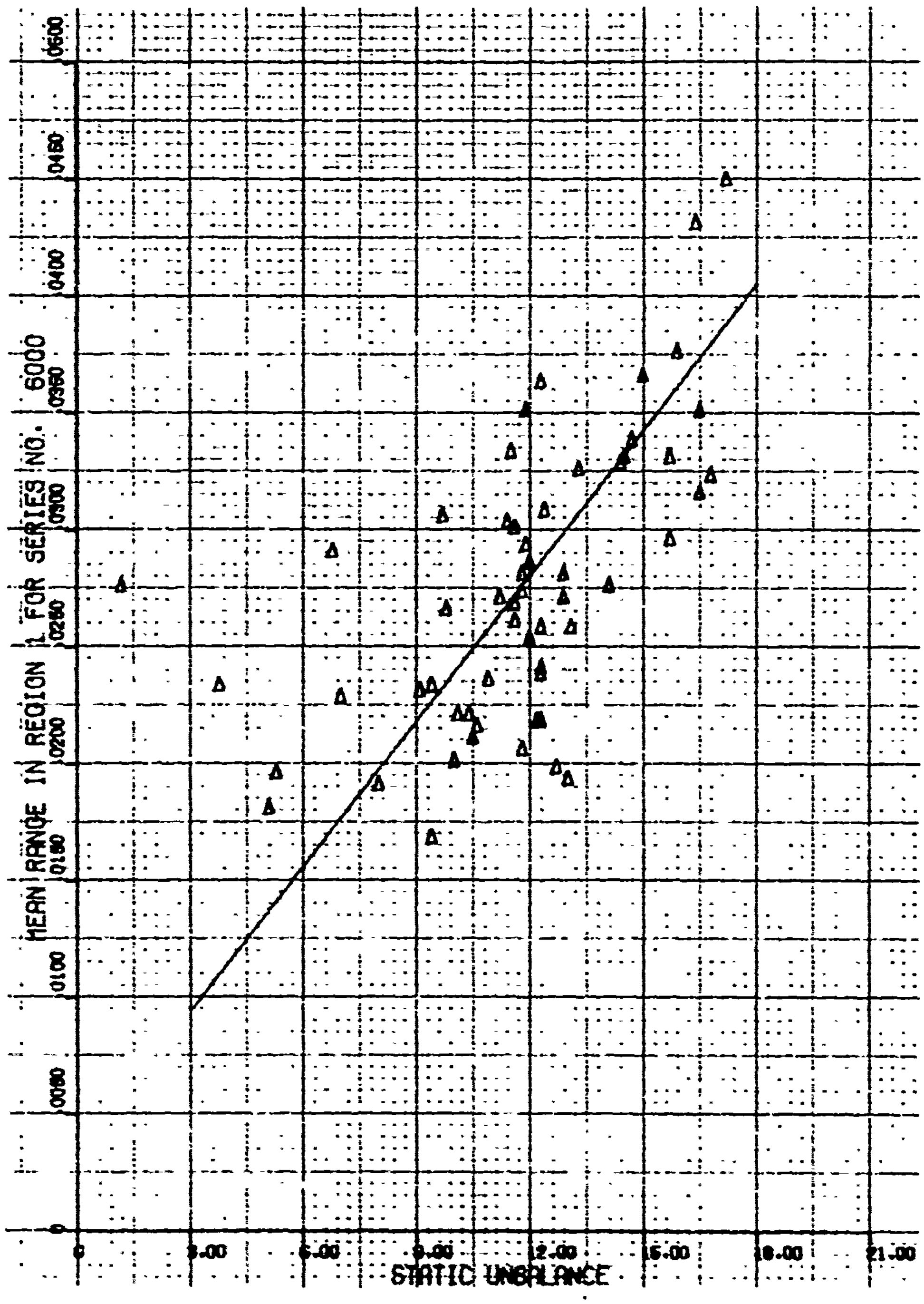

Figure 158 - Mean Wall Thickness Variation Versus Static Unbalance, 6000 Series, Region 1, Full

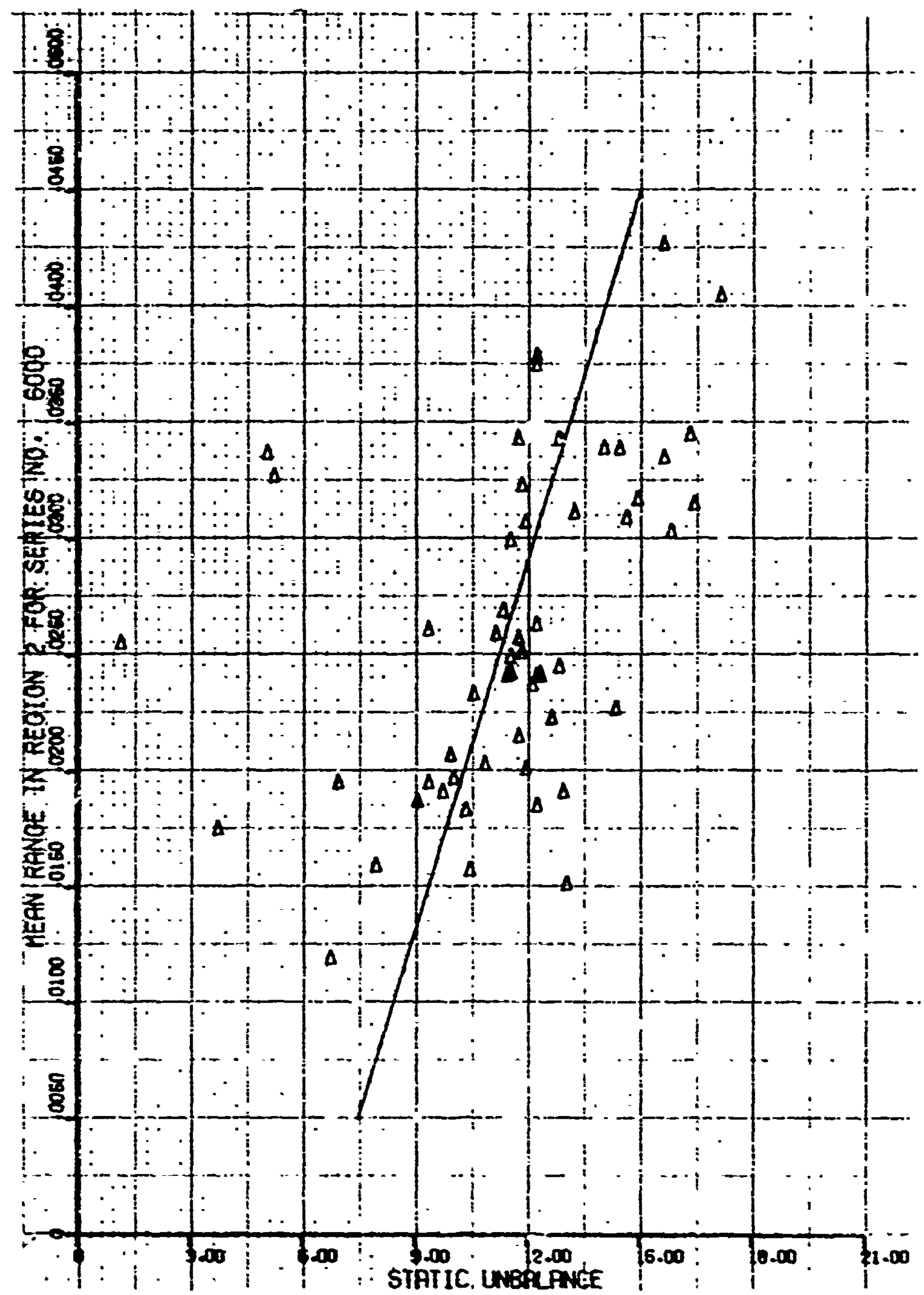

Figure 159 - Mean Wall Thickness Variation Versus Static Unbalance, Series 6000, Region 2, Full

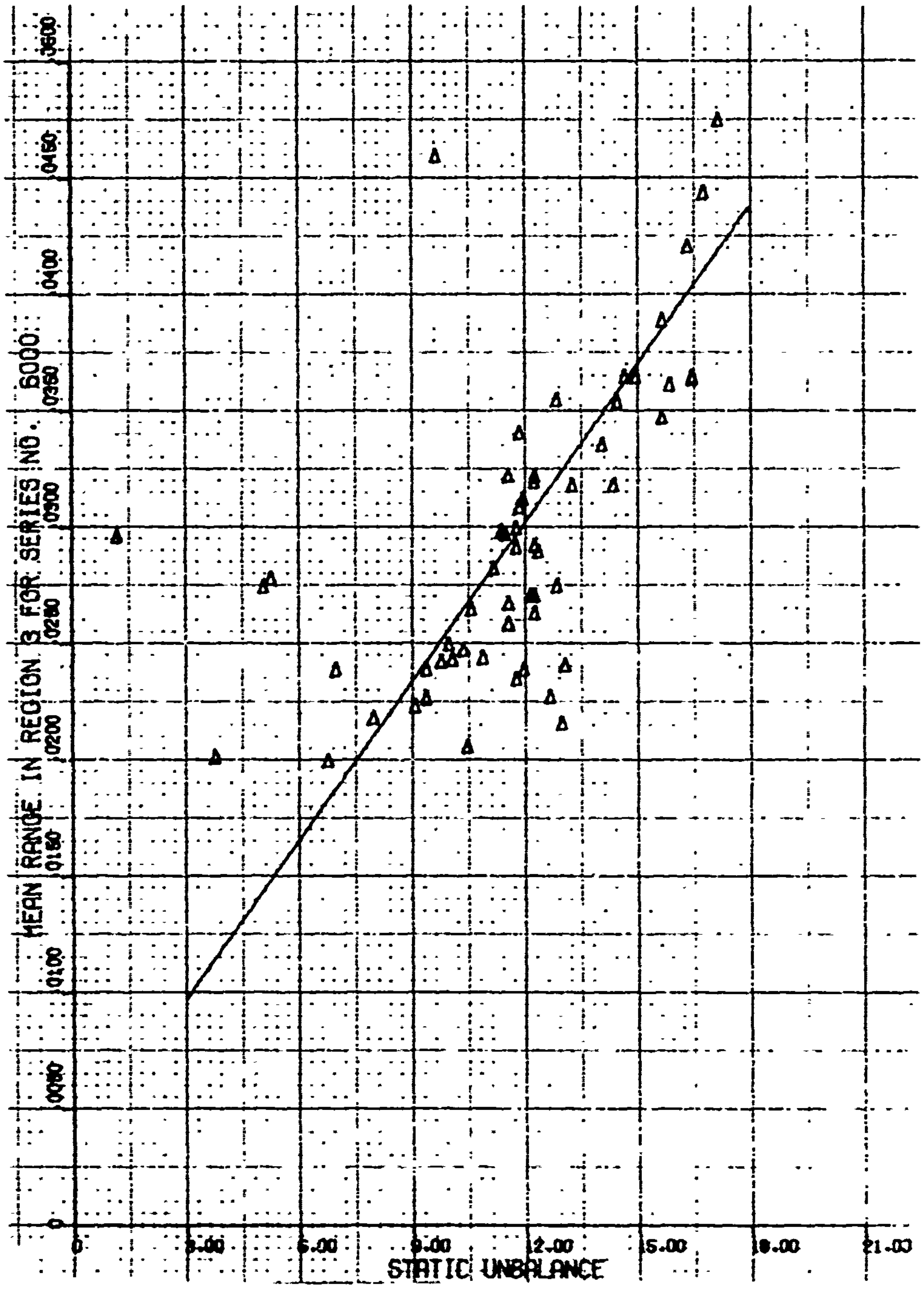

Figure 160 - Mean Wall Thickness Variation Versus Static Unbalance, Series 6000, Region 3, Full

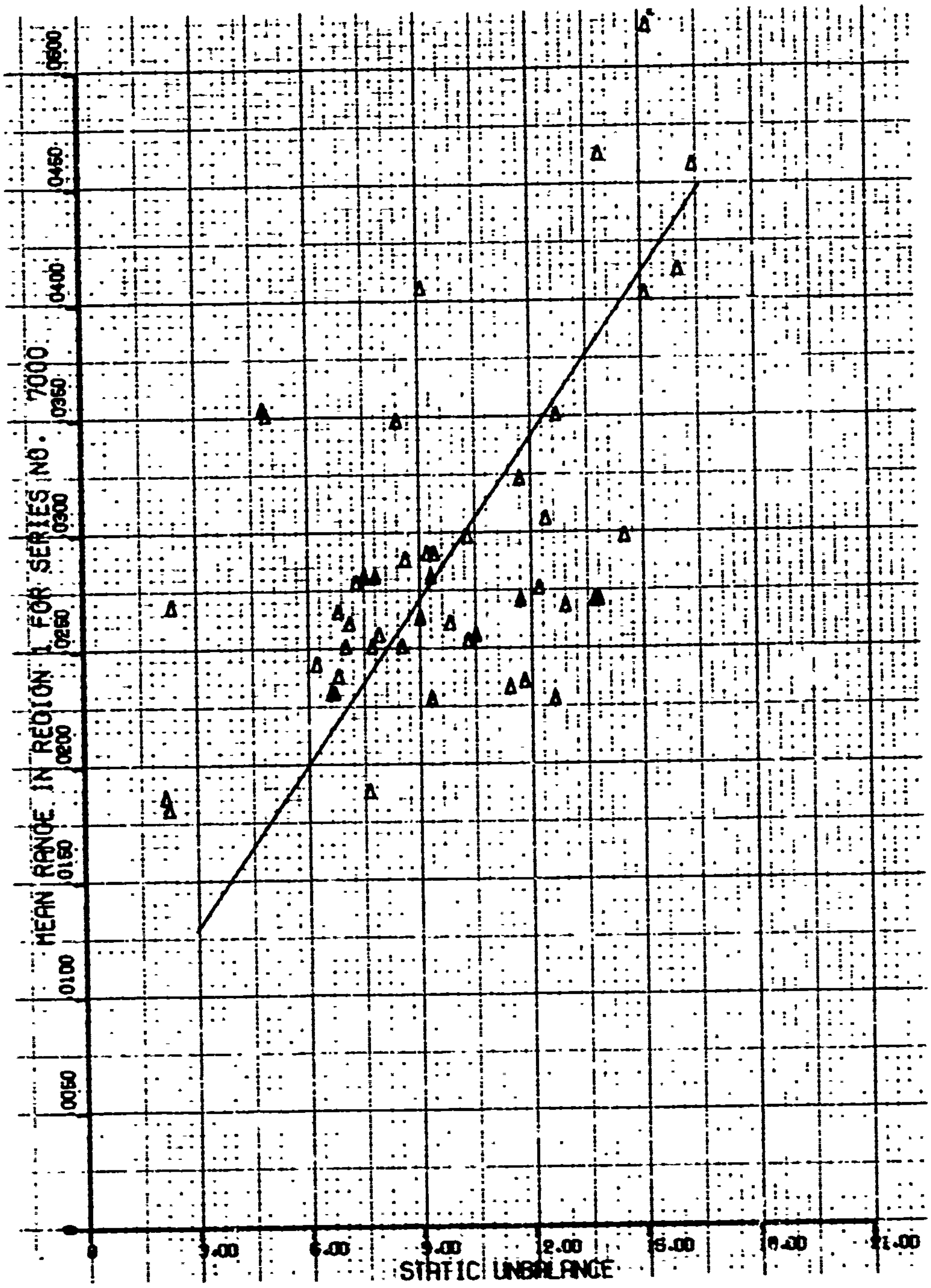

Figure 161 - Mean Wall Thickness Variation Versus Static Unbalance, Series 7000, Region 1, Full

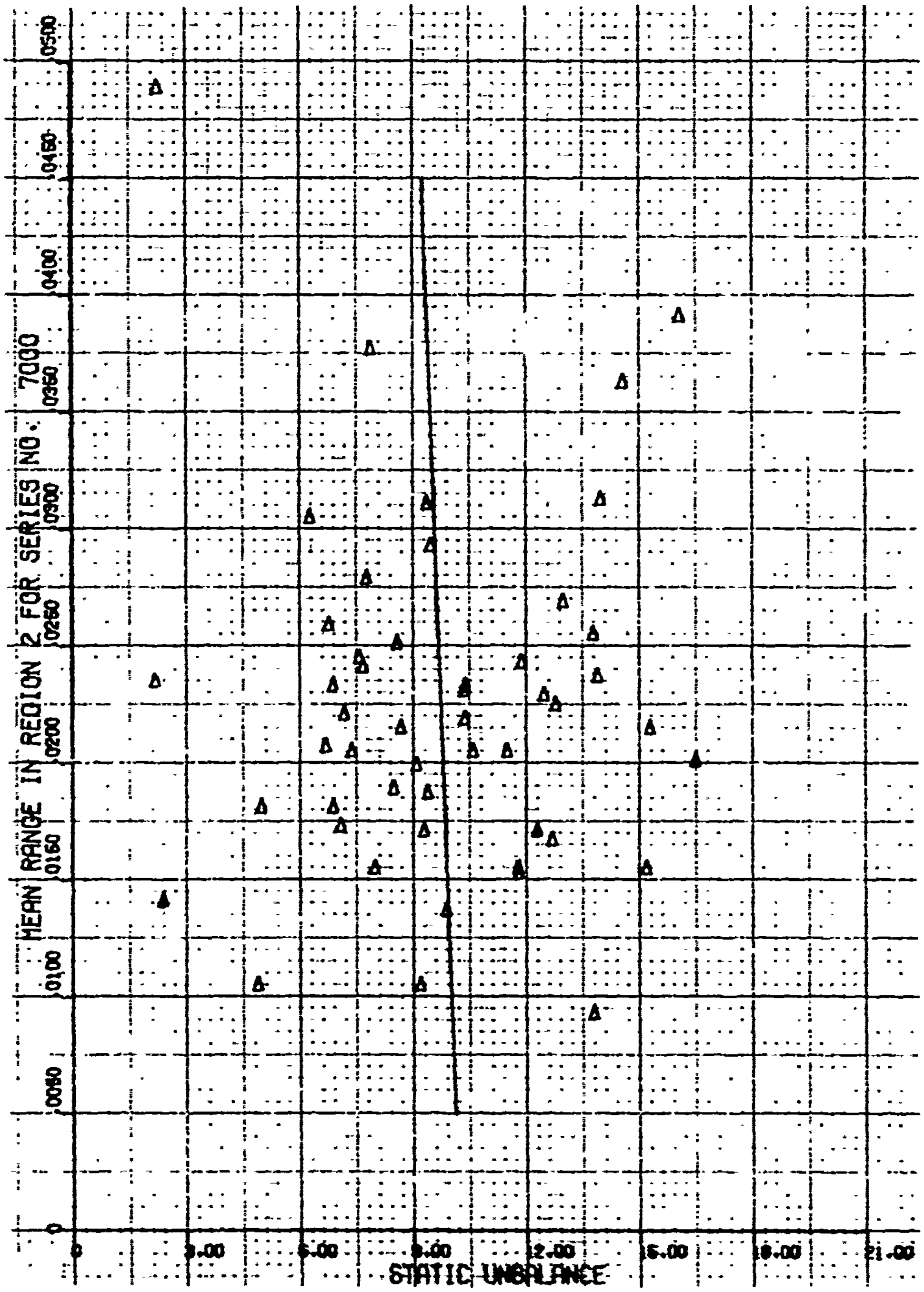

Figure 162 - Mean Wall Thickness Variation Versus Static Unbalance, Series 7000, Region 2, Full

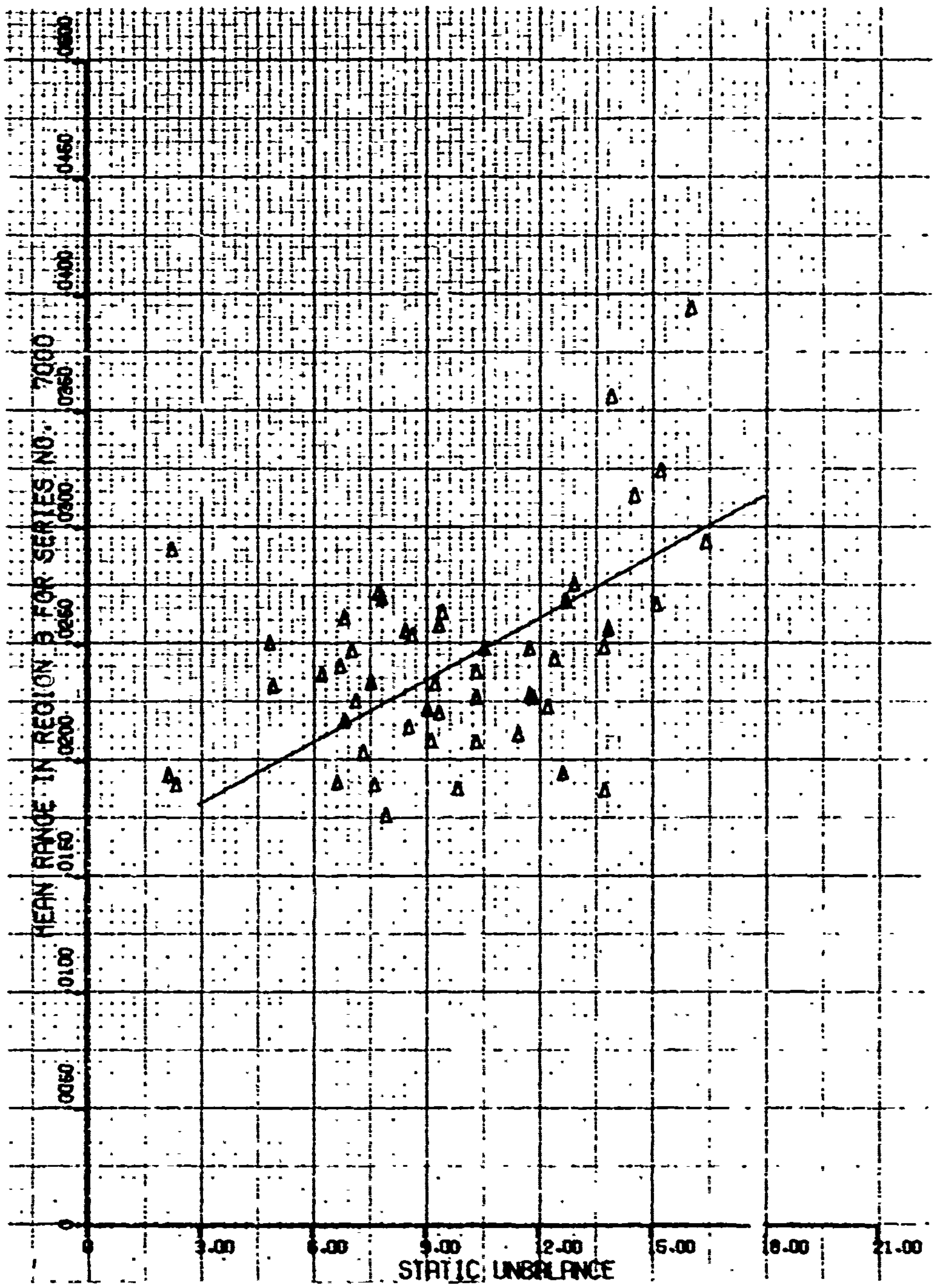

Figure 163 - Mean Wall Thickness Variation Versus Static Unbalance, Series 7000, Region 3, Full

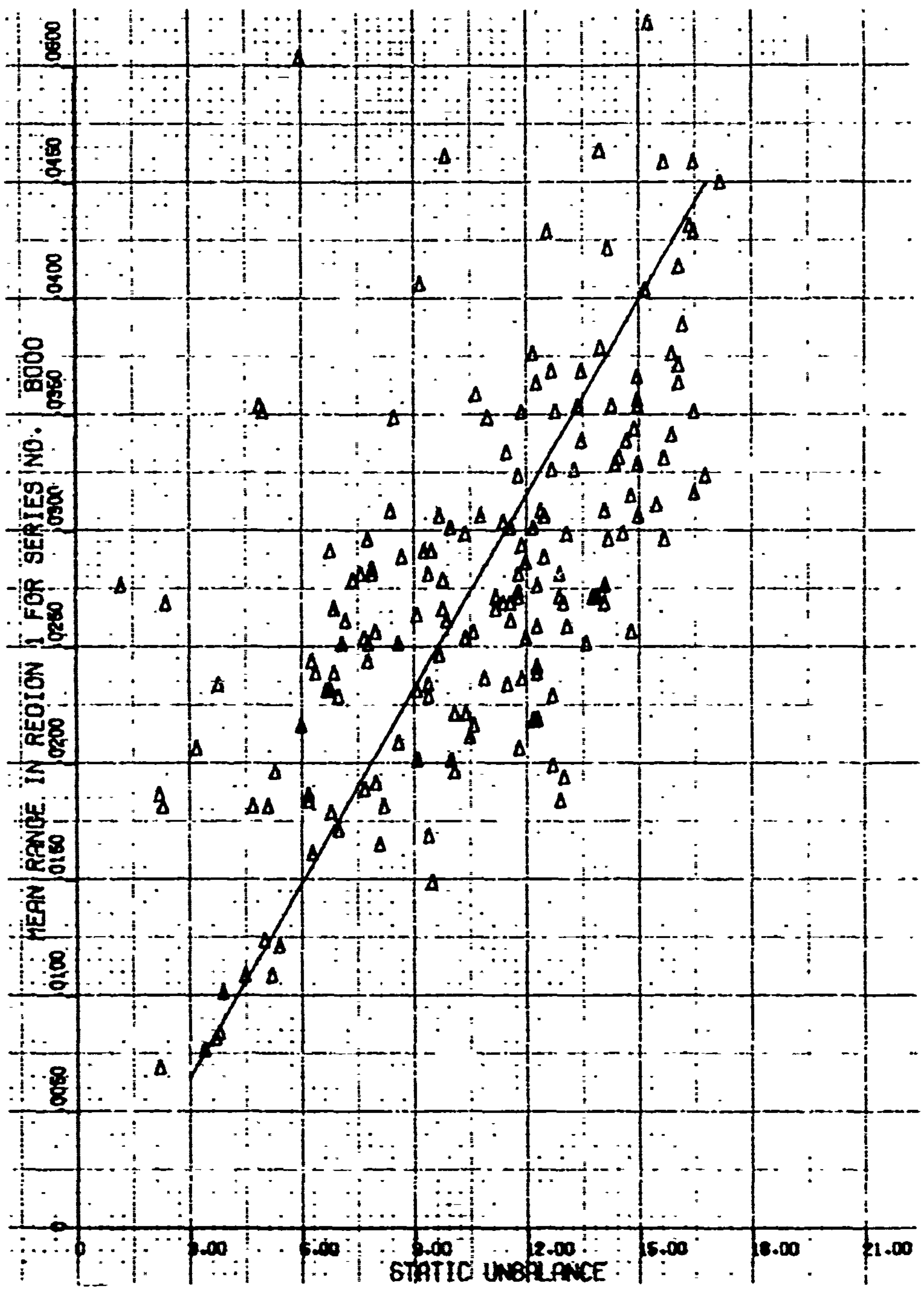

Figure 164 - Mean Wall Thickness Variation Versus Static Unbalance, Series 8000, Region 1, Full

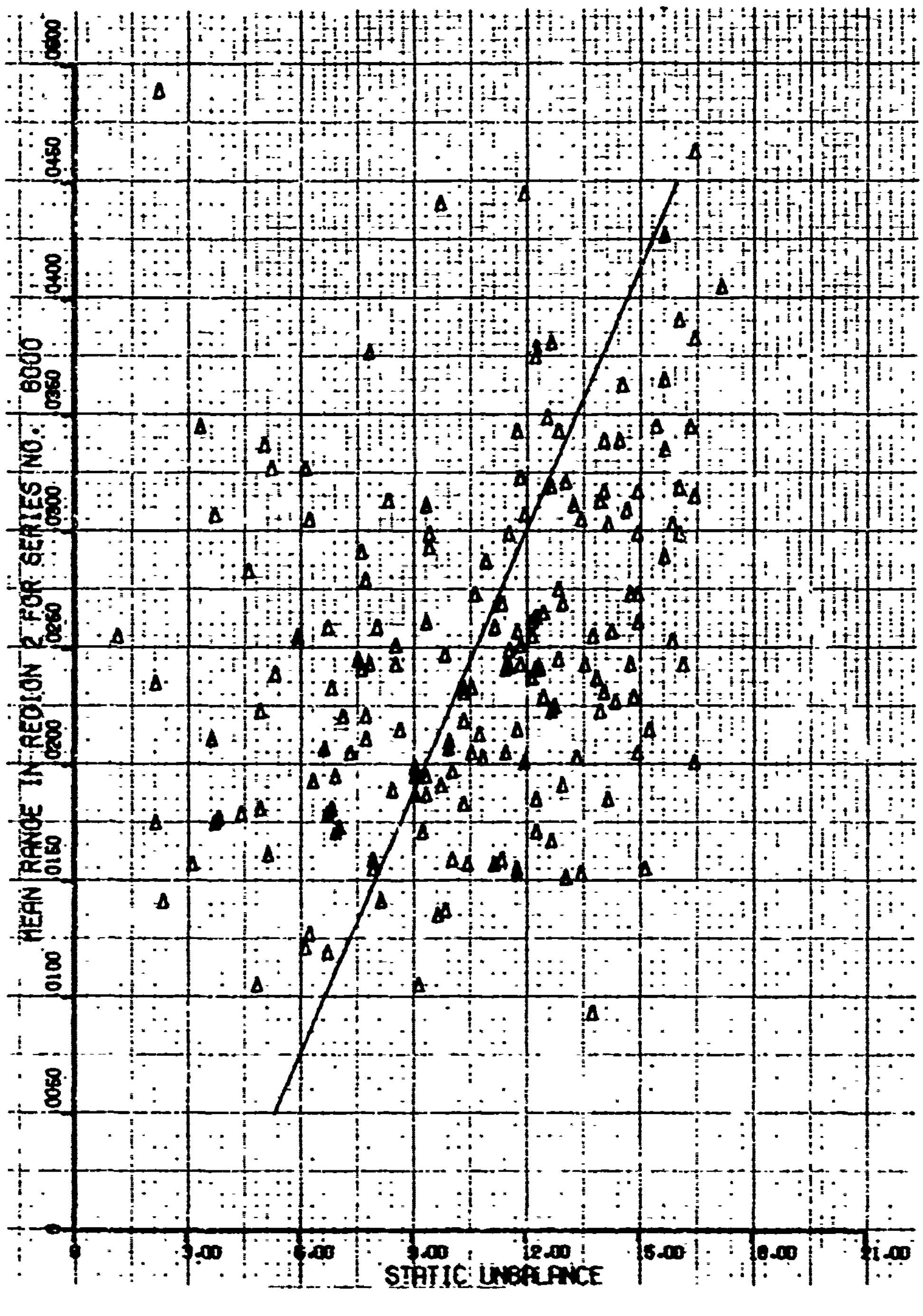

Figure 165 - Mean Wall Thickness Variation Versus Static Unbalance, Series 8000, Region 2, Full

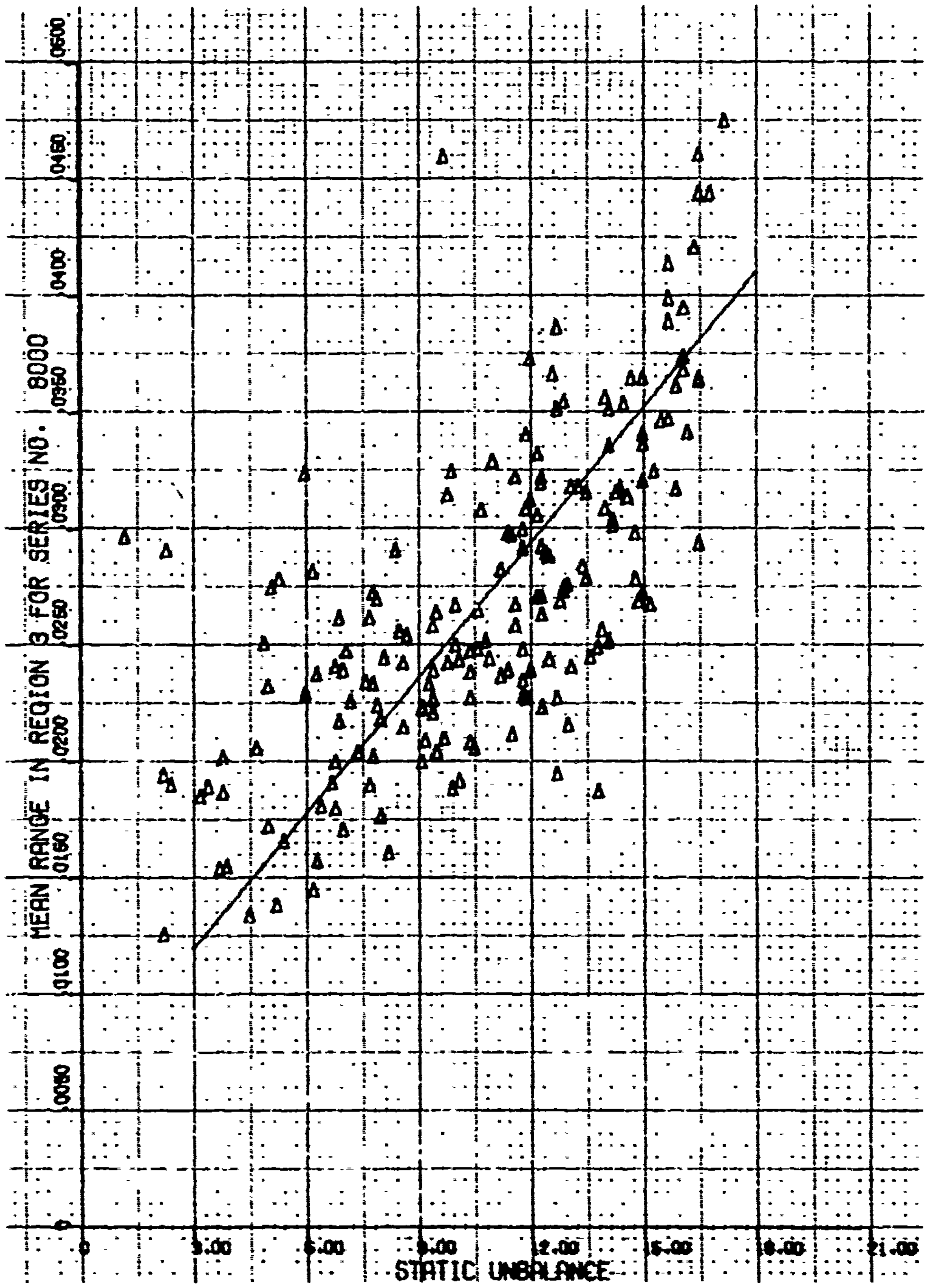

Figure 166 - Mean Wall Thickness Variation Versus Static Unbalance, Series 8000, Region 3, Full

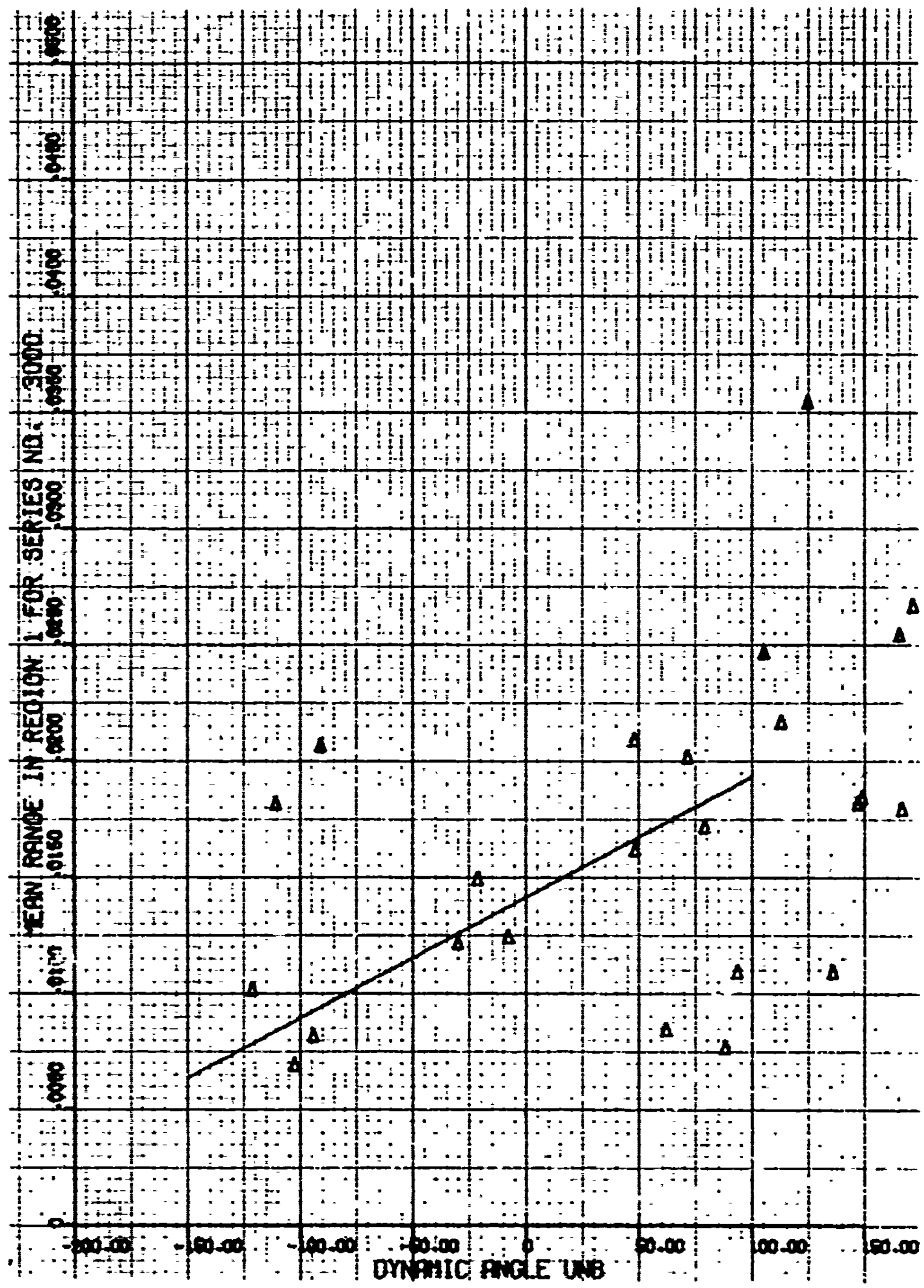

Figure 167 - Mean Wall Thickness Variation Versus Azimuth of Dynamic Unbalance, Series 3000, Region 1, Empty

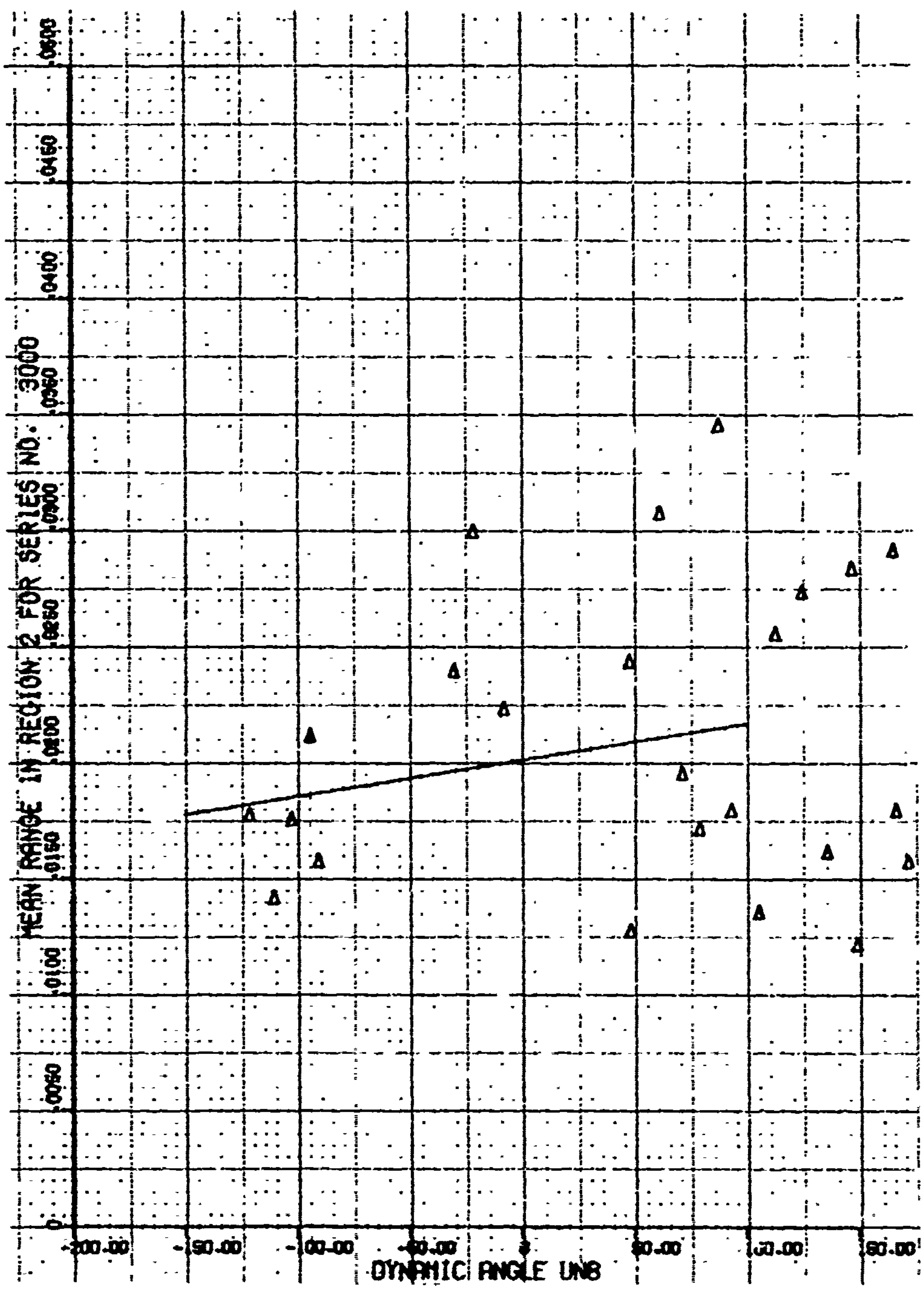

Figure 168 - Mean Wall Thickness Variation Versus Azimuth of Dynamic Unbalance, Series 3000, Region 2, Empty

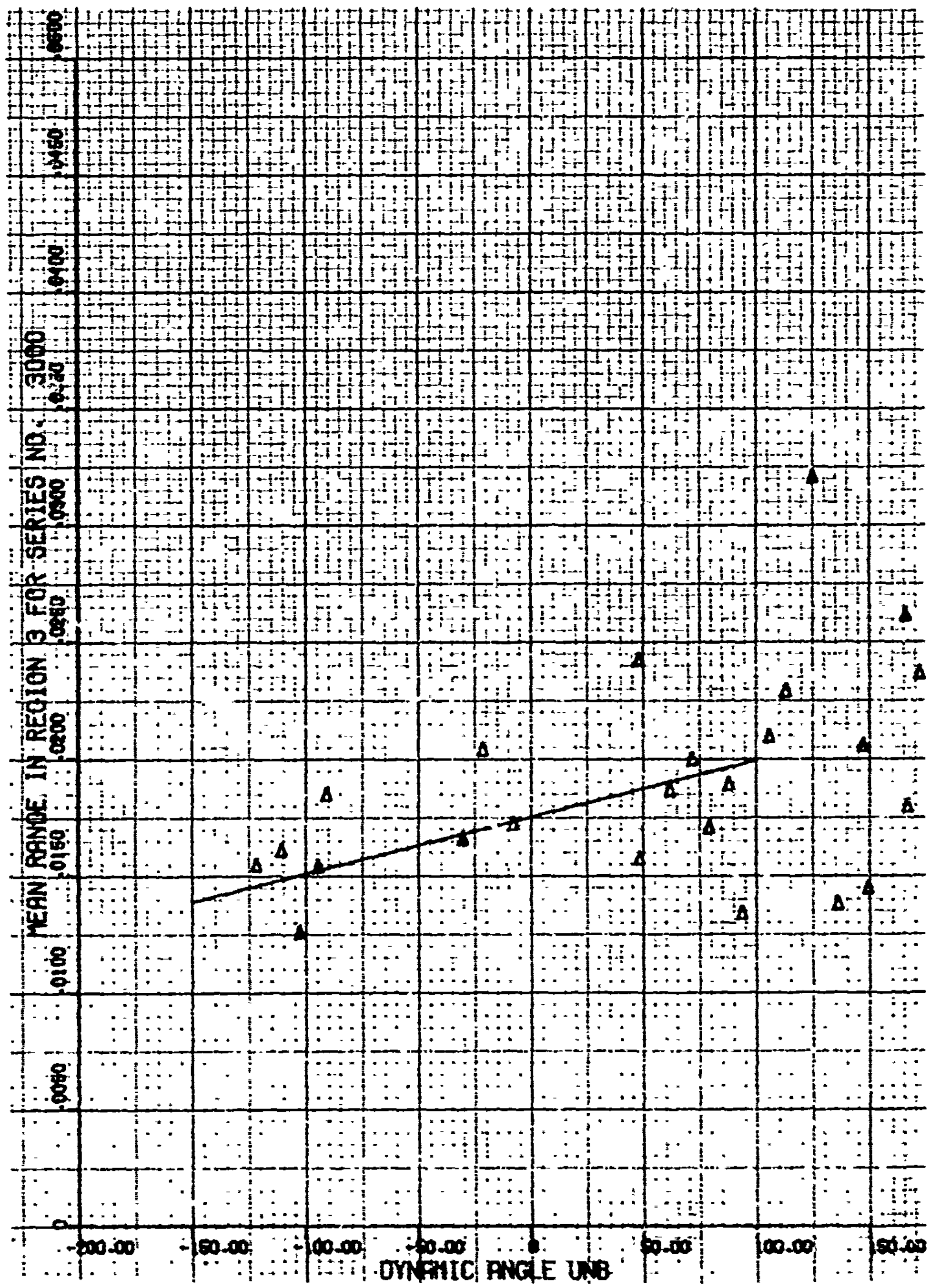

Figure 169 - Mean Wall Thickness Variation Versus Azimuth of Dynamic Unbalance, Ser[illegible]s 3000, Region 3, Empty

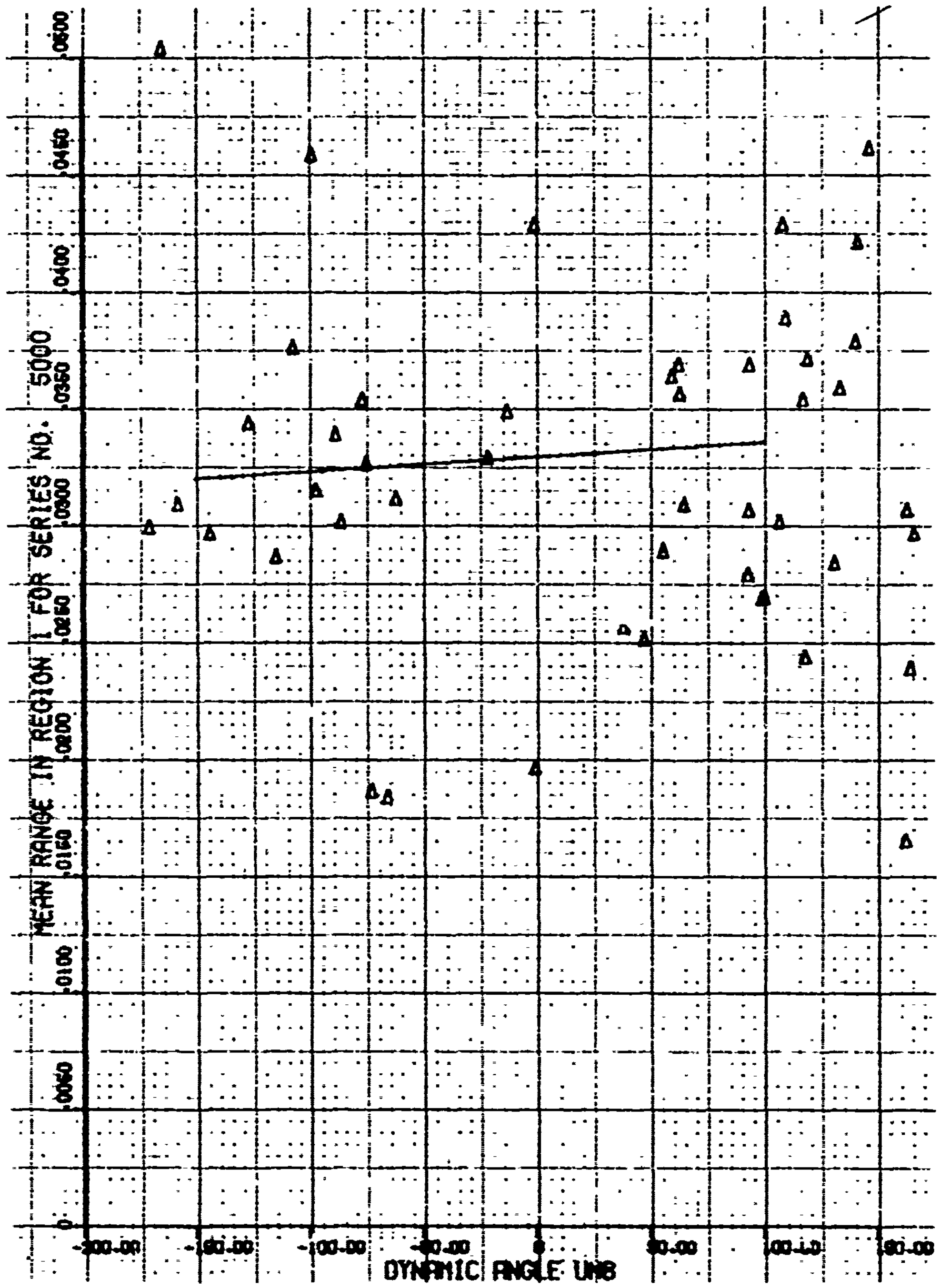

Figure 170 - Mean Wall Thickness Variation Versus Azimuth of Dynamic Unbalance, Series 5000, Region 1, Empty

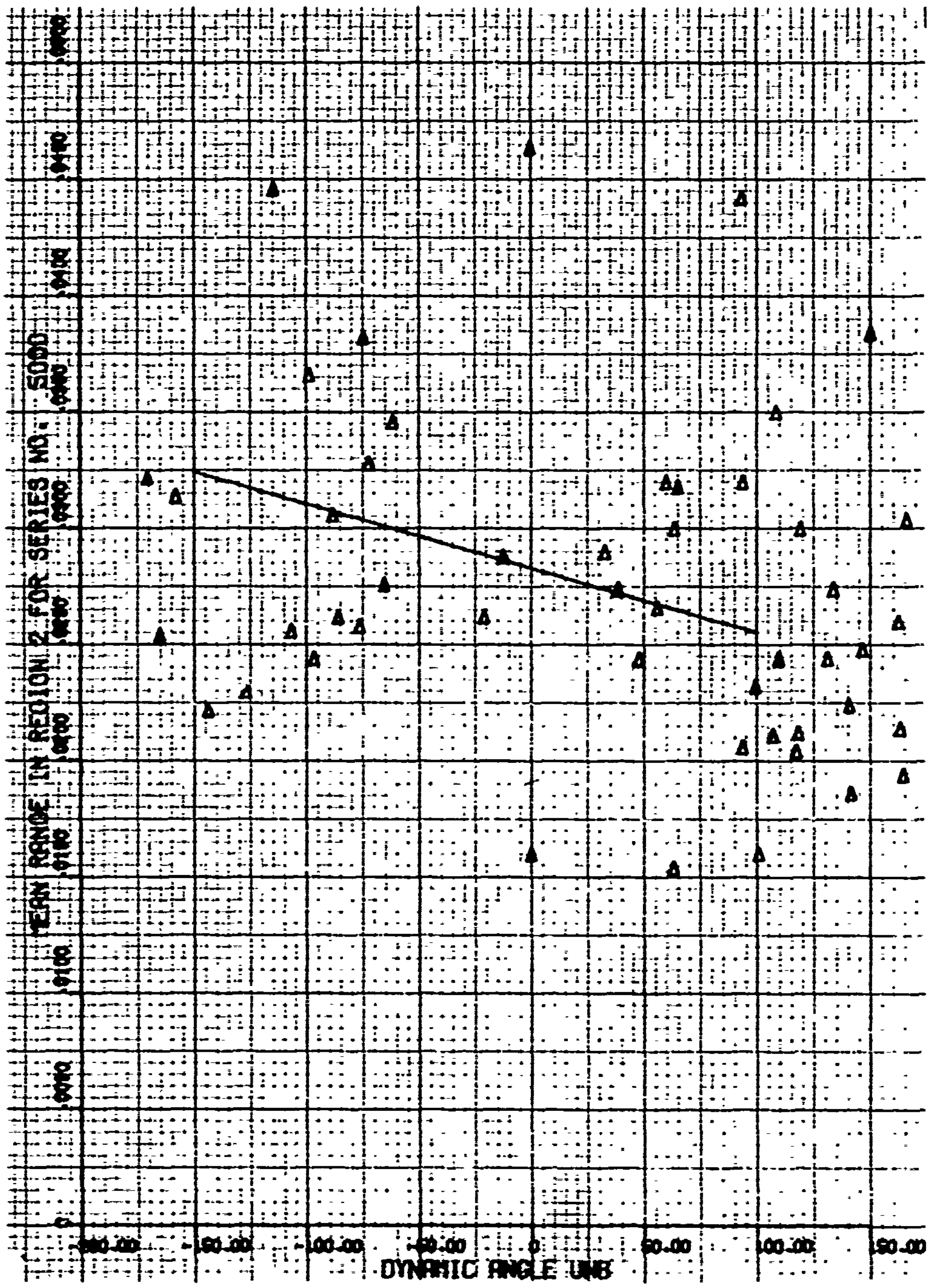

Figure 171 - Mean Wall Thickness Variation Versus Azimuth of Dynamic Unbalance, Series 5000, Region 2, Empty

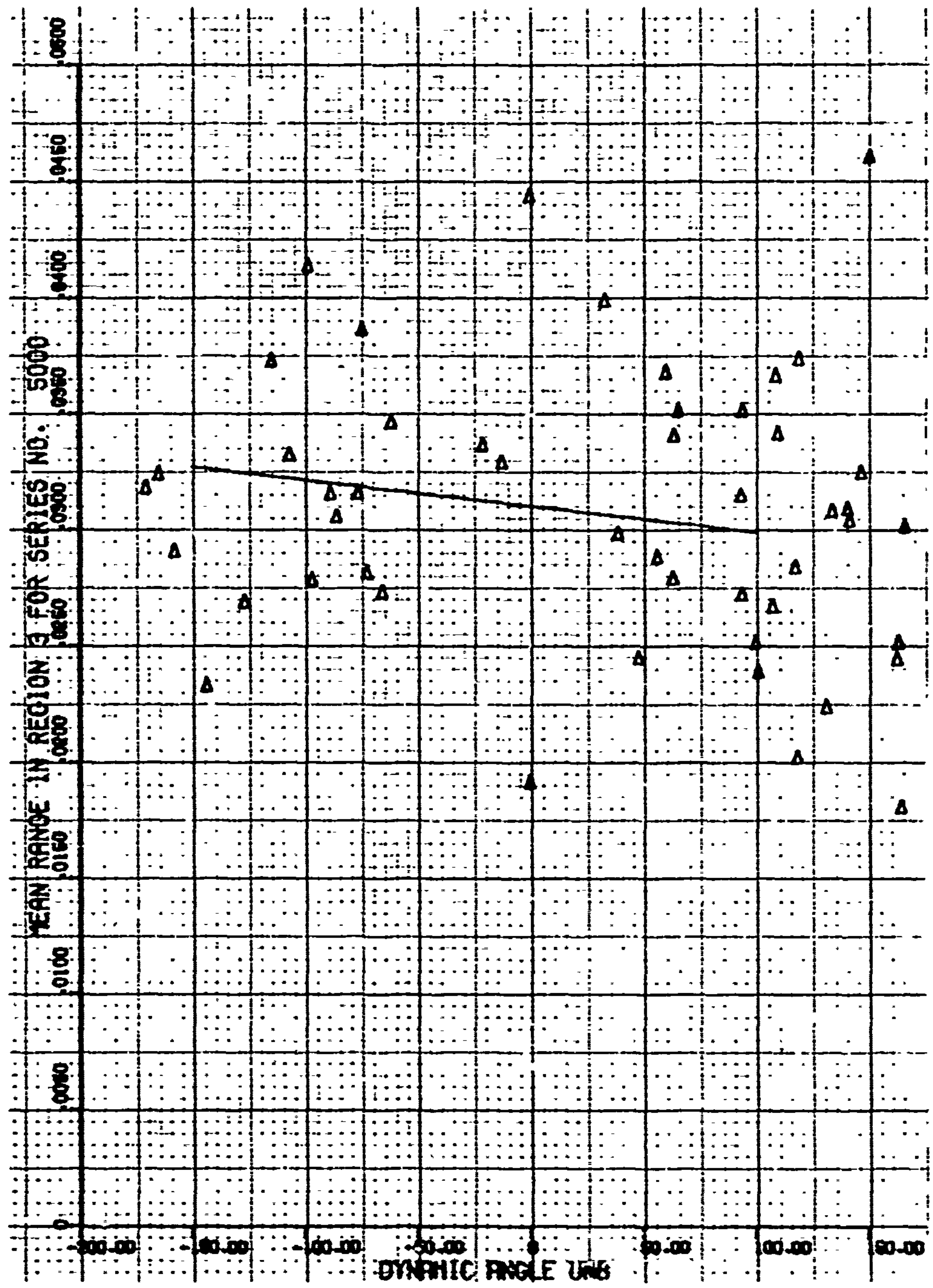

Figure 172 - Mean Wall Thickness Variation Versus Azimuth of Dynamic Unbalance, Series 5000, Region 3, Empty

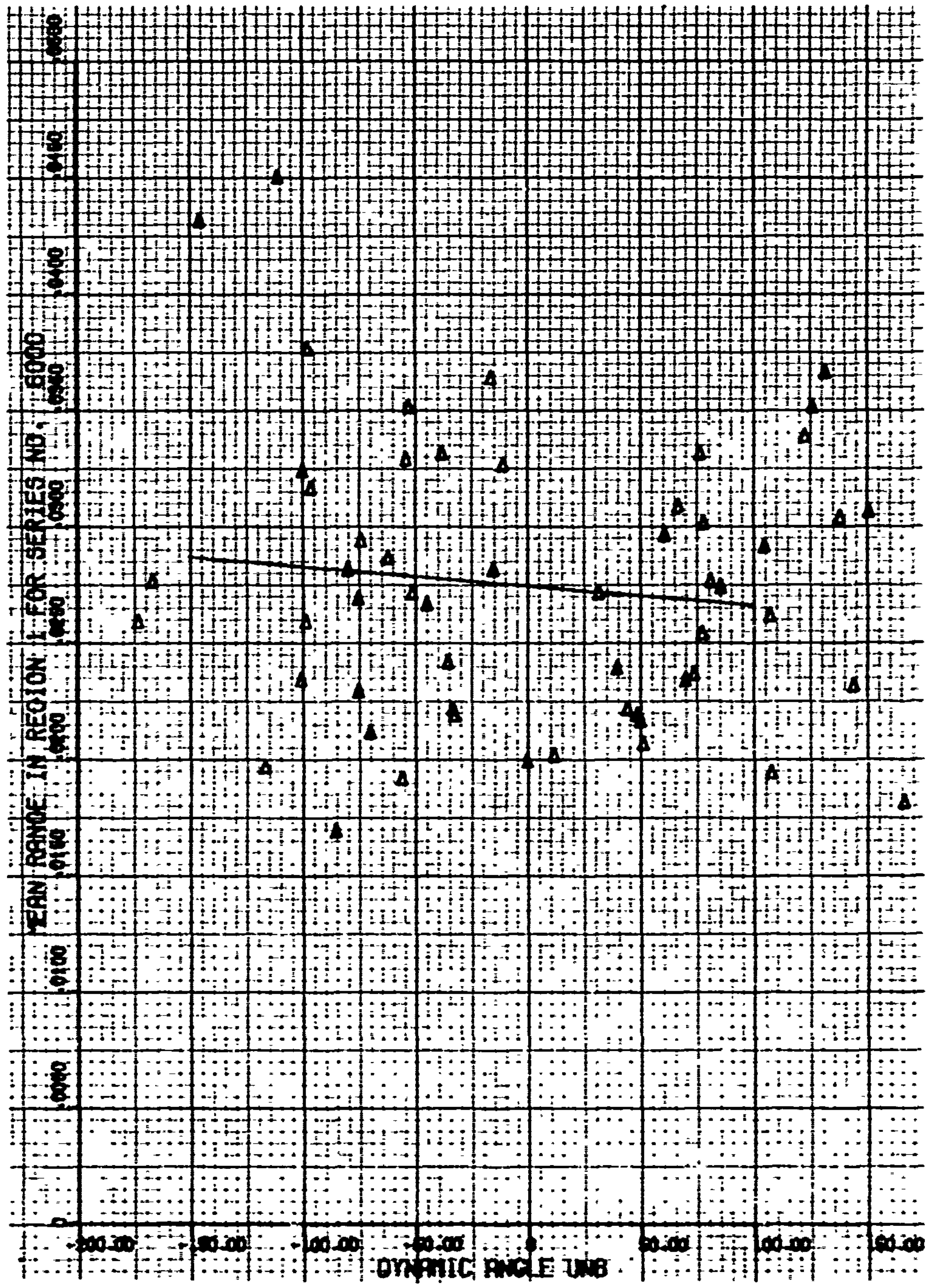

Figure 173 - Mean Wall Thickness Variation Versus Azimuth of Dynamic Unbalance, Series 6000, Region 1, Empty

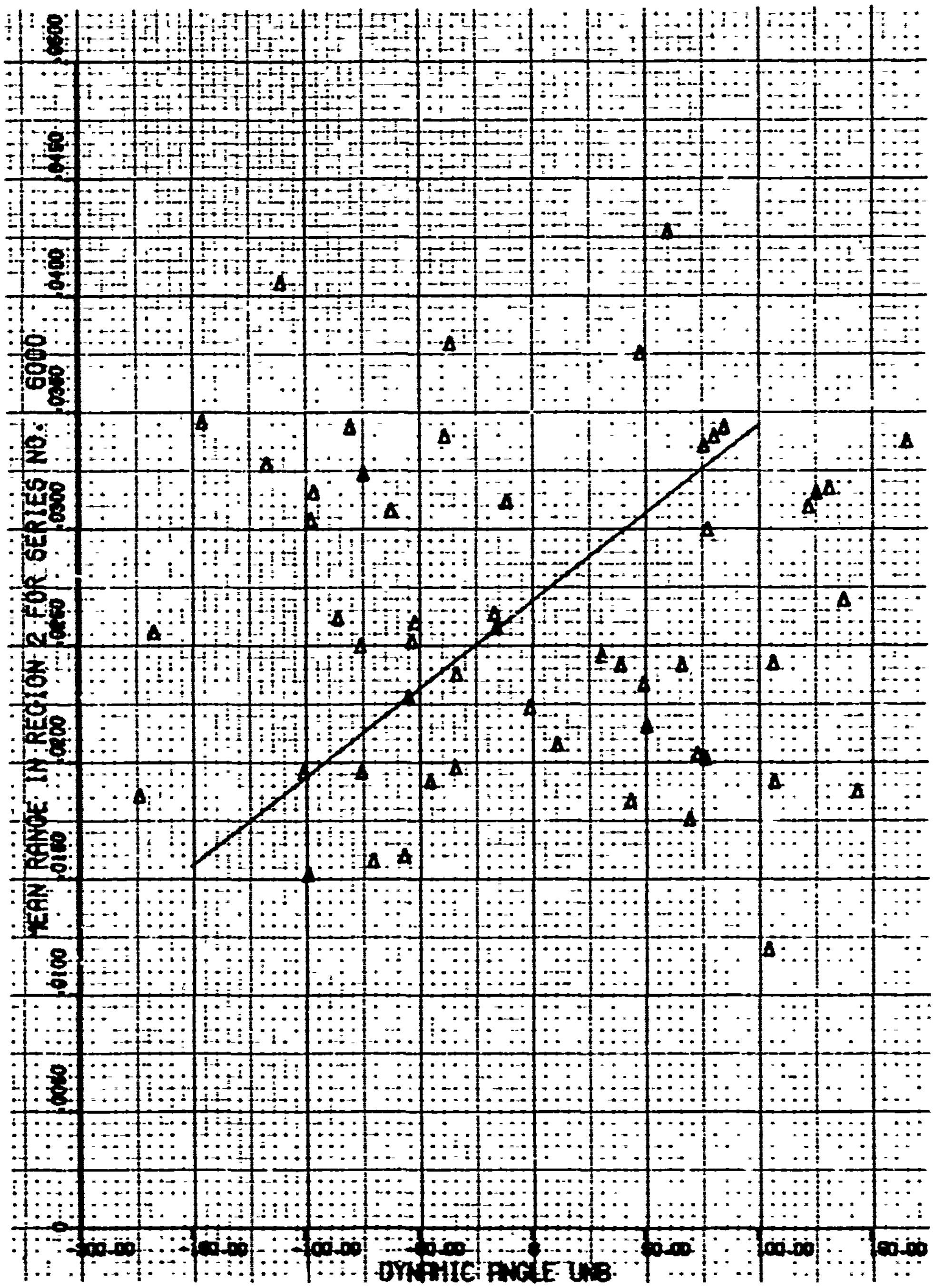

Figure 174 - Mean Wall Thickness Variation Versus Azimuth of Dynamic Unbalance, Series 6000, Region 2, Empty

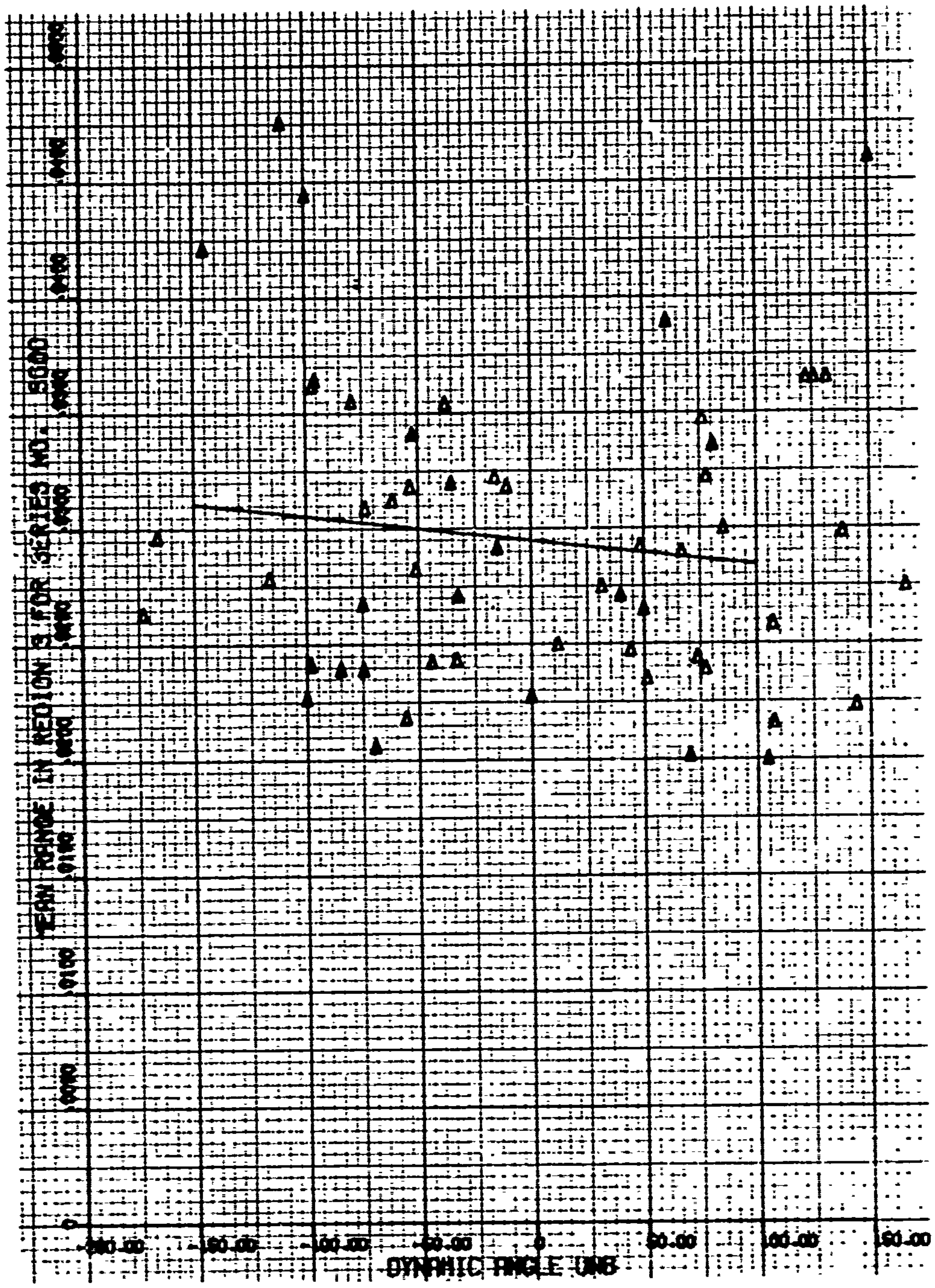

Figure 175 - Mean Wall Thickness Variation Versus Azimuth of Dynamic Unbalance, Series 6000, Region 3, Empty

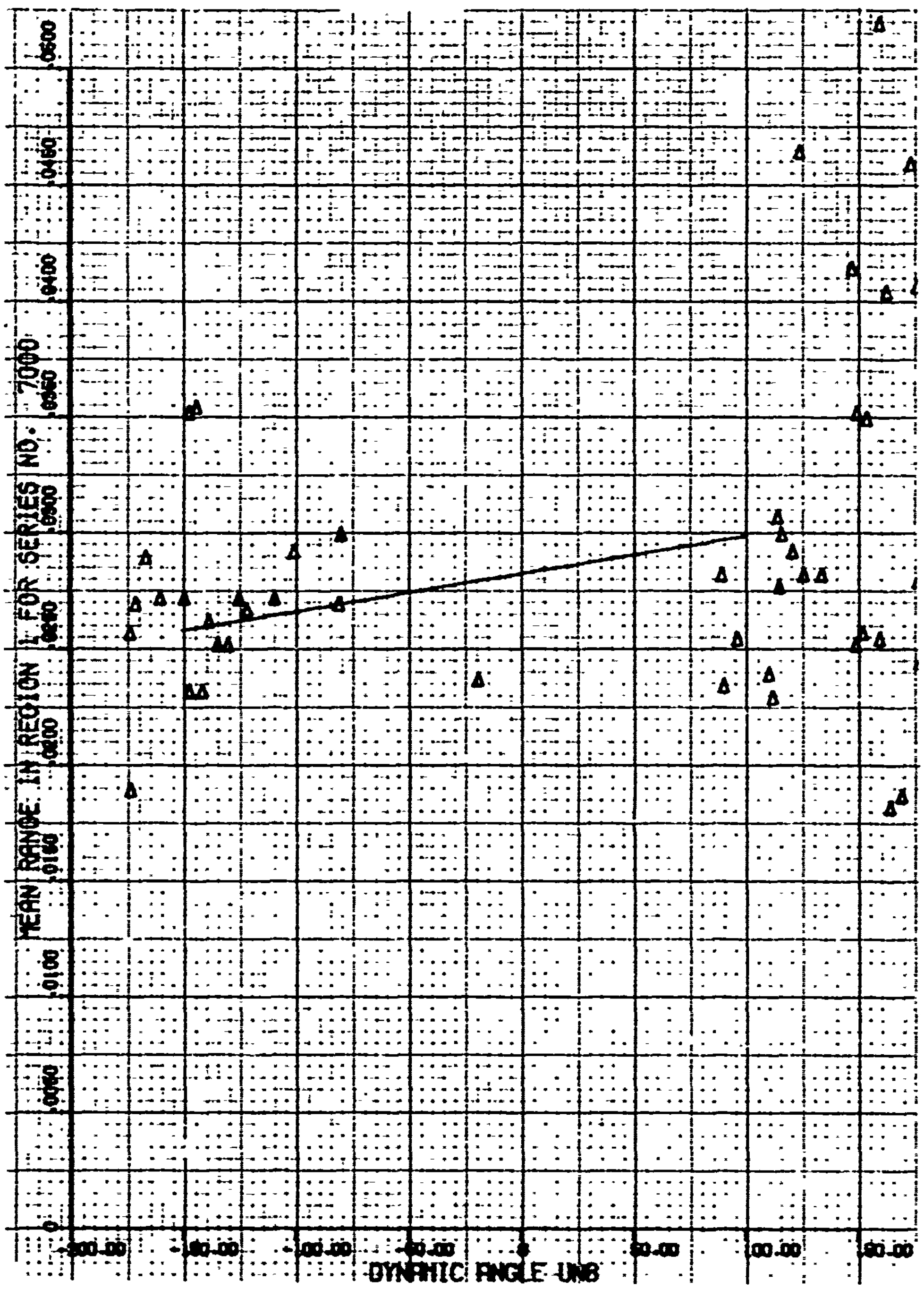

Figure 176 - Mean Wall Thickness Variation Versus Azimuth of Dynamic Unbalance, Series 7000, Region 1, Empty

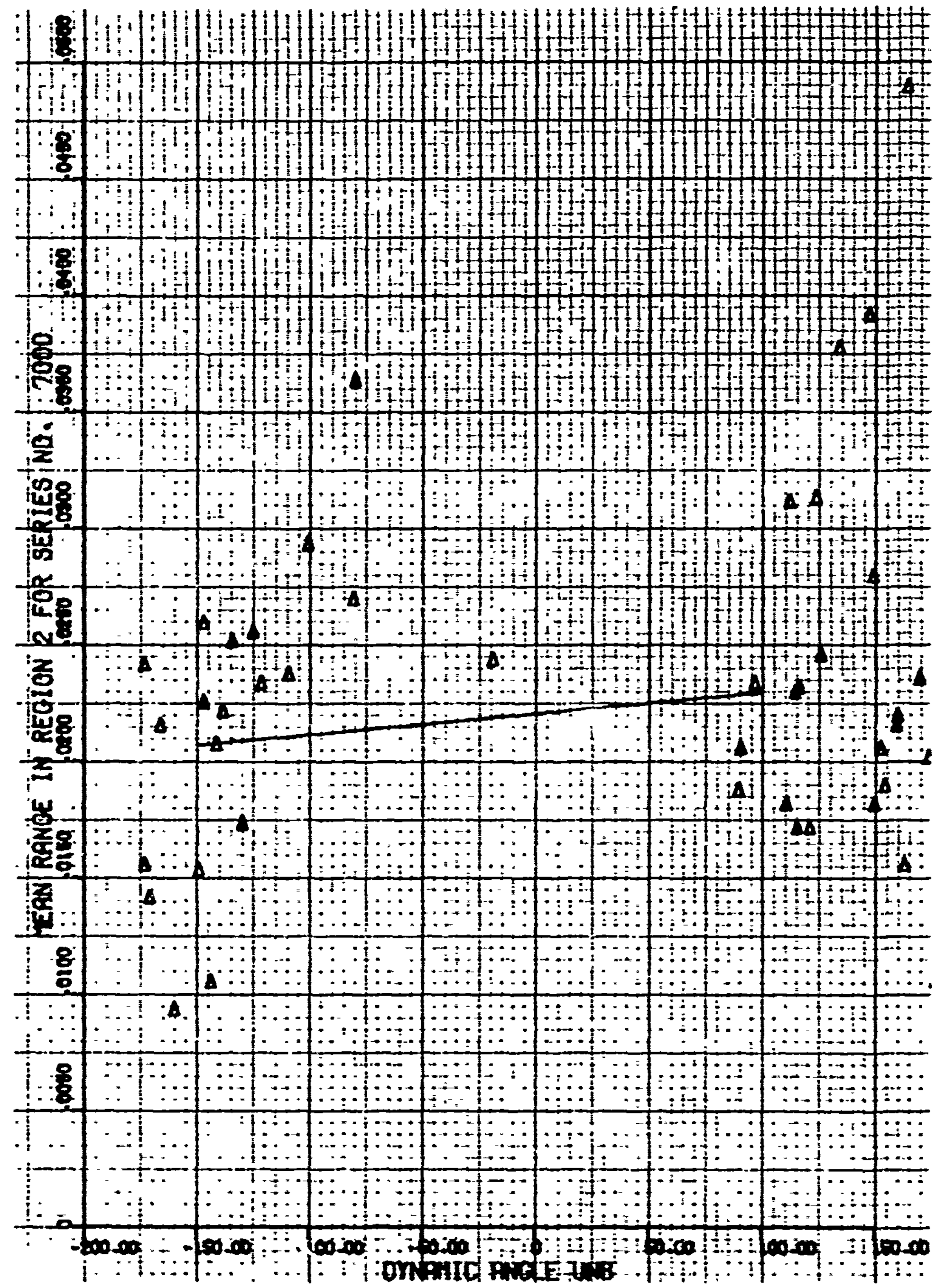

Figure 177 - Mean Wall Thickness Variation Versus Azimuth of Dynamic Unbalance, Series 7000, Region 2, Empty

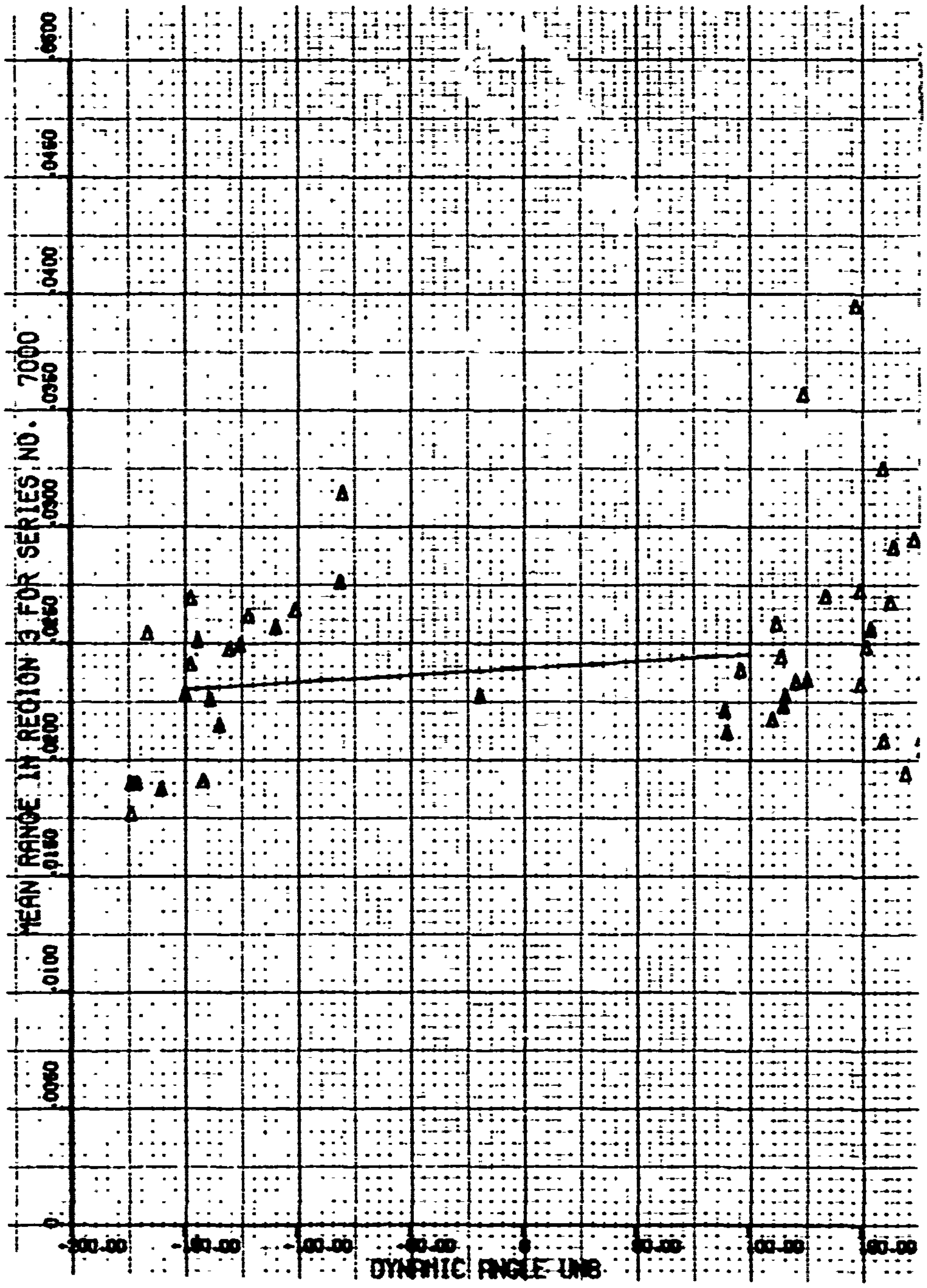

Figure 178 - Mean Wall Thickness Variation Versus Azimuth of Dynamic Unbalance, Series 7000, Region 3, Empty

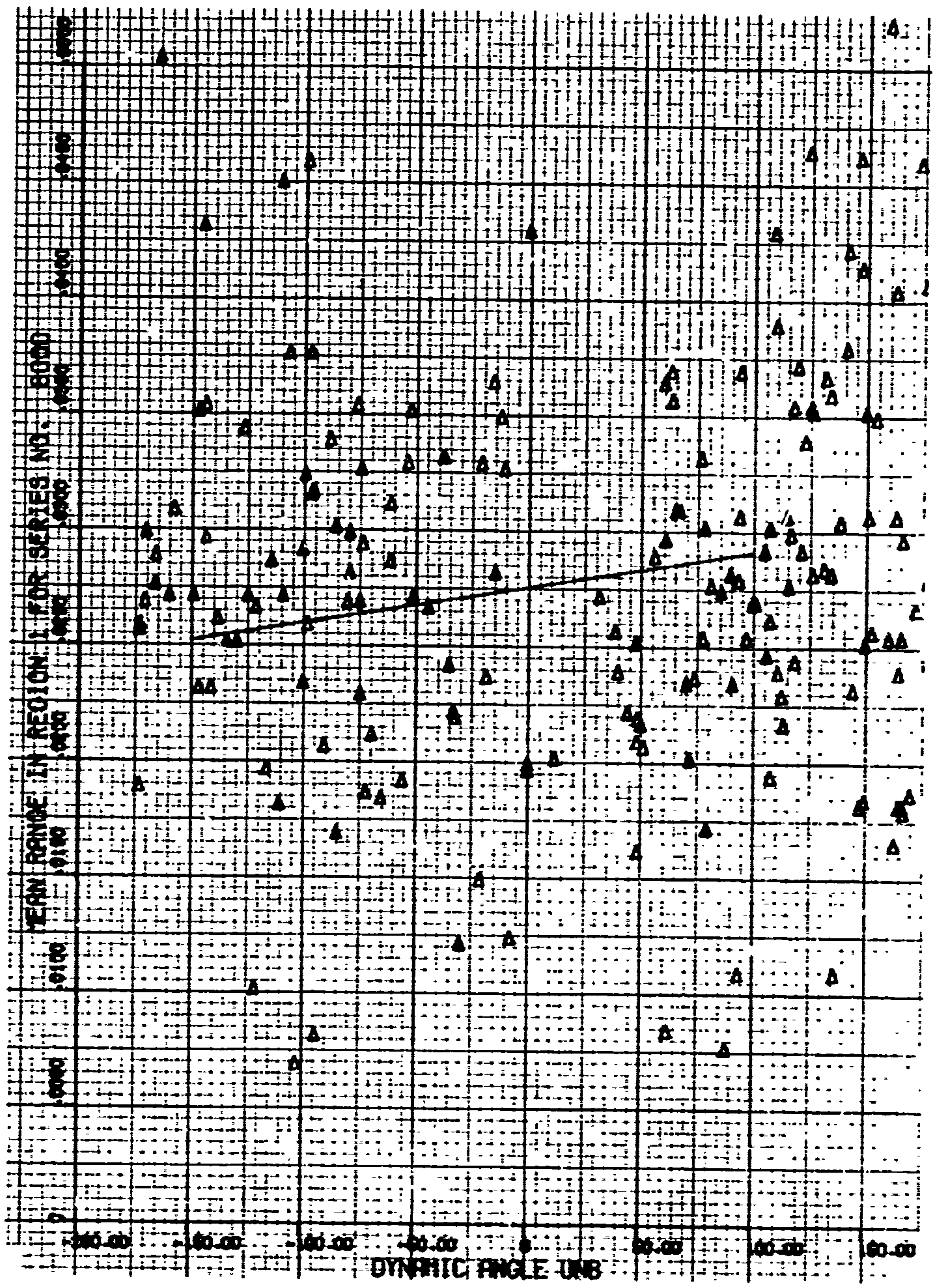

Figure 179 - Mean Wall Thickness Variation Versus Azimuth of Dynamic Unbalance, Series 8000, Region 1, Empty

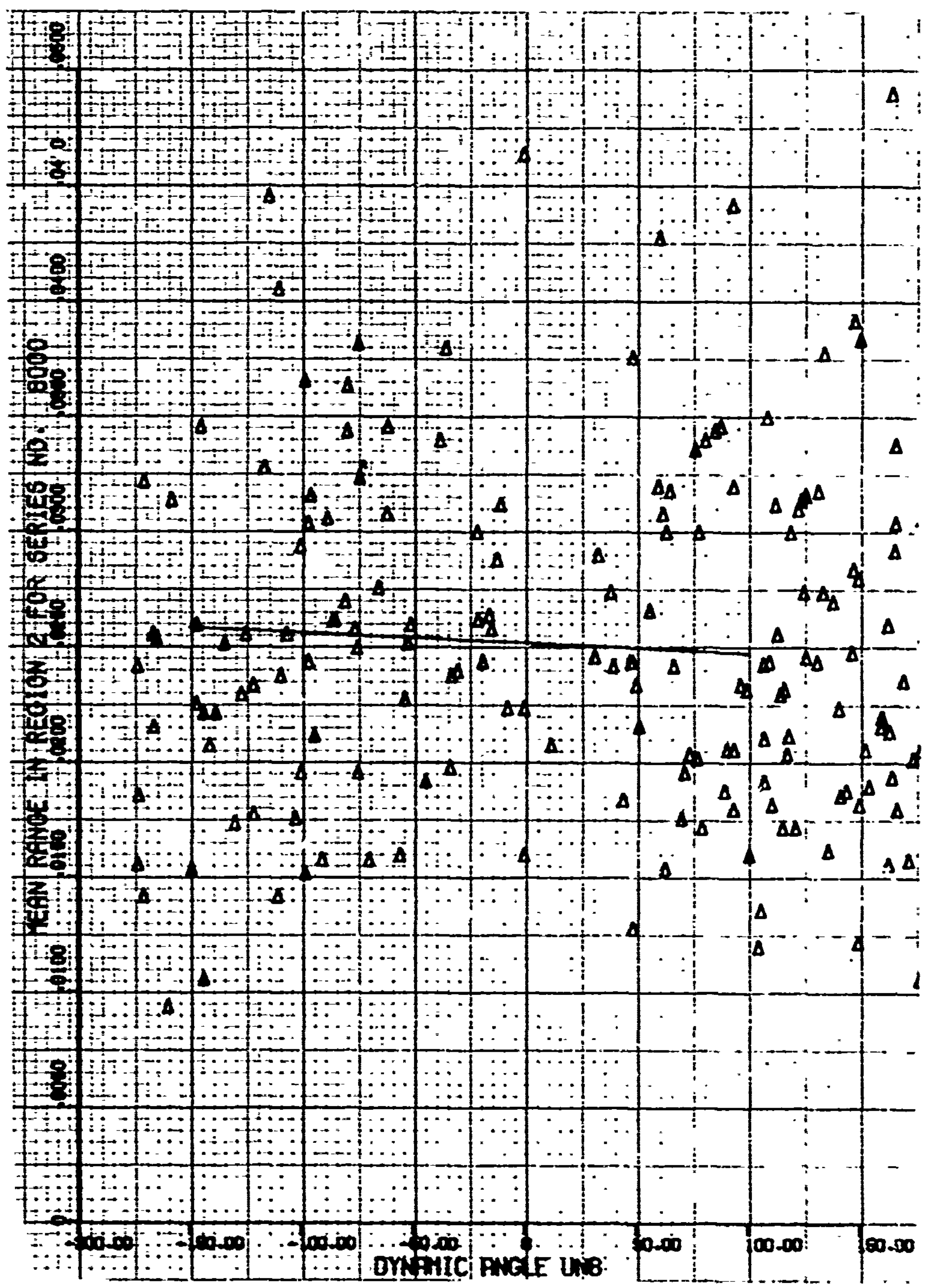

Figure 180 - Mean Wall Thickness Variation Versus Azimuth of Dynamic Unbalance, Series 8000, Region 2, Empty

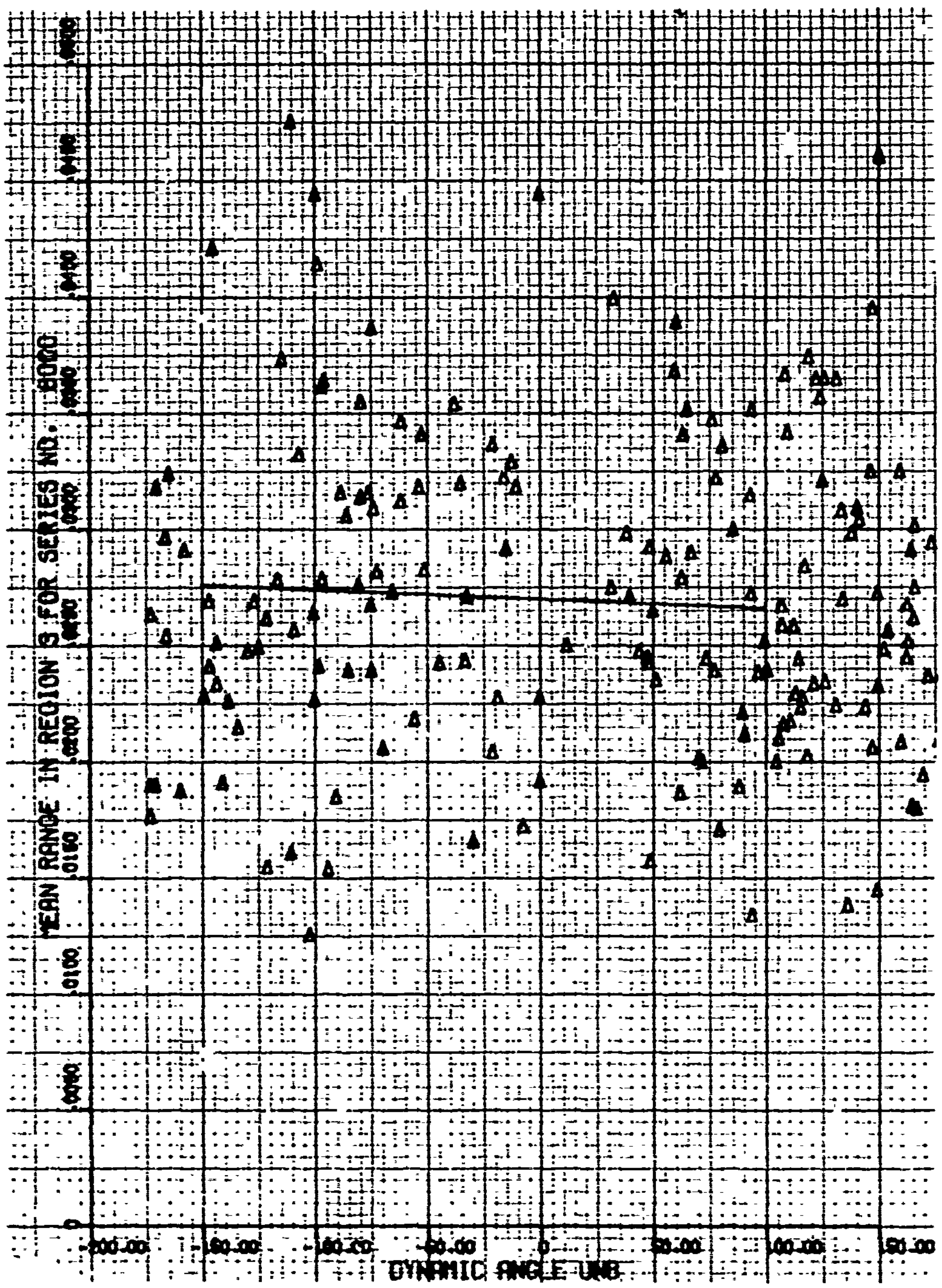

Figure 181 - Mean Wall Thickness Variation Versus Azimuth of Dynamic Unbalance, Series 8000, Region 3, Empty

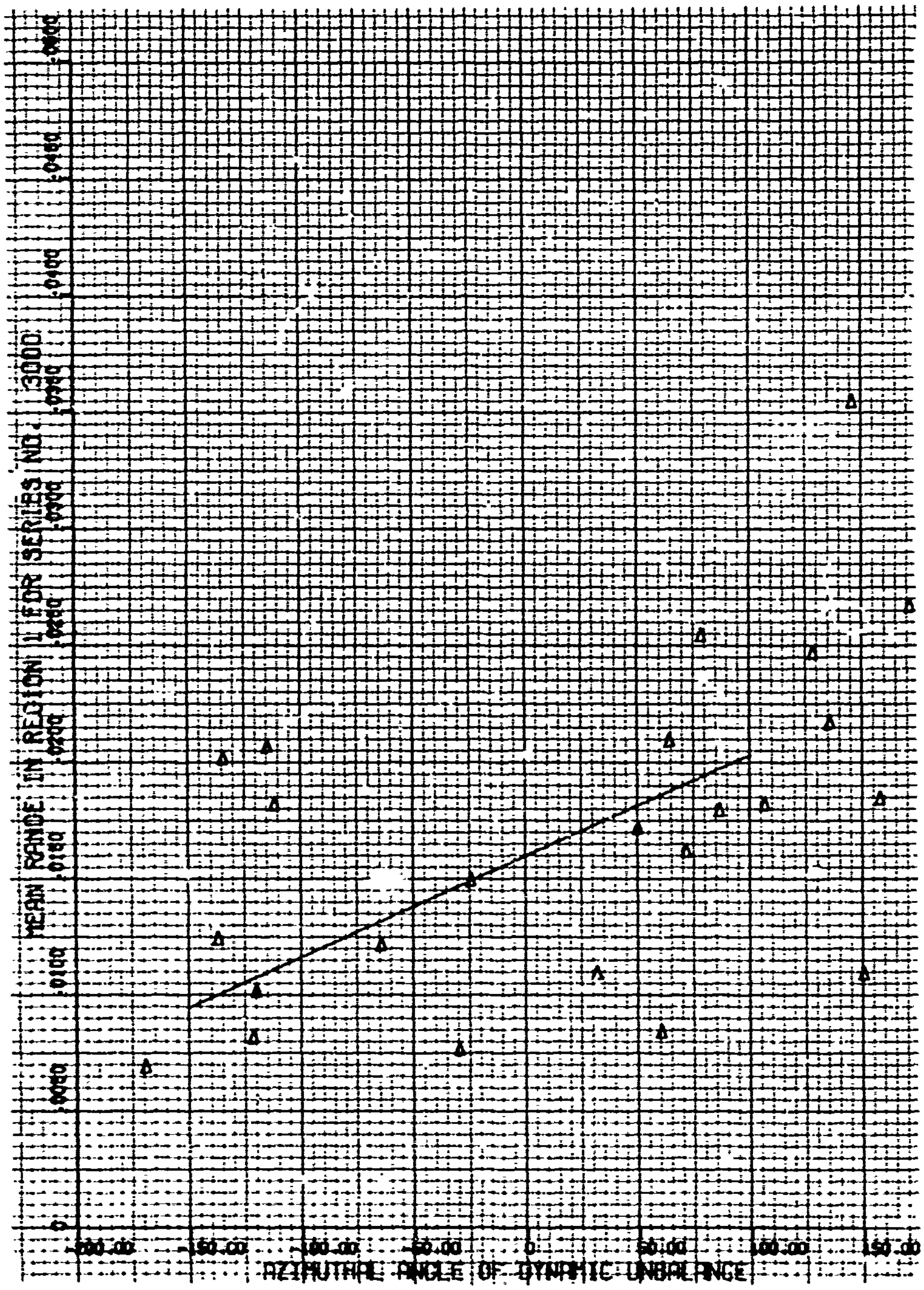

Figure 182 - Mean Wall Thickness Variation Versus Azimuth of Dynamic Unbalance, Series 3000, Region 1, Full

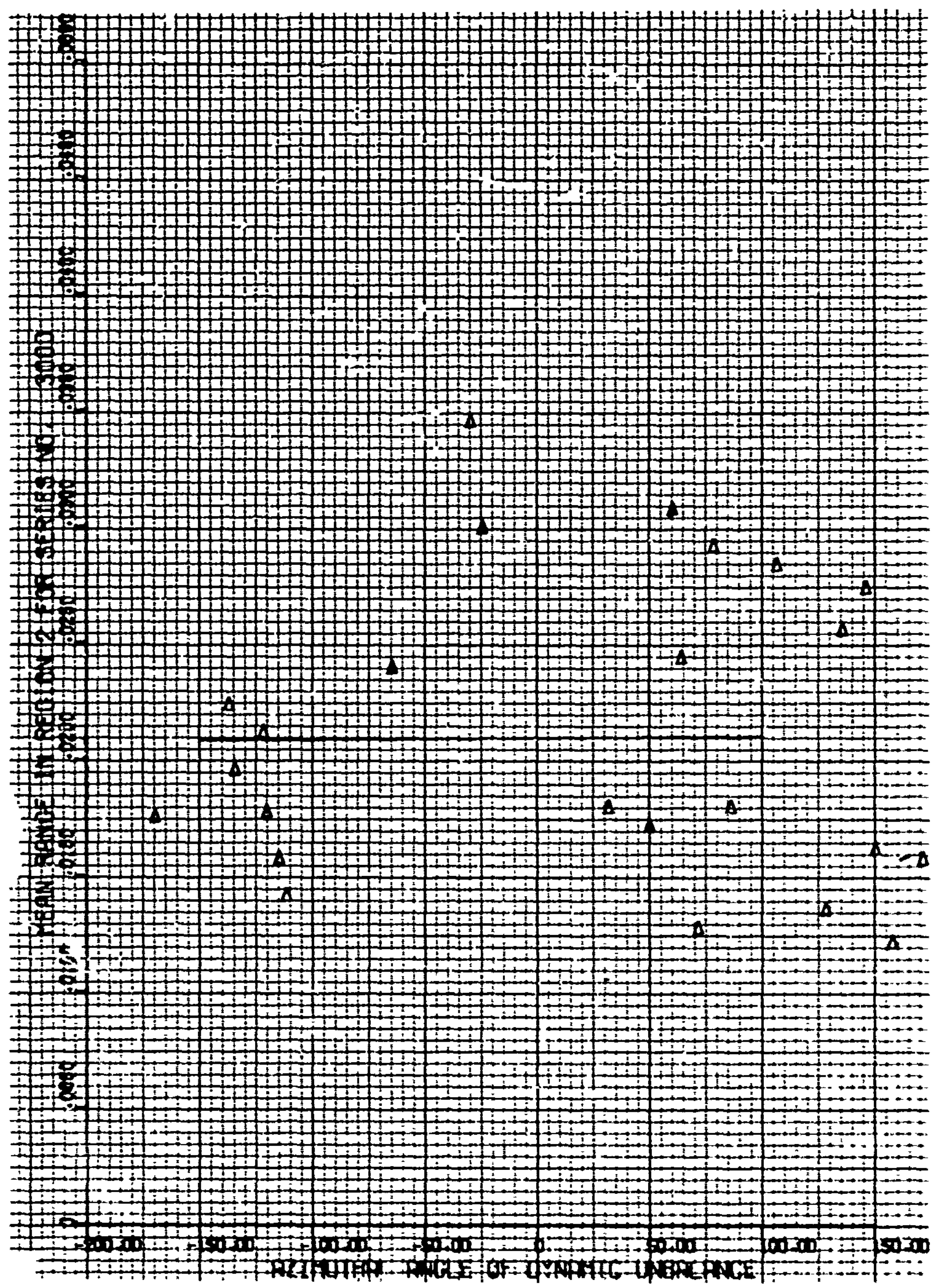

Figure 183 - Mean Wall Thickness Variation Versus Azimuth of Dynamic Unbalance, Series 3000, Region 2, Full

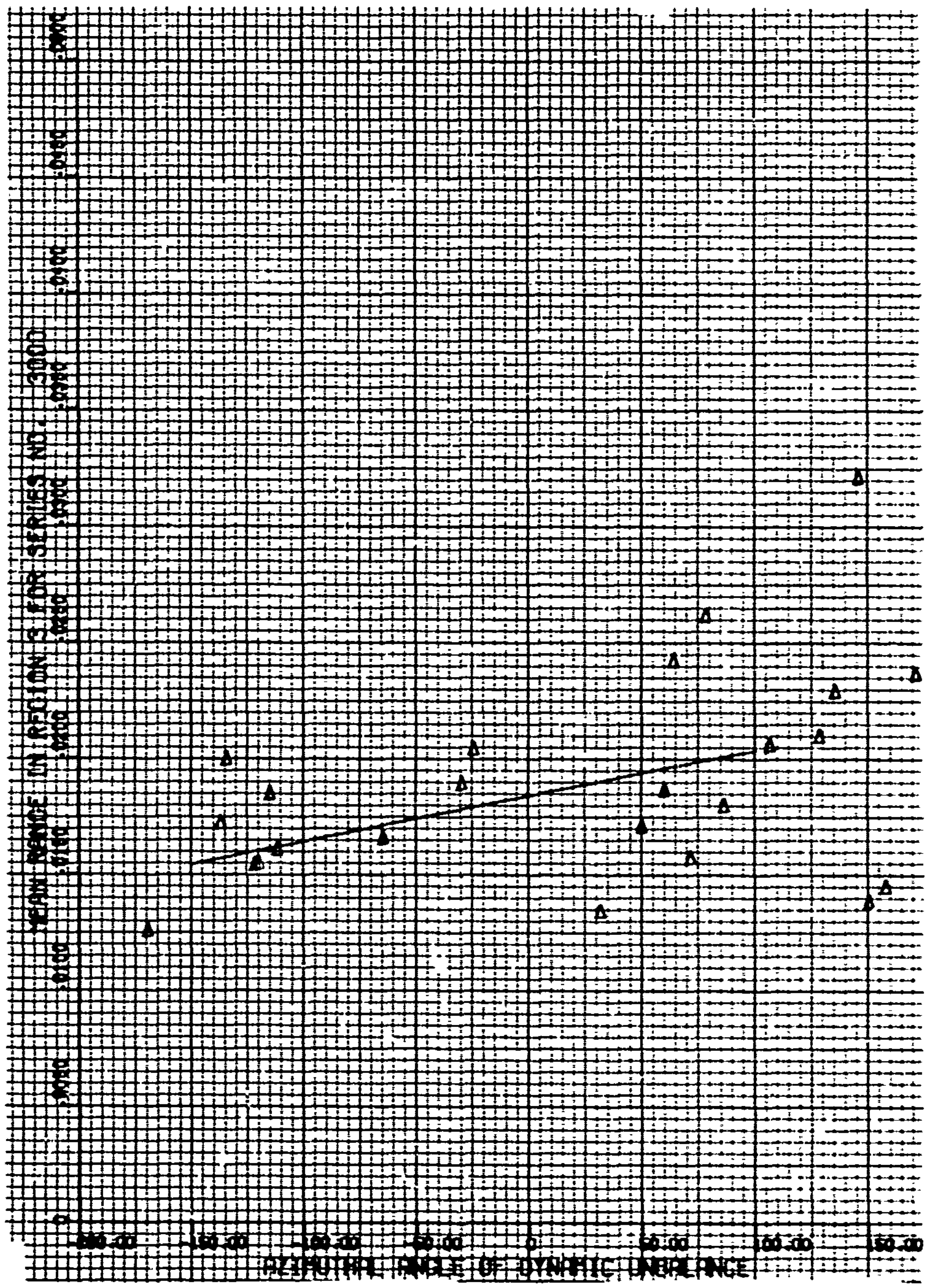

Figure 134 - Mean Wall Thickness Variation Versus Azimuth of Dynamic Unbalance, Series 300C, Region 3, Full

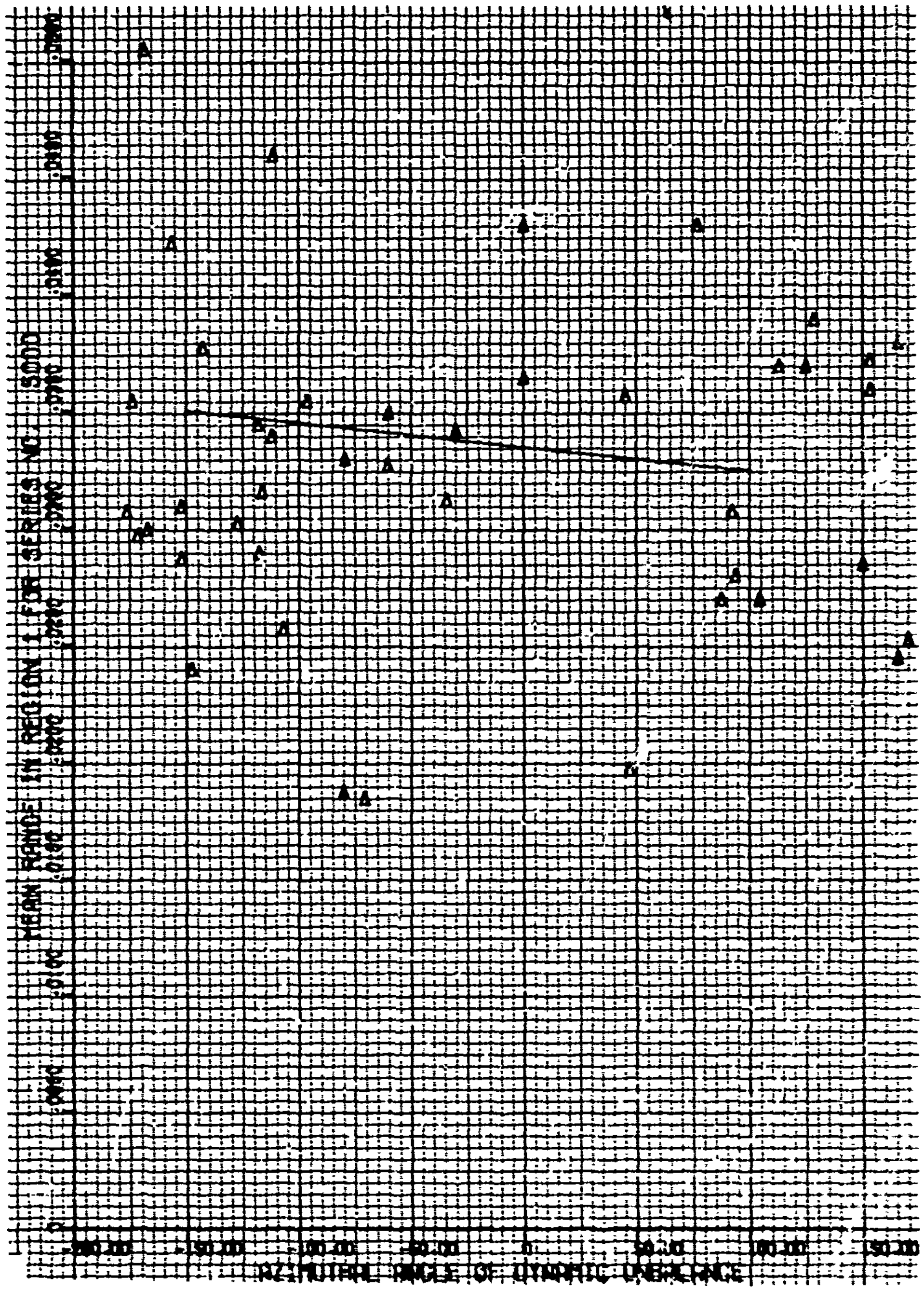

Figure 135 - Mean Wall Thickness Variation Versus Azimuth of Dynamic Unbalance, Series 500C, Region 1, Full

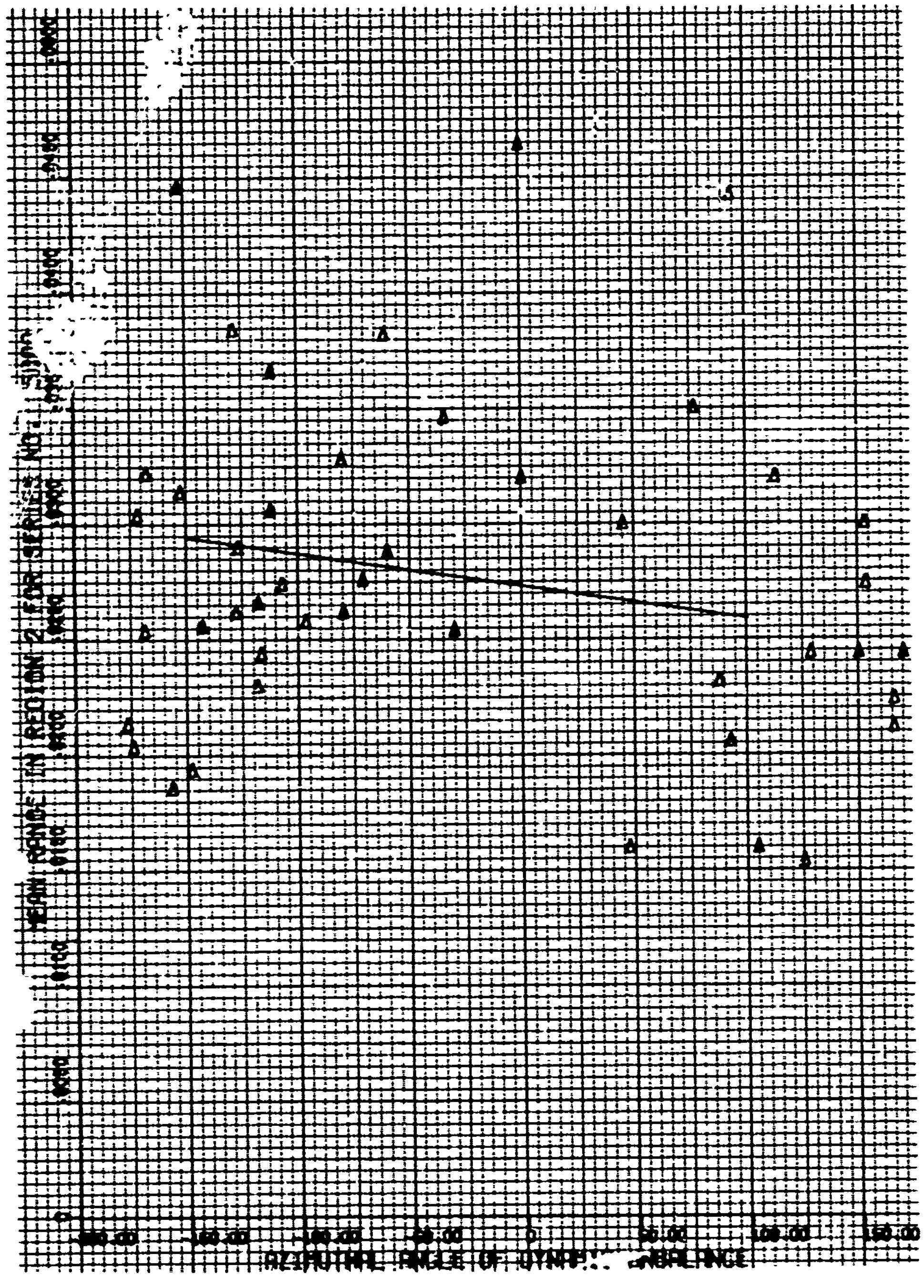

Figure 186 - Mean Wall Thickness Variation Versus Azimuth of Dynamic Unbalance, Series 5000, Region 2, Full

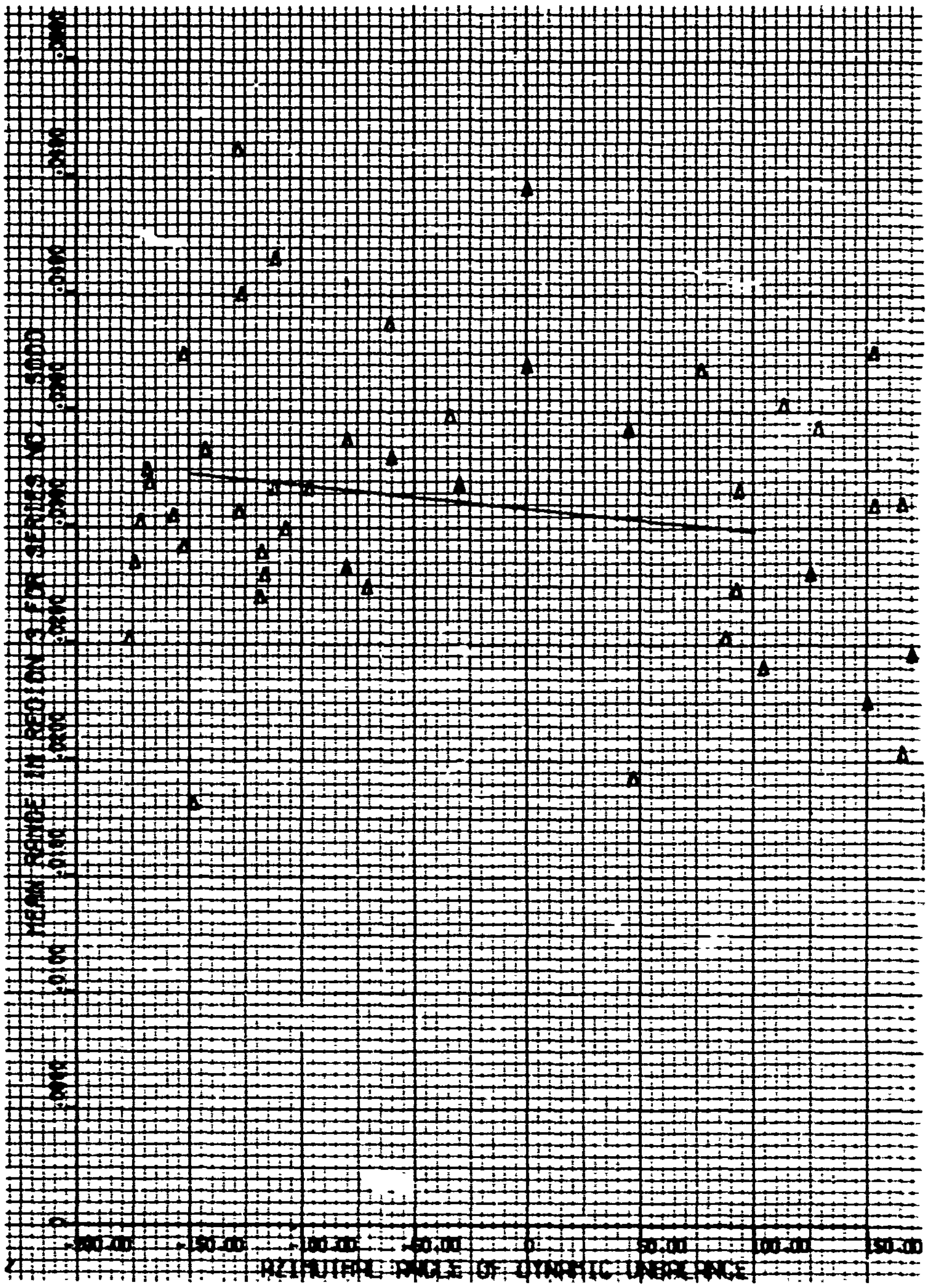

Figure 187 - Mean Wall Thickness Variation Versus Azimuth of Dynamic Unbalance, Series 5000, Region 3, Full

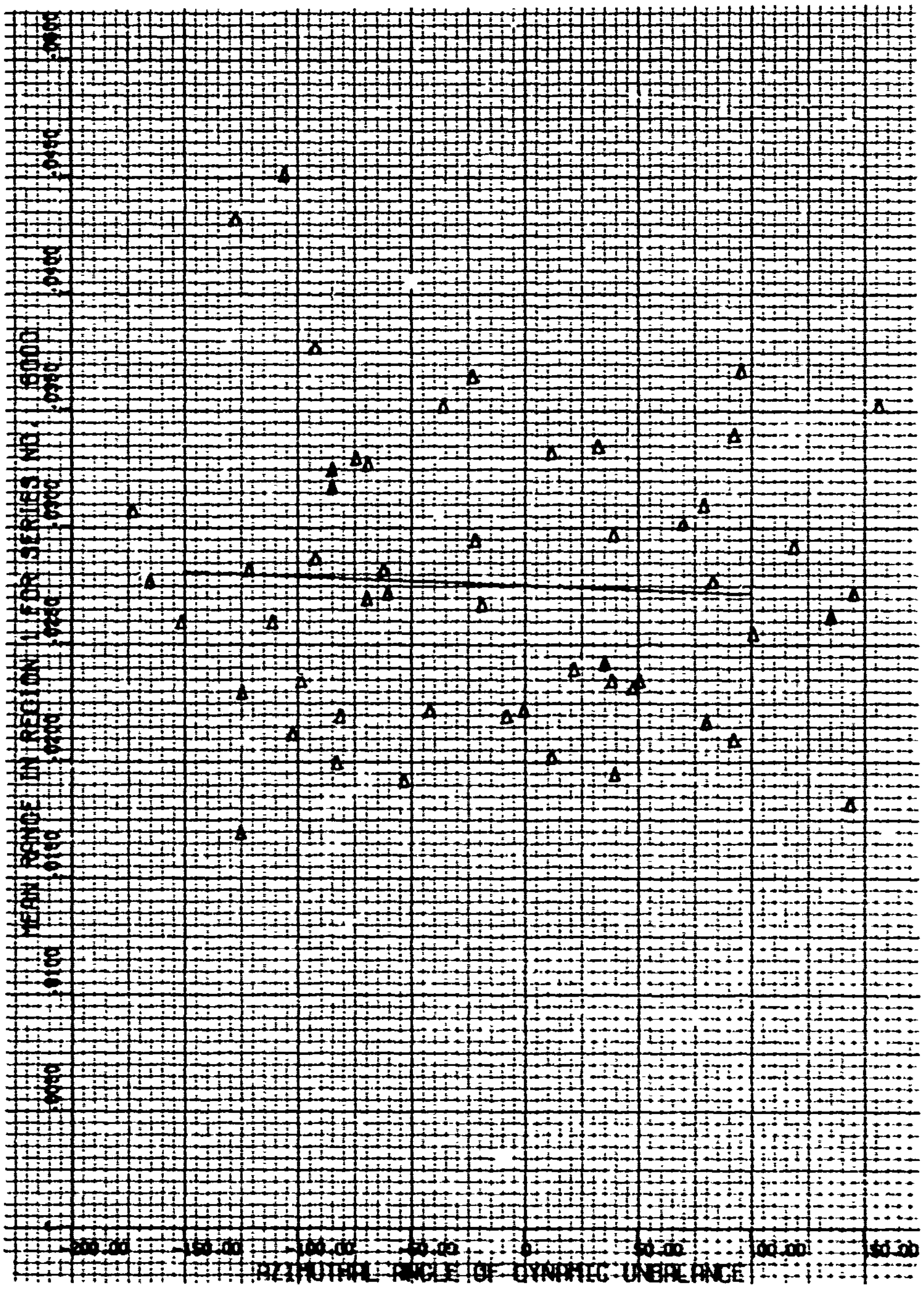

Figure 138 - Mean Wall Thickness Variation Versus Azimuth of Dynamic Unbalance, Series 6000, Region 1, Full

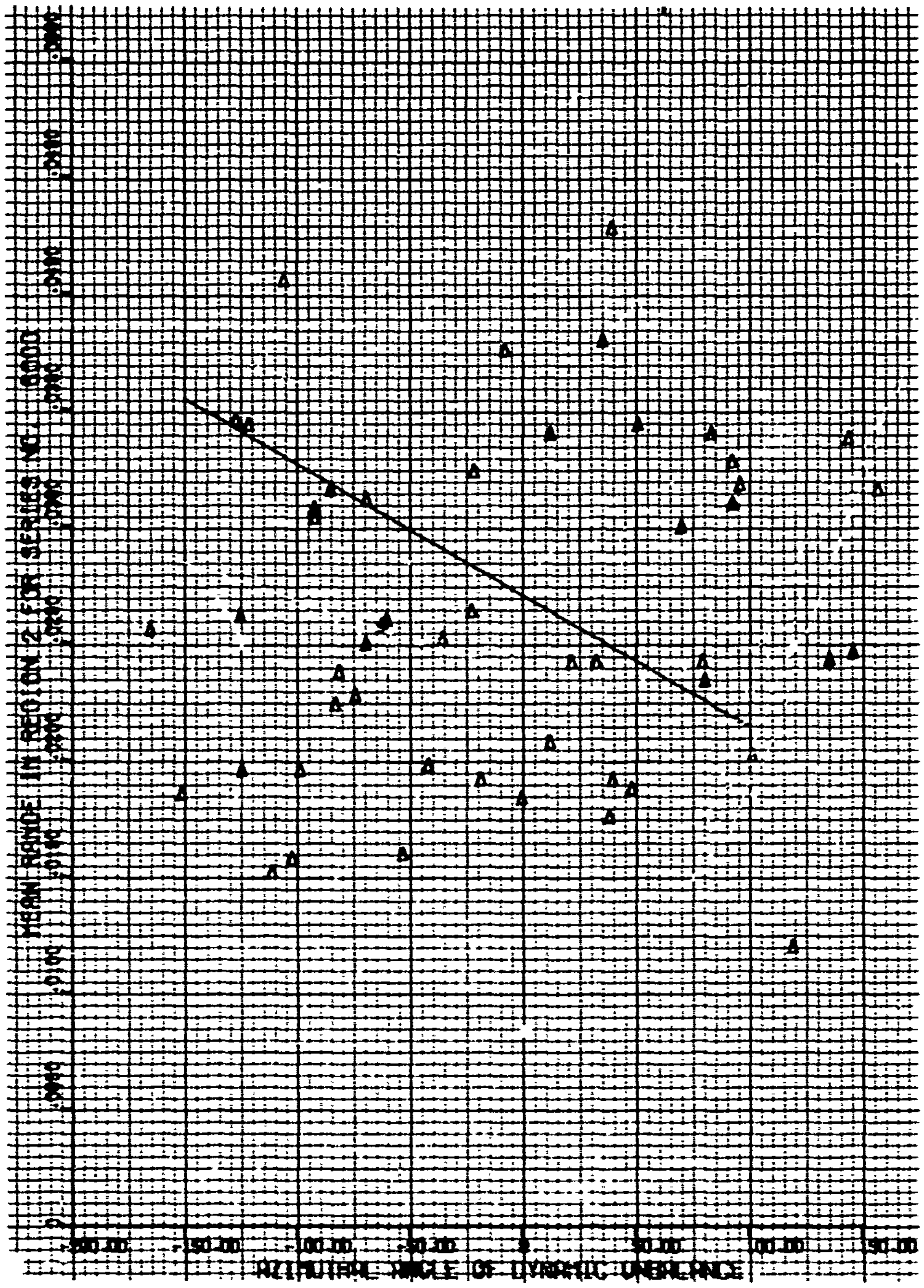

Figure 189 - Mean Wall Thickness Variation Versus Azimuth of Dynamic Unbalance, Series 6000, Region 2, Full

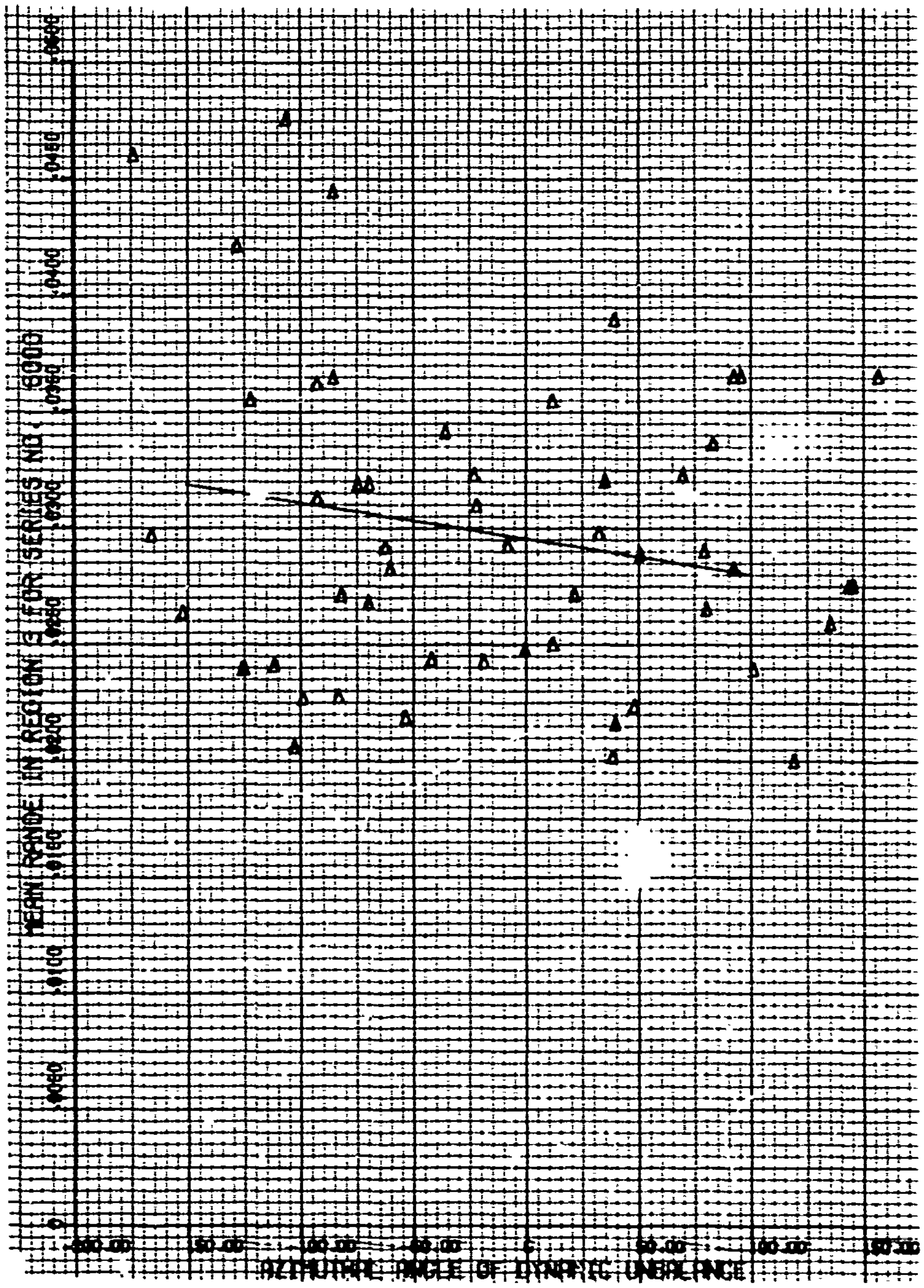

Figure 190 - Mean Wall Thickness Variation Versus Azimuth of Dynamic Unbalance, Series 6000, Region 3, Full

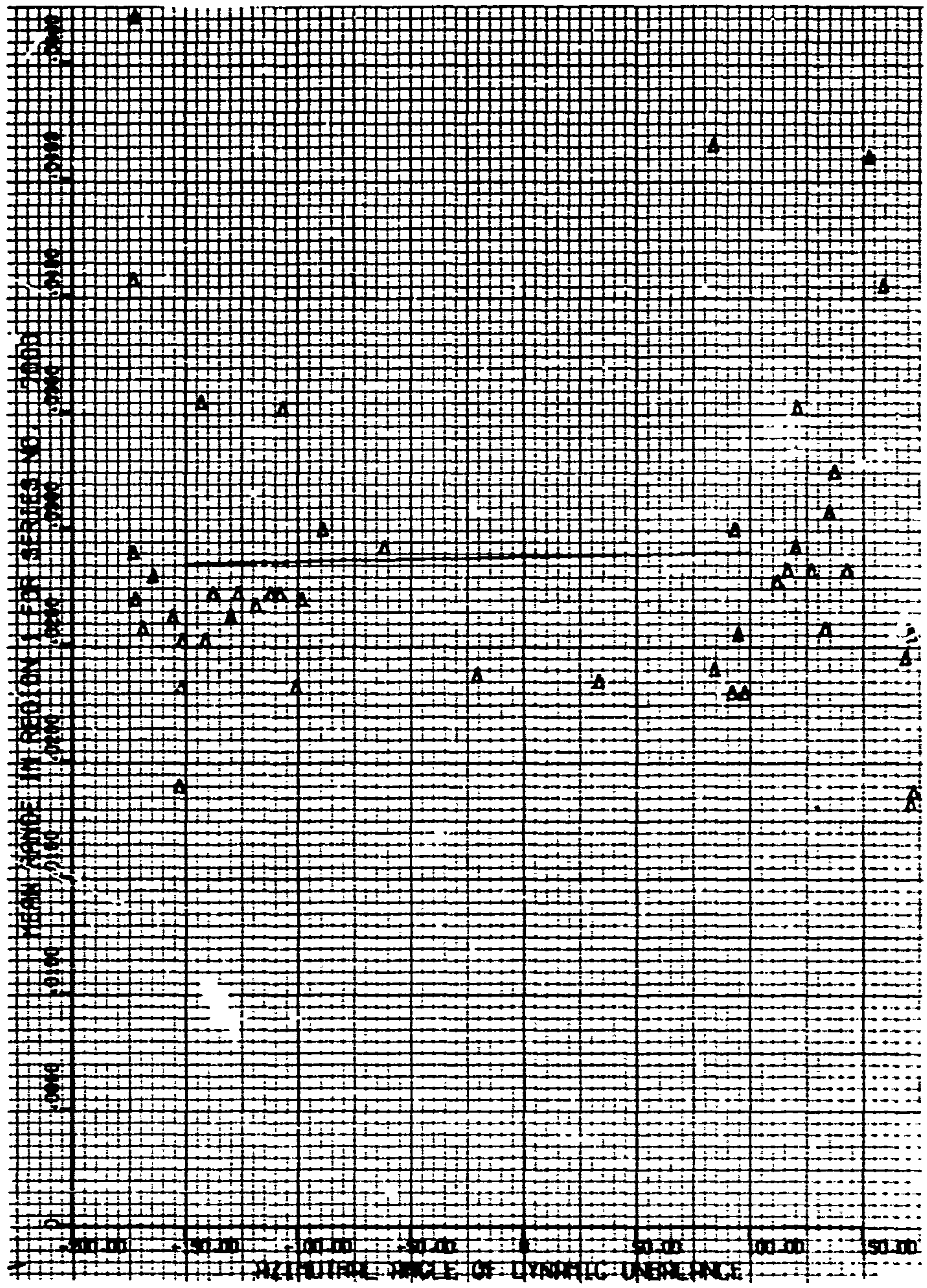

Figure 191 - Mean Wall Thickness Variation Versus Azimuth of Dynamic Unbalance, Series 7000, Region 1, Full

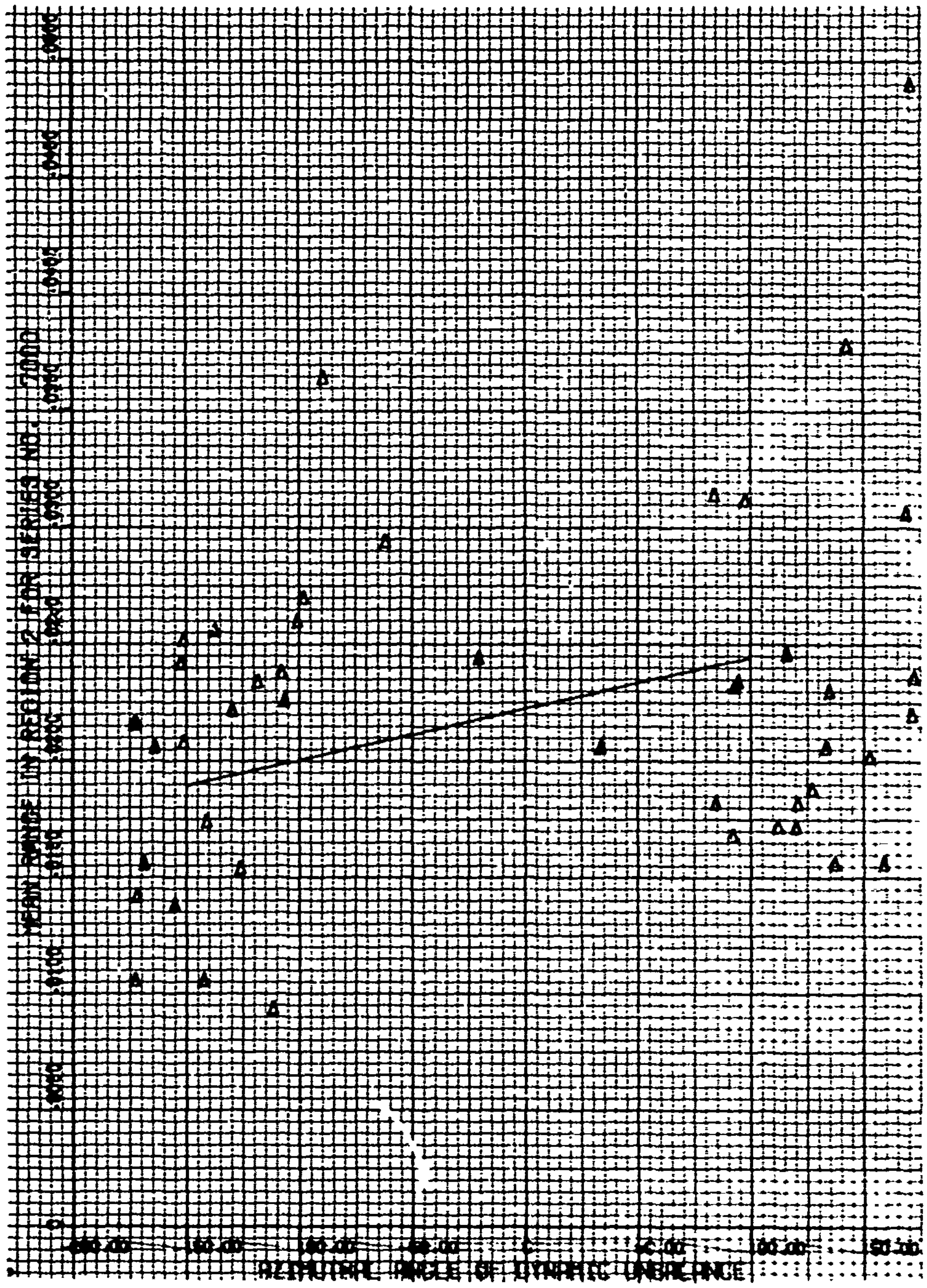

Figure 192 - Mean Wall Thickness Variation Versus Azimuth of Dynamic Unbalance, Series 7000, Region 2, Full

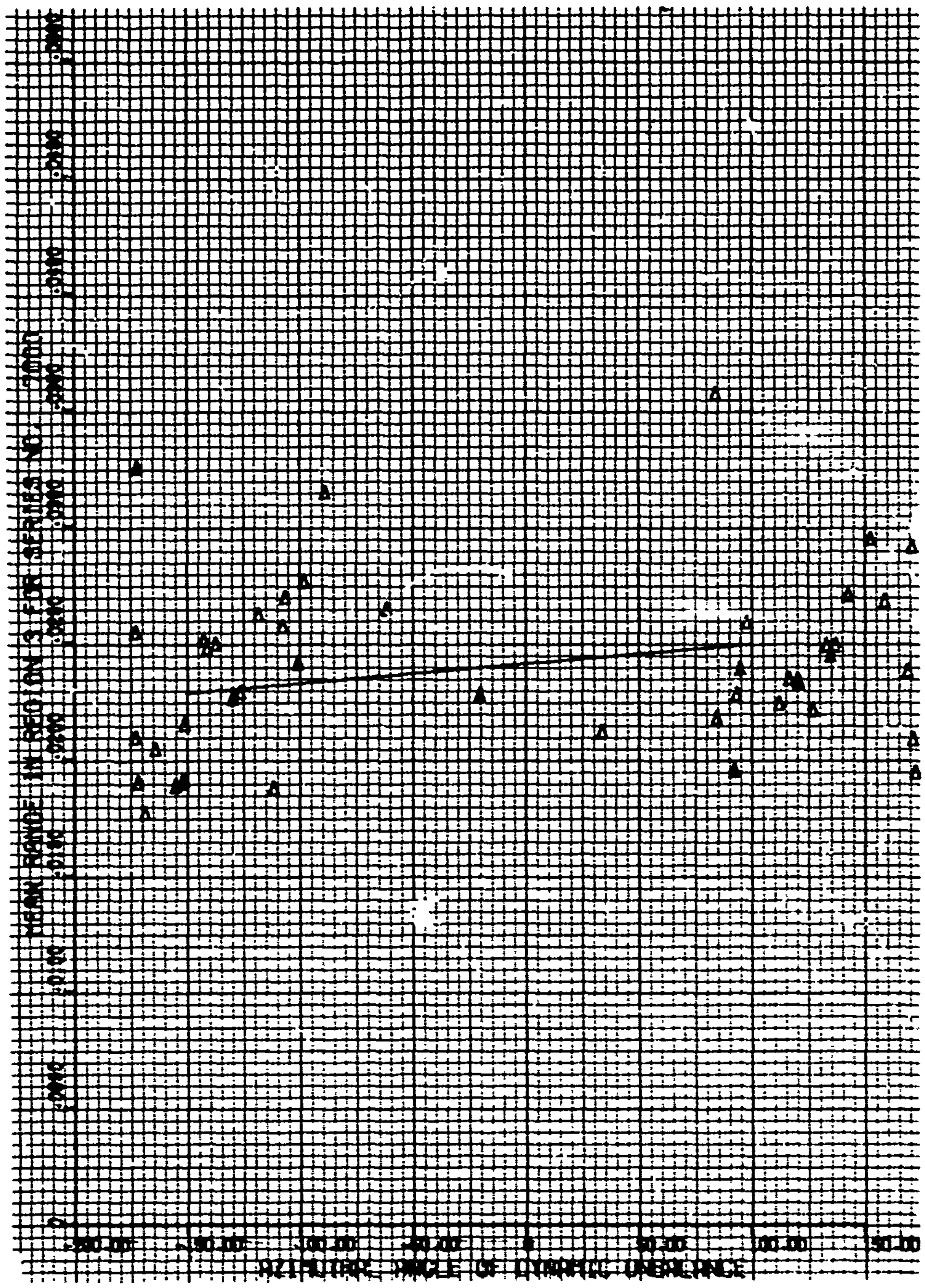

Figure 193 - Mean Wall Thickness Variation Versus Azimuth of
Dynamic Unbalance, Series 70C0, Region 3, Full

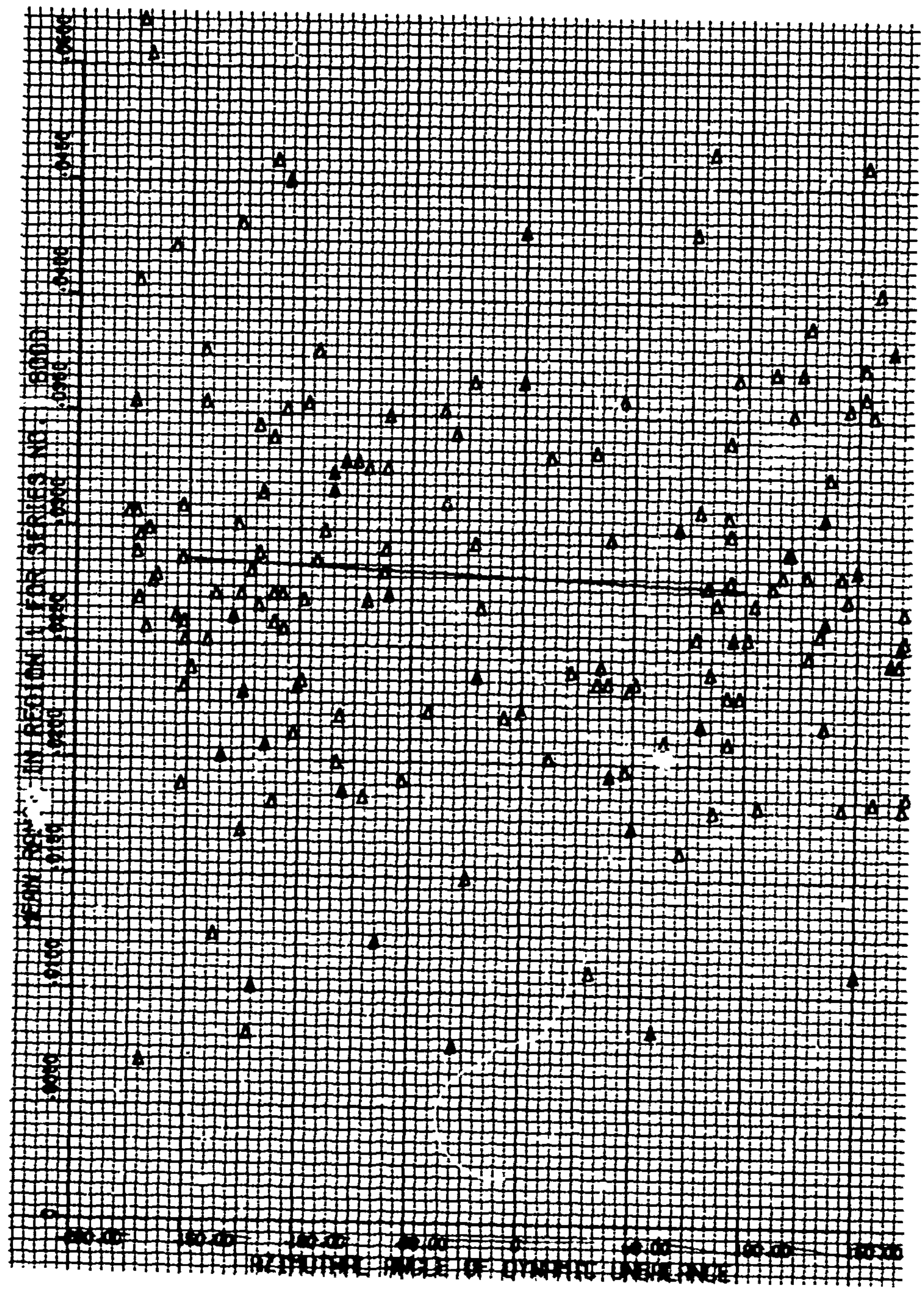

Figure 194 - Mean Wall Thickness Variation Versus Azimuth of Dynamic Unbalance, Series 8000, Region 1, Full

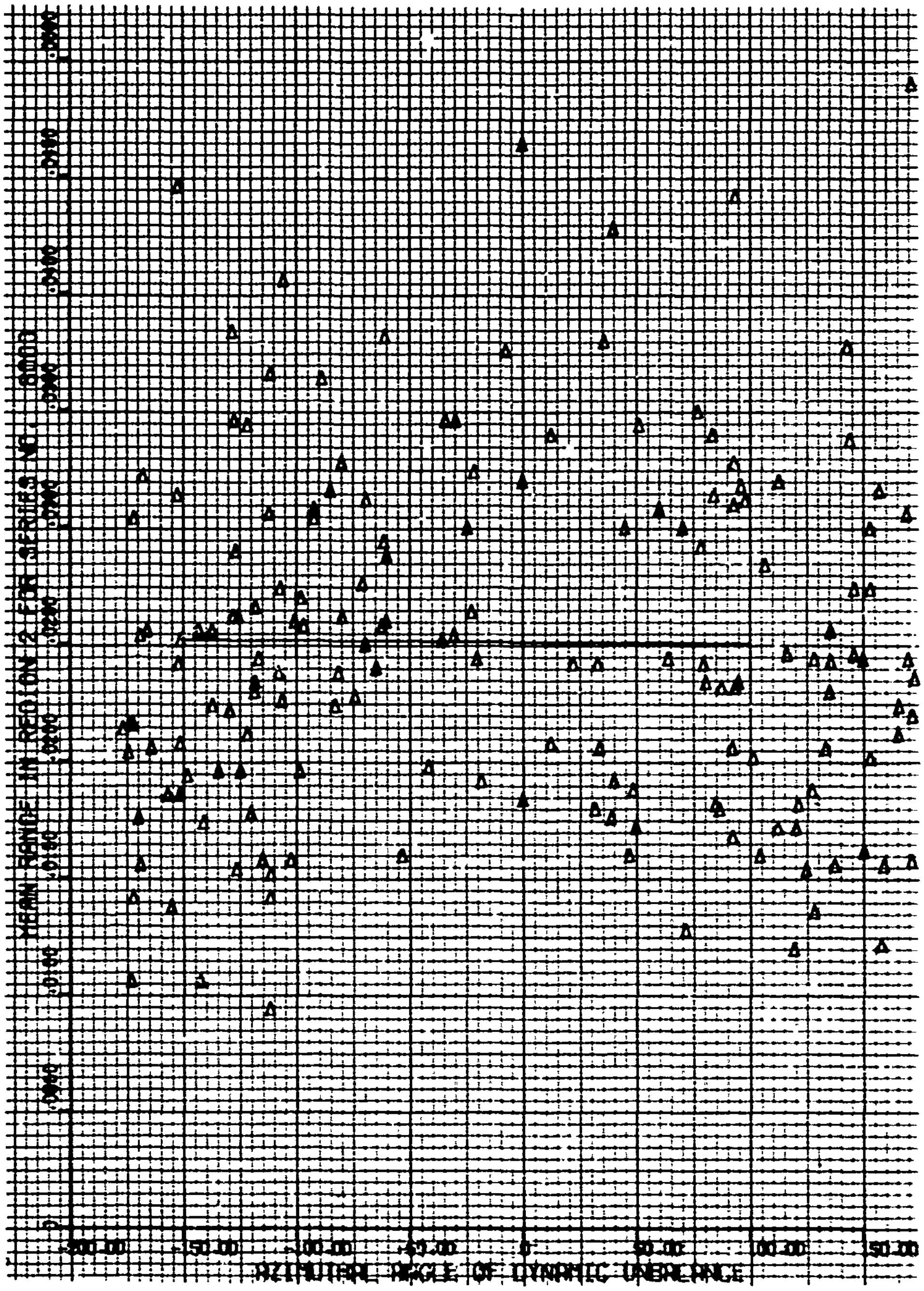

Figure 195 - Mean Wall Thickness Variation Versus Azimuth of Dynamic Unbalance, Series 8000, Region 2, Full

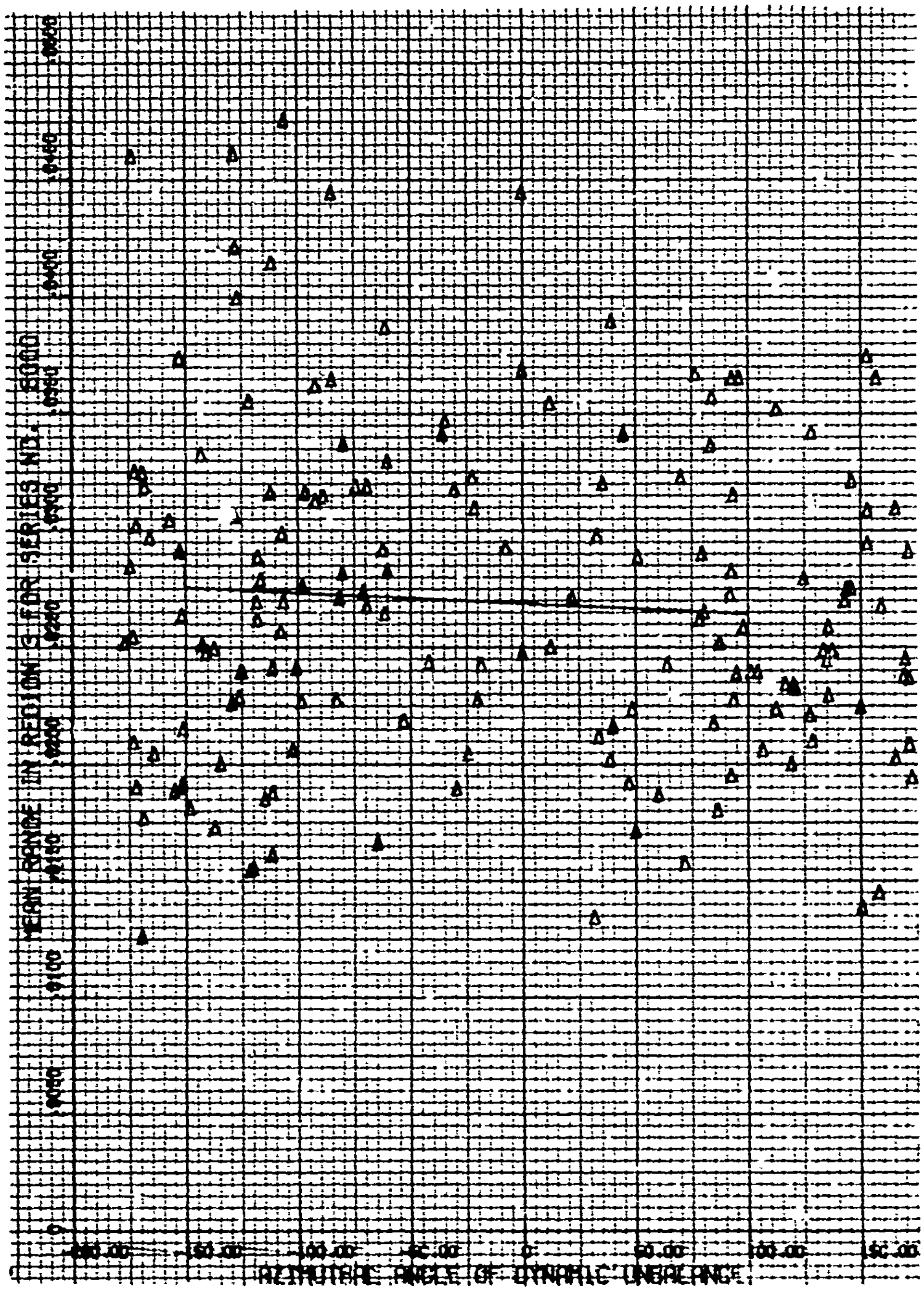

Figure 196 - Mean Wall Thickness Variation Versus Azimuth of Dynamic Unbalance, Series 8000, Region 3, Full

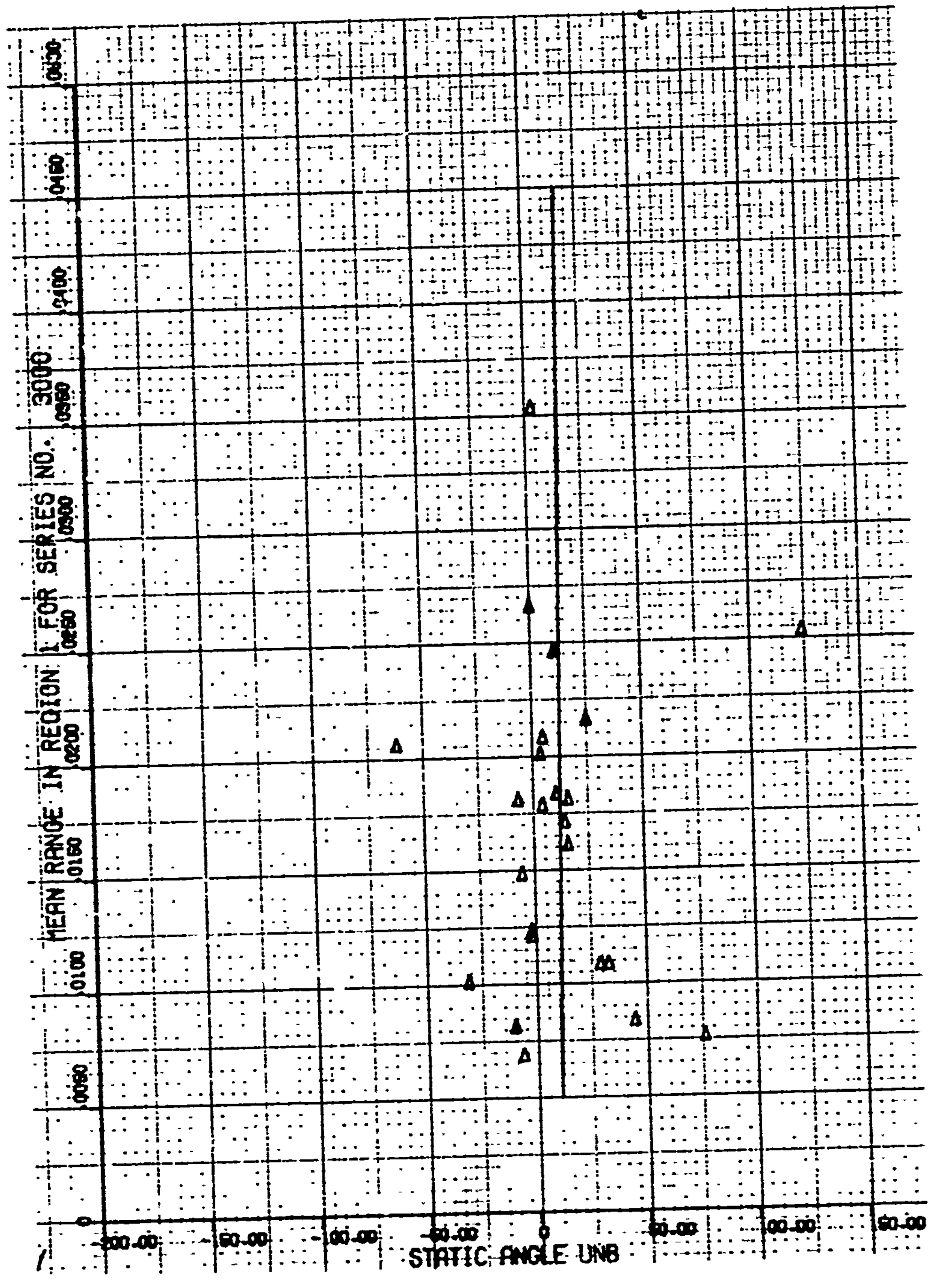

Figure 197 - Mean Wall Thickness Variation Versus Azimuth of Static Unbalance, Series 3000, Region 1, Empty

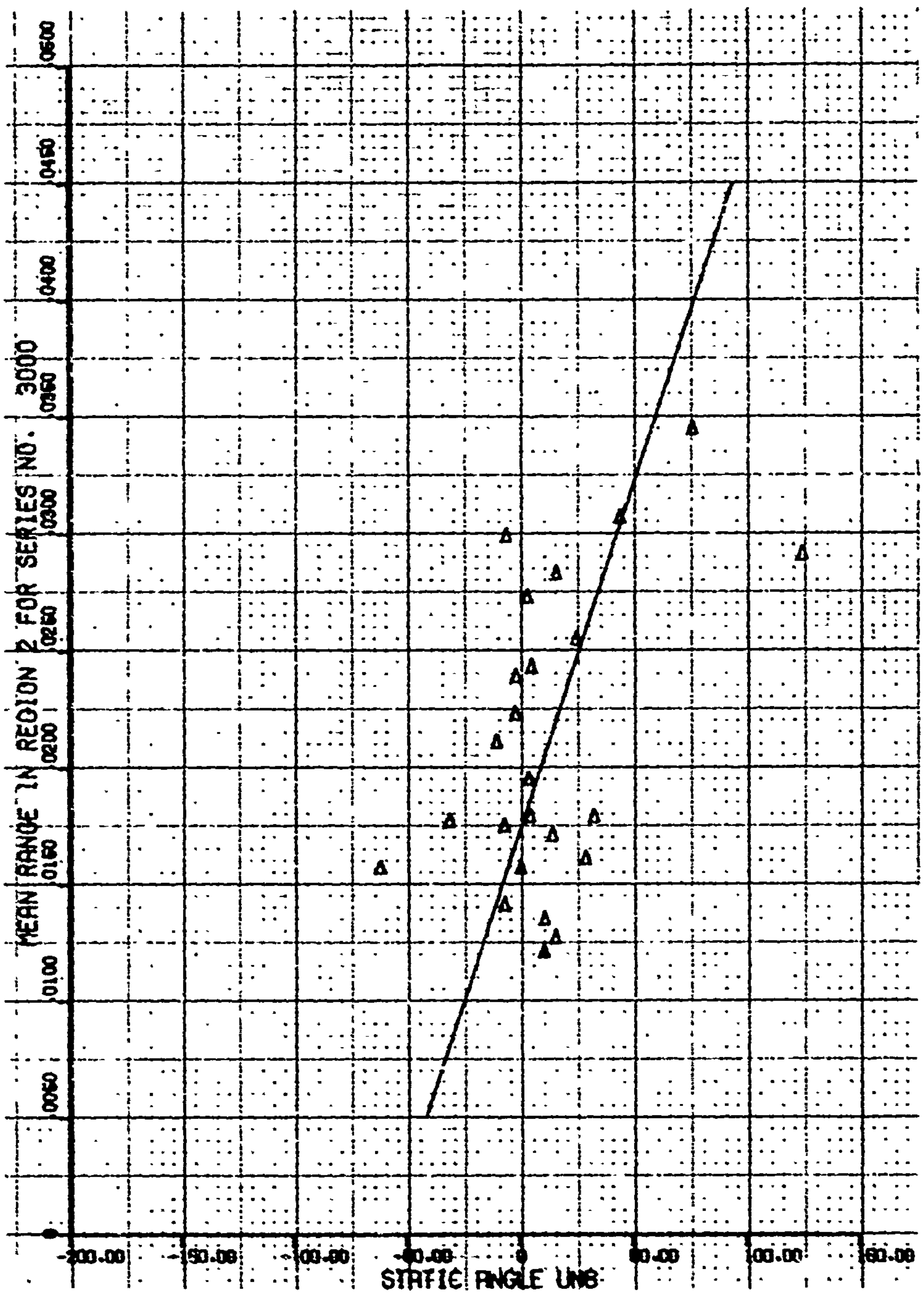

Figure 198 - Mean Wall Thickness Variation Versus Azimuth of Static Unbalance, Series 3000, Region 2, Empty

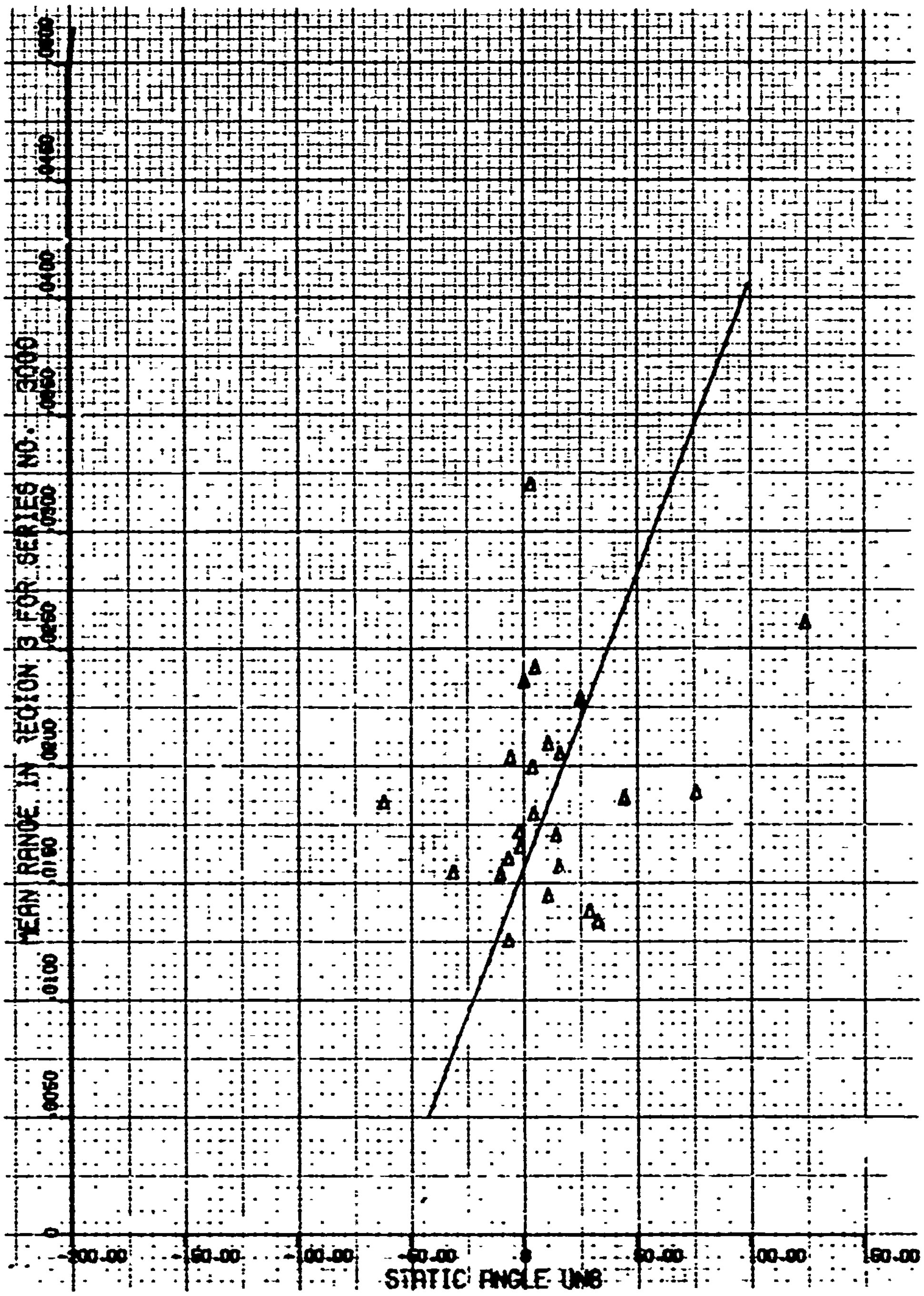

Figure 199 - Mean Wall Thickness Variation Versus Azimuth of Static Unbalance, Series 3000, Region 3, Empty

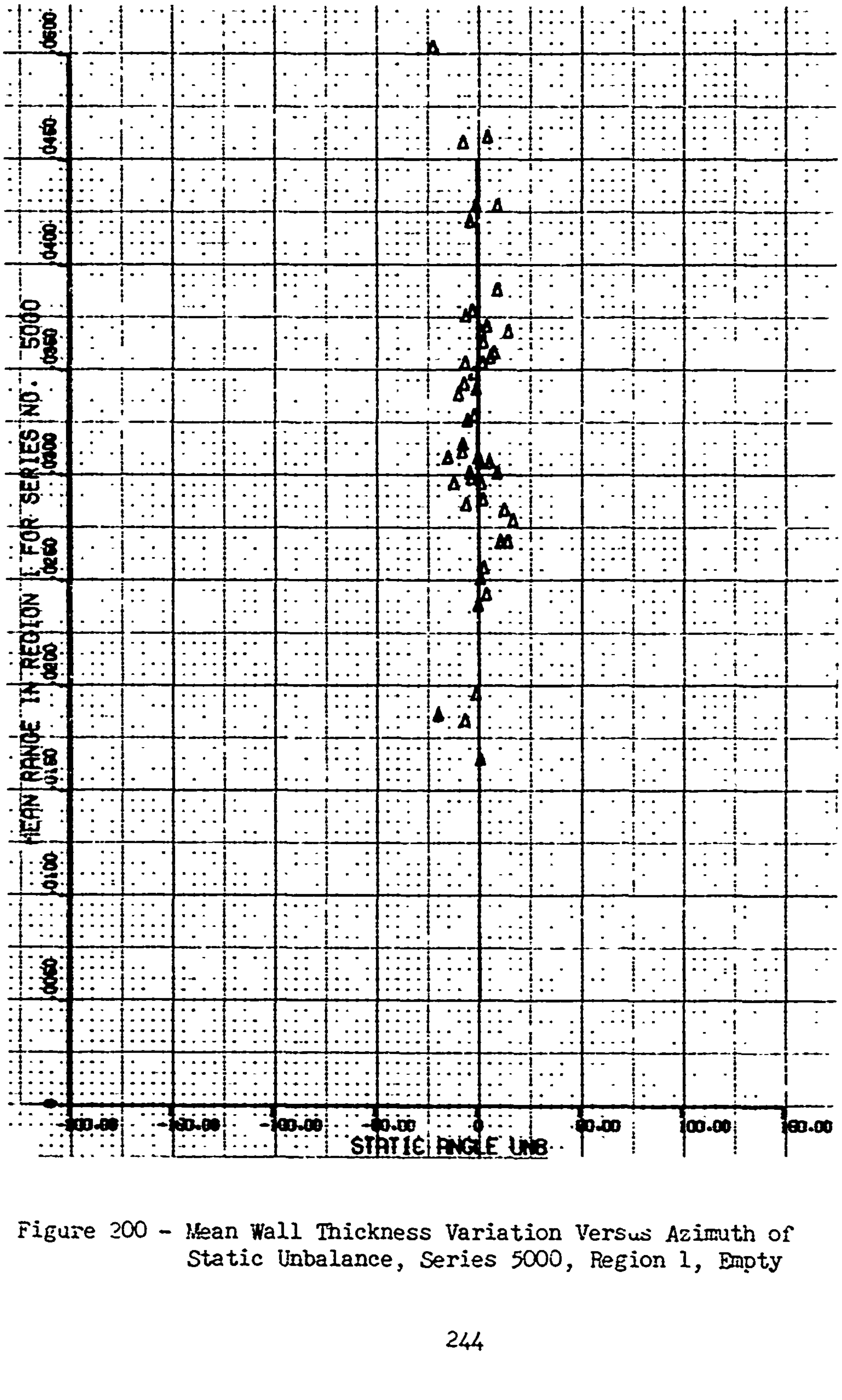

Figure 200 - Mean Wall Thickness Variation Versus Azimuth of Static Unbalance, Series 5000, Region 1, Empty

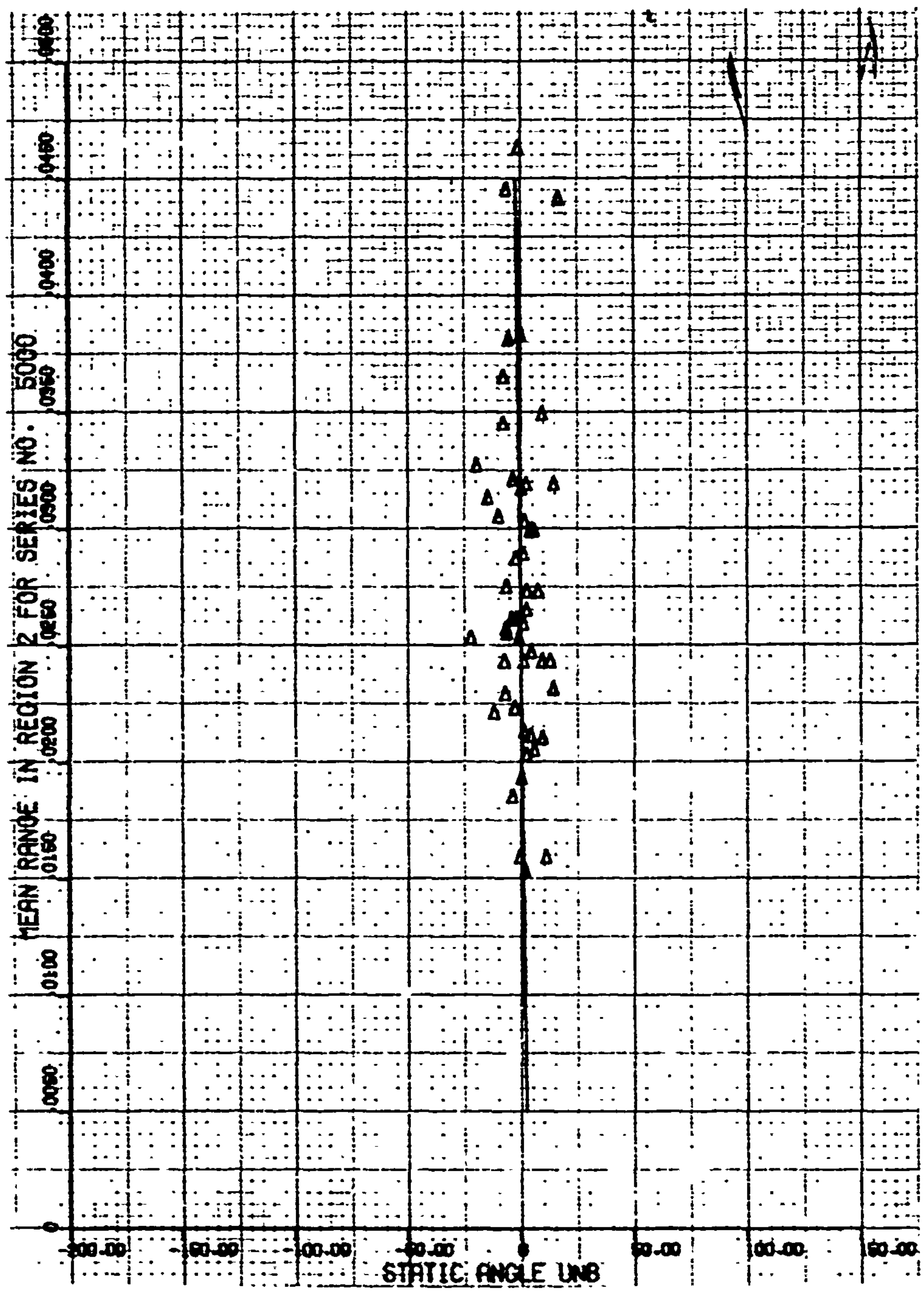

Figure 201 - Mean Wall Thickness Variation Versus Azimuth of Static Unbalance, Series 5000, Region 2, Empty

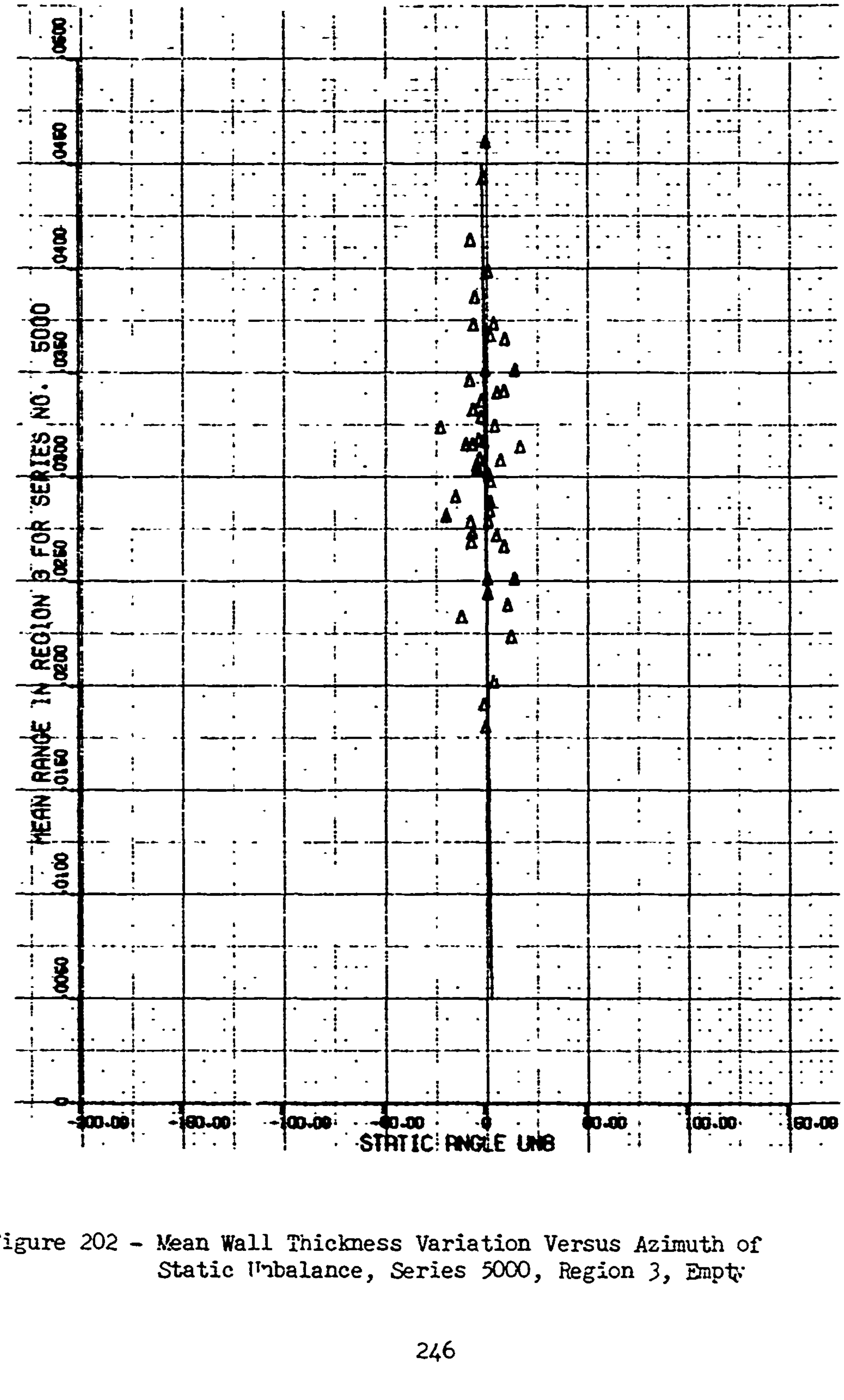

Figure 202 - Mean Wall Thickness Variation Versus Azimuth of
Static Unbalance, Series 5000, Region 3, Empty

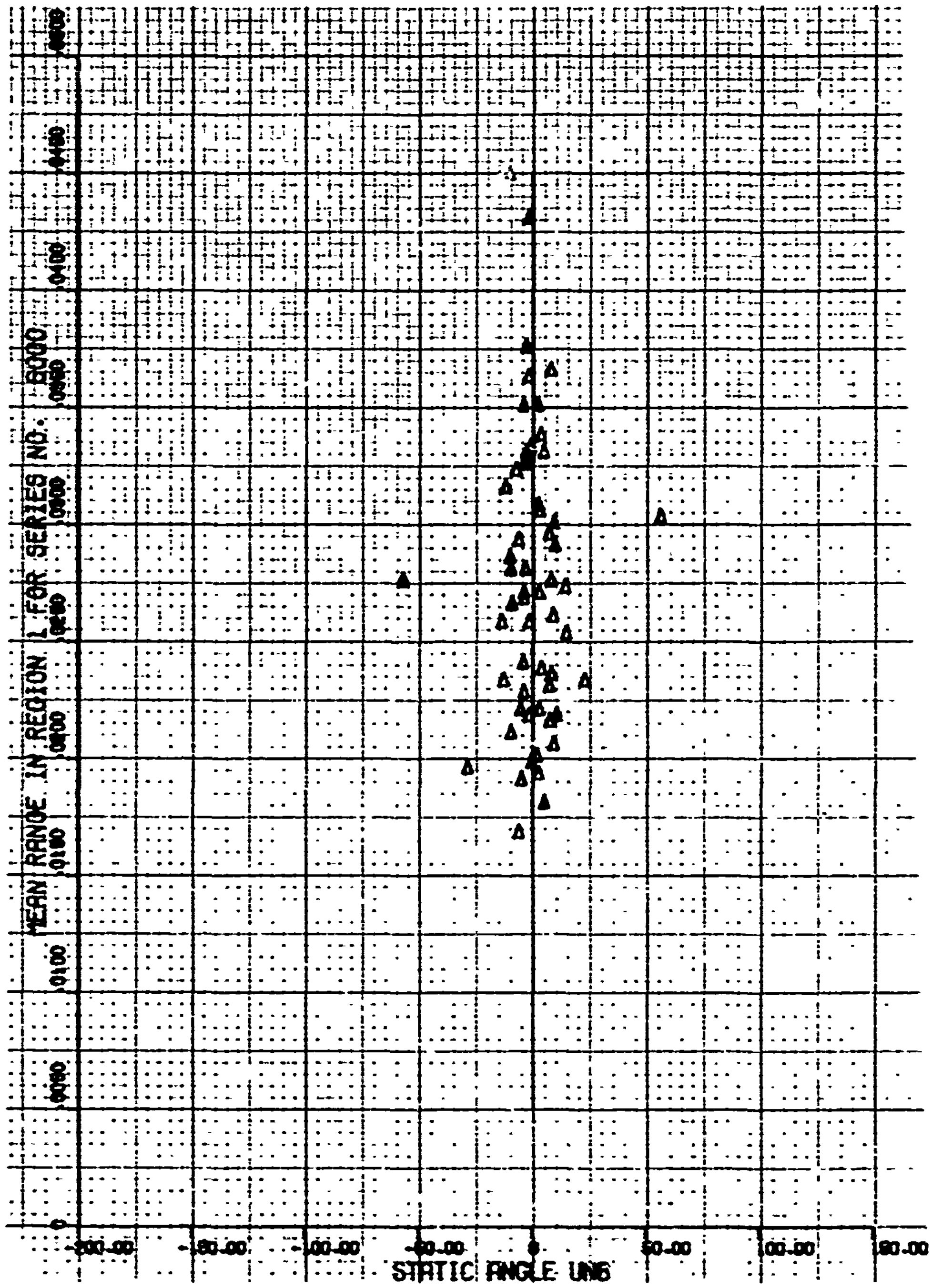

Figure 203 - Mean Wall Thickness Variation Versus Azimuth of Static Unbalance, Series 6000, Region 1, Empty

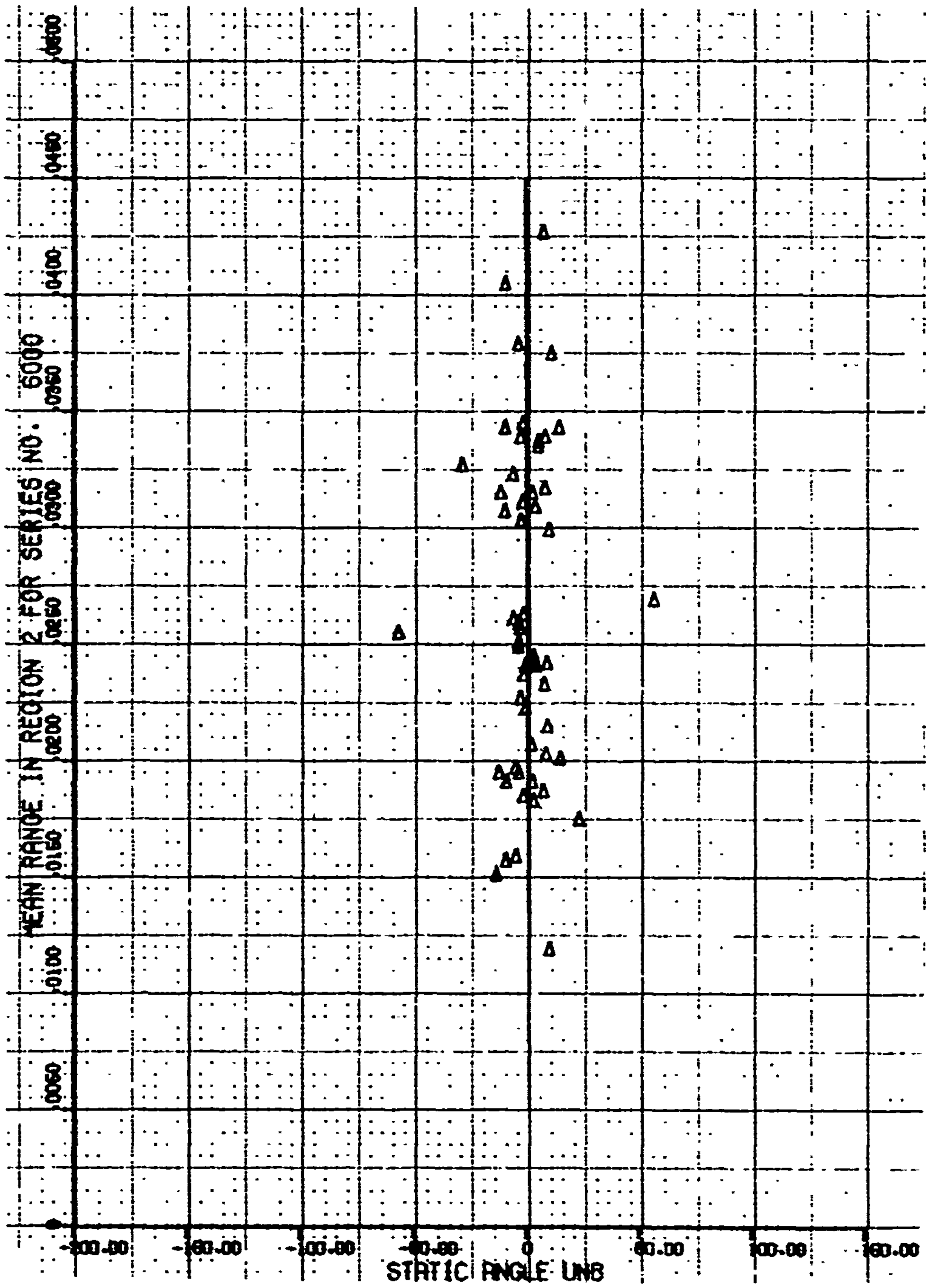

Figure 204 - Mean Wall Thickness Variation Versus Azimuth of Static Unbalance, Series 6000, Region 2, Empty

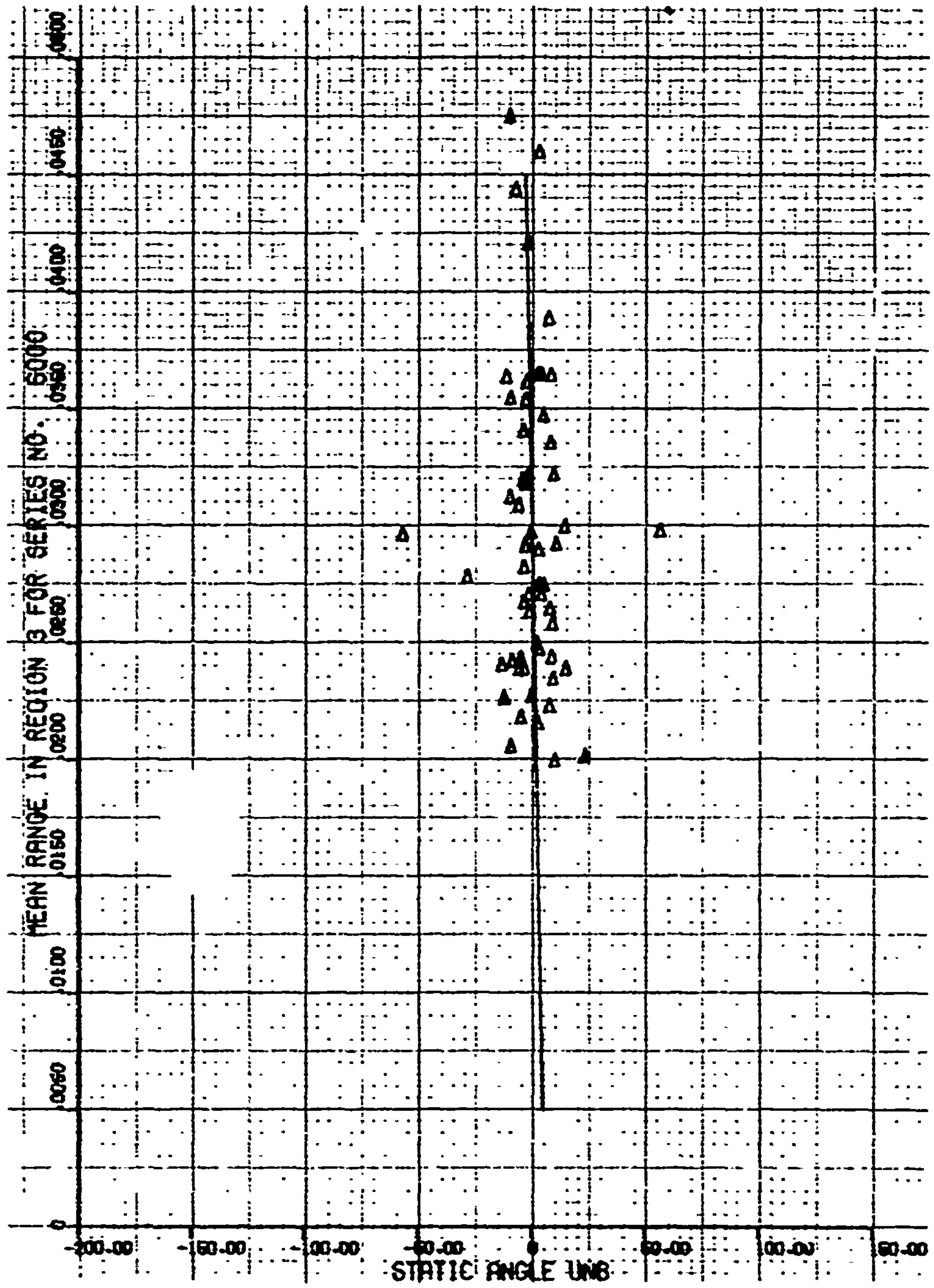

Figure 205 - Mean Wall Thickness Variation Versus Azimuth of Static Unbalance, Series 6000, Region 3, Empty

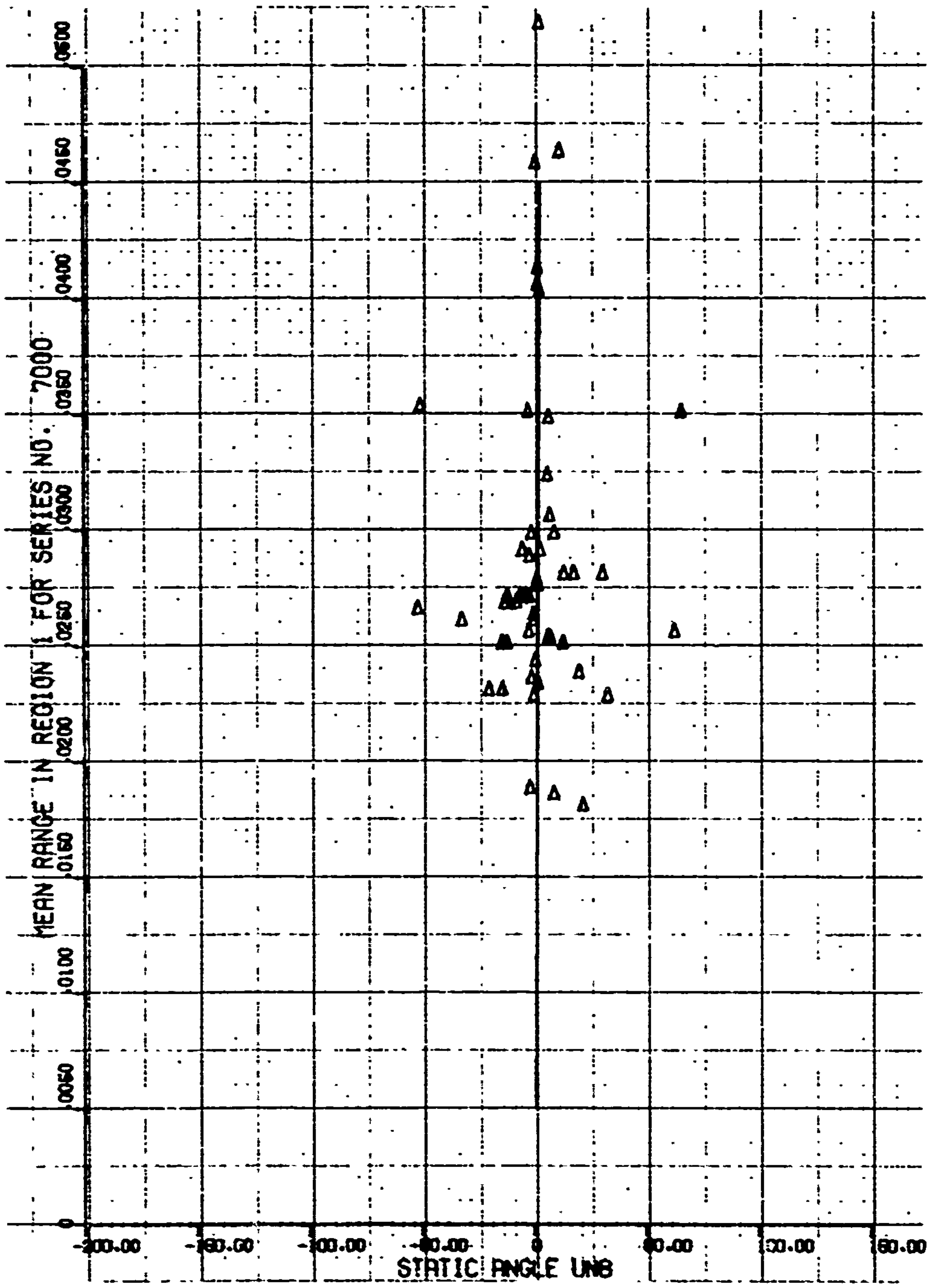

Figure 206 - Mean Wall Thickness Variation Versus Azimuth of Static Unbalance, Series 7000, Region 1, Empty

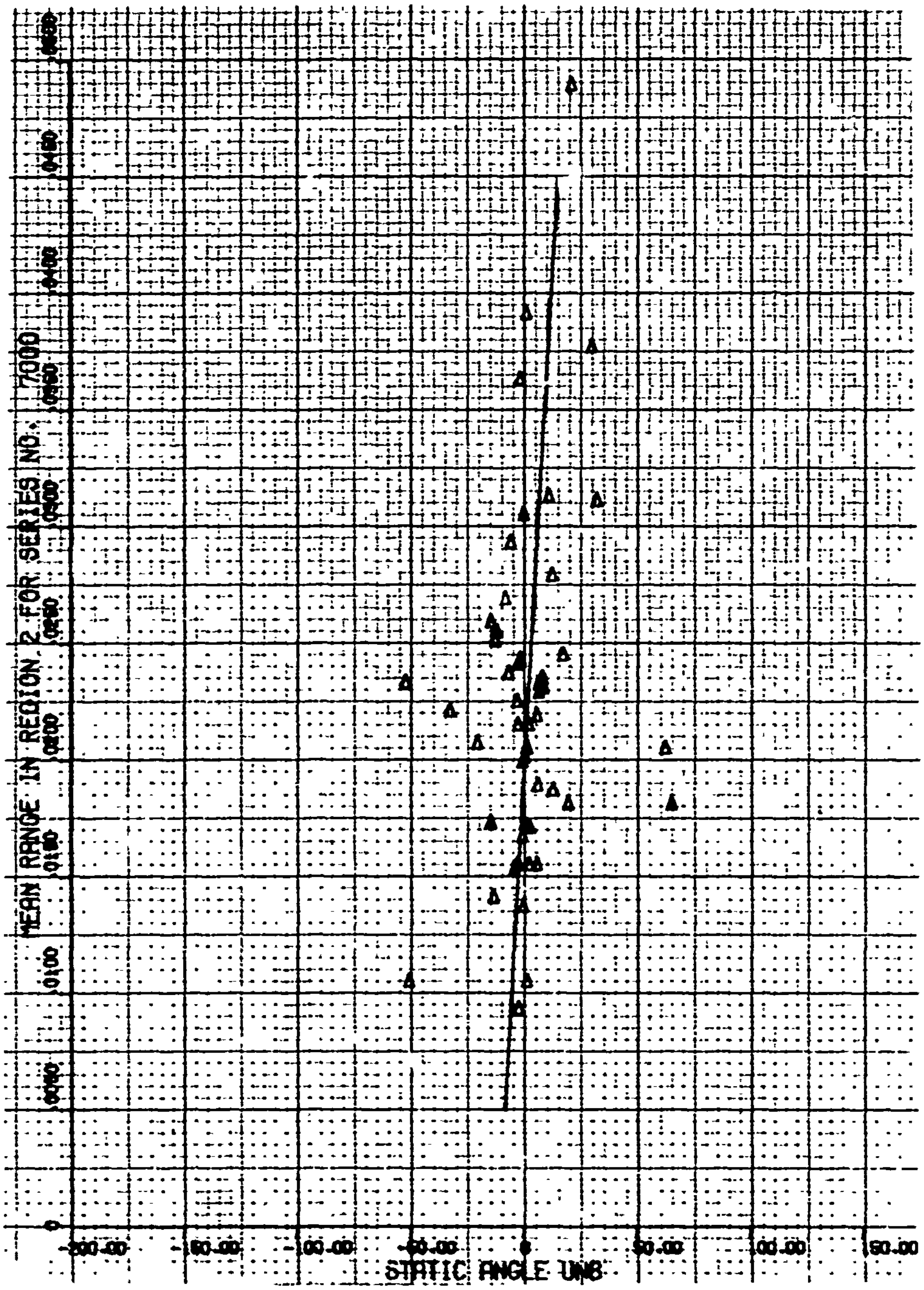

Figure 207 - Mean Wall Thickness Variation Versus Azimuth of Static Unbalance, Series 7000, Region 2, Empty

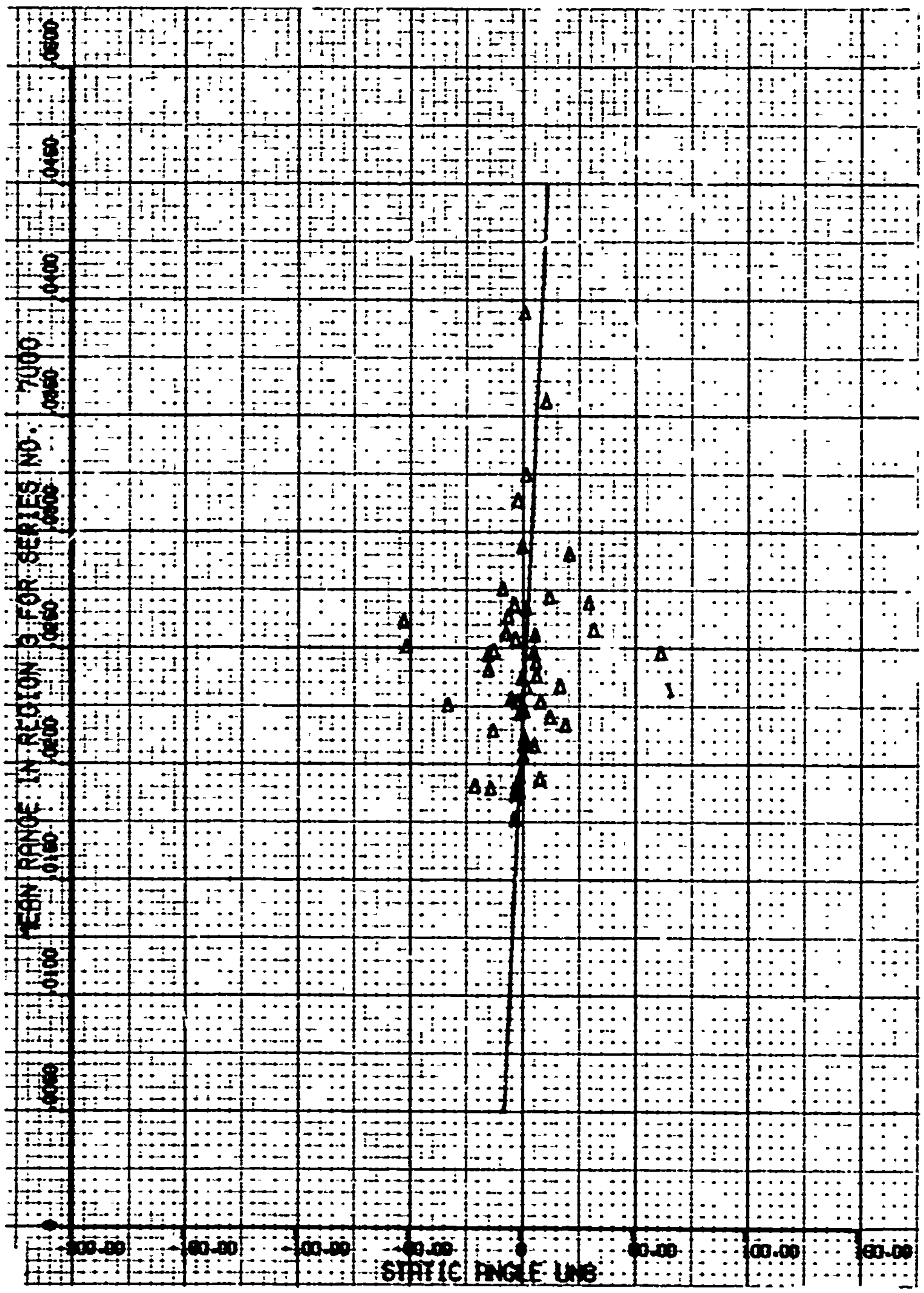

Figure 208 - Mean Wall Thickness Variation Versus Azimuth of Static Unbalance, Series 7000, Region 3, Empty

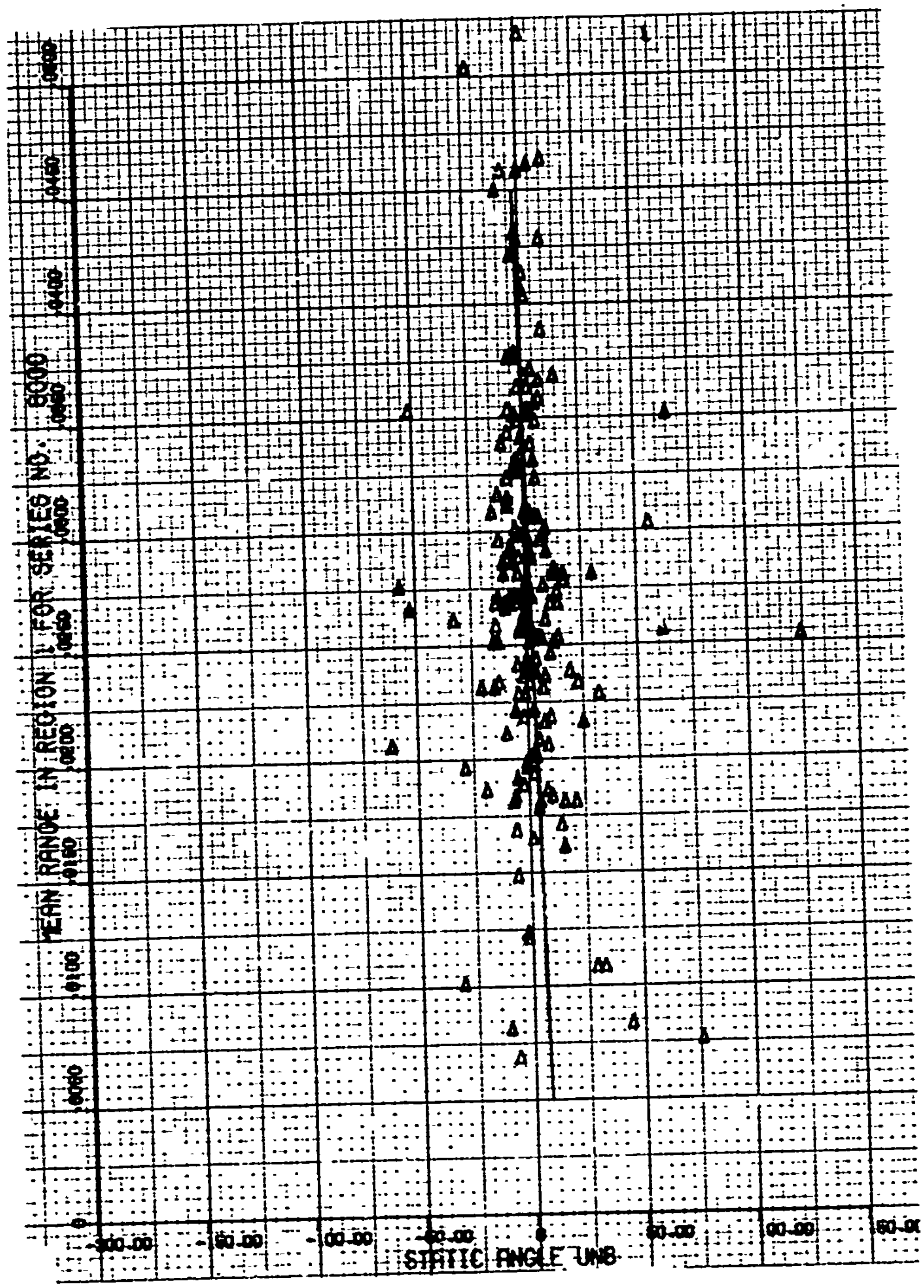

Figure 209 - Mean Wall Thickness Variation Versus Azimuth of Static Unbalance, Series 8000, Region 1, Empty

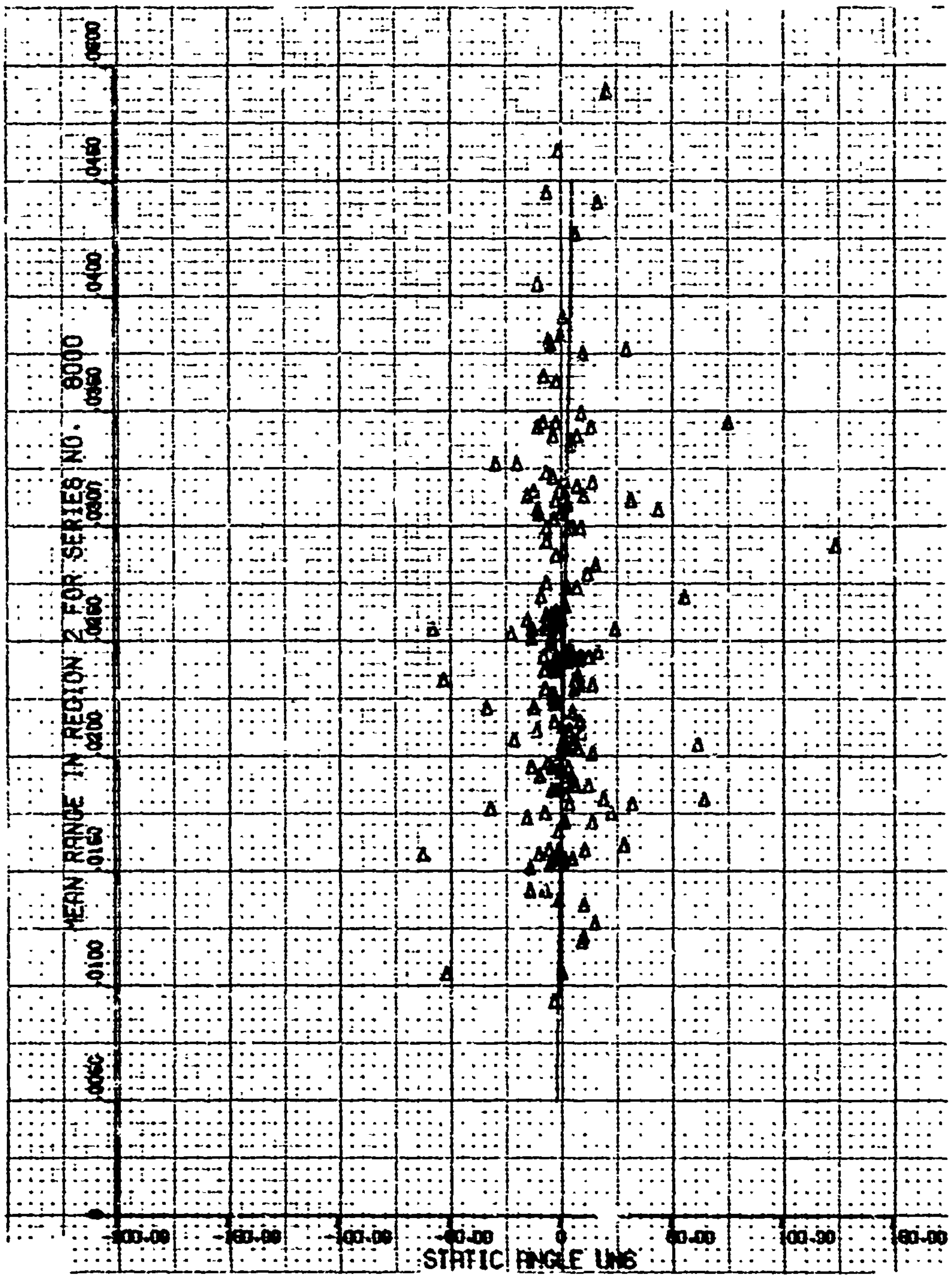

Figure 210 -Mean Wall Thickness Variation Versus Azimuth of Static Unbalance, Series 3000, Region 2, Empty

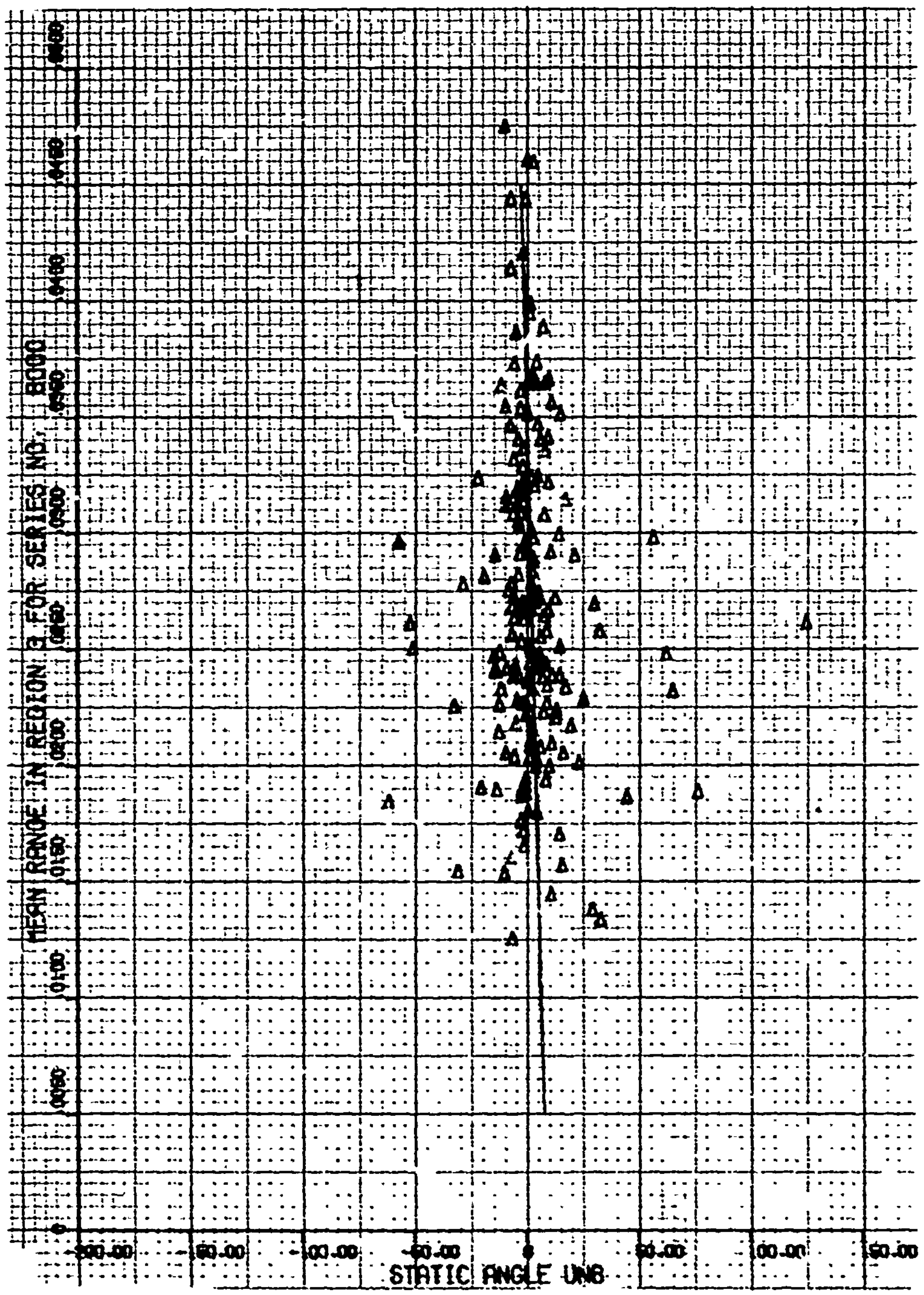

Figure 211 - Mean Wall Thickness Variation Versus Azimuth of Static Unbalance, Series 8000. Region 3, Empty

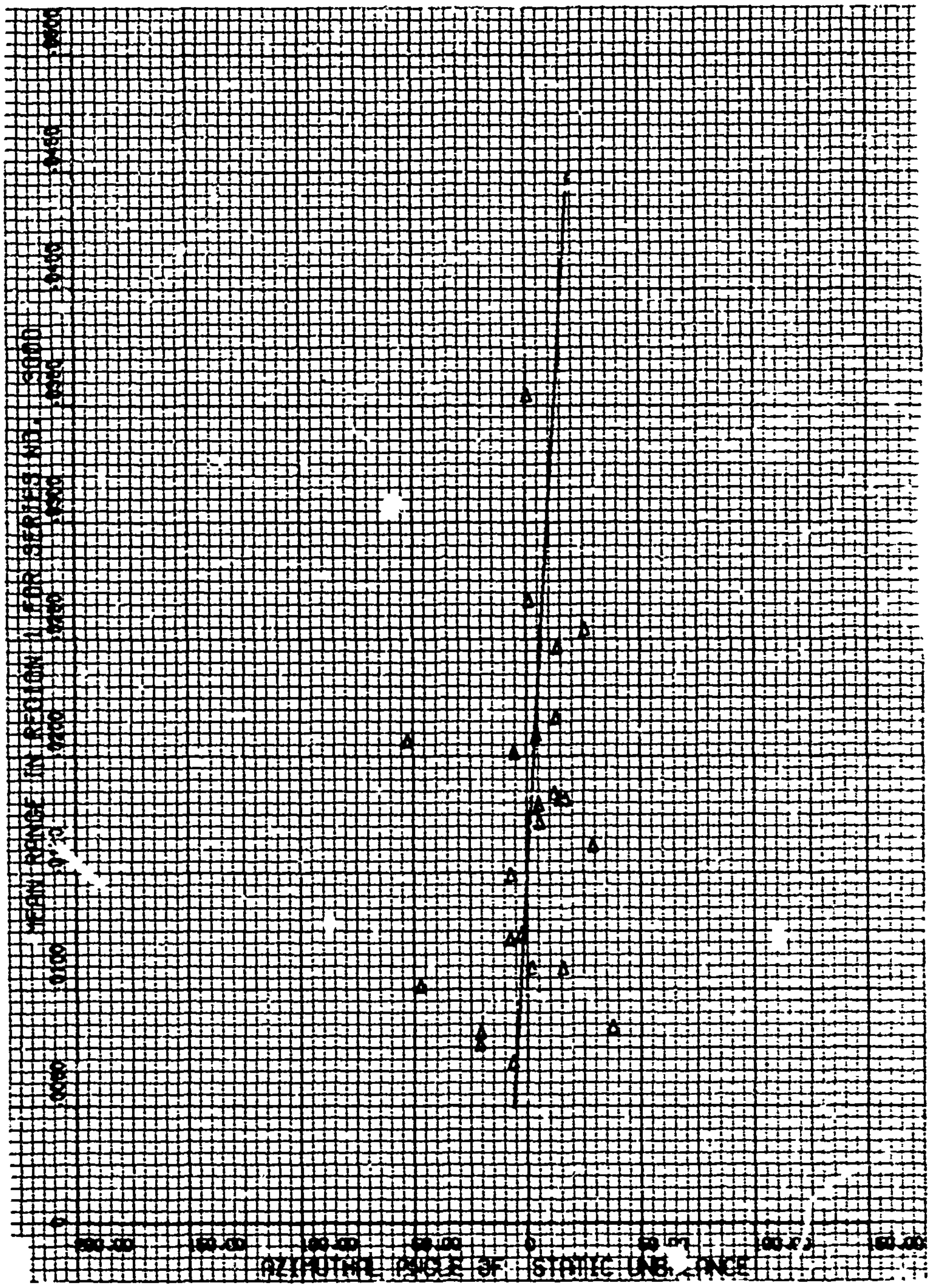

Figure 212 - Mean Wall Thickness Variation Versus Azimuth of Static Unbalance, Series 3000, Region 1, Full

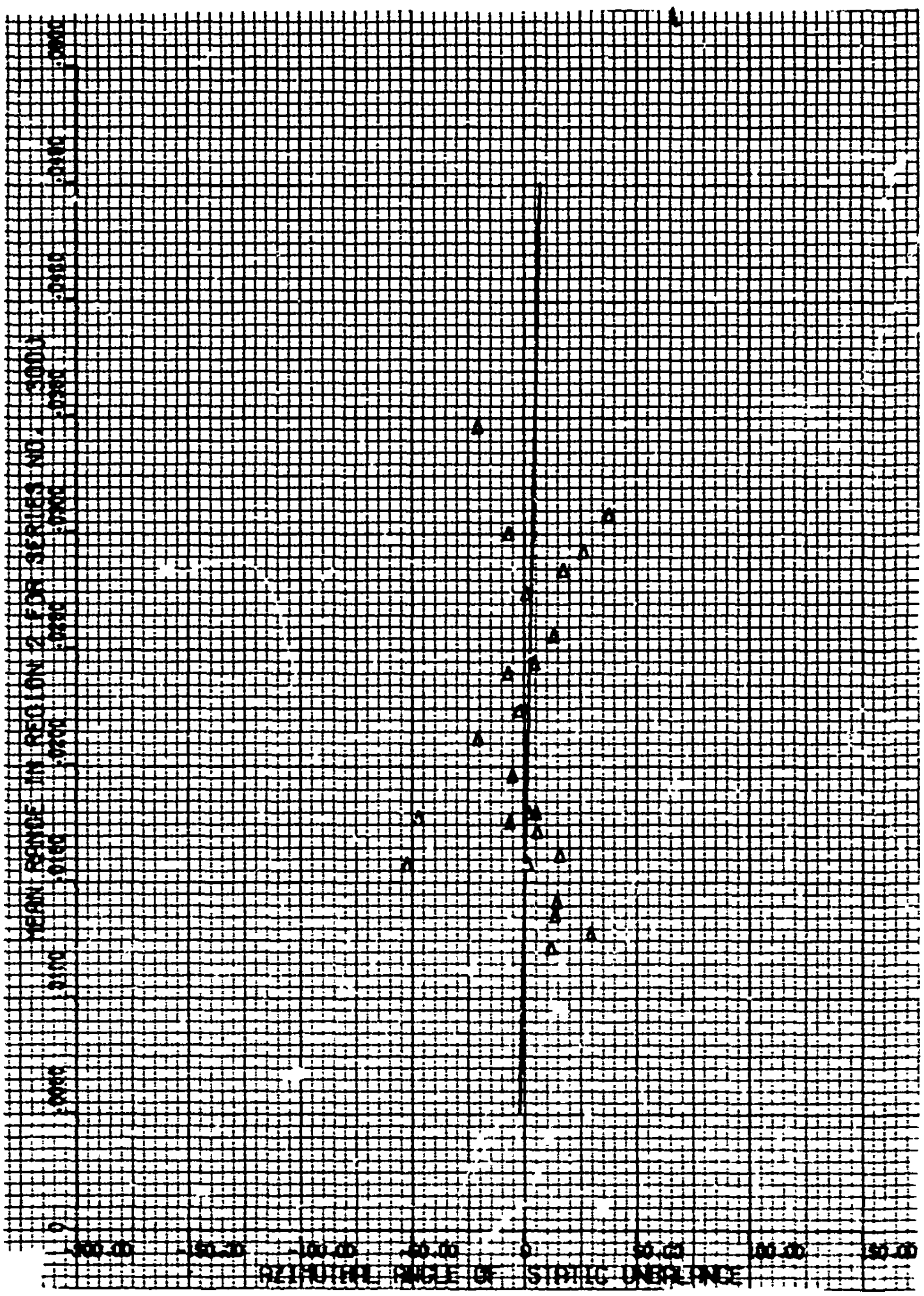

Figure 213 - Mean Wall Thickness Variation Versus Azimuth of Static Unbalance, Series 3000, Region 2, Full

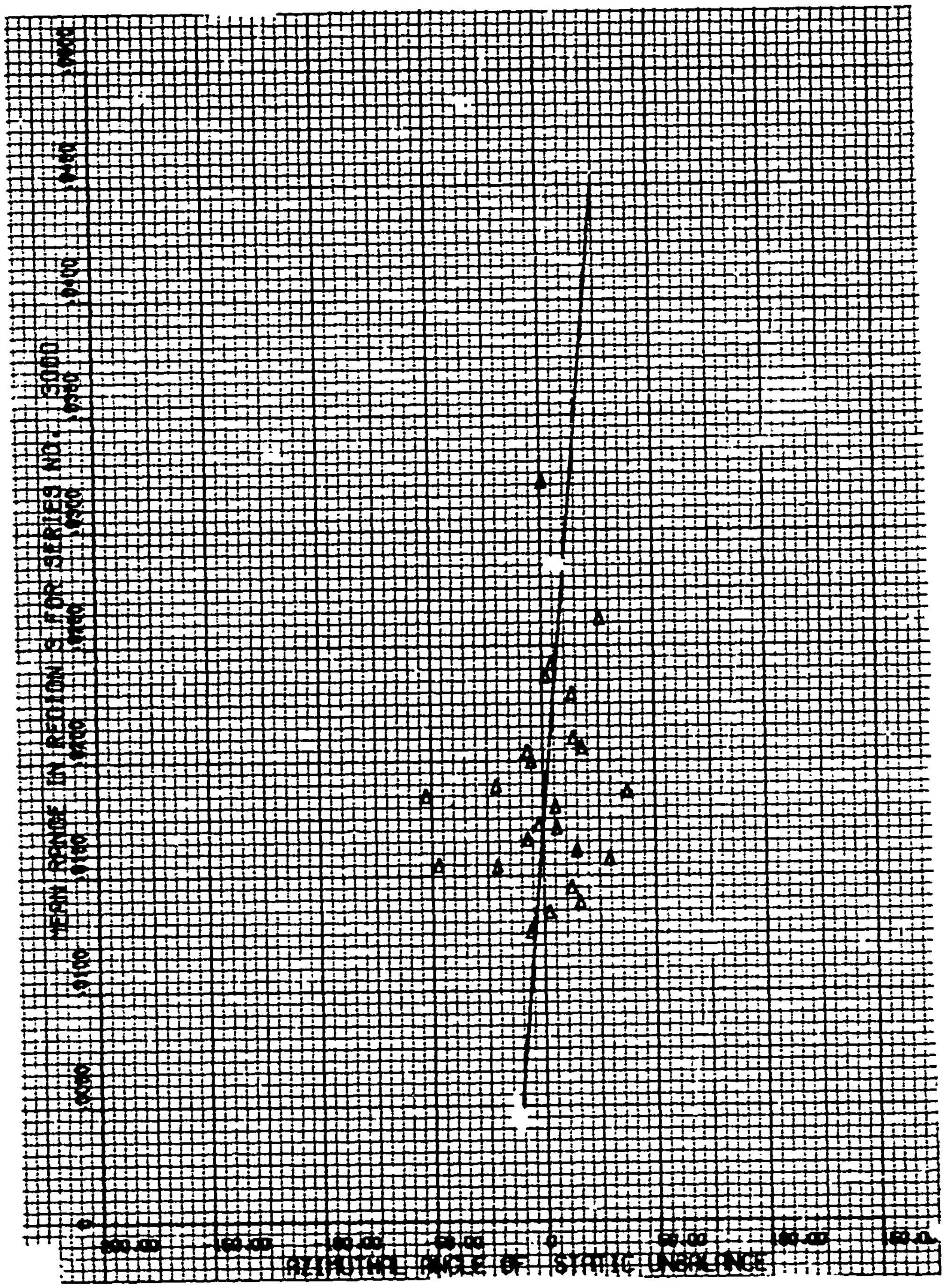

Figure 214 - Mean Wall Thickness Variation Versus Azimuth of Static Unbalance, Series 300C, Region 3, Full

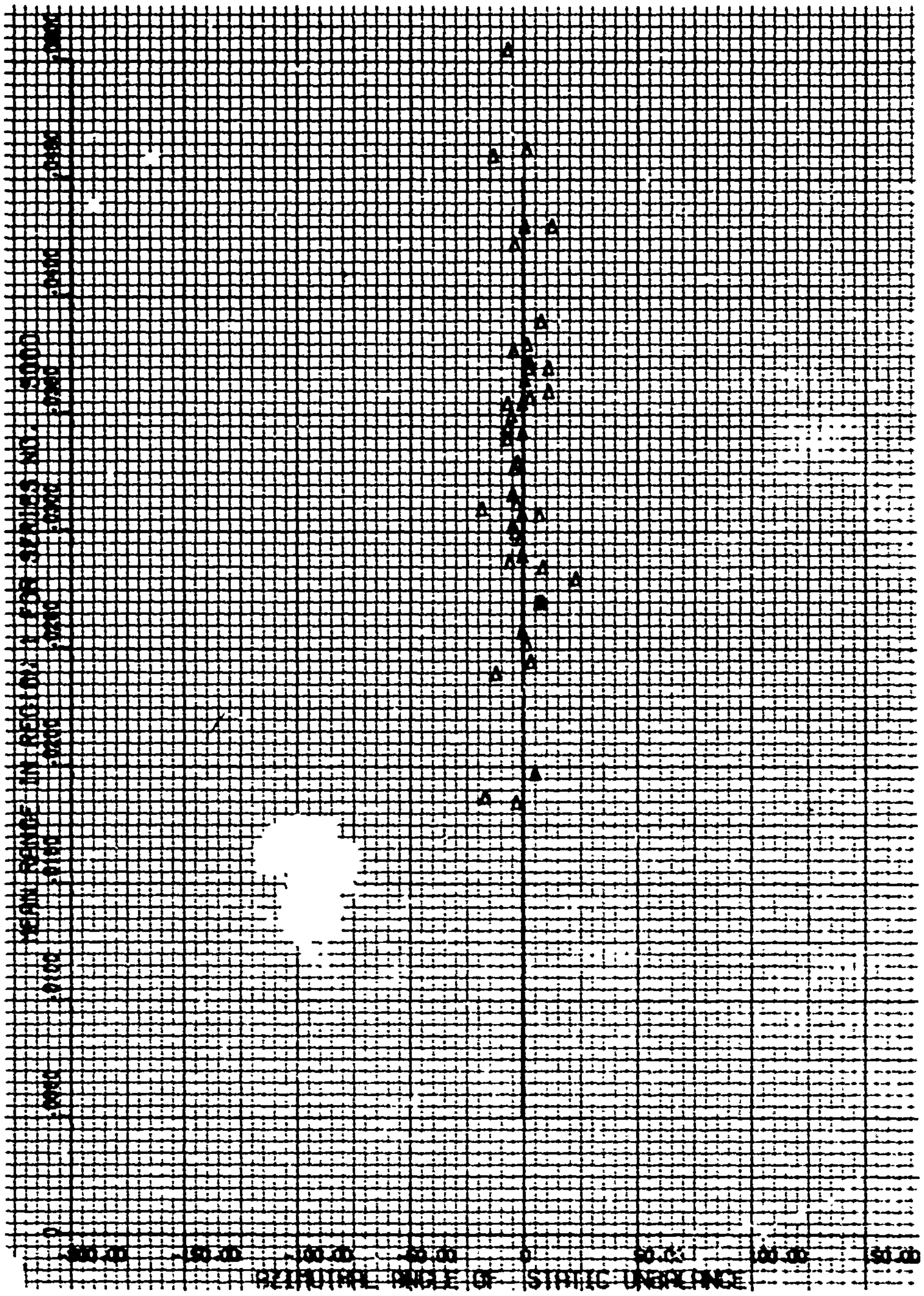

Figure 215 - Mean Wall Thickness Variation Versus Azimuth of Static Unbalance, Series 5000, Region 1, Full

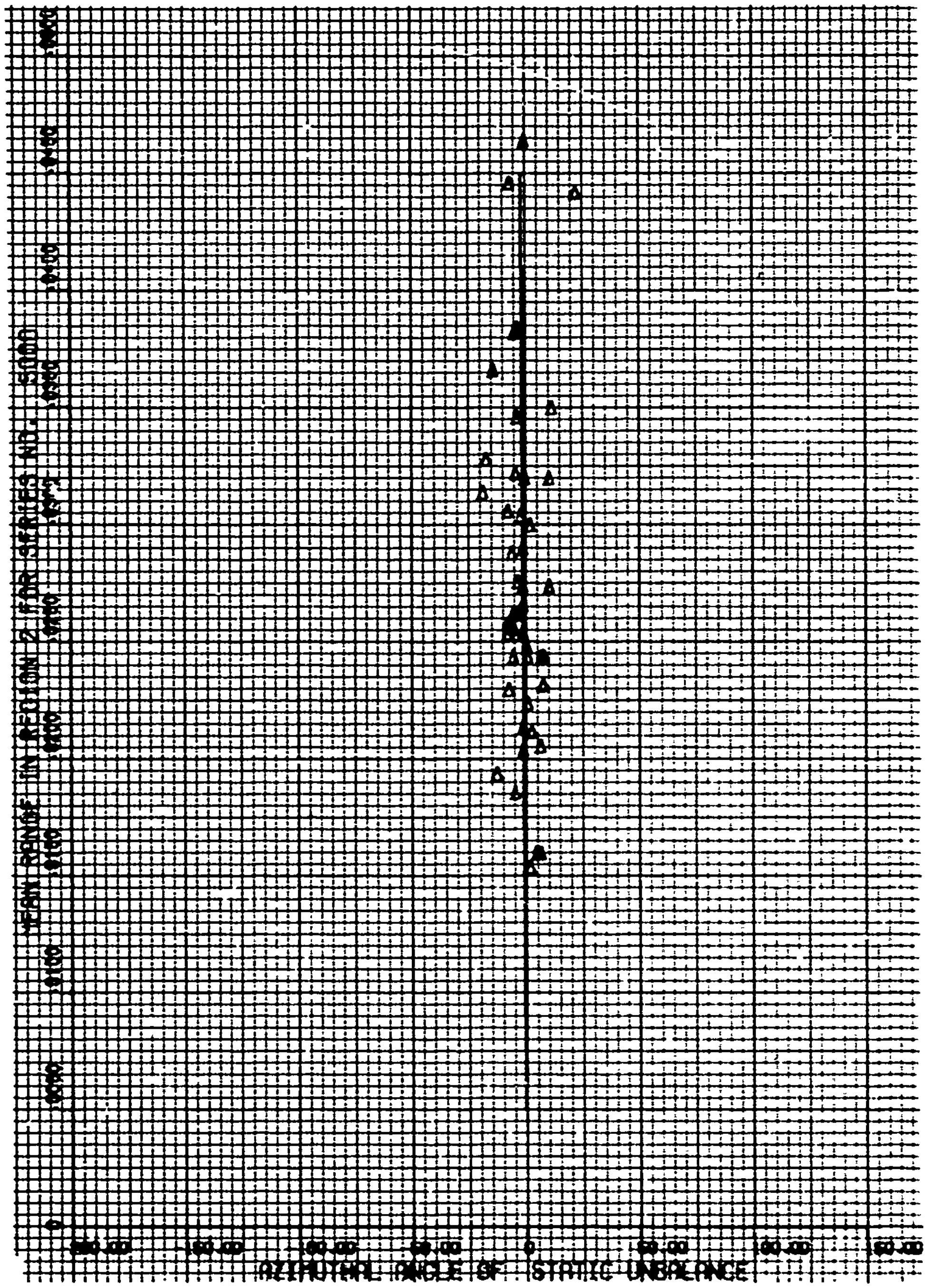

Figure 216 - Mean Wall Thickness Variation Versus Azimuth of Static Unbalance, Series 5000, Region 2, Full

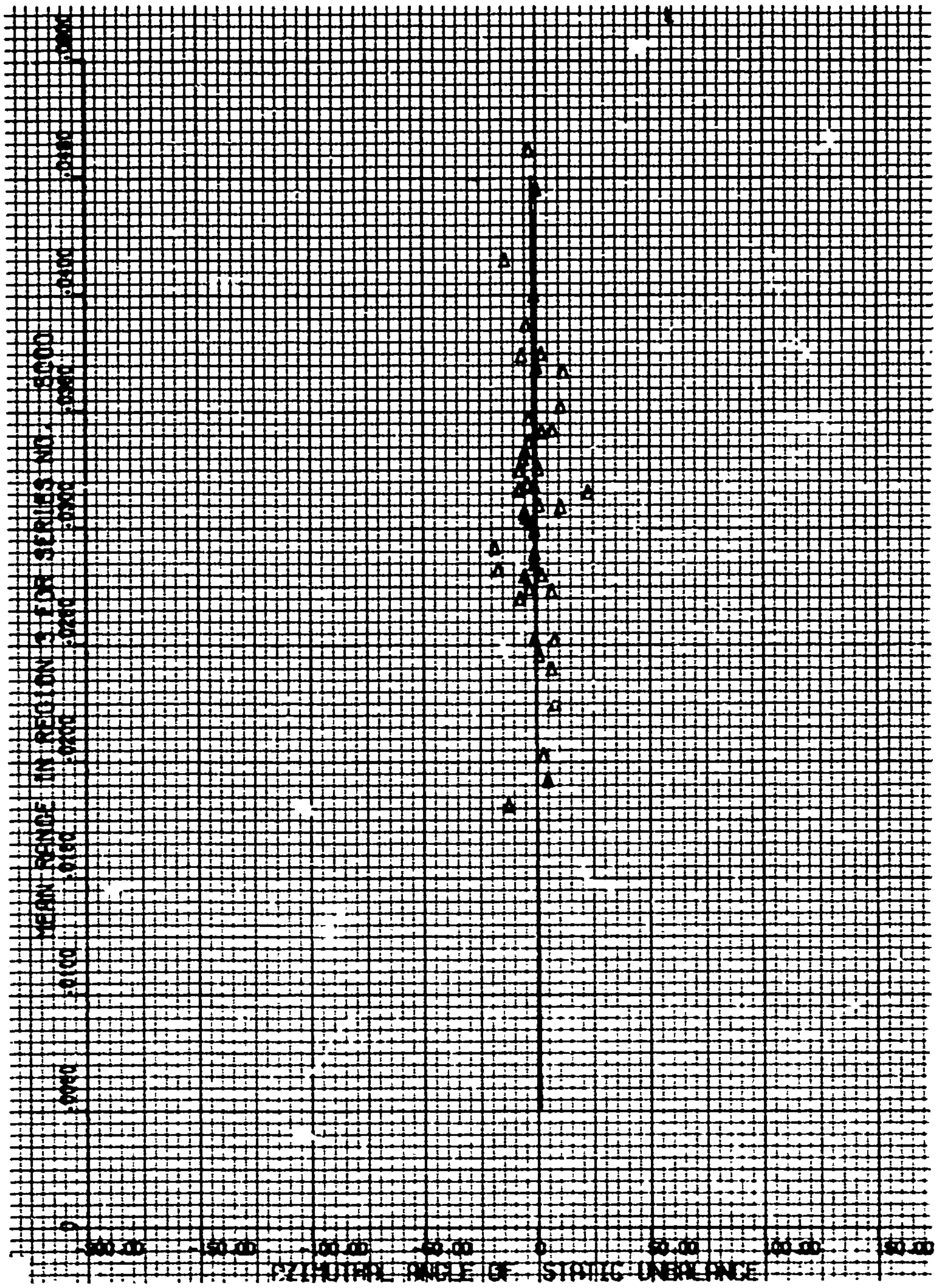

Figure 217 - Mean Wall Thickness Variation Versus Azimuth of Static Unbalance, Series 5000, Region 3, Full

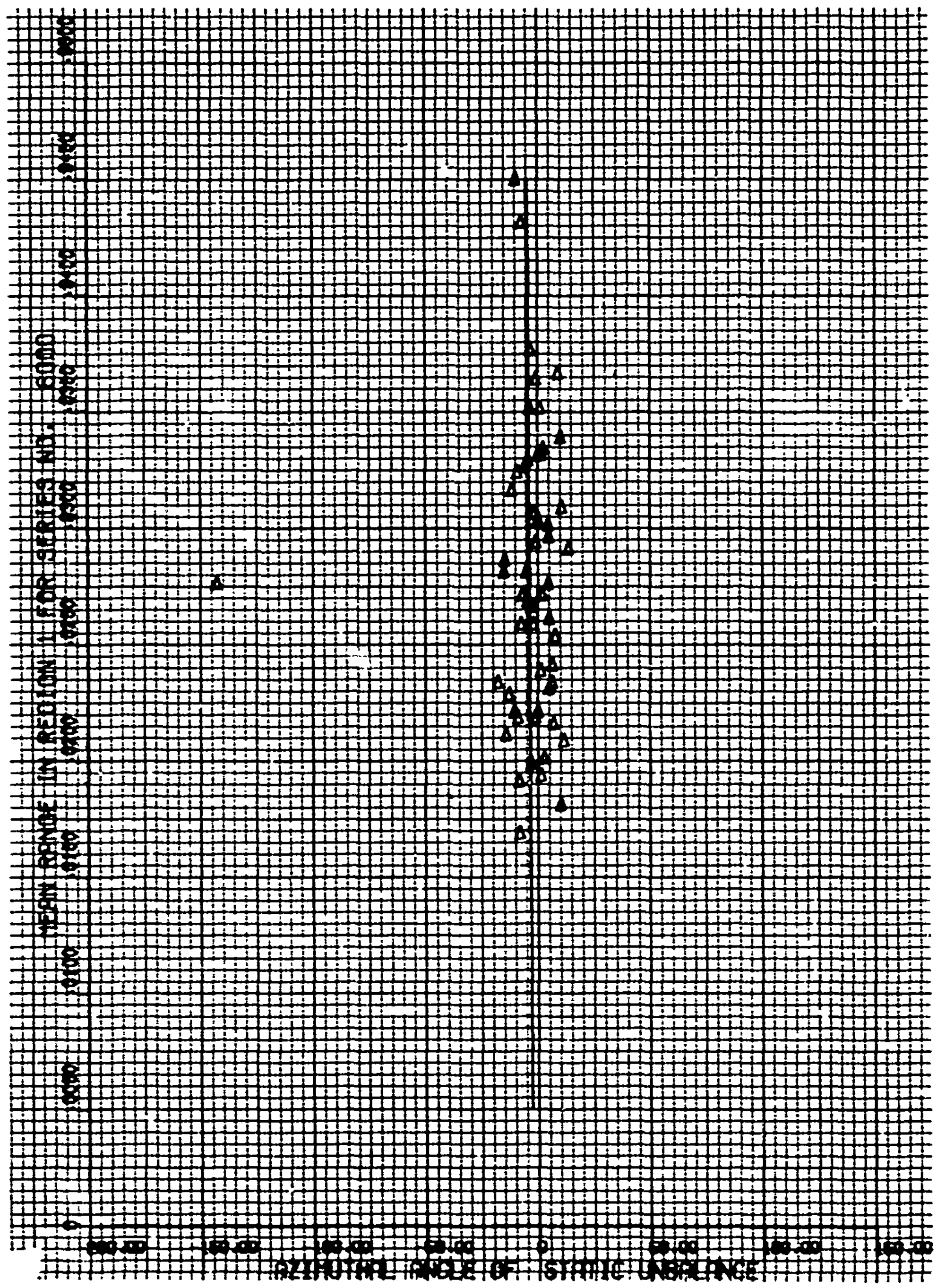

Figure 218 - Mean Wall Thickness Variation Versus Azimuth of Static Unbalance, Series 6000, Region 1, Full

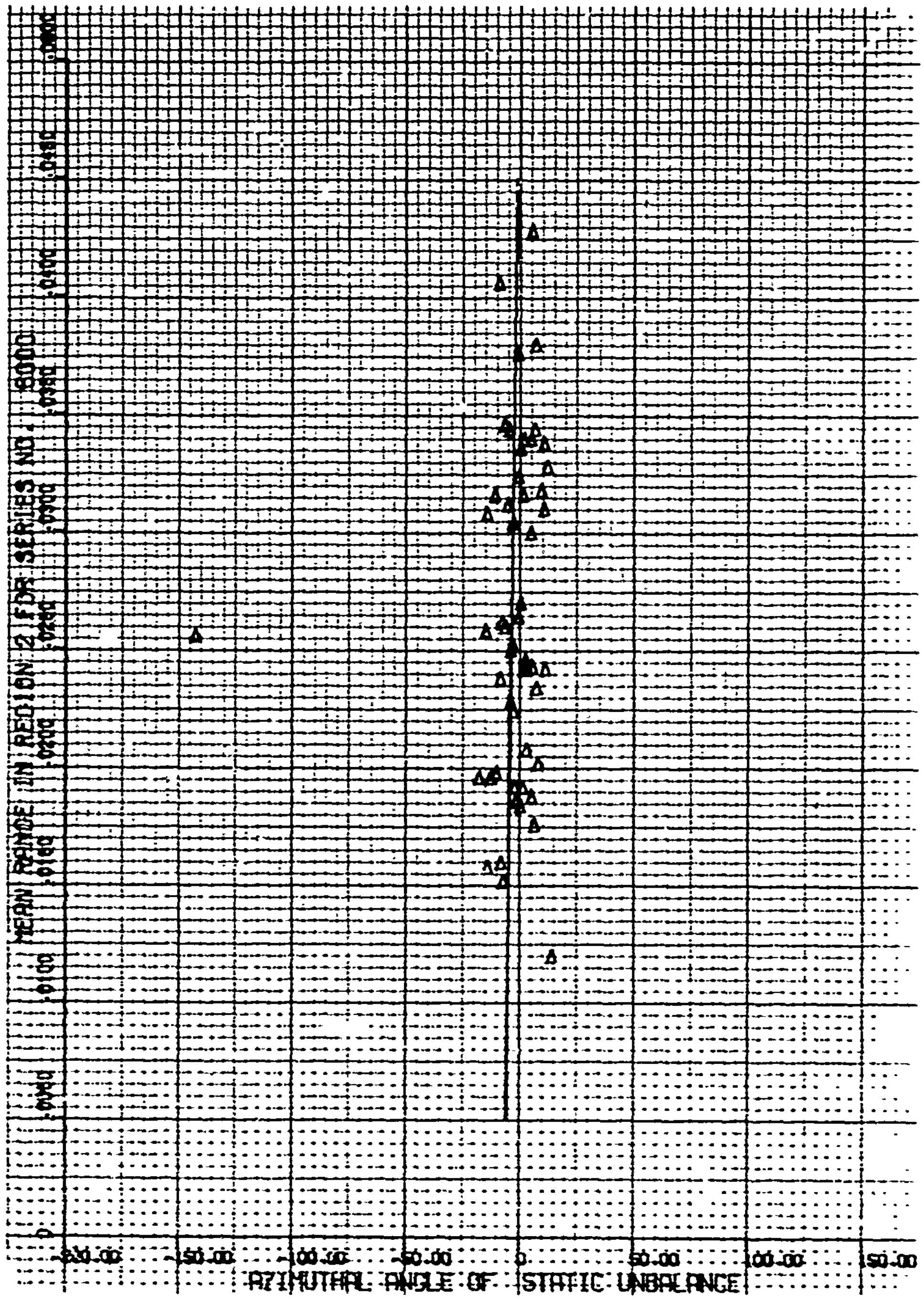

Figure 219 - Mean Wall Thickness Variation Versus Azimuth of Static Unbalance, Series 6000, Region 2, Full

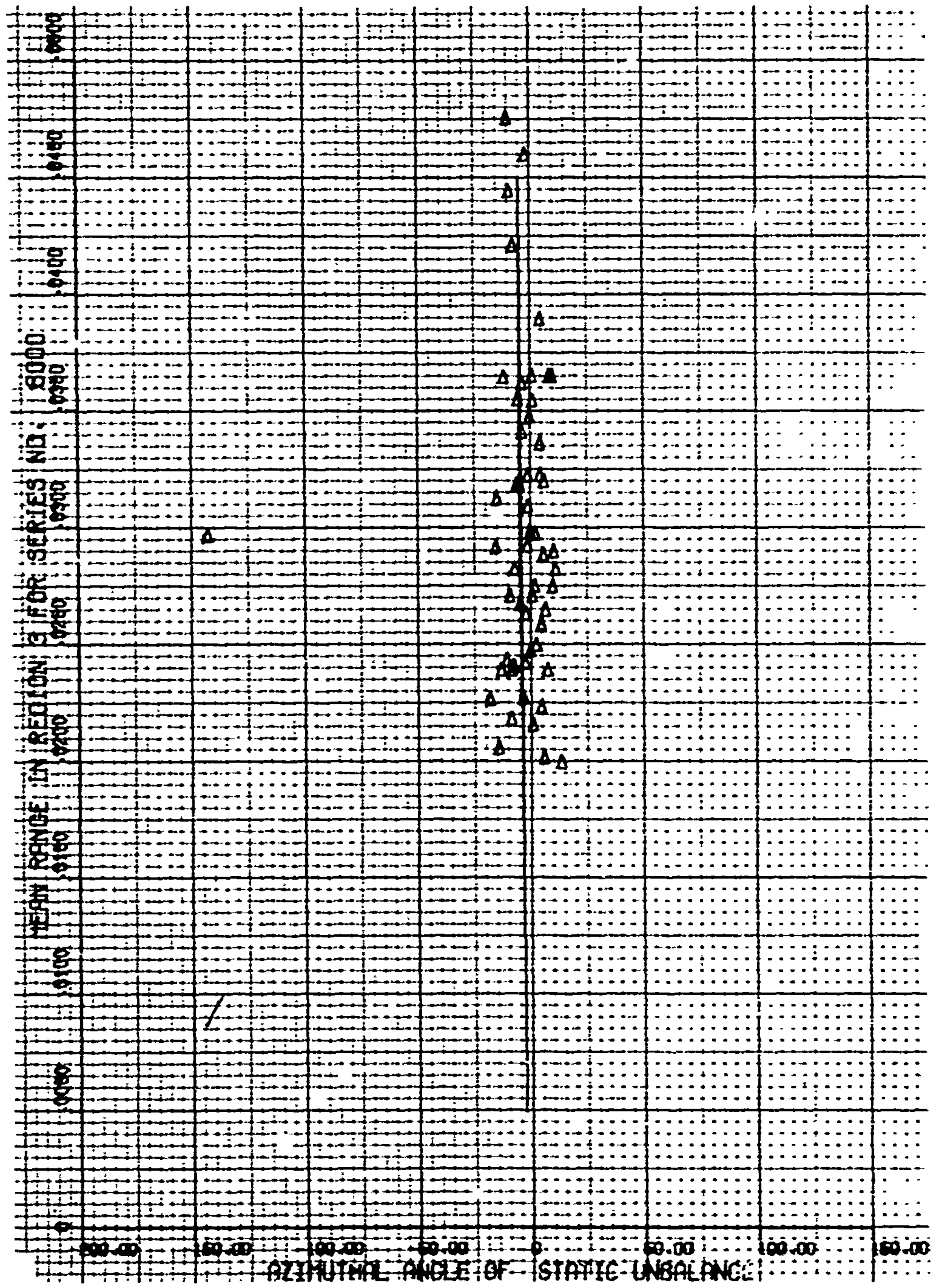

Figure 220 - Mean Wall Thickness Variation Versus Azimuth of Static Unbalance, Series 6000, Region 3, Full

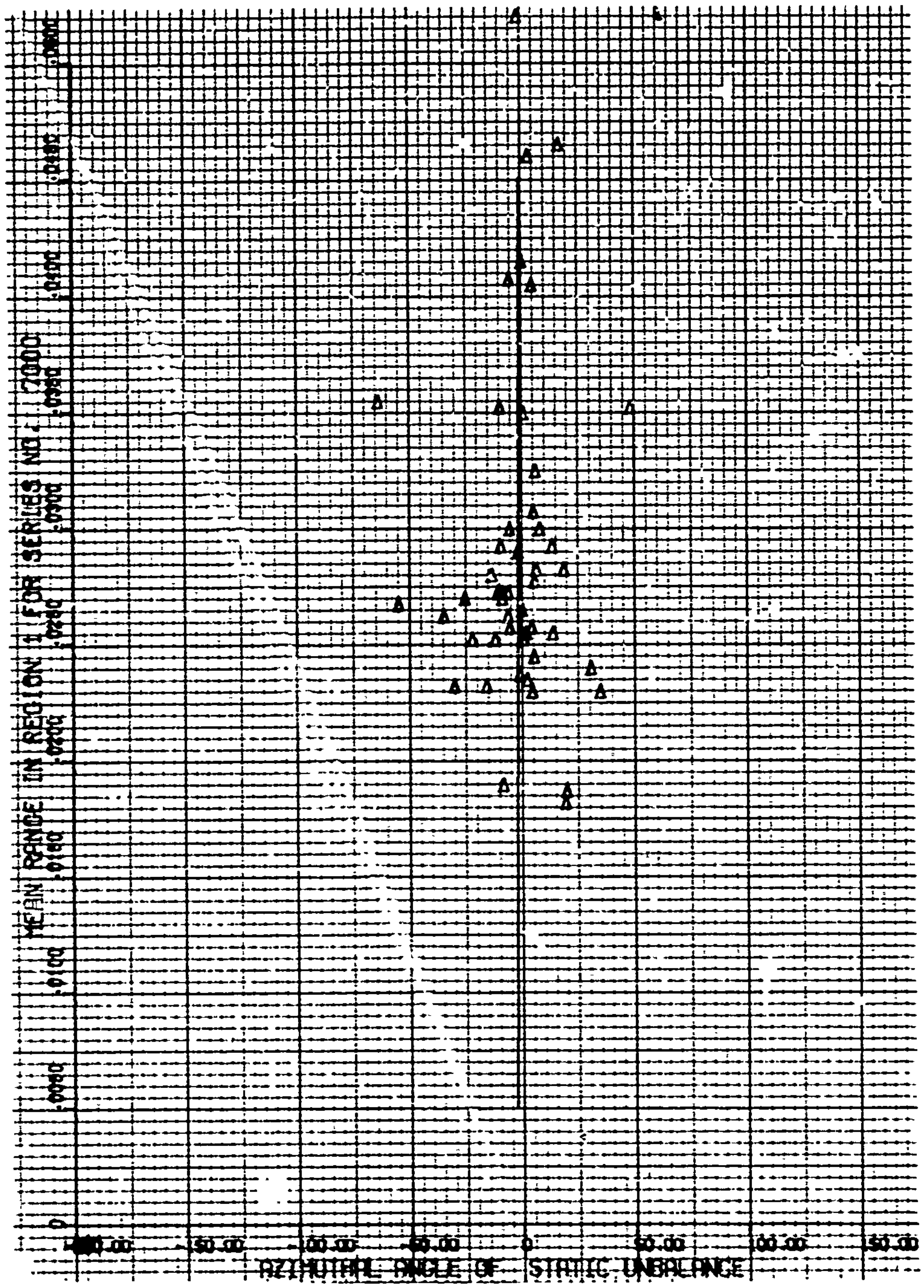

Figure 221 - Mean Wall Thickness Variation Versus Azimuth of Static Unbalance, Series 7000, Region 1, Full

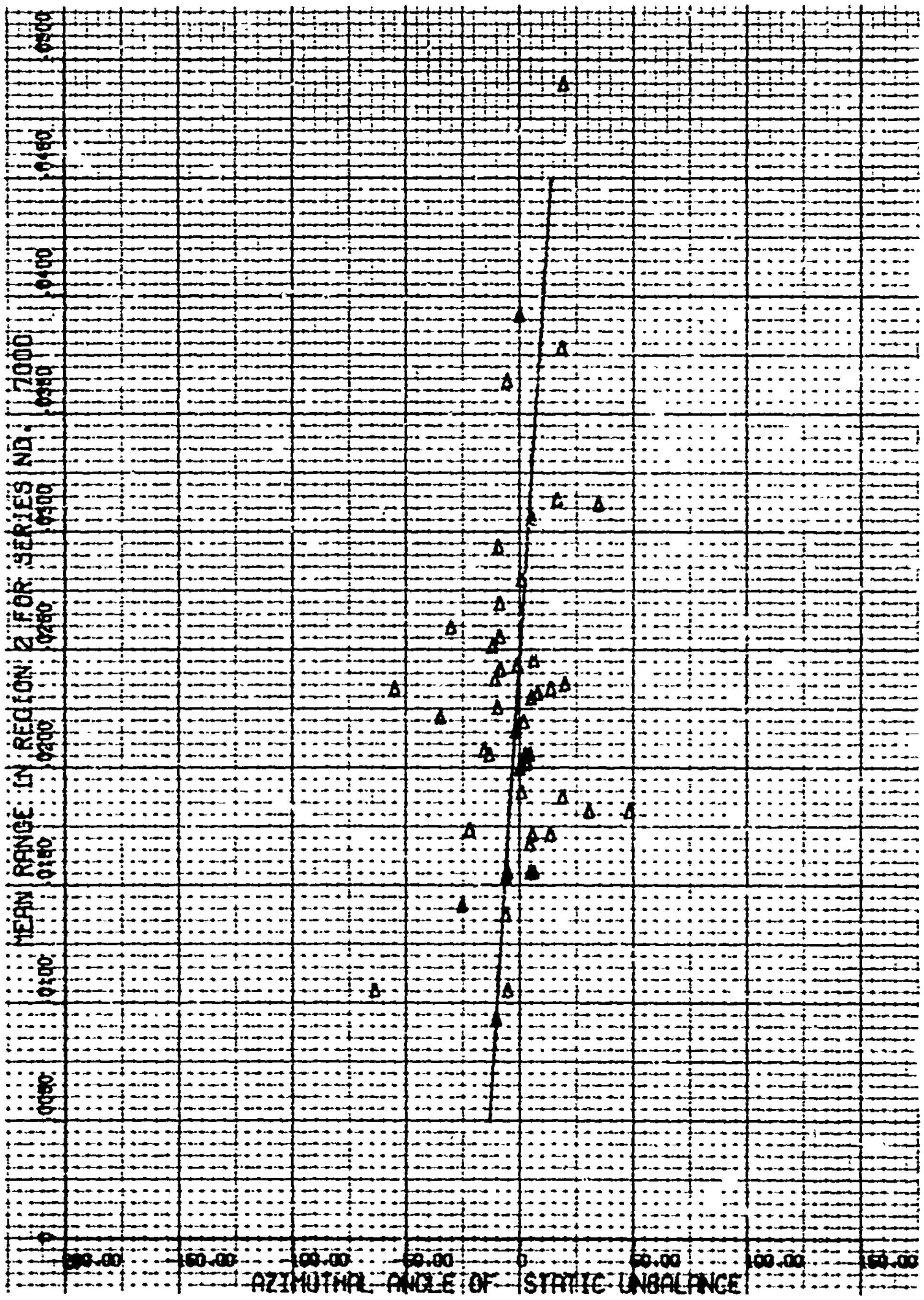

Figure 222 - Mean Wall Thickness Variation Versus Azimuth of Static Unbalance, Series 7000, Region 2, Full

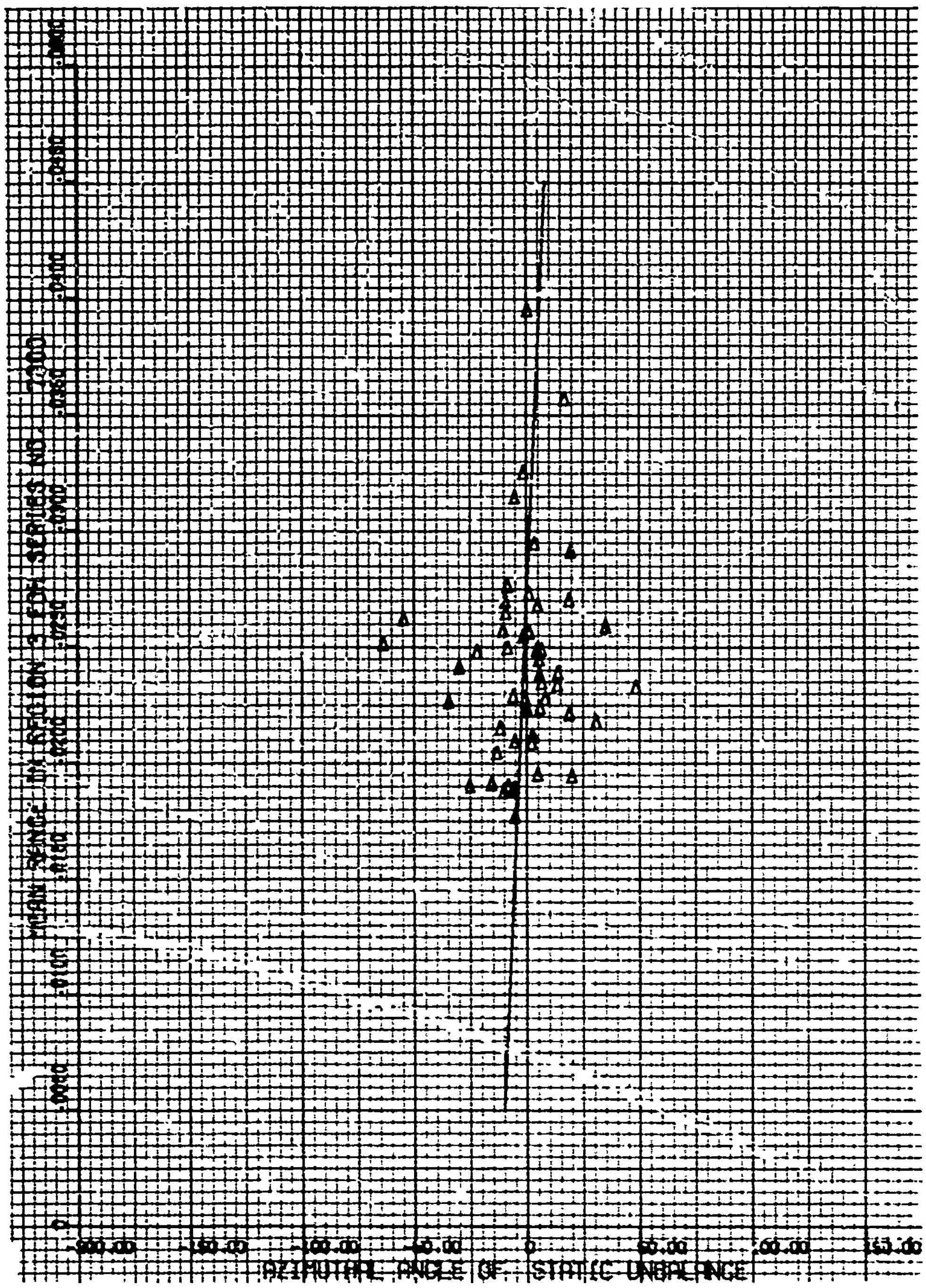

Figure 223 - Mean Wall Thickness Variation Versus Azimuth of Static Unbalance, Series 7000, Region 3, Full

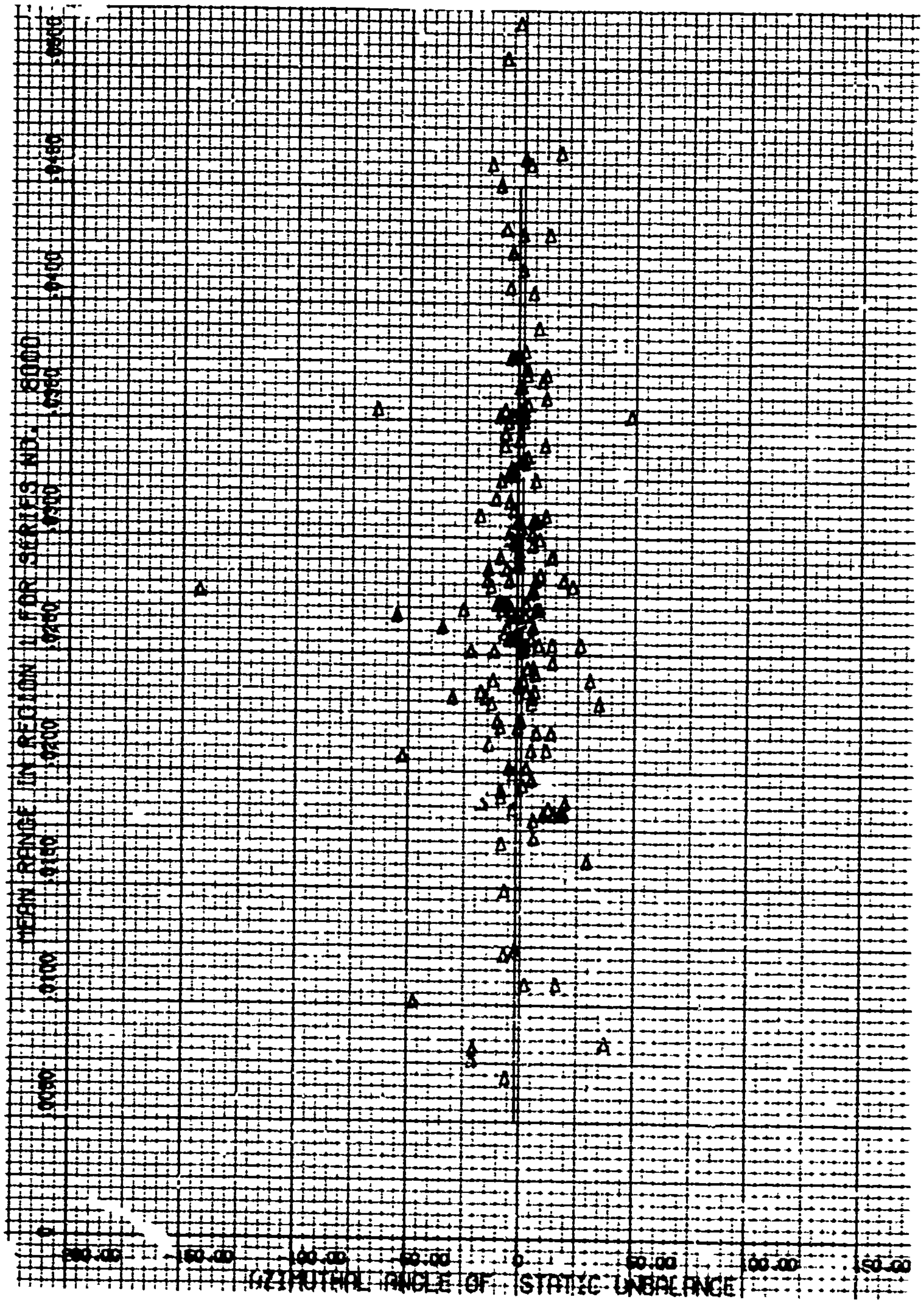

Figure 224 - Mean Wall Thickness Variation Versus Azimuth of Static Unbalance, Series 3000, Region 1, Full

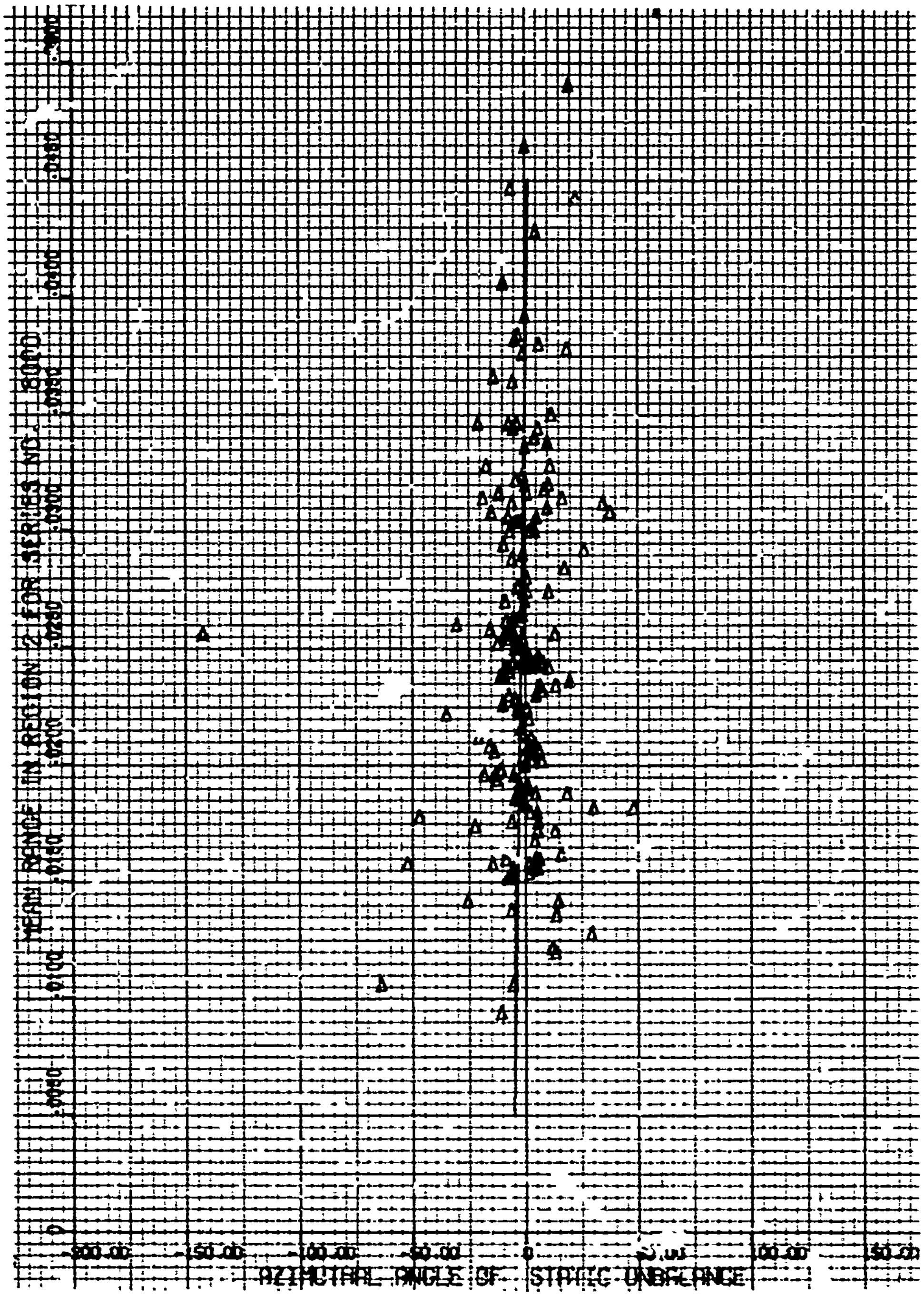

Figure 225 - Mean Wall Thickness Variation Versus Azimuth of Static Unbalance, Series 8000, Region 2, Full

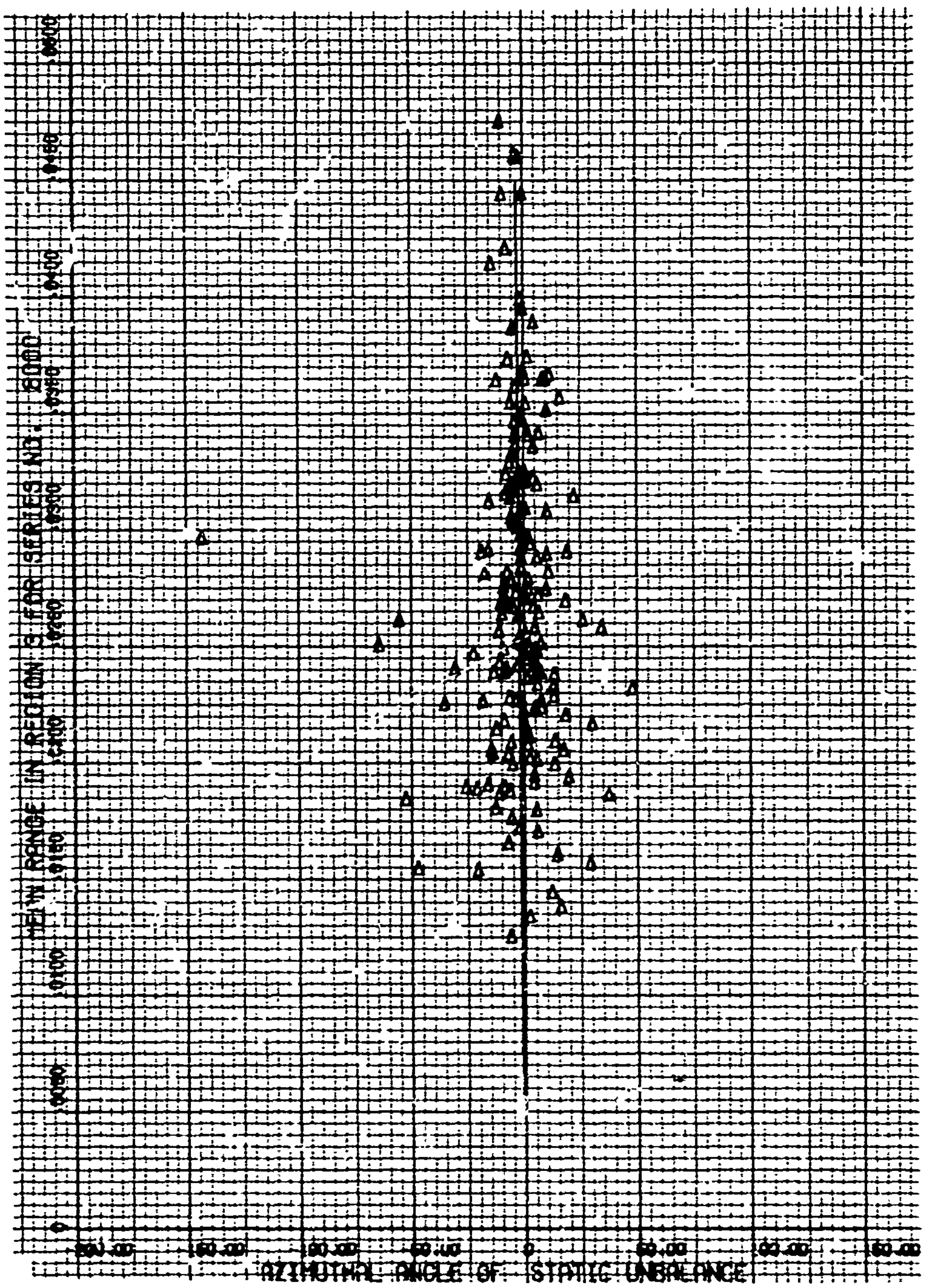

Figure 226 - Mean Wall Thickness Variation Versus Azimuth of Static Unbalance, Series 8000, Region 3, Full

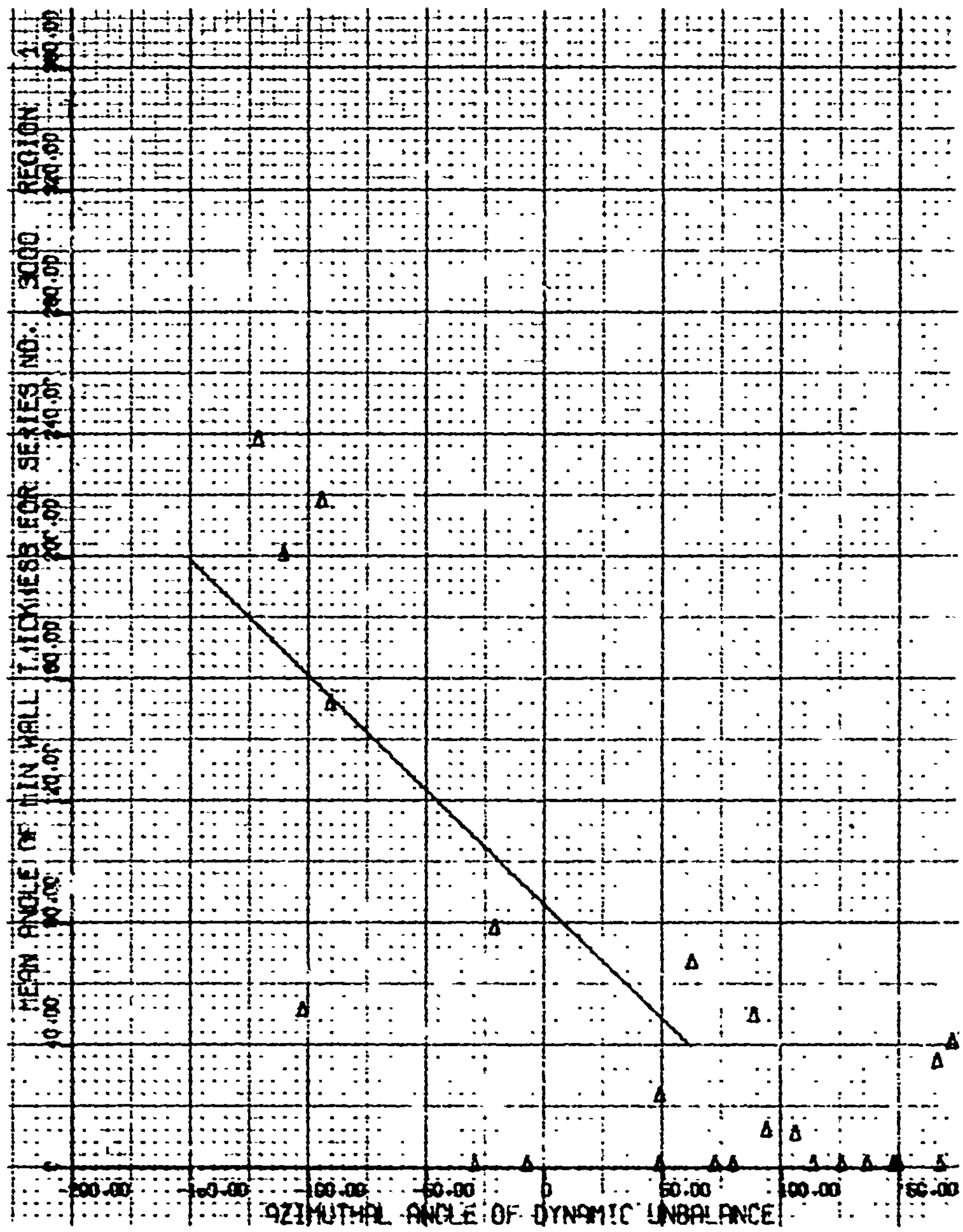

Figure . 27 - Mean Azimuth of Minimum Wall Thickness Versus Azimuth of Dynamic Unbalance, Series 3000, Region 1, Empty

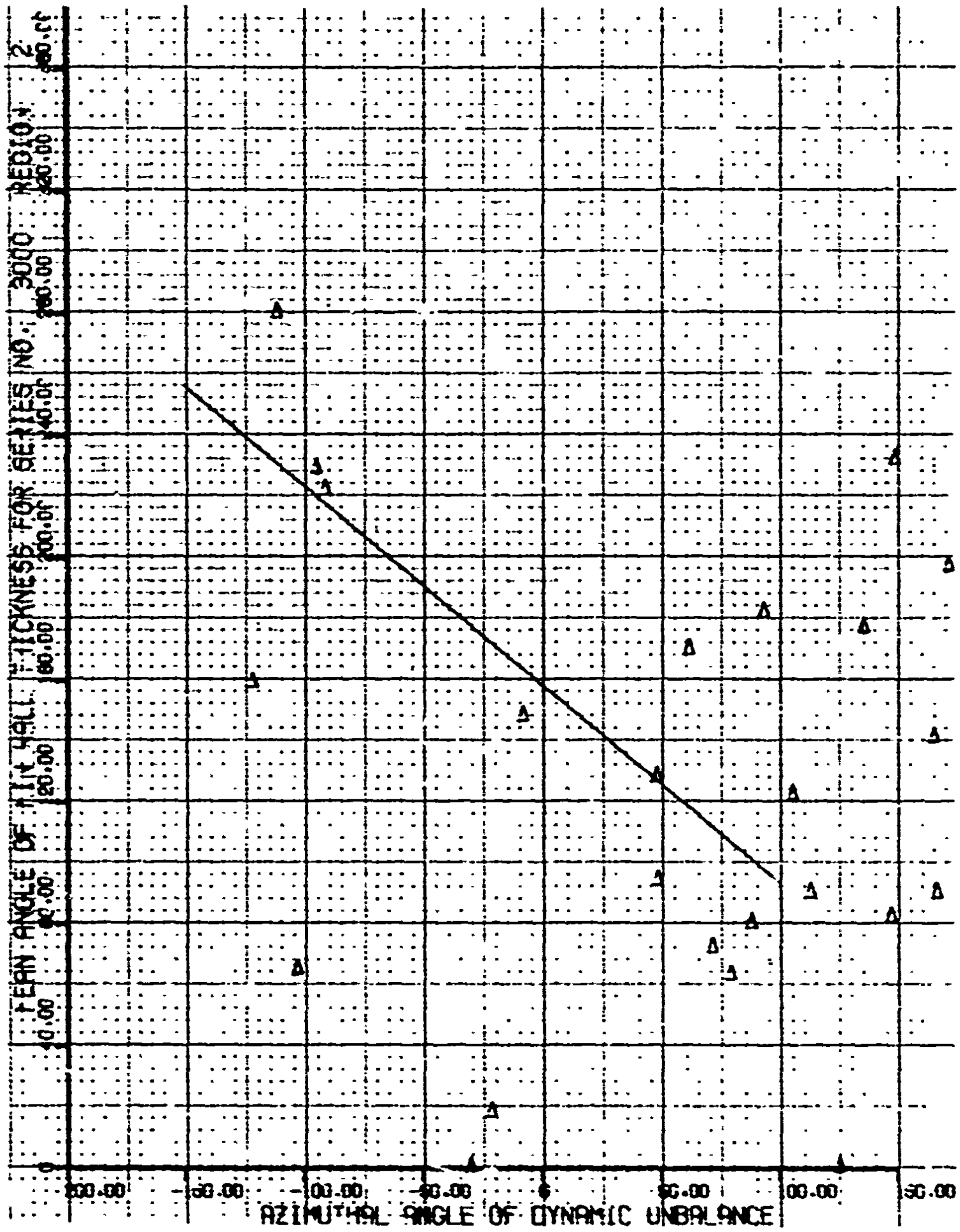

Figure 228 - Mean Azimuth of Minimum Wall Thickness Versus Azimuth of Dynamic Unbalance, Series 3000, Region 2, Empty

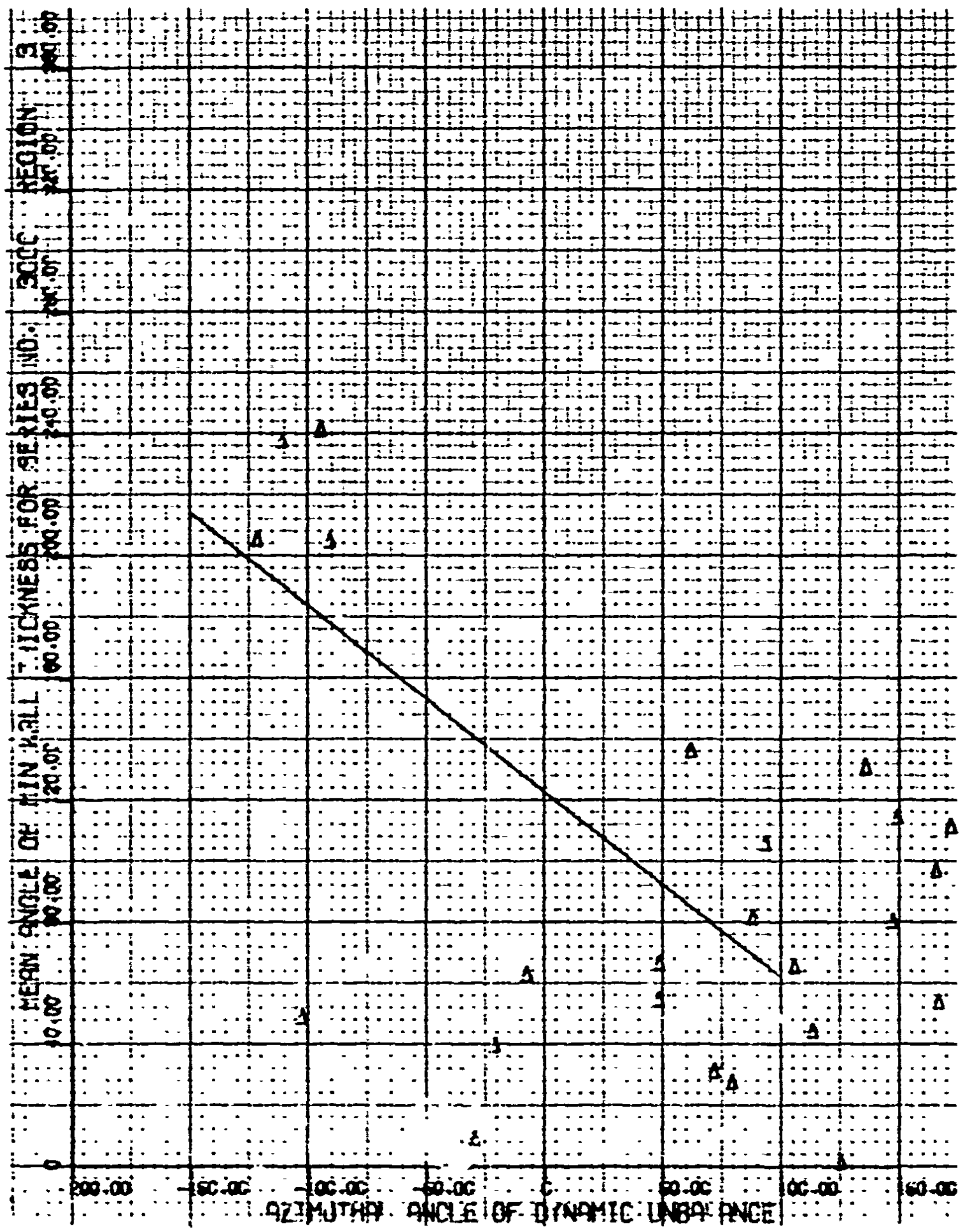

Figure 229 - Mean Azimuth of Minimum Wall Thickness Versus Azimuth of Dynamic Unbalance, Series 3000, Region 3, Empty

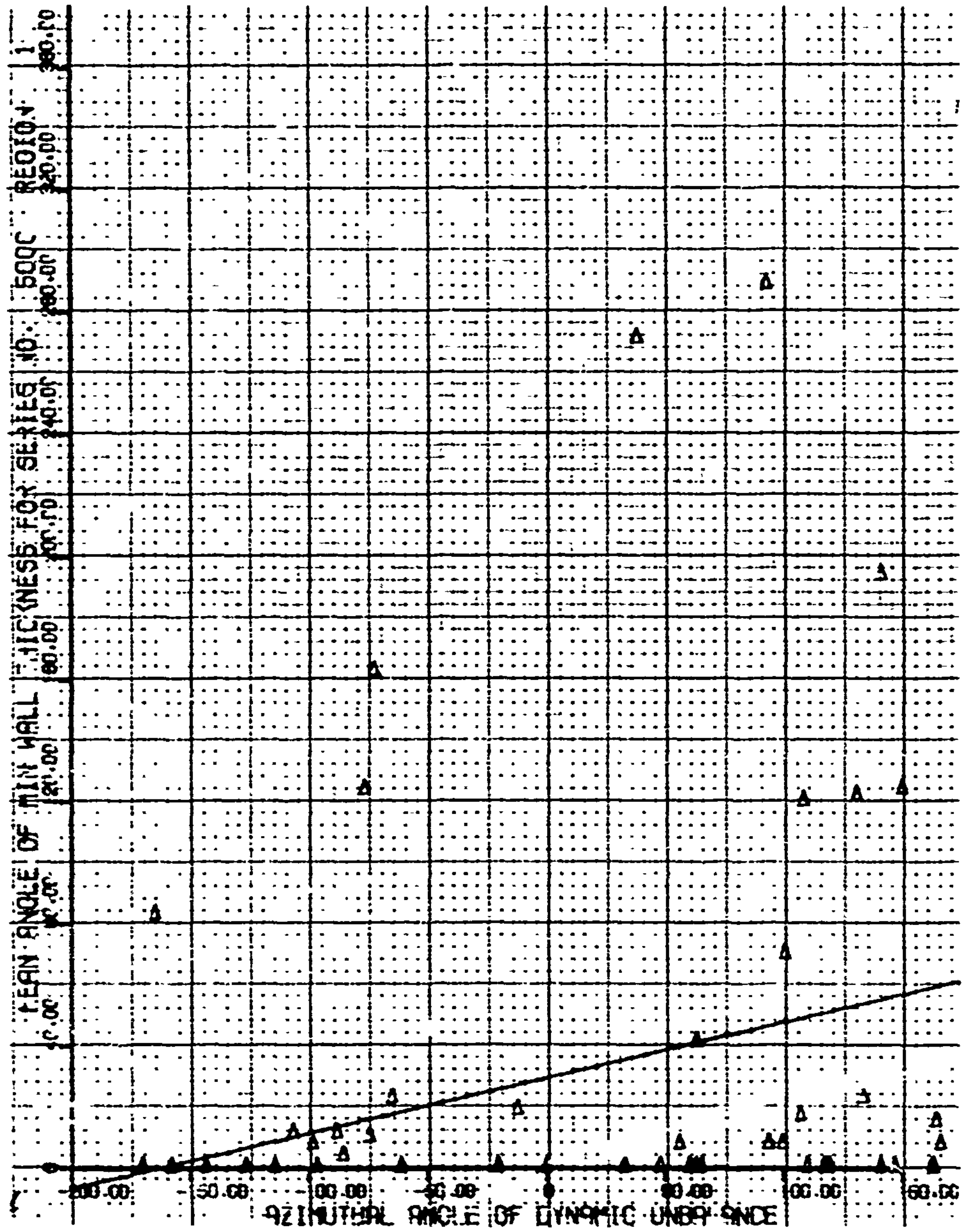

Figure 230 - Mean Azimuth of Minimum Wall Thickness Versus Azimuth of Dynamic Unbalance, Series 5000, Region 1. Empty

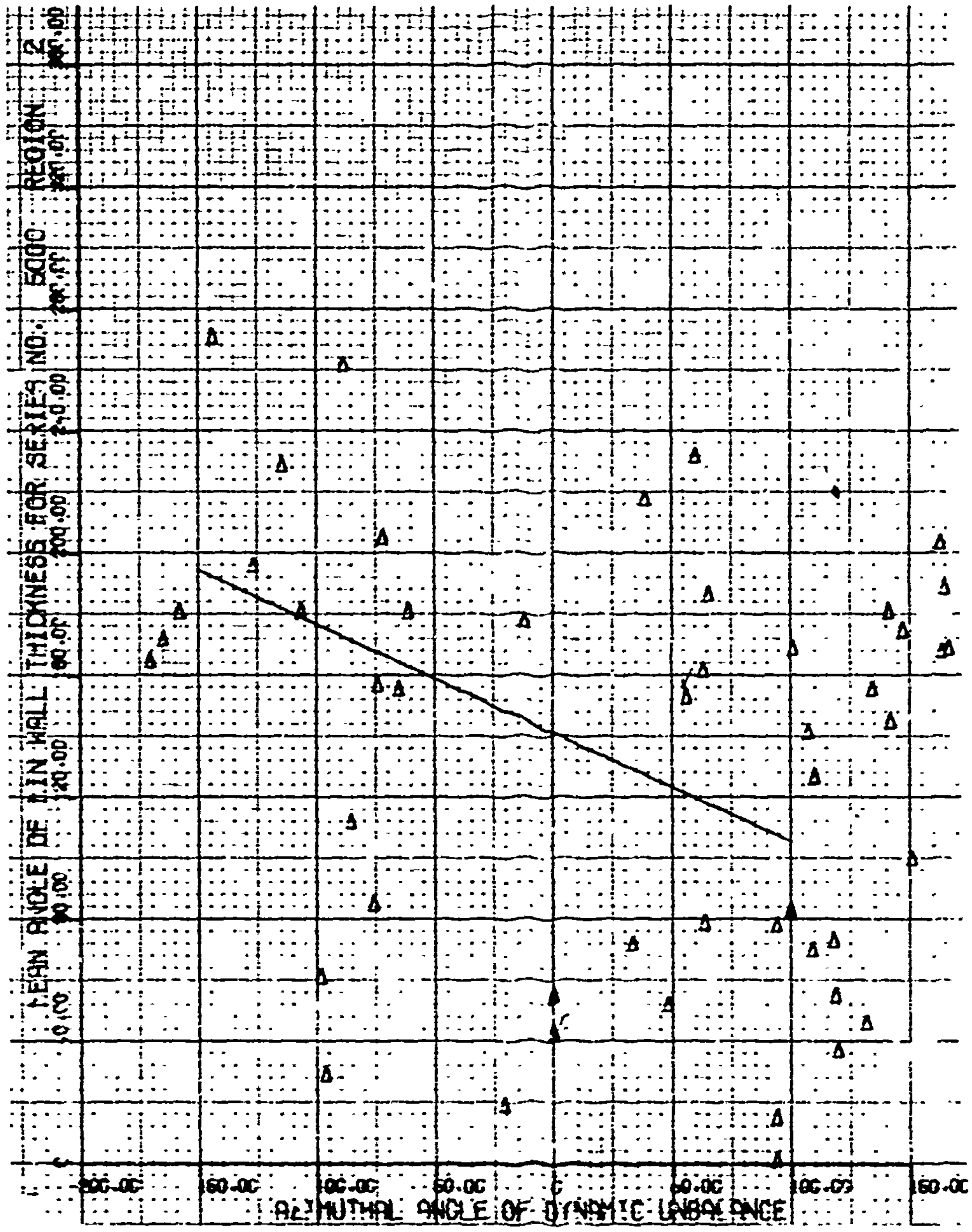

Figure 231 - Mean Azimuth of Minimum Wall Thickness Versus Azimuth of Dynamic Unbalance, Series 5000, Region 2, Empty

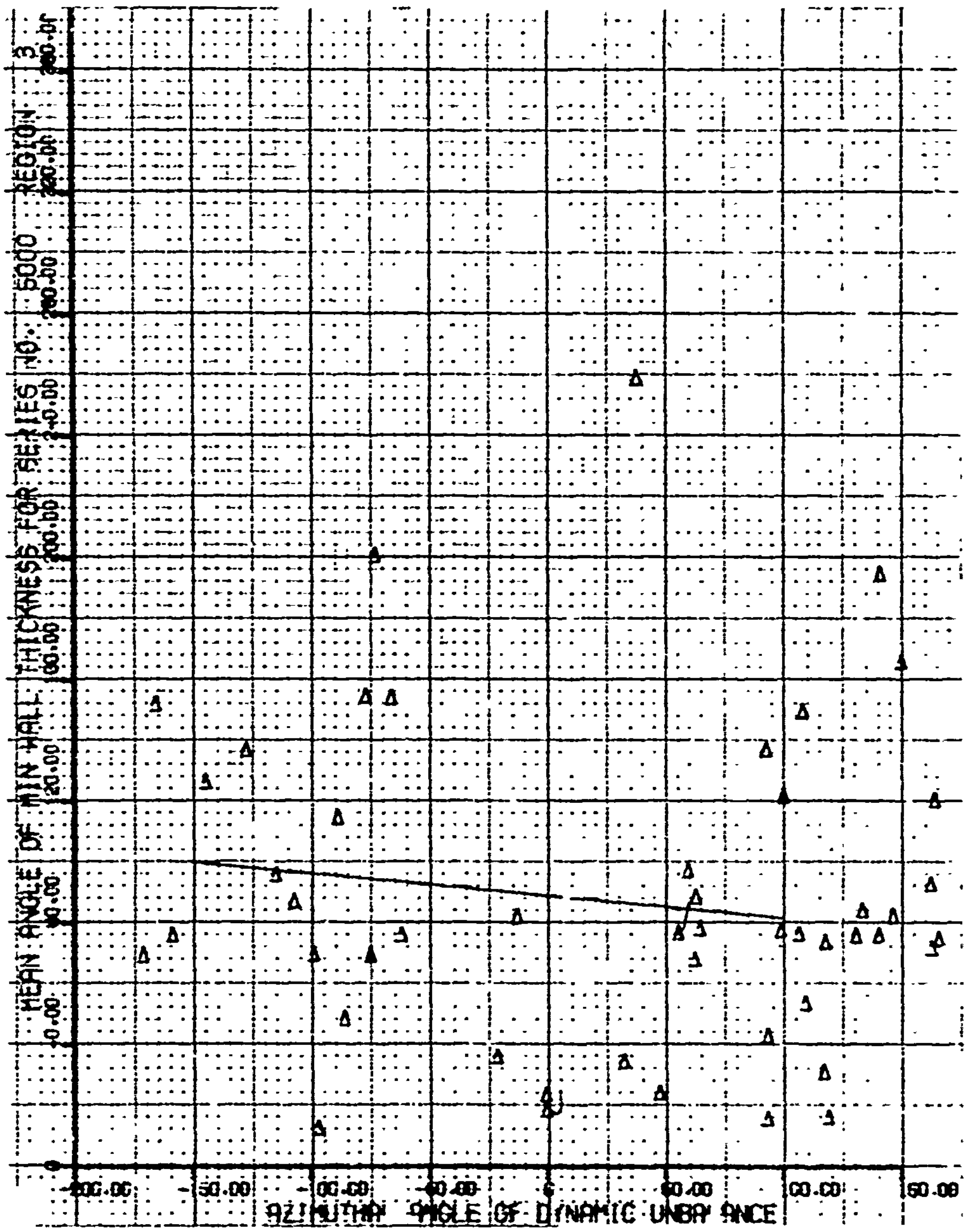

Figure 232 - Mean Azimuth of Minimum Wall Thickness Versus Azimuth of Dynamic Unbalance, Series 5000, Region 3, Empty

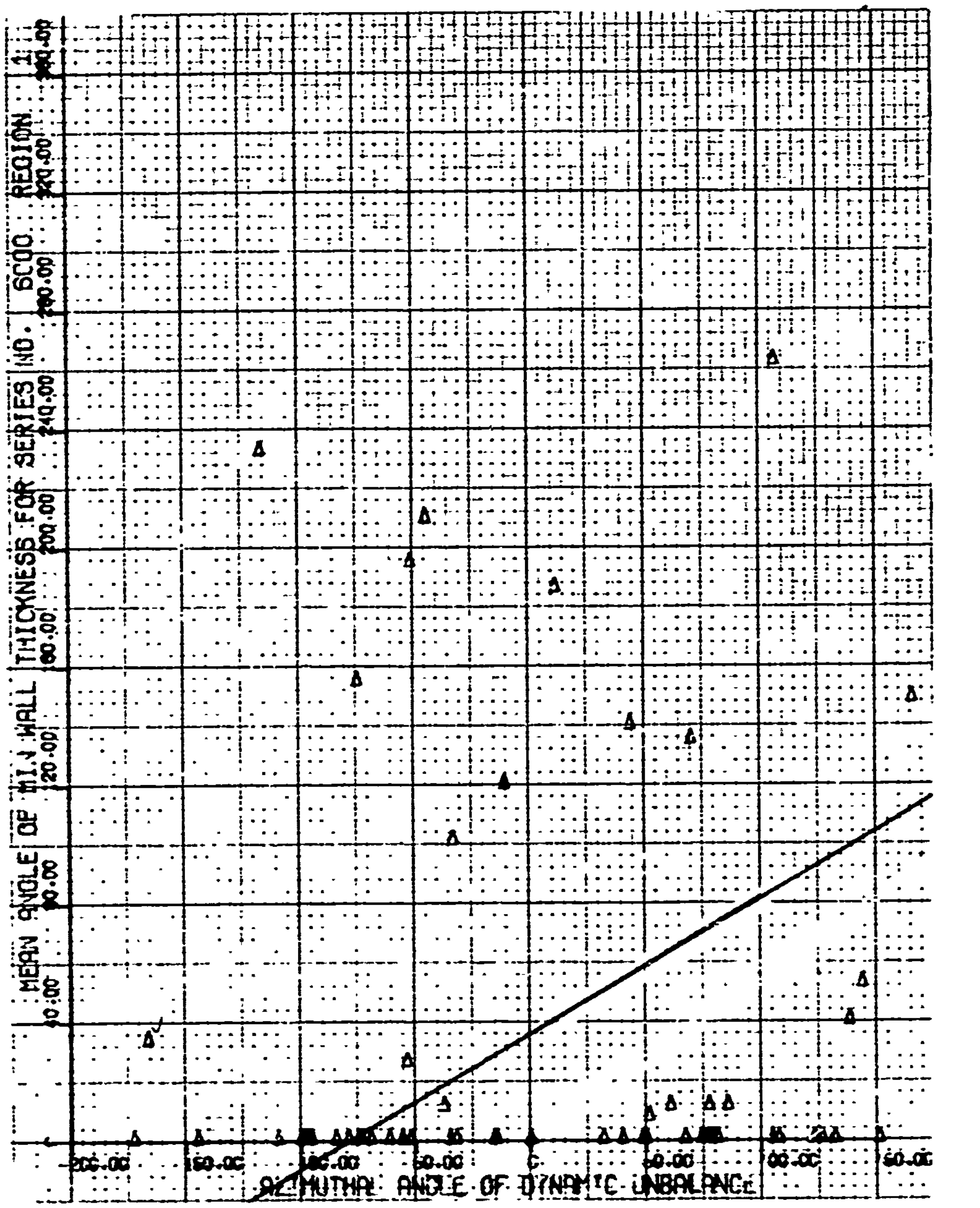

Figure 233 - Mean Azimuth of Minimum Wall Thickness Versus Azimuth of Dynamic Unbalance, Series 6000, Region 1, Empty

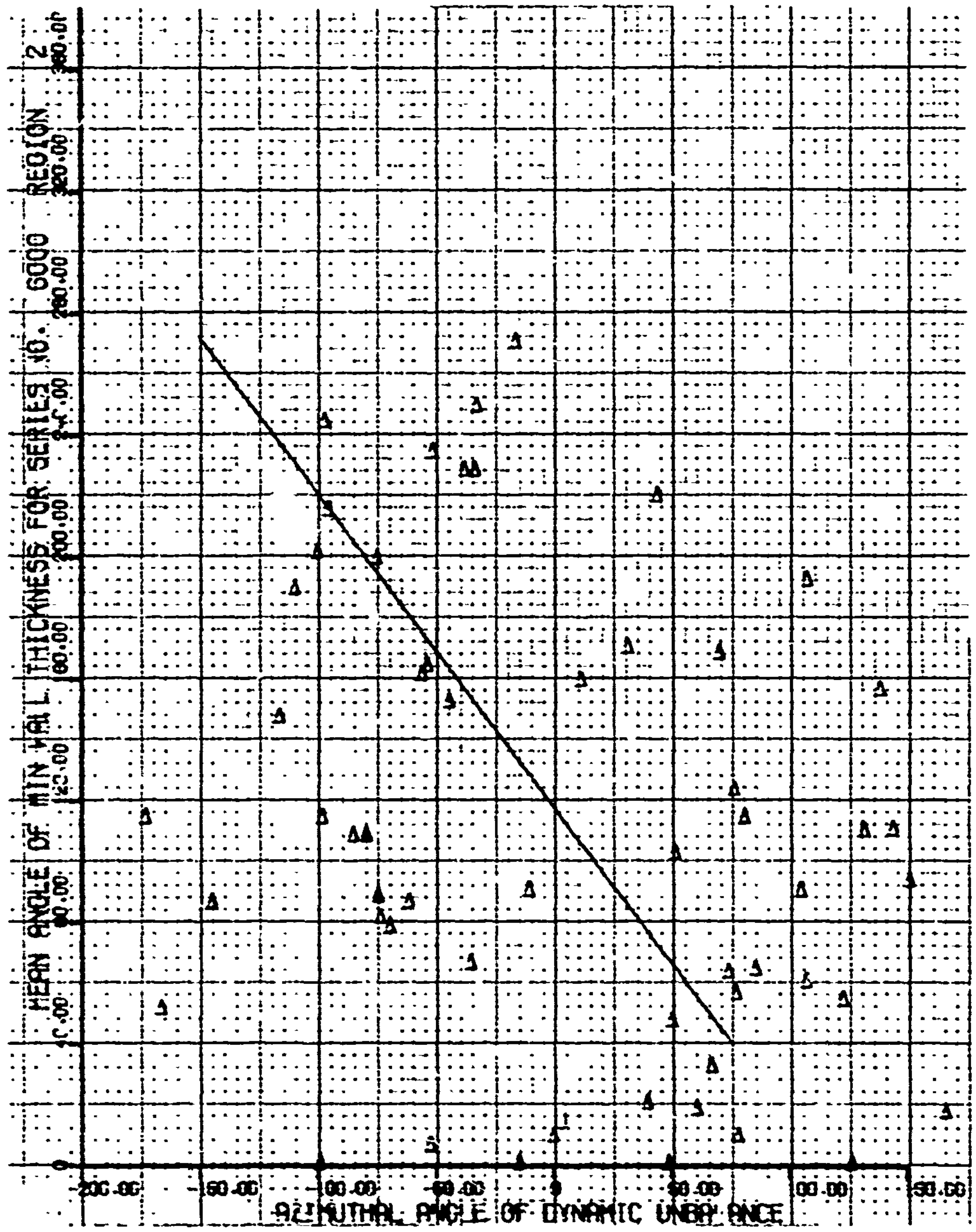

Figure 234 - Mean Azimuth of Minimum Wall Thickness Versus Azimuth of Dynamic Unbalance, Series 6000, Region 2, Empty

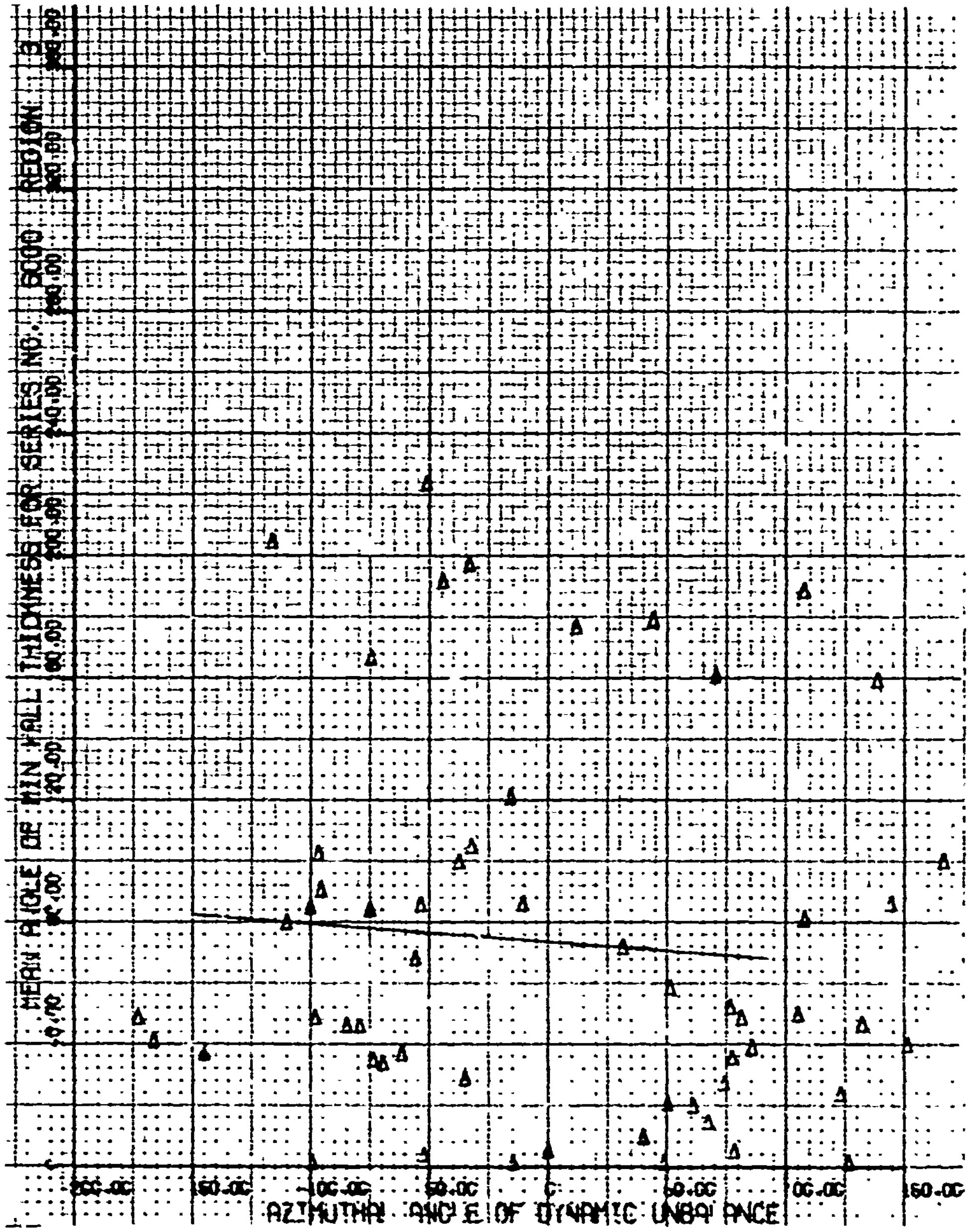

Figure 235 - Mean Azimuth of Minimum Wall Thickness Versus Azimuth of Dynamic Unbalance, Series 6000, Region 3, Empty

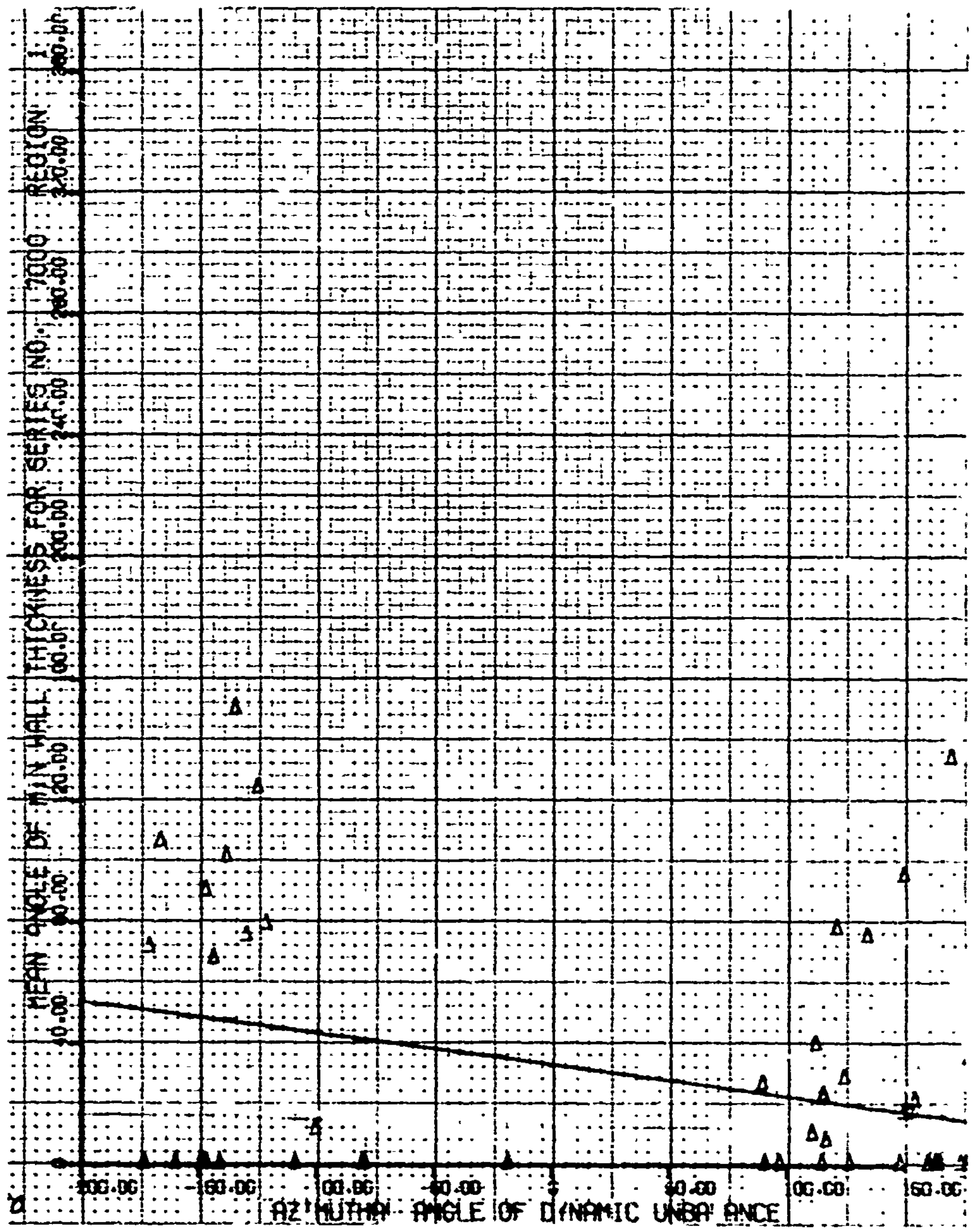

Figure 236 - Mean Azimuth of Minimum Wall Thickness Versus Azimuth of Dynamic Unbalance, Series 7000, Region 1, Empty

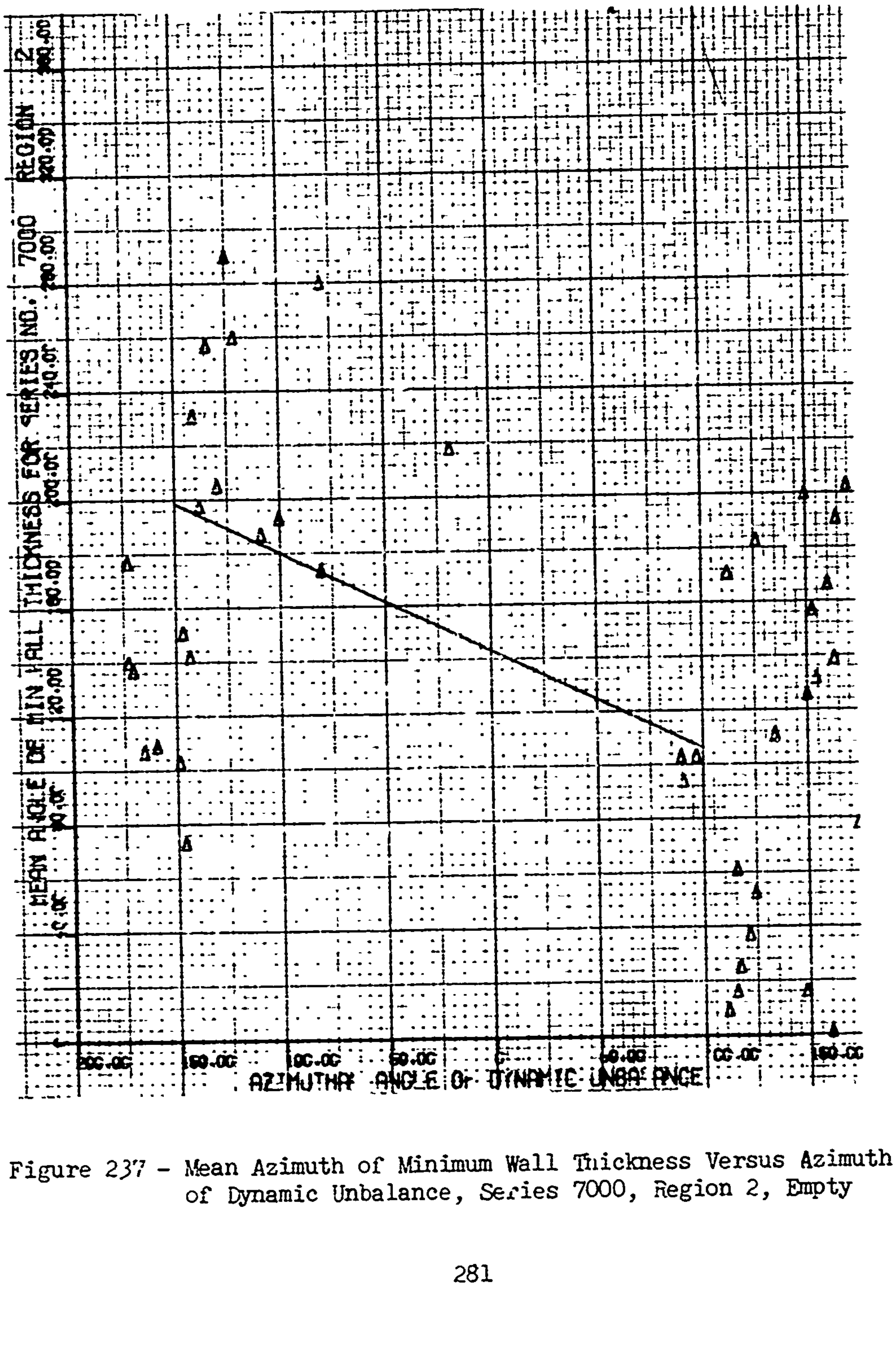

Figure 237 - Mean Azimuth of Minimum Wall Thickness Versus Azimuth of Dynamic Unbalance, Series 7000, Region 2, Empty

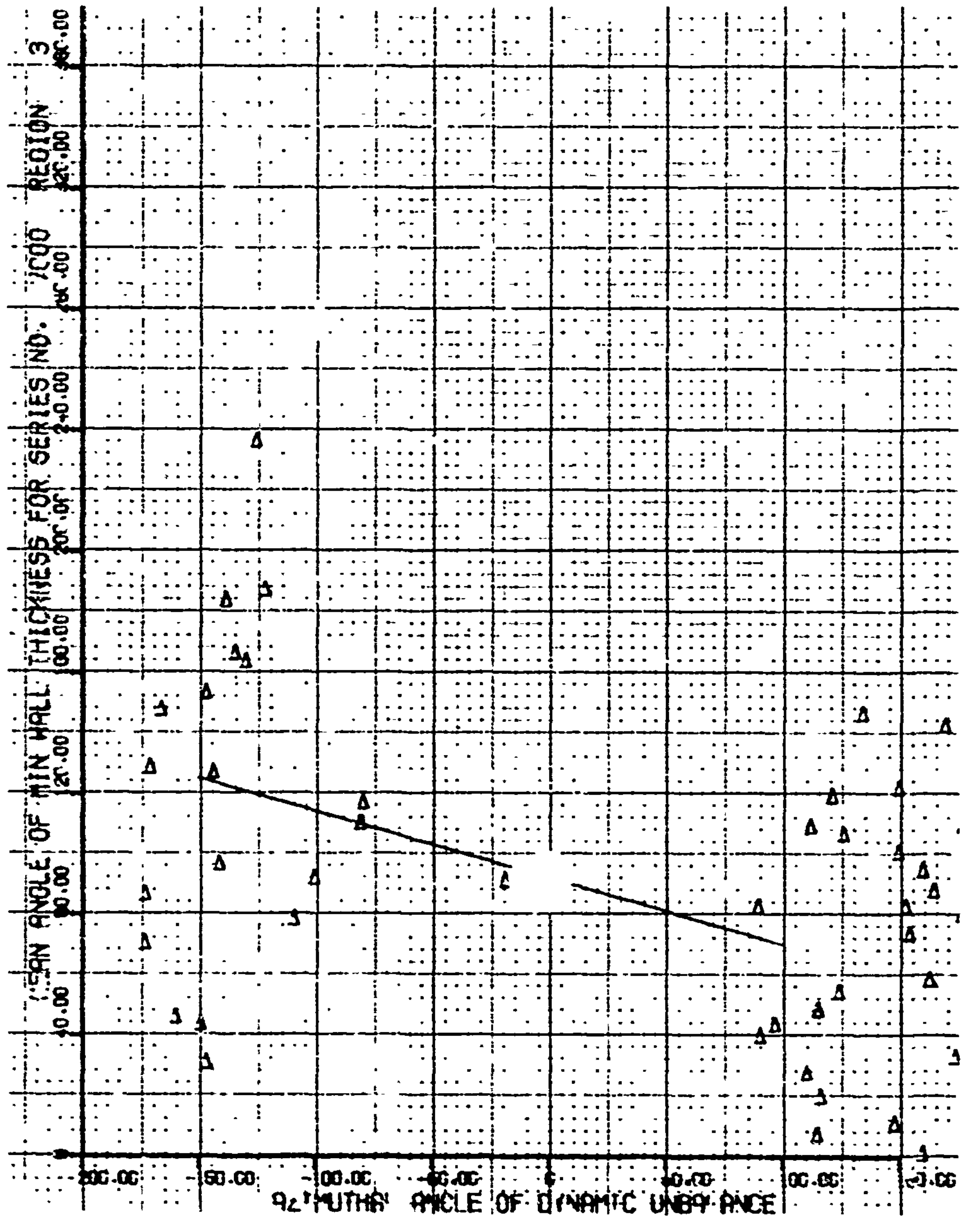

Figure 238 - Mean Azimuth of Minimum Wall Thickness Versus Azimuth of Dynamic Unbalance, Series 7000, Region 3, Empty

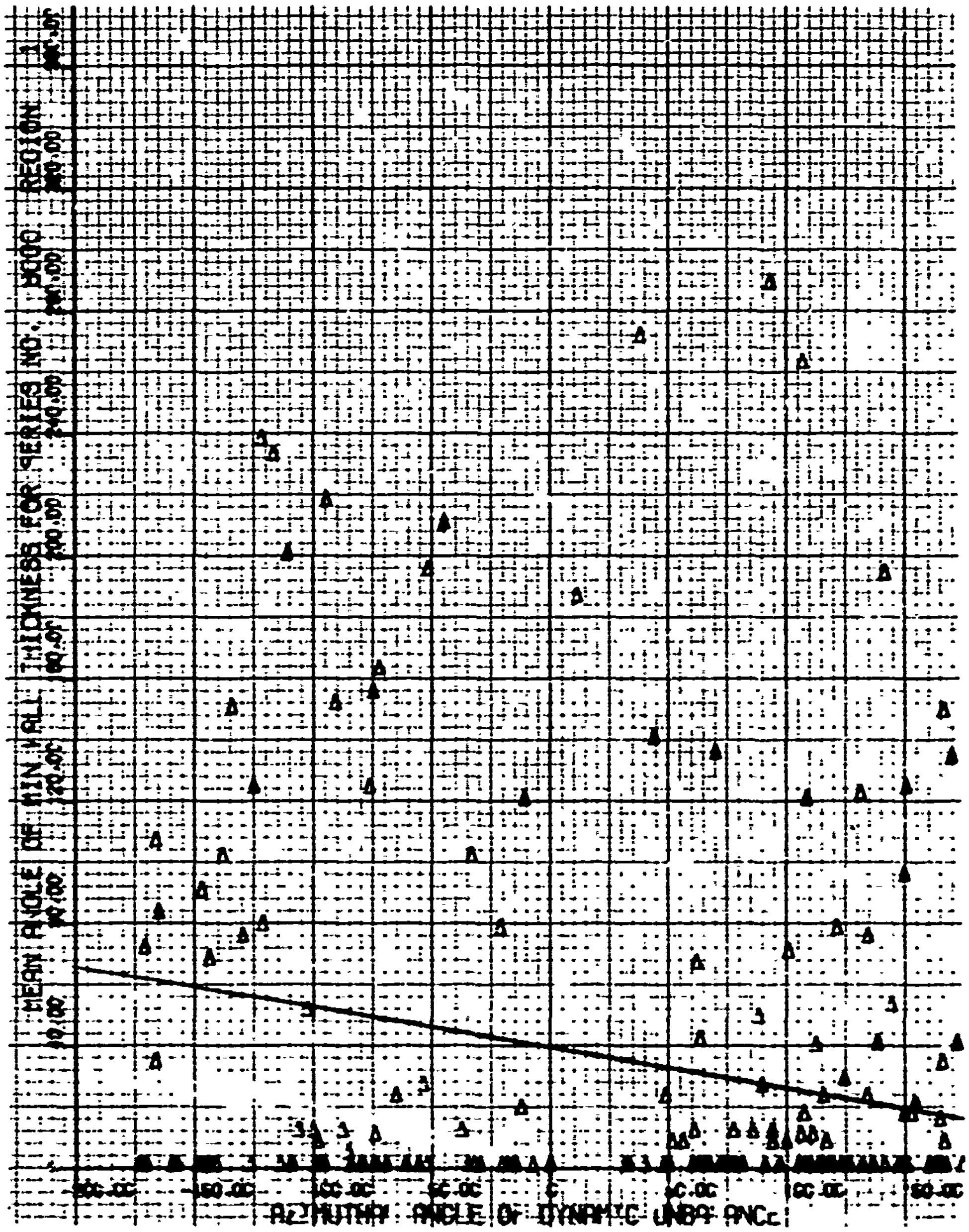

Figure 239 - Mean Azimuth of Minimum Wall Thickness Versus Azimuth of Dynamic Unbalance, Series 8000, Region 1, Empty

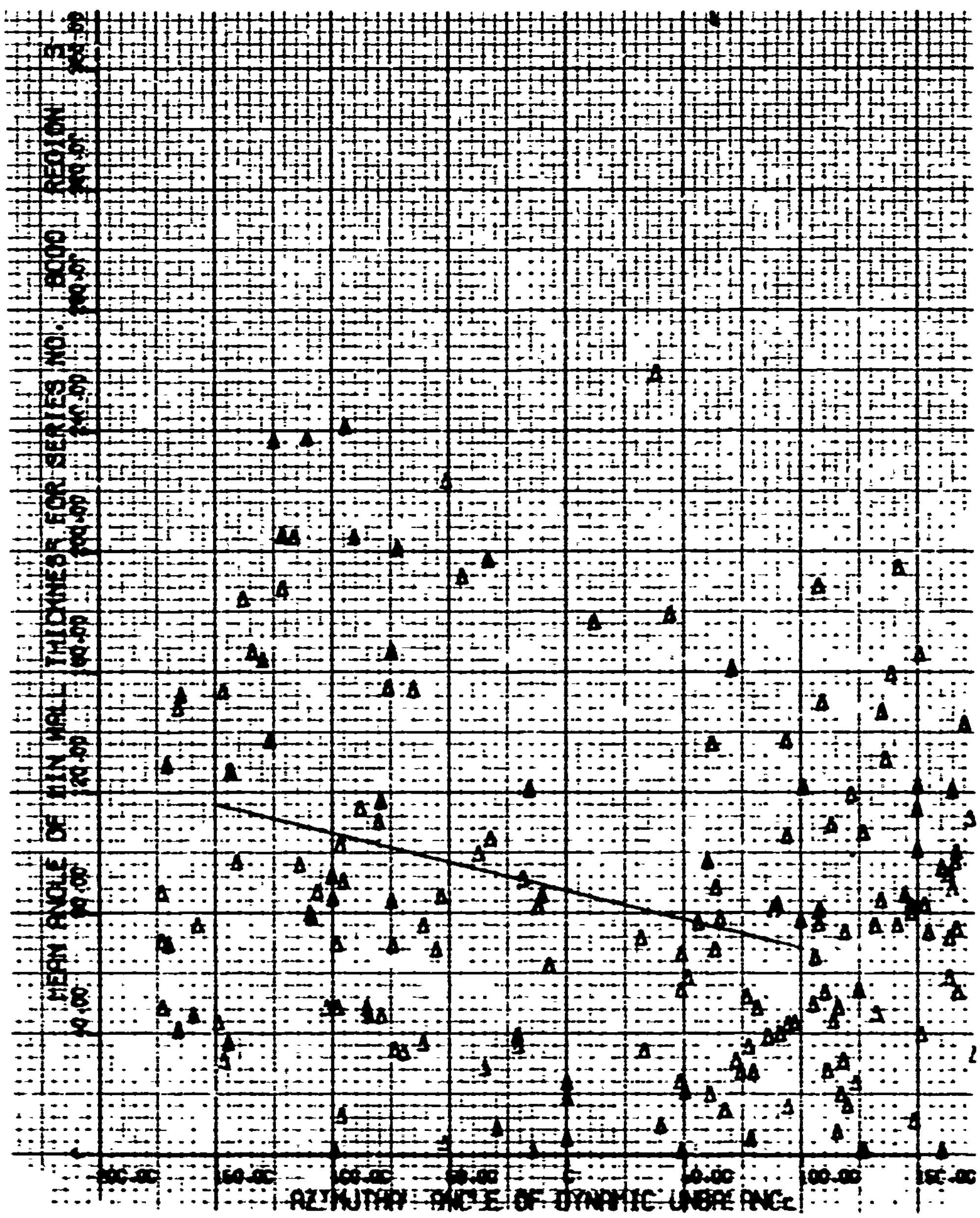

Figure 241 - Mean Azimuth of Minimum Wall Thickness Versus Azimuth of Dynamic Unbalance, Series 8000, Region 3, Empty

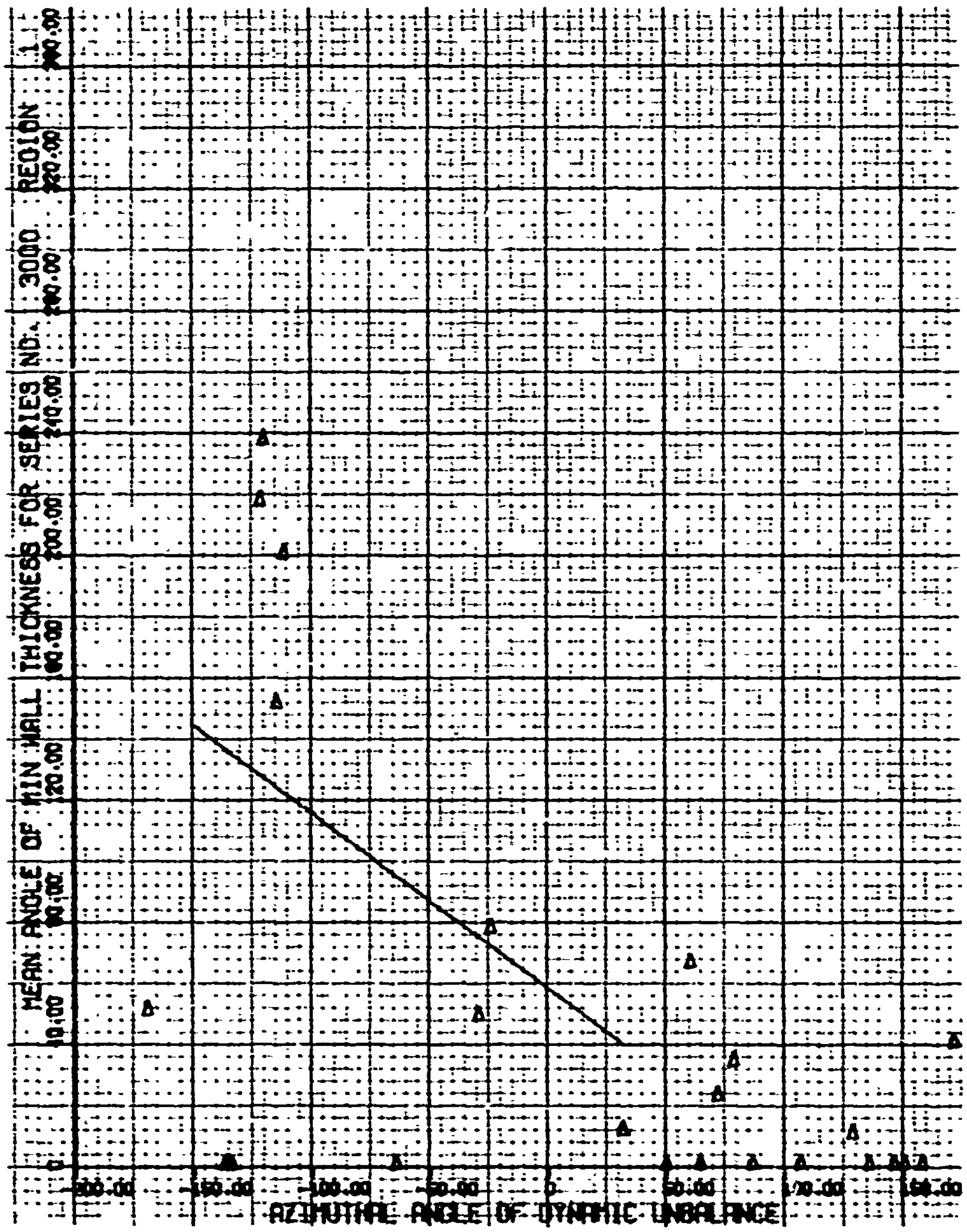

Figure 242 - Mean Azimuth of Minimum Wall Thickness Versus Azimuth of Dynamic Unbalance, Series 3000, Region 1, Full

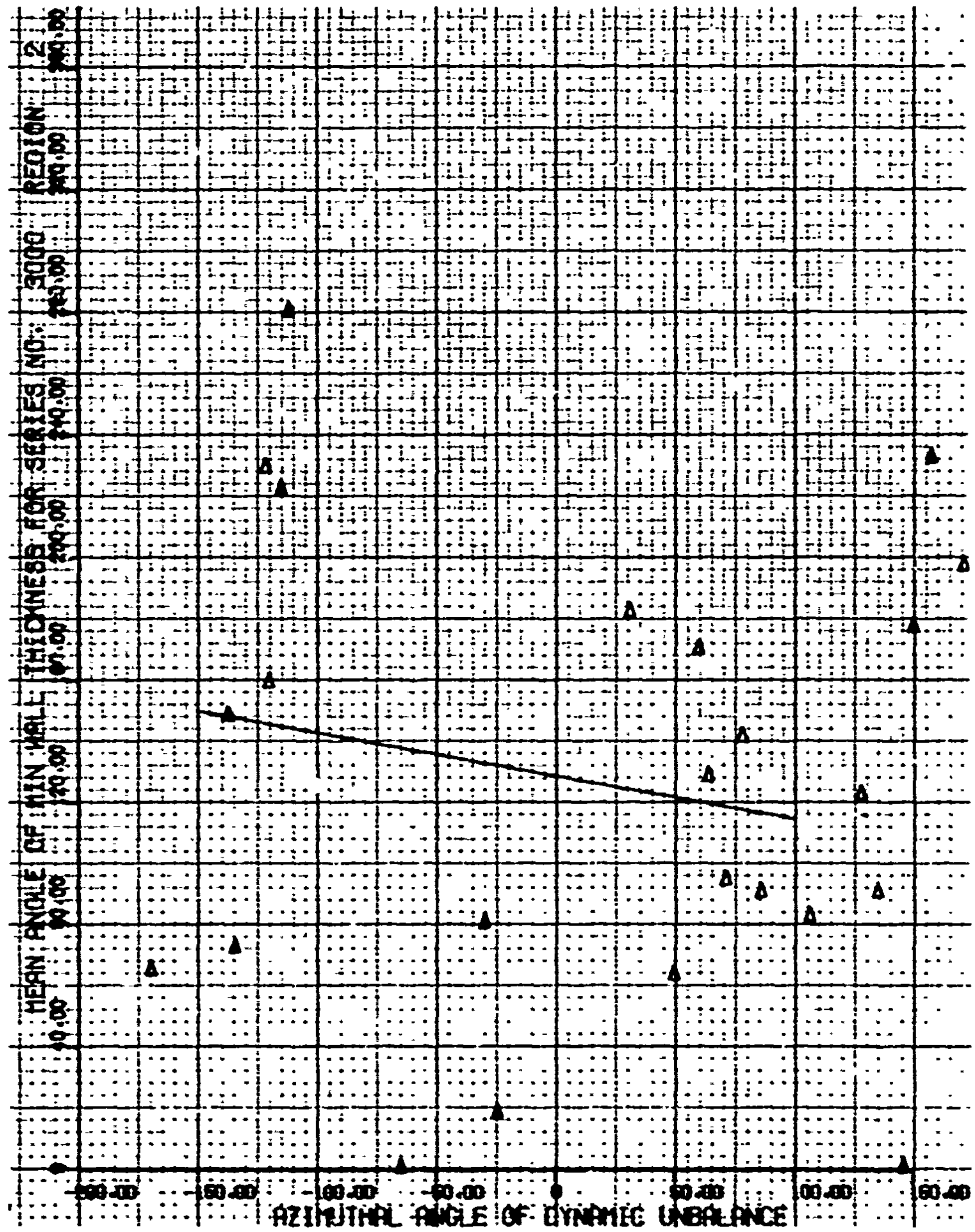

Figure 243 - Mean Azimuth of Minimum Wall Thickness Versus Azimuth of Dynamic Unbalance, Series 3000, Region 2, Full

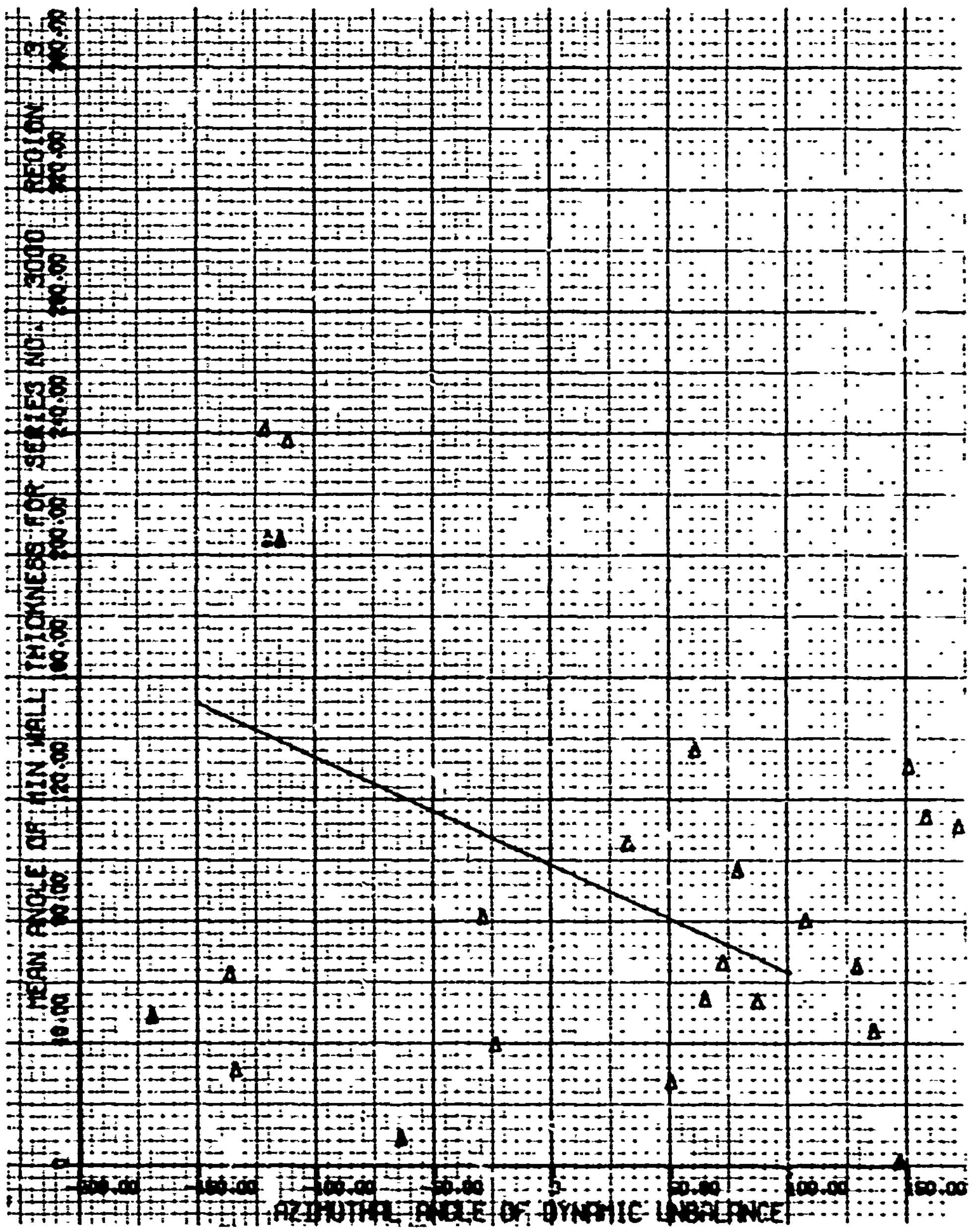

Figure 244 - Mean Azimuth of Minimum Wall Thickness Versus Azimuth of Dynamic Unbalance, Series 3000, Region 3, Full

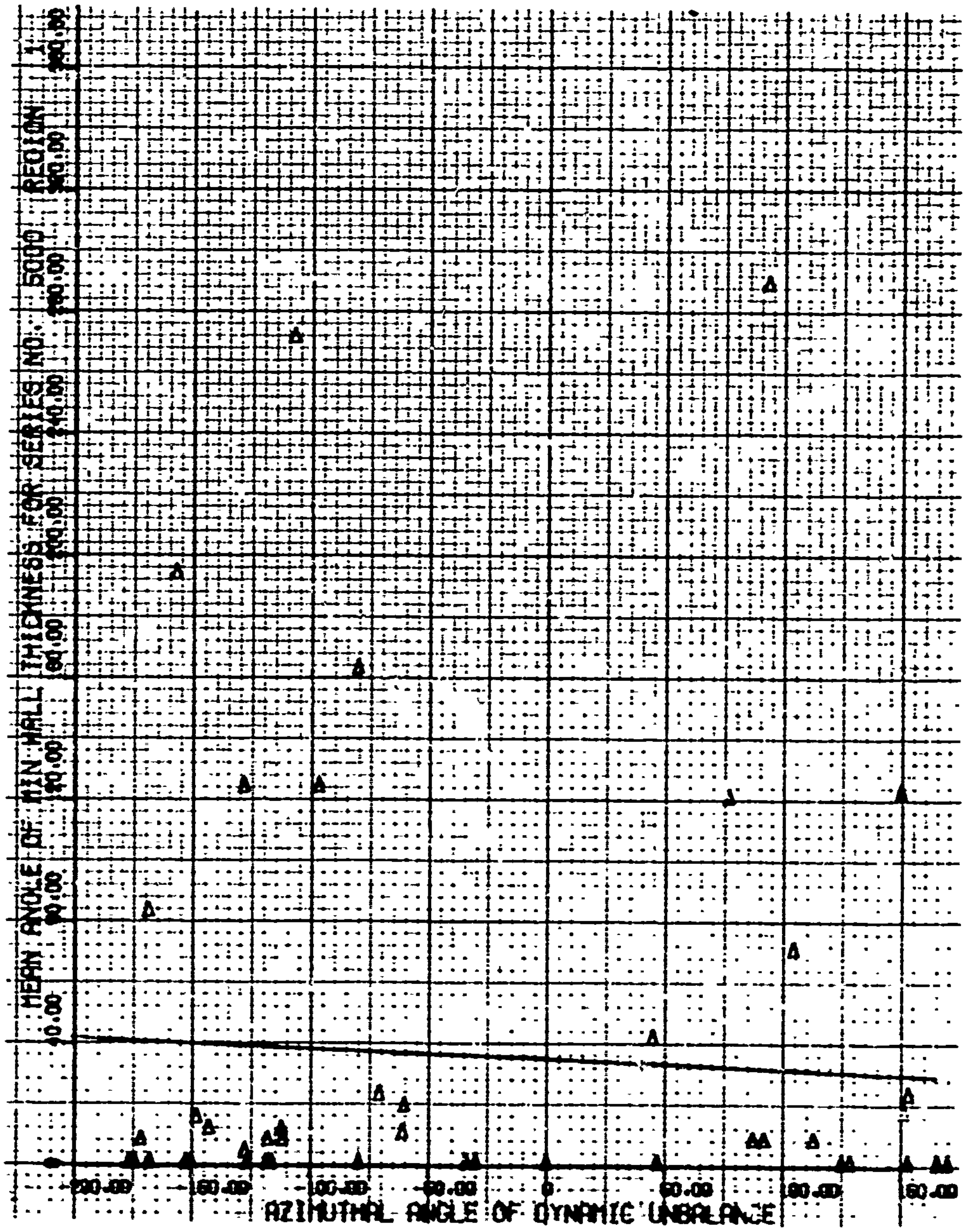

Figure 245 - Mean Azimuth of Minimum Wall Thickness Versus Azimuth of Dynamic Unbalance, Series 5000, Region 1, Full

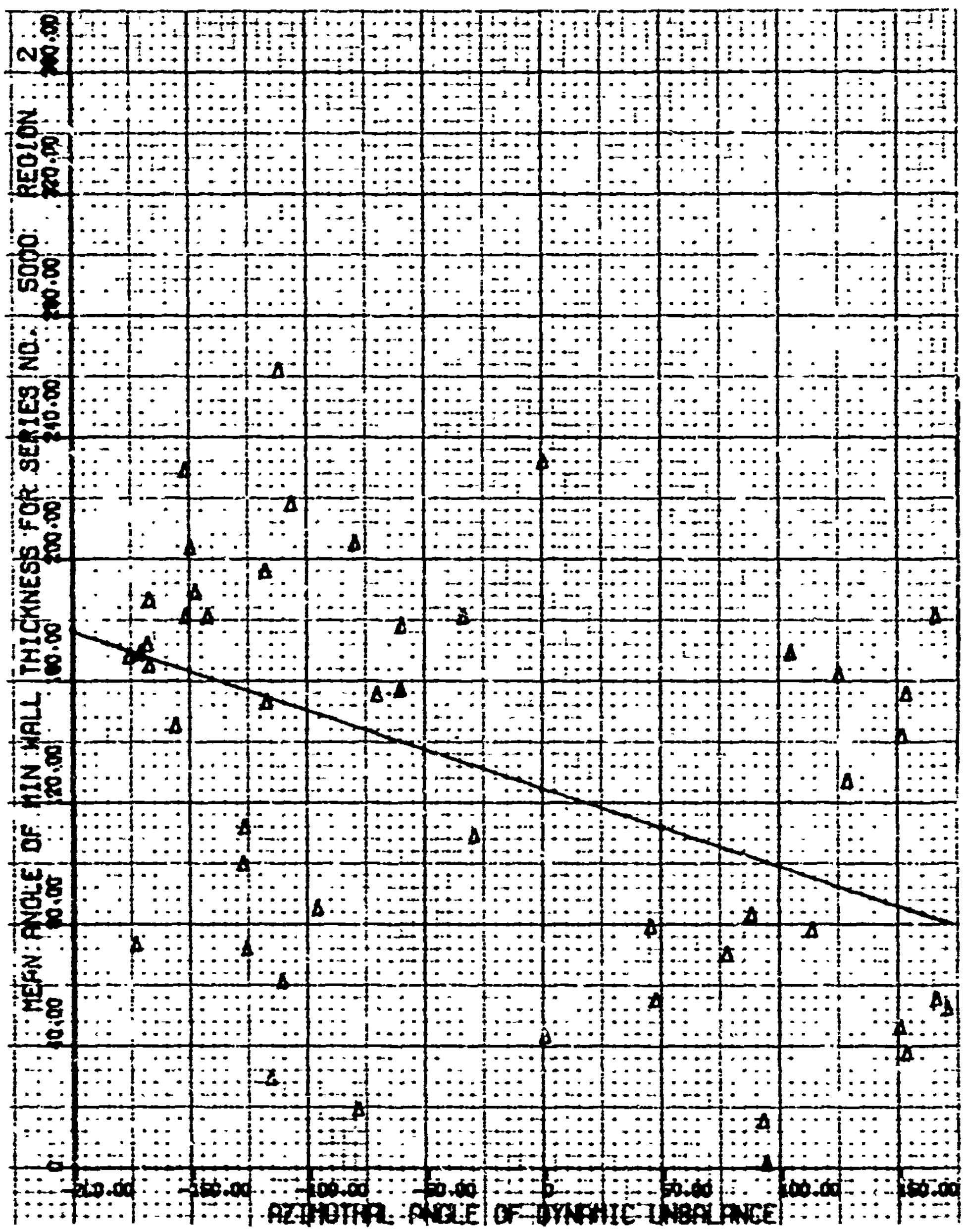

Figure 246 - Mean Azimuth of Minimum Wall Thickness Versus Azimuth of Dynamic Unbalance, Series 5000, Region 2, Full

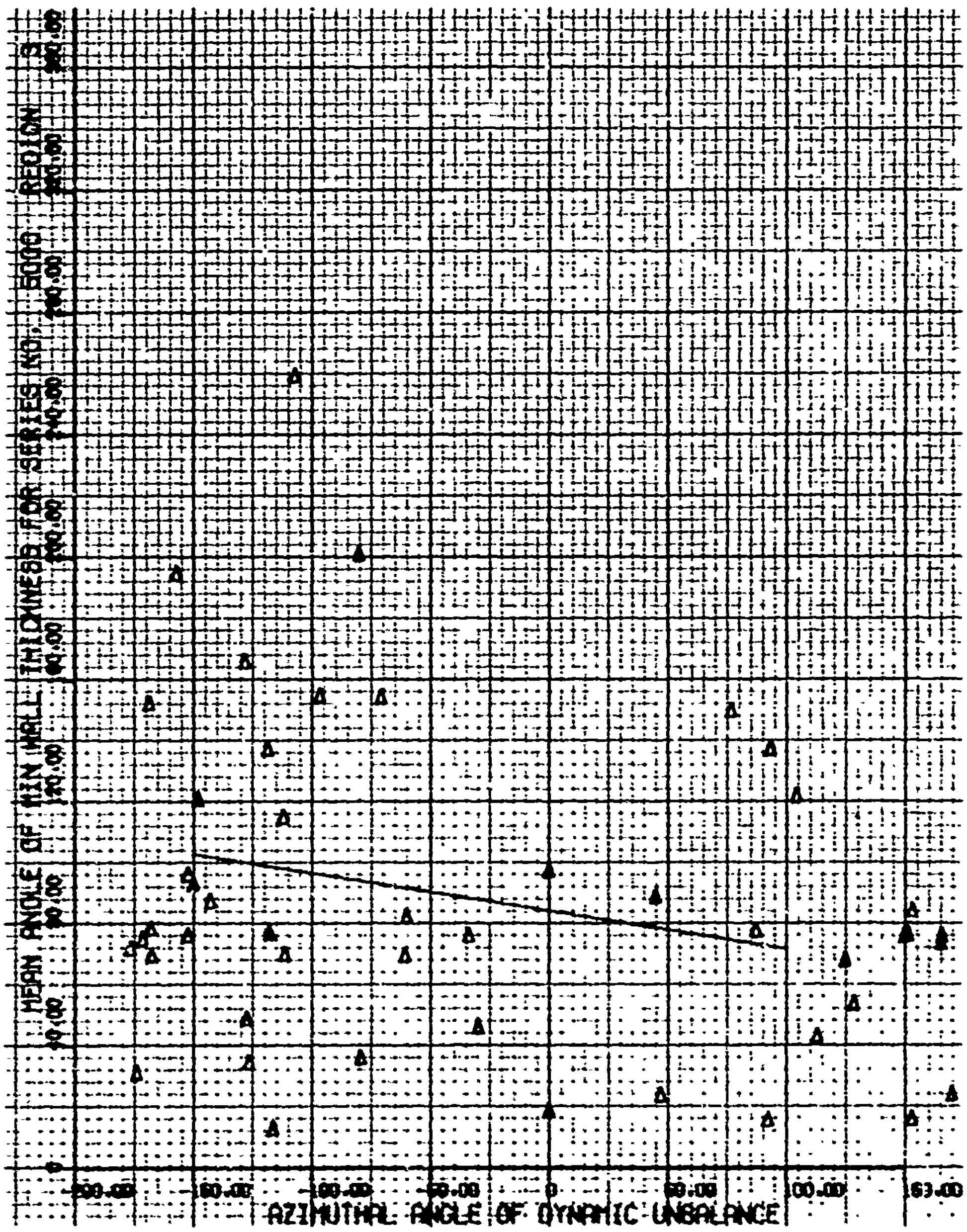

Figure 247 - Mean Azimuth of Minimum Wall Thickness Versus Azimuth of Dynamic Unbalance, Series 5000, Region 3, Full

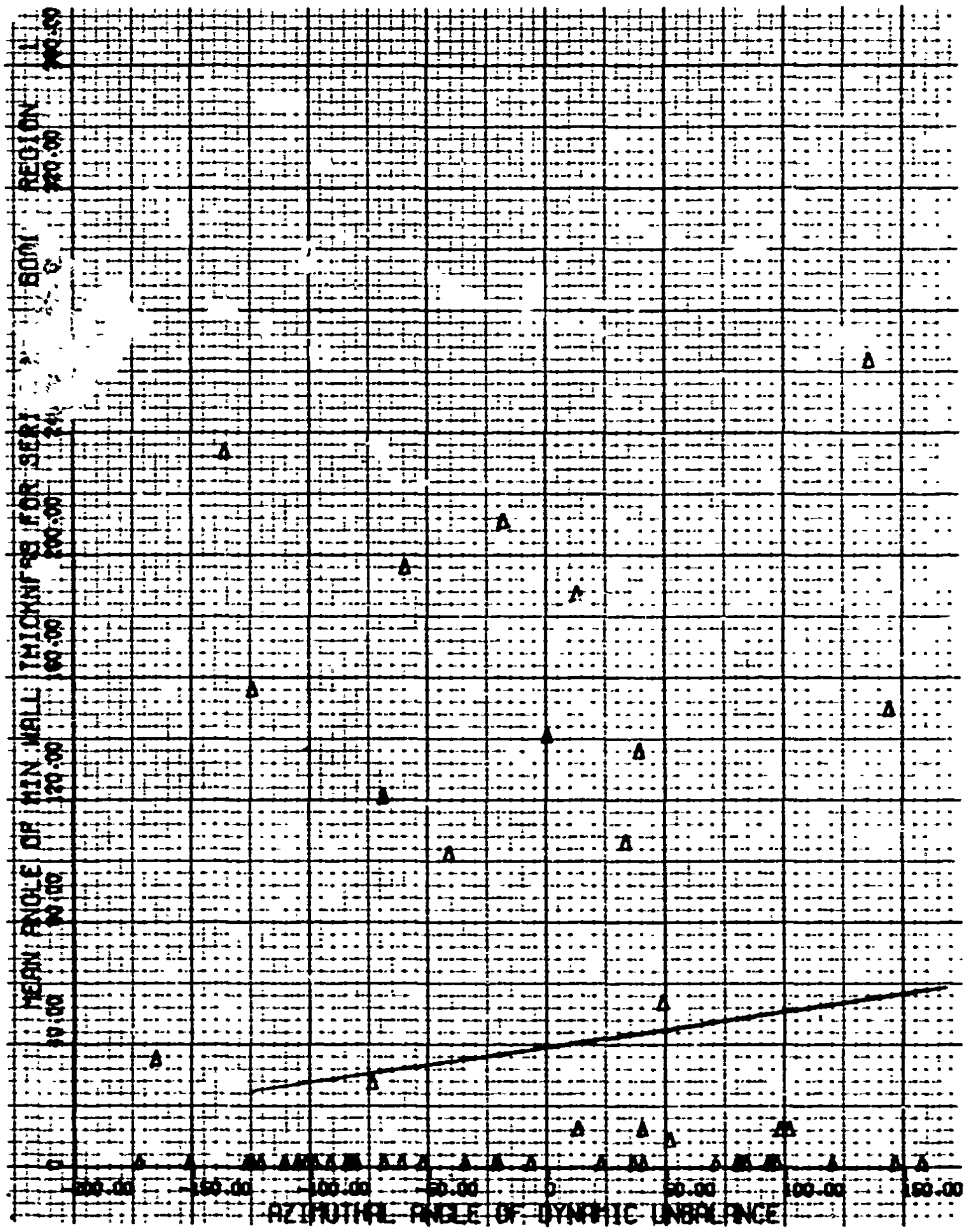

Figure 248 - Mean Azimuth of Minimum Wall Thickness Versus Azimuth of Dynamic Unbalance, Series 6000, Region 1, Full

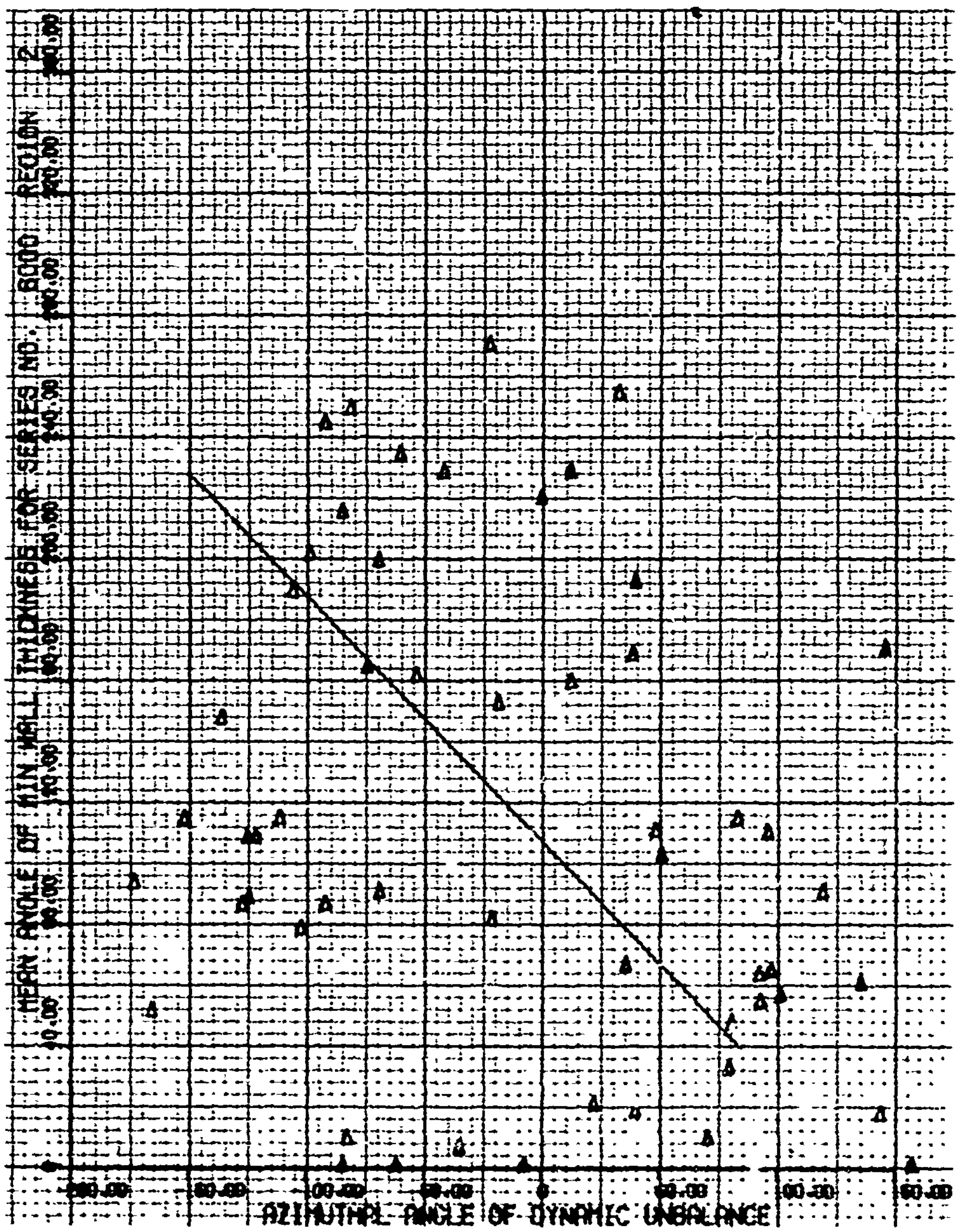

Figure 249 - Mean Azimuth of Minimum Wall Thickness Versus Azimuth of Dynamic Unbalance, Series 6000, Region 2, Full

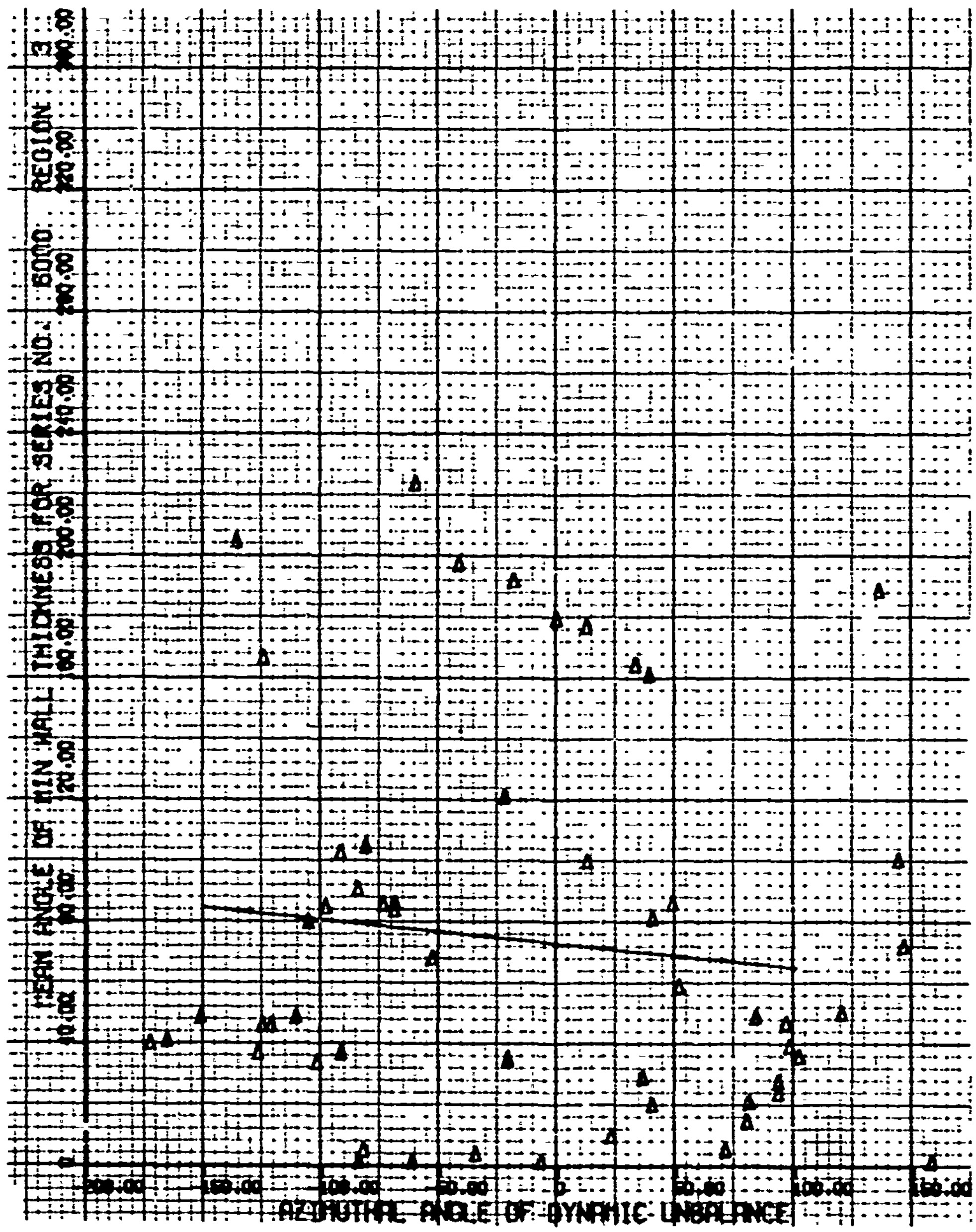

Figure 250 - Mean Azimuth of Minimum Wall Thickness Versus Azimuth of Dynamic Unbalance, Series 6000, Region 3, Full

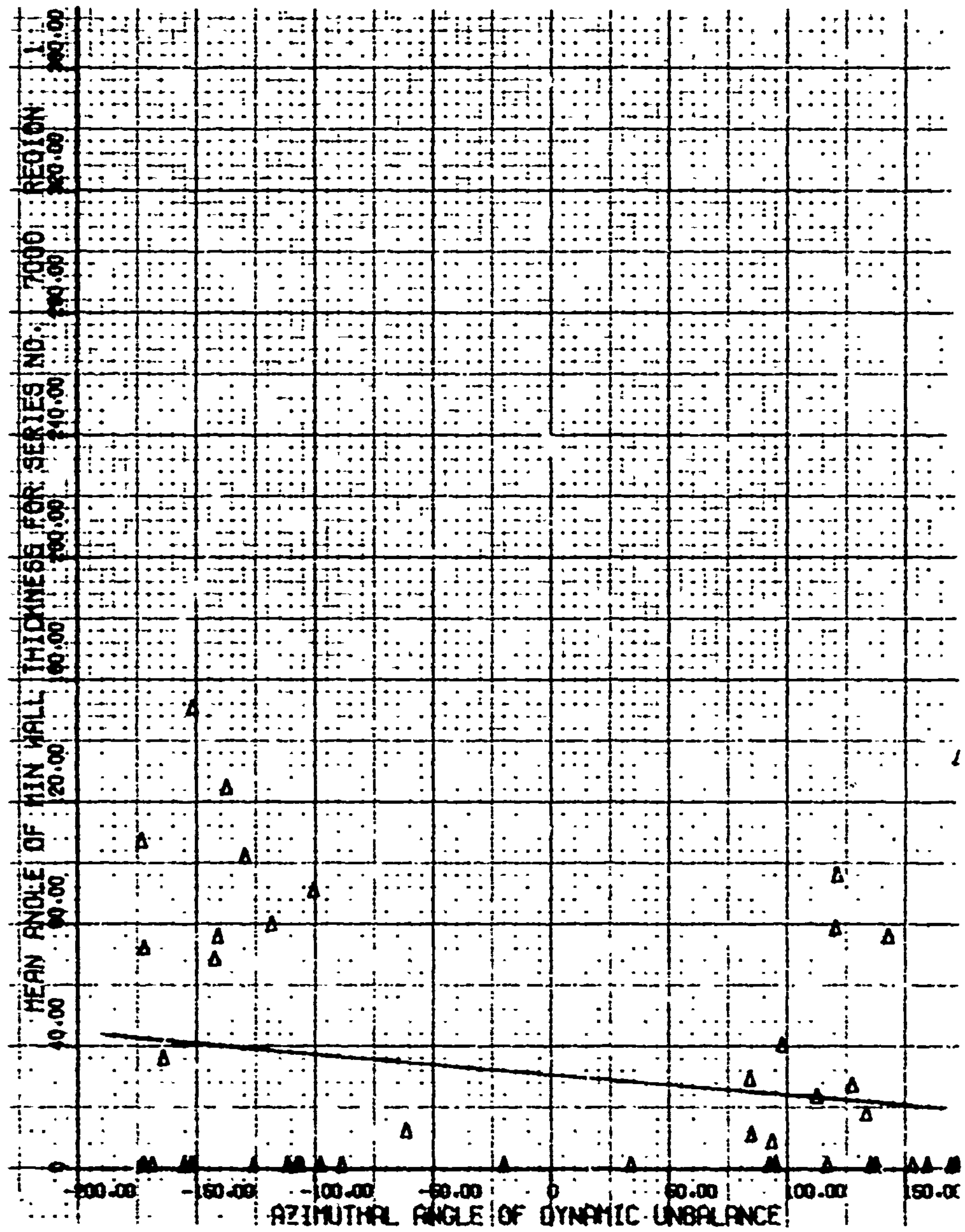

Figure 251 - Mean Azimuth of Minimum Wall Thickness Versus Azimuth of Dynamic Unbalance, Series 7000, Region 1, Full

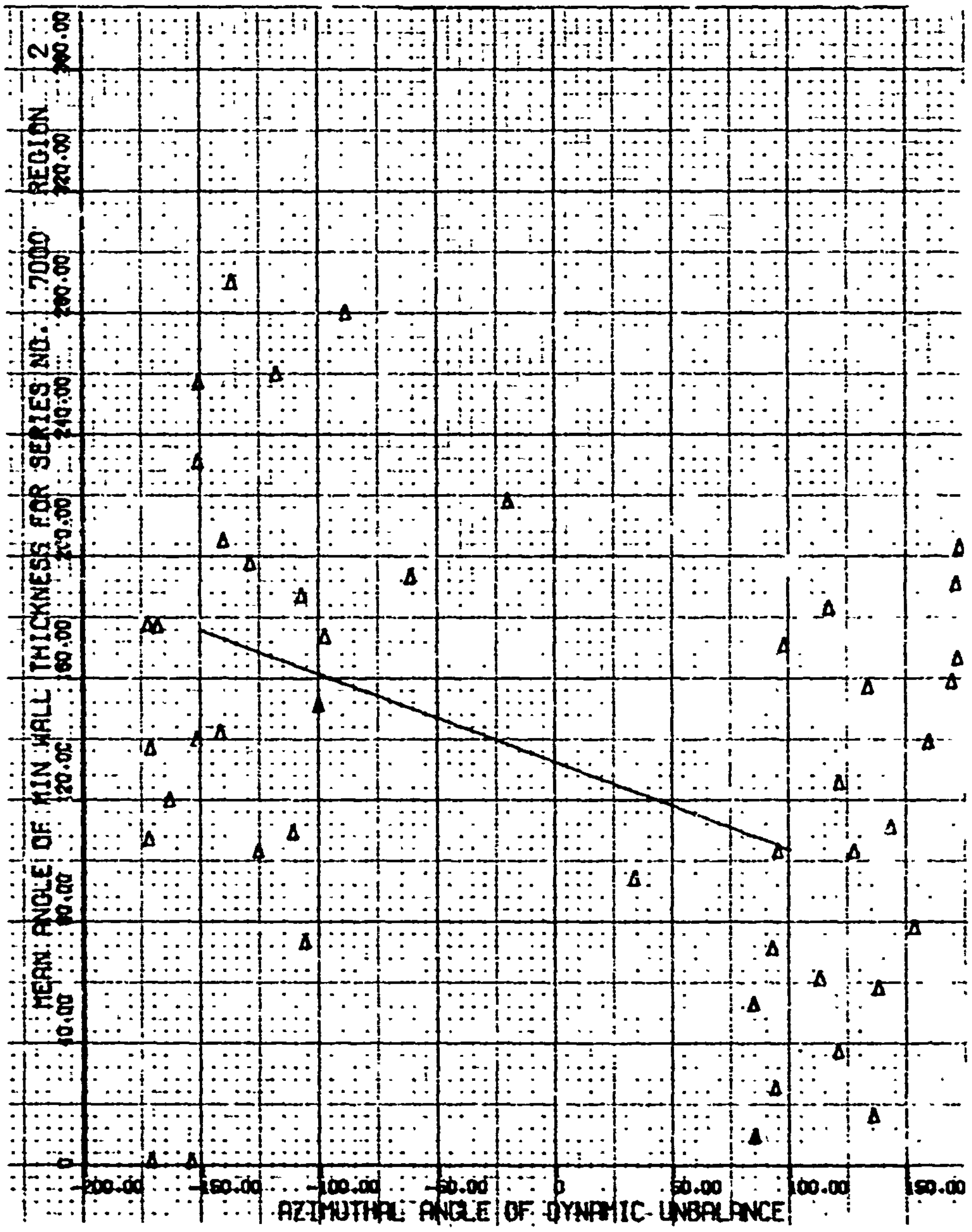

Figure 252 - Mean Azimuth of Minimum Wall Thickness Versus Azimuth of Dynamic Unbalance, Series 7000, Region 2, Full

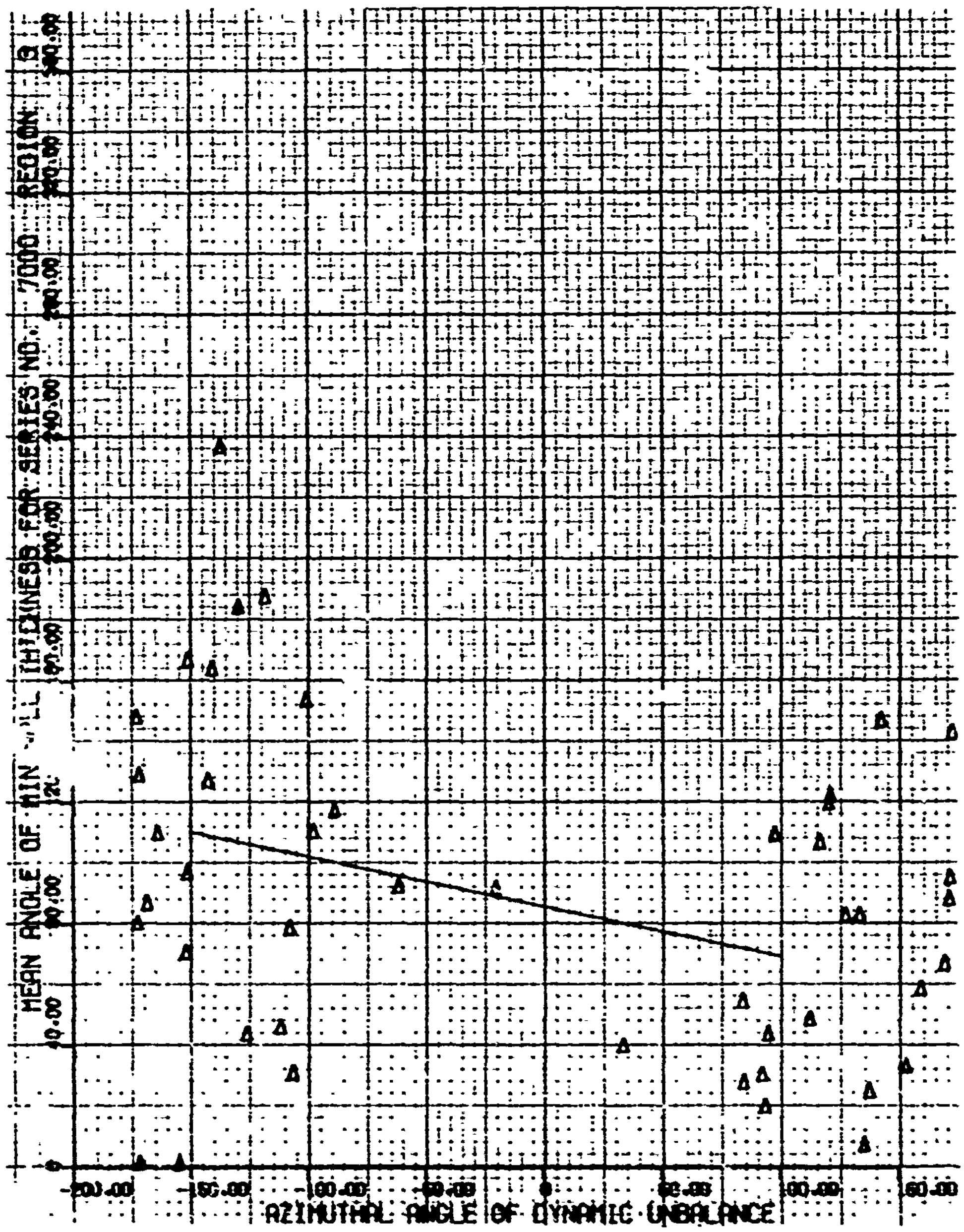

Figure 253 - Mean Azimuth of Minimum Wall Thickness Versus Azimuth of Dynamic Unbalance, Series 7000, Region 3, Full

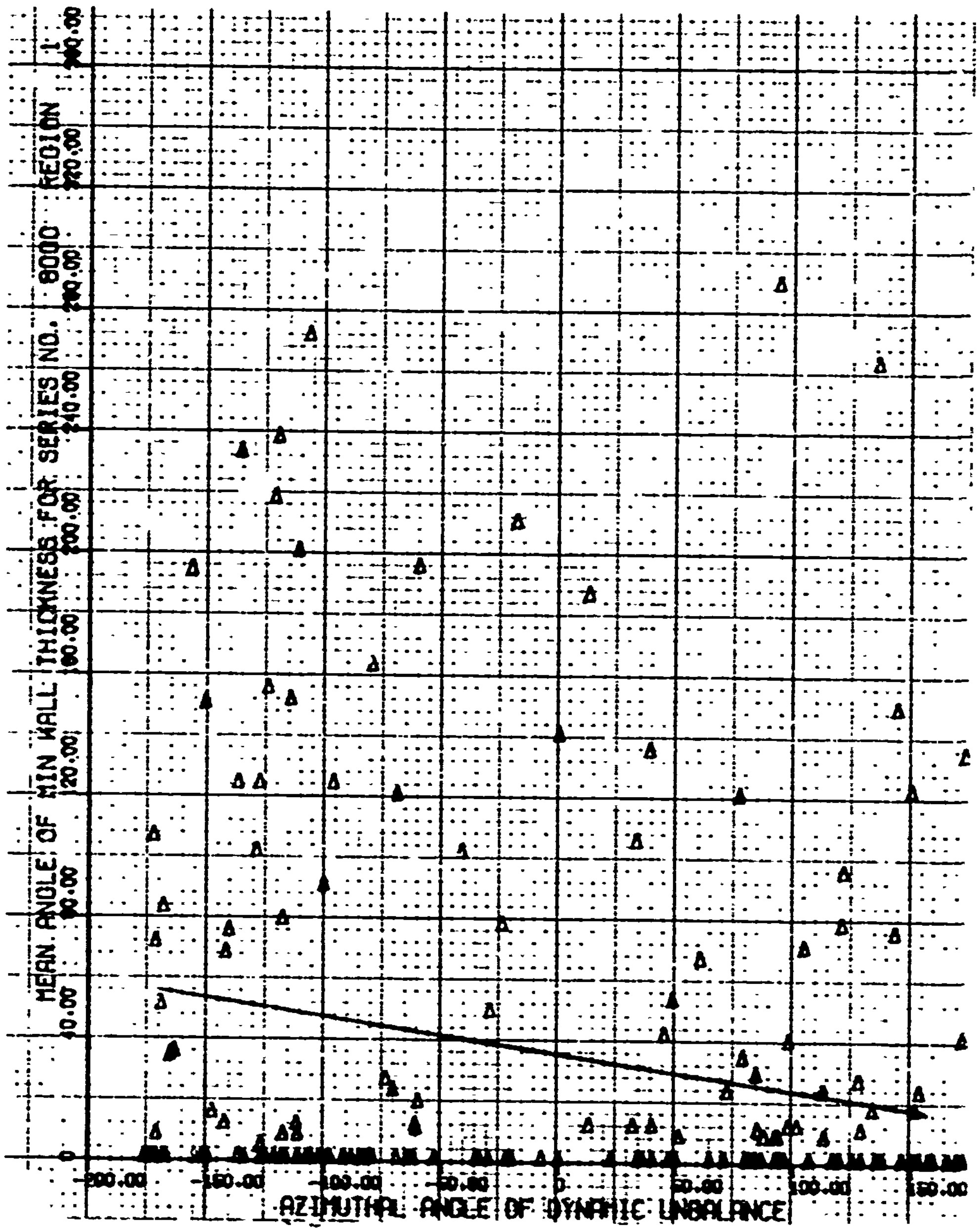

Figure 254 - Mean Azimuth of Minimum Wall Thickness Versus Azimuth of Dynamic Unbalance, Series 8000, Region 1, Full

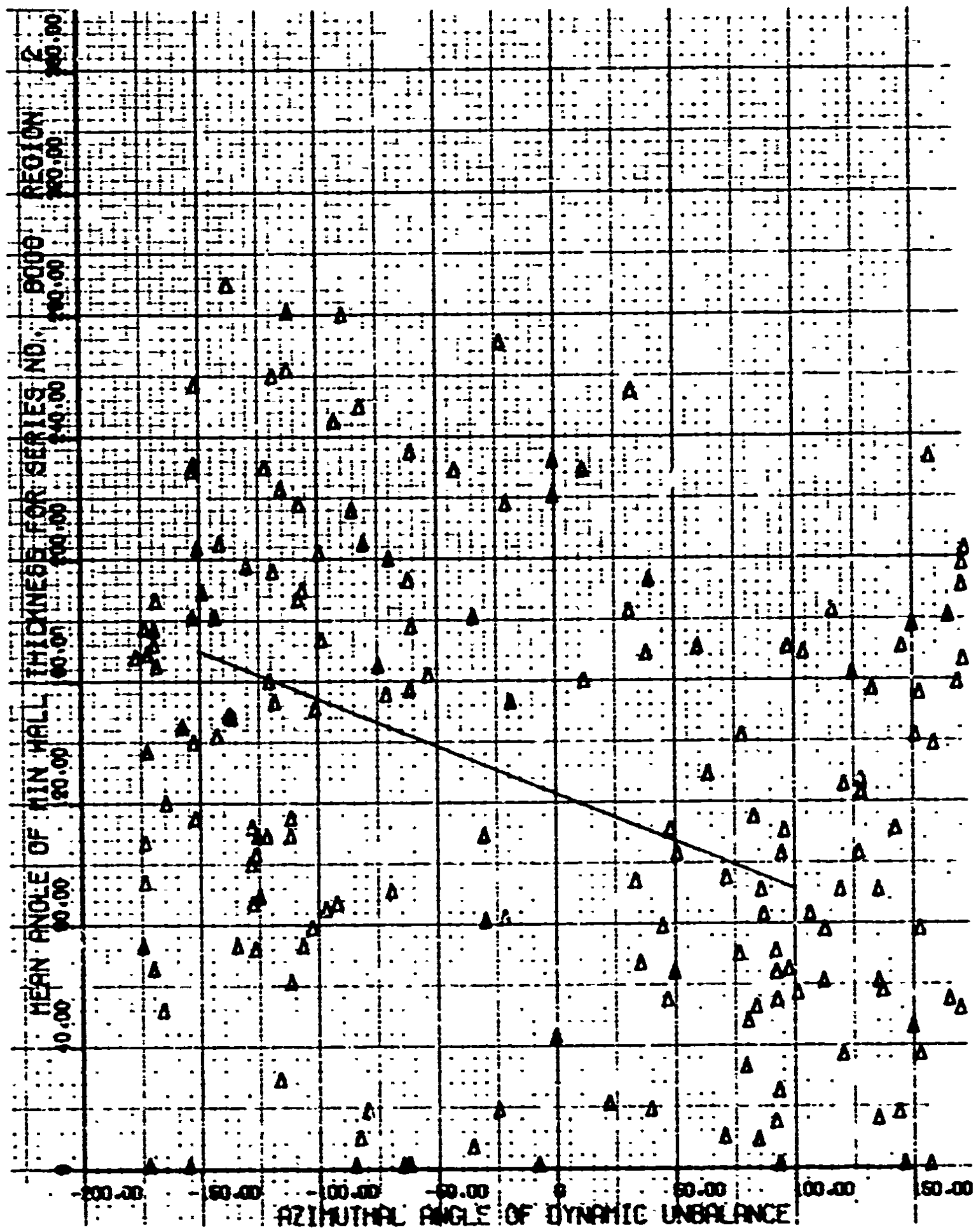

Figure 255 - Mean Azimuth of Minimum Wall Thickness Versus Azimuth of Dynamic Unbalance, Series 8000, Region 2, Full

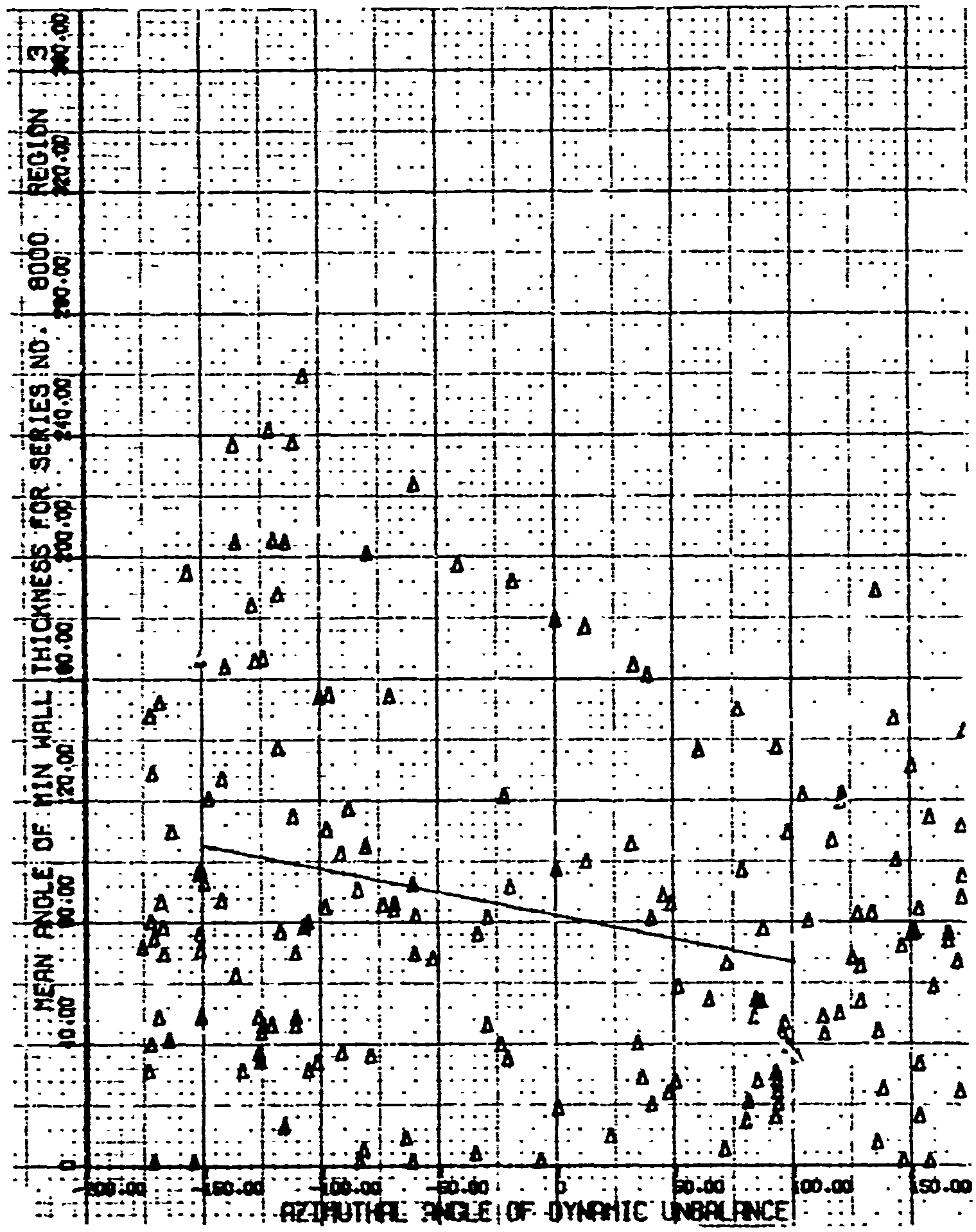

Figure 256 - Mean Azimuth of Minimum Wall Thickness Versus Azimuth of Dynamic Unbalance, Series 8000, Region 3, Full

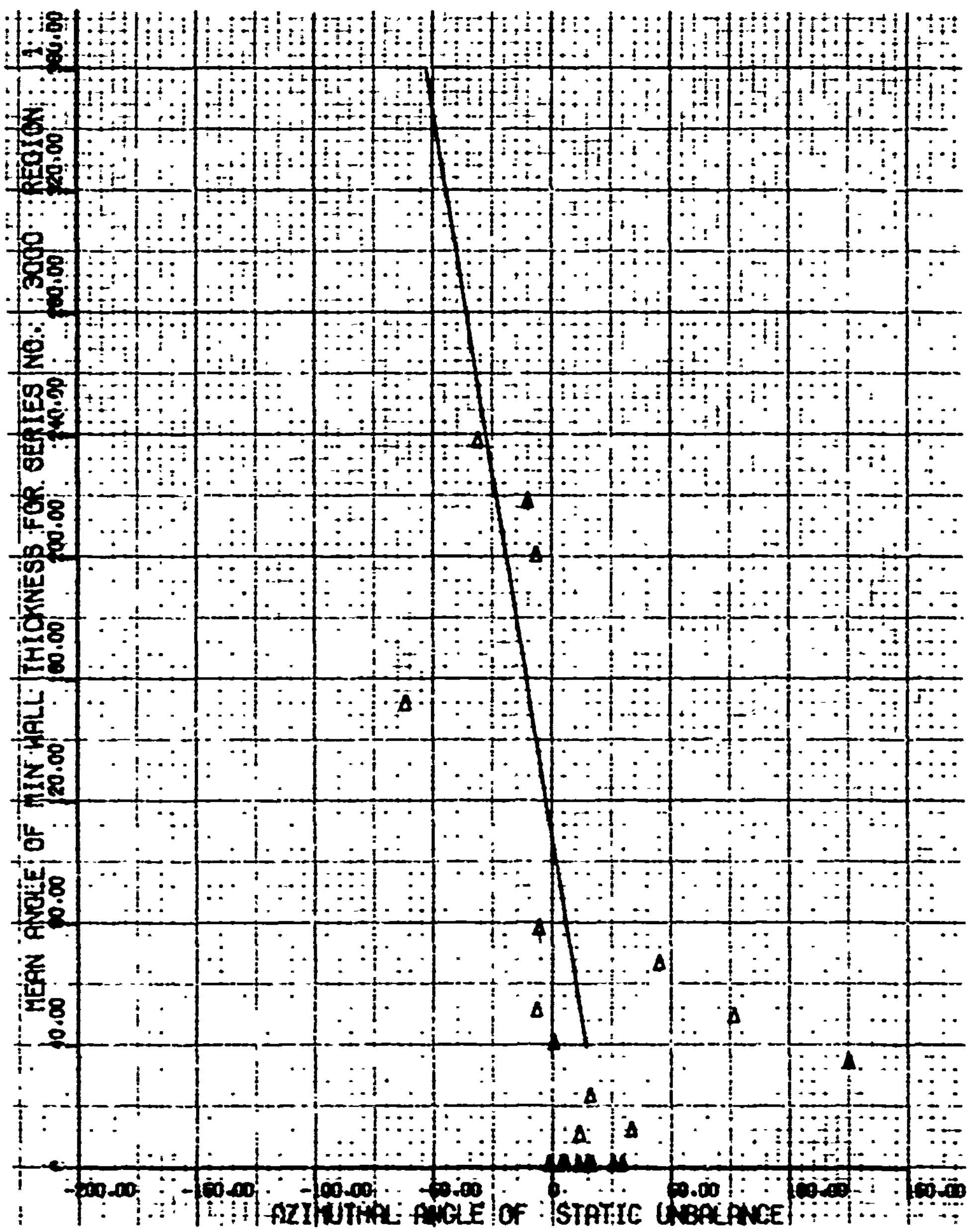

Figure 257 - Mean Azimuth of Minimum Wall Thickness Versus Azimuth of Static Unbalance, Series 3000, Region 1, Empty

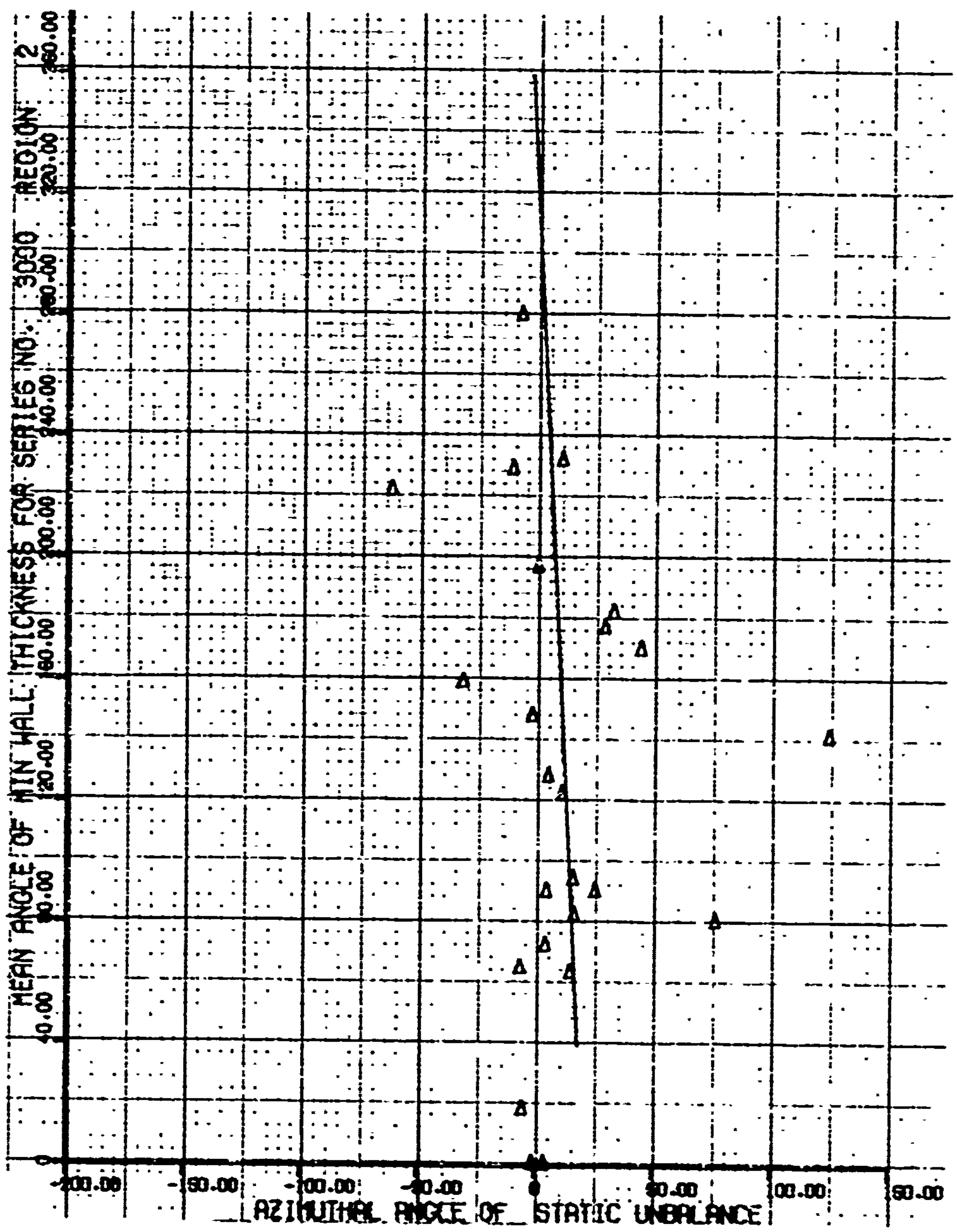

Figure 258 - Mean Azimuth of Minimum Wall Thickness Versus Azimuth of Static Unbalance, Series 3000, Region 2, Empty

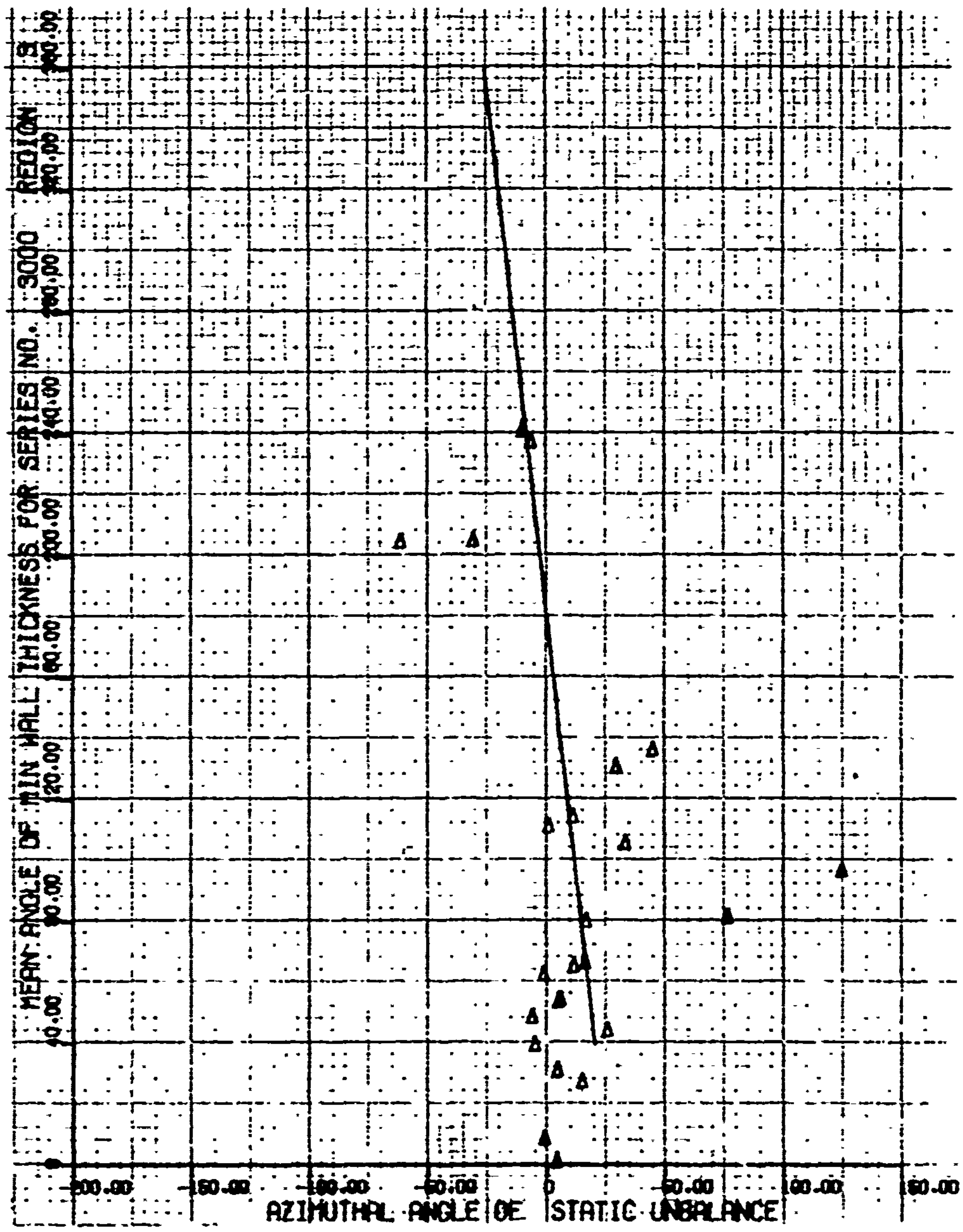

Figure 259 - Mean Azimuth of Minimum Wall Thickness Versus Azimuth of Static Unbalance, Series 3000, Region 3, Empty

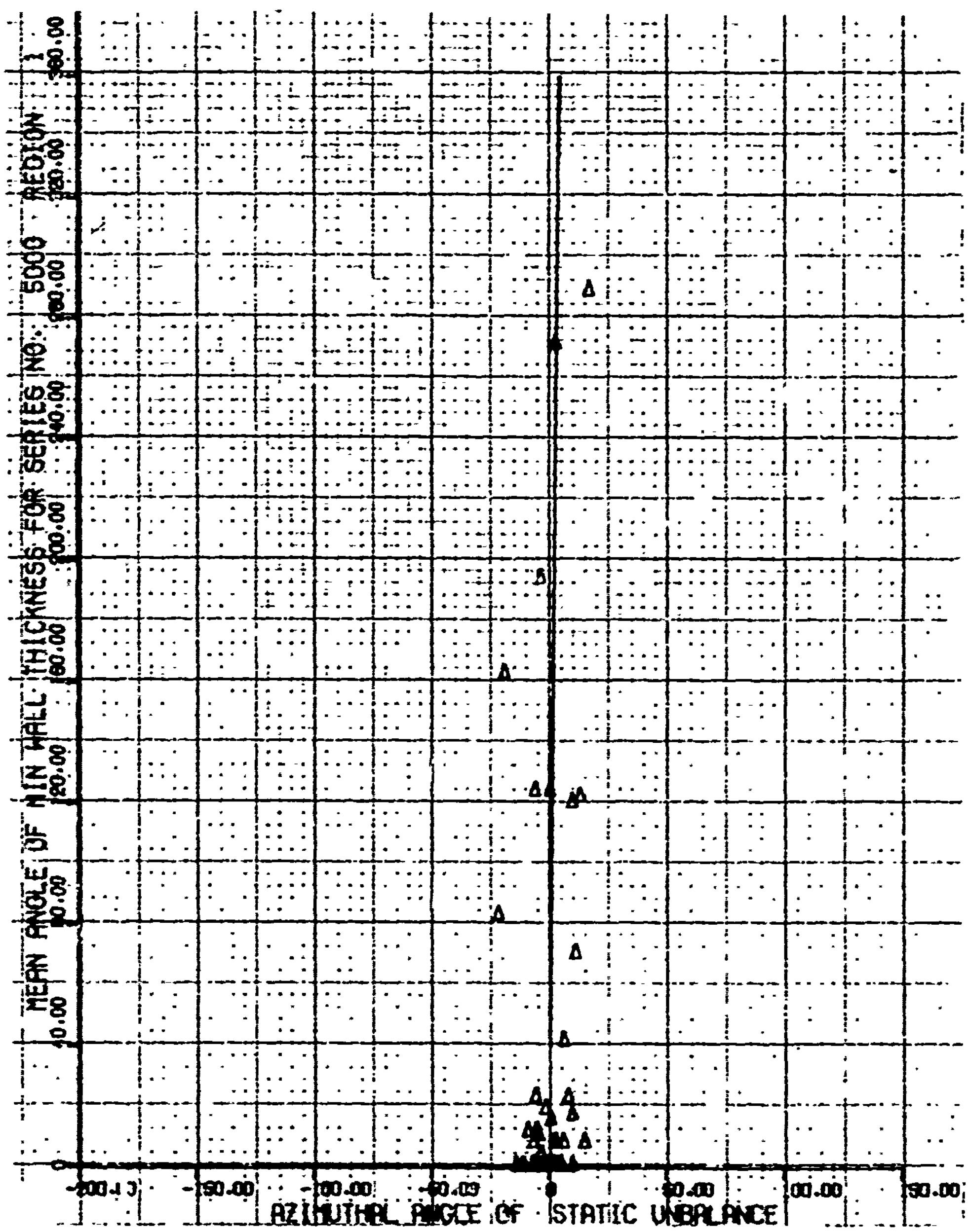

Figure 260 - Mean Azimuth of Minimum Wall Thickness Versus Azimuth of Static Unbalance, Series 5000, Region 1, Empty

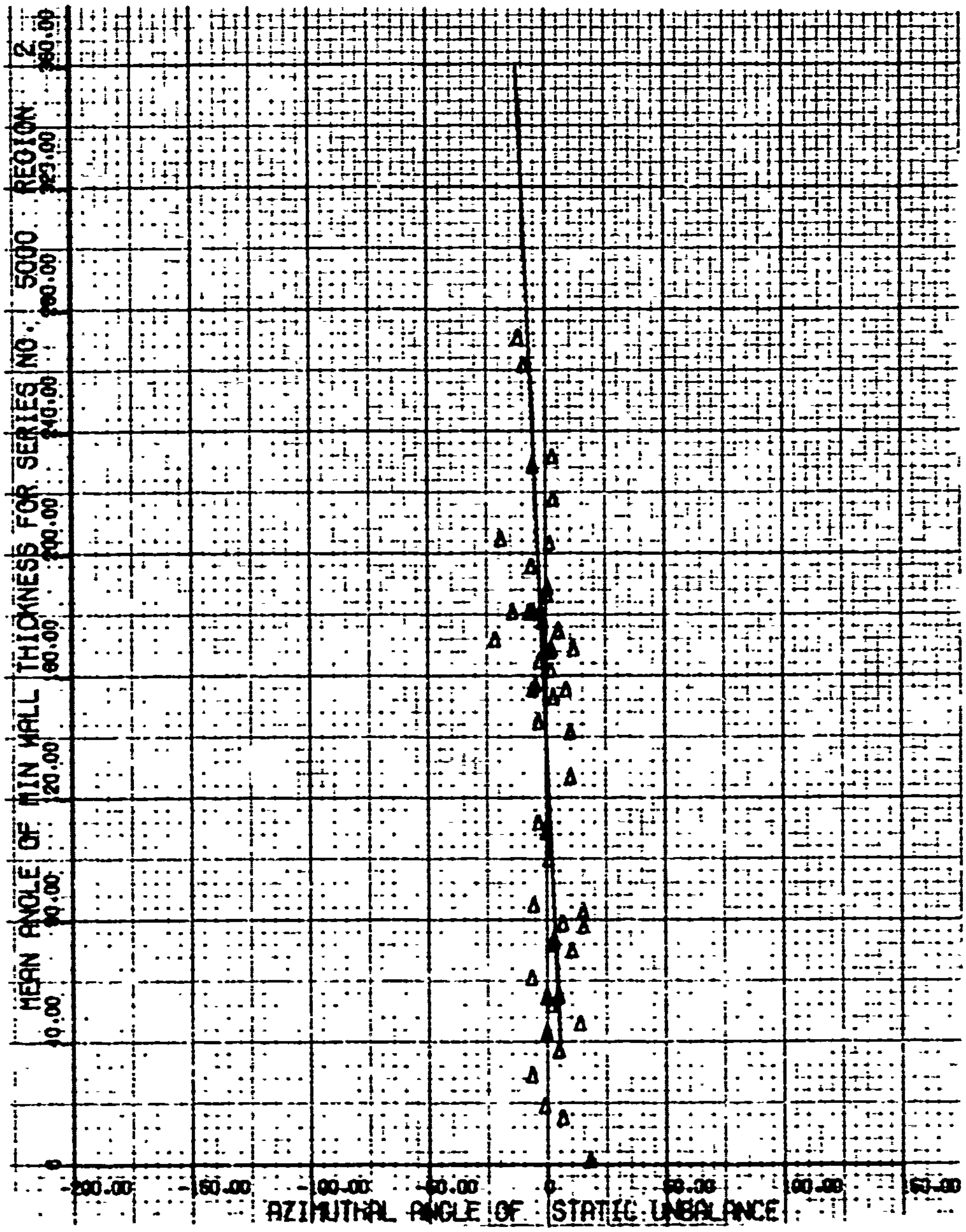

Figure 261 - Mean Azimuth of Minimum Wall Thickness Versus Azimuth of Static Unbalance, Series 5000, Region 2, Empty

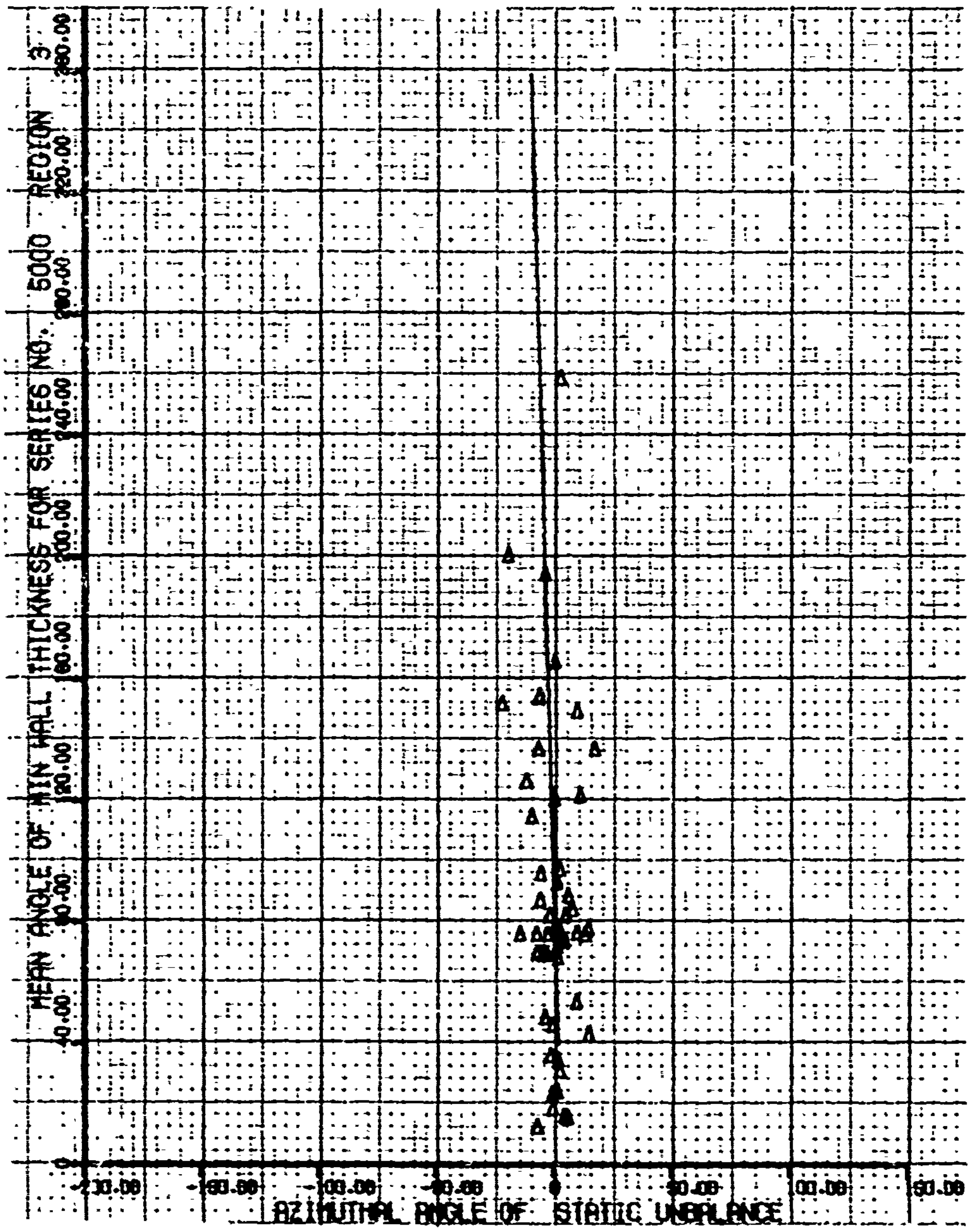

Figure 262 - Mean Azimuth of Minimum Wall Thickness Versus Azimuth of Static Unbalance, Series 5000, Region 3, Empty

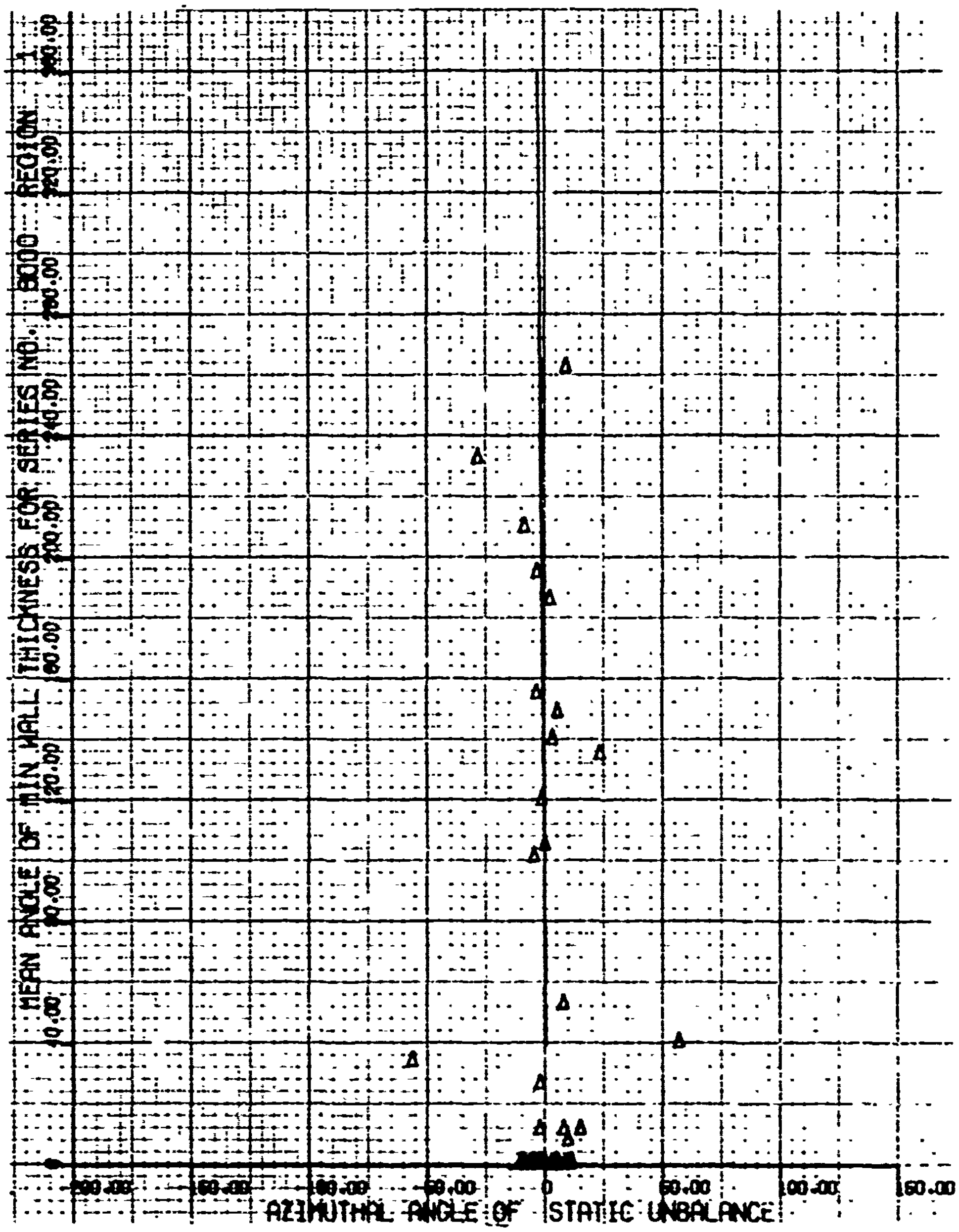

Figure 263 - Mean Azimuth of Minimum Wall Thickness Versus Azimuth of Static Unbalance, Series 6000, Region 1, Empty

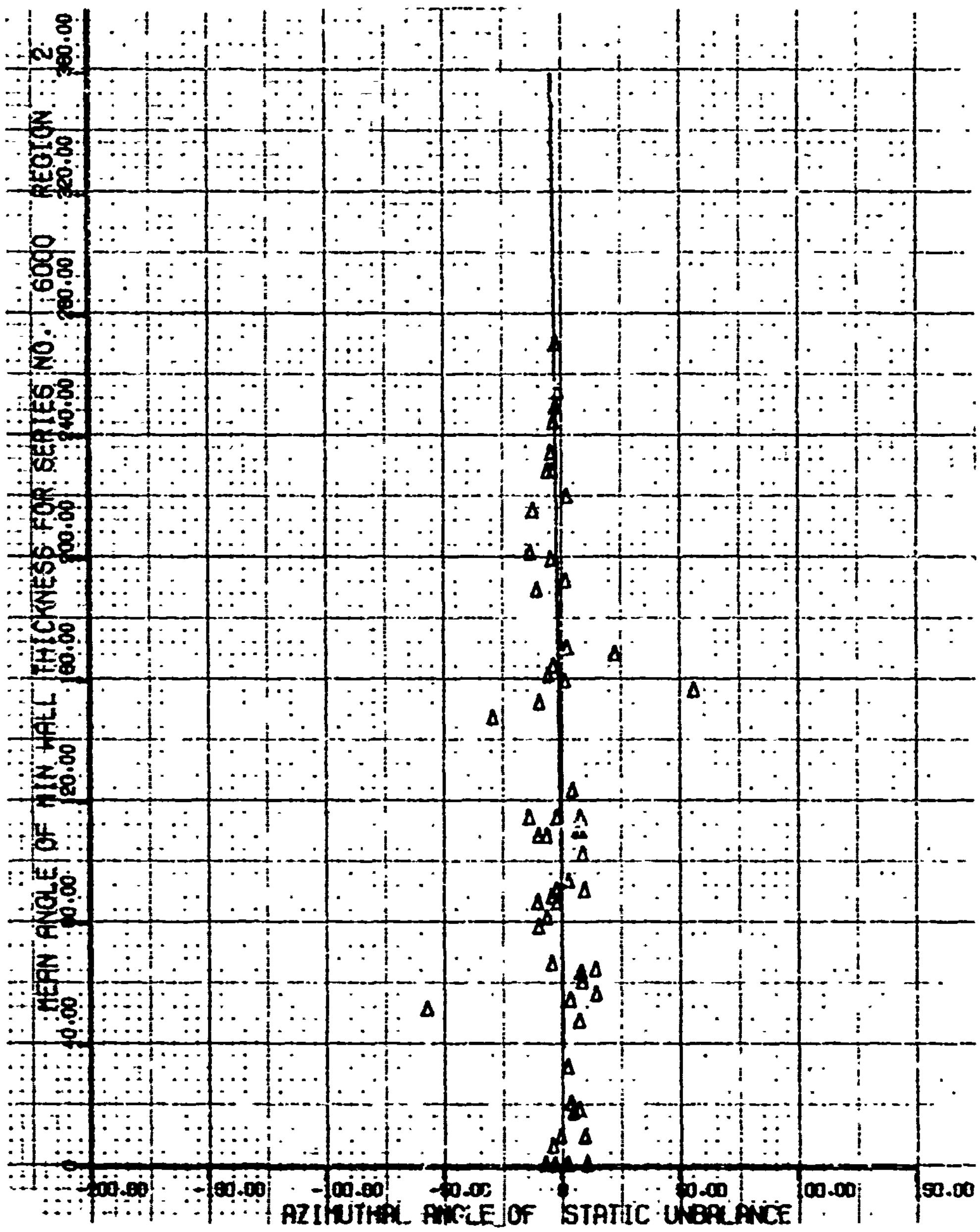

Figure 264 - Mean Azimuth of Minimum Wall Thickness Versus Azimuth of Static Unbalance, Series 6000, Region 2, Empty

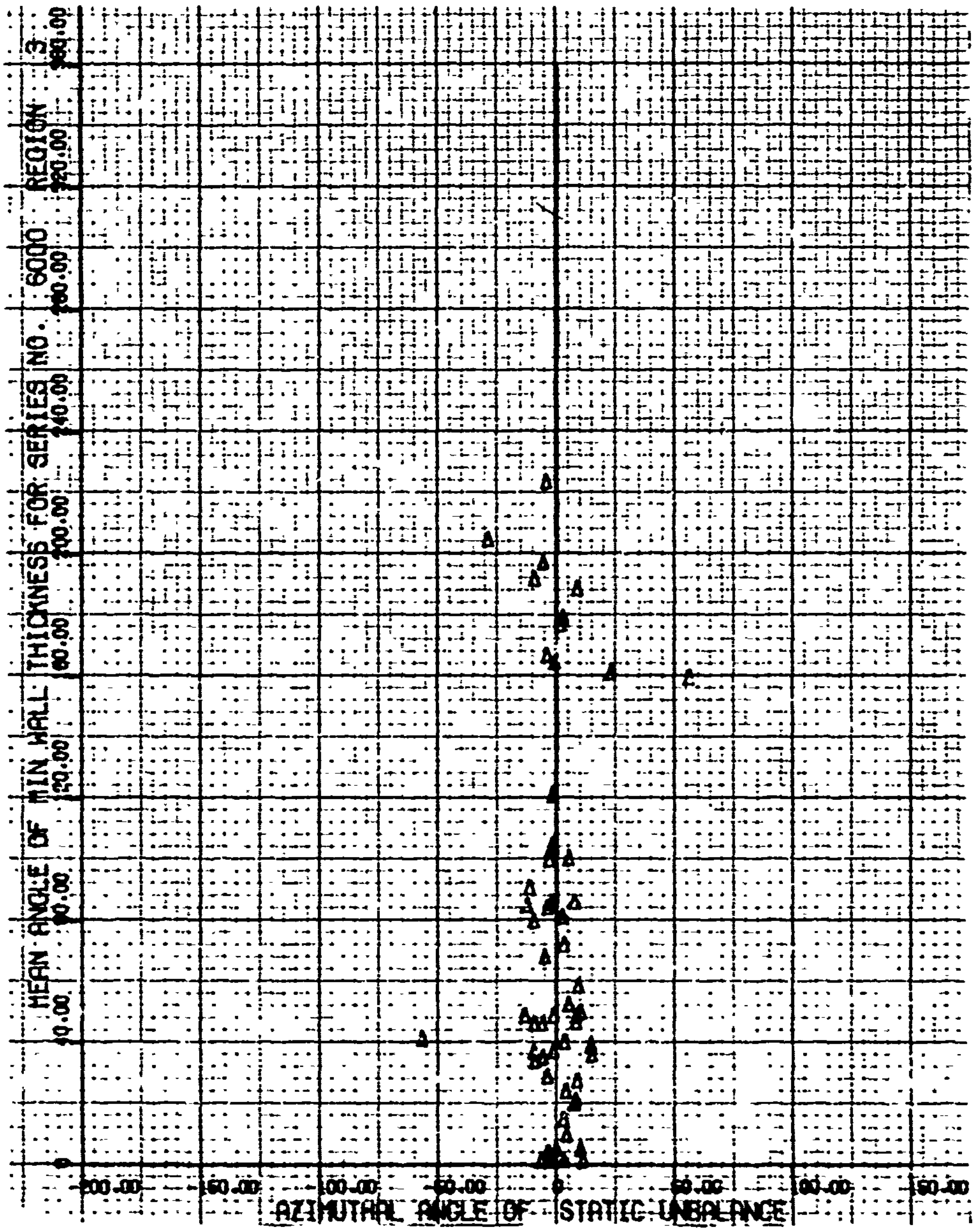

Figure 265 - Mean Azimuth of Minimum Wall Thickness Versus Azimuth of Static Unbalance, Series 6000, Region 3, Empty

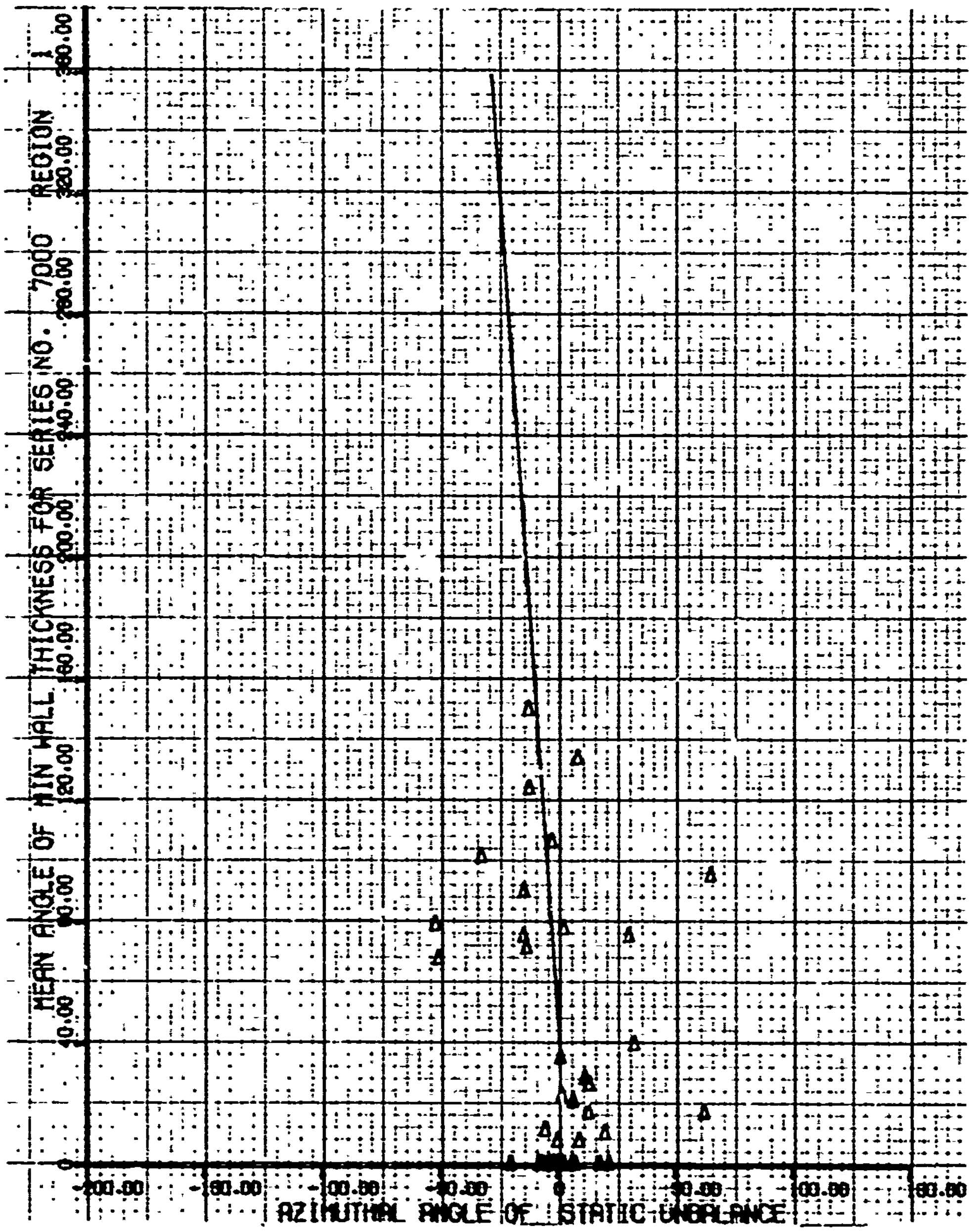

Figure 266 - Mean Azimuth of Minimum Wall Thickn. . Versus Azimuth of Static Unbalance, Series 7000, Region 1, Empty

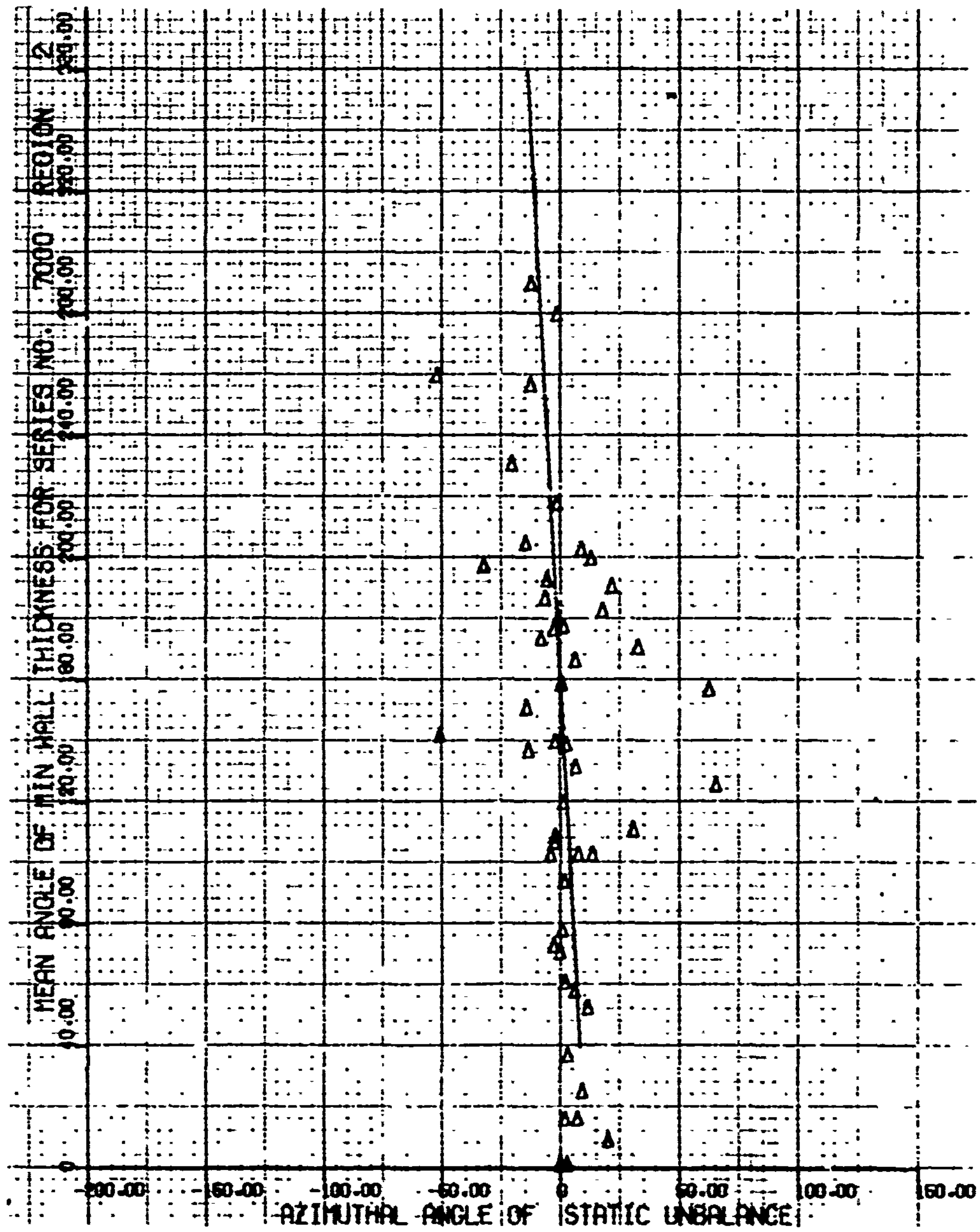

Figure 267 - Mean Azimuth of Minimum Wall Thickness Versus Azimuth of Static Unbalance, Series 7000, Region 2, Empty

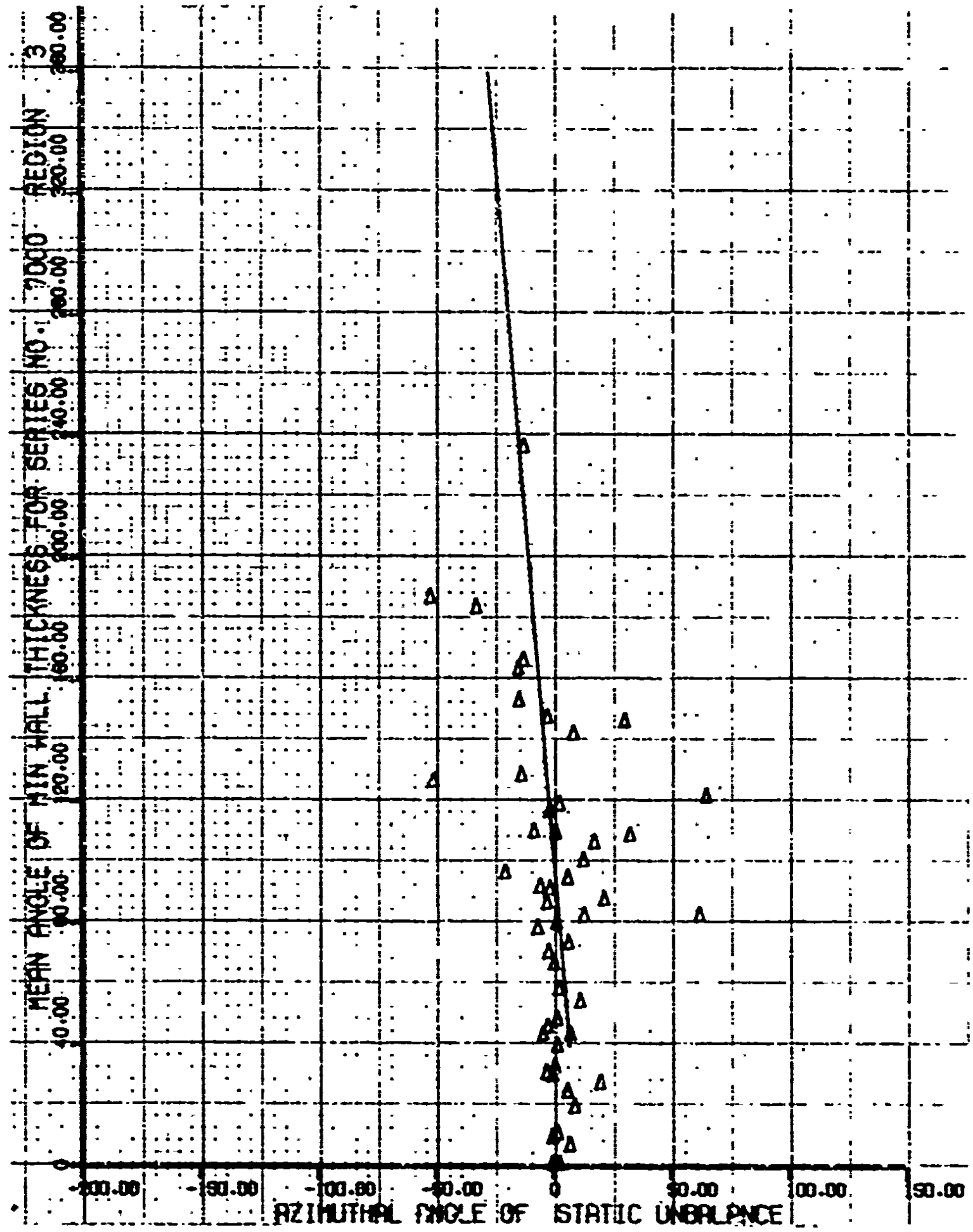

Figure 268 - Mean Azimuth of Minimum Wall Thickness Versus Azimuth of Static Unbalance, Series 7000, Region 3, Empty

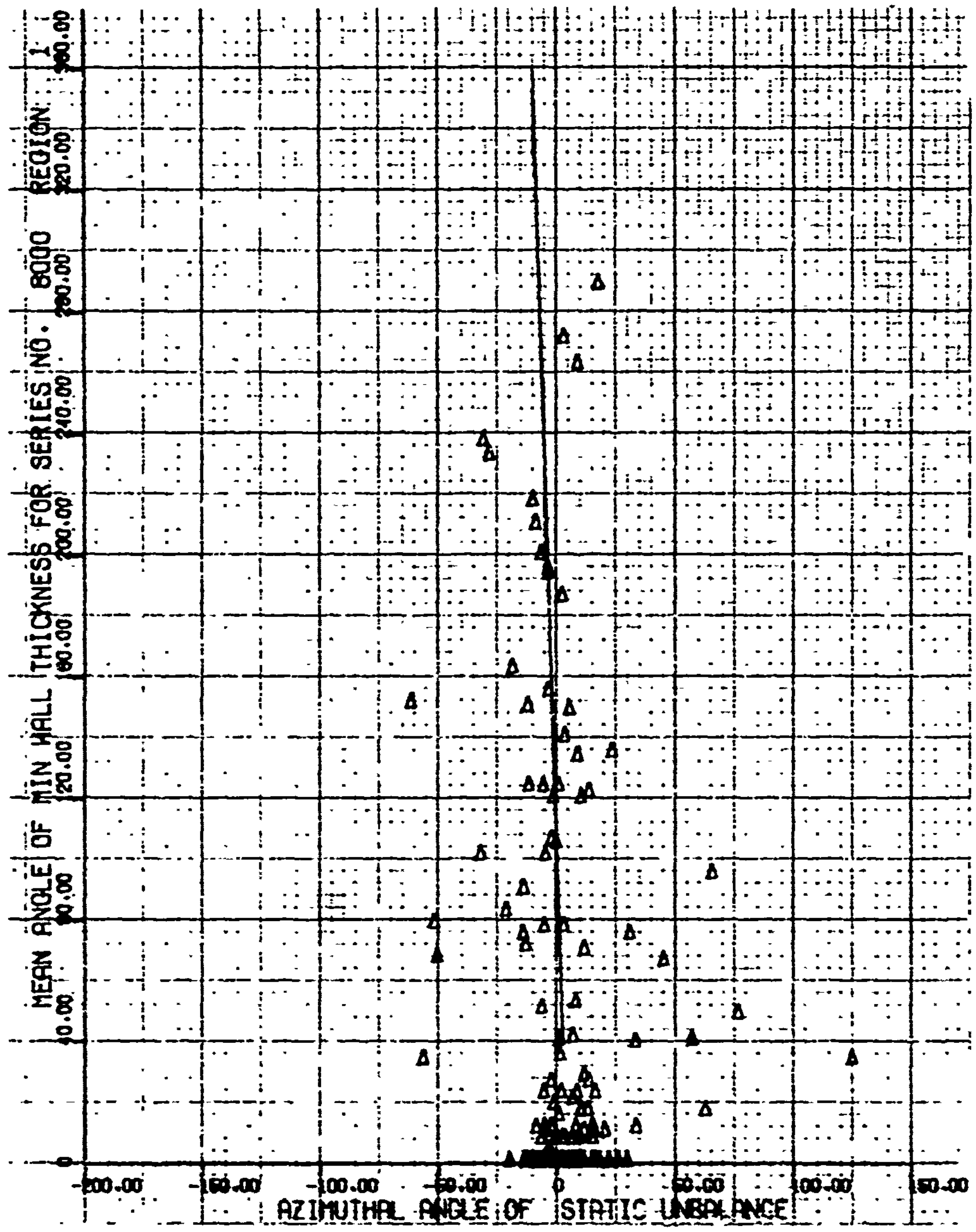

Figure 269 - Mean Azimuth of Minimum Wall Thickness Versus Azimuth of Static Unbalance, Series 8000, Region 1, Empty

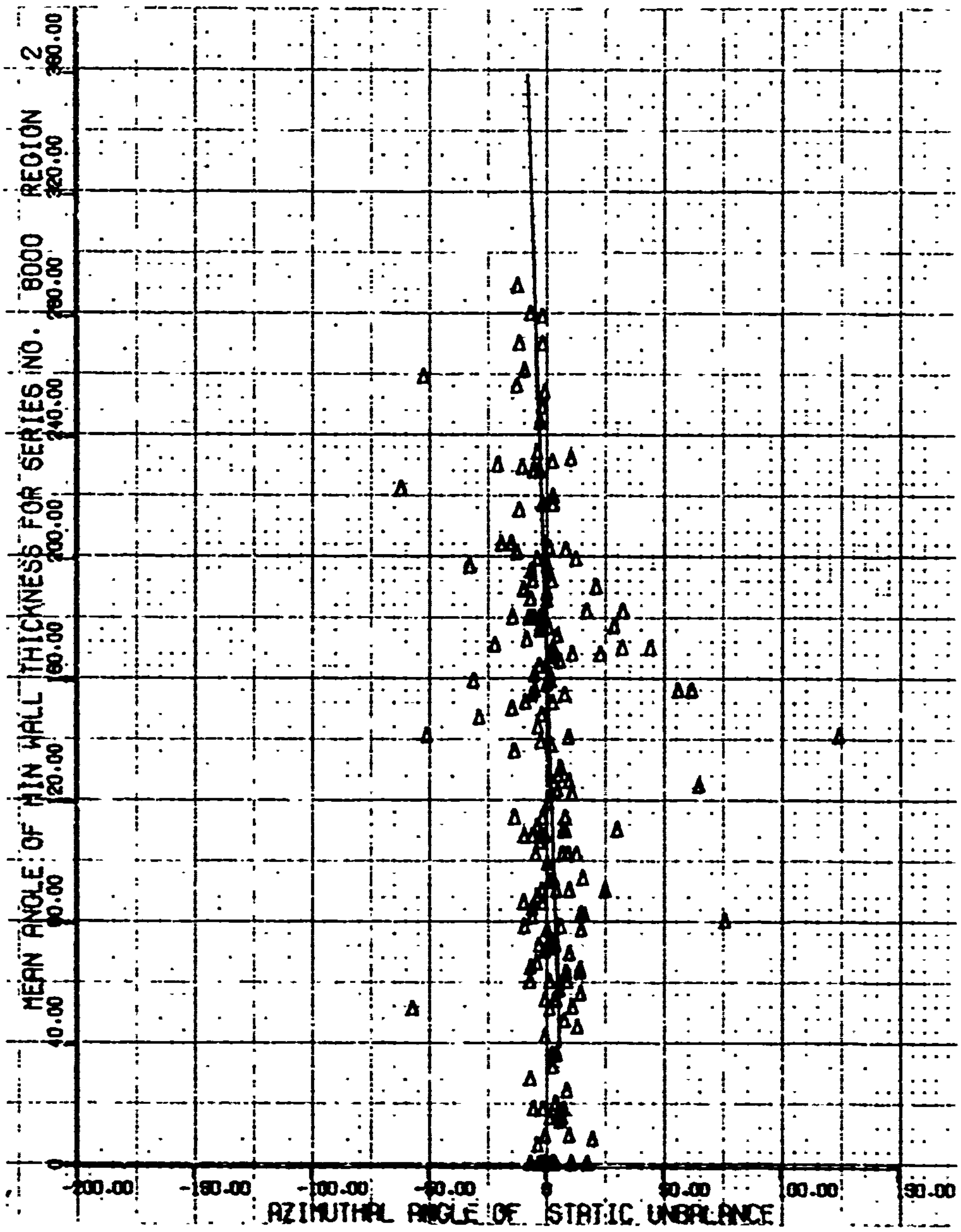

Figure 270 - Mean Azimuth of Minimum Wall Thickness Versus Azimuth of Static Unbalance, Series 8000, Region 2, Empty

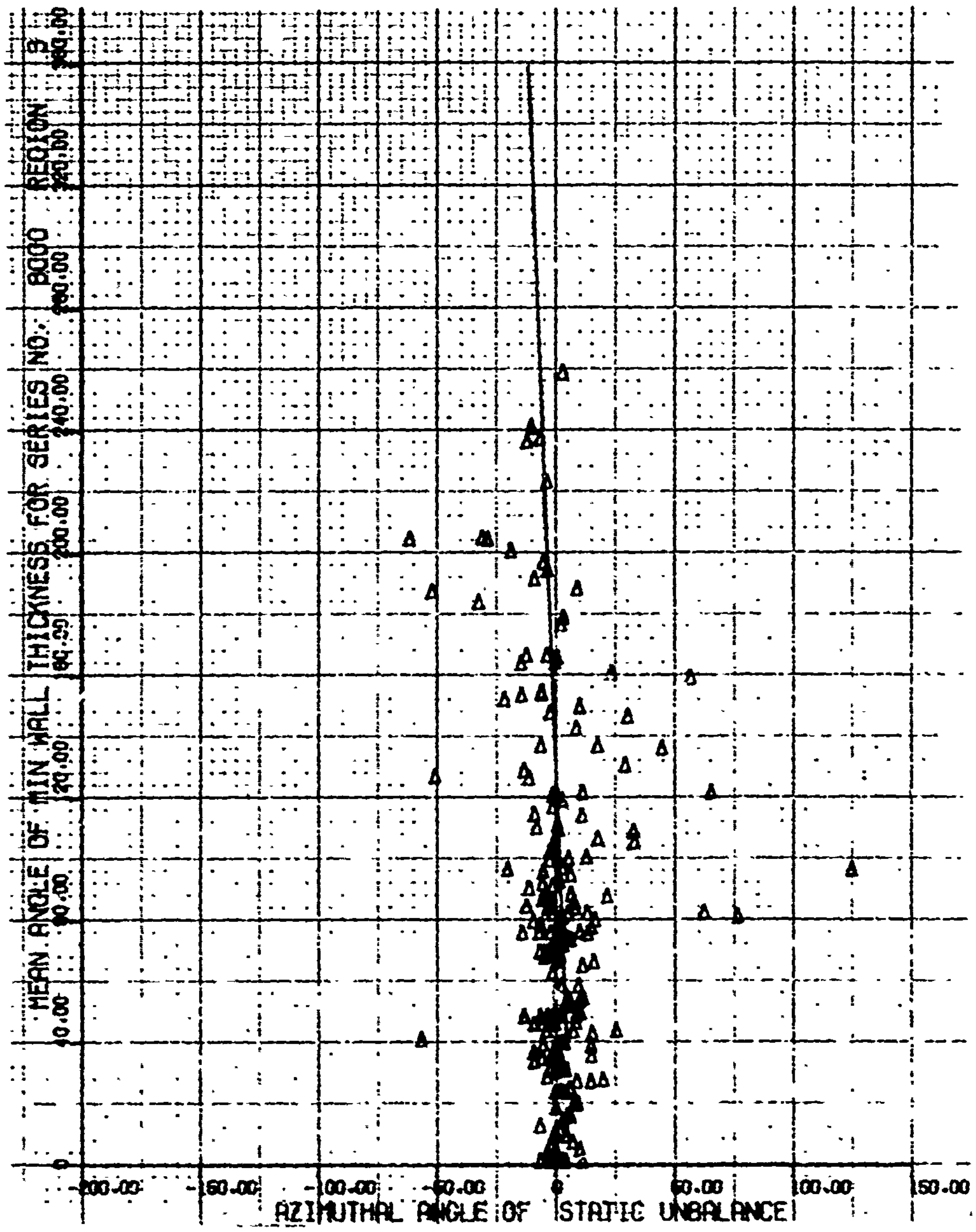

Figure 271 - Mean Azimuth of Minimum Wall Thickness Versus Azimuth of Static Unbalance, Series 8000, Region 3, Empty

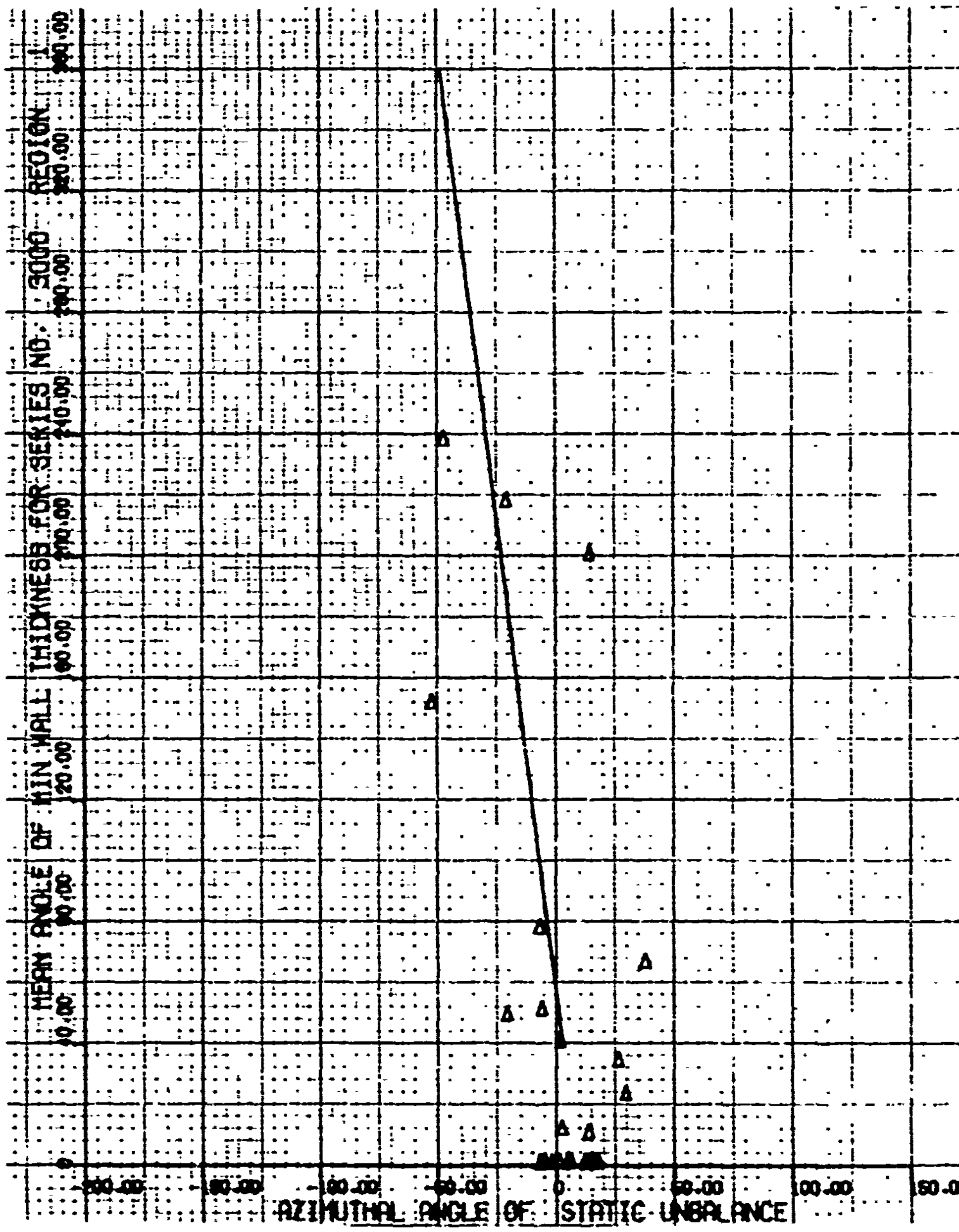

Figure 272 - Mean Azimuth of Minimum Wall Thickness Versus Azimuth of Static Unbalance, Series 3000, Region 1, Full

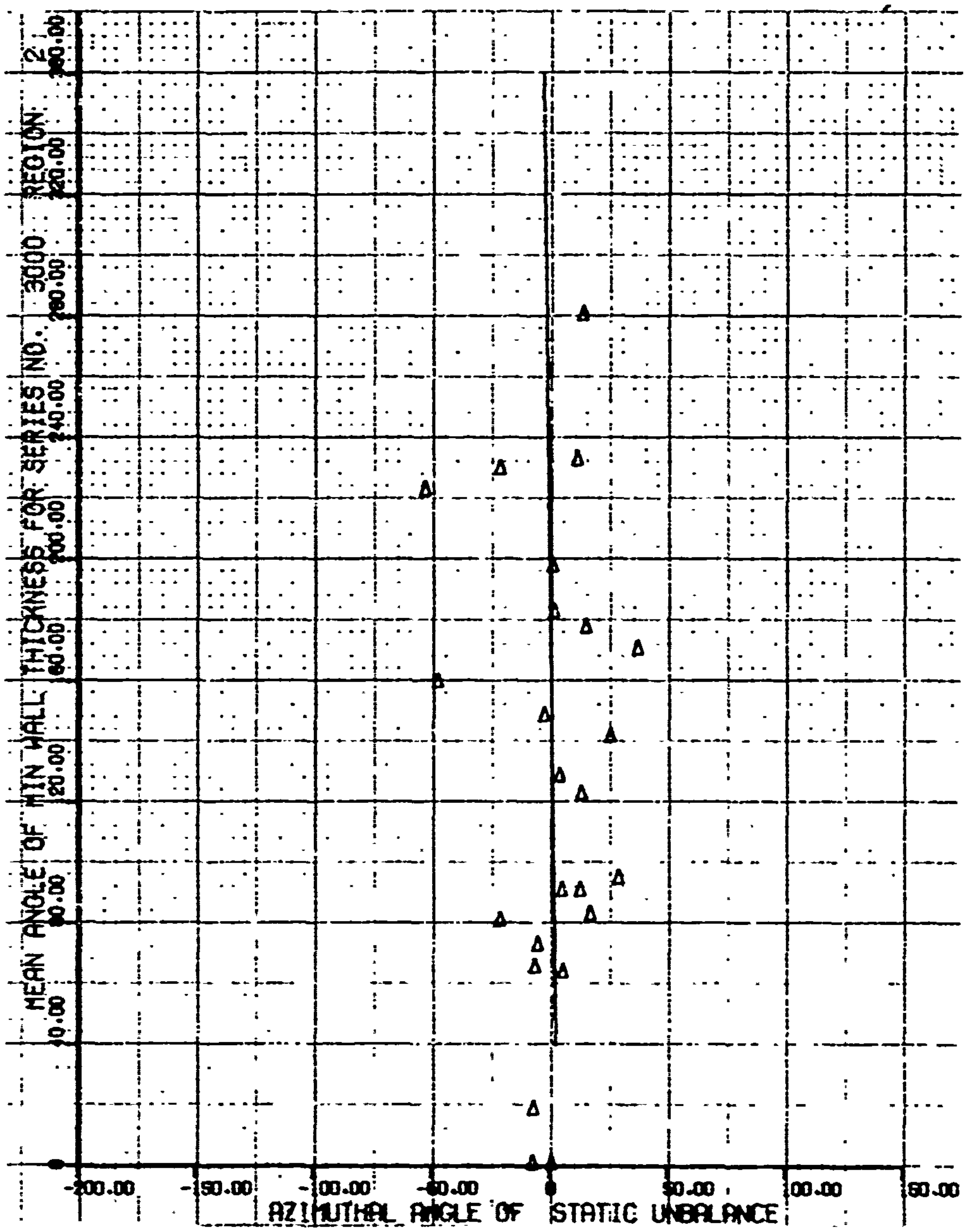

Figure 273 - Mean Azimuth of Minimum Wall Thickness Versus Azimuth of Static Unbalance, Series 3000, Region 2, Full

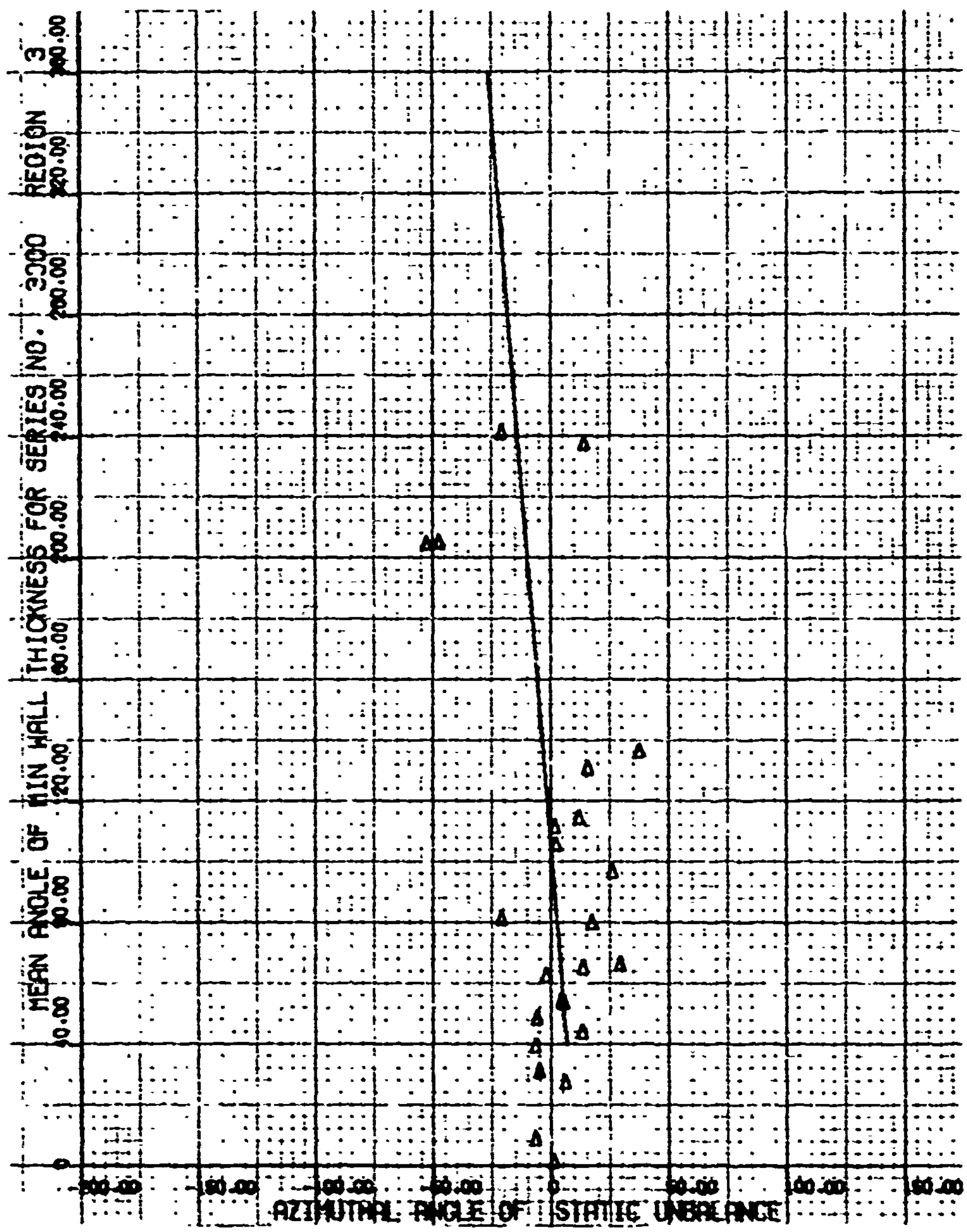

Figure 274 - Mean Azimuth of Minimum Wall Thickness Versus Azimuth of Static Unbalance, Series 3000, Region 3, Full

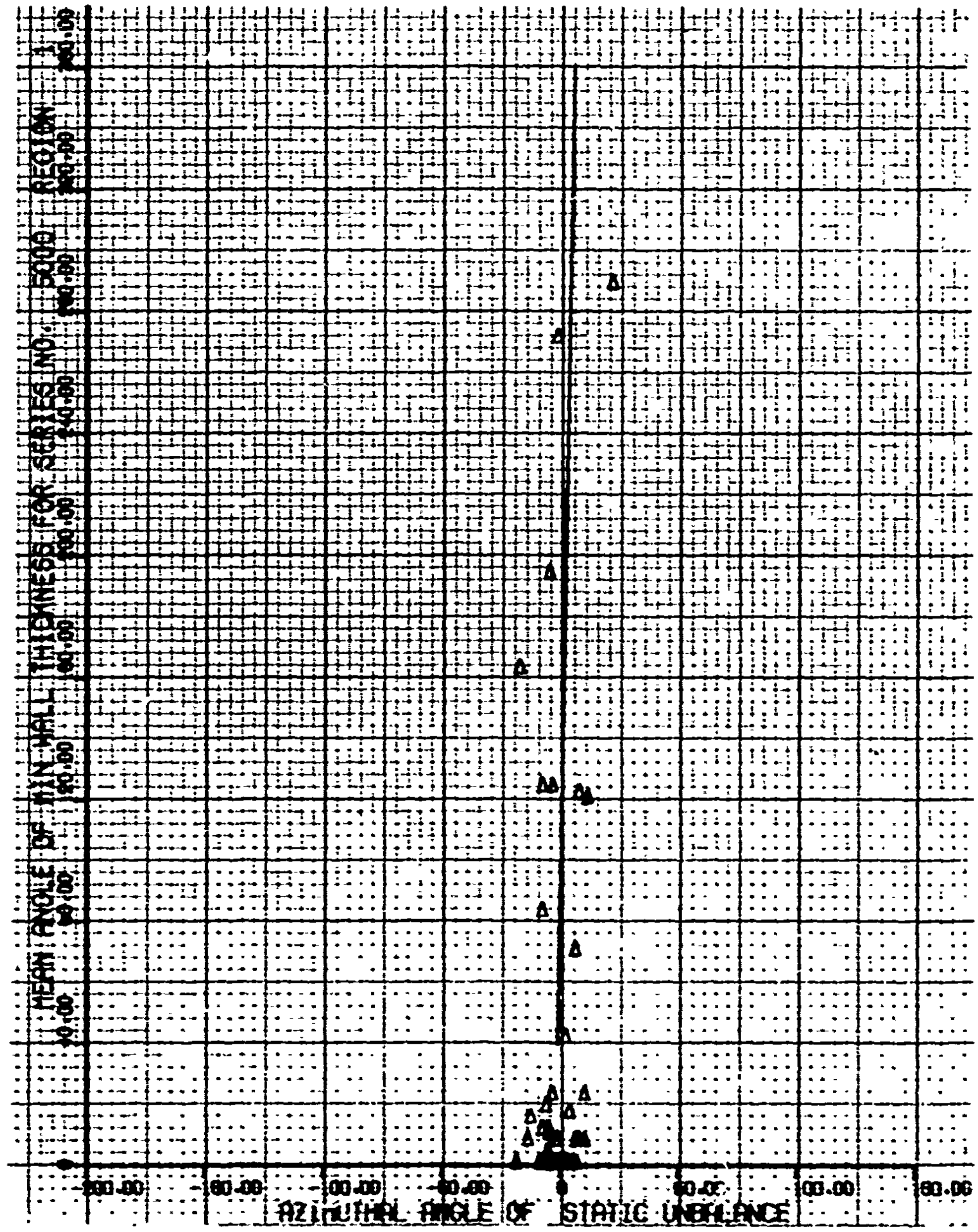

Figure 275 - Mean Azimuth of Minimum Wall Thickness Versus Azimuth of Static Unbalance, Series 5000, Region 1, Full

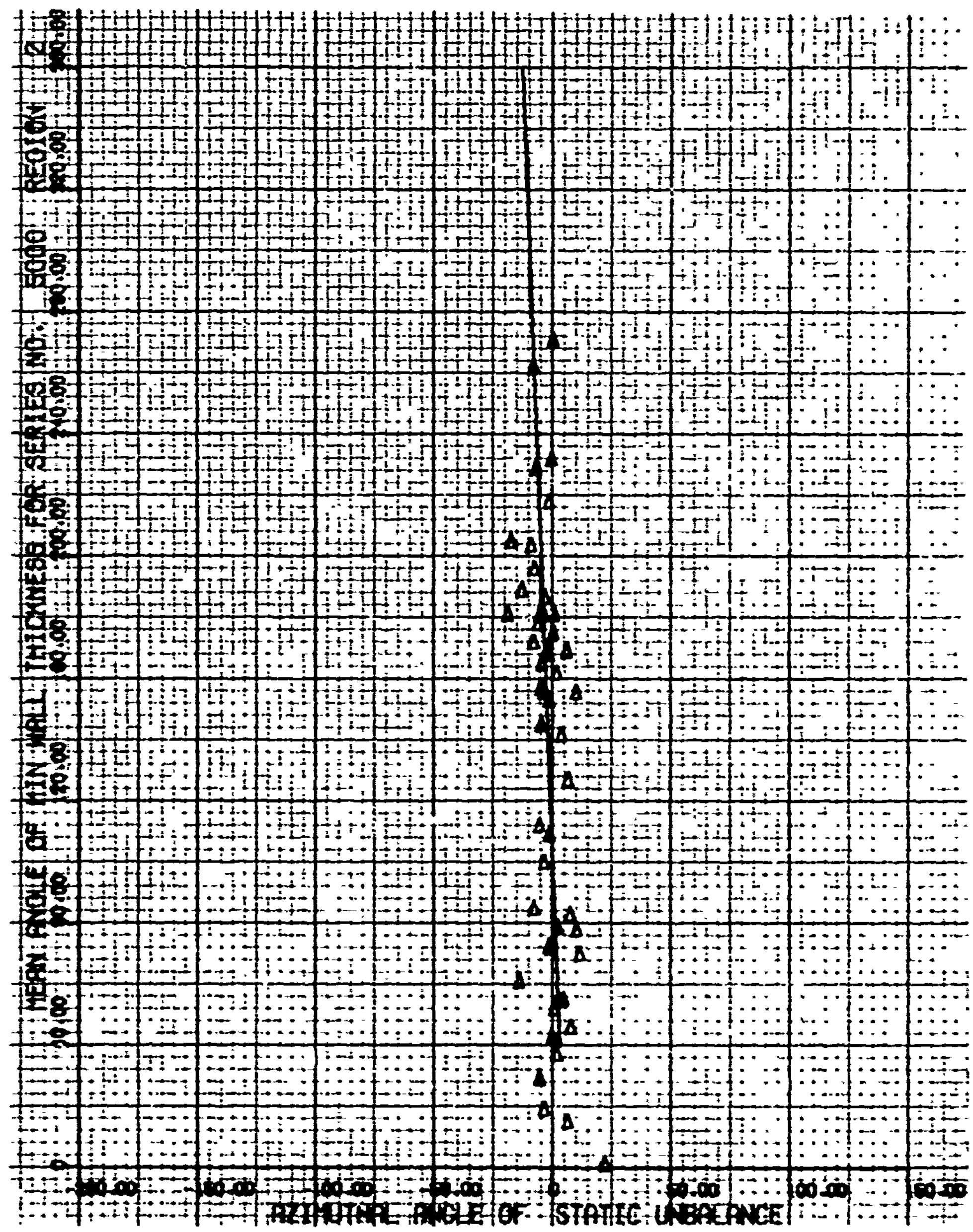

Figure 276 - Mean Azimuth of Minimum Wall Thickness Versus Azimuth of Static Unbalance, Series 5000, Region 2, Full

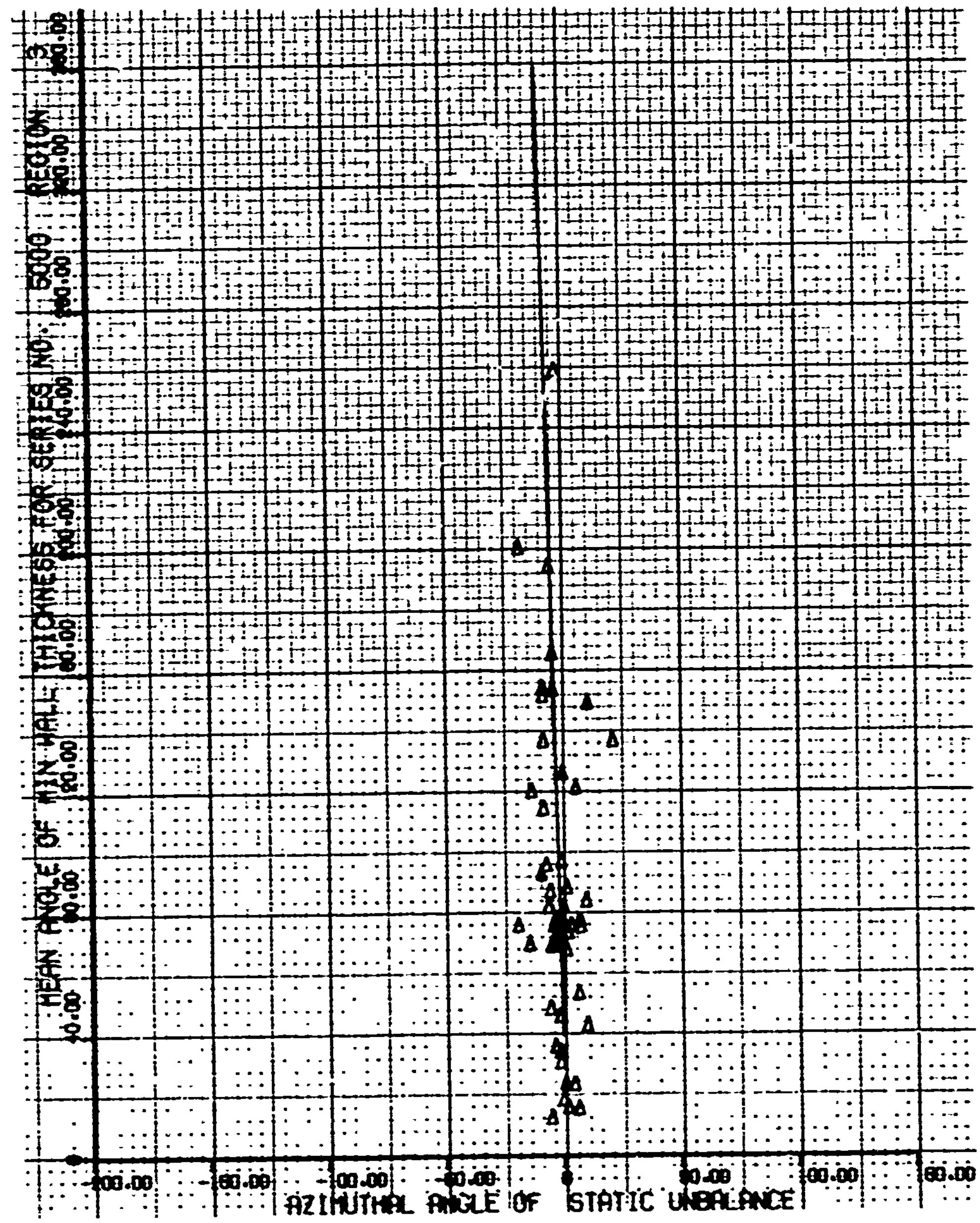

Figure 277 - Mean Azimuth of Minimum Wall Thickness Versus Azimuth of Static Unbalance, Series 5000, Region 3, Full

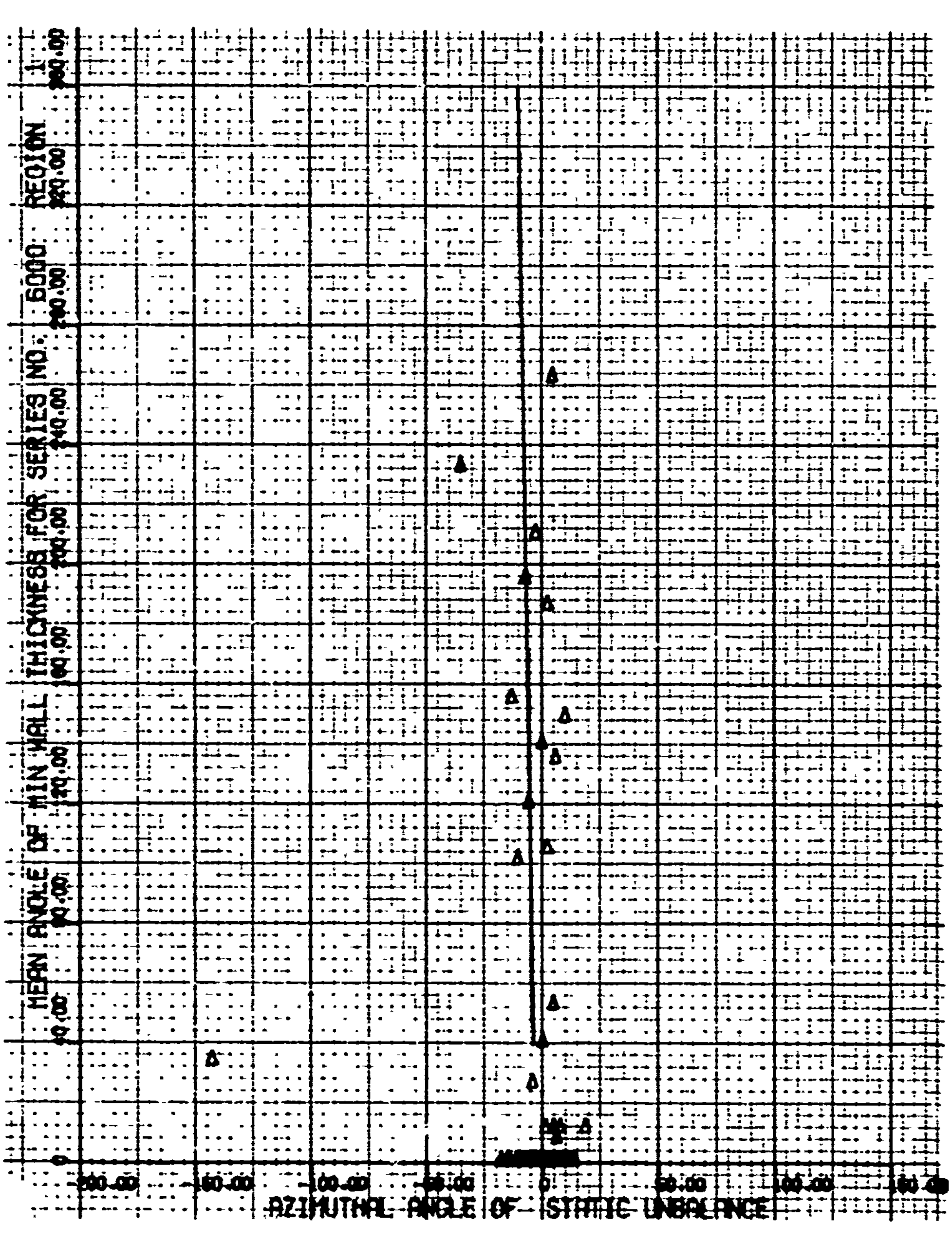

Figure 278 - Mean Azimuth of Minimum Wall Thickness Versus Azimuth of Static Unbalance, Series 6000, Region 1, Full

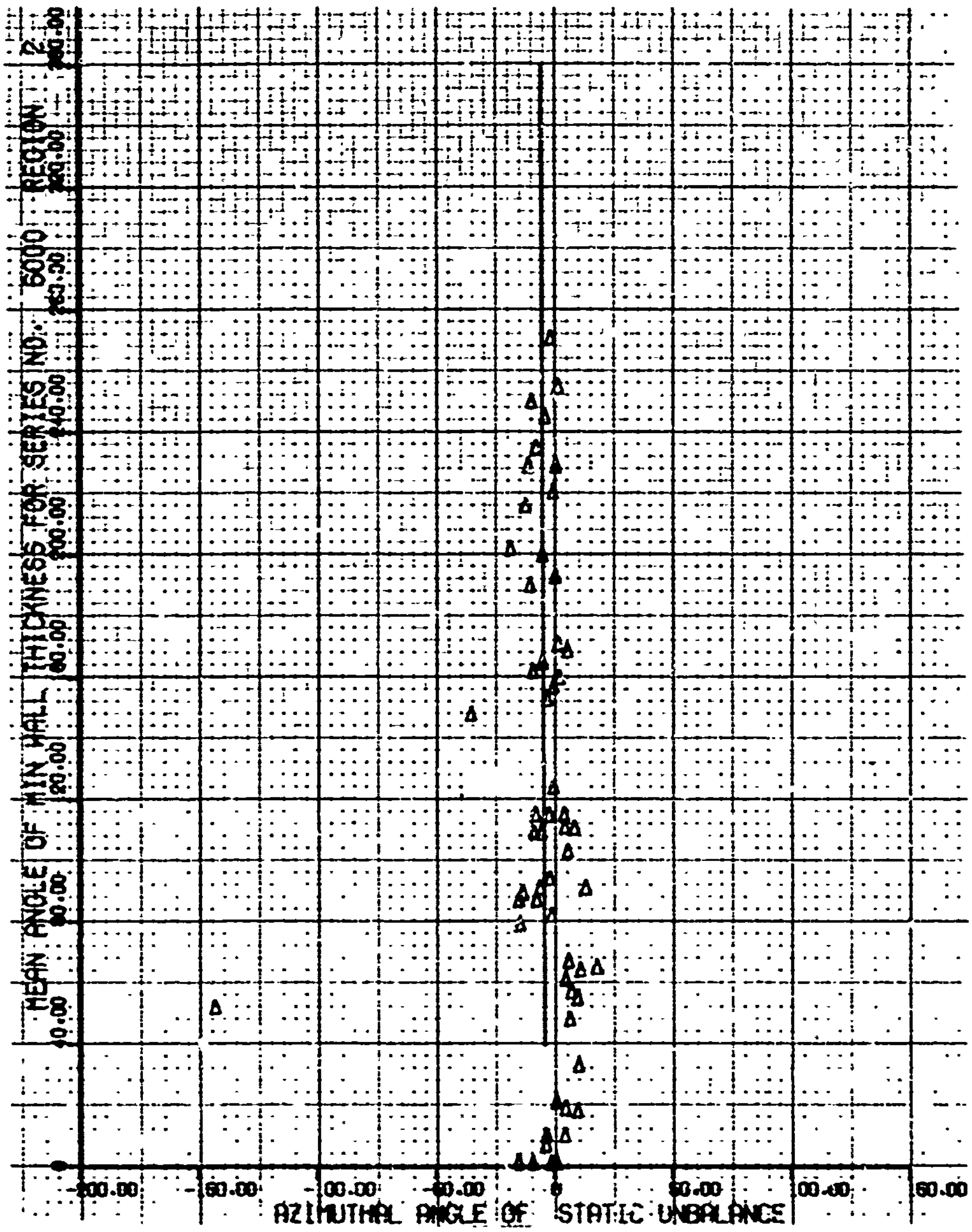

Figure 279 - Mean Azimuth of Minimum Wall Thickness Versus Azimuth of Static Unbalance, Series 6000, Region 2, Full

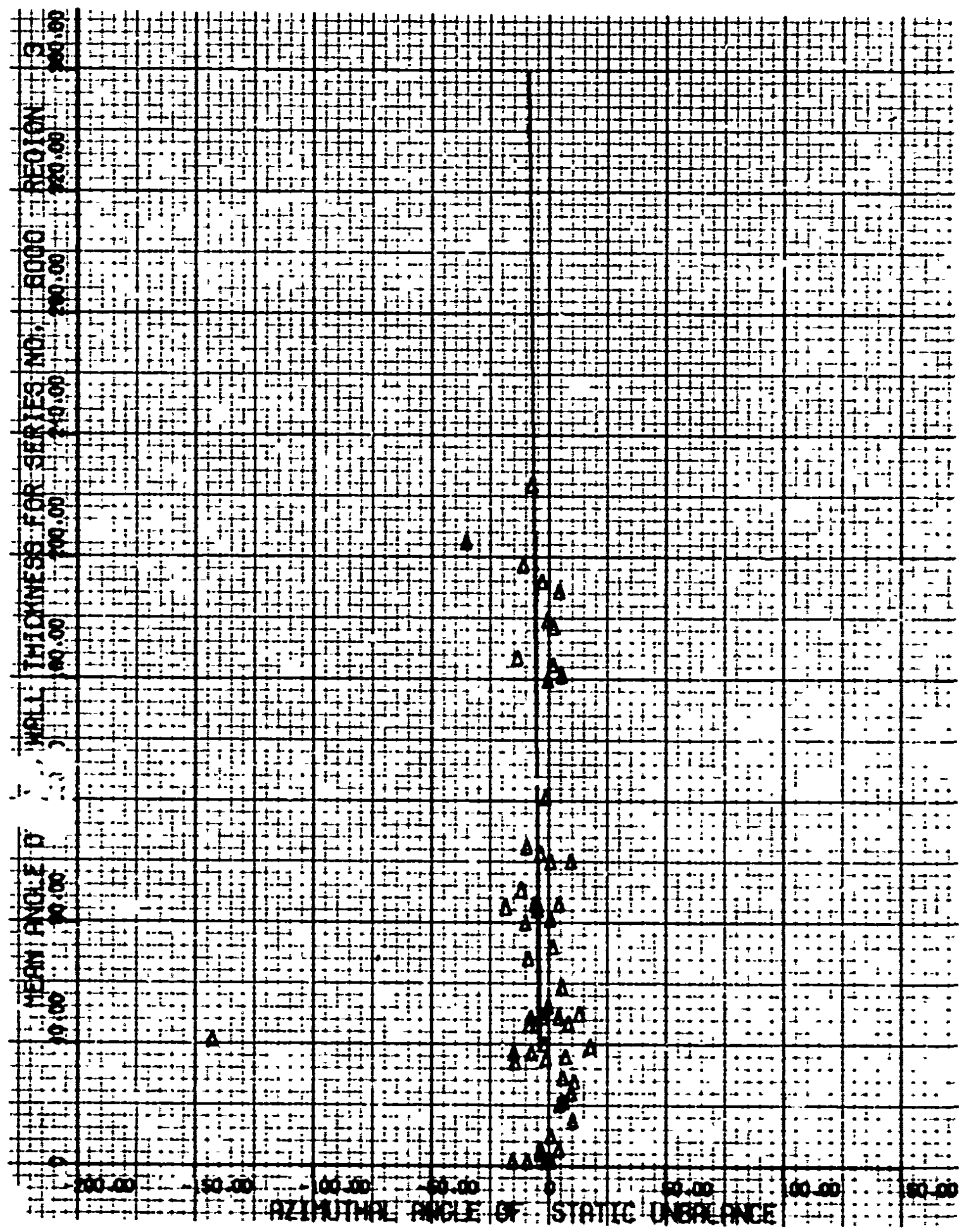

Figure 280 - Mean Azimuth of Minimum Wall Thickness Versus Azimuth of Static Unbalance, Series 6000, Region 3, Full

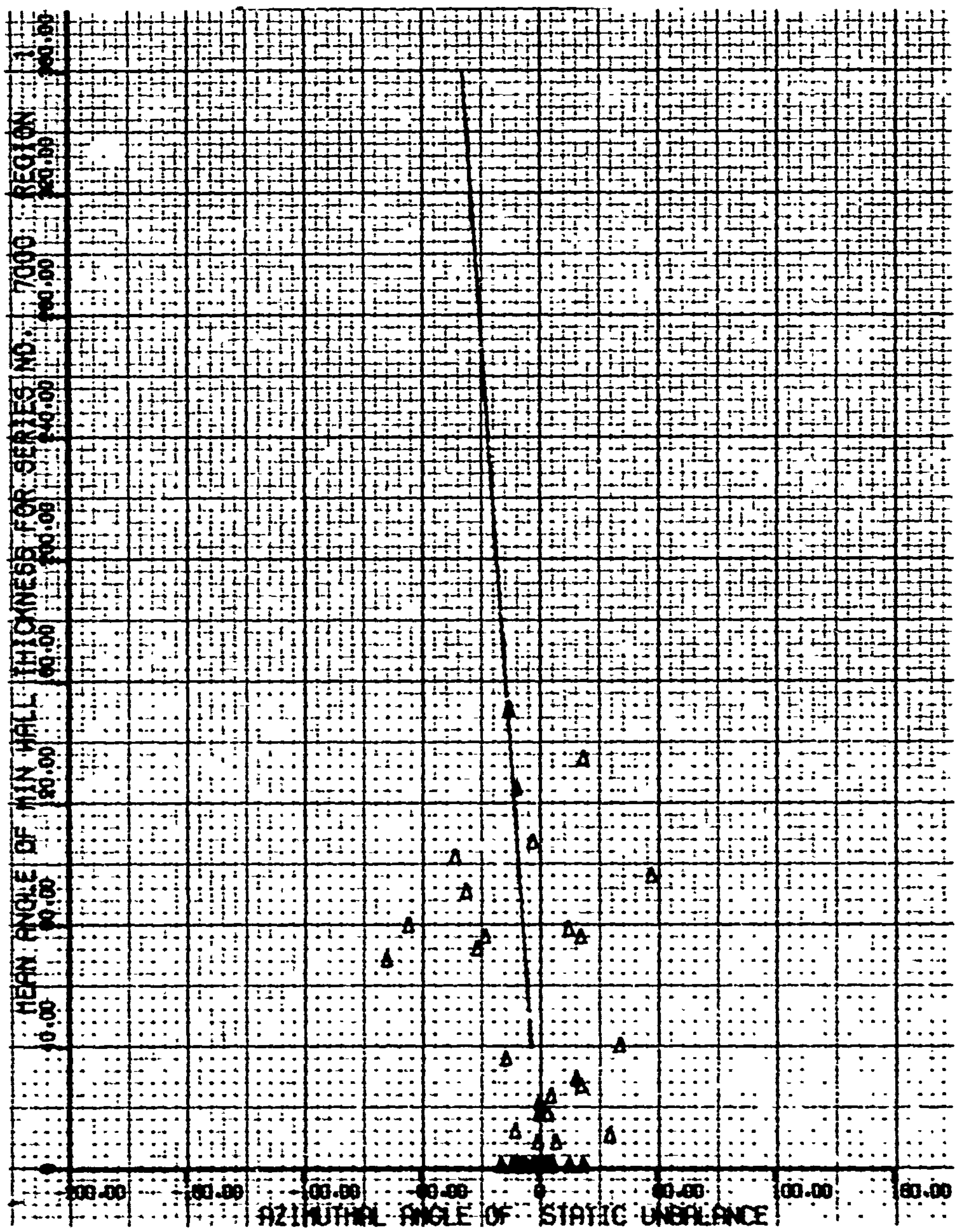

Figure 281 - Mean Azimuth of Minimum Wall Thickness Versus Azimuth of Static Unbalance, Series 7000, Region 1, Full

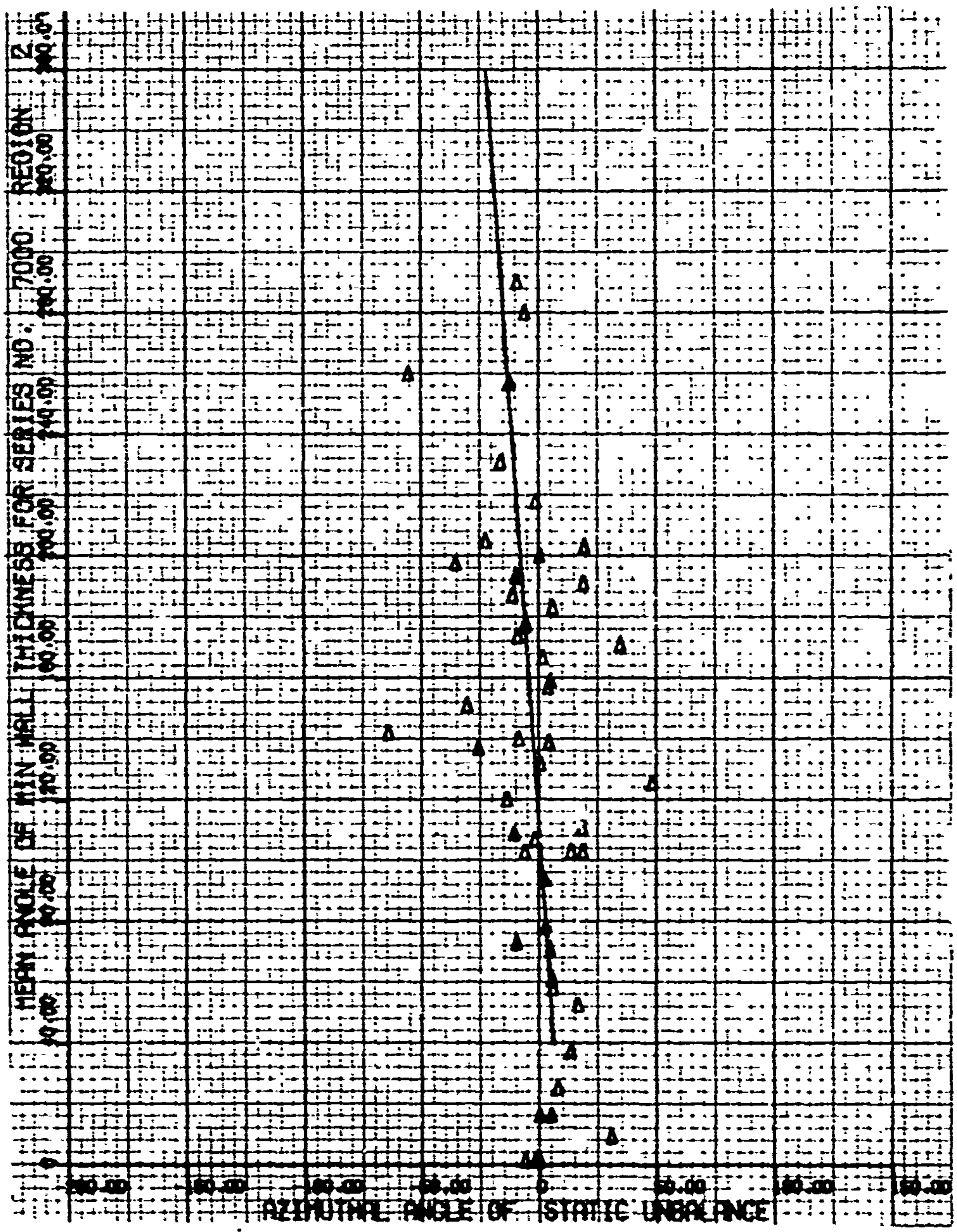

Figure 282 - Mean Azimuth of Minimum Wall Thickness Versus Azimuth of Static Unbalance, Series 7000, Region 2, Full

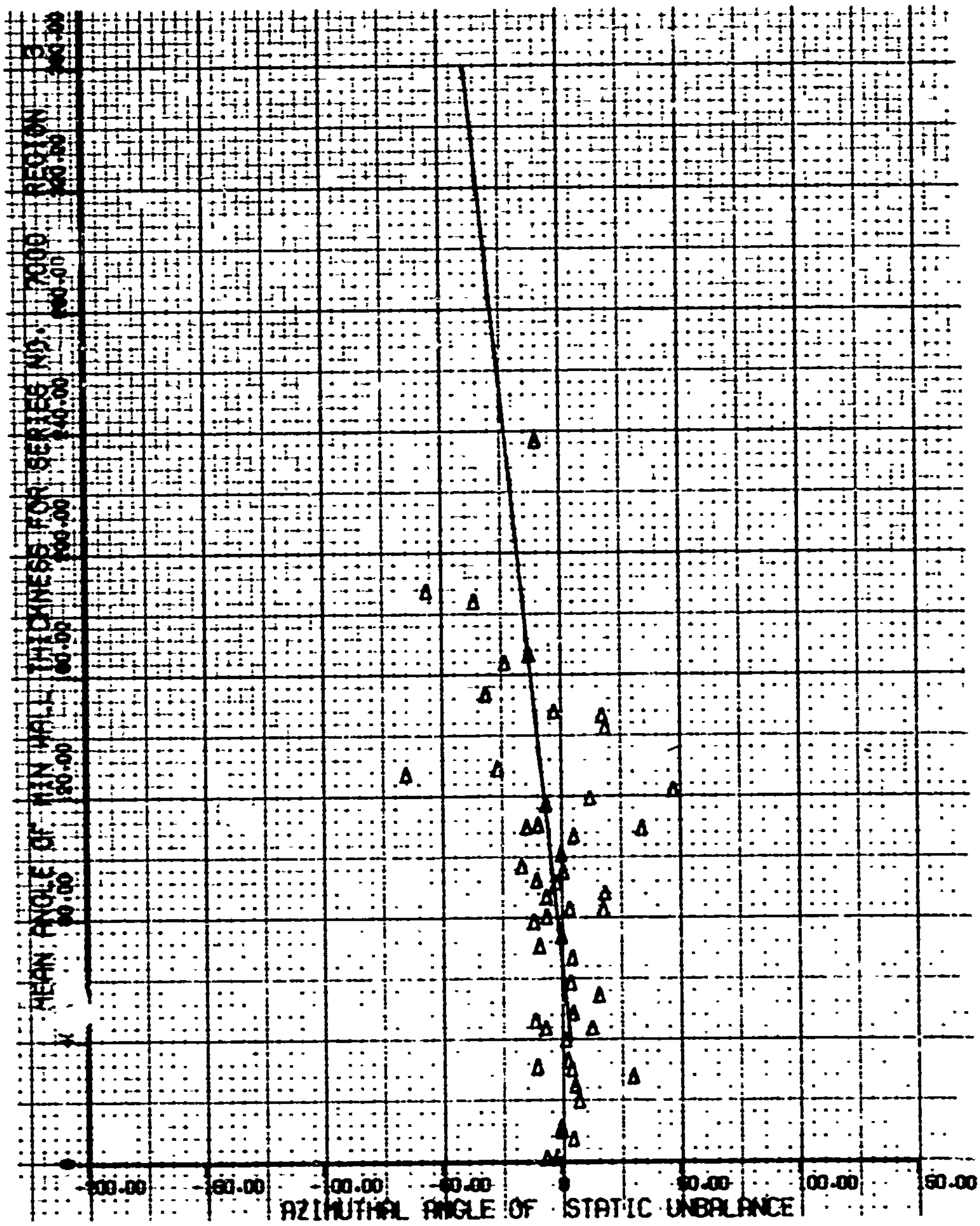

Figure 283 - Mean Azimuth of Minimum Wall Thickness Versus Azimuth of Static Unbalance, Series 7000, Region 3, Full

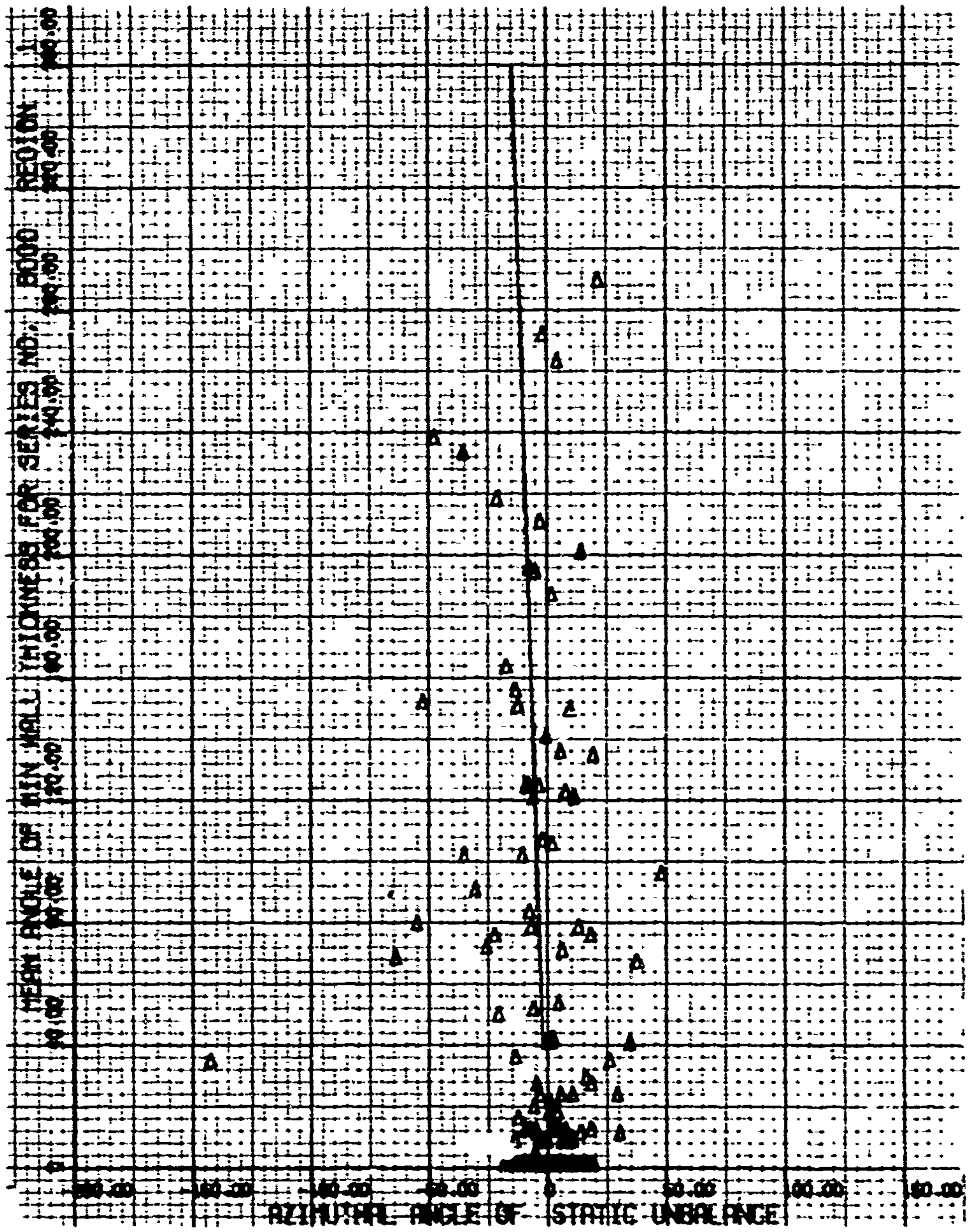

Figure 284 - Mean Azimuth of Minimum Wall Thickness Versus Azimuth of Static Unbalance, Series 8000, Region 1, Full

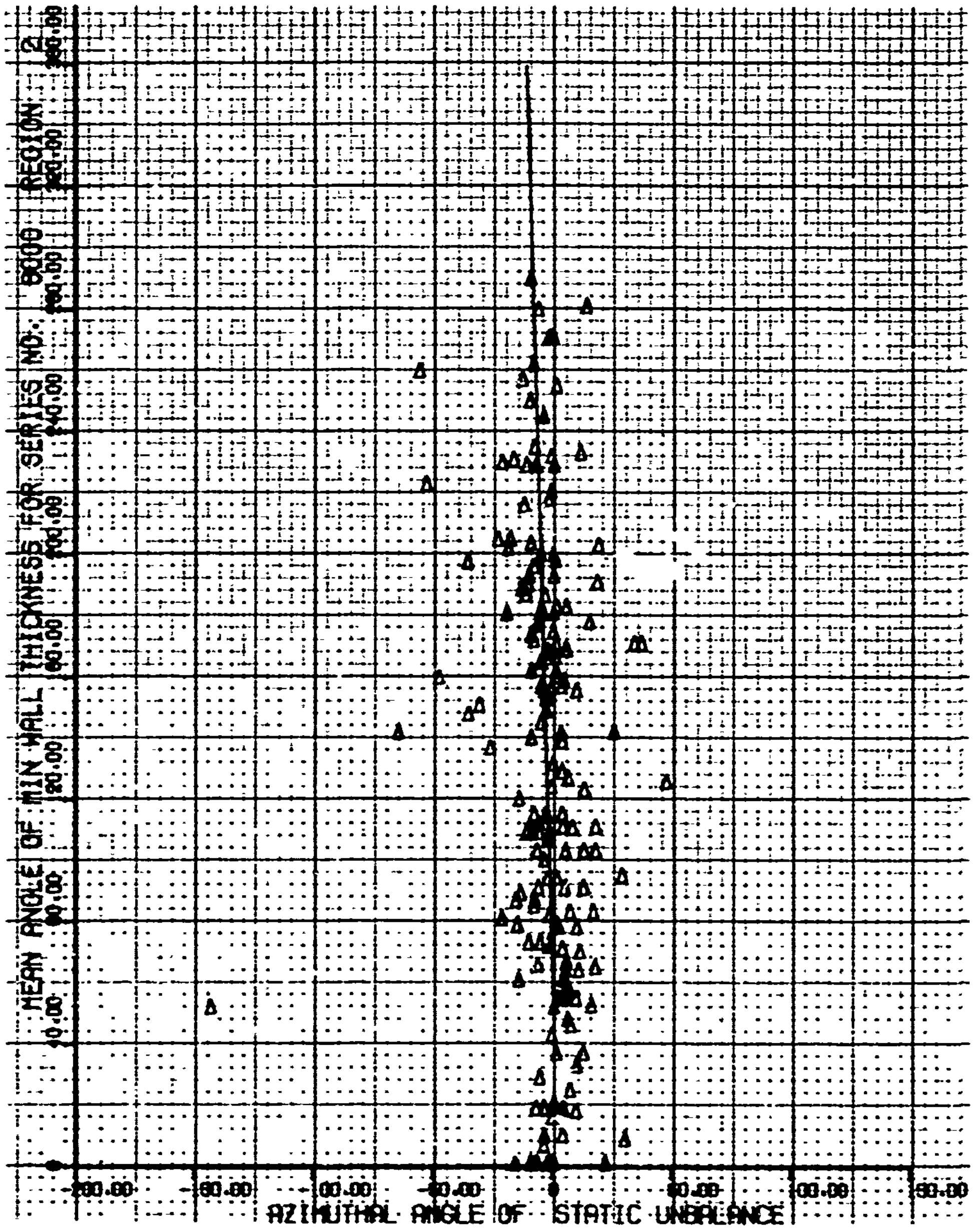

Figure 285 - Mean Azimuth of Minimum Wall Thickness Versus Azimuth of Static Unbalance, Series 8000, Region 2, Full

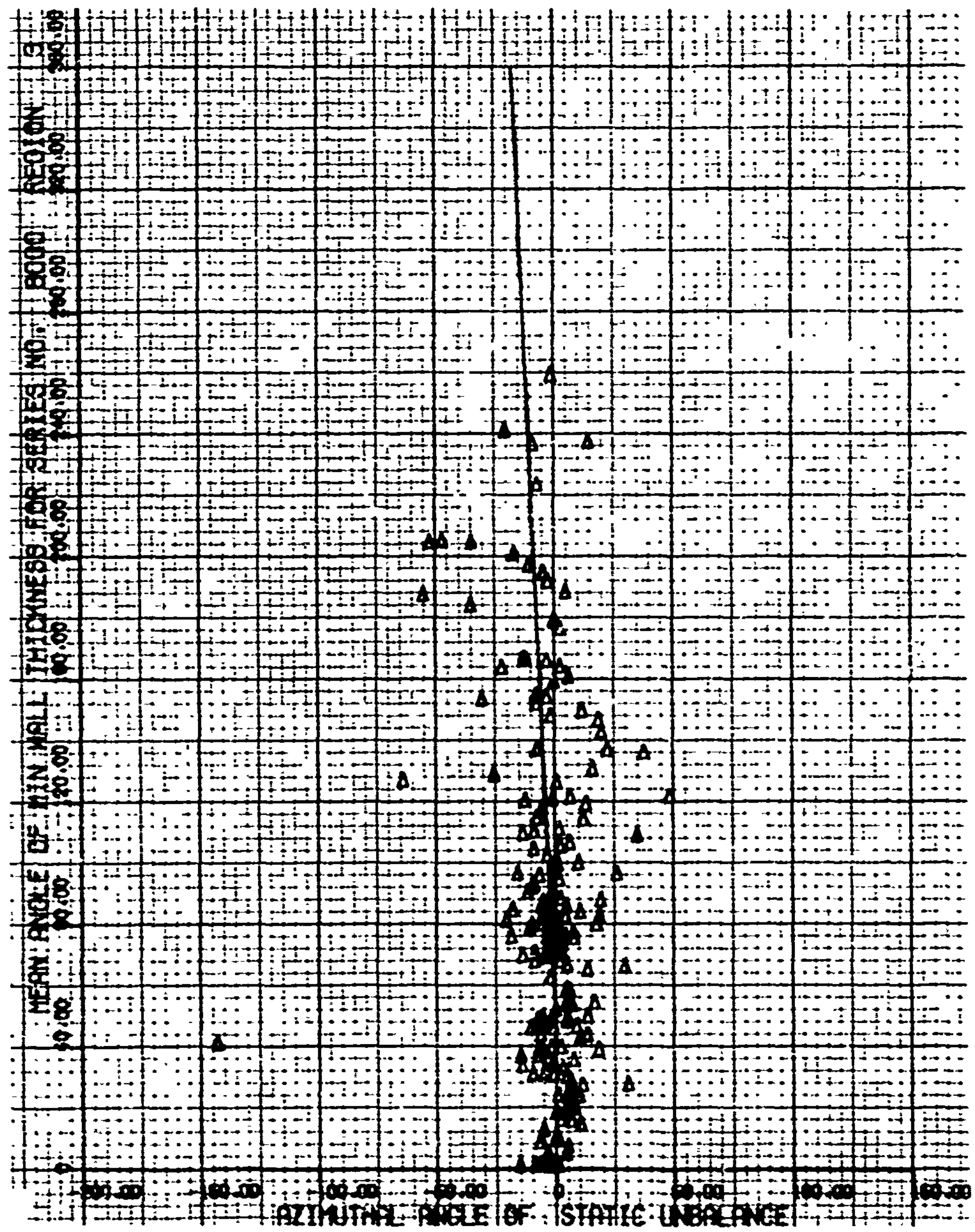

Figure 286 - Mean Azimuth of Minimum Wall Thickness Versus Azimuth of Static Unbalance, Series 8000, Region 3, Full

CORRELATION COEFFICIENTS FOR SERIES 3000

y \ x		z	α		ϵ		τ		λ	
		all	empty	full	empty	full	empty	full	empty	full
ϵ			-0.0740	0.0340						
λ							0.636	0.627		
$\bar{\beta}_{min}$	Region 1	—					-0.749	-0.565	-0.391	-0.544
	Region 2	—					-0.176	-0.0661	-0.117	-0.0489
	Region 3	-0.915					-0.467	-0.303	-0.236	-0.312
$\bar{\Delta}_t$	Region 1		0.220	0.00272	0.686	0.837	0.475	0.525	0.0217	0.192
	Region 2		0.277	-0.138	-0.161	-0.00309	0.141	0.00875	0.491	0.0600
	Region 3		0.285	-0.0773	0.526	0.741	0.434	0.430	0.247	0.152

Figure 287 - Linear Correlation Coefficients for Series 3000

CORRELATION COEFFICIENTS FOR SERIES 5000

y \ x		z	α		ϵ		τ		λ	
		al.	empty	full	empty	full	empty	full	empty	full
ϵ			-0.509	-0.505						
λ							0.671	0.699		
$\bar{\beta}_{min}$	Region 1	—					0.106	-0.0329	0.121	0.208
	Region 2	—					-0.244	-0.279	-0.441	-0.441
	Region 3	-0.936					-0.0957	-0.225	-0.227	-0.178
$\bar{\Delta}_t$	Region 1		0.0444	0.0470	0.357	0.403	0.0295	-0.0790	-0.0406	-0.0122
	Region 2		0.0610	0.156	0.168	0.219	-0.257	-0.159	-0.0776	-0.0294
	Region 3		-0.0532	-0.0643	0.478	0.593	-0.140	-0.154	-0.0770	-0.0659

Figure 288 - Linear Correlation Coefficients for Series 5000

CORRELATION COEFFICIENTS FOR SERIES 6000

y \ x		z	α		ϵ		τ		λ	
		all	empty	full	empty	full	empty	full	empty	full
ϵ			-0.100	-0.0699						
λ							0.674	0.512		
$\bar{\beta}_{min}$	Region 1	—					0.0689	0.0261	-0.0493	-0.0570
	Region 2	—					-0.194	-0.195	-0.0746	-0.0133
	Region 3	-0.917					-0.0263	-0.0453	-0.0171	-0.0386
$\bar{\Delta t}$	Region 1		-0.171	0.0479	0.489	0.600	-0.0711	-0.0354	0.00374	-0.0101
	Region 2		0.0838	0.291	0.339	0.387	0.0456	-0.0712	-0.0263	-0.0431
	Region 3		-0.0589	0.235	0.490	0.607	-0.0782	-0.126	-0.0805	-0.0141

Figure 289 - Linear Correlation Coefficients for Series 6000

CORRELATION COEFFICIENTS FOR SERIES 7000

y \ x		z	α		ϵ		τ		λ	
		all	empty	full	empty	full	empty	full	empty	full
ϵ			-0.654	-0.604						
λ							0.581	0.647		
$\bar{\beta}_{min}$	Region 1	—					-0.298	-0.206	-0.164	-0.173
	Region 2	—					-0.464	-0.311	-0.246	-0.325
	Region 3	-0.980					-0.473	-0.330	-0.263	-0.339
$\bar{\Delta t}$	Region 1		-0.0574	0.0269	0.531	0.535	0.248	0.0296	0.0181	0.0142
	Region 2		0.0446	-0.0860	-0.0312	-0.0179	0.120	0.299	0.211	0.249
	Region 3		-0.0351	-0.108	0.435	0.454	0.173	0.242	0.0810	0.0797

Figure 290 - Linear Correlation Coefficients for Series 7000

CORRELATION COEFFICIENTS FOR SERIES 8000

y \ x		z	α		ϵ		τ		λ	
		all	empty	full	empty	full	empty	full	empty	full
ϵ			-0.275	-0.222						
λ							0.548	0.532		
$\bar{\beta}_{min}$	Region 1	—					-0.115	-0.124	-0.123	-0.126
	Region 2	—					-0.279	-0.234	-0.162	-0.151
	Region 3	-0.984					-0.225	-0.207	-0.142	-0.173
$\overline{\Delta t}$	Region 1		-0.0235	0.0632	0.609	0.642	0.0818	-0.0252	-0.103	0.00126
	Region 2		-0.0118	-0.0264	0.275	0.312	-0.0285	-0.00409	0.0815	0.0709
	Region 3		-0.123	-0.0967	0.644	0.698	-0.0399	-0.0497	-0.0813	-0.0183

Figure 291 - Linear Correlation Coefficients for Series 8000

APPENDIX A

Derivation of Normal Distance Least Squares Fit

Given the line $y = ax + b$ and the arbitrary point (x_1, y_1) find the point on the line that minimizes the distance, d, between (x_1, y_1) and the line $y = ax + b$:

$$d^2 = (x_2 - x_1)^2 + (y_2 - y_1)^2 = (x_2 - x_1)^2 + (a x_2 + b - y_1)^2 \qquad \text{(A-1)}$$

$$\frac{d}{dx_2}(d^2) = 0 = (x_2 - x_1) + a(a x_2 + b - y_1) \qquad \text{(A-2)}$$

or

$$x_2 = \frac{x_1 + a y_1 - b}{a^2 + 1} \qquad \text{(A-3)}$$

to satisfy d being a minimum.

Therefore the minimum distance (or normal distance) squared from any given point (x_i, y_i) to the line $y = ax + b$ is obtained by:

$$d_i^2 = (x_2 - x_i)^2 + (a x_2 + b - y_i)^2 \qquad \text{(A-4)}$$

$$d_i^2 = \left(\frac{x_i + a y_i - ab}{a^2 + 1} - x_i\right)^2 + \left[a\left(\frac{x_i + a y_i - ab}{a^2 + 1}\right) + b - y_i\right]^2 \qquad \text{(A-5)}$$

or

$$d_i^2 = \frac{(a x_i - y_i + b)^2}{a^2 + 1} \qquad \text{(A-6)}$$

For N points

$$D \triangleq \sum_{i=1}^{N} d_i^2 = \frac{1}{a^2+1} \sum_{i=1}^{N} (a x_i - y_i + b)^2 \qquad \text{(A-7)}$$

or

$$D = \frac{1}{a^2+1}\Big(a^2 \sum_{i=1}^{N} x_i^2 + \sum_{i=1}^{N} y_i^2 - 2a \sum_{i=1}^{N} x_i y_i + \qquad \text{(A-8)}$$

$$+ 2ab \sum_{i=1}^{N} x_i - 2b \sum_{i=1}^{N} y_i + b^2 N \Big)$$

Let

$$\sigma_x \equiv \sum_{i=1}^{N} x_i \ , \quad \sigma_y \equiv \sum_{i=1}^{N} y_i \ , \quad \sigma_{xy} \equiv \sum_{i=1}^{N} x_i y_i$$

$$\sigma_{xx} \equiv \sum_{i=1}^{N} x_i^2 \ , \quad \sigma_{yy} \equiv \sum_{i=1}^{N} y_i^2$$

Then

$$D = \frac{1}{a^2+1}\left(a^2 \sigma_{xx} + \sigma_{yy} - 2a\sigma_{xy} + 2ab\sigma_x - 2b\sigma_y + b^2 N \right) \qquad \text{(A-9)}$$

We want to minimize D through the proper choice of a and b. Partially differentiating D by both a and b and setting the results equal to zero:

$$\frac{\partial D}{\partial b} = 0 = \frac{2}{a^2+1}\left(a\sigma_x - \sigma_y + bN \right) \qquad \text{(A-10)}$$

or

$$b = \frac{\sigma_y - a\sigma_x}{N} \qquad \text{(A-11)}$$

and

$$\frac{\partial D}{\partial a} = 0 = (N\sigma_{xy} - Nb\sigma_x)a^2 + (N\sigma_{xx} + -N\sigma_{yy} + 2Nb\sigma_y - N^2b^2)a + -(N\sigma_{xy} - Nb\sigma_x) \qquad \text{(A-12)}$$

substituting $Nb = \sigma_y - a\sigma_x$ from (A-11)

$$0 = (N\sigma_{xy} - \sigma_x\sigma_y)a^2 + (N\sigma_{xx} - N\sigma_{yy} + \sigma_y^2 - \sigma_x^2)a - (N\sigma_{xy} - \sigma_x\sigma_y) \qquad \text{(A-13)}$$

or

$$a^2 + 2Ga - 1 = 0 \qquad \text{(A-14)}$$

where

$$G = \frac{1}{2}\left(\frac{N\sigma_{xx} - N\sigma_{yy} + \sigma_y^2 - \sigma_x^2}{N\sigma_{xy} - \sigma_x\sigma_y}\right) \qquad \text{(A-15)}$$

Therefore

$$a = -G \pm \sqrt{G^2 + 1} \qquad \text{(A-16)}$$

While

$$b = \frac{(\sigma_y - a\sigma_x)}{N} \qquad \text{(A-17)}$$

Both values of a will produce a local minimum. To find the value of a that produces the smaller D we substitute our values of a and b into equation (A-9). Then using equation (A-17) for b:

$$ND = \frac{1}{a^2+1}\Big[(N\sigma_{xx} - \sigma_x^2)a^2 - 2(N\sigma_{xy} - \sigma_x\sigma_y)a +$$

$$+ (N\sigma_{yy} - \sigma_y^2)\Big] \tag{A-18}$$

Then using our relation for a in terms of G, (A-16):

$$ND = N\sigma_{xx} - \sigma_x^2 \mp \frac{2\sqrt{G^2+1}}{a^2+1}\left(N\sigma_{xy} - \sigma_x\sigma_y\right) \tag{A-19}$$

Then, since

$$\mp \frac{2\sqrt{G^2+1}}{a^2+1} = -G \mp \sqrt{G^2+1} \tag{A-20}$$

$$ND = N\sigma_{xx} - \sigma_x^2 + (N\sigma_x - \sigma_x\sigma_y)\left(-G \mp \sqrt{G^2+1}\right) \tag{A-21}$$

Since,

$$ND = N\sum_{i=1}^{N} d_i^2 > 0$$

ND and D are minimums when

$$(N\sigma_{xy} - \sigma_x\sigma_y)\left(-G \mp \sqrt{G^2+1}\right) < 0 \tag{A-22}$$

The condition that (A-22) be true can always be met since

$$-G - \sqrt{G^2+1} < 0 \tag{A-23}$$

while

$$-G + \sqrt{G^2+1} > 0 \tag{A-24}$$

However, $a = -G \pm \sqrt{G^2+1}$ always has the opposite sign of $-G \mp \sqrt{G^2+1}$ so that the condition that (A-22) be true is equivalent to the condition

$$(N\sigma_{xy} - \sigma_x \sigma_y)(-G \pm \sqrt{G^2+1}) > 0 \tag{A-25}$$

or

$$(N\sigma_{xy} - \sigma_x \sigma_y) > 0 \tag{A-26}$$

by (A-24).